The Thesis Committee for Panos Andonyadis Certifies that this is the approved version of the following thesis:

Decision Support for Enhanced Oil Recovery Projects

APPROVED BY
SUPERVISING COMMITTEE:

Supervisor:

Robert B. Gilbert, Supervisor

Larry W. Lake

Decision Support for Enhanced Oil Recovery Projects

by

Panos Andonyadis, B.S.E

Thesis

Presented to the Faculty of the Graduate School of

The University of Texas at Austin

in Partial Fulfillment

of the Requirements

for the Degree of

Master of Science in Engineering

The University of Texas at Austin

August 2010

Dedication

To my parents, Manol and Sula.

Acknowledgements

I would like to extend my gratitude to my advisor, Dr. Robert B. Gilbert, for his guidance and support throughout my graduate studies. I am also appreciative for the support and assistance from Dr. Larry Lake. My family's encouragement and unconditional support gave me the necessary strength for completing my studies. In particular my father's mentorship provided with me with the motivation to work through all obstacles.

I would like to extend my gratitude and thanks for the financial support from the Center for Petroleum Asset Risk Management, Chevron, and the University of Texas.

Abstract

Decision Support for Enhanced Oil Recovery Projects

Panos Andonyadis, M.S.E

The University of Texas at Austin, 2010

Supervisor: Robert B. Gilbert

Recently, oil prices and oil demand are rising and are projected to continue to rise over the long term. These trends create great potential for enhanced oil recovery methods that could improve the recovery efficiency of reservoirs all over the world. The greatest challenges for enhanced oil recovery involve the technical uncertainty with design and performance, and the high financial risk. Pilot tests can help mitigate the risk associated with such projects; however, there is a question about the value of information from the tests. Decision support can provide information about the value of an enhanced oil recovery project, which can assist with alleviating financial risk and create more potential opportunities for the technology.

The first objective of this study is to create a new simplified method for modeling oil production histories of enhanced oil recovery methods. The method is designed to satisfy three criteria: 1) it allows for quick simulations based on only a few physically

meaningful input parameters; 2) it can create almost any potential type of realistic production history that may be realized during a project; and 3) it applies to all non-thermal enhanced oil recovery methods, including surfactant-polymer, alkali-surfactant-polymer, and CO_2 floods. The developed method is capable of creating realistic curves with only four unique parameters.

The second objective is to evaluate the predictive method against data from pilot and field scale projects. The evaluations demonstrate that the method can fit most realistic production histories as well as provided ranges for the input parameters. A sensitivity analysis is also performed to assist with determining how all of the parameters involved with the predictive method and the economic model influence the forecasted value for a project. The analysis suggests that the price of oil, change in oil saturation, and the size of the reservoir are the most influential parameters.

The final objective is to establish a method for a decision analysis that determines the value of information of a pilot for enhanced oil recovery. The analysis uses the predictive method and economic model for determining economic utilities for every potential outcome. It uses a decision-based method to ensure that the non-informative prior probability distributions have an unbiased, consistent, and rational starting point. A simple example demonstrating the process is discussed and it is used to show that a pilot test provides some valuable information when there is minimal prior information.

For future work it is recommended that more evaluations are performed, the decision analysis is expanded to include more input parameters, and a rational and logical method is developed for determining likelihood functions from existing information.

Table of Contents

List of Tables

List of Figures

CHAPTER 1: INTRODUCTION

1.1 Background on Enhanced Oil Recovery

As oil prices and global for oil continue to steadily rise, oil producers have two options; start new fields or attempt recovering oil left behind in existing reservoirs (Belhaj and Lay 2008). Accessibility and start-up costs associated with producing oil from new fields make only large and rare fields economically viable options, and therefore enhanced oil recovery (EOR) is receiving more attention.

Most fields depend on primary and secondary isothermal recovery methods for oil production, which leaves approximately 40 to 60% of the oil in a reservoir unrecovered. EOR methods such as surfactant-polymer (SP), alkali-surfactant-polymer (ASP), and CO_2 flooding all have the ability to recover a fraction of the oil remaining in the reservoirs. Such methods can economically recover upwards of 15% of the original oil in place (Lake 1989).

Each method has its advantages and disadvantages. SP and ASP floods improve oil recovery through the mobilization of residual oil and improved sweep through the reservoir (Austad and Milter 2000). SP flooding is more expensive than ASP flooding, but arguably more dependable because of more field experience. CO_2 flooding mobilizes residual oil at a considerably lower cost than the other methods, but it usually reduces the sweep of the reservoir (Walsh and Lake 2008). Therefore, careful consideration of the advantages and disadvantages is required during the selection process between the three methods to ensure that the economically most attractive option is selected.

1.2 The Motivation for the Research

The technologies associated with EOR have existed for over half a century, with early pilot tests performed in the 1960's. However, the financial risks associated with the projects have prevented widespread use (Hartshorne and Nikonchik 1984; Stover 1988; and Bae 1995). Furthermore, the lack of history and experience with the technologies has created uncertainty with designing and predicting the performance of EOR projects. Therefore, as companies look towards EOR, they must balance the technological risk with economic potential.

Several researchers and engineers have attempted to minimize the risk associated with EOR by creating complex models that attempt to accurately predict the performance of projects (Paul et al. 1982, Saad et al. 1989, and Walsh and Lake 2008). Such models are limited by the uncertainty associated with the large number of required inputs.

Another popular method for analyzing and minimizing risk is to perform a decision making analysis that allows for a fair and unbiased selection process between the different methods. Such analyses typically take into account all possible outcomes; therefore, they require simple models that allow for many simulations to capture all of the outcomes. Several researchers have used simple models in decision analyses, but failled to create close representations of the oil recovery history (Barua et al., and 1986, Sanz and Miller 1994). Furthermore, the approaches used by many to set up the decision analyses typically create unintentional bias that alters the decision (Min 2008). Therefore, there is a need for a simplified but physically meaningful model of EOR

performance and a need to use this model to evaluate EOR in a formal decision framework.

1.3 Objectives of this Study

The main objective of this study is to provide decision support for EOR projects. The support comes in the form of decision analysis framework laid out for a value of information analysis of a pilot for EOR. To meet the objective several steps and sub-objectives have to be completed.

1.3.1 One: Establish a Predictive Model

A model for predicting the oil production history of an EOR project such as SP, ASP, and CO_2 floods is necessary. It must be simple with as few physically meaningful variables as possible for predicting technical performance. The predictions must be able to capture the general shape of the oil production history curve so that accurate economical predictions are possible. Along with the predictive model there must be an economic model that properly accounts for all expenses and revenue associated with an EOR project so that an accurate economic value of the project can be created.

1.3.2 Two: Evaluate the Predictive Model

The predictive model must be evaluated against actual pilot and field scale projects to assess the model's ability to forecast accurate oil production history. This evaluation also provides and typical values data and ranges associated with the input variables for the model that match real data.

1.3.3 Three: Establish a Decision Analysis Process and Demonstrate the Process through an Example

A decision analysis framework is needed to support the decision analysis. To establish an unbiased and consistent starting point, for assessing probabilities in this framework, a decision-based method is evaluated and used. A realistic example using this framework provides generic insight about the value of information of a pilot test.

1.4 Organization of Thesis

The thesis is organized in an order similar to the layout of the sub-objectives. Chapter 2 is generic overview of EOR processes and a review of similar decision analysis work. Chapter 3 explains the development of the predictive model and the meaning of the parameters associated with it. The evaluation of the predictive model and ranges for the parameters associated with the parameters of the model are discussed in Chapter 4. Chapter 5 explains the economic model and how revenue and expenses are accounted. Chapter 6 is a sensitivity analysis of all of the parameters associated with the predictive model and the economic model. This chapter provides some insight into how all the parameters influence value of an EOR project. The set up of the decision analysis is discussed in Chapter 7. The method for performing a value of information analysis of a pilot test for an EOR project is discussed and illustrated in Chapter 8. Conclusions about the predictive model and the decision analysis process are reviewed in Chapter 9. In the appendices are a collection of the all fields used in the evaluation of the predictive model (Appendix A), a collection of plots showing correlations between predictive model's parameters and field properties (Appendix B), collection of the plots created for the

sensitivity analyses (Appendix C), plots demonstrating the decision based method (Appendix D), and a summary of the nomenclature used throughout the thesis (Appendix E).

CHAPTER 2: BACKGROUND ON ENHANCED OIL RECOVERY METHODS, MODELLING, AND DECISION ANALYSES

2.1 Introduction

Countries all around the world are currently industrializing and therefore require large amounts of energy, especially petroleum. Figure 2-1 shows how the per capita demand of several countries has grown over the past century. Developed countries, such as the US and Japan, have leveled off in terms of per capita demand; however, over the past couple of decades, the heavily populated countries of China and India have begun to industrialize and their development will cause a significant increase in demand.

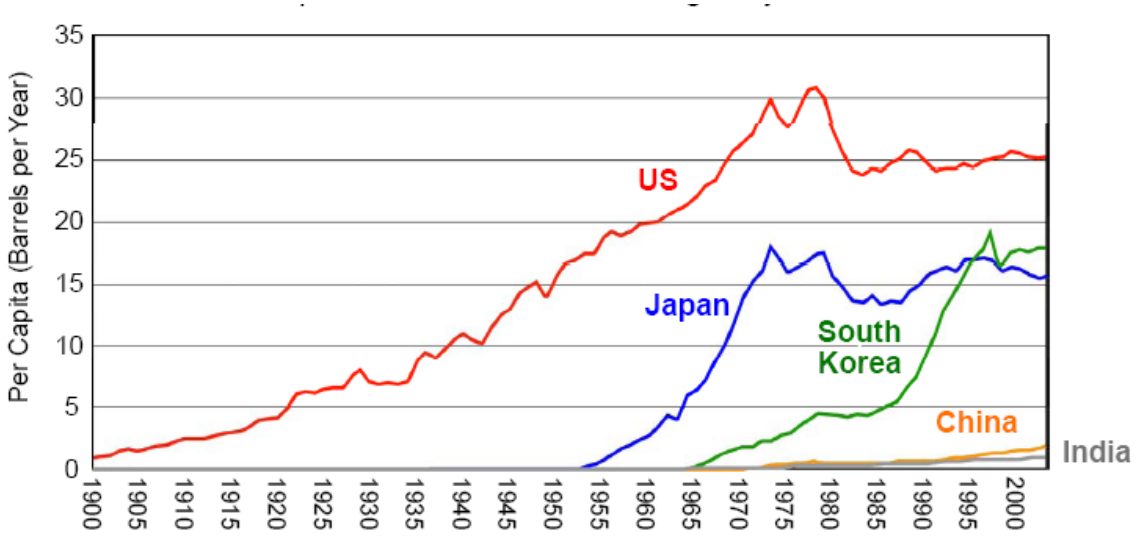

Figure 2-1 Plot of Oil Consumption during Industrialization of US, Japan, South Korea, China, and India (Jackson 2007)

The new demand will strain current resources of oil and force oil companies to look towards either new fields or become more efficient with existing ones. Starting a new field is an economic endeavor that is not attractive unless it is a huge field.

Therefore, companies are considering a wide variety of techniques to recover oil that is often unrecovered under conventional methods. These techniques fall under the category of enhanced oil recovery (EOR) methods (Lake 2008).

2.2 General Background on Conventional Recovery

The life of a typical reservoir goes through several stages of recovery. The first stage, known as primary recovery, uses the natural pressure gradient that exists within a reservoir to drive oil production. Once the pressure in the reservoir decreases to a point where recovery is no longer economical, secondary recovery is initiated. In general, about 12 to 15 percent of a reservoir's original oil in place (OOIP) is recovered during primary (Walsh and Lake 2003).

Secondary recovery is where either external energy is supplied into the reservoir through means, such as pumps, or a pressure gradient is regenerated through the injection of a fluid, such as water. A common form of secondary recovery is water flooding, a process where water is injected into the reservoir that displaces a fraction of the remaining oil. About another 15 to 20 percent of the OOIP is economically recovered by secondary flooding (Walsh and Lake 2003).

Once water flooding is no longer economical, oil companies must decide whether to attempt tertiary recovery or to abandon the reservoir. There may be as much as 65 to 70 percent of the OOIP may not be recovered. Figure 2-2 is a comparison of the ultimate oil recovery efficiencies with conventional methods for projects from around the world.

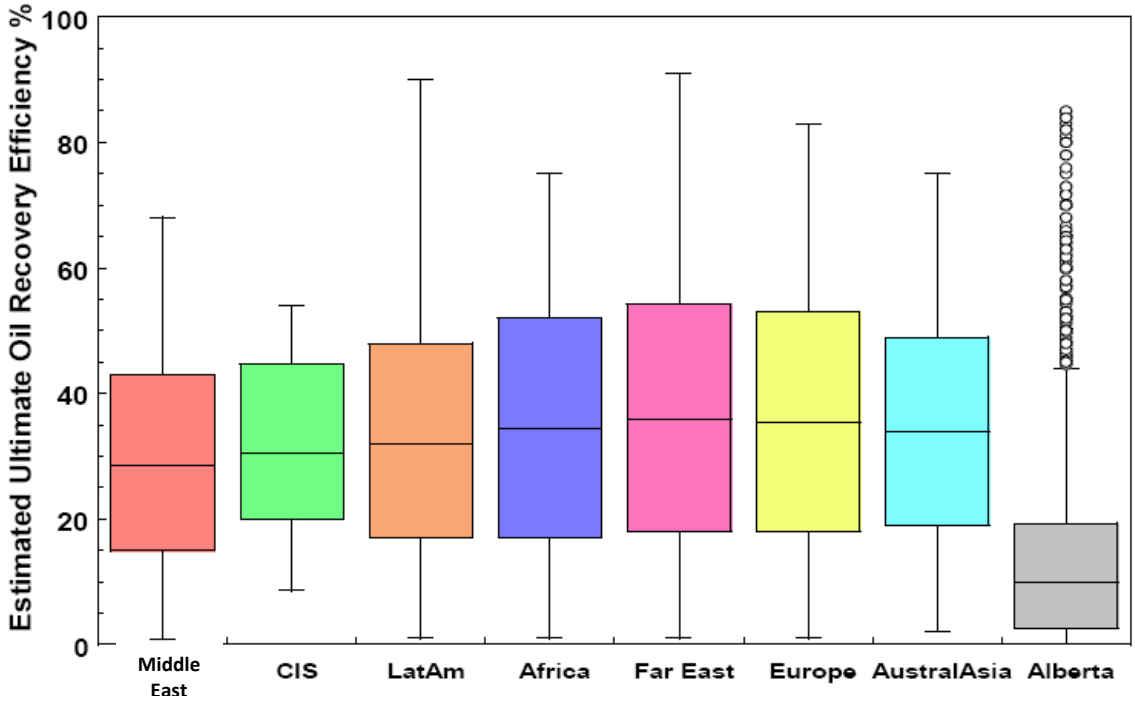

Figure 2-2 Comparison of the Distribution of Ultimate Oil Recovery Efficiencies with Conventional Methods for Projects from around the World (Lake 2008)

There are a variety of options for tertiary recovery including chemical injection, steam injection, in-situ combustion, and solvent injection. Tertiary recovery is often referred to as EOR. EOR methods improve recovery by mobilizing oil not typically mobilized by conventional recovery. The newly mobilized oil leads to an increase in rate of oil production and the final volume of produced oil. These methods have the potential to recover some of the remaining OOIP; however, economical limitation allow for them to only recover about five to 15 percent of the OOIP. The technology has existed for decades with particular interest during the 1980s when oil prices spiked (Lake 2008).

This thesis focuses on a specific group of isothermal EOR methods including surfactant-polymer (SP), alkali-surfactant-polymer (ASP), and carbon dioxide (CO_2)

injection. SP and ASP floods are often referred to as chemical EOR methods and CO_2 flooding is a form of a gas EOR method.

2.3 Discussion of the Isothermal Enhanced Oil Recovery Methods

Oil is not recovered during a water flood because it is either trapped by capillary forces or the water completely bypasses the oil. The capillary forces are due to surface tension, and they compete with the flow velocity, and viscosity of the injected water. The forces trap oil in small pores that make it very difficult to recover with water because extremely high pressure gradients are required. This trapped oil is often referred to as residual oil. The effect of the capillary force is characterized by the capillary number, N_C, which is defined as

$$N_C = \frac{\mu_w v}{\sigma} \propto \frac{\text{Driving Force}}{\text{Resisting Force}}$$

Equation 2-1

where σ is the oil-water interfacial tension, μ_w is the viscosity of the displacing fluid, and v is the effective flow rate. Figure 2-3 is a plot of residual oil saturation (S_{or}) against N_C for a typical reservoir. To mobilize residual oil, either the surface tension of the water must be reduced, or the water's viscosity must greatly increase (Austad and Milter 2000).

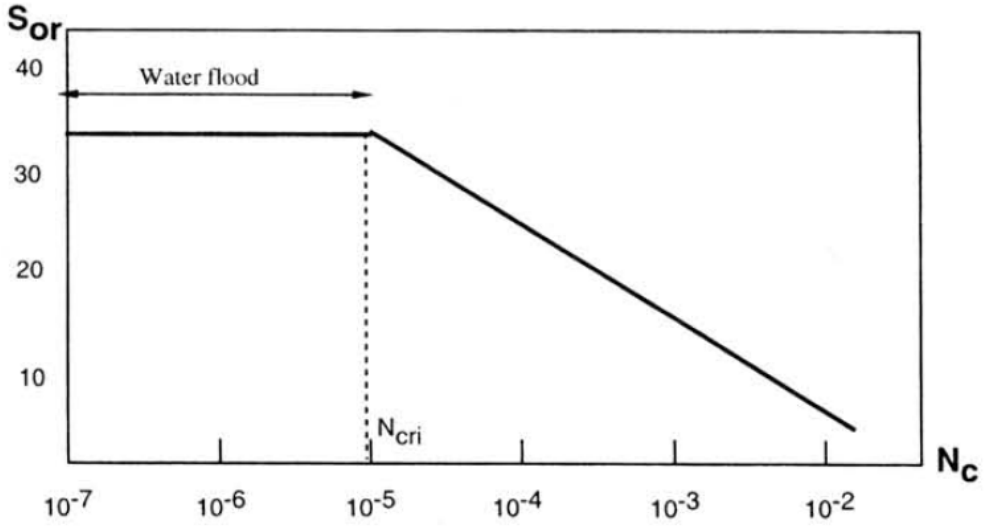

Figure 2-3 Residual Oil Saturation against Capillary Number for a Typical Reservoir (Austad and Milter 2000)

The oil that is bypassed is missed because of poor sweep between the injectors and producers. The injected water tends to miss the oil because of either an unfavorable mobility between the oil and water or because of the heterogeneity of the reservoir. Mobility is the ratio of the permeability of a porous material to a given phase divided by the viscosity of that phase. Poor areal sweep is often a result of instability between the water and oil, which creates fingering of the low viscosity water into the oil. Poor vertical sweep is typically caused by heterogeneity of the layers of the reservoir (Sorbie 1991). As a result of the poor sweep, a very large volume of water must be injected so that water can come into contact with all of the oil that is not trapped by capillary pressures.

Each isothermal EOR method addresses the aforementioned issues to some degree; however, each method has its own benefits and restrictions that must be considered prior to project initiation.

2.3.1 Polymer Flooding

A very common form of EOR is polymer flooding. Polymer floods are floods where polymer is mixed with water to create a viscous fluid that is injected into the reservoir. The more viscous fluid reduces the mobility ratio between the oil and water, which improves the sweep of the injected fluid for the reservoir. The mobility ratio, M, is the ratio of the mobilities of oil and the displacing fluid, as shown

$$M = \frac{\left(k/\mu\right)_w}{\left(k/\mu\right)_o}$$

Equation 2-2

where k is permeability, μ is viscosity, and the subscripts w and o stand for the displacing fluid and oil, respectively (Sorbie, 1991). The displacing fluid is water mixed with admixtures or solvents.

As a result of the better sweep, a spike in oil cut is generated and the remaining non-residual oil is recovered more rapidly, which reduces the life of the field (Sorbie 1991). The higher rate of recovery leads to a higher economical value for the produced oil than would exist if water flooding were continued, because early returns are more valuable when considering the time value of money.

Polymer floods also mobilize a small fraction of the residual oil because of the increase in viscosity; however, this effect is often neglected. The viscosity of the water usually needs to be increased by several orders of magnitude in order to mobilize a significant volume of residual oil (Sorbie 1991, Austad and Milter 2000).

Polymer floods are best suited for fields where the mobility ratio between water and oil causes fingering and heterogeneity causes channeling. Floods with mobility ratios greater than five typically experience these effects (Sorbie 1991). Other factors that to be considered include temperature, permeability, porosity, pH, clay content, fluid injectivity, salinity, and hardness of both the injected and in-situ fluids. These factors influence the degradation and adsorption of the polymer which in turn affect the effectiveness of the flood (Sorbie 1991). Injectivity of a fluid is the rate and pressure at which the fluid can be pumped into the reservoir without creating fractures in the formation. Injectivity could be of considerable importance because it may limit the injection rate for a significant portion of the flood's life which in turn leads to a lower production rate and lower overall profits when considering the time value of money.

Despite the wide range of factors, there is considerable comfort with designing polymer floods because they are relatively inexpensive, extensive flood preparations are not usually necessary and a wide variety of case histories and research exists. The most critical economic aspect is to build a mixing plant and the cost of the polymer. Other types of EOR floods include polymers because of the low cost and the added benefits with sweep (Sorbie 1991).

2.3.2 Surfactant-Polymer Flooding

Surfactant-polymer (SP) floods are designed to both improve the sweep of the reservoir as well as mobilize residual oil. SP floods are often referred to as micellar-polymer flooding or microemulsion flooding. A surfactant is a substance that lowers the surface tension between the two immiscible phases of oil and water. By reducing the

surface tension, the capillary forces are reduced and more oil is mobilized. Common forms of surfactants are detergents and soaps (Lake 1989).

There are several phases to an SP flood that involve the injection of distinctly different slugs. Historically, the first phase involves the injection of preflush slug designed to establish more favorable reservoir conditions for the surfactant slug by adjusting the salinity of the fluids in the reservoir. The second phase is injecting a slug of surfactant mixed with injection brine. The slug size is typically small (less than 0.25 total pore volumes of the reservoir) and the concentration of surfactant ranges between two and eight percent of the weight of injected fluids. The surfactant slug is followed by a slug of polymer and then followed by chase water. Some studies suggest that polymer could be mixed with surfactant as well as a polymer slug and the preflush may not be necessary (Lake 1989).

The ideal scenario for a SP flood is for reservoirs where the S_{or} is high, heterogeneity and mobility is an issue, the in-situ conditions are favorable for the surfactant and polymer, and the price of oil is high. Designing for a SP flood is challenging because the chemicals are sensitive to wide variety of factors including rock type, salinity, pH, heterogeneity of the reservoir, injectivity, hardness of fluids, clay content, viscosities, temperature, and pressure. Co-solvents such as alcohol may be needed to prevent gel formation and other complications (Austad and Milter 2000). Furthermore, there are few case histories of full-scale implementations and therefore little experience to draw from for assistance. The few case studies that do exist are mostly

from the 1970s and 1980s when SP flooding was popular and considered to be a viable option (Lake 2008).

There are several lab studies and research projects regarding SP flooding. The overall conclusion is that SP floods can provide a significant technical success as a large volume of the S_{or} can be recovered from core floods. However, at the field-scale there tend to be issues when trying to ensure good contact between oil and injected chemicals. Therefore, the field scale projects are not as technically successful as flooded lab cores. There also appears to be a shift in recommended flood design. Early projects injected very small slugs with high surfactant concentration. More recent projects seem to lean towards larger slug sizes with lower concentrations of surfactant.

The costs associated with a surfactant flood are high because the surfactant is expensive and most fields will need some development. The development includes new injection and production wells because smaller well spacings are needed in order to improve chemical and oil contact (White et al. 1986).

Since the 1980s, the overall consensus of the oil companies is that this method is a technical risk and uneconomical unless the price of oil is very high (Austad and Milter 2000). With the current oil prices hovering around $80/STB (Bloomberg 2010), SP flooding has once again become economically viable. The issue that remains to be overcome is the technical uncertainty involved with such a project.

2.3.3 Alkali-Surfactant-Polymer Flooding

Alkali-surfactant-polymer (ASP) floods are very similar to SP floods. Both EOR methods improve oil recovery by mobilizing residual oil and improving volumetric

sweep of the reservoir. The most significant difference between the two is that in ASP floods, alkaline chemicals are used along with surfactants and polymers. The alkali helps to reduce the adsorption of the surfactant and produces additional surfactant when reacting with in-situ oil. The alkali therefore produces a surfactant in the reservoir that works with the synthetic surfactant to mobilize residual oil (Hirasaki et al. 2008).

Overall, ASP floods have similar sensitivity to the same factors as SP floods. ASP floods are more sensitive to the rock type of the reservoir and have the added challenge of dealing with alkali consumption because of the alkali reacting with the oil. Furthermore, ASP floods are more likely to need a preflush to condition the reservoir, which delays profitable recovery for the project (Hirasaki et al. 2008).

Just as with SP floods, ASP floods have similar stages of injection. They start with a preflush, followed by an ASP slug, followed by a polymer slug, and then the chase water. The hardness of the injected fluid needs to be carefully monitored and maintained during the injection of the alkali (Wyatt et al. 2008).

Similar economic costs are associated with ASP floods as SP, including building new wells, mixing plants, and chemical costs. Overall, the cost of the chemicals are significantly lower as only a fraction of surfactant is needed and alkaline chemicals are not very expensive (Wyatt et al. 2008).

As long as the in-situ properties allow an ASP flood to work and the S_{or} is high, then an ASP flood can be a strong option because it is not a very expensive method, especially when compared to SP floods. However, ASP flooding is a relatively young technology and there are very few case studies at the field level.

2.3.4 CO_2 Flooding

CO_2 flooding is a type of solvent flooding method. It can be either be a miscible or immiscible process (Walsh and Lake 2008).

The main mechanism of oil recovery for CO_2 flooding is its ability to reduce surface tension between oil and water. Under lab conditions, it can recover nearly all of the residual oil in a core. At the field-scale a project typically produces less sweep of the reservoir than predicted. The viscosity of the CO_2 solvent is a very low compared to the oil, creating a poor mobility ratio between the solvent and the oil. To improve mobility, CO_2 is injected with water to increase the viscosity of the solvent. This process is known as a water alternating gas (WAG) process. CO_2 floods are designed with a WAG ratio in mind. The WAG ratio is the ratio of water to CO_2 solvent for the injected fluid. Lower WAG ratios have a higher CO_2 concentration and tend to lead to better residual oil mobilization, but poorer sweep. A balanced design is required for an economically optimal recovery (Walsh and Lake 2008).

The most critical criteria for a CO_2 candidate reservoir are low oil viscosity and high S_{or}. Rock type, pressure, and injectivity are other factors to be considered (Lake 2008).

The costs associated with CO_2 flooding are usually lower than for SP and ASP because less initial preparation work is required and the cost of the solvent is relatively inexpensive. The initial costs are low because larger well spacings, such as those used with water flooding, can be adequately used with CO_2 flooding (Mohan et al. 2008).

2.4 Enhanced Oil Recovery Models

Several models and methods exist to assist with designing and predicting the performance of an EOR process. Each method has its advantages and disadvantages. Some look to accurately and precisely forecast the production history of a field, while others attempt to predict only basic features with a simple model.

2.4.1 Koval's Method

Koval (1963) discusses a simple method to predict the behavior of a secondary recovery process through the use of a variable known as a Koval factor. The Koval factor is used to account for the effect of heterogeneity on a flood's behavior. Some have attempted to apply the model directly to EOR floods as well as secondary recovery.

The main advantage to the method is its simplicity. The method is a set of equations based on a single non-dimensional factor, the Koval factor. The simplicity of the method limits it from being able to capture all aspects of a flood. For example Koval's method predicts an instantaneous jump in oil cut that remains constant until breakthrough of the injected fluids. This behavior is not the case for a tertiary flood in the field or even the lab, because there is typically a delay between start of injection and the peak oil cut at the producers. Furthermore, there is typically an increase in oil cut rather than an instantaneous jump. Missing these characteristics can impact the economics of the project. The method is however able to capture the overall behavior of a declining oil cut and to some degree characterize the life of the flood in non-dimensional terms.

2.4.2 Chemical Flood Predictive Model

A simple model known as the chemical flood predictive model (CFPM) was developed for SP floods by Paul et al. (1982). The model is designed to use correlations to relate factors that influence oil recovery. Particular attention is paid to the capillary number, heterogeneity (Dykstra-Parsons coefficient), wettability, and surfactant sorption. From the correlations and fractional flow theory, oil breakthrough, peak oil rate, and project life are estimated.

CFPM produces a trianglular pattern of oil production history, as shown in Figure 2-4. The left vertex reflects zero oil production and occurs when oil breakthrough is expected to occur. The apex is at the level and time when the peak oil production is expected. The right vertex is at an oil production of zero at the time when the flood is expected to end. The area under the curve estimates the total volume of recoverable oil. Figure 2-4 is an example of a prediction from CFPM compared with field data.

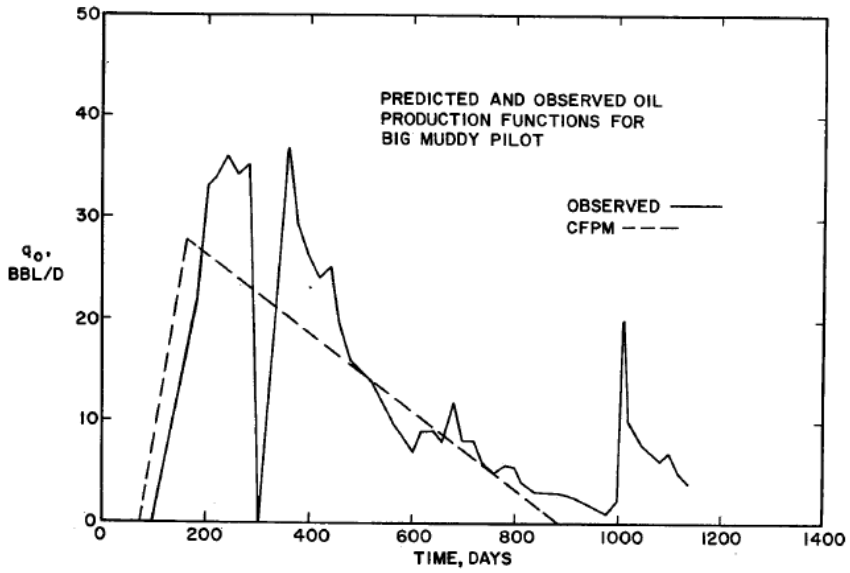

Figure 2-4 Example of CFPM against Data from a Field Surfactant-Polymer Flood (Paul et al. 1982)

CFPM is a simple model that does a better job than Koval's method in dealing with delay and increasing oil cut. The triangular curve does capture several important aspects of the flood behavior. Even though it does not create a close representative shape of the flood behavior, the triangular curve probably allows for a decent rough approximation of the monetary value of the project. Furthermore, because it is based on real tangible values, it can provide reasonable starting points when going through multiple simulations.

The main limitation of CFPM is that it creates a rough approximation of the production history curve. Another issue with the model is that it is strictly limited to sandstone reservoirs and SP floods.

2.4.3 UTCHEM

UTCHEM was developed at The University of Texas at Austin. It is designed to create accurate three dimensional reservoir simulations for chemical flooding. The simulator takes into account three-phases and up to 19-component flow. It is based on material mass-balance equations and accounts for several major physical phenomena. UTCHEM can handle any of the factors that are thought to influence the effectiveness of a chemical flood. It has been evaluated against several sets of lab, pilot, and field data (Saad et al. 1989).

UTCHEM is the "gold standard" simulator when compared to the other models discussed. Simulations generated by UTCHEM require dozens of input variables and multiple simulations are time-consuming. Table 2-1 is an example of the required inputs for UTCHEM. Most of the inputs are immeasurable and therefore contain considerable

uncertainty. Figure 2-5 is an example of the fit possible with the simulator. The simplified enhanced oil recovery model (SEORM) was also fitted against the production history in Figure 2-5.

Table 2-1 Example of the Required Simulation Parameters for UTCHEM, from the Big Muddy Pilot (Saad et al. 1989)

Parameter	Value	Parameter	Value	Parameter	Value
C^*_{2PLC}	0.0	S_{1rw}	0.32	A_{P2}	2,700.0
C^*_{2PRC}	1.0	S_{2rw}	0.32	A_{P3}	2,500.0
C_{3min}	0.0001	S_{3rw}	0.32	β_p	2.0
m_{A0}	0.131	k^0_{r1w}	0.144	C_{SE1}	0.01
c_{A0}	0.1	k^0_{r2w}	0.8	S_p	0.17
m_{A1}	0.191	k^0_{r3w}	0.11	γ_c	20.0
c_{A1}	0.026	e_{1w}	1.5	$\gamma_{\frac{1}{2}}$	20.0
m_{A2}	0.363	e_{2w}	1.9	P_α	1.8
c_{A2}	0.028	e_{3w}	1.5	b_{rk}	1,000.0
β_6	0.8	S_{1rc}	0.0	C_{rk}	0.0186
β_7	−2.0	S_{2rc}	0.0	c_{pc}	9.0
C_{SEL7}	0.177	S_{3rc}	0.0	n_{pc}	2.0
C_{SEU7}	0.344	k^0_{r1c}	1.0	D	0.0
G_{11}	13.0	k^0_{r2c}	1.0	α_L	16.0
G_{12}	−14.8	k^0_{r3c}	1.0	α_T	4.0
G_{13}	0.007	e_{1c}	1.5	a_{31}	1.0
G_{21}	13.0	e_{2c}	1.98	a_{32}	0.5
G_{22}	−14.5	e_{3c}	0.48	b_3	1,000.0
G_{23}	0.010	μ_1	0.7	a_4	2.0
$\log(\sigma_{wo})$	1.3	μ_2	4.0	b_4	100.0
T_{11}	−0.778	α_1	4.0	Q_v	0.05
T_{12}	−0.329	α_2	5.0	M_s	427.0
T_{21}	−0.662	α_3	−30.0	λ_1	1.549×10^{-4}
T_{22}	2.5	α_4	0.9	F_{R1}	0.2
T_{31}	−0.411	α_5	0.7	F_{R2}	0.15
T_{32}	−0.903	A_{P1}	81.0		

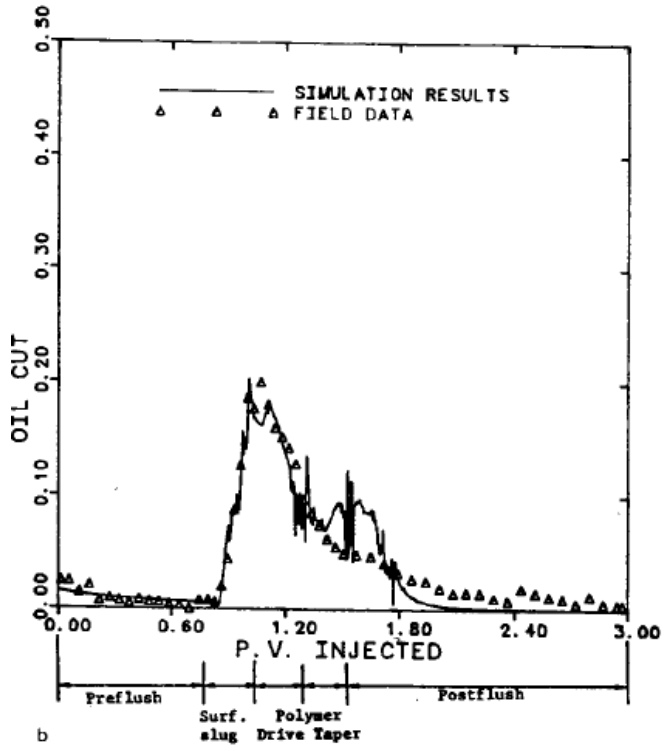

Figure 2-5 Example of UTCHEM Fit against Data from the Big Muddy Pilot (Saad et al. 1989)

2.4.4 Enhanced Oil Recovery Rate Model

The EOR rate model was developed by Walsh and Lake (2008) for the purpose of predicting a tertiary miscible flood. The approach is based on a hyperbolic decline curve and material balance. The model breaks down an EOR flood into three parts. The first part is the delay between when the flood is initiated and first response occurs at the producer. During this part, it is assumed that the decline curve modeling the water flood is continued. The second part is a linear increase in oil production till an assumed peak oil rate is reached. The third part is a decline in production till the production becomes zero. The model involves up to nine input parameters. The values used for the parameters are based on empirical correlations or ranges based on previous fits. Figure

2-6 is an example of the EOR rate model being applied. The example is from the Wertz field and is of a CO_2 flood. The model can be altered to fit most data sets well.

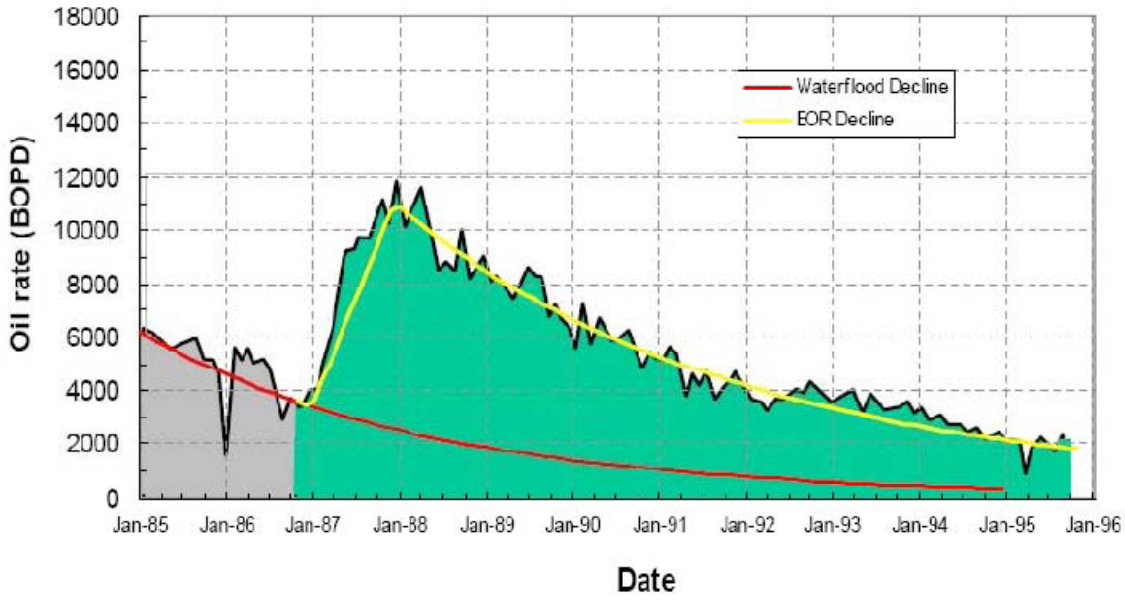

Figure 2-6 Example of EOR Rate Model Fit against Data from the Wertz Field (Walsh and Lake 2008)

The advantage of the model is that it provides a closer match than the other simple models with relatively few inputs. This model does allow one to perform multiple simulations quickly and could provide a more precise prediction of the monetary value of a project. However, there are nine parameters that are essentially unknown and not easily predicted prior to a flood because they are empirical. Distributions and correlations do exist to help predict these values, but they are based on very few data sets, all of which are CO_2 floods. Therefore, considerable evaluation would be required to ensure the model can work with other types of floods and to determine more accurate ranges and correlations.

2.5 Decision Analyses

Most simulators and models are not very accurate at prediction, even if they involve a significant amount of detail. A decision analysis that takes into account all of the possible outcomes for an EOR flood is no longer handicapped by a model's inaccuracy. By taking in account extremes, one can interpret the entire spectrum of possible outcomes.

Several papers have been published that attempt to demonstrate how one can use a simple model as part of decision analysis that either tries to determine the optimal design or decision for an EOR project. Two papers in particular are Sanz and Miller's (1994) and Barua et al. (1986).

2.5.1 Sanz and Miller's Paper

Sanz and Miller created a decision analysis method designed to assist with determining the probability that a design input is optimal for an SP flood. The authors used a model known as MCPALK. The utilities for any outcome were based on the monetary value of the project, as determined by the discounted cash flow. The input parameters for the model were divided into decision variables and stochastic variables. All stochastic variables were assumed to have continuous distributions, while finite distributions were used for the design variables. Sensitivity analyses were performed as a means to rank and identify the most influential stochastic parameters.

The authors created a method that studies and determines the optimal value for a design variable individually, based on the outcomes of the stochastic variables. Monte

Carlo simulation was implemented to represent the possible combinations of values to occur.

Their method applies for scenarios where the engineer has already determined the scale of the SP flood. The analysis does not explicitly take into account information from a pilot nor does it properly explains how the probability distributions for the stochastic variables are determined. The authors suggest that a user inputs probabilities for the variables based on their judgment.

2.5.2 Barua et al. Paper

The purpose of the paper was to develop a method that allows one to make technical and business decisions about SP flooding when there is considerable uncertainty. Their method allows an engineer to quickly evaluate the economic potential a field for an EOR flood and to compare EOR methods against other alternatives. The authors used CFPM as the SP flood modeling tool and discounted cash flow for creating the utilities. A Monte Carlo simulator was used to reflect the uncertainty.

The authors performed a similar analysis as Sanz and Miller, except fewer parameters were studied. Barua's work has the advantage that it can handle comparing different project alternatives as well as determining how a particular parameter influences the decision. Barua's has the same issue with the input probabilities and lack of pilot information as Sanz and Miller.

2.6 Summary

Enhanced oil recovery methods inherently have significant risk because of the uncertainty of the characteristics of a reservoir and the economic future. They are also very expensive and time consuming endeavors that must be carefully evaluated prior to a project's commencement. Several researchers have created models designed for both preliminary analysis as well as more detailed forecasting of the technical performance of an EOR flood. These models allow an engineer to study the potential outcomes as well as determine where the majority of uncertainty lies for a project. Decision analyses allow the engineer to then determine what the expected value of a project based on certain parameters. Researchers have used decision analyses and simple models to evaluate a field's potential for EOR and to determine starting points for creating optimal designs for the EOR flood.

Based on the review of existing literature on EOR and relevant modeling and decision analyses, a new simple model that better handles the shape of a typical EOR oil production curve is needed. Also needed is a method that defensibly establishes probabilities for the input parameters and a decision analysis that accounts for the value of pilot information.

CHAPTER 3: DEVELOPMENT OF THE SIMPLIFIED ENHANCED OIL RECOVERY METHOD

3.1 Introduction

A model is necessary to predict how a field will behave through the course of its life so that possible production and economic performance can be represented. Currently, several models exist to model a reservoir during a chemical flood; however, they require many input variables that require an in depth understanding of the input parameters and how the programs work. Furthermore, such programs can be cumbersome when one tries to run through multiple scenarios. The objective of this chapter is to explain the development and theory behind the simplified enhanced oil recovery method, which is designed for quick simulations of accurate oil production history curves.

The simplified enhanced oil recovery method (SEORM) models oil recovery in one dimension and it is based on fractional flow theories. The method also has Koval's model at its foundation.

3.2 Idealized One Dimensional Flow Model

3.2.1 Description of the Simplest Case

As a starting point for envisioning the problem, a basic one dimensional flow model between the injector and producer is considered. The following assumptions are made:

1) mass is conserved
2) the system is linear
3) the fluids are ideal and incompressible
4) one dimensional flow through a homogenous, isotropic, and isothermal material
5) the initial distribution of the fluids are uniform
6) no more than two phases flowing at once
7) no more than three flowing banks
8) Darcy's law applies
9) there is continuous flow
10) there is continuous and constant injection of displacing fluid
11) the banks are locally segregated
12) gravity and capillary effects are negligible
13) dispersion can be ignored
14) the top and bottom boundary of the reservoir are no-flow boundaries

If these assumptions are applied to a two bank flood, much like in a water flood, the reservoir will experience a piston like displacement between the injector and producer, as shown in Figure 3-1. The flood will consist of two banks, one for the initial condition and another for the injected fluid. Point A marks the front of the injected bank.

A bank is a portion of the fluids within a reservoir that has similar composition of its components in terms of fractional flow and saturation. A component is a distinct molecular entity, such as water or oil. For example, the initial bank is characterized by the saturations of the components that initially existed prior to flooding.

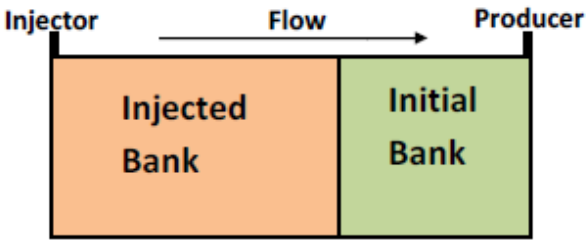

Figure 3-1 Profile of a Snap Shot in Time of a One Dimensional Flow for a Piston Like Two Bank Flow

The two banks in Figure 3-1 consist of the same components, oil and water, but at different saturations. The initial bank will have a higher oil saturation and lower water saturation than the injected bank. Each bank will also have different fractional flows of each component. The fractional flow of a component is the fraction of the total flow that the component compromises. For example if the 40% of the total volumetric flow of fluids is water, then the fractional flow of water is 0.4. The fractional flow of a component is also known as the cut of that component when it is being measured at the producer (Walsh and Lake 2003).

In the simple case, the oil cut at the producer will remain constant until the displacing fluid, the injected bank, arrives, at which point the oil cut will experience a step change. This type of behavior is captured with the equations

$$f_o(t_D) = \begin{cases} f_{oI} & t_D < \dfrac{1}{v_{disp}} \\ f_{oF} & t_D > \dfrac{1}{v_{disp}} \end{cases}$$

Equation 3-1

where $f_o(t_D)$ is the oil cut at a given time, f_{oI} and f_{oF} are the oil cut for the initial and injected banks, respectively, and v_{disp} is the specific shock velocity of the displacing fluid

front, and t_D is dimensionless time. The specific shock velocity is a dimensionless velocity that describes the relative velocity of the front of a bank. The dimensionless time is in terms of injected total pore volumes of the reservoir. Equation 3-1 can also be written as

$$f_o = f_{oI} + (f_{oF} - f_{oI})F(t_D)$$

Equation 3-2

where $F(t_D)$ is a set of step equations that describe the fractional flow of the displacing component as follows

$$F(t_D) = \begin{cases} 0 & t_D < \dfrac{1}{v_{disp}} \\ 1 & t_D > \dfrac{1}{v_{disp}} \end{cases}$$

Equation 3-3

3.2.2 Description of the Simple Case for an EOR Flood

The previous example can be extended to apply to a simple and ideal EOR flood. It is assumed that upon injection of the chemicals, the reservoir would begin to form three distinct banks, because of newly mobilized oil within the reservoir. The first bank represents the initial condition that existed before the flood. The second bank consists of oil released from previously trapped oil that is mobilized by the injected chemicals. The injected bank represents the injected chemicals. All previous assumptions continue to be applied. Figure 3-2 is a diagram of the piston-like case for an EOR flood.

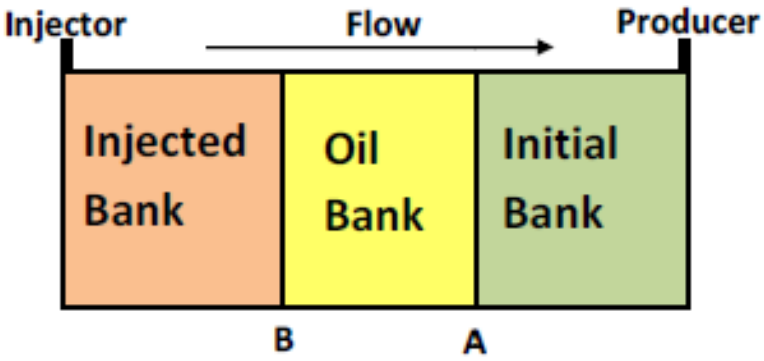

Figure 3-2 Profile of a Snap Shot in Time of a One Dimensional Flow for a Piston Like Three Bank Flow

There are two fronts, one for the bank of mobilized oil and another for the injected chemicals. Again, there is constant oil saturation and fractional flow of oil within each section. Before the oil bank reaches the producer, the producer will continue to behave as it did during the previous production by holding a constant oil cut. Once the oil bank reaches the producer, a shock occurs in the oil cut and it would again remain constant until the injected fluid reaches the producer. Figure 3-3 is a plot of how the oil cut will behave under these ideal conditions.

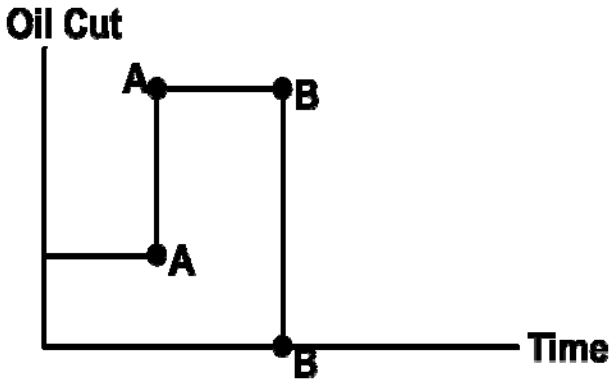

Figure 3-3 Oil Cut for a Three Bank Piston Like Flow

The oil cut experienced over the life of the flood can be expressed as step equations in terms t_D

$$f_o(t_D) = \begin{cases} f_{oI} & 1 < v_{oB}t_D \\ f_{oB} & v_{oB}t_D < 1 < v_C t_D \\ f_{oF} & 1 > v_C t_D \end{cases}$$

Equation 3-4

where f_{oB} is the oil cut for the oil bank, v_{oB} is the specific shock velocity of the oil bank, and v_C is the specific shock velocity of the injected bank. The oil cut is assumed to be zero when the injected fluid reaches the producer because the piston model assumes perfect displacement of all mobilized oil in the system. Equation 3-4 can also be written as

$$f_o(t_D) = f_{oI} + (f_{oB} - f_{oI})F_{oB}(t_D) + (f_{oF} - f_{oB})F_{oF}(t_D)$$

Equation 3-5

where $F_{oB}(t_D)$ is the fractional flow of the oil bank and is described by the step equations

$$F_{oB}(t_D) = \begin{cases} 0 & t_D < \dfrac{1}{v_{oB}} \\ 1 & t_D > \dfrac{1}{v_{oB}} \end{cases}$$

Equation 3-6

and $F_{oF}(t_D)$ is the fractional flow of the injected fluids as described by similar step equations

$$F_{oF}(t_D) = \begin{cases} 0 & t_D < \dfrac{1}{v_C} \\ 1 & t_D > \dfrac{1}{v_C} \end{cases}$$

Equation 3-7

3.3 The Actual Condition with Two Banks

The piston model does not accurately represent actual flow due to channeling caused by the heterogeneity of the reservoir and relatively large mobility ratio between the oil and the injected chemicals. Channeling occurs when the majority of the displacing fluid follows a path of least resistance through the medium between the injector and producer, preventing even displacement of the original in-place fluids. Hence, there is no instantaneous rise or fall in oil cut and the flow of the oil is not simply characterized by the velocity of the injected bank front. Figure 3-4 is a generic profile representing the more realistic condition with a two component flow. Figure 3-5 is a plot of the oil cut against time for a heterogeneous two bank system for a water flood.

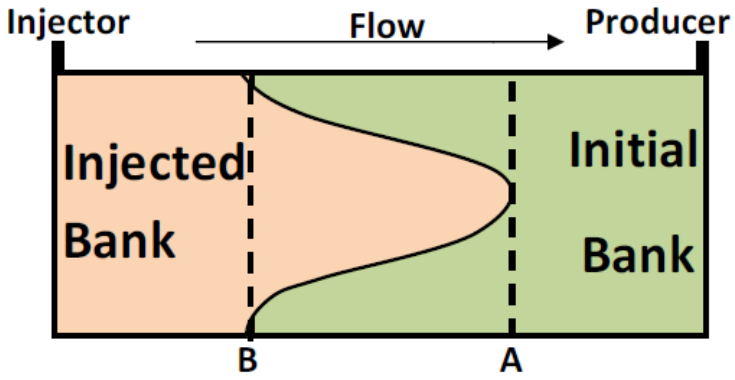

Figure 3-4 Profile of a Snap Shot in Time of a Generic for a Two Bank Flow with Channeling

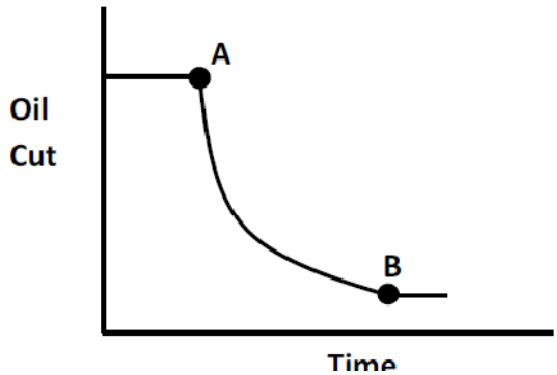

Figure 3-5 Oil Cut against Time for a Heterogeneous Two Bank Flow

3.4 The Actual Condition with Three Banks

Figure 3-6 is a generic profile for an EOR flood. It is still assumed that upon injection of the chemicals, three distinct banks will form within the reservoir and that the fractional flow theory continues to apply locally. The oil bank will also experience channeling because of the heterogeneity of the medium and the mobility between the fluids in the system.

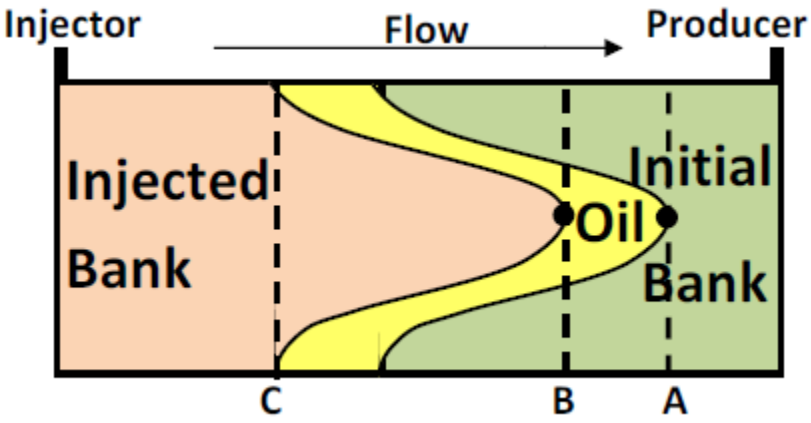

Figure 3-6 Profile of Generic for a Three Bank Flow with Channeling

The producer will continue to experience an oil cut similar to the one experienced during water flooding until the tip of the oil bank, point "A," reaches the producer. Then the producer will begin to experience a gradual rise in oil cut until the most advanced point of the injected chemicals, point "B", reaches the producer. The producer will then experience either a decline in oil cut or a more gradual rise in oil cut and then begin to decline. Figure 3-7 is a typical oil cut against time plot for a reservoir.

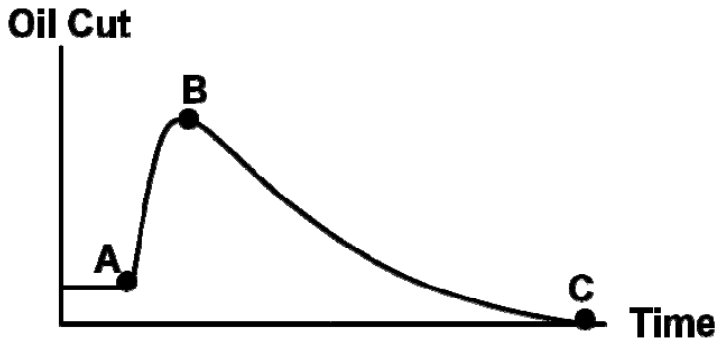

Figure 3-7 Oil Cut for a Three Component Flow with Channeling

Equation 3-6 and Equation 3-7 can be altered to account for less shock-like changes in fractional flow by adding an intermediate step that is defined by a variable that captures the channeling, C, as follows

$$F(t_D) = \begin{cases} 0 & F_{disp}(C, t_D) < 0 \\ F_{disp}(C, t_D) & 0 > F_{disp}(C, t_D) > 1 \\ 1 & F_{disp}(C, t_D) > 1 \end{cases}$$

Equation 3-8

3.5 Predicting Frontal Velocities

Pope (1980) noted that the specific velocity of a front for isothermal recovery methods can be found through the application of fractional flow theory. Equations were

developed as means to estimate the specific velocities of the two assumed fronts during an EOR flood.

3.5.1 Application of the Conservation of Mass

The law of the conservation of mass is used as a starting point in relating saturation and the fractional flow of a fluid. Buckley and Leverett (1942) showed from material balance that the equation for the conservation of a displacing fluid is

$$\frac{\partial S_{disp}}{\partial t} + u_{disp}\frac{\partial F_{disp}}{\partial x} = 0$$

Equation 3-9

where t is time, x is the distance from the injector, S_{disp} is the saturation of the displacing fluid, F_{disp} is the fractional flow of the displacing fluid, and u_{disp} is the interstitial velocity for the displacing fluid as defined by the following

$$u_{disp} = \frac{q}{A\varphi}$$

Equation 3-10

where q is volumetric flow, A is cross sectional area, and φ is porosity. The interstitial velocity is the average velocity of a fluid's front.

To help make the equation applicable with any size media, dimensionless units are used in place of t and x. The relative distance, x_D, is

$$x_D(x) = \frac{\int_0^x A\varphi d\xi}{\int_0^L A\varphi d\xi} = \frac{\text{Volume of pores filled by injected slug}}{\text{Total volume of pores}}$$

Equation 3-11

where L is the distance between the injector and producer. If φ and A are constant throughout the reservoir, then there is the special case

$$x_D(x) = \frac{x}{L}$$

Equation 3-12

The value for x equals zero at the injector, and L at the producer. Dimensionless time, t_D, is the total volume of injected fluid up to time t divided by the total pore volume of the medium, as shown

$$t_D(t) = \frac{\int_0^t q d\xi}{\int_0^L A\varphi d\xi} = \frac{\text{Injected volume}}{\text{Total pore volume}}$$

Equation 3-13

For the special case that φ and A are constant throughout the reservoir Equation 3-13 becomes

$$t_D(t) = \frac{qt}{A\varphi L} = \frac{qt}{V_p}$$

Equation 3-14

where V_p is the total pore volume of the system.

Taking the derivatives of Equation 3-12 and Equation 3-14 produces

$$dx_D = \frac{dx}{L}$$

Equation 3-15

$$dt_D = \frac{qdt}{V_p}$$

Equation 3-16

Substitutions of Equation 3-10, Equation 3-15, and Equation 3-16 into Equation 3-9 yields

$$\frac{\partial S_{disp}}{\partial t_D} + \frac{\partial F_{disp}}{\partial x_D} = 0$$

Equation 3-17

This equation demonstrates a correlation between saturation and fractional flow in dimensionless terms.

3.5.2 Application of the Frontal Advance Formula

Buckley and Leverett (1942) determined the frontal advance formula by transforming the material balance equation, Equation 3-9, into the following form

$$J_{disp} = \frac{q}{A\varphi}\frac{dF_{disp}}{dS_{disp}}$$

Equation 3-18

where J_{disp} is the saturation velocity, which is a dimensional velocity of the constant saturation front. Similarly, Equation 3-17 can be transformed to

$$v_{disp} = \frac{dx_D}{dt_D} = \frac{dF_{disp}}{dS_{disp}}$$

Equation 3-19

where v_{disp} is the specific shock velocity of the displacing front. The specific shock velocity is the dimensionless form of the saturation velocity.

3.5.3 Application of the Fractional Flow Curve for the Surfactant-Polymer and Alkali-Surfactant-Polymer Cases

The discussion for this section focuses on the construction and application of the fractional flow curves for SP and ASP floods.

To determine the fractional flow of the displacing fluid for different times and parts of the flood, a fractional flow curve is implemented. According to Buckley and Leverett (1942), if gravity effects and capillary pressure differences are neglected, then the fractional flow of the displacing chemicals is described by

$$F_w = \frac{1}{1 + \frac{k_{ro}}{k_{rw}} \frac{\mu_w}{\mu_o}}$$

Equation 3-20

where F_w is the fractional flow of the injected water, k_{ro} and k_{rw} represent the relative permeability of oil and the injected water, respectively, and μ_o and μ_w are the viscosities of the oil and the injected water, respectively.

As the displacing fluids move from a highly water saturated region to a lower one, oil is removed, reducing the oil saturation and increasing the displacing fluid concentration. As a result, the permeability of both the oil and displacing fluid change and the permeability values are a function of the saturation of the displacing fluid (Buckley and Leverrett 1942). Corey-type equations help define this relationship through the functions (Brooks and Corey, 1966).

$$k_{rw} = k_{rw}^{o}(S)^{n}$$

$$k_{ro} = k_{ro}^{o}(1 - S)^{m}$$

Equation 3-21

where k_{rw}^{o} and k_{ro}^{o} are end-point relative permeability values for water and oil respectively, m and n are constants that characterize the functions, and S is the relative saturation of the system. S is defined by the equation

$$S = \frac{S_w - S_{wr}}{1 - S_{or} - S_{wr}}$$

Equation 3-22

where S_w is the water saturation, S_{wr} and S_{or} are the residual saturations of the displacing fluid and oil, respectively. Figure 3-8 is a plot of generic relative permeability curves based on properties from Table 3-1.

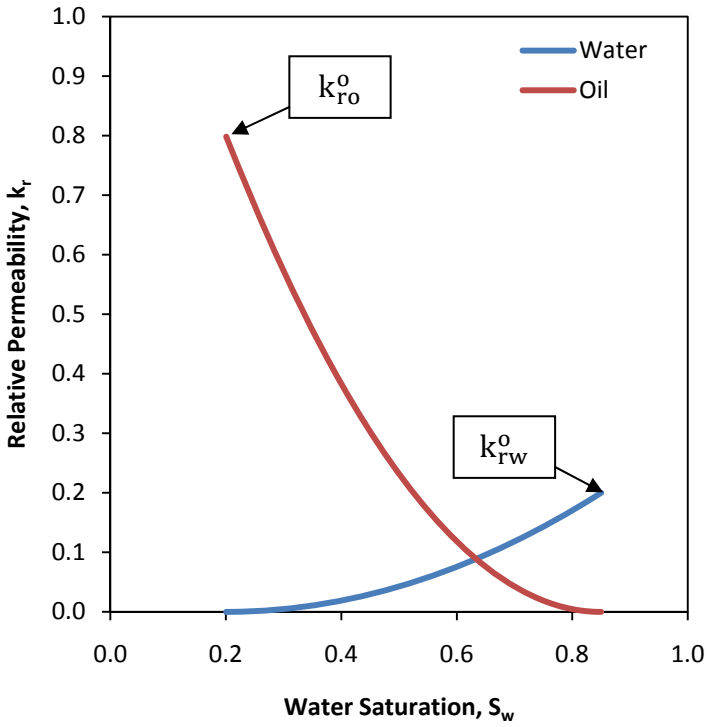

Figure 3-8 Generic Relative Permeability Curves

Substituting Equation 3-20 into Equation 3-21 yields

$$F_w = \frac{1}{1 + \frac{k^o_{ro}(1-S)^m}{k^o_{rw}(S)^n}\frac{\mu_w}{\mu_o}}$$

Equation 3-23

Figure 3-9 is a generic plot for a fractional flow curve as defined by the parameters in Table 3-1. The curve is a typical example of a water flood. The fractional flow is in terms of water cut because it is assumed the measurement is being made at the producer.

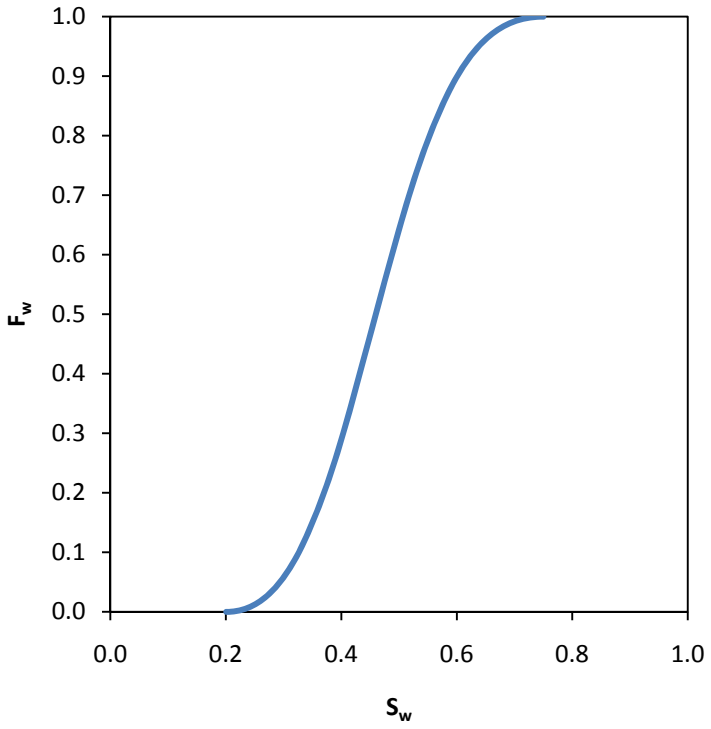

Figure 3-9 Generic Fractional Flow Curve Based on Values in Table 3-1

Table 3-1: Summary of Input Values for the General Fractional Flow Curve

Input	Variable	Value	Units
Viscosity of water	μ_w	1	cp
Viscosity of oil	μ_o	5	cp
End point relative permeability of water	k^o_{rw}	0.2	--
End point relative permeability of oil	k^o_{ro}	0.8	--
Corey type exponent for water	n	2	--
Corey type exponent for oil	m	2	--
Residual water saturation	S_{wr}	0.2	--
Residual oil saturation	S_{or}	0.25	--

Based on Equation 3-19, the curve predicts the specific velocities for different saturation fronts of various types of floods.

The simplest case is a water flood. The velocity of a continuous saturation front is defined as the slope of the fractional curve at a given saturation. At some saturation there is a maximum velocity. If the initial saturation is lower than the maximum, then that would suggest that upstream saturations fronts are travelling at faster rate than the downstream fronts, which creates situations where the slower velocity fronts are overtaken. Therefore, multiple saturations would exist at one point. This does not happen in nature because a shock front forms. The specific shock velocity is defined as the slope of a line between the initial condition for the flood, I, and a point tangent to the fractional flow curve, known as the saturation point, Z. Between the saturation point and the final condition point, J, the specific shock velocity decreases, creating a gradual change in the fractional flow of water over time. Figure 3-10 is a fractional flow curve demonstrating how the specific shock velocity for a water flood is estimated. Figure 3-11 is the saturation profile for the example water flood at t_D equals 0.3 V_P.

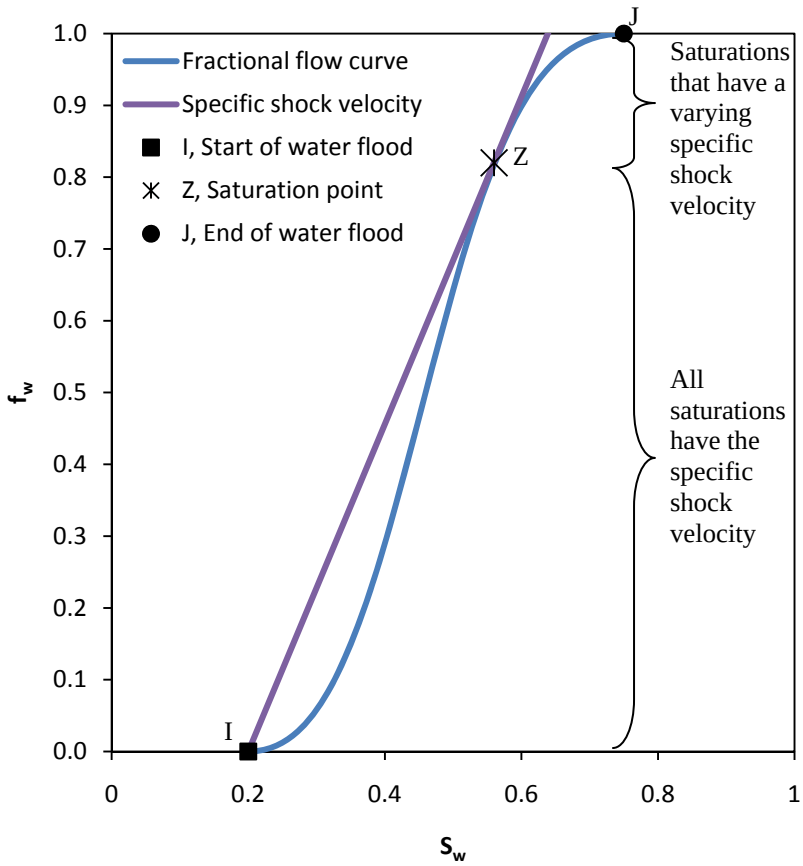

Figure 3-10 Fractional Flow Curve with Specific Shock Velocity for a Water Flood (Lake 1989)

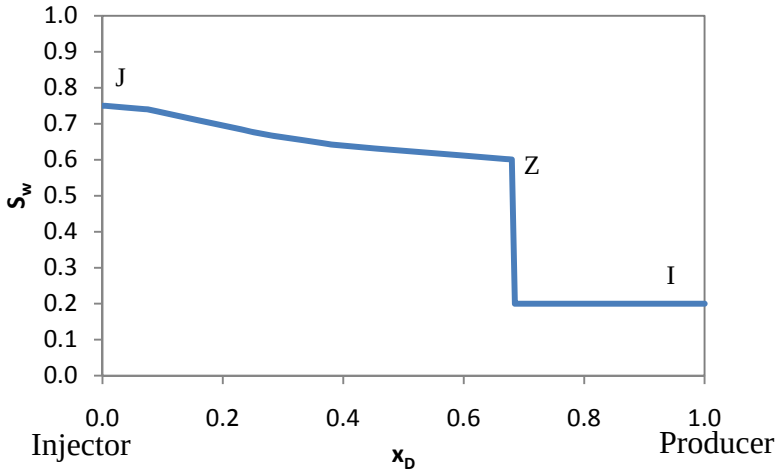

Figure 3-11 Approximation of the Saturation Profile for the Example Water Flood

An EOR process involves the formation of an oil bank and the injection of chemicals with significantly different properties than the in-situ oil or brine. Careful attention is required to calculate the specific velocities of the bank and injected chemicals.

Two fractional flow curves are necessary to capture the EOR process. The first is oil and water curve, similar to Figure 3-10. This curve is used to capture how the oil bank will displace the initial in place fluids. The second curve is for the displacing agent and oil and it is used to capture how the bank is displaced by the injected displacing agents. Figure 3-12 is a schematic plot of the two curves with the critical points marked.

For each curve, the points that define the specific velocities are the initial and final conditions. The arrows show how the saturations and fractional flow change over time. The specific shock velocity for the bank is no longer tangent to the curve as for the water flood; the specific shock velocity will only decrease between the initial and final condition, as the highest velocity for the displacing fluid exists where the lowest saturation exists. Therefore, in the special case where the oil bank is the displacing fluid and has a higher oil saturation than the displaced fluid, typically only one specific shock velocity is expected to exist. See Lake (1989, Chapter 5) for more details and background about the construction of fractional flow curves.

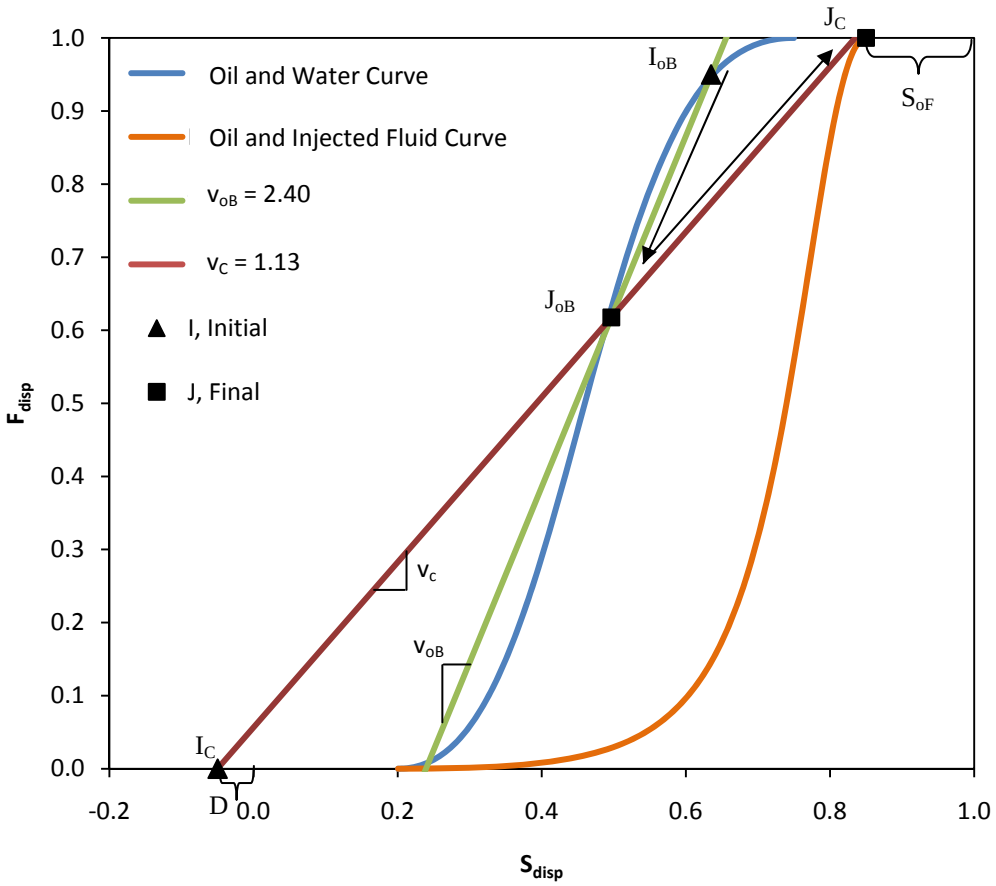

Figure 3-12 Fractional Flow Curves for a Generic EOR Scenario

Finding the specific shock velocity of the injected chemical is similar to the water flood condition except the initial point must start from a point less than zero and be tangent the chemical fractional flow curve. The value D on Figure 3-12 represents the effect of adsorption of the injected chemicals in terms of injected pore volumes. From Pope (1980), D usually is negligible; therefore, it can be assumed that the v_C line instead passes through the origin. Furthermore, the point of tangency is very close to the final condition of the flood, so as simplification, it is assumed that the specific shock velocity can be defined by a single value. With these assumptions, Figure 3-12 simplifies to

Figure 3-13. The assumptions create minor changes for v_{oB} and v_C; however the sensitivity analysis (Chapter 5) shows them to be relatively insignificant.

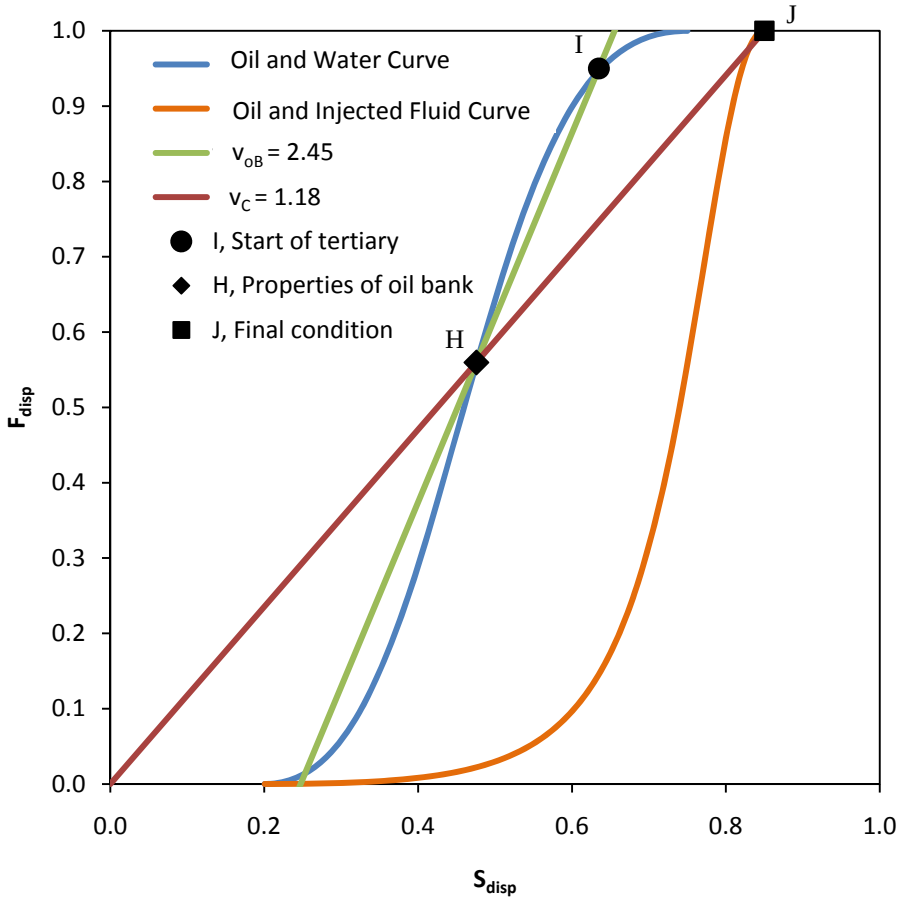

Figure 3-13 Simplified Fractional Flow Curves for a Generic EOR Scenario

From Equation 3-19 and the simplifying assumptions for fractional flow behavior, the specific velocities of both the oil bank and the injected chemical fronts can be captured by

$$v_{disp} = \frac{F_{disp|F} - F_{disp|I}}{S_{disp|F} - S_{disp|I}}$$

Equation 3-24

where the subscripts I, and F refer to initial and final condition, respectively. For the oil bank

$$F_{disp|F} = 1 - f_{oB}$$

$$F_{disp|I} = 1 - f_{oI}$$

$$S_{disp|F} = 1 - S_{oB}$$

$$S_{disp|I} = 1 - S_{oI}$$

Equation 3-25

where the subscripts "oB" refer to the oil bank and "oI" refer to the oil saturation at the initial in-situ condition. Oil cuts are used instead of fractional flow of oil at a certain x_D because what occurs at the producer is most important. Therefore v_{oB} equals

$$v_{oB} = \frac{f_{oB} - f_{oI}}{S_{oB} - S_{oI}}$$

Equation 3-26

Similarly for the injected chemicals

$$F_{disp|F} = 1$$

$$F_{disp|I} = 0$$

$$S_{disp|F} = 1 - S_{oF}$$

$$S_{disp|I} = 0$$

Equation 3-27

where S_{oF} is the EOR flood residual oil saturation at the end of the flood. Therefore v_C equals

$$v_C = \frac{1}{1 - S_{oF}}$$

Equation 3-28

The line for v_C also must pass through the bank condition because the injected chemical will displace the bank as well. Therefore, the following is also true

$$F_{disp|F} = 1$$

$$F_{disp|I} = 1 - f_{oB}$$

$$S_{disp|F} = 1 - S_{oF}$$

$$S_{disp|I} = 1 - S_{oB}$$

Equation 3-29

and

$$v_C = \frac{f_{oB}}{S_{oB} - S_{oF}}$$

Equation 3-30

Figure 3-14 is the saturation profile for the simplified case represented by the fractional flow curves in Figure 3-13.

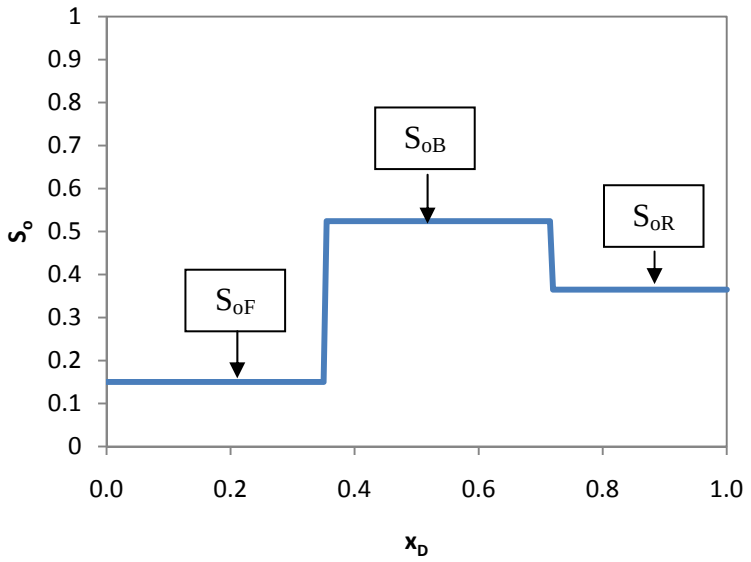

Figure 3-14 Oil Saturation Profile of the Simplified Fractional Flow Curves for the Generic EOR Scenario

Referring to Equation 3-5, Equation 3-26, and Equation 3-30, several variables are necessary to produce a prediction. Based on the history of the flood and core data, f_{oI} and S_{oI} may be estimated. The properties of the oil bank and S_{oF} are the remaining unknowns. S_{oF} captures the amount of oil recovered from the flood, where the lower S_{oF} is, the better the recovery. Hence it is a value that is not easily known. As for finding the properties of the oil bank, one must determine whether to assume values for f_{oB} and S_{oB} or to make assumptions about v_{oB} and v_C. From Figure 3-13, the line representing v_{oB} must go through both the points representing the initial conditions at the start of the flood and the oil bank, as it is these two points that define the slope. The line representing v_C must also go through the points representing the origin, oil bank and final condition, S_{oF}. Therefore, there are three critical points needed to define the two frontal velocities; however, the only point known with any confidence is the initial condition point. The

point representing the bank can be found from the intersection of the v_C line and the bank's fractional flow curve (relative permeability values and viscosities). Ultimately, this suggests that with a known fractional flow curve for the oil bank and assumed final oil saturation at the end of the flood, one could determine the specific velocities and the properties of the bank.

3.5.4 Application of the Fractional Flow Curve for the CO_2 Flood Case

The discussion for this section focuses on the construction and application of the fractional flow curves for CO_2 floods. The behavior of CO_2 flooding is different from other miscible processes because the CO_2 has appreciable solubility into both oil and water (Pope 1980). Therefore the construction is altered, in particular the construction for the line representing the specific shock velocity of the injected CO_2 solvent.

Walsh and Lake (1988) created a method to apply fractional flow theory to solvent flooding. The theories and assumptions made for SP and ASP cases continue to apply. Once again two curves are required for determining the fractional flow velocities of the oil bank and the chasing solvent. One curve is the oil and water curve and the other is solvent and water curve. Both curves are constructed with the same parameters, except different viscosities. For the solvent and water curve the viscosity of the solvent is used in place of the oil. Table 3-2 is a summary of generic parameters used to create generic oil and water, and solvent and water fractional flow curves shown in Figure 3-15.

Table 3-2 Summary of the Input Values for the General Oil and Water and Solvent, and Water Fractional Flow Curves

Input	Variable	Value	Units
Viscosity of water	μ_w	1	cp
Viscosity of oil	μ_o	1.5	cp
Viscosity of solvent	μ_s	0.07	cp
End point relative permeability of water	k^o_{rw}	0.2	--
End point relative permeability of oil	k^o_{ro}	0.8	--
Corey type exponent for water	n	2	--
Corey type exponent for oil	m	2	--
Residual water saturation	S_{wr}	0.2	--
Residual oil saturation	S_{or}	0.4	--

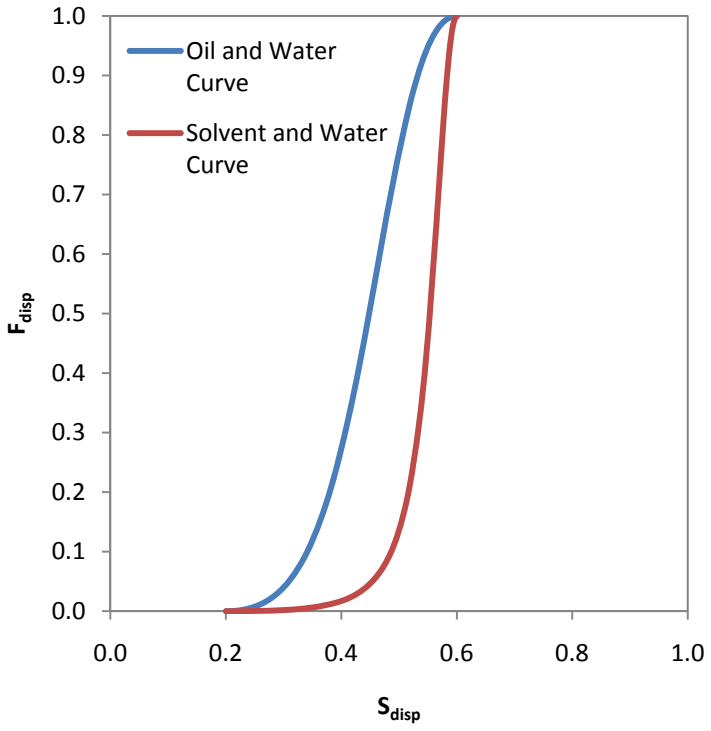

Figure 3-15 Generic Fractional Flow Curves Based on Values in Table 3-2

CO_2 flooding involves injecting water with CO_2 as a means to improve the mobility between the solvent and oil. This process is done by either alternating injection of water solvent or by mixing the two together. The ratio of water to gas is known as the WAG ratio and it based on volume. The WAG ratio is a design parameter and it is important parameter for determining the specific shock velocity of the fractional flow of the solvent. Walsh and Lake determined that the WAG ratio controls the fractional flow of water at the injector end at the beginning of the flood, f_{wJ}, with the following relationship

$$f_{wJ} = \frac{WAG}{1 + WAG}$$

Equation 3-31

The line representing the specific shock velocity of the solvent passes through a point on the solvent and water curve at f_{wJ}. The line also passes through the point where the line for the specific shock velocity of the oil passes through the oil and water curve. The specific shock velocity of the solvent is v_C and the specific shock velocity of the oil bank is v_{oB}. The line for v_C also passes through the point representing the final oil saturation, S_{oF}, at the end of the flood. Figure 3-16 is a plot of the fractional flow curves and the specific shock velocities. A line could be used to approximate the solvent and water curve.

Figure 3-16 is very similar to Figure 3-13. The most significant difference is with the line for v_C. For SP and ASP floods the line is anchored in at the origin and for CO_2 it is anchored into a point along the solvent and water curve at a point designated by the WAG ratio.

See Walsh and Lake (1988) for more details and background about the construction of fractional flow curves for solvent flooding.

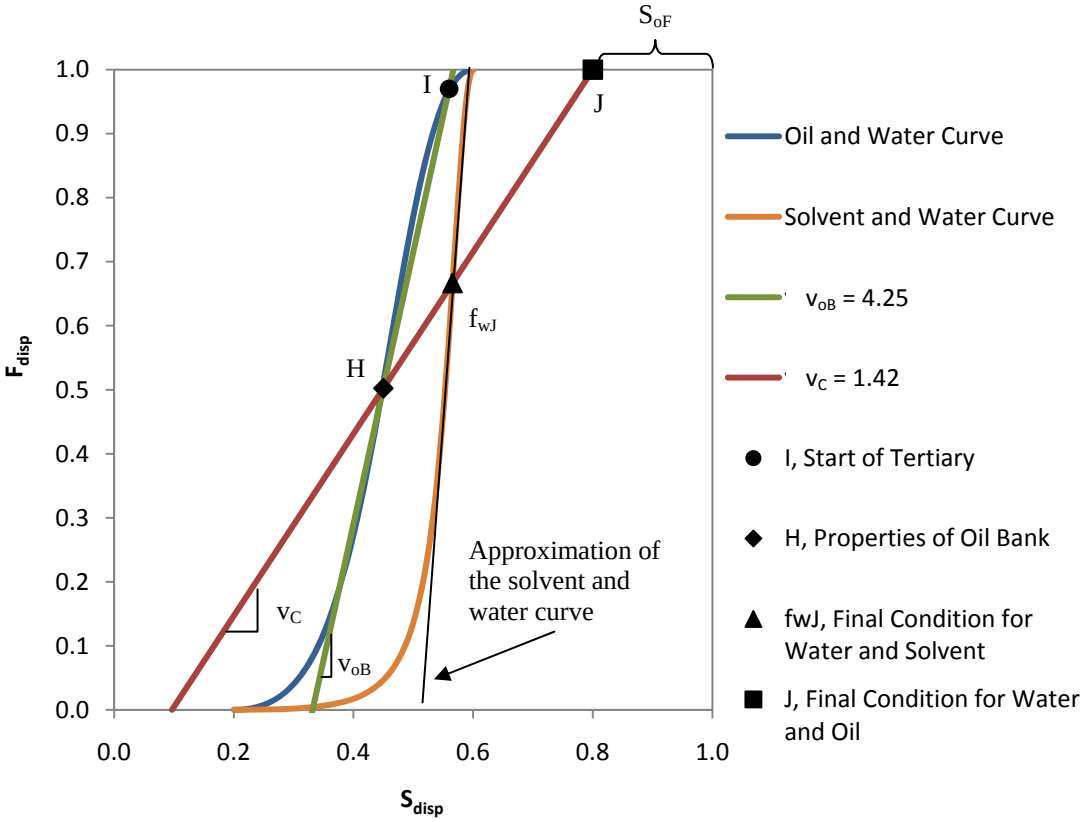

Figure 3-16 Generic Fractional Flow Curve CO_2 Floods

Equation 3-26 and Equation 3-30 can be used to calculate v_{oB} and v_C, respectively. If the WAG ratio and the properties of the fractional flow curves are known or assumed then the location and value of f_{wJ} is known. With that information Equation 3-30 can also be defined as

$$v_C = \frac{f_{wJ}}{S_{wJ} - S_{oF}}$$

Equation 3-32

where S_{wJ} is the water saturation at f_{wJ}. With v_C known, the starting point for the line for v_{oB} defined by the properties at the start of tertiary flooding, the oil and water curve known, then v_{oB} can be determined. Also with v_C known, S_{oF} can be determined. Therefore, with information about the fractional flow curves and the WAG ratio, the specific shock velocities and the final oil saturation can be determined.

3.6 Koval's Method

Koval (1963) attempted to capture the behavior of an unstable miscible flood through simple equations called Koval's method. The method is centered on the concept that heterogeneity and mobility of the fluids can be captured under one variable, a Koval factor, which is used to describe bypassing or channeling.

3.6.1 Koval's Assumptions

The method follows similar assumptions as mentioned before and includes that the solvent is miscible with the oil in place and the fractional flow curve is simplified. It is based on fractional flow curves that go from S_{disp}=0 and F_{disp}=0 to S_{disp}=1 and F_{disp}=1. This approach suggests that all of the fluid in the system is mobilized. Furthermore the method is based on the Buckley-Leverett theory and material balance (Koval, 1963).

3.6.2 Development of Koval's Equations

The Buckley-Leverett theory provides two critical relationships, the frontal advance formula, and the fractional flow equation. Koval's method begins with the fractional flow equation as shown in Equation 3-20 and, based on the assumption of

locally segregated flow between the solvent and oil, the interaction between the oil and the displacing fluid can be determined the following relationships

$$k_{rdisp} = k^{o}(S_{disp})$$

$$k_{ro} = k^{o}(1 - S_{disp})$$

Equation 3-33

where k is permeability, k_{rdisp} is the relative permeability of the displacing fluid and S_{disp} is the displacing fluid saturation. Equation 3-33 is the Corey-type assumption, Equation 3-21, with m = n = 1. Koval assumed that there was considerable evidence to suggest that a heterogeneity factor, H, and effective viscosity ratio, E, are critical to the recovery of oil. The Koval factor, K_{disp}, is defined as the product of the heterogeneity factor and effective viscosity ratio. The effective viscosity can be estimated with the following

$$E = \left(0.78 + 0.22\nu^{\frac{1}{4}}\right)^{4}$$

Equation 3-34

where E is the effective viscosity and ν is μ_o/μ_{disp}. The heterogeneity factor is a value estimated based on experimental data.

Substitution of Equation 3-33 into Equation 3-20 and following his assumptions, Koval determined that

$$F_{disp} = \frac{1}{1 + \frac{(1 - S_{disp})}{(S_{disp})} \frac{1}{K_{disp}}}$$

Equation 3-35

Figure 3-17 is a plot showing various ranges of fractional flow curves as they apply to the Koval method. Note that the displacing fluid has an initial condition of zero saturation and flow and final condition of 100% saturation and flow.

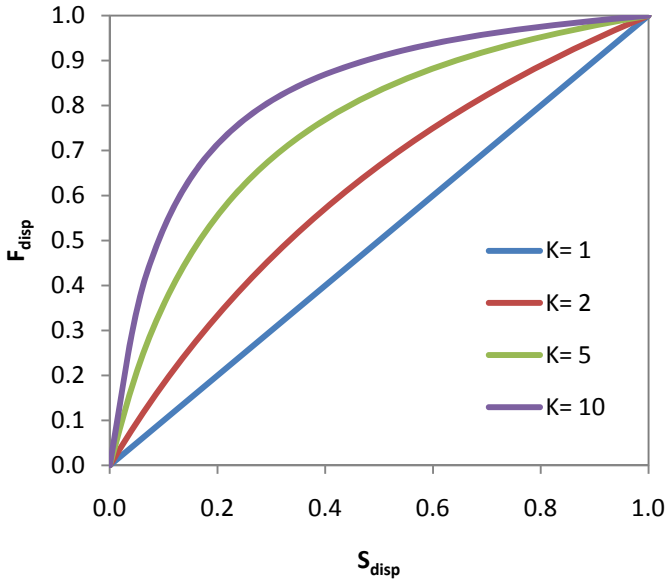

Figure 3-17 Range of Fractional Flow Curves for the Koval Method

Referring back to the frontal advance formula, Equation 3-19, and by taking the derivative of Equation 3-35 in terms of S, it is found that

$$\frac{dF_{disp}}{dS_{disp}} = \frac{dx_D}{dt_D} = \frac{K_{disp}}{\left[1 + (K_{disp} - 1)S_{disp}\right]^2}$$

Equation 3-36

By taking Equation 3-35 and setting it equal to S_{disp}, substituting it back into Equation 3-36, and then applying it to Equation 3-8, Koval developed the following set of simple equations designed to capture the behavior of the fractional flow of the displacing fluid

$$F_{disp}(x_D, t_D) = \begin{cases} 0 & t_D < \dfrac{x_D}{K_{disp}} \\ \dfrac{K_{disp} - \sqrt{\dfrac{K_{disp} x_D}{t_D}}}{(K_{disp} - 1)} & \dfrac{x_D}{K_{disp}} < t_D < x_D K_{disp} \\ 1 & t_D > x_D K_{disp} \end{cases}$$

Equation 3-37

Figure 3-18 is a collection of water cut curves for various K values. Higher K values imply higher heterogeneity of the medium.

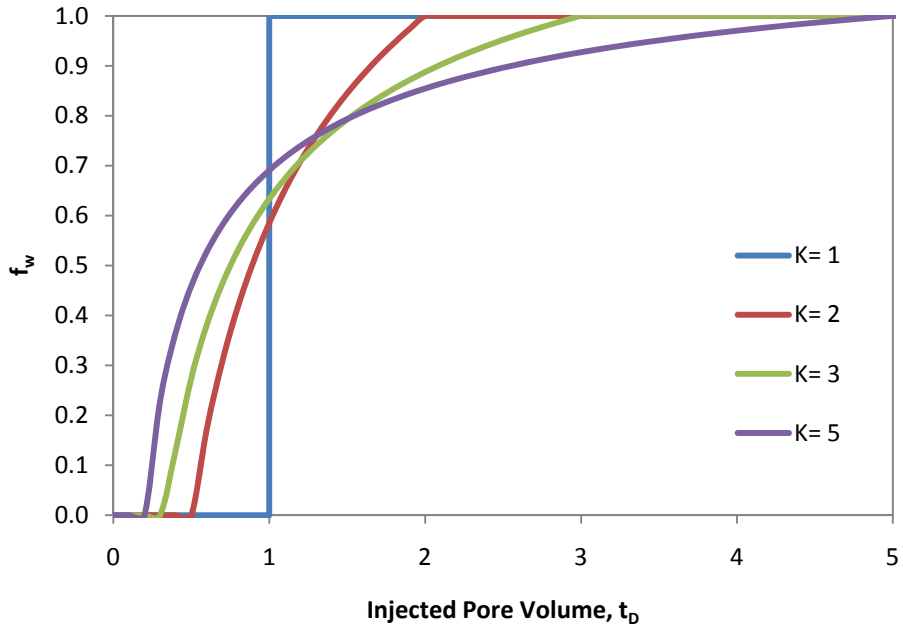

Figure 3-18 Example of Fractional Flow of Water Curves for Various Koval Factors

Koval's model worked with two bank flow; therefore f_o is

$$F_o(x_D, t_D) = 1 - F_{disp}(x_D, t_D)$$

Equation 3-38

For more details refer to Koval (1963).

3.7 Development of the Simplified Enhanced Oil Recovery Model

The simplified enhanced oil recovery method (SEORM) has Koval's model as its foundation. SEORM is designed to maintain the simplicity of Koval's method, while still addressing its short comings as discussed in Chapter 2.

3.7.1 Derivation of the Fractional Flow Equation for the Simplified Enhanced Oil Recovery Method

The Koval model essentially works with a two component flow for moveable pore volume is the same as pore volume. The first step in building SOERM is to use the Koval model as a starting point with Equation 3-36. Up to this point the total pore volume was assumed to also be the sweepable pore volume at any time during the flood. This is not the case typically as residual saturations will prevent complete sweep of the total pore volume. Therefore the frontal advance formula is redefined as

$$\frac{dF_{disp}}{dS_{disp}} = \frac{x_D}{t_{D|s}}$$

Equation 3-39

where $t_{D|s}$ is dimensionless time in terms of sweepable pore volume defined as

$$t_{D|s} = \frac{tq(\Delta F_{disp})}{V_p(\Delta S_{disp})}$$

Equation 3-40

The change in fractional flow of the displacing fluid, ΔF_{disp}, refers to the change that occurs between banks. The injection rate, q, multiplied by the change in fractional flow expresses the amount of the injected fluid that is moving though the sweepable pore volume, which captures the change in rate through the sweepable pore volume. The total pore volume, V_p, multiplied by the change in saturation represents the change in sweepable pore volume.

From Equation 3-40, $t_{D|s}$ is the product of t_D and the specific shock velocity of the displacing fluid, v_{disp}. Thus, Equation 3-36 becomes

$$\frac{dF_{disp}}{dS_{disp}} = \frac{dx_D}{dv_{disp}t_D} = \frac{K_{disp}}{\left[1 + (K_{disp} - 1)S_{disp}\right]^2}$$

Equation 3-41

Equation 3-41 is then set equal to S_{disp} and then substituted into Equation 3-35 to get

$$F_{disp}(x_D, t_D) = \frac{K_{disp}\sqrt{\frac{t_D v_{disp}}{K_{disp}x_D}} - 1}{(K_{disp} - 1)\sqrt{\frac{t_D v_{disp}}{K_{disp}x_D}}}$$

Equation 3-42

3.7.2 Derivation of the Oil Cut Equation

Recall that Equation 3-5 captures the oil cut for an ideal three component case. With Equation 3-42 as the definition for the change in fractional flow of the displacing fluid in Equation 3-8, Equation 3-42 becomes

$$F_{disp}(x_D, t_D) = \begin{cases} 0 & t_D < \dfrac{x_D}{K_{disp} v_{disp}} \\ \dfrac{K_{disp}\sqrt{\dfrac{t_D v_{disp}}{K_{disp} x_D}} - 1}{(K_{disp} - 1)\sqrt{\dfrac{t_D v_{disp}}{K_{disp} x_D}}} & \dfrac{x_D}{K_{disp} v_{disp}} < t_D < \dfrac{x_D K_{disp}}{v_{disp}} \\ 1 & \dfrac{x_D K_{disp}}{v_{disp}} > t_D \end{cases}$$

Equation 3-43

Note how the limits for each step are now defined. As Equation 3-43 is applied to the oil bank component it becomes

$$F_{oB}(x_D, t_D) = \begin{cases} 0 & t_D < \dfrac{x_D}{K_1 v_{oB}} \\ \dfrac{K_1\sqrt{\dfrac{t_D v_{oB}}{K_1 x_D}} - 1}{(K_1 - 1)\sqrt{\dfrac{t_D v_{oB}}{K_1 x_D}}} & \dfrac{x_D}{K_1 v_{oB}} < t_D < \dfrac{x_D K_1}{v_{oB}} \\ 1 & t_D > \dfrac{x_D K_1}{v_{oB}} \end{cases}$$

Equation 3-44

where K_1 is the Koval factor for the flow between the oil and initial banks. Similarly for the injected chemical component, Equation 3-43 becomes

$$F_{oF}(x_D, t_D) = \begin{cases} 0 & t_D < \dfrac{x_D}{K_2 v_c} \\ \dfrac{K_2\sqrt{\dfrac{t_D v_C}{K_2 x_D}} - 1}{(K_2 - 1)\sqrt{\dfrac{t_D v_C}{K_2 x_D}}} & \dfrac{x_D}{K_2 v_c} < t_D < \dfrac{x_D K_1}{v_c} \\ 1 & t_D > \dfrac{x_D K_2}{v_c} \end{cases}$$

Equation 3-45

where K_2 is the Koval factor for the flow between the injected and oil banks. Equation 3-5 still applies as mentioned earlier.

3.7.3 Summary of Critical Equations for the Simplified Enhanced Oil Recovery Method

The following equations are summarized for SEORM. To simplify the equations slightly, it is assumed that the main concern for a flood is how the producers react during the EOR process; therefore, x_D is set to equal one so that the equations describe the behavior of the flood at the producers.

$$f_o(t_D) = f_{oI} + (f_{oB} - f_{oI})F_{oB}(t_D) + (f_{oF} - f_{oB})F_{oF}(t_D)$$

Equation 3-46

$$F_{oB}(t_D) = \begin{cases} 0 & t_D < \dfrac{1}{K_1 v_{oB}} \\ \dfrac{K_1\sqrt{\dfrac{t_D v_{oB}}{K_1}} - 1}{(K_1 - 1)\sqrt{\dfrac{t_D v_{oB}}{K_1}}} & \dfrac{1}{K_1 v_{oB}} < t_D < \dfrac{K_1}{v_{oB}} \\ 1 & t_D > \dfrac{K_1}{v_{oB}} \end{cases}$$

Equation 3-47

$$F_{oF}(t_D) = \begin{cases} 0 & t_D < \dfrac{1}{K_2 v_c} \\ \dfrac{K_2\sqrt{\dfrac{t_D v_C}{K_2}} - 1}{(K_2 - 1)\sqrt{\dfrac{t_D v_C}{K_2}}} & \dfrac{1}{K_2 v_C} < t_D < \dfrac{K_2}{v_C} \\ 1 & t_D > \dfrac{K_2}{v_C} \end{cases}$$

Equation 3-48

$$v_{oB} = \frac{f_{oB} - f_{oI}}{S_{oB} - S_{oI}}$$

Equation 3-49

$$v_C = \frac{1}{1 - S_{oF}} = \frac{1 - f_{oB}}{1 - S_{oB}}$$

Equation 3-50

Figure 3-19 is a typical plot of SEORM. The rise and decline of the oil cut are captured by the cumulative sum of the changes in $F_{oB}(t_D)$ and $F_{oF}(t_D)$, as described in

Equation 3-47and Equation 3-48. Note the close resemblance to the expected behavior of the actual case for an EOR flood.

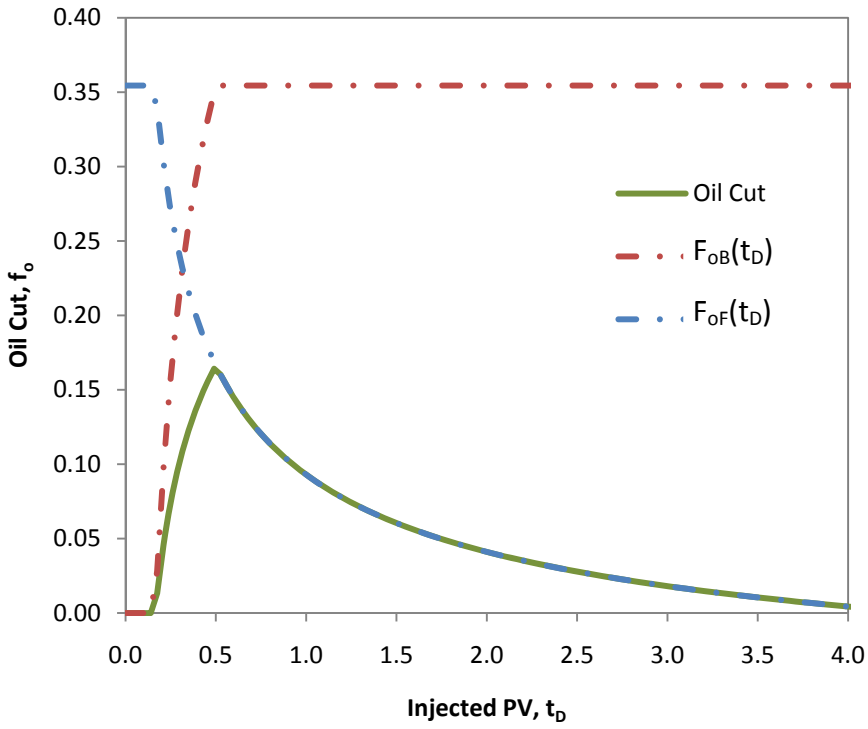

Figure 3-19 Example of SEORM Predicting Oil Cut

3.7.4 Discussion of the Input Parameters for the Simplified Enhanced Oil Recovery Method

Table 3-3 summarizes the input variables for Equation 3-46 through Equation 3-50.

Table 3-3 Summary of Input Parameters for SEORM

Input Parameter	Description
t_D	Dimensionless time in terms of injected pore volume
f_{oI}	Oil cut at start of EOR flood
f_{oB}	Peak oil cut for mobilized oil bank
f_{oF}	Oil cut at the end of EOR flood, assumed to be zero
S_{oI}	Average oil saturation at the start of EOR flood
S_{oB}	Oil saturation within the mobilized oil bank
S_{oF}	Average oil saturation at the end of the EOR flood
K_1	The Koval factor for the flow between the mobilized oil and initial banks
K_2	The Koval factor for the flow between the injected and mobilized oil banks
v_{oB}	The specific shock velocity of the mobilized oil bank
v_C	The specific shock velocity of the injected chemical bank
WAG	The WAG ratio, applies only to CO_2 flooding

Of the 12 inputs listed in Table 3-3, eight must be input by the user: f_{oI}, f_{oF}, S_{oI}, S_{oF}, K_1, K_2, v_{oB}, and WAG. Of the eight user inputs, only three have considerable uncertainty.

The values for f_{oI} and S_{oI} are usually estimated based on careful observation from previous recovery methods. Also, f_{oF} is typically assumed to be zero because under normal circumstances it would be a small value ranging between zero and one percent. Oil cuts within this low range are typically uneconomical to recover and therefore, can be neglected.

The parameter WAG is a design parameter and may be well understood; however, the actual water to solvent ratio that may exist during the flood could be different from what was intended. Therefore, there may be some uncertainty with WAG.

The parameters f_{oB}, S_{oB}, v_{oB}, and v_C can all be calculated from the fractional flow curve with an assumed value for S_{oF} or WAG, depending on the type of flood. If no

fractional flow curve is available, then v_{oB} is used as an input parameter because this value is a strong reflection of the fractional flow curve; however, the uncertainty in f_{oB} and S_{oB} then becomes a function of v_{oB}. The final three parameters, K_1, K_2, and S_{oF} contain significant meaning as they each capture special aspects of the behavior of an EOR flood.

The Koval factors, K_1 and K_2, are direct reflections of the magnitude of the heterogeneity of the reservoir, the mobility between displacing and displaced fluids, and adsorption of injected chemical. Overall, the Koval factors are indicators of the effectiveness of the flood's sweep through the mobilized fluids. Small values insinuate that the sweep is efficient, for example K values equal to one represent an ideal sweep similar to the piston like condition as shown in Figure 3-2 and Figure 3-3. Larger values of K imply that the flood has significant channeling and it is likely that the mobilizing agent in the injected bank, such as polymer, had considerable adsorption into the media. These effects reduce sweep efficiency and create longer floods with lower peak oil cuts. Furthermore, K_1 and K_2 are independent with certain limitations. K_2 cannot exceed a certain values that would cause the appearance that the injected bank breaks through before the oil bank. Equation 3-51 defines the upper limit for K_2.

$$K_{2|max} = \frac{K_1 v_{oB}}{v_C}$$

Equation 3-51

A situation where the injected bank breaks through before the oil bank can technically occur; however, the model is unable to handle such a situation and creates an error. Also, K_1 or K_2 cannot be less than one because a value of one represents the piston condition.

The parameter S_{oF} is a strong reflection of how effective the injected chemicals are at mobilizing the residual oil in the reservoir. Small values indicate efficient recovery of the residual oil. A large value may imply poor recovery because of a low injected agent volume, lost chemical, poor contact between the mobilizing agent and the residual oil, or deterioration or absorption of the agent into the media. S_{oF} also somewhat reflects the total pore volumes of the reservoir. For example a high S_{oF} may mean the sweep volume is overestimated.

3.7.5 Discussion of Other Important Parameters for the Simplified Enhanced Oil Recovery Method

There are a couple of other inputs for SEORM that are not directly part of the equations; however, they do influence the prediction. The first is the total pore volume of the reservoir, V_p. The assumed V_p alters various attributes of the floods such as the scale of the dimensional time axis and the total recovered volume of oil. A large V_p value means that the reservoir is large and requires a higher volume of chemical agents for the flood to be effective. Furthermore, a large V_p value suggests it would take a longer time to flood the reservoir and see a change in oil cut. Assuming that the original prediction for the oil saturation of the reservoir is accurate, the volume of recovered oil is directly proportional to V_p.

Other critical input parameters are the expected injection rate for the life of the flood, q_I, and the expected production rate, q_p. The parameter q_I scales the time axis and, along with V_p, is used to convert dimensionless time to real time. A high injection rate would mean a faster flood where the oil is recovered sooner. The model creates this by predicting a higher oil cut over the life of the flood as well as a shorter flood life. The q_p parameter is influential in the economics because it controls the total volume of fluids recovered. The recovered fluids must be treated and therefore have costs associated with them.

3.8 Summary of the Simplified Enhanced Oil Recovery Method

The simplified enhanced oil recovery method is based on fractional flow theory and Koval's method. It is designed to characterize an oil production history curve with a few simple parameters that are used to generically represent the effects of a larger number of parameters.

The method allows for quick easy simulations that create accurately representative production history curves, which creates significant advantages over conventional models for predicting the recovery of oil. These attributes are important to a decision analysis that is designed to account for a wide range of possible outcome and uses probabilities determine the expected value of a project.

CHAPTER 4: EVALUATION OF THE SIMLIFIED ENHANCED OIL RECOVERY METHOD

4.1 Introduction

The simplified enhanced oil recovery method (SEORM) is based on theory about the flow of oil and displacing fluids, as discussed in Chapter 3. The method must be evaluated with field data in order to develop confidence in the method's forecasting abilities. SEORM is evaluated using data for surfactant-polymer (SP), alkali-surfactant-polymer (ASP), and CO_2 floods.

The method hinges heavily on the input of several technical variables, including: K_1, K_2 (or K_f), v_{oB}, S_{oF} (or ΔS_o), and WAG (for CO_2 floods). Each parameter accounts for several characteristics associated with enhanced oil recovery (EOR) projects. For example, the Koval factors, K_1 and K_2, help describe the shape or behavior of the oil recovery through the life of the flood. These factors account for the influence of the reservoir's heterogeneity, the mobility of the fluids in the reservoir, the affects of salinity, clay content, adsorption of chemical agents, and other influencing properties of the flood or reservoir. Therefore, the Koval factors by themselves cannot be calculated easily or predicted based on data existing before EOR flooding. Through the evaluation of SEORM, the technical inputs were calibrated based on the EOR flood type so that at least ranges could be determined. From these ranges, various potential scenarios of oil recovery can be simulated. The objective of this chapter is to discuss how the evaluation

is performed and to discuss ranges of values for certain parameters as well as any conclusions about the method and the fits.

4.2 General Discussion of the Data Used for Validation

The evaluation of SEORM is based on 30 field and pilot scale projects. Of the 30, 19 are SP floods, three are ASP floods, and eight are CO_2 floods. The information for the fields comes from papers published in journals and conferences. Therefore, much of the data used for the evaluation comes from sources that have already summarized and reduced the data from field performances. There was difficulty in finding complete data necessary for project evaluation for ASP and CO_2 floods; hence, there are fewer field validations.

The majority of the SP floods occurred between the 1960s and 1990s, while most of the ASP and CO_2 floods occurred after 1990.

The majority of the fields studied are from the US. Only a couple of international projects are included in the evaluation, due to the general lack of necessary information for many international projects in the literature.

4.3 The Evaluation Process

A typical method is used for fitting SEORM against field data. To illustrate the process, an example fitting is discussed with data from the Bell Creek field.

4.3.1 Necessary Field Data

All of the data used for the fitting came from Hartshorne and Nikonchik's (1984) paper. The paper provided a comprehensive review of the field's history, properties, and

performance of the SP flooding. Table 4-1 is a summary of the inputs provided the paper.

Table 4-1 Summary Inputs Determined from Hartshorne and Nikonchik (1984)

Field Layout

Size	179	acres
Spacing	20	acres
Pattern	Five spot	
Number of Injectors	9	
Number of Producers	16	

Reservoir Properties

S_{oI}	0.800	
S_{oR}	0.330	
B_o	1.026	RB/STB
Pore volume	8.600E+06	RB
Oil Viscosity	6	cp
Brine Viscosity	1.2	cp
f_{oI}	0.029	

Performance/Design Properties

Injected Fluid	**Water**	**Polymer**	**Surfactant**	**Units**
Injection Rate	7300	7300	2800	STB/day
Production Rate	17800	17800	8900	STB/day
Slug size (injected)	--	0.93	0.046	Frac. V_p

There are various injection and production rates used in the fitting because the rates varied considerably over the life of the flood. It is common for there to be multiple injection rate for SP floods because each part of the chemical slug is injected at a different rate due to the infectivity of the fluids. The model used with SEORM can handle three different rates, one for each part of the flood: surfactant injection, polymer injection, and chase water injection. In the future, the model could be adapted to handle more volatile rates.

The data provided in Nikonchik's paper did not include much information about properties for fractional flow curves. Therefore, the descriptive values come from Vargo's (1978) paper.

The most critical piece of information for the fit is the history of the flood. Figure 4-1 is a plot of the provided oil production history. The data is digitized and put into Microsoft EXCEL and then matched with SEORM.

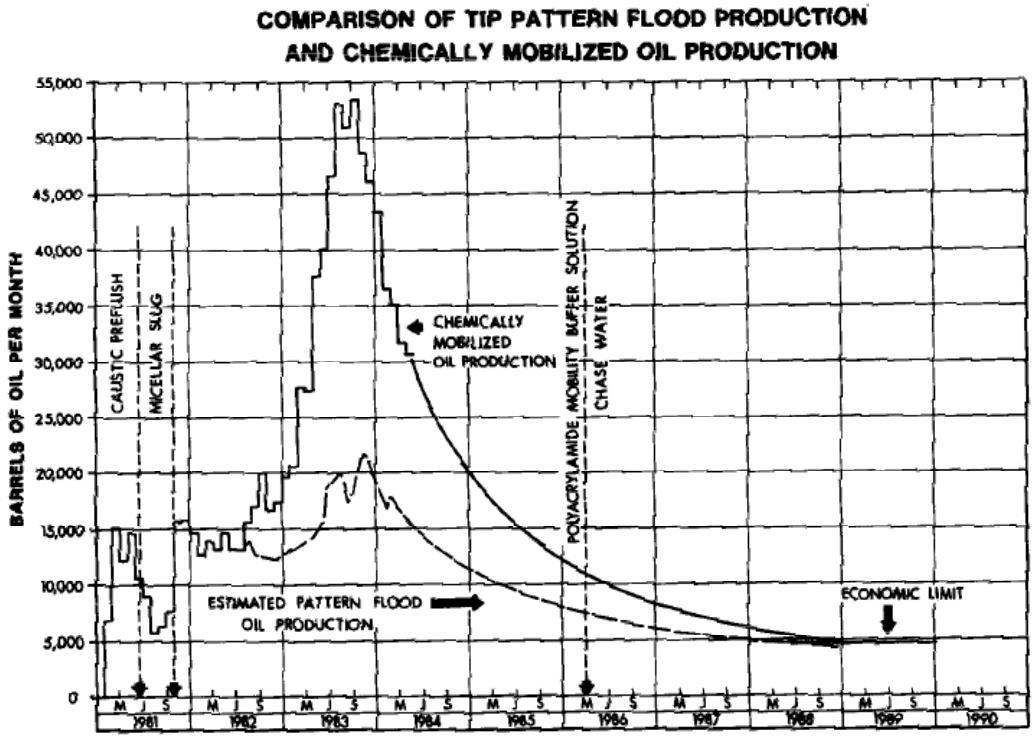

Fig. 13—Comparison of TIP patternflood production and chemically mobilized oil production.

Figure 4-1 Plot of the Provided Flood Performance of the Field for Bell Creek from Hartshorne and Nikonchik (1984)

The data from Figure 4-1 is then converted into dimensionless time of injected pore volumes, t_D. The following equation is used for the conversion

$$t_D(t) = \frac{qt}{V_p}$$

Equation 4-1

where t is time, q is the injection rate, and V_P is the total pore volumes of the reservoir. The data is plotted in terms of oil saturation and oil cut against dimensionless time for the fitting. Figure 4-2 is a plot with the digitized data.

4.3.2 The Fitting Process for Surfactant-Polymer and Alkali-Surfactant-Polymer Floods

The following process is applied to surfactant-polymer (SP) and alkali-surfactant-polymer (ASP) floods.

The fits used for the evaluation are based on the oil cut against dimensionless time curves. The oil cut curves are used because they represent the history of oil production, which is important to economics. Furthermore, by using both oil cut and dimensionless time, two dimensionless variables, the fits could be compared to one another between different field results, regardless of scale.

The fits are based on a coefficient of determination, R^2, as defined by the following

$$R^2 = 1 - \frac{\text{Average squared difference}}{\text{Variance}} = 1 - \frac{\frac{\sum\left(f_o^{data} - f_o^{model}\right)^2}{n}}{\frac{\sum\left(f_o^{data}\right)^2}{n} - \frac{\left(\sum f_o^{data}\right)^2}{n^2}}$$

Equation 4-2

where f_o^{model} is the average oil cut from SEORM, f_o^{data} is the average oil cut from the data, and n is the number data points (Ang and Tang 2007). R^2 values close to one

signify strong fits with one being a perfect fit. Negative valued fits are possible because the model does not create perfectly linear curves to represent no fit.

To create the fits, the parameters S_{oF}, K_1, K_2, and v_{oB} are adjusted until a seemingly a good fit is attained. S_{oF} is the assumed final oil saturation attainable for the EOR flood, K_1 and K_2 are Koval factors, and v_{oB} is the specific shock velocity of the oil bank. Most of the fits for SP and ASP floods could be improved by altering V_p by either increasing or decreasing the value; however, the V_p provided is never altered for the SP or ASP flood data because it considerably opens up the flexibility of the fits. Altering V_p means that the dimensionless time and the volume of recoverable oil is changed. These changes allow for different Koval factors, S_{oF}, and v_{oB} values to fit with different V_p. Therefore, allowing V_p to be adjustable leads to a wide range of potential fits.

Initially trial and error and "eye-balling" are used to create fits. The excel program, Solver, is then used to perform a maximization of the fit. Trial and error is necessary to determine a starting point for maximizing the fit because Solver is unable to find a good fit from arbitrary starting points.

The results produced by Solver are reviewed and adjusted if they seem irregular. For example, corrections are made if it would be impossible to fit a fractional curve to the provided results. Overall, corrections are rare. Table 4-2 summarizes the fitted parameters for Bell Creek. Figure 4-2 through Figure 4-4 are plots of SEORM with the data. The fit are strong against the provided data. For the Bell Creek case, the full life of the flood is not provided and therefore a significant portion is extrapolated.

Table 4-2 Summary of Fitted Parameters for Bell Creek Field

Fitted Parameters	
S_{oF}	0.198
ΔS_o	0.13
K_1	1.25
K_2	2.00
v_{oB}	2.00

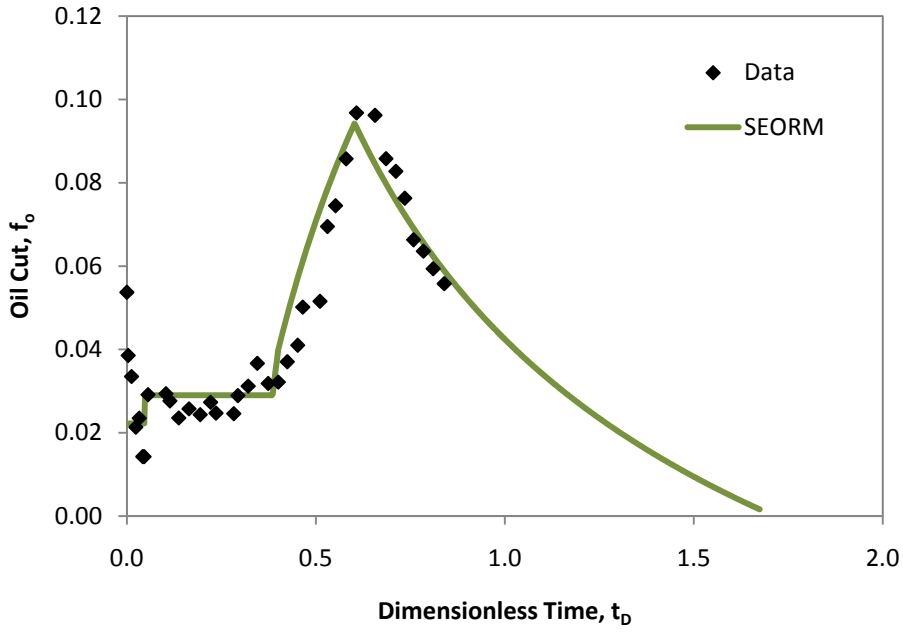

Figure 4-2 Plot of Oil Cut against Dimensionless Time for the Bell Creek Field

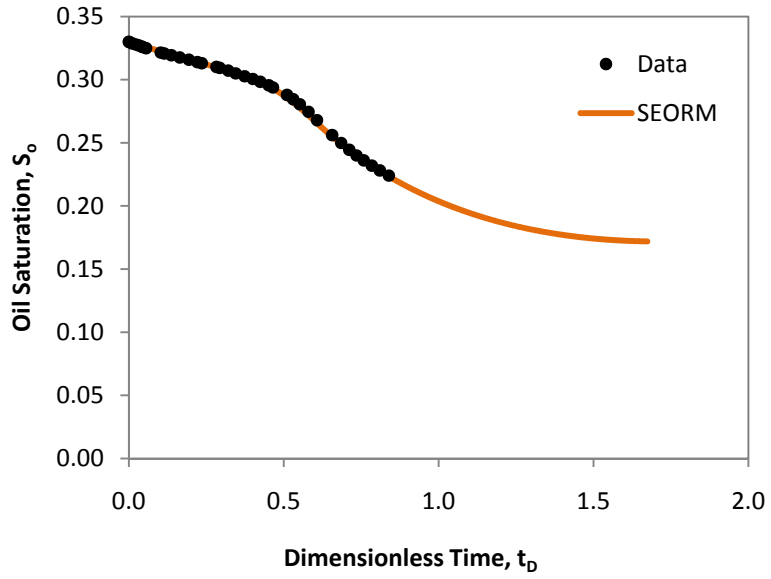

Figure 4-3 Plot of Oil Saturation against Dimensionless Time for the Bell Creek Field

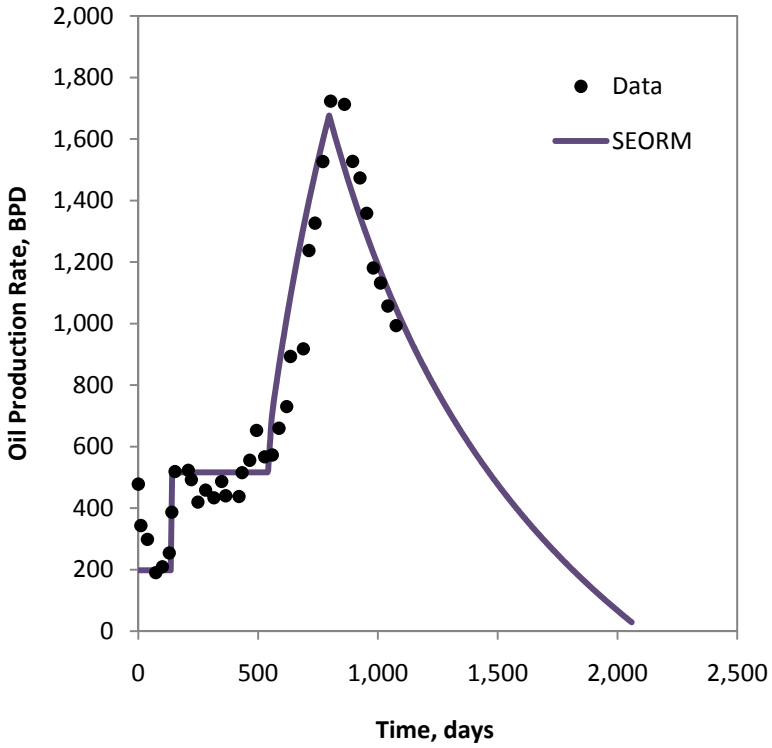

Figure 4-4 Plot of Oil Production Rate against Time for the Bell Creek Field

In Figure 4-4 there appears to be a jump in oil rate at about 100 days. This jump is because of an instantaneous jump in injection rate as well as production rate. If the spreadsheet is designed to better handle varying rates, then a smoother transition could be modeled. In Appendix A several plots have a jump appear in either in the oil production or oil cut plot because of the jumps in rates.

4.3.3 Fitting the Fractional Flow Curve

The fractional flow curves are also fitted to ensure that the theory behind the fit was maintained. Parameters of S_{oF} and v_{oB} are the most critical for the curve. The values for parameters S_{oF} and v_{oB} are based on the best fits to the field history data. The critical points for the curve are the initial and the final points for the flood. The initial point for the EOR flood is defined by the oil cut, f_{oI}, and the oil saturation, S_{oR}, at the time the EOR flood is initiated. It is assumed that the values provided in the paper are accurate and therefore a point on the curve is known. Another important point is the starting point of the water-oil curve, S_{oI} or S_{wr}, which in the case of Bell Creek is provided. Assuming that the fit matches the theory, then the intersection of the lines for v_{oB} and v_C is a second point on the curve. The parameter v_C is specific shock velocity of the injected fluids. The parameter v_C is defined by S_{oF} for SP and ASP floods. The provided viscosities for the water and oil in the reservoir give some information on the shape of the curve. The remaining parameters for the field came from another paper about the Bell Creek field. Vargo's 1978 paper provided information on the fractional flow curve for the field.

Data from Vargo's paper is used to help define the end point relative permeability of water (k^o_{rw}), end point relative permeability of oil (k^o_{ro}), Corey type exponent for water (n), Corey type exponent for oil (m), and residual oil saturation (S_{or}). The parameters k^o_{rw}, k^o_{ro}, n, and m control the shape of the curve, while S_{or} controls an end point of the curve. Table 4-3 is a summary of the fitted parameters and Figure 4-5 is a plot of the curve.

For most fields, data about the fractional flow curve for the field is not provided and therefore values for the defining parameters are fitted. Based on the best fitting v_{oB}, S_{oF}, and the initial condition at the start of the flood, there are two points that could be used to fit a curve. The one point is the initial condition of the flood and the other is the intersection of the v_{oB} and v_C lines. Typically the viscosity of the oil is provided, but the viscosity of the brine is assumed to be one cp. The values for, n, m, k^o_{rw}, k^o_{ro}, S_{oI}, and S_{or} are altered till the curve passes through the two points. Table 4-4 is summary of typical starting values. For equations of how the fractional flow curve is constructed, refer to section 3.5.3.

Table 4-3 Summary of Fitted Parameters for the Fractional Flow Curve for Bell Creek Field from Vargo (1978) and Hartshorne and Nikonchik (1984)

Fitted Parameter	
k^o_{rw}	0.18
k^o_{rw}	0.80
n	1.75
m	2
S_{wr}	0.20
S_{or}	0.24

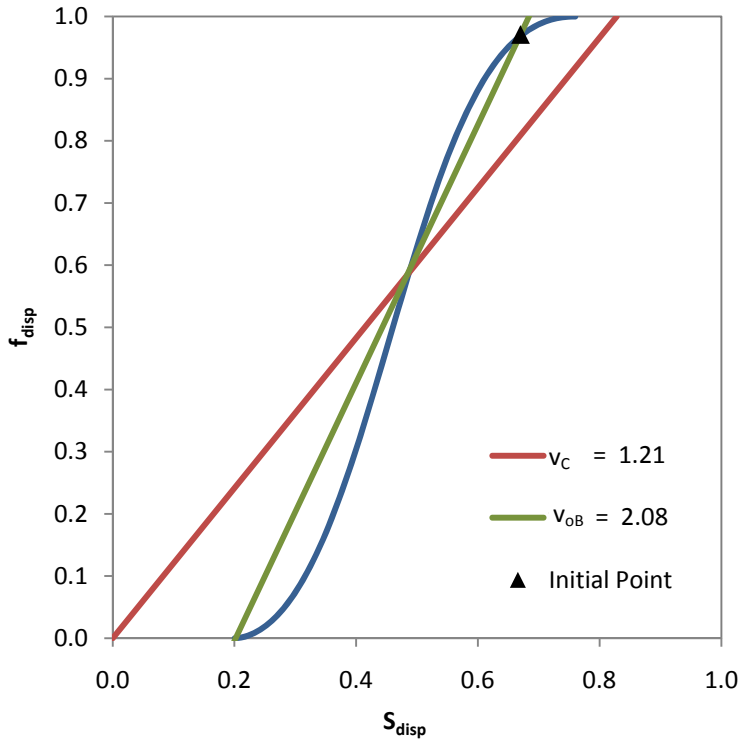

Figure 4-5 Plot of the Fitted Fractional Flow Curve for the Bell Creek Field

Table 4-4 Summary of Assumed Starting Values for Fractional Flow Curve Fits

Parameter	Starting Value
k_{rw}^o	0.2
k_{ro}^o	0.8
n	2
m	2
S_{or}	0.3 (or a value less than S_{oR})
S_{ol}	0.8
μ_w (cp)	1
μ_o (cp)	5 (for SP and ASP floods) 1.5 (for CO_2 floods)

4.3.4 The Fitting Process for CO_2 Floods

There fitting process is a bit different for CO_2 floods from the process used for SP and ASP floods because of the importance of the design parameter of water to solvent (WAG) ratio.

The methodology for the fittings is the same as with SP and ASP. The key difference in the process is which parameters were used for fitting. The parameters S_{oF}, K_1, v_{oB}, WAG, and V_P are adjusted until a strong fit based on R^2 is established. Instead of using K_2 as a fitting parameter, $K_{2,max}$ is used because it is assumed that the solvent and the oil bank arrive at the producer at the same time. For CO_2 floods it is very typical for the solvent to arrive before the oil shock; however, the model is unable to handle that condition and the best approximation was to assume the oil and solvent banks breakthrough at the same time.

The total pore volume, V_P, is also a fitting parameter for CO_2 floods because the estimated V_P provided in the literature is typically very high and fits are not possible. The WAG ratio values provided in the literature are used for the fits. The model cannot handle WAG ratios of zero and therefore a minimum value is set at one. If substantial fractional flow curve data is also provided then v_{oB} is essentially provided and not altered much for the fits. Therefore, only S_{oF}, K_1, and V_P are altered for most cases. For cases where there is not much fractional flow data or the WAG ratio is zero or unknown then the fits include more parameters.

There is not as much of an issue with V_P being a fitting parameter for CO_2 floods as there is for SP and ASP floods because K_2 is set at $K_{2,max}$ and the WAG ratio is typically another piece of information for the field. The extra information helps to limit the potential number of satisfactory fits. The decision analysis considers a varying V_p because of SEORM's sensitivity to the parameter and the belief that the originally predicted V_p could be inaccurate.

4.4 Summary of the Fits for All of the Flood Types

SEORM is able to fit every field relatively closely. Table 4-5 through Table 4-7 are summaries of the fits for the two flood types. Appendix A includes the fitted plots and fitting parameters for each field. The fits are constructed so that the provided data from the literature and SEORM matched as closely as possible.

In Table 4-5 through Table 4-7, ΔS_o is the change in average saturation and is defined as

$$\Delta S_o = S_{oR} - S_{oF}$$

Equation 4-3

"Rec. Eff." Stands for recovery efficiency and is defined as

$$\text{Rec. Eff.} = \frac{\Delta S_o}{S_{oI}}$$

Equation 4-4

The parameter K_f is a factor term that scales K_2 so that it falls between K_1 and $K_{2,max}$. $K_{2,max}$ is the upper bound limit for K_2 values and it is defined as

$$K_{2,max} = \frac{K_1 v_{oB}}{v_C}$$

Equation 4-5

K_f is defined as

$$K_f = \frac{K_2 - K_1}{K_{2,max} - K_1}$$

Equation 4-6

All of the fits are relatively strong with having an R^2 value of over 0.7. The only glaring exception is the Manvel pilot. The fit appears weak because the project was unsuccessful and it did not experience a notable increase in oil cut, as shown in Figure 4-6. Therefore, SEORM is unable to create a satisfying fit to the data. However, the best fitting values did produce a curve that demonstrated poor performance.

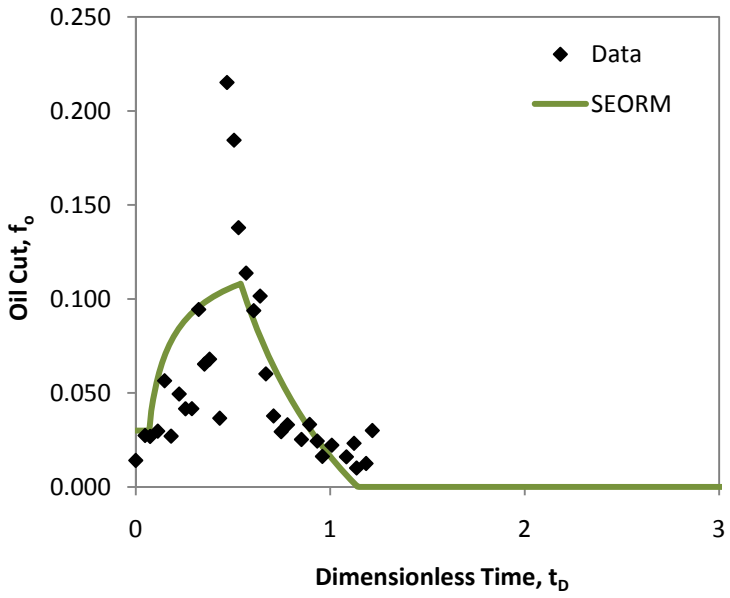

Figure 4-6 Plot of the Manvel Data with the SEORM Fit for the Oil Cut Curve

Table 4-5 Summary of Fitted Parameters for Surfactant Polymer Pilot Floods

Field Name	Field Size (acres)	Well Spacing (acres)	Total Pore Volume (RB)	S_{oF}	ΔS_o	Rec. Eff.	K_1	K_2	K_f	v_{oB}	v_C	R^2
Benton	1	1.0	4.90E+03	0.26	0.09	0.11	1.71	2.66	1.00	2.11	1.36	0.74
Berryhill	18	4.5	7.24E+05	0.22	0.08	0.12	2.50	3.90	0.88	2.10	1.28	0.68
Big Muddy	1	1.0	1.40E+05	0.22	0.11	0.21	1.24	2.17	0.14	8.05	1.29	0.91
Borregos	1.25	1.25	7.20E+03	0.22	0.09	0.13	1.50	2.00	0.20	3.47	1.28	0.74
Chateaurenard	19.4	4.85	6.30E+04	0.00	0.50	0.63	2.49	7.34	0.56	4.5	1.00	0.75
Loudon	0.71	0.71	1.72E+04	0.08	0.17	0.25	1.31	1.83	0.32	2.42	1.08	0.97
Manvel	5.5	2.75	7.00E+05	0.25	0.05	0.09	3.72	5.58	1.00	2.00	1.33	0.04
Robinson	0.75	0.75	2.70E+04	0.27	0.13	0.18	1.50	2.20	0.44	2.80	1.37	0.82
Sloss	9	9.0	1.20E+05	0.15	0.15	0.19	2.00	3.37	0.98	2.00	1.18	0.83
Wilmington	10.3	2.58	1.39E+06	0.20	0.15	0.18	1.71	2.85	0.91	2.17	1.25	0.96

Table 4-6 Summary of Fitted Parameters for Surfactant Polymer Field Floods

Field Name	Field Size (acres)	Well Spacing (acres)	Total Pore Volume (RB)	S_{oF}	ΔS_o	Rec. Eff.	K_1	K_2	K_f	v_{oB}	v_C	R^2
Bell Creek	179	20	8.60E+06	0.17	0.16	0.20	1.25	2.07	0.94	2.05	1.21	0.85
Berryhill	92	4.38	1.20E+07	0.21	0.09	0.13	3.75	7.36	0.99	2.50	1.27	0.79
Big Muddy	90	10	8.60E+06	0.23	0.09	0.17	1.50	4.10	0.30	8.70	1.30	0.88
Bradford 7	46.2	2.89	1.50E+06	0.28	0.13	0.19	1.59	5.00	0.95	4.50	1.38	0.82
Bradford 8	220	4.0	5.60E+06	0.35	0.06	0.08	1.50	2.25	0.78	2.50	1.53	0.83
M1-2.5	200	2.5	9.00E+06	0.31	0.09	0.12	1.62	2.42	0.43	3.10	1.45	0.91
M1-5.0	200	5.0	9.00E+06	0.32	0.08	0.11	1.60	2.40	0.43	3.20	1.47	0.79
North Burbank	90	10.0	4.80E+06	0.27	0.07	0.12	2.00	4.30	0.97	3.00	1.37	0.89
Salem	60	5	3.57E+06	0.17	0.13	0.19	3.81	6.85	0.40	3.60	1.20	0.67

Table 4-7 Summary of Fitted Parameters for Alkali Surfactant Polymer Floods

Field Name	Field Size (acres)	Scale	Well Spacing (acres)	Total Pore Volume (RB)	S_{oF}	ΔS_o	Rec. Eff.	K_1	K_2	K_f	v_{oB}	v_C	R^2
Cambridge	4	Pilot	4	5.83E+06	0.22	0.44	0.56	1.97	2.8	0.20	4.0	1.28	0.94
Karamay	7.7	Pilot	1.93	2.50E+05	0.05	0.29	0.48	2.5	6.0	0.63	3.4	1.05	0.78
Tanner	40	Pilot	40	2.56E+06	0.41	0.20	0.24	2.5	2.5	0.00	5.0	1.73	0.85

Table 4-8 Summary of Fitted Parameters for CO_2 Floods

Field Name	Field Size (acres)	Well Spacing (acres)	Fitted WAG	Fitted Total Pore Volume (RB)	Frac. of Fitted to Provided V_P	S_{oF}	ΔS_o	Rec. Eff.	K_1	$K_{2,max}$	v_{oB}	v_C	R^2
Lost Soldier	---	10	1	1.30E+08	0.43	0.20	0.30	0.33	5.4	22.7	7.0	1.7	0.57
Rangely	2590	10	1	1.60E+09	0.84	0.33	0.17	0.21	6.9	22.9	10.0	3.0	0.49
SACROC 4	600	40	3	2.40E+07	0.44	0.29	0.17	0.22	2.3	6.4	3.8	1.4	0.95
SACROC 17	2700	40	5	7.10E+07	0.45	0.33	0.13	0.17	3.0	7.9	3.2	1.2	0.75
Slaughter	12	3	1	7.20E+05	0.83	0.23	0.32	0.35	2.4	4.9	3.1	1.5	0.64
Twofreds	80	40	1	4.00E+07	1.18	0.38	0.08	0.15	3.1	9.0	15.0	5.3	0.85
Wertz	370	10	1	8.30E+07	0.37	0.24	0.26	0.28	7.0	24.7	7.0	2.0	0.91
West Sussex	9.6	9.6	4	3.00E+05	0.94	0.36	0.07	0.10	2.7	3.9	5.0	3.5	0.49

4.5 Analysis of the Fits

To create a better understanding about the results of the fits, some basic statistical information is calculated for each flood type. Included in the analysis is the range of values, the mean value, standard deviation, and coefficient of variation for each parameter as shown in Table 4-9. The SP floods are also divided between field and pilot scale. The ASP flood data is not analyzed in this manner because there is not enough data sets yield anything insightful. One must be careful when looking at these comparisons because there only a few sets of data for each scale and flood type. A larger sample space would yield more confidence for the comparison. Along with the table, box plots are made to help visualize the distribution of values.

Table 4-9 Summary of Statistical Information for the Fitted Parameters for SP and CO_2 Flood Data

SP Pilot					
Parameter	**Low**	**High**	**Average**	**St. Dev.**	**C.O.V.**
S_{oR}	0.24	0.50	0.34	0.08	0.24
S_{oF}	0.00	0.27	0.19	0.09	0.47
ΔS_o	0.05	0.50	0.15	0.13	0.92
K_1	1.24	3.72	1.99	0.75	0.38
K_2	1.83	7.34	3.37	1.80	0.53
K_f	0.04	1.00	0.63	0.37	0.59
v_{oB}	2.00	8.05	3.18	1.90	0.60

SP Field					
Parameter	**Low**	**High**	**Average**	**St. Dev.**	**C.O.V.**
S_{oR}	0.30	0.40	0.30	0.04	0.12
S_{oF}	0.17	0.37	0.28	0.06	0.22
ΔS_o	0.06	0.16	0.10	0.03	0.32
K_1	1.21	3.75	1.97	0.94	0.48
K_2	1.78	7.36	3.86	2.04	0.53
K_f	0.30	0.99	0.75	0.27	0.35
v_{oB}	2.00	8.70	3.38	0.94	0.28

CO_2 All					
Parameter	**Low**	**High**	**Average**	**St. Dev.**	**C.O.V.**
S_{oR}	0.43	0.55	0.48	0.04	0.08
S_{oF}	0.20	0.38	0.30	0.07	0.22
ΔS_o	0.07	0.32	0.19	0.10	0.51
K_1	2.30	7.00	4.11	2.01	0.49
K_2	3.90	24.70	12.79	8.97	0.70
K_f	0.99	1.01	1.00	0.01	0.01
v_{oB}	3.10	15.00	6.76	4.08	0.60

4.5.1 Comparison of Scale for SP Floods

A review of Table 4-9 leads to several important observations about the difference between scale and flood type. There appears to be a distinction between the field and pilot scale projects. The field scale projects for the SP floods seem to have similar S_{oR}, which was expected because EOR is typically considered at the end of water flooding, but higher S_{oF} and lower ΔS_o than the pilot projects. This result is expected since good contact between chemical and oil is less likely with larger scale projects because the chemical agents are more likely to degrade, be adsorbed, or leak out the expected reservoir leading to a lower volume of mobilized oil.

Figure 4-7 is a comparison of the distribution of ΔS_o based on project scale. The pilot cases seem to have a wider distribution that is more oriented towards higher values than the field cases. This suggests that when studying smaller reservoir increments, one may observe higher variability in ΔS_o. Data from Chateaurenard is considered to be an outlier because the results from that project are significantly different when compared to other projects. The change in oil saturation for the project is almost three times higher

than the next highest value. This likely suggests that the either the assumed total pore volumes for the project is low or that the oil saturation at the start of tertiary is low.

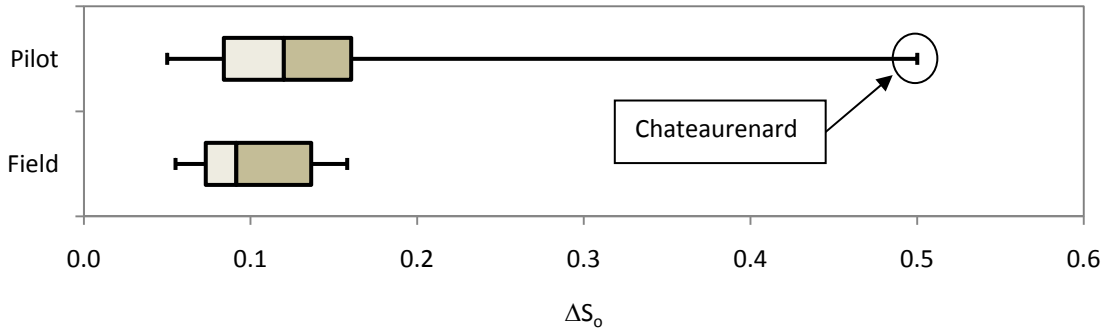

Figure 4-7 Distribution of ΔS_o for Pilot and Field Scale SP Floods

Figure 4-8 is a plot of the distribution for the values of K_1 and K_2 for both pilot and field cases for the SP flood data. The distribution of both Koval factors is wider for the field cases with a tendency to be skewed towards higher values. Also, the distribution of K_1 for both field and pilot projects are skewed towards higher values while K_2 appears to have a more symmetrical distribution. The average value for K_1 does not vary significantly between field and pilot scale projects. However, the distribution for K_1 seems to have a greater skew towards larger values for field projects. This is again likely for the same reasons as for K_2.

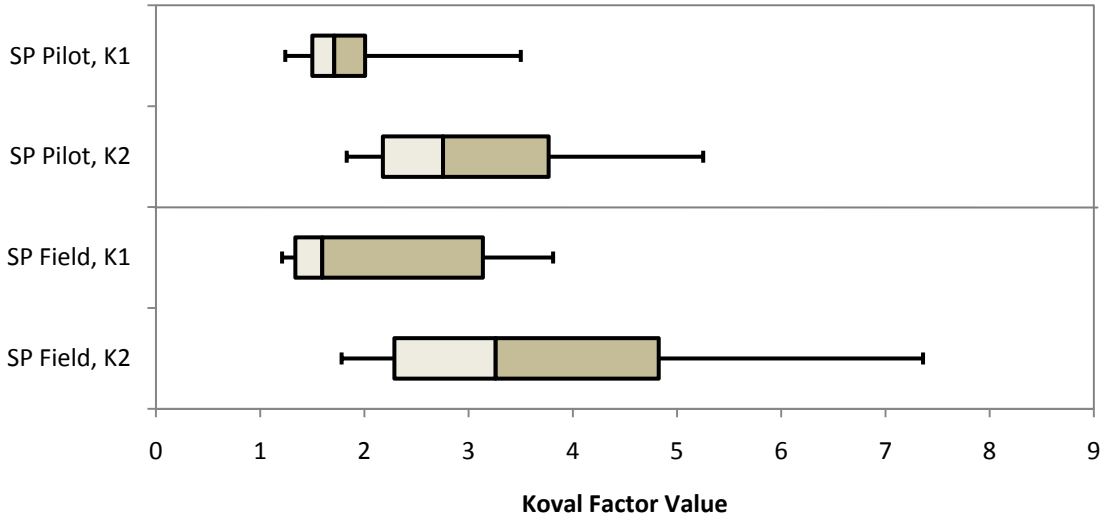

Figure 4-8 Distribution of Koval Factors for Pilot and Field Scale SP Floods

Figure 4-9 is a plot of the distribution of K_f for field and pilot projects. It is surprising to see that the distribution for K_f is narrower for the field scale projects than for the pilot scale. However, the field distribution is more restricted to the higher region with a slight skew to the left.

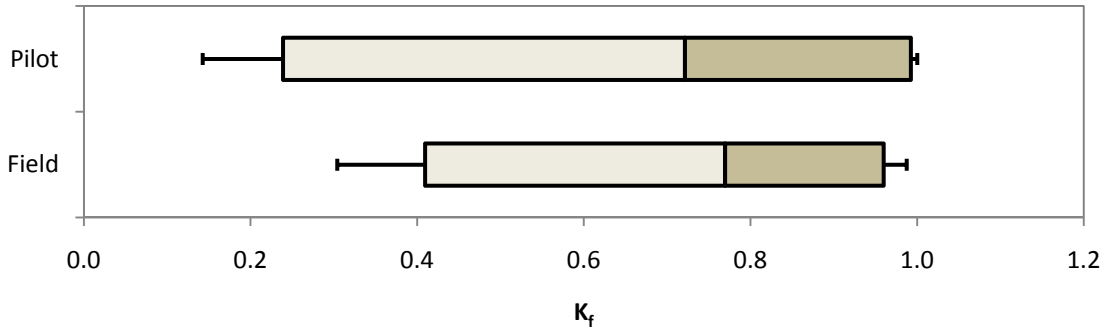

Figure 4-9 Distribution of K_f for Pilot and Field Scale SP Floods

The field projects are better fitted with higher K_2 and K_f values than the pilot projects. This implies that field scale projects are more likely to behave more heterogeneously. Again, this is expected as larger scale projects are expected to have

more heterogeneity in the medium and mobility would be more likely to be less favorable because of polymer deterioration and adsorption.

In regards to the parameter v_{oB}, the field scale projects tend to have larger values. This may suggest that channeling is a more significant issue at the field scale than pilot scale. At larger scales, there tends to be more heterogeneity meaning that there is a higher likelihood that channeling would occur; therefore, this result makes sense. Figure 4-10 is a plot of the distributions for v_{oB}. The distribution for the field projects tends to have a slightly larger median; yet the two distributions do compare somewhat closely.

Data from the Big Muddy field and pilot scale projects are marked as outliers because they are significantly higher than the rest of the data. The next highest v_{oB} value for both the field and pilot data is 4.5. It is peculiar that both the pilot and field data produced similar high v_{oB} results, suggesting that the high v_{oB} is because of field properties. It could also be a direct result of an inaccurately reported total pore volume.

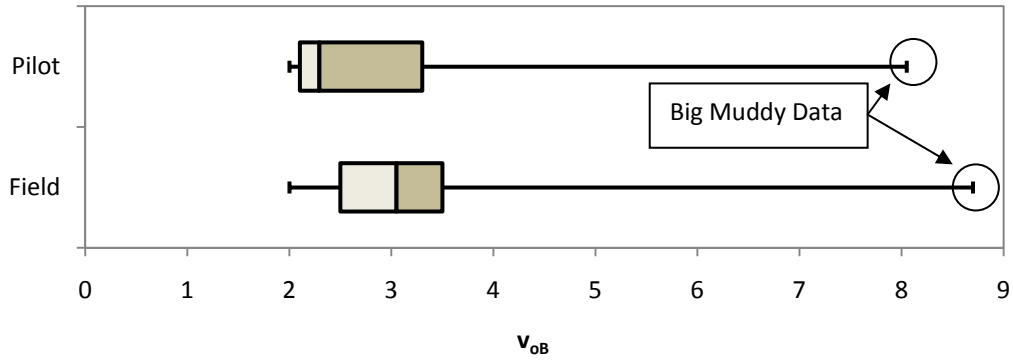

Figure 4-10 Distribution of v_{oB} for Pilot and Field Scale SP Floods

ASP and SP floods should behave similarly because the two flood types have similar mechanisms for oil recovery. The ASP data is not added to the SP data because it would skew the data regarding saturations. The ASP floods reviewed injected the

chemicals relatively early in the field's life when compared to SP floods. Therefore, they have higher S_{oR} and ΔS_o values. The values for S_{oF}, K_1, K_2, K_f, and v_{oB} are not out of reason when looking at the summary for SP data; however, more data is required before any conclusions can be made.

4.5.2 Comparison of Flood Types; SP and CO_2

There are differences between flood types between the SP and CO_2 data for all of the fitting parameters. Figure 4-11 is a plot of the distributions comparing The CO_2 floods appear to have larger S_{oF} values than SP, which is consistent with theory because CO_2 floods do not mobilize as much residual oil as surfactants.

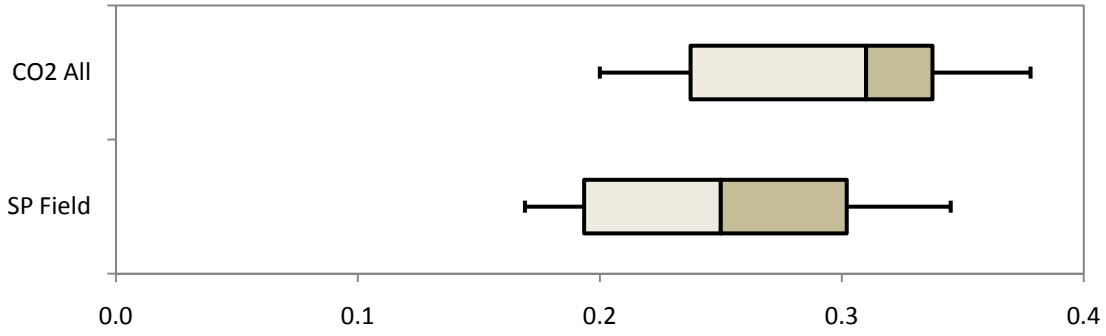

Figure 4-11 Distribution of S_{oF} for SP and CO_2 Floods

Figure 4-12 is a comparison of the distribution of ΔS_o between SP and CO_2 floods. Despite the higher S_{oF}, CO_2 floods have ΔS_o values that are larger than for SP floods, because CO_2 floods typically start at higher oil saturations and a slightly earlier in the life of the field than SP floods. The CO_2 data is compared to the SP field data because most of the CO_2 data is from field scale projects. The CO_2 floods distribution is larger and is more oriented towards the larger values. The higher ΔS_o values and large

distribution may be a direct result of allowing V_P to be a fitting parameter for the CO_2 fittings. Smaller V_P values than estimated may suggest lower S_{oF} and higher ΔS_o values for the flood because if the recovered volume of oil does not change. Therefore, if V_P decreases then ΔS_o must increase to maintain mass balance. If the fits for the SP flood are redone with a varying V_P, then the distribution and value for ΔS_o could potentially increase.

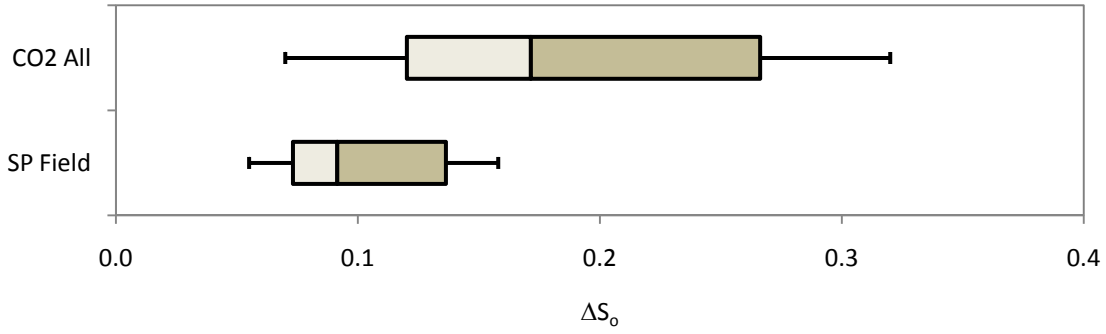

Figure 4-12 Distribution of ΔS_o for SP and CO_2 Floods

Figure 4-13 compares the distributions for v_{oB} for CO_2 and SP floods. The v_{oB} values are considerably larger for CO_2 floods. The distribution for the CO_2 is larger and it is situated at higher values than the SP flood distribution. It does appear that the v_{oB} values are generally higher than SP, especially if the Big Muddy outlier is to be neglected. This is likely a result of the miscibility of CO_2 gas with the oil as direct result of pressure variation that occurs between layers within the reservoir during the flood. The large mobility ratio that is typical for CO_2 also leads to channeling and larger v_{oB} values.

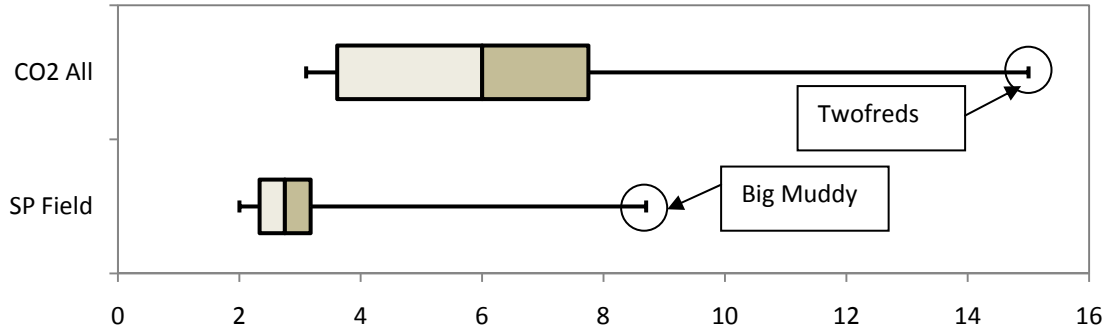

Figure 4-13 Distribution of v_{oB} for SP and CO_2 Floods

Figure 4-14 is a comparison of the Koval factors for SP and CO_2 floods. The average values of both Koval factors are higher for CO_2 floods than for SP floods. The distributions are also larger for CO_2 floods. These distributions suggest that CO_2 floods are more likely to experience heterogeneous behavior and therefore have a longer recovery period than SP floods. This result is consistent with historical performances of CO_2 floods. The heterogeneous behavior is most likely a result of the relatively poor mobility of the solvent water mix and the oil.

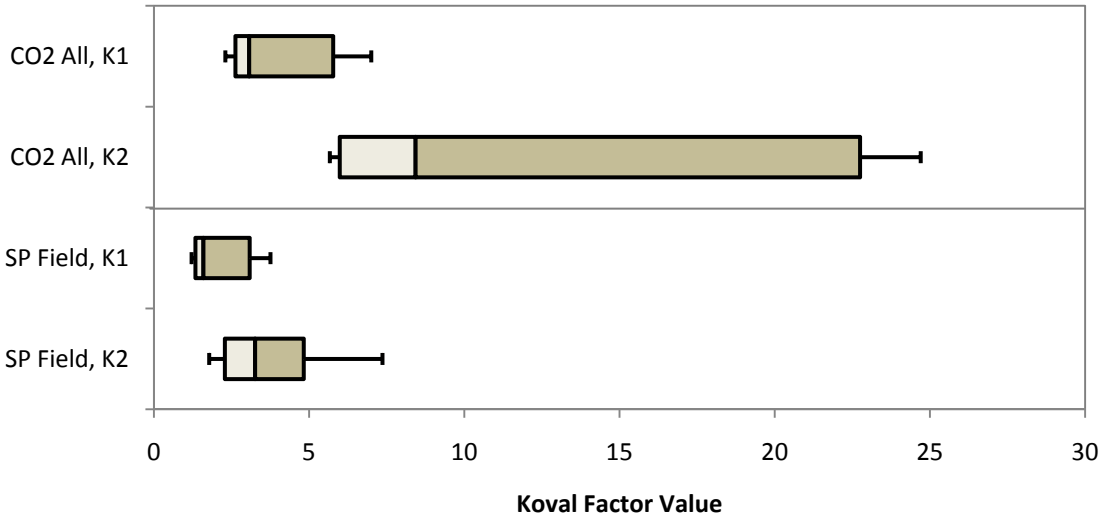

Figure 4-14 Distribution of Koval Factors for SP and CO_2 Floods

Although the above discussion calls out certain effects for the cause of certain trends, a review of the data does not actually find any strong correlations between any reservoir characteristic parameters and either the Koval factors, ΔS_o, S_{oF}, or v_{oB}. This is likely because so many different factors contribute to how a flood behaves and each parameter essentially captures how all of the factors work together, rather than singling out one or two. Attempts at determining linear relationships between different reservoir characteristics and fitting parameters can be found in Appendix B.

4.5.3 Discussion of the Outliers and Fitting Issues

All of the data sets are fitted relatively well by SEORM. It is, however, observed that some fits are questionable. Some projects appear to be outliers. As an example the Big Muddy data is best fitted with large v_{oB} values that are considerably larger than those used for other SP floods. One possible explanation for this is that the reported V_p is inaccurate. Inaccuracy with the reported V_P could be common because it is an estimate based on an assumed porosity and net pay thickness. It is also unknown if the injected chemicals will ever be able to sweep the entire reservoir as well. In the case of Big Muddy, if a lower V_p is assumed, then the fit can be improved considerably. New values can be found that fit both the Big Muddy field and pilot data reasonably well.

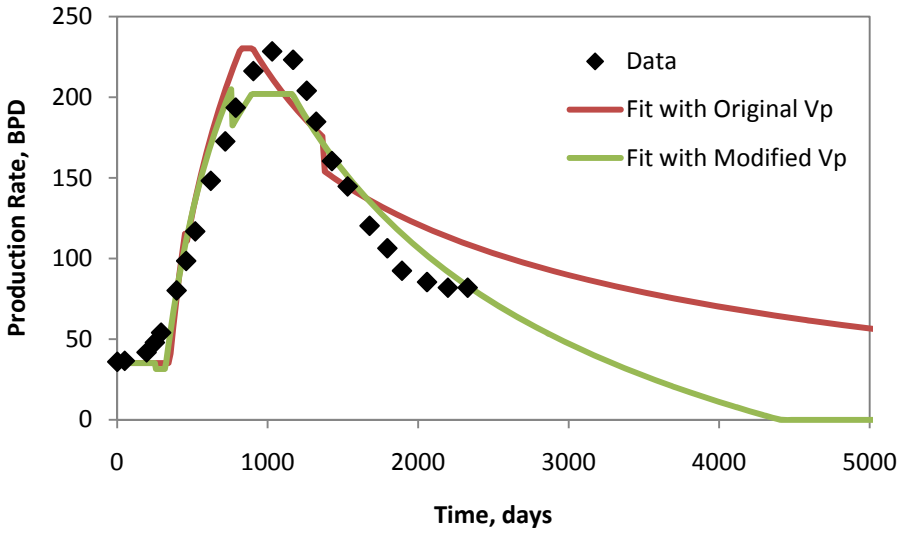

Figure 4-15 Plot Comparing Fits for the Big Muddy Field with Altered V_p

Another standout outlier is the data from the Chateaurenard pilot. The pilot appeared to perform exceptionally well with almost perfect recovery predicted. Such high recovery is unlikely and assuming that the oil production data is accurate, then the there is likely an error with the total pore volumes. Chances are that the reservoir may actually be larger than estimated.

Other sources of error with the fits include problems with handling the varying injection rates and inaccuracies with the assumed S_{oR}. As mentioned earlier, SEORM is able to handle up to three different injection and production rates; however, most of the data sets have varying rates for various reasons. Assuming up to three values works well for most of the fields.

Errors involving S_{oR} are likely because of the difficulty associated with measuring an accurate value that is representative of the entire project. An error with S_{oR} is not significant in regards to the actual fit with SEORM, but it does create issues for the fitting

with the fractional flow curve because it influences the location of the start of flood point, a point the curve must pass through.

4.6 Comparison of Fittings for Similar Projects

There are several sets of data from the same oil reservoir. Some of these projects are pilot and field scale projects and others are of the same scale. It is important to see if SEORM produces consistent results between projects from the same reservoir, assuming similar injection techniques and chemicals are used.

4.6.1 Comparison of Pilot and Field Scale Projects

There are three reservoirs with pilot and field scale data used in the evaluation, Berryhill, Big Muddy, and Robinson (M-1). The results of their fits are summarized in Table 4-10. There appears to be a decent correlation between pilot and field results. The data and fit for Berryhill is used as example to explain how pilot and field scale projects from the same reservoir are treated, the following discusses the Berryhill project.

Table 4-10 Summary of Fitted Values for Pilot and Field Scale Projects: Big Muddy, Robinson, and Berryhill

	Big Muddy (Original)		Robinson/M-1			Berryhill	
Parameter	Pilot	Field	Pilot	Field	Field	Pilot	Field
WS (acres)	1	10	0.8	2.5	5	4.5	20
V_P (RB)	1.40E+05	8.60E+06	2.70E+04	9.00E+06	9.00E+06	7.24E+05	1.20E+07
S_{oF}	0.22	0.23	0.27	0.31	0.32	0.22	0.22
ΔS_o	0.10	0.09	0.13	0.09	0.08	0.08	0.09
K_1	1.24	1.50	1.50	1.62	1.6	2.50	3.75
K_2	2.17	4.10	2.20	2.42	2.4	3.90	7.36
K_f	0.14	0.30	0.44	0.43	0.43	2.10	2.50
v_{oB}	8.05	8.70	2.80	3.10	3.2	0.88	1.00

The Berryhill field, also known as Glenn Pool field, is in Creek County, Oklahoma. The chemical EOR project began in the late 1970s with a pilot that was later expanded to a field project in the early 1980s. Data for the pilot and field came from three papers: Crawford and Crawford 1985; Bae and Syed 1988; Bae 1995. Figure 4-16 is a figure of the fits for the pilot and field data.

Table 4-11 is a summary of the parameters that describe the characteristics of the reservoir that should be the same for the two projects. Shaded values are those that are assumed and not provided by the papers. The assumed values are altered until they best fit both the pilot and field data. Table 4-12 is a summary of parameters unique to each project. Again the shaded values are fitted.

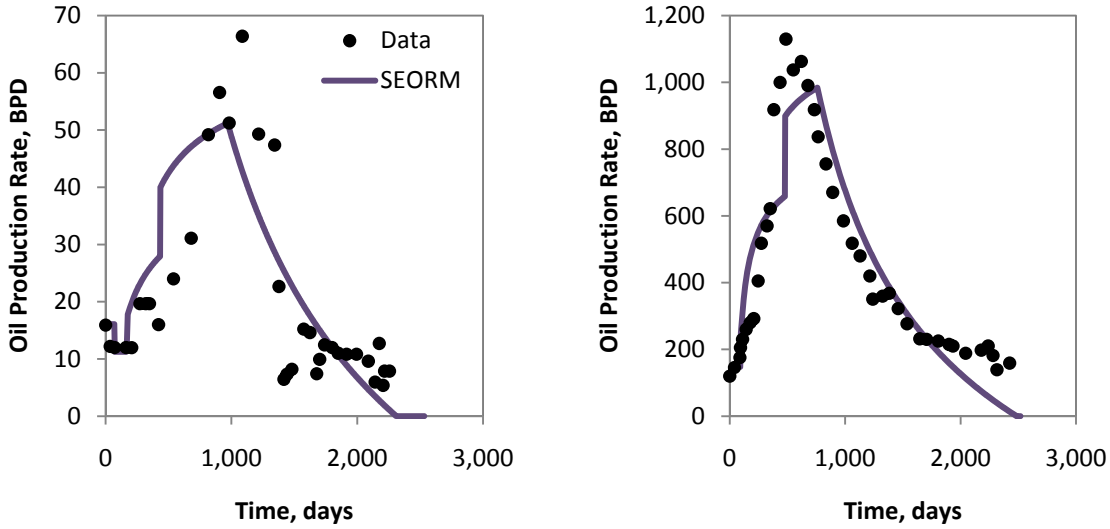

Figure 4-16 Fits of the Berryhill Pilot (Left) and Field (Right) with SEORM

Table 4-11 Summary of Common Parameters for Berryhill Pilot and Field Projects

Parameter	Value	Units
S_{oI}	0.710	
S_{oR}	0.303	
S_{or}	0.27	
B_o	1	RB/STB
μ_o	4	cp
μ_w	1	cp
f_{oI}	0.010	
k_{rw}^o	0.175	
k_{ro}^o	0.8	
n	3	
m	2	

Table 4-12 Summary of Fitted Parameters for Berryhill Pilot and Field Projects

Fitted Parameters	Pilot	Field	Units
Size	18	160	acres
Spacing	4.5	20	acres
Injection Scheme	5-spot	5-spot	
V_p	7.24E+05	1.20E+07	RB
S_{oF}	0.220	0.215	
ΔS_o	0.083	0.088	
K_1	2.50	3.75	
K_2	3.90	7.36	
v_{oB}	2.10	2.50	
K_f	0.88	1.00	

Various conclusions can be drawn from comparing the results of the fits for the two scales. The first is that both scales had a similar ΔS_o value which is a critical parameter regarding a project's potential for profitability because it describes how much volume of oil could be recovered.

Another observation is the well spacing for the two scales. As is common practice, the pilot has a smaller well spacing than the field; however, the overall recovery does not appear to have been adversely affected. Rather the behavior of the flood seems to strongly reflect the effects of the well spacing. The pilot is fitted with lower Koval factors, K_f, and v_{oB} values than the field, as is expected.

The magnitude of the increase in the values for the Koval factors is a bit surprising, in particular K_1. Even though the pilot under predicted the field's K_1 value, the higher than average value and the tendency for field scale projects to have higher Koval factors suggest to one to use a relatively high K_1 for predicting field scale behavior. Based on the pilot data, a reasonable prediction for the field would be a K_1 of about 3.0 to 3.25.

Observations from the summary in Table 4-10 include that the conclusions made for Berryhill seem to apply to the Big Muddy and Robinson/M-1 cases. Overall the Koval factors and K_f values increased, ΔS_o decreased, and v_{oB} remained constant when going between the two scales. It is also observed that an extreme, such as the high v_{oB} value for Big Muddy, is consistent between the two scales. This seems to reaffirm the idea that fitted pilot data could be used to predict field performance.

4.6.2 Comparison of Same Scale Projects

There is some data for a few large scale projects from the same field, including the M-1 project (part of the Robinson Field), the SACROC project, and the Bradford project. For each field set, the fractional flow curves are the same Table 4-13 is a

summary of the fits for these projects. Of these three projects, the M-1 and SACROC projects demonstrate consistency between its two sets of data.

Table 4-13 Summary of Fitted Values for Projects from the Same Field

Field Name	M1-2.5	M1-5.0	Bradford 7	Bradford 8	SACROC 4	SACROC 17
Size (acres)	200	200	46.2	220	600	2700
Well Spacing (acres)	2.5	5	2.89	4.00	40	40
S_{oF}	0.31	0.32	0.28	0.34	0.29	0.33
ΔS_o	0.09	0.08	0.13	0.06	0.17	0.13
K_1	1.62	1.60	1.59	1.50	2.30	3.00
K_2	2.42	2.40	5.00	2.25	6.35	7.90
K_f	0.43	0.43	0.95	0.77	1.00	1.00
v_{oB}	3.10	3.20	4.50	2.50	3.75	3.20

The fits for the Bradford projects are not close and do not show consistency to the trends discussed in the earlier sections. For example, with the Bradford field it appears that a larger project size and well spacing leads to a more uniform recovery with less channeling, but also a lower ΔS_o. There could be various reasons for the discrepancy including a different polymer injection schedule, surfactant slug size, and surfactant concentration.

In the SACROC case, the Koval factors and S_{oF} and ΔS_o follow the trends associated with larger field size. The v_{oB} does not follow the trend but the values are similar between the two projects. Furthermore, this project has the most complete data for the fractional flow and the fitted parameters also fit the curves, see Appendix A.

4.7 Conclusions

SEORM fit well to all of the data sampled and ranges now exist for key SEORM parameters. These ranges provide good starting points when studying fields as potential

EOR candidates. Table 4-14 is a summary of the ranges and average values recommended for a decision analysis for a field scale project. The ranges are based on eight sets of data for SP floods and eight sets for CO_2 fields, and ASP is assumed to behave similarly as SP fields. It is assumed that the field is approaching the end of its economic life and has a low oil cut. If the field is younger, the oil saturation at the start of the flood would be high, then ΔS_o should be adjusted to reflect the difference. The ranges are empirical and user judgment is needed when determining the most appropriate values to be used for a decision analysis or EOR forecasting.

Table 4-14 Recommended Ranges for SEORM Input Parameters

Parameter	ASP and SP Flood			CO_2 Flood		
	Low	High	Average	Low	High	Average
ΔS_o	0.06	0.16	0.10	0.06	0.14	0.10
K_1	1.25	3.5	1.6	1.5	2.5	2.0
K_2	2.0	5.0	3.0	2.0	6.0	3.5
K_f	0.4	1.0	0.75	0.0	1.0	0.5
v_{oB}	2.0	4.0	3.0	3.0	7.0	4.0

The evaluation also demonstrated that values fitted to pilot scale projects do provide some insight as to what to expect for a field scale project and therefore can provide useful information for a decision analysis. For example, if pilot data does exist then there could be more confidence in the appropriate input parameters for SEORM.

Certain trends regarding the fits are also noted. Larger scale projects tend to have higher Koval factors, higher v_{oB} values, and lower ΔS_o values. CO_2 floods tend to have higher Koval factors, v_{oB} values, and ΔS_o values than SP floods. The trends seem to agree with expectations based on the history for each flood type.

CHAPTER 5: DEVELOPMENT OF AN ECONOMIC MODEL

5.1 Introduction

Economics are commonly the attribute used to value a project and to make decisions. The simplified enhanced oil recovery method (SEORM) predicts possible technical outcomes for an enhanced oil recovery (EOR) flood: including the volumes of oil and water produced versus time. The objective of this chapter is to develop a model that quantifies the economic value of each possible technical outcome. The model is intended to account for how the scale, duration, and timing of various expenses influence the value of the project.

5.1.1.1 Economic Criteria

The economic model adopted herein is based on the cumulative discounted cash flow method (CDCFM) to characterize the economic value. From the CDCFM, one finds the net present value (NPV) of the project at various times, which is the difference between the initial investment and the sum of the total discounted cash flows. The cash flows include all costs and earnings throughout the life of the project. CDCFM uses a discount rate to describe the present day worth of a cash flow. The discount rate reflects the opportunity cost is expected on an investment made today and it represents the rate of return that could be realized with an investment with similar risk (Bosch, Montllor-Serrats and Tarrazon 2007). If the NPV is positive, then the project is profitable. A typical discount rate for an oil production project ranges between five and 15% per year.

There is uncertainty in what the actual discount rate will be; however, assuming zero for this rate is not considered appropriate because any dollar invested in the project could be invested in another project with some kind of expected rate of return greater than zero. The discount rate, d, is applied as follows

$$PV = \frac{FV}{(1 + d)^t}$$

Equation 5-1

where PV is the present value, FV is the future value, and t is time (Bosch et al. 2007).

The advantage to implementing NPV is that it provides an easy way to directly compare different economic outcomes for projects of comparable scale. Furthermore the method also incorporates the effect of time on the attractiveness of an option, where a longer period of waiting on a financial return reduces its value.

5.2 Economic Parameters

The literature on reports of several field and pilot scale projects of EOR was reviewed to develop an economic model that represented the state of practice reasonably well.

5.2.1 Generic Factors

The following sections address the factors that can be generically applied to each EOR method, including price of oil, taxes and royalties, start-up costs, maintenance costs, injection costs, treatment costs, and inflation.

5.2.1.1 Oil Price

The price of oil is arguably the most critical economic factor, as it strongly influences the profitability of a project. For example, chemical-based EOR projects are generally not economical options unless the oil price is relatively high because the chemicals are expensive. Projects such as the Bell Creek, M-1, and the Berryhill floods were considered to be technically successful projects because additional oil was mobilized and recovered. However they were not economically profitable (Hartshorne and Nikonchik 1984; Stover 1988; and Bae 1995).

Oil price is volatile. According to recent records from the US Department of Energy, the price of oil has fluctuated from $50/STB in February 2007 to a peak at $145/STB in July 2008, and then dropped to $40/STB in December 2008. This is a variation in price of about $100 over a period of a year and half. A large-scale EOR project is expected to last over a decade and is likely to experience several wide fluctuations in oil price.

Predicting oil price for the life of a flood with certainty is impossible. Many have tried to create models to forecast price, with some of the most comprehensive ones implementing thousands of inputs. Such inputs include global politics, energy consumption, technological trends, country development, and predicted production rates. Though no model can claim to be accurate over the span of decades, they do seem to imply that the general trend is for the price to be on the rise as more developing countries increase their energy demands (Belhaj and Lay 2008).

5.2.1.2 Taxes and Royalties

Several types of taxes typically apply to oil recovery projects: ad-valorem tax, severance tax, income tax, and royalties (White, Gorring and Odeh 1986). An income tax is a tax applied to the profits made by an individual or company (Forbes 2010). For the economic model it was neglected because the tax is applied to a company as whole, which makes it difficult to determine how much an individual project would be taxed. The ad-valorem tax is a tax that is applied to the value of the land of any real-estate. It can vary from state to state, but is typically between two percent of five percent of the total value of a company's assets. The severance tax is a tax that is applied to the removal of non-renewable resources. Some wells may be exempt from severance tax based on their production rate. Royalties refers to money owed to owner of the property from which oil is recovered. This fee is applied to the earnings from the sold recovered oil. Typically royalties are either 12.5% or 16.7% (American Petroleum Institute 2009). The ad-valorem tax is applied to property that is owned by the oil company and the royalty is applied to oil recovered from property owned by others. Table 5-1 is a summary of typical rates.

Table 5-1 Typical Values for Taxes and Royalties

Tax	Rate (%)
Ad-valorem	5.0
Severance	5.0
Royalty	12.5

These rates do vary somewhat from field to field, though they should be well understood when evaluating a field and therefore are not uncertain. Some projects have the potential to qualify for a tax credit for using EOR methods.

5.2.1.3 Injection, Treatment, and Disposal Costs

The injection cost, applied per barrel of injected fluid, accounts for all steps and measures necessary for the preparation and injection of fluids. The cost is applied both during the injection of the chemical slugs and the chasing water.

The treatment cost is applied per barrel of oil recovered. It is supposed to account for extra expenses involved with separating the chemicals from the oil. The water disposal cost captures the expenses for treating recovered water before disposal or reinjection (White, Gorring and Odeh 1986). These values may contain some uncertainty. Table 5-2 is a summary of typical values (Anderson et al. 2006).

Table 5-2 Typical Values for Injection, Treatment, and Disposal Costs

Cost	Rate ($/STB)
Fluid Injection	0.10
Oil Treatment	0.10
Water Disposal	0.15

5.2.1.4 Start Up and Maintenance Costs

At the start of an EOR project, there are several initial expenses that must be considered. These include creating a mixing plant for preparing the injected chemical, building water supply lines, building new wells, converting some wells from producers to injectors, and investigation and engineering expenses. All expenses are typically

proportional to the scale of the project. Of the fore-mentioned upfront expenses, the most significant is the development and preparation of new wells (White, Gorring and Odeh 1986). Generally, a field being developed for an EOR project will require smaller well spacing to promote better sweep. The only exception may be for CO_2 floods, which can be implemented without the development of new wells.

EOR projects also require maintenance and observation of all of the wells. The maintenance expense accounts for well operation costs, fracturing expenses, engineering expenses over the life of the flood, and maintenance of the wells and other equipment. Typical values are about $150/day/well (White, Gorring and Odeh 1986; and Anderson et al. 2006) (White, Gorring and Odeh 1986; and Anderson et al. 2006).

Both the upfront and maintenance costs are uncertain. Various problems with the geology or shape of the formation can create issues making well spacing and development problematic. Furthermore problems with well operations have been frequently reported and could become an issue for any flood.

5.2.1.5 Inflation

Inflation is used to account for the potential of a general increase in expenses over time. Inflation does have moderate uncertainty and a typical value is between five and ten percent (White, Gorring and Odeh 1986).

5.2.2 Factors Unique to Specific Floods

Each type of isothermal flood has its own unique expenses. These unique expenses primarily deal with the price of the injected chemical.

5.2.2.1 Polymer Expenses

The cost for polymer captures the costs of the raw material at market price and shipping the material to the site. A typical value for the price of polymer is in the range of about $1/lb to $2/lb, and higher oil price often implies higher polymer cost because the polymer is a hydrocarbon product (Wyatt, Pitts and Surkalo 2008). There is uncertainty with the value of the polymer as it may fluctuate over the life of a flood.

5.2.2.2 Surfactant-Polymer Expenses

Surfactant-polymer (SP) floods include the expenses associated with polymer floods as well as additional ones involving the surfactant. Usually admixtures are injected with a surfactant such as a cosurfactant, cosolvent, and salt. The cost of the surfactant mixture includes shipping of the raw material to the site. The cost of the surfactant can range significantly with a typical range of about $2/lb to $3/lb (Wyatt, Pitts and Surkalo 2008). There is considerable uncertainty with this parameter, in particular because the composition of the admixture is uncertain.

5.2.2.3 Alkaline-Surfactant-Polymer Expenses

Alkaline-surfactant-polymer (ASP) floods involve expenses associated with SP floods as well as additional ones for the alkali agents. ASP floods use either caustic soda (NaOH) or soda ash (Na_2CO_3) as the alkaline agents. Typical costs for caustic soda and soda sash are approximately $0.10/lb to $0.50/lb (Wyatt, Pitts and Surkalo 2008).

ASP floods are unique in that they may require higher treatment costs than the other floods because the injected brine must be softened to some degree. The softening cost may range between $0.05/STB to $1.00/STB (Wyatt, Pitts and Surkalo 2008).

There is considerable uncertainty with the price for injecting the alkali resulting from uncertainty over the identity of the alkali agent and the necessary softening cost.

5.2.2.4 CO_2 Expenses

CO_2 floods use a gas that it is often mixed with water to mobilize oil. The price of the gas varies considerably based on whether it comes from a natural or industrial source. Currently, the price range is between one and four dollars per thousand standard cubic feet (Mohan 2008). The implemented unit costs account for expenses from transporting the gas to the site. The CO_2 price is proportional to the price of oil because most sources of CO_2 are related fossil fuels (Mohan 2008). The high variability in the cost of CO_2 suggests there is substantial uncertainty.

5.2.3 Summary of Input Parameters

Table 5-3 summarizes typical values for the economic parameters that affect the value of an EOR project.

Table 5-3 Summary of Economic Parameters

Economic Parameter	Variable	Typical Value (2008)	Potential Range			Rate
Price of Oil	P_O	70	40	-	120	$/STB
Escalation Factor	R_E	3.0	-2	-	6	%/year
Severance Tax	T_S	5.0	4	-	6	%
Ad-Valorem Tax	T_V	5.0	4	-	6	%
Royalty	T_R	12.5	12.5	-	16.7	%
Inflation	i	5.0	3.0	-	8.0	%/year
Discount Rate	d	5.0	3.0	-	8.0	%/year
Fluid Injection Cost	C_q	0.10	0.05	-	0.20	$/STB
Oil Treatment Cost	C_T	0.10	0.05	-	0.20	$/ STB
Water Disposal Cost	C_{WD}	0.15	0.05	-	0.30	$/ STB
Start Up Cost	C_I	1,500	750	-	3,000	$M/well
Maintenance Cost	C_M	150	100	-	300	$/day/well
Polymer Price	C_P	1.00	0.70	-	1.50	$/lbm
Surfactant Price	C_{Sur}	2.00	1.50	-	3.00	$/lbm
Alkali Price	C_A	0.30	0.10	-	0.50	$/lbm
Softening Cost	C_{Soft}	0.50	0.00	-	1.00	$/STB
CO_2 Price	C_{CO2}	2.00	1.00	-	4.00	$/Mcf

5.3 Economic Model

The economic model is implemented by marching forward through time in discrete steps of Δt. For each time step, it calculates the discounted present value of the earnings and expenses and then sums all of the steps together to calculate the net present value of the project at a specified time.

5.3.1 Income

The first step is to establish the price of oil at a given time, t_j, during the flood. For this work, a constant oil price that represents the average price over the life of the flood is used. In addition, the model includes an escalation factor that captures an

annually compounded trend of increasing or decreasing oil price with time over the life of the project. The following defines oil price

$$P_o(t_j) = P_o(1 + R_E)^{t_j}$$

Equation 5-2

where $P_o(t)$ is the price of oil at time t_j.

The total income or earnings, $E(\Delta t_j)$, over a time step, Δt_j, centered about t_j is

$$E(\Delta t_j) = P_o(t_j)N_P(\Delta t_j)$$

Equation 5-3

where $N_P(\Delta t_j)$ is the cumulative oil produced during Δt_j.

5.3.2 Expenses

From the earnings, the total owed in taxes and royalties in time step Δt_j, $T(\Delta t_j)$, is calculated from

$$T(\Delta t_j) = (T_R + T_S)E(\Delta t_j) + (T_V L)(1 + i)^{t_j}$$

Equation 5-4

where L is the value of the property at the start of the project. In this model, inflation is applied to all cost and expenses. Inflation is applied to the ad-valorem expense because as time passes the value of the land is expected to increase.

To calculate the cost of the injected chemical, $I(\Delta t_j)$, over Δt_j, the following is applied

$$I(\Delta t_j) = \left(m_P(\Delta t_j)C_P + m_{Sur}(\Delta t_j)C_{Sur} + m_A(\Delta t_j)C_A + V_{CO_2}(\Delta t_j)C_{CO_2} + C_q + C_{Soft}\right)(q_i \Delta t_j)(1+i)^{t_j}$$

Equation 5-5

where $m(\Delta t_j)$ is the quantity of injected barrels during time step Δt_j, the subscripts P, Sur, and A stand for polymer, surfactant, and alkali, respectively, $V_{CO_2}(\Delta t_j)$ is the volume of CO_2 per injected barrel during time step Δt_j, and q_i is the injection rate during Δt_j.

The cost of treating the recovered oil during time step Δt_j, $J(\Delta t_j)$, is

$$J(\Delta t_j) = C_t N_p(\Delta t_j)(1+i)^{t_j}$$

Equation 5-6

The expense for water disposal during time step Δt_j, $W(\Delta t_j)$, is

$$W(\Delta t_j) = C_{WD}\left(q_p \Delta t - N_p(\Delta t_j)\right)(1+i)^{t_j}$$

Equation 5-7

where q_p is the production rate during Δt_j.

The maintenance cost during time step Δt_j, $M(\Delta t_j)$, is calculated as

$$M(\Delta t_j) = nC_M \Delta t_j (1+i)^{t_j}$$

Equation 5-8

where n is the total number of injection and production wells for the entire EOR project.

The economic model developed for this work treats initial expenses as a function of the number of new wells that will be needed based on the scale of the project and the initial well spacing of existing wells. An overall expense is then applied per new

necessary well. For example a 5,000-acre field that initially had 40-acre well spacing during a water flood may need a 20-acre well spacing, requiring approximately 250 new wells. If one assumes 1.5 million dollars per new well, then the upfront cost is $375 million.

The initial upfront cost, U, is

$$U = bC_I(1+i)^{t_i}$$

Equation 5-9

where b is the number of new production and injection wells for the project and t_i is the time of the well constructions relative to the initiation of the EOR project.

5.3.3 Net Profit

Based on Equation 5-3 through Equation 5-8, the profits during time step Δt_j, $P(\Delta t_j)$, is simply

$$P(\Delta t_j) = E(\Delta t_j) - T(\Delta t_j) - I(\Delta t_j) - J(\Delta t_j) - W(\Delta t_j) - M(\Delta t_j)$$

Equation 5-10

5.3.4 Cumulative Discounted Cash Flow

Finally, the cumulative discounted cash flow, CDCF, of the project at time t is

$$CDCF(t_j) = \sum_{j=1}^{z}\left[\frac{P(\Delta t_j)}{(1+d)^{t_j}}\right] - \frac{U}{(1+d)^{t_i}}$$

Equation 5-11

where z is the number time intervals between the beginning of the project and time t_j.

The model follows the CDCF through time and selects the max value that is realized after chemical injection is completed. It is assumed that engineers working at the project will continuously monitor the profitability of the project carefully and will select to terminate the project when the project is no longer profitable based on an assumed oil price that is reasonable for the foreseeable future.

5.4 Discussion of the Economical Cap

The decision analysis applies a profit cap for both the WF and EOR. It is based on the amount that is invested in the project with taxes and royalties neglected. The cap is designed to take into account the fact that the economic model neglects external economic, political, and social factors that typically limit the max profits that a company or individual can experience on an investment. The cap is a factor of the total investment, where a 100% cap means that the total earnings, after taxes, are equal to the total investment. For the analyses discussed in this chapter, the cap factor accounts for the time value of money where the time period of interest is when the peak profit is realized.

To demonstrate how the cap is applied, an example is shown in Table 5-4. All values in the table are in terms of present value worth. In both scenarios 1 and 2 the project has $1.155 billion dollars of expenses with a 200% cap and therefore the limit for the profits is set at $1.155 billion dollars. For scenario 1 the total profits experienced, after taxes and royalties, is $466 million, which is under the cap. Therefore, the selected value used in the decision analysis is $466 million. In scenario 2 the profits are $1.546

billion which is larger than the cap limit and therefore the cap is selected for the decision analysis.

Table 5-4 Example of the Economic Cap

Scenario	Cap	Total Costs	Total Earnings	Total Taxes and Royalties	Total Profits	Cap Profit Limit
	%	$MM	$MM	$MM	$MM	$MM
1	200	1155	1964	344	466	1155
2	200	1155	3274	573	1546	1155

5.5 Example of the Economic Model

Figure 5-1 is an example of results from the economic model for a surfactant flood. Figure 5-2 is a plot of the oil production rate versus time in this example.

The most significant expense for the flood is associated with the cost of injecting the surfactant. The project does not become profitable until about five years after initiation. After payout, the project continues to make money until the oil production rate falls below 500 BPD or an oil cut of less than two percent, which represents the economic limit. At this point it is assumed that the project is terminated as profits can no longer be realized based on the oil price and escalation factors assumed.

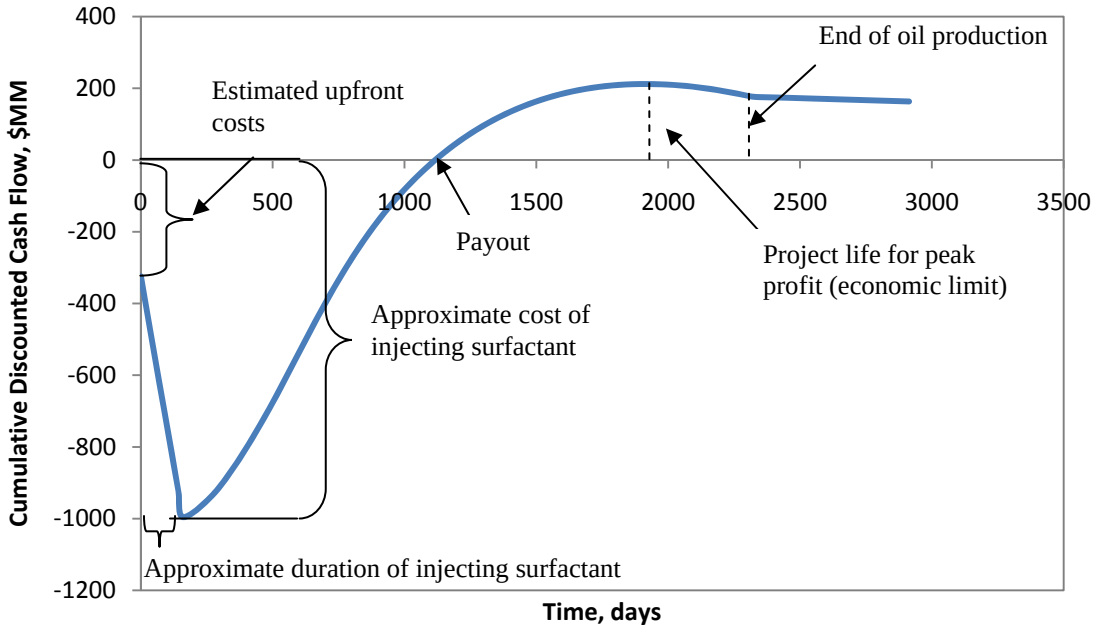

Figure 5-1 Example of Economic Model Predicting NPV

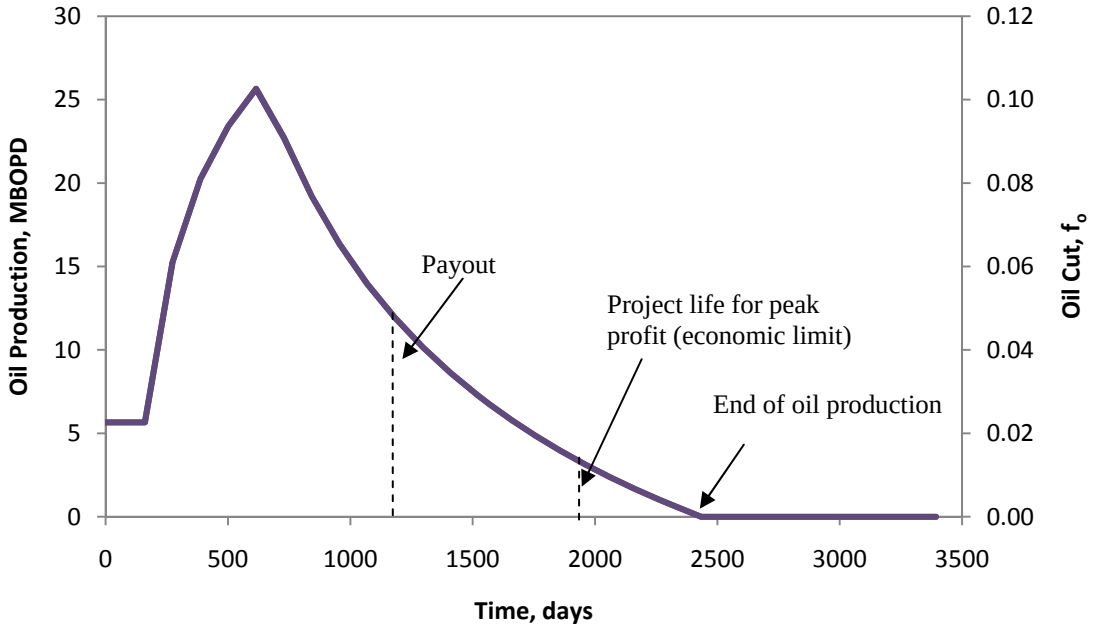

Figure 5-2 Oil Production Rate Associated with Figure 5-1

CHAPTER 6: SENSITIVITY ANALYSIS

6.1 Introduction

The economic model and the simplified enhanced oil recovery method (SEORM) together use dozens of parameters that all influence the monetary value of an enhanced oil recovery (EOR) project's financial outcome. It is important to understand how the parameters influence the value and behavior of an EOR project. A sensitivity analysis studies the magnitude of influence a value has on the outcome of a model. The results indicate how much influence the uncertainty a parameter has on the economic value. The results also provide insight about which input parameters requires the most user attention, how the model performs, and what the range of potential outcomes are. The objection of this chapter is to identify the critical parameters in order to improve the efficiency of the decision analysis.

6.2 Sensitivity Analysis Process

A local sensitivity analysis is an analysis that studies the sensitivity of the outcome to each parameter (Singh et al. 2007).

The outcomes are characterized by the maximum cumulative discounted cash flow (CDCF), as discussed in Chapter 5. The maximum CDCF, also referred to as the maximum net present value (MNPV) of the project, removes certain issues that may arise if the value of a project at a certain time is considered instead. For example, some parameters may cause the outcomes to experience early peak profitability, while other

parameters may create significant delay in peak profitability; if the selected time of interest is too early, the project's peak value may be missed. Therefore, this analysis considers the entire life of the project.

The sensitivity analysis is related to a base case to appreciate the magnitude of influence a variable has on the MNPV. The base case is presented in section **Error! Reference source not found.**. A sensitivity index, S, as defined by Singh et al. (2007) is expressed as follows

$$S_i = \frac{\Delta \mathrm{MNPV}}{\mathrm{MNPV}_{\mathrm{Base}|i}} \left(\frac{\mathrm{x}_{\mathrm{Base}|i}}{\Delta \mathrm{x}_i} \right)$$

Equation 6-1

where

$$\Delta \mathrm{MNPV} = \mathrm{MNPV}_{\mathrm{High}|i} - \mathrm{MNPV}_{\mathrm{Low}|i}$$

Equation 6-2

$$\Delta \mathrm{x}_i = \mathrm{x}_{\mathrm{High}|i} - \mathrm{x}_{\mathrm{Low}|i}$$

Equation 6-3

where x is the input value for parameter *i*, and the subscripts High, Low, and Base, represent the upper, lower, and base case condition respectively. The index S_i can range from negative infinity to positive infinity.

As a means to determine the influence that each parameter has on the model when compared to one another, the following relation is used

$$S_i' = \frac{|S_i|}{\sum_1^i |S_i|}$$

Equation 6-4

where S_i' is the magnitude influence of parameter *i*. S_i' can range from zero to one. If the model was equally sensitive to every parameter, then each S_i' would be equal.

Each type of EOR flood, surfactant-polymer (SP), alkali-surfactant-polymer (ASP), and CO_2, is analyzed separately because each flood has unique input parameters and base cases. For each flood there are from 23 to 29 parameters.

The sensitivity indices for the parameters are classified into four groups (High, Moderate, Low, and None). Table 6-1 summarizes the rating ranges. To put the S_i' values in perspective, an S_i' value of 0.1 would mean the parameter accounts for 10% of the overall impact that all of the parameters together have on the outcome. If there are 20 parameters, then the parameter would also be two times more influential than the average of all parameters.

Table 6-1 Sensitivity Classification System

Range	Rating
$S_i' > 0.1$	High
$0.05 < S_i' < 0.1$	Moderate
$0.02 < S_i' < 0.05$	Low
$S_i' < 0.02$	--

6.3 Base Cases

A base case is required to be able to establish a standard from which to measure the amount of deviation created by an input.

6.3.1 Review of the input variables

Table 6-2 is a summary of all of the input parameters for SEORM, the economic model, and other design parameters. The parameters listed in the table are those that are used to describe flood behavior and economic cash flows directly. They are sorted to show for which flood types they are applicable.

All input values for SEORM are based on ranges and mean values determined from the model validation, Chapter 4. The input values for the economic parameters, based on ranges from the literature, are summarized in Chapter 5. It is assumed for the analysis that SP floods and ASP floods will behave the same, therefore their SEORM values will be the same. However, CO_2 floods typically behave differently from SP and ASP floods. In particular the values for the specific shock velocity of the oil bank, v_{oB}, and the well spacing can vary significantly. Therefore, the values for the bases cases are similar between SP and ASP, but CO_2 is significantly different. For more details about the listed parameters, refer to Chapters 3 and 5.

The Koval factor for the flow between the injected chemical bank and the mobilized oil bank, K_2, depends on v_{oB} and the Koval factor for the flow between the mobilized oil bank and the initial bank, K_1. Therefore, to assist with the analysis, a factor term, referred to as K_f, is used in place of altering K_2 alone. The term K_f scales K_2 so that it falls between K_1 and $K_{2,max}$. Equation 6-5 shows how K_2 is calculated from K_f.

$$K_2 = K_1 + K_f\left(K_{2,max} - K_1\right)$$

Equation 6-5

where

$$K_{2,max} = \frac{K_1 v_{oB}}{v_c}$$

Equation 6-6

and v_c is the specific shock velocity of the injected chemical bank. When K_f is zero, K_2 equals K_1, and when K_f equals one, K_2 equals $K_{2,max}$.

There are also several other inputs required to help describe the properties of the reservoir and the field. These variables are mostly describe the generic fractional flow curve and the scale of the project. The analyses for SP and ASP are based on similar values, while CO_2 is significantly different. However, the values selected for each flood type do represent similar scale projects. The values for the fractional flow curves for each flood type are listed in Table 6-2. The fractional flow curves associated with the parameters are shown on Figure 6-1.

The fractional flow curves associated with the parameters are provided in Table 6-3. The only difference is for the assumed oil viscosity because CO_2 typically only is applied to oils of very low viscosity compared to ASP and SP floods. These values are based on interpreted averages from real field data, Chapter 4.

Table 6-2 Base Case Input Parameters and Values for SEORM and the Economic Model

Model	Flood	Par.	Description	Units
SEORM	All	ΔS_o	Change in oil saturation over life of EOR flood	--
		K_1	Koval factor for mobilized oil & initial banks	--
		K_f	Scale factor for determining K_2	--
		v_{oB}	Specific shock velocity of mobilized oil bank	--
		q_i	Injection rate (constant for entire flood)	STB/day
		q_p	Production rate (constant for entire flood)	STB/day
		V_p	Total pore volume of reservoir	RB
Flood Design	All	WS	Well spacing	Acres
	SP & ASP	V_{Poly}	Polymer slug size	V_p
		Z_{Poly}	Polymer concentration	ppm
		V_{Chem}	Surfactant or alkali slug size	V_p
		Z_{Sur}	Surfactant concentration	% conc.
	ASP	Z_{Alk}	Alkali agent concentration	% conc.
	CO_2	V_{CO2}	CO_2 slug size	V_p
		Z_{CO2}	CO_2 WAG ratio	--
Economic Model	All	P_O	Price of Oil	$/STB
		R_E	Escalation Factor	%/yr.
		T_S	Severance Tax	%
		T_V	Ad-Valorem Tax	%
		T_R	Royalty	%
		i	Inflation	%/yr.
		d	Discount Rate	%/yr.
		C_q	Fluid Injection Cost	$/STB
		C_T	Oil Treatment Cost	$/STB
		C_{WD}	Water Disposal Cost	$/STB
		C_I	Start Up Cost	$/well
		C_M	Maintenance Cost	$/day/well
	SP & ASP	C_P	Polymer Price	$/lbm
		C_{Sur}	Surfactant Price	$/lbm
	ASP	C_A	Alkali Price	$/lbm
		C_{Soft}	Softening Cost	$/STB
	CO_2	C_{CO2}	CO_2 Price	$/MCF

Table 6-3 Summary of Other Descriptive Parameters

Parameter	Variable	Value	Units
Initial oil saturation post primary recovery (SP and ASP)	S_{ol}	0.70	--
Initial oil saturation post primary recovery (CO_2)	S_{ol}	0.60	--
Oil saturation at start of EOR flooding	S_{oR}	0.35	--
Water flood residual oil saturation (SP and ASP)	S_{or}	0.31	--
Water flood residual oil saturation (CO_2)	S_{or}	0.33	--
Oil cut at start of EOR flood	f_{ol}	0.02	--
Formation Volume Factor for oil	B_o	1	RB/STB
Oil Viscosity (ASP and SP)	μ_o	5	cp
Oil Viscosity (CO_2)	μ_o	1.5	cp
Water Viscosity	μ_w	1	cp
End point relative permeability of water	k_{rw}^{o}	0.2	--
End point relative permeability of oil	k_{ro}^{o}	0.8	--
Corey type exponent for water	n	2	--
Corey type exponent for oil	m	2	--
Surface Area of Project	SA	5000	Acres
Pre-EOR Well Spacing	WS	40	Acres/well

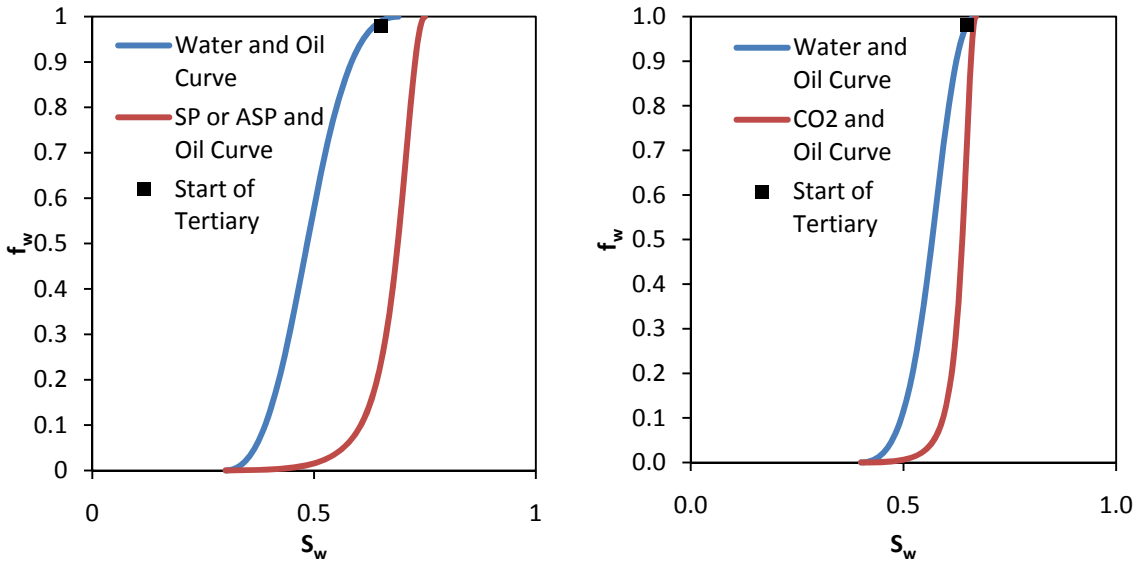

Figure 6-1 Fractional Flow Curves for Each Flood Type as Based on Table 6-3 (SP and ASP Flood on the Left and CO_2 Flood on the Right)

6.3.2 Base Case Plots

From the values in Table 6-2 and Table 6-3, the base case plots showing oil cut, oil saturation, oil recovery, and CDCF are created for each flood type. Figure 6-2 through Figure 6-5 show these plots. SEORM values for SP and ASP floods are assumed to be the same, therefore the oil cut, oil saturation plots, and oil recovery plots are all the same. All plots of CDCF depict the economics of the project from initiation to about 2500 days (SP and ASP floods) or 4000 days (CO_2 floods). The MNPV and the time at which oil production ends are also depicted.

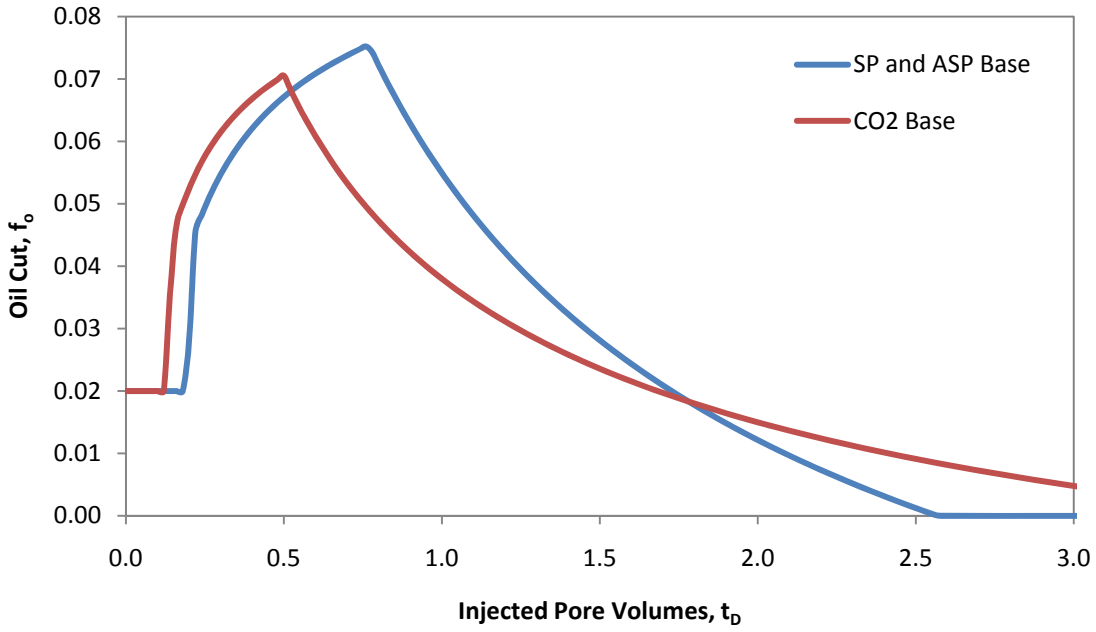

Figure 6-2 Plot of Oil Cut against Dimensionless Time for the Base Cases

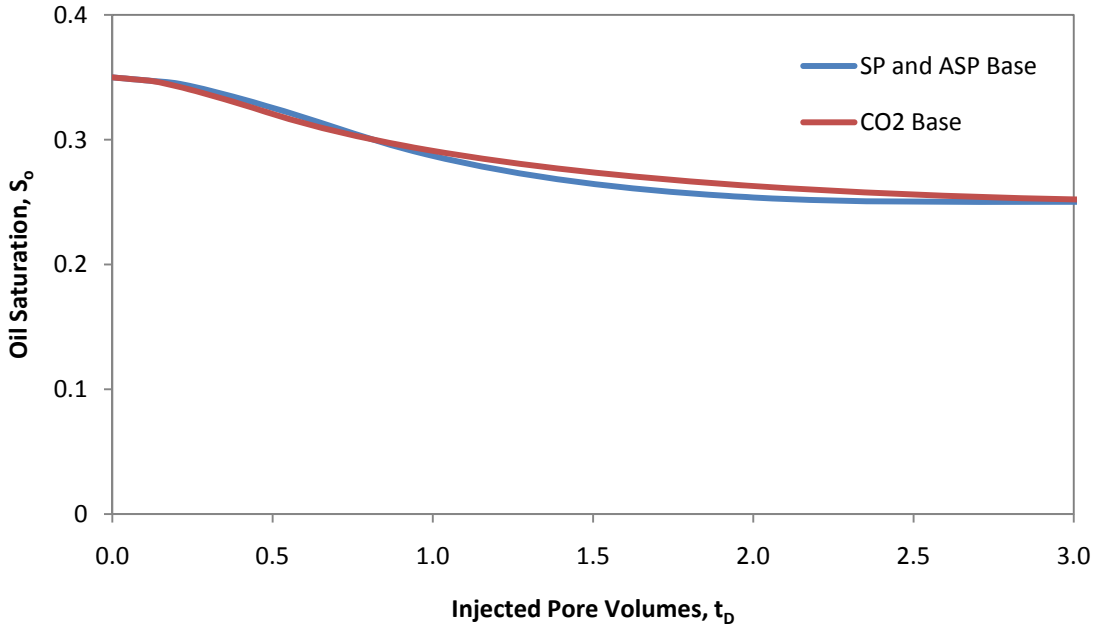

Figure 6-3 Plot of Oil Saturation against Dimensionless Time for the Base Cases

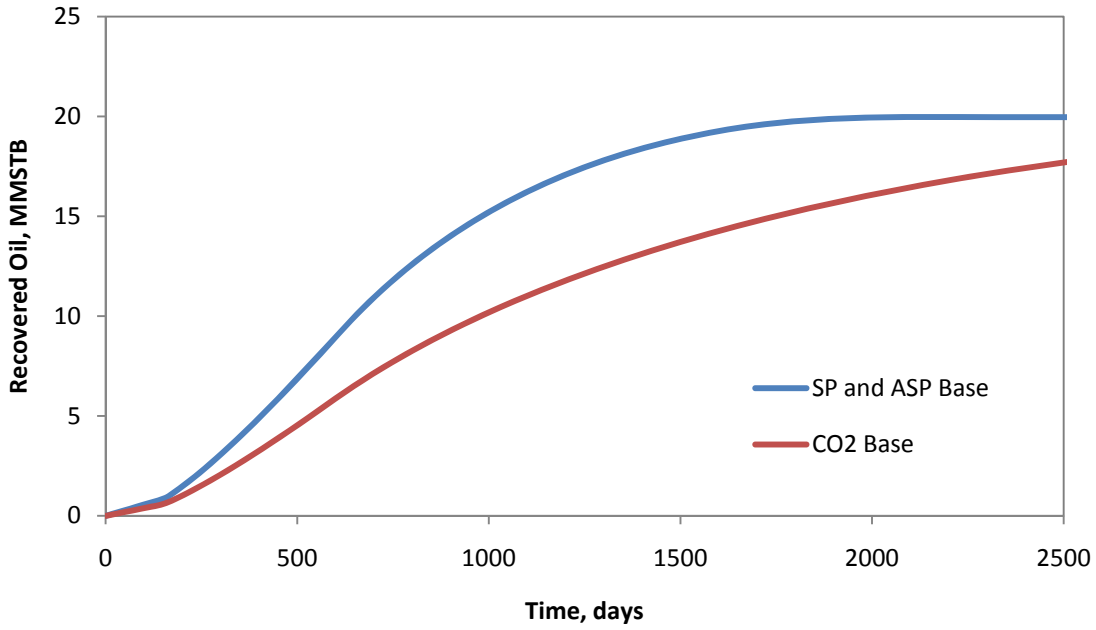

Figure 6-4 Plot of Oil Recovery against Time for the Base Cases

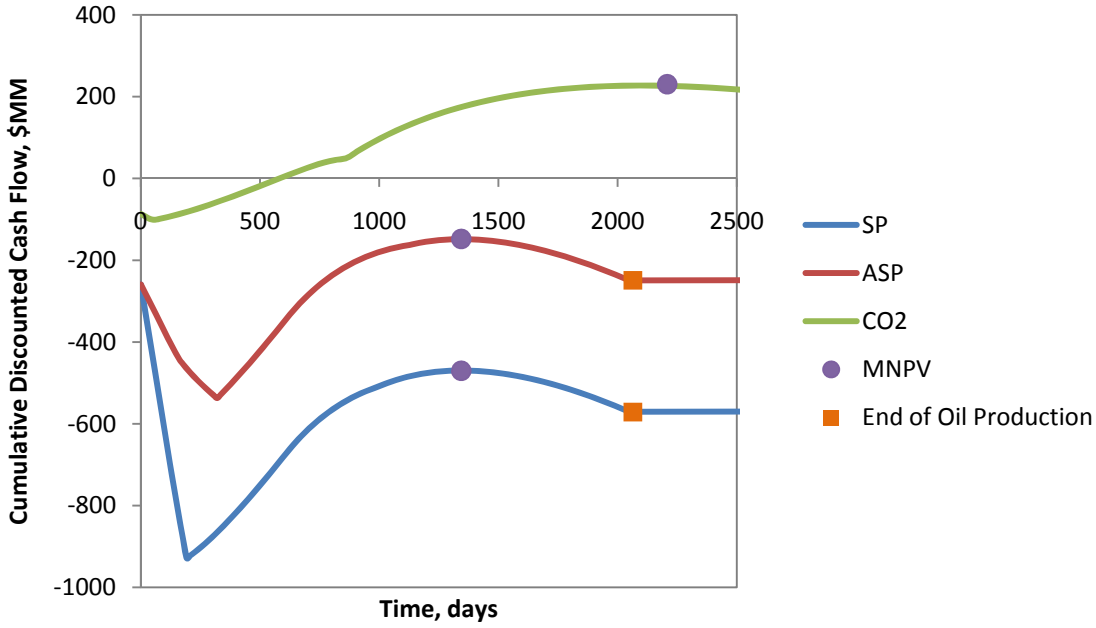

Figure 6-5 Plot of CDCF against Time for the Base Cases

The high cost of performing an SP flood is relatively high compared to the others; SP floods have more economic obstacles, which are discussed in the subsequent sections. Also, the flood life expected for a CO_2 flood is longer than others.

6.4 Sensitivity Analysis of Surfactant-Polymer Floods

6.4.1 Setup for Surfactant-Polymer Floods

The input variables used for the SP flood analysis are summarized in Table 6-4. The table includes the assumed base values and upper and lower limits for a range of values that are evaluated for each parameter. The range is assumed to be one standard deviation from the base and the standard deviations are assumed.

Table 6-4 Summary of All Inputs Used for the SP Flood Sensitivity Analysis

#	Var.	Base	Std. Dev.	Range			Units
1	ΔS_o	0.10	0.03	0.08	-	0.13	--
2	K_1	2.00	0.50	1.50	-	2.50	--
3	K_f	0.75	0.20	0.55	-	0.95	--
4	v_{oB}	2.60	0.60	2.00	-	3.20	--
5	q_i	1000	250	750	-	1250	STB/day/well
6	q_p	1000	250	750	-	1250	STB/day/well
7	V_p	2.00E+08	5.00E+07	1.50E+08	-	2.50E+08	RB
8	WS	20	5	15	-	25	Acres
9	V_{Poly}	1.00	0.25	0.75	-	1.25	V_p
10	Z_{Poly}	1000	250	750	-	1250	ppm
11	V_{Chem}	0.25	0.06	0.19	-	0.31	V_p
12	Z_{Sur}	2.00	0.50	1.50	-	2.50	% conc.
13	P_O	70.00	17.50	52.50	-	87.50	$/STB
14	R_E	4.00	1.00	3.00	-	5.00	%/yr.
15	T_S	5.0	1.3	3.8	-	6.3	%
16	T_V	5.0	1.3	3.8	-	6.3	%
17	T_R	14.5	3.5	11.0	-	18.0	%
18	i	5.0	1.3	3.8	-	6.3	%/yr.
19	d	10.0	2.5	7.5	-	12.5	%/yr.
20	C_q	0.10	0.03	0.08	-	0.13	$/ STB
21	C_T	0.10	0.03	0.08	-	0.13	$/STB
22	C_{WD}	0.15	0.04	0.11	-	0.19	$/ STB
23	C_I	1.00E+06	2.50E+05	7.50E+05	-	1.25E+06	$/well
24	C_M	200	50	150	-	250	$/day/well
25	C_P	1.00	0.25	0.75	-	1.25	$/lbm
26	C_{Sur}	2.00	0.5	1.50	-	2.50	$/lbm

6.4.2 Results for the Surfactant-Polymer Flood Analysis

Table 6-5 is a summary of the results for the analysis. Of the original 26 parameters analyzed, 13 are somewhat sensitive. The two most sensitive parameters contribute about 25% of the sensitivity when compared to the other parameters. This result suggests that about a quarter of the variability in MNPV can be attributed to only two of the 26 parameters. Of the sensitive parameters, four are associated with SEORM and nine are economic parameters.

6.4.2.1 Change in Oil Saturation

Figure 6-6 through Figure 6-9 are plots of the oil cut, oil saturation, oil recovery, and CDCF for varying ΔS_o. The change in oil saturation, ΔS_o, is a sensitive parameter because it influences several critical characteristics of the flood. The most important property that ΔS_o captures is the volume of oil recovered. Large ΔS_o implies that a large volume of oil is recovered. Altering ΔS_o only has a marginal effect on increasing the life of the flood; therefore, larger ΔS_o causes an increase in oil cut, which leads to faster oil recovery and higher rate of profits over the life of the flood.

Table 6-5 Summary of Results for the Sensitivity Analysis for SP Floods

#	Variable	S_i'	Rating
1	ΔS_o	0.123	High
2	K_1	0.056	Moderate
3	K_f	0.024	Low
4	v_{oB}	0.007	--
5	q_i	0.031	Low
6	q_p	0.006	--
7	V_p	0.085	Moderate
8	WS	0.071	Moderate
9	V_{Poly}	0.007	--
10	Z_{Poly}	0.012	--
11	V_{Chem}	0.100	Moderate
12	Z_{Sur}	0.095	Moderate
13	P_O	0.131	High
14	R_E	0.009	--
15	T_S	0.008	--
16	T_V	0.027	Low
17	T_R	0.024	Low
18	i	0.007	--
19	d	0.008	--
20	C_q	0.002	--
21	C_T	0.000	--
22	C_{WD}	0.007	--
23	C_I	0.037	Low
24	C_M	0.019	--
25	C_P	0.012	--
26	C_{Sur}	0.095	Moderate

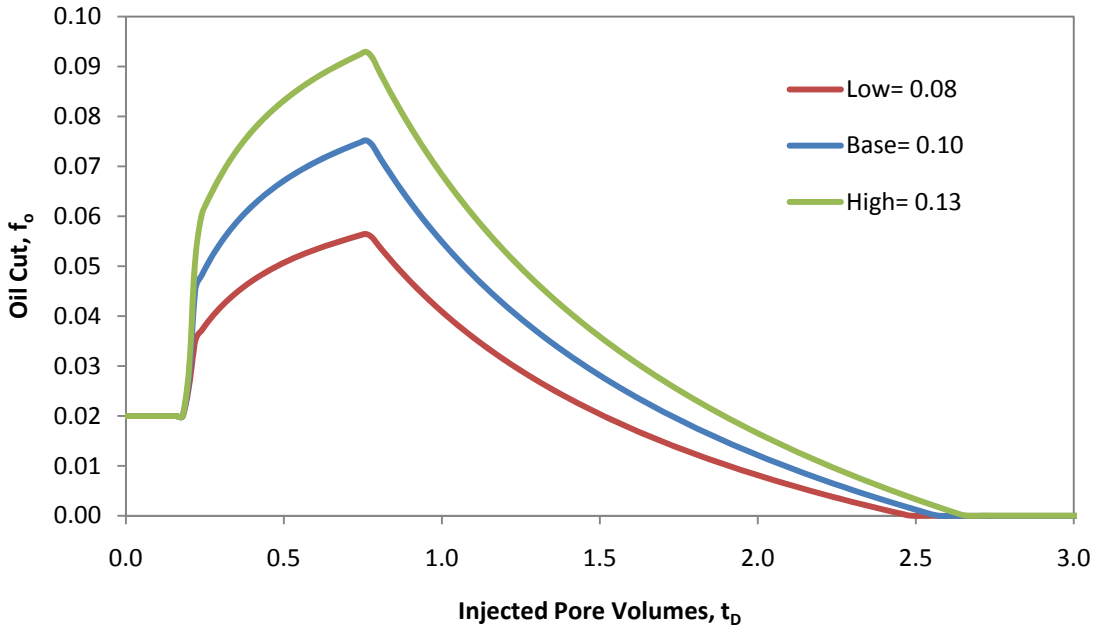

Figure 6-6 Plot of Oil Cut against Dimensionless Time for Varying ΔS_o for SP Floods

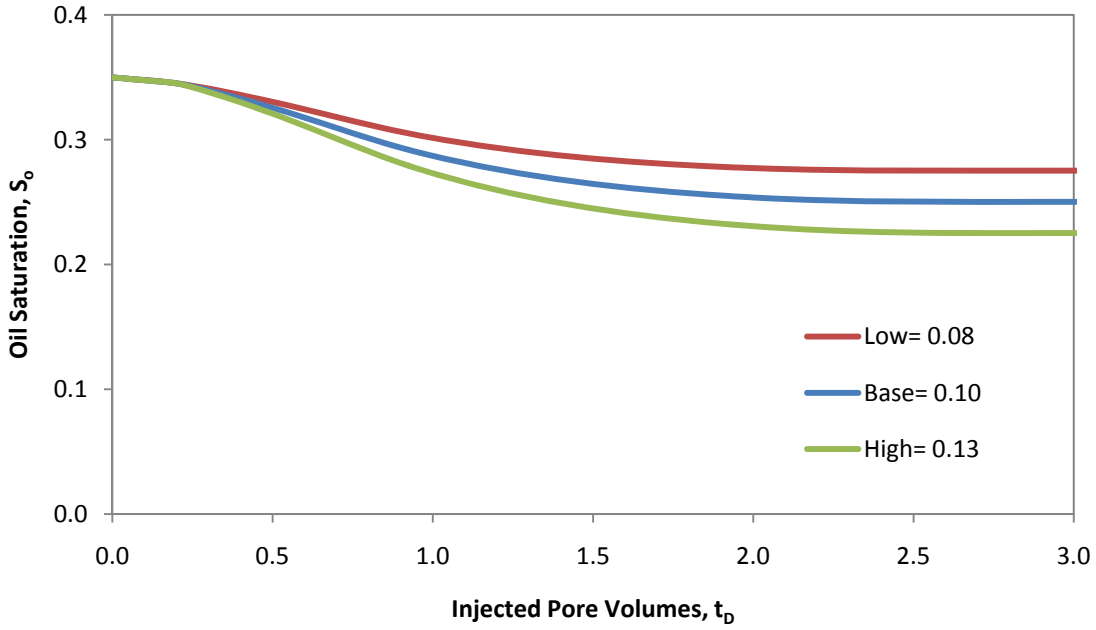

Figure 6-7 Plot of Oil Saturation against Dimensionless Time for Varying ΔS_o for SP Floods

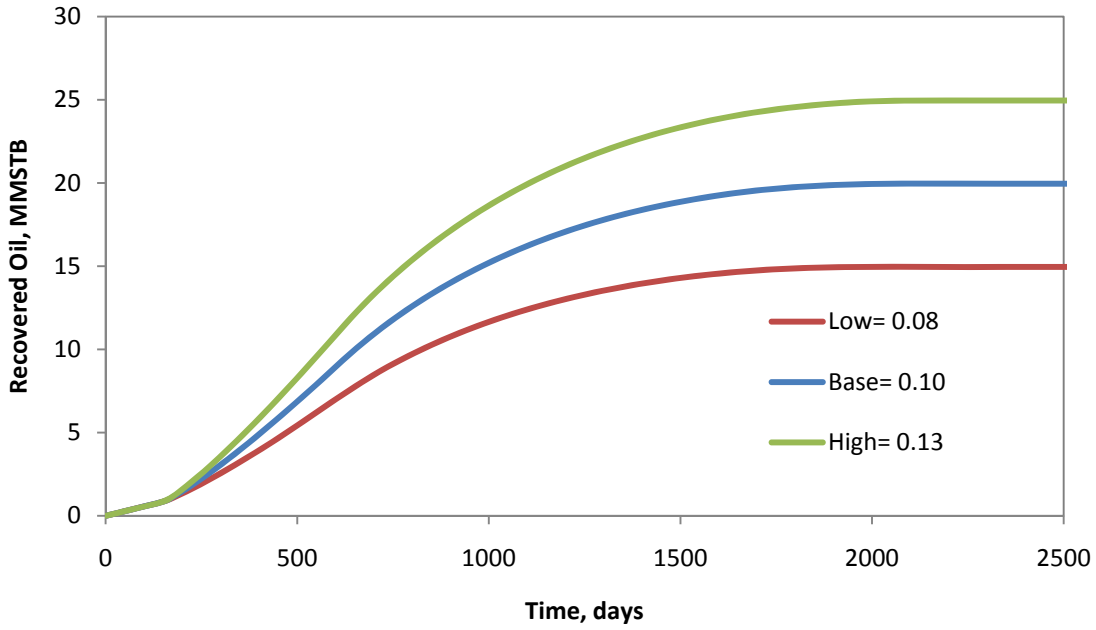

Figure 6-8 Plot of Oil Recovery against Time for Varying ΔS_o for SP Floods

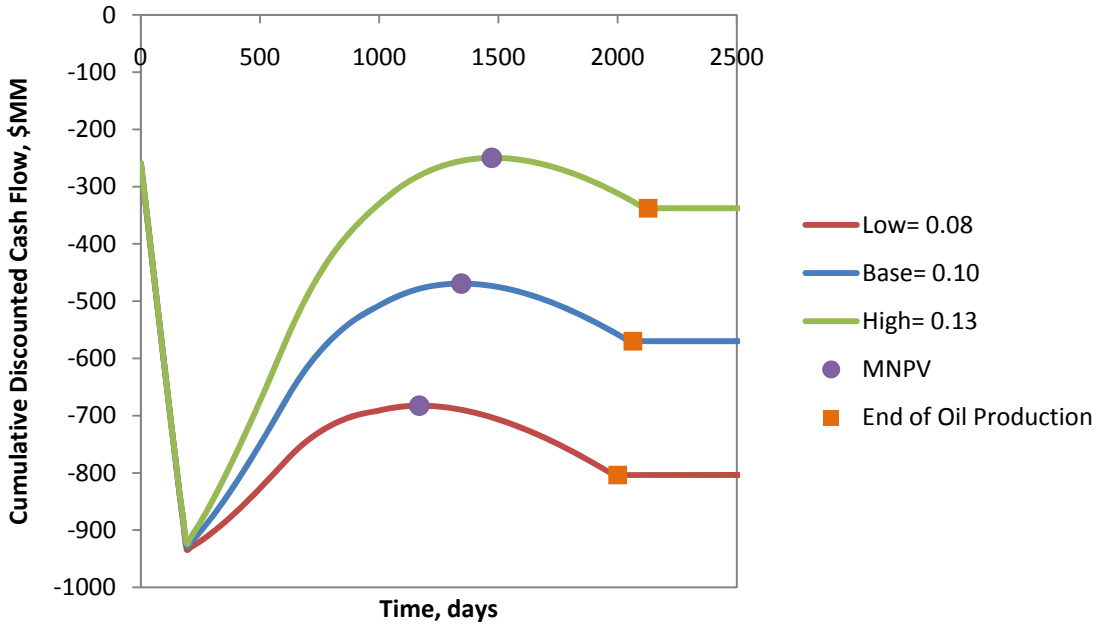

Figure 6-9 Plot of CDCF against Time for Varying ΔS_o for SP Floods

6.4.2.2 Total Pore Volume

Figure 6-10 through Figure 6-13 are plots of the oil cut, oil saturation, oil recovery, and CDCF for varying V_p. The total pore volume, V_p, of the reservoir is a sensitive parameter because of how it influences the total recovered volume of oil. A large V_p value implies that a larger volume of oil can be recovered. Furthermore, the life of the flood increases significantly. The oil cut and the oil saturation, when compared against dimensionless time, do not change from the base case; however, if compared against dimensioned time, then both the oil cut and oil saturation plots become stretched horizontally. Therefore, times to oil breakthrough, peak oil cut, and sweep out occur at later periods as the pore volume increases.

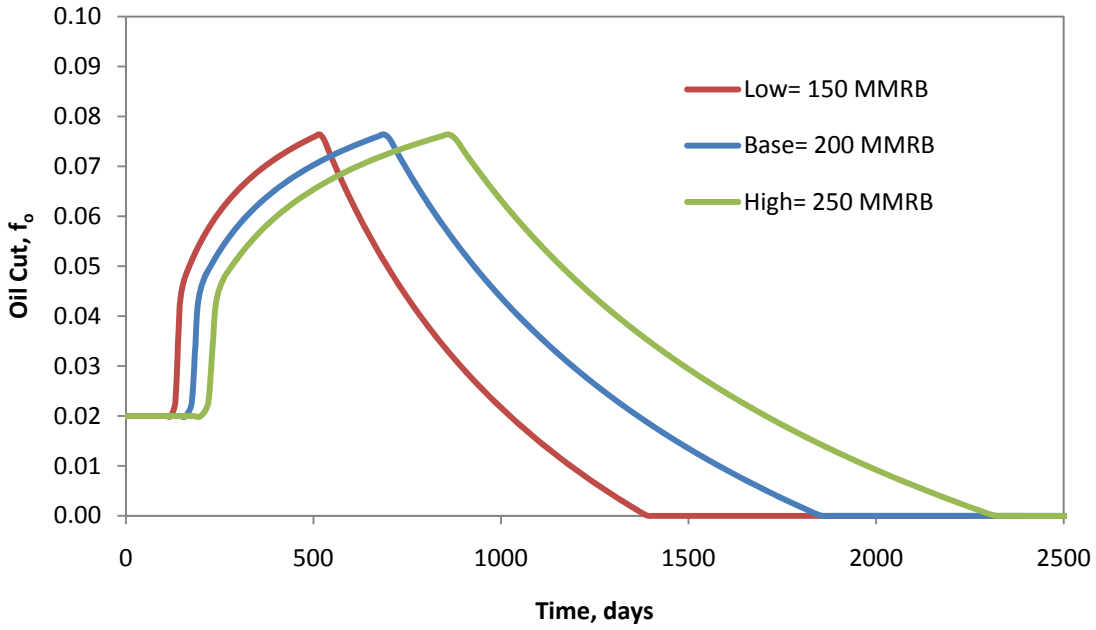

Figure 6-10 Plot of Oil Cut against Time for a Varying V_p for SP Floods

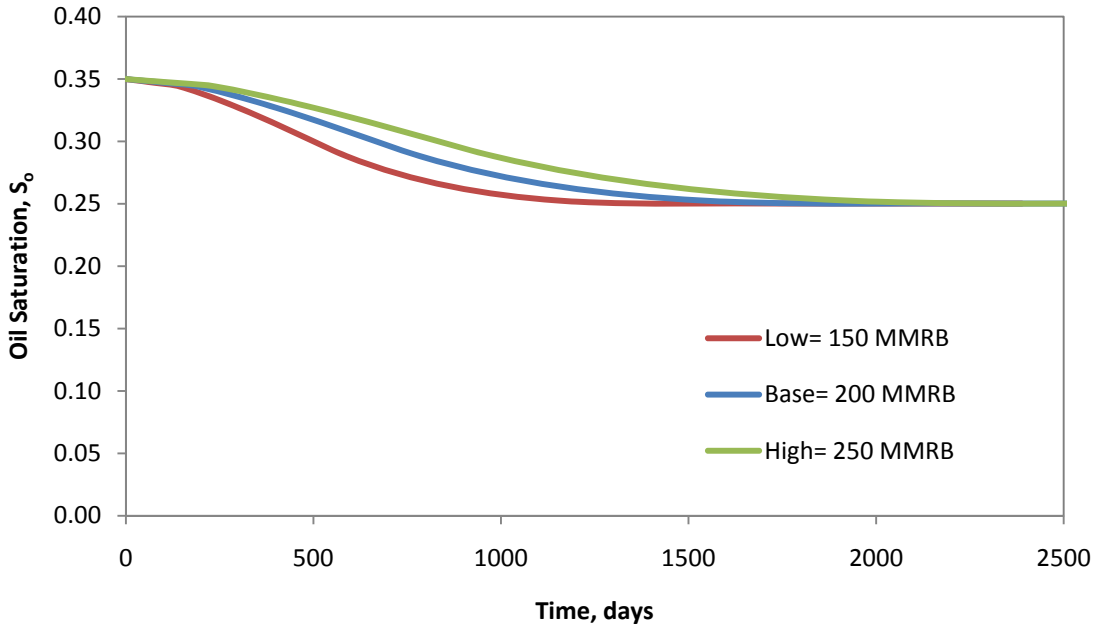

Figure 6-11 Plot of Oil Saturation against Time for a Varying V_p

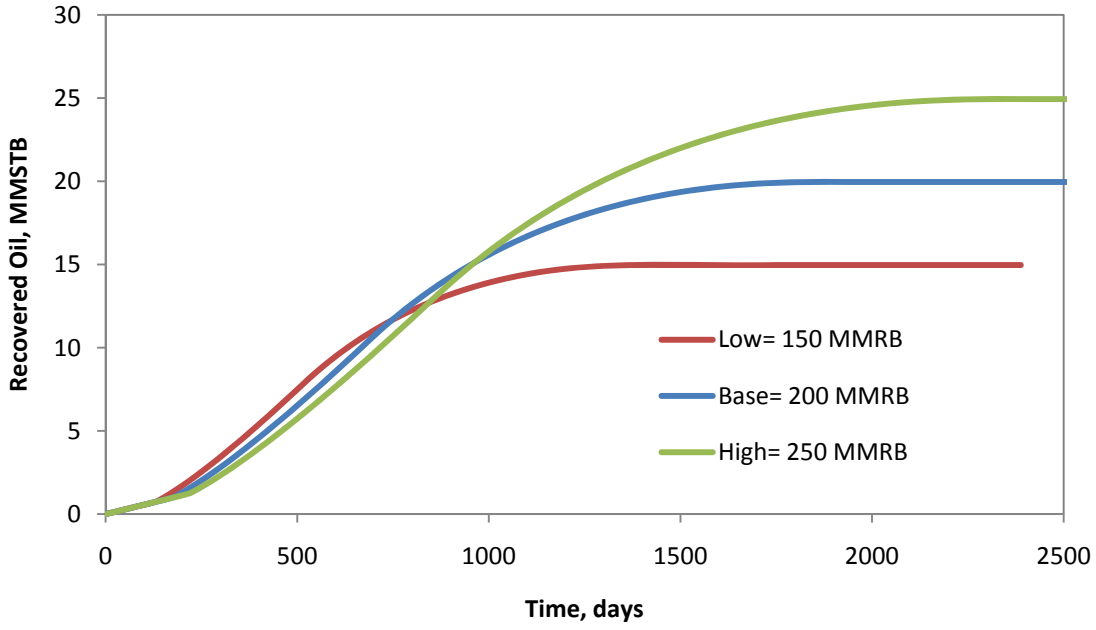

Figure 6-12 Plot of Oil Recovery against Time for a Varying V_p for SP Floods

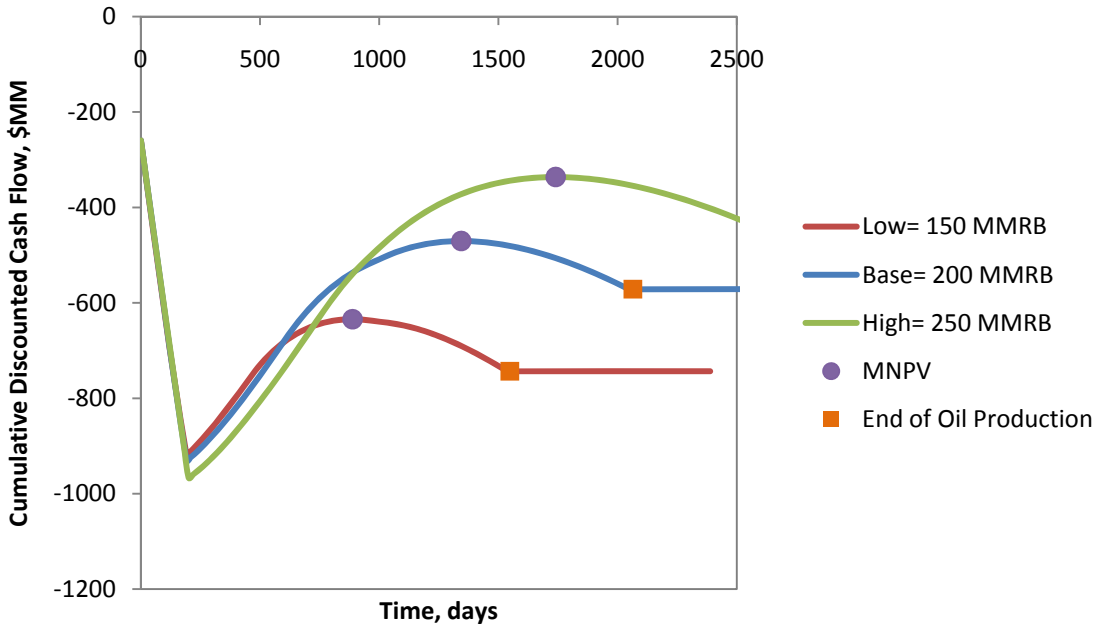

Figure 6-13 Plot of CDCF against Time for a Varying V_p for SP Floods

6.4.2.3 Price of Oil

Figure 6-14 is a plot of the CDCF for varying oil price. The price of oil, P_o, is the most sensitive parameter for SP floods. This result is not surprising as the parameter is the most critical economic input since it directly impacts the profits of a project. Altering the price of oil has no impact on the oil cut, oil saturation, or oil recovery. It does influence the economic limit for the oil cut, thereby altering the volume of profitable oil that can be recovered. For example, a high oil price allows for profitable oil recovery at a lower oil cut. In general, the extra oil recovered between a high oil price condition and a low one is significant.

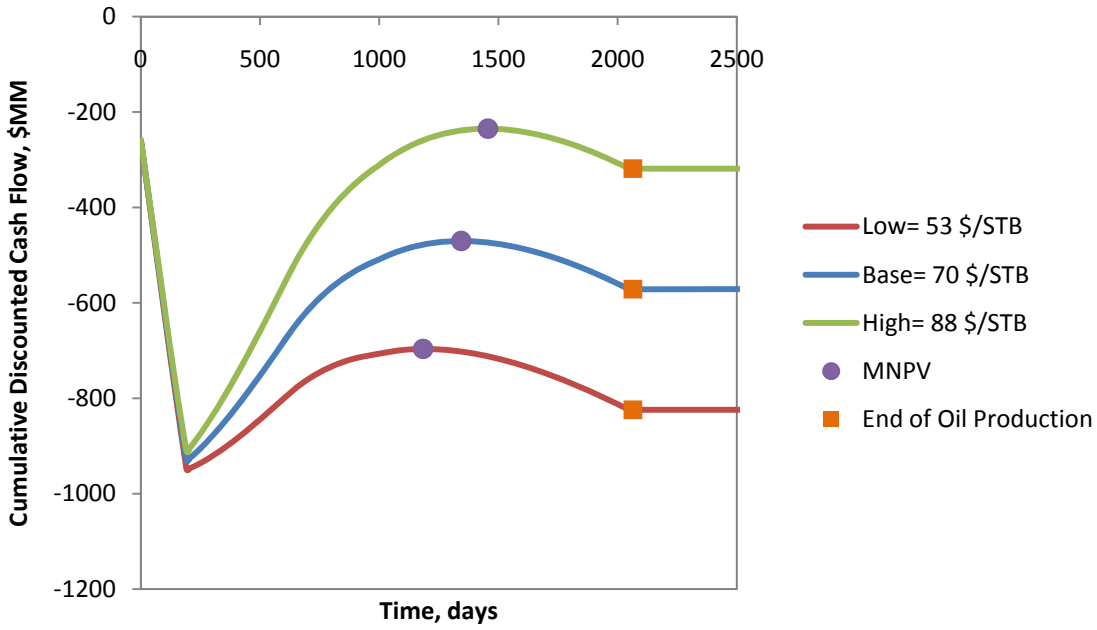

Figure 6-14 Plot of CDCF against Time for Varying P_o for SP Floods

6.4.2.4 Well Spacing

Figure 6-15 and Figure 6-16 are plots of the oil recovery and CDCF for varying well spacing, WS. Well spacing is a sensitive parameter because it influences the expenses of and life of a project. Smaller values imply that the field will have more new wells installed, leading to higher upfront expenses for installation and higher maintenance expenses. More wells also increases the injection rate for the entire field, shortening the expected life of the flood by increasing the rate of oil recovery. The higher recovery rate can be beneficial since there is an earlier monetary return on the project, though the benefit typically does not outweigh the added expenses. Furthermore the model and the analysis do not take into account the potential benefit that a smaller well spacing may

induce a higher ΔS_o because of better sweep through the reservoir. For each well spacing value, ΔS_o is kept constant.

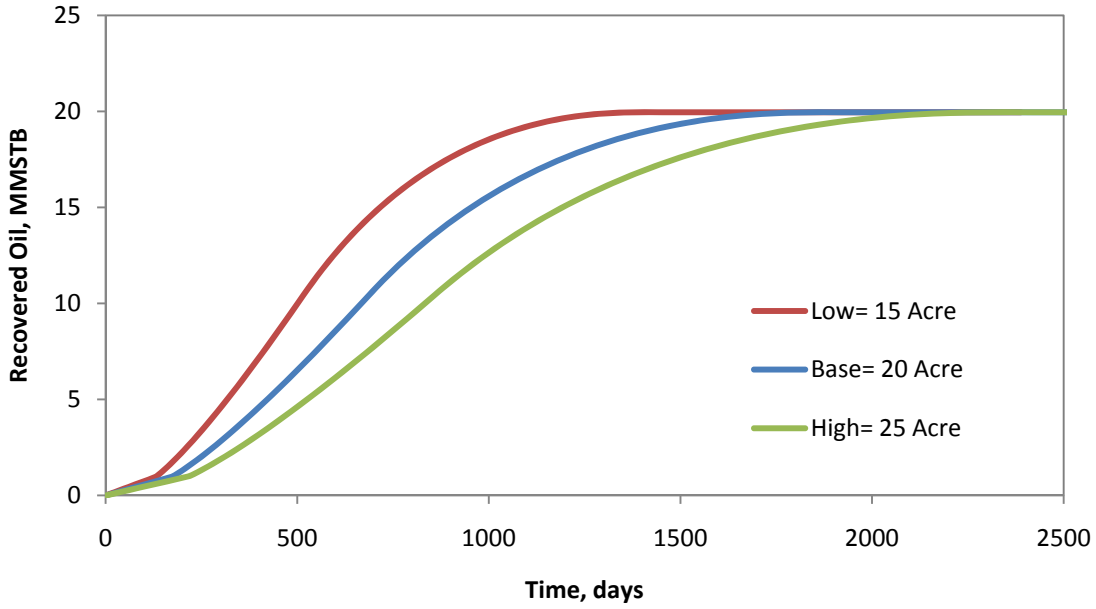

Figure 6-15 Plot of Oil Recovery against Time for a Varying WS for SP Floods

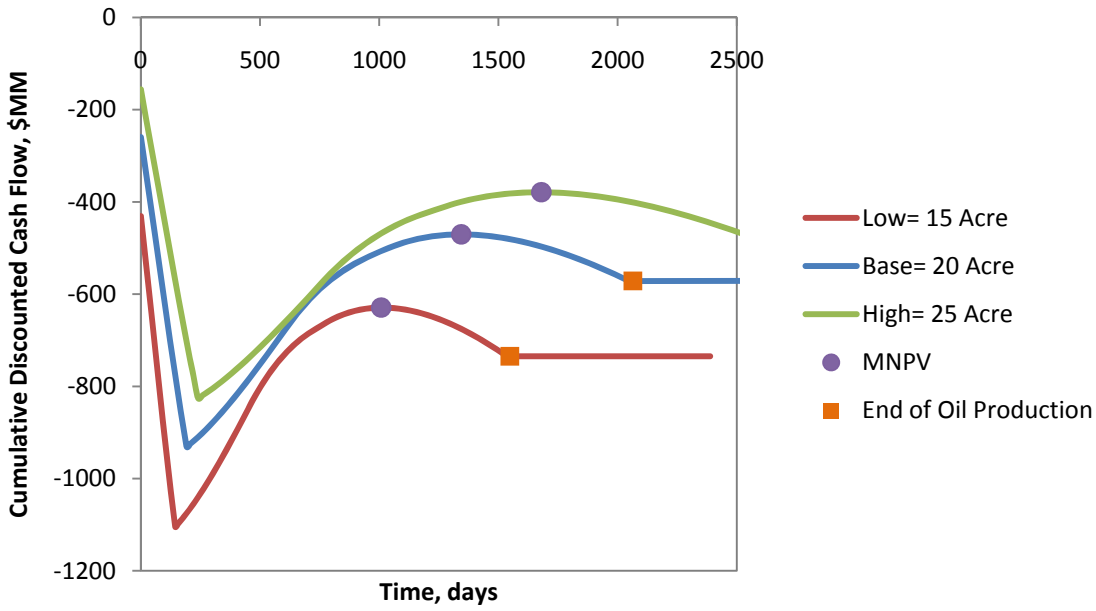

Figure 6-16 Plot of CDCF against Time for Varying WS for SP Floods

6.4.2.5 Surfactant Expenses

The cost of injecting the surfactant is the most significant expense, and three parameters directly influence the magnitude of the expense. Altering either the slug size, V_{Chem}, or the surfactant concentration, Z_{Sur}, has a similar effect on the profitability of the project because they change the volume of the injected surfactant. The cost of surfactant, C_{Sur}, controls the cost of the surfactant. Together, the three parameters account for about 25% of the sensitivity when compared to the other parameters.

Figure 6-17 and Figure 6-18 compare how varying the volume of the injected surfactant alters the economics of an EOR project. Changing V_{Chem} alters the duration of the chemical injection; while changing the concentration alters the rate the expense is applied. Therefore, the means used to inject the volume of surfactant can influence early economics slightly, which is why V_{chem} is a bit more sensitive than Z_{sur}.

The economic model is sensitive to the cost of the surfactant because of the high volume required during injection. Varying the cost is analogous to varying the concentration because they both alter the rate of the expense. For this reason the results in Figure 6-18 are very similar to those in Figure 6-19.

In terms of this sensitivity analysis, the three parameters only influence economics and not the behavior of the flood. It can be argued that a higher volume of injected surfactant will result in higher ΔS_o; however, the ΔS_o is assumed to be constant when analyzing the parameters.

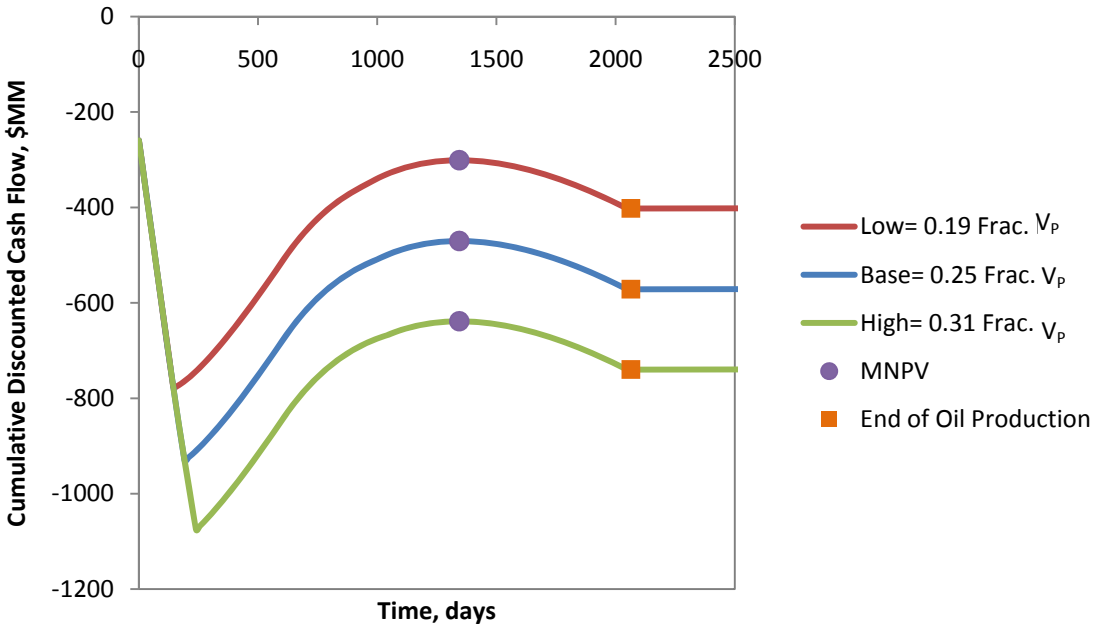

Figure 6-17 Plot of CDCF against Time for Varying V_{Chem} for SP Floods

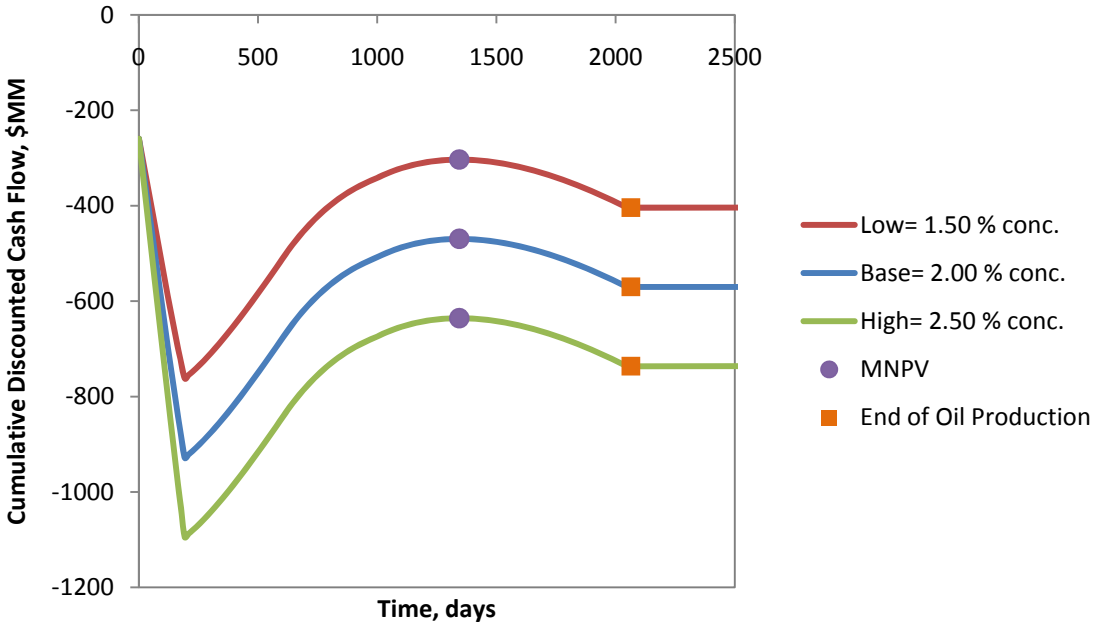

Figure 6-18 Plot of CDCF against Time for Varying Z_{Sur} for SP Floods

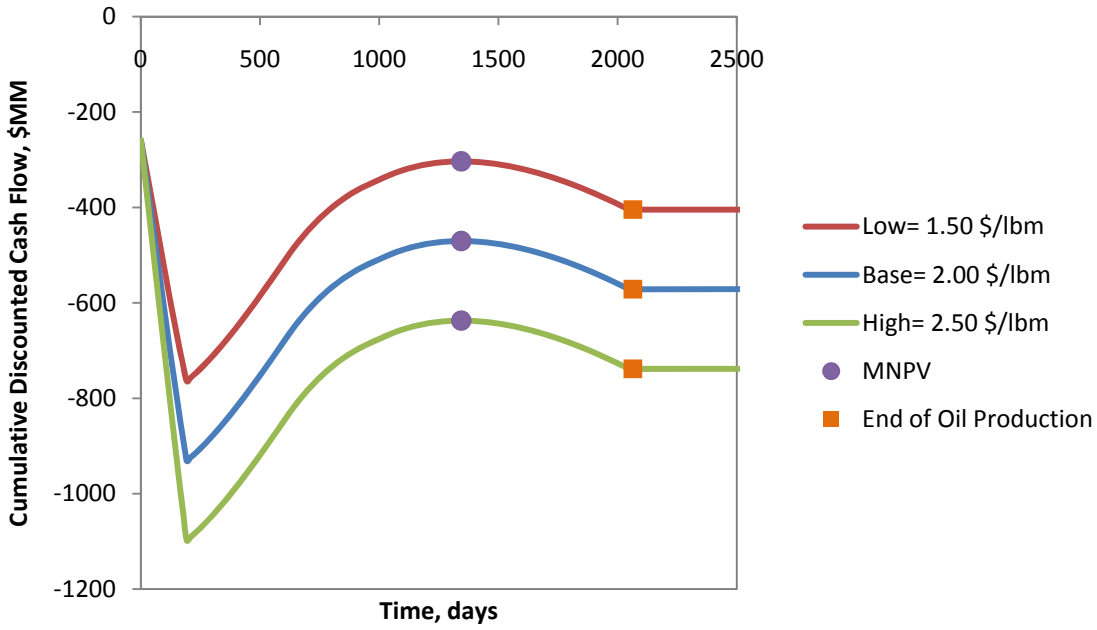

Figure 6-19 Plot of CDCF against Time for Varying C_{Sur} for SP Floods

6.4.2.6 Heterogeneity Factors

Figure 6-20 through Figure 6-23 are plots of oil cut, oil saturation, oil recovery, and CDCF for varying K_1. Recall from section 6.3.1 that K_2 will vary as K_1 varies. The K_2 parameter influences the declining portion of the oil cut curve. It is expected that the parameters that capture the heterogeneity and mobility of the fluids would be important, since they control the behavior of the flood. However, the Koval factors, K_1 and K_2, do not alter any expenses or earnings economically, or the total oil recovered, therefore the sensitivity of the parameters is somewhat limited. They do alter the rate of profits through the life of the flood which is how the MNPV is influenced.

Changes to K_1 directly impacts the peak oil cut experienced as well as the life of the flood. High Koval values suggest floods with lower peak oil cuts and longer lives. A

high Koval value suggests significant channeling and therefore also experiences an earlier breakthrough time.

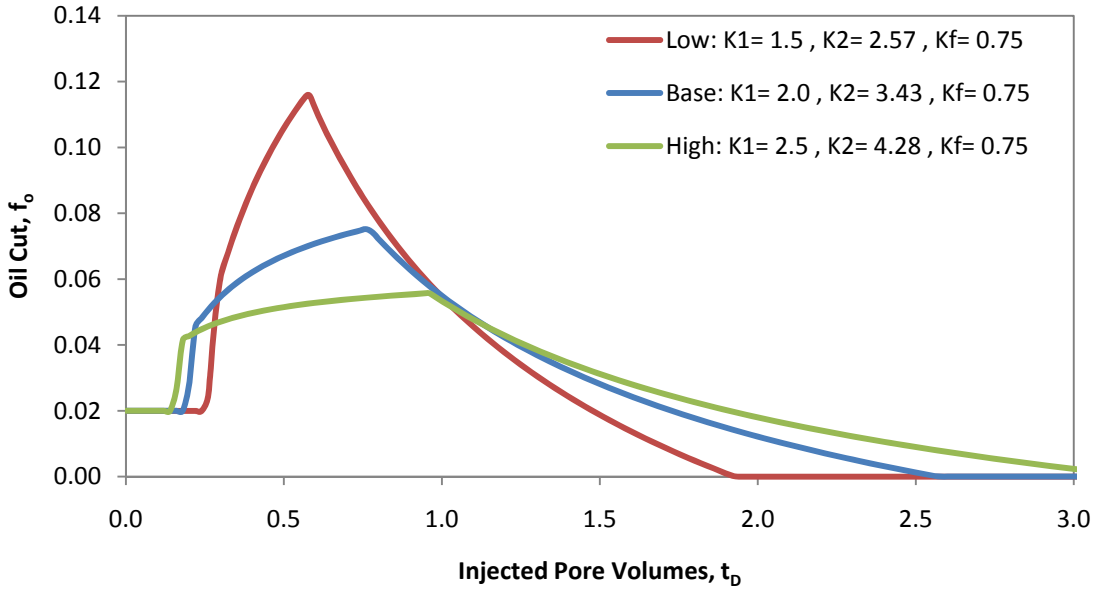

Figure 6-20 Plot of Oil Cut against Dimensionless Time for a Varying K_1 for SP Floods

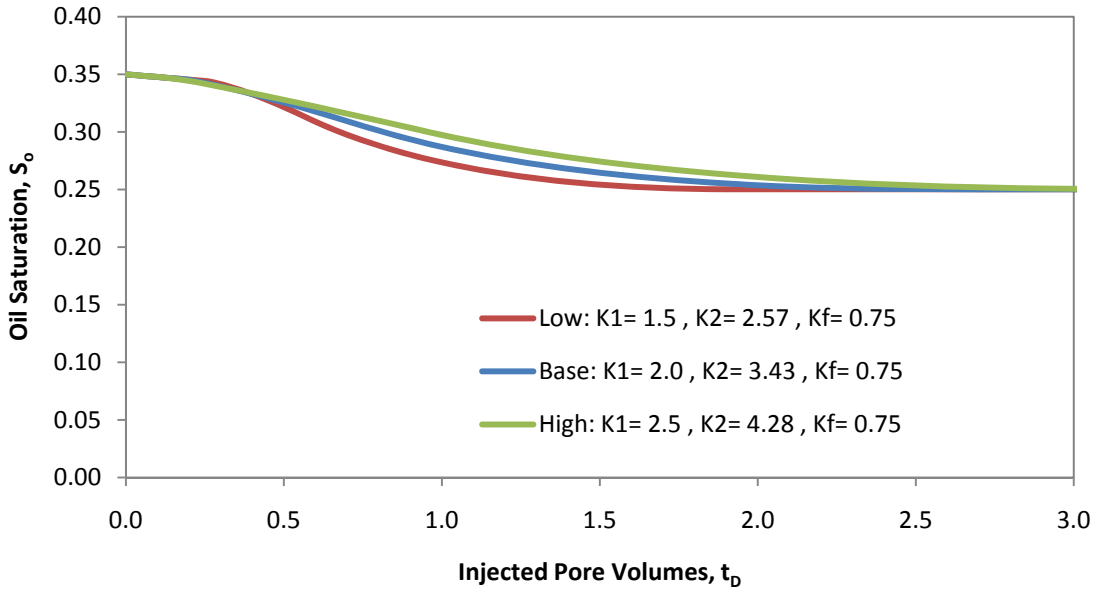

Figure 6-21 Plot of Oil Saturation against Dimensionless Time for a Varying K_1 for SP Floods

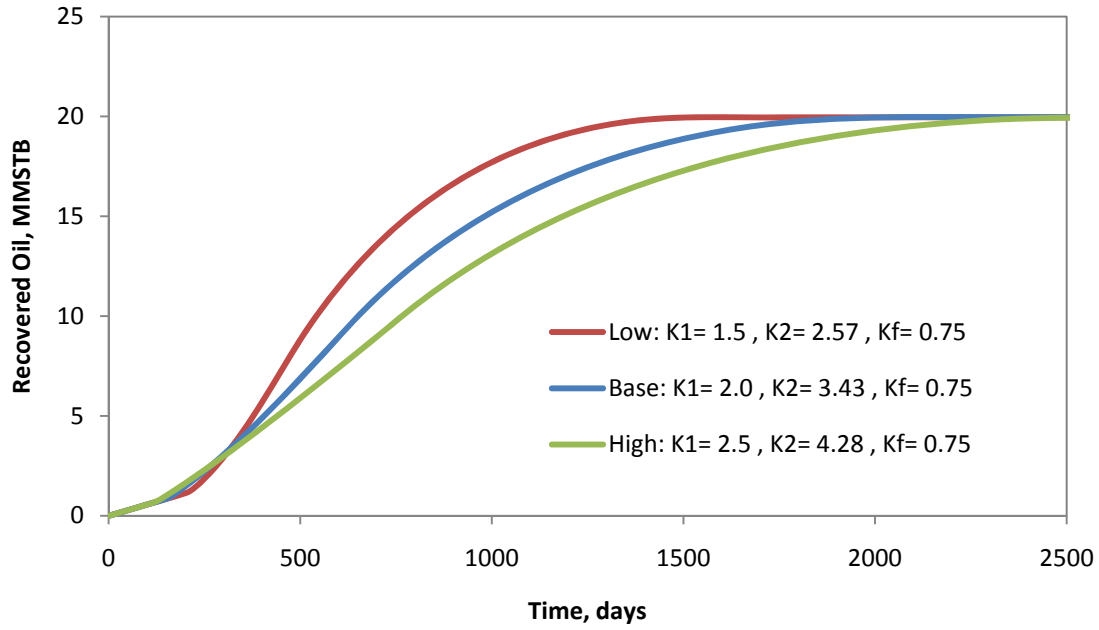

Figure 6-22 Plot of Oil Recovery against Time for a Varying K_1 for SP Floods

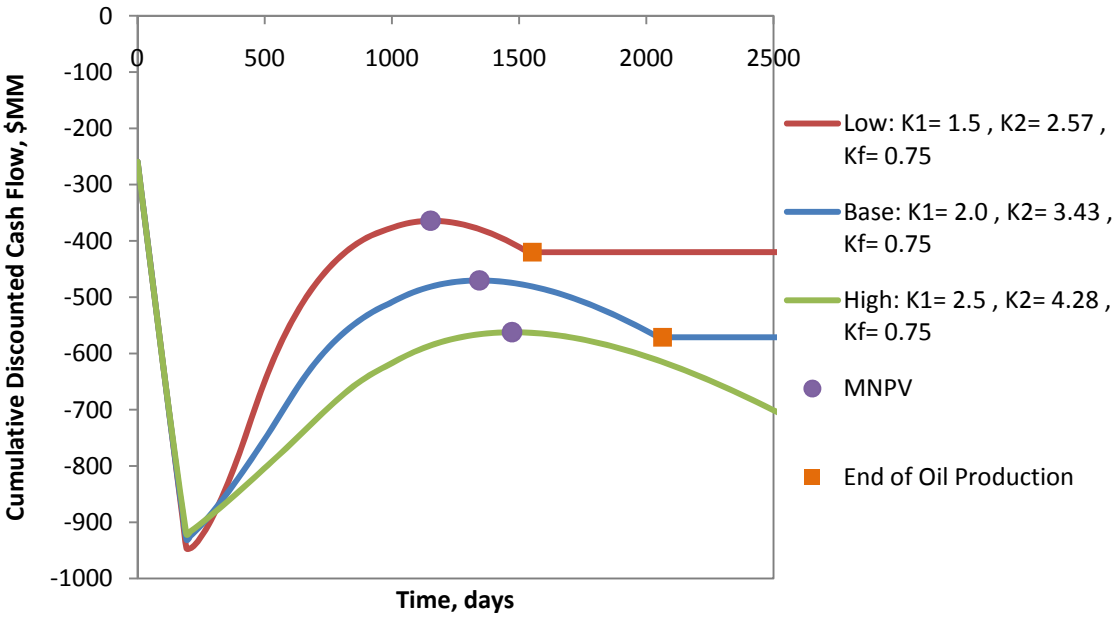

Figure 6-23 Plot of CDCF against Time for a Varying K_1 for SP Floods

Figure 6-24 and Figure 6-25 are plots of the oil cut and CDCF for varying K_f. The parameter K_f controls K_2, but it is not as influential as K_1 because the range of values that K_2 can take is controlled by K_1, v_{oB}, and S_{oF}. The parameter K_f is only a factor that selects a value for K_2 between K_1 and $K_{2,max}$. Altering K_f does alter the early oil cut and the life of the flood; however, the changes translate to a minimal change in MNPV for the project. A lower K_f is a desirable condition because it suggests a more even flow through the life of the flood.

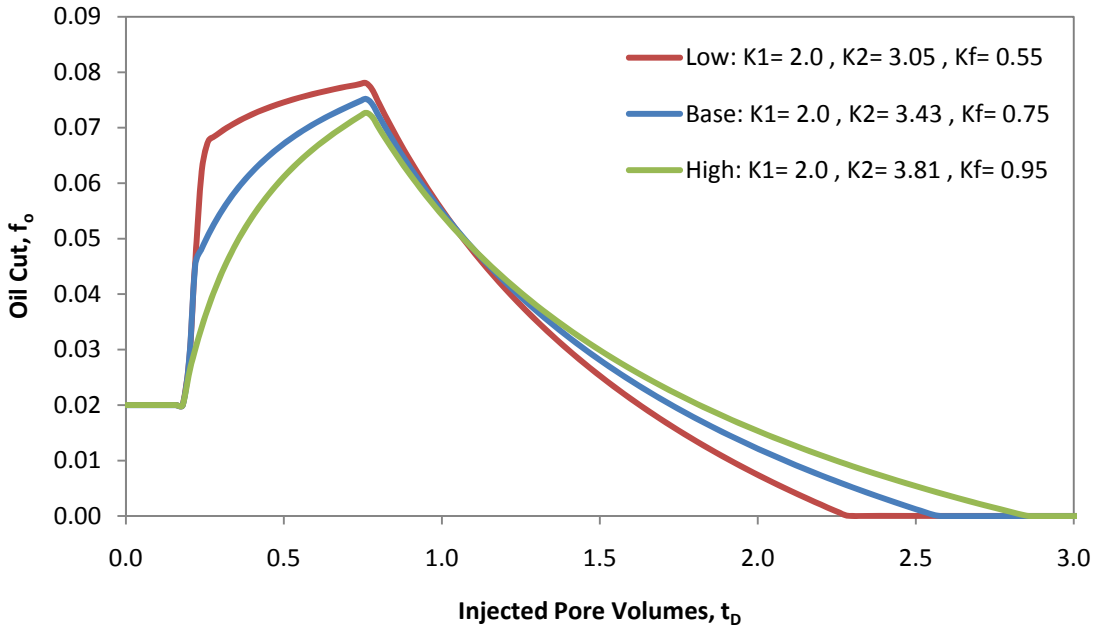

Figure 6-24 Plot of Oil Cut against Dimensionless Time for a Varying K_f for SP Floods

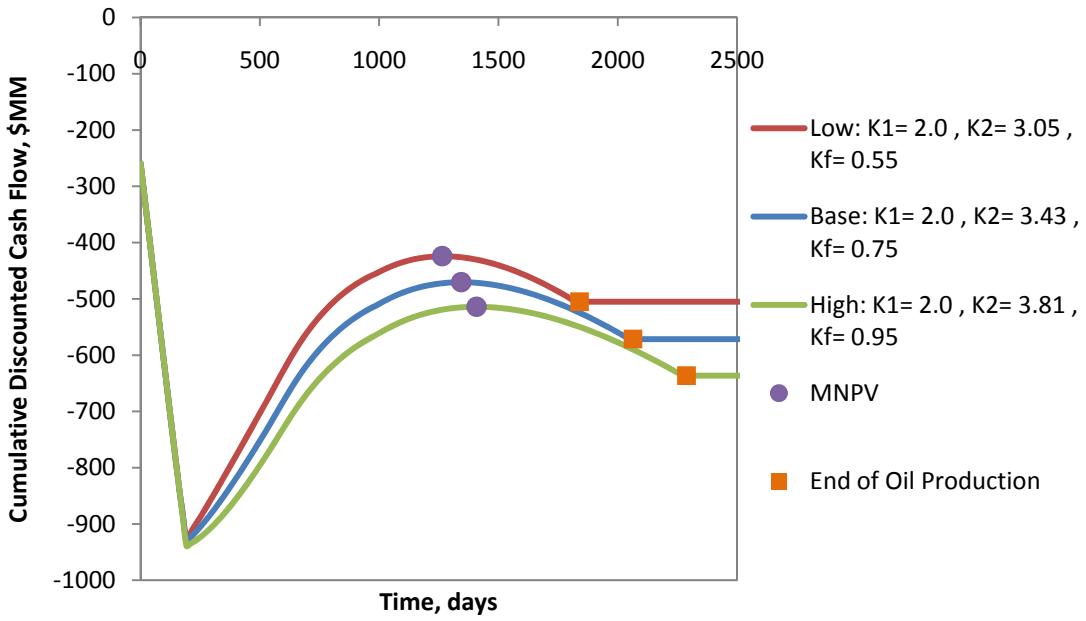

Figure 6-25 Plot of CDCF against Time for a Varying K_f for SP Floods

6.4.2.7 Least Sensitive Parameters for the Simplified Enhanced Oil Recovery Method

The parameters v_{oB}, q_i, and q_p had very little influence on the MNPV for SP floods. Figure 6-26 and Figure 6-27 are plots of the oil and CDCF for varying specific shock velocity of the oil bank, v_{oB}. The v_{oB} parameter controls the break through time and the upper limit for K_2. A higher v_{oB} implies an earlier break through time and a longer flood life. However, v_{oB} has minimal influence on the oil cut over the life of the flood and therefore does not appreciably alter the MNPV.

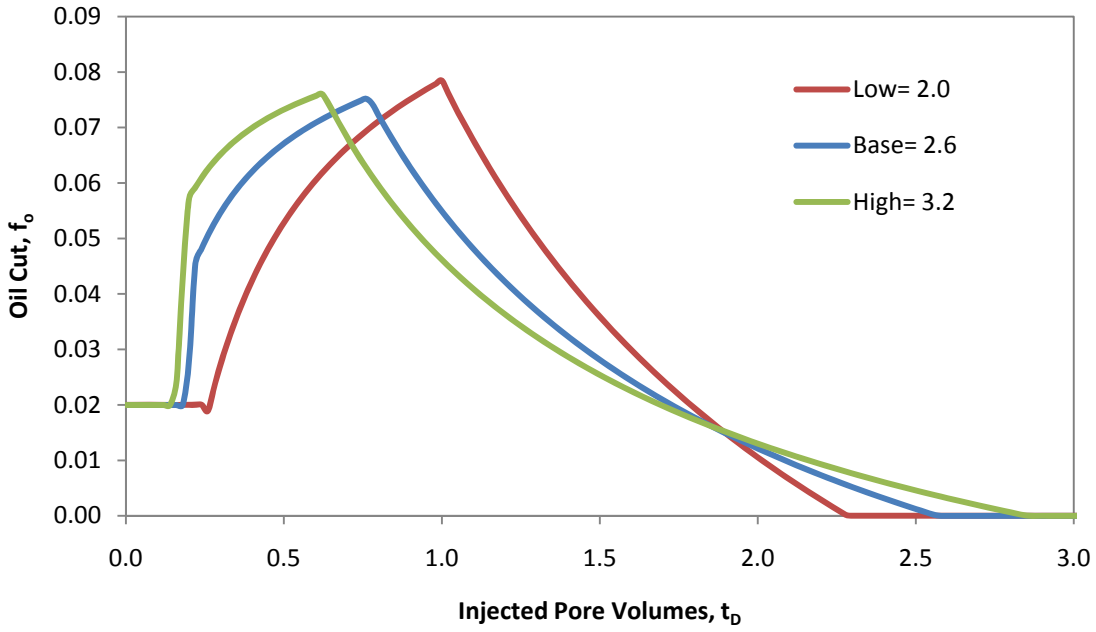

Figure 6-26 Plot of Oil Cut against Dimensionless Time for a Varying v_{oB} for SP Floods

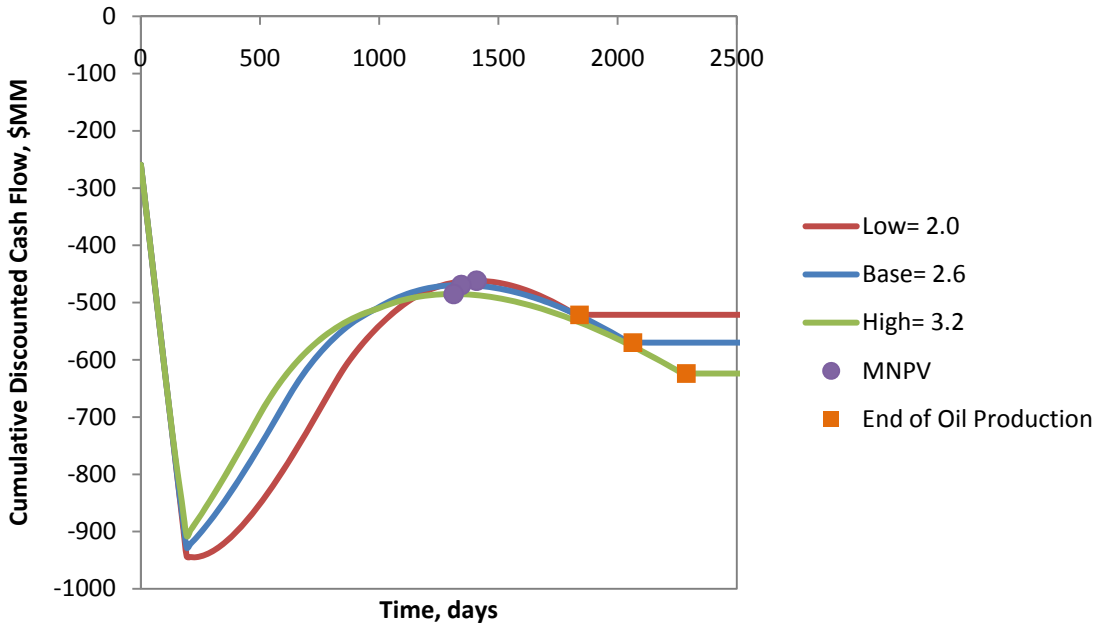

Figure 6-27 Plot of CDCF against Time for a Varying v_{oB} for SP Floods

The low sensitivity of the injection and production rates, q_i and q_p, is surprising because they are expected to influence the dimensioned time behavior of the flood. Figure 6-28 is a plot of the CDCF for varying q_p, and Figure 6-29 and Figure 6-30 are figures of oil cut and CDCF against time for varying q_i, respectively. The only rate to be a factor of any degree is q_i because SEORM relates oil production to injection rate, including oil cut. Therefore the production rate does not influence the time scale of the project or the rate of recovery. Altering the production rate has a minor influence on the economics because a higher production rate suggests a larger volume of water must be treated.

The sensitivity of the results to the injection rate is limited because even though the rate of oil recovery and life of the flood can be varied, the volume of recovered oil and expenses are not. The analysis suggests that the desirable condition is for the injection rate to be as high as allowable because a higher injection rate leads to an earlier response in oil cut.

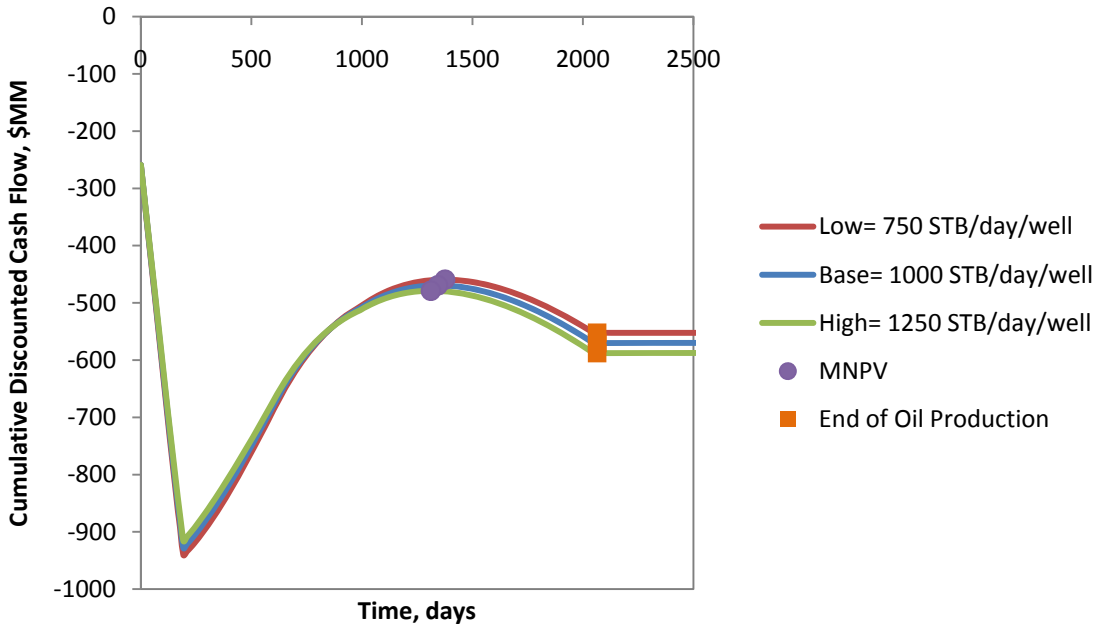

Figure 6-28 Plot of CDCF against Time for Varying q_p for SP Floods

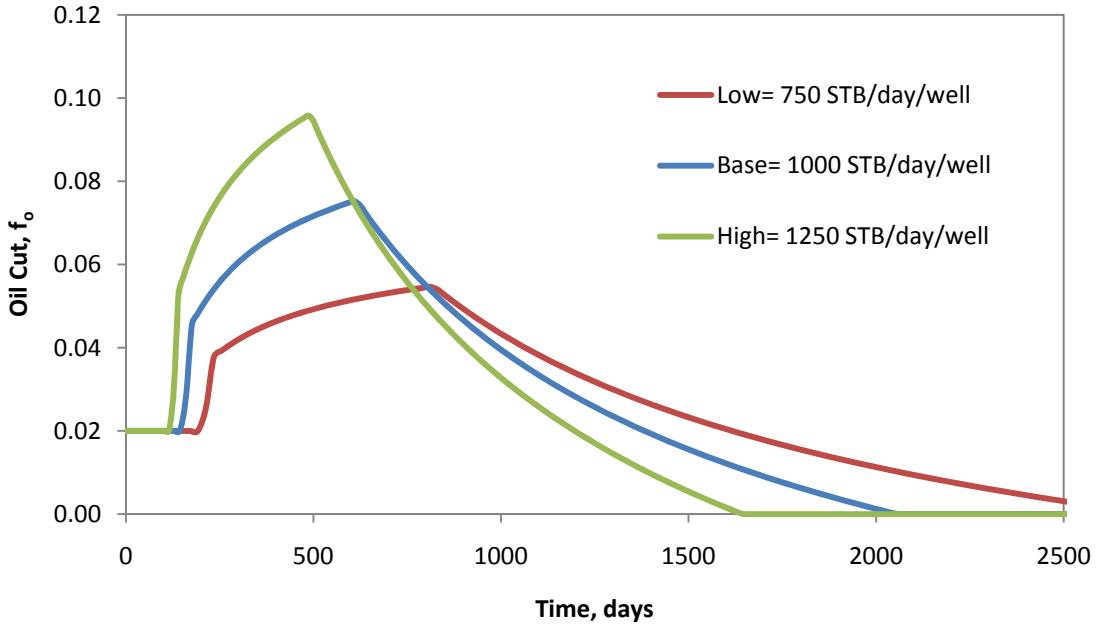

Figure 6-29 Plot of Oil Cut against Time for a Varying q_i for SP Floods

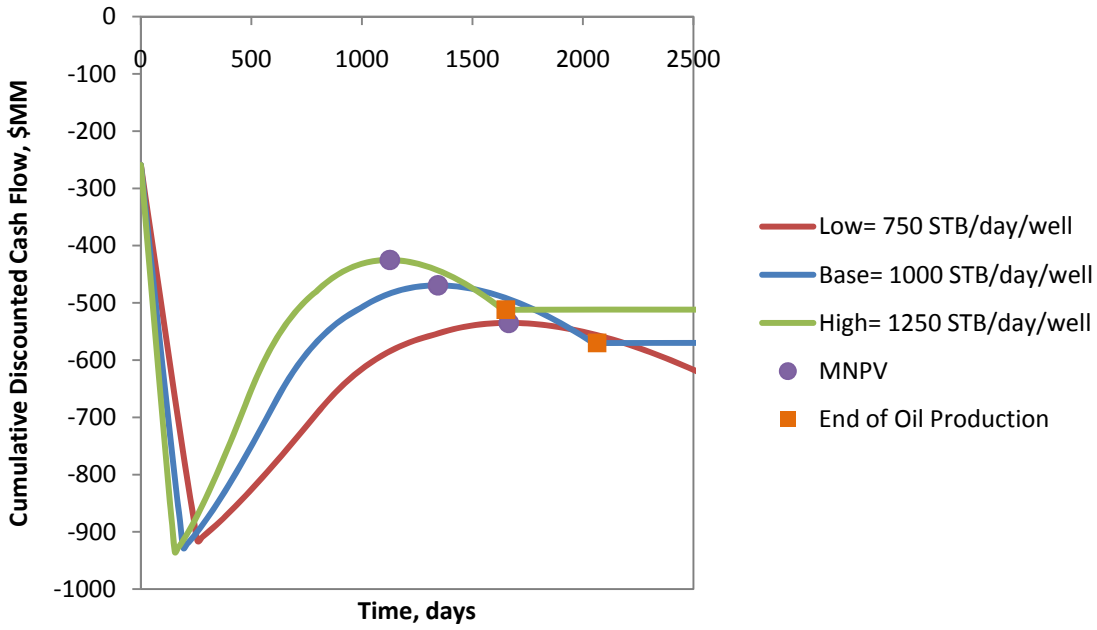

Figure 6-30 Plot of CDCF against Time for a Varying q_i for SP Floods

6.4.2.8 Upfront and Maintenance Expenses

Both the upfront cost, C_I, and maintenance cost, C_M, are strictly economic parameters that are directly related to the number of wells in the field. C_I is a onetime expense based on the number of new wells that must be installed for the project. Figure 6-31 is a plot of the CDCF for varying C_I. C_M is a daily rate that is applied to every well in the field. Figure 6-32 is a plot of the CDCF for varying C_M. Both expenses are not very significant when compared against surfactant costs, hence their low sensitivity.

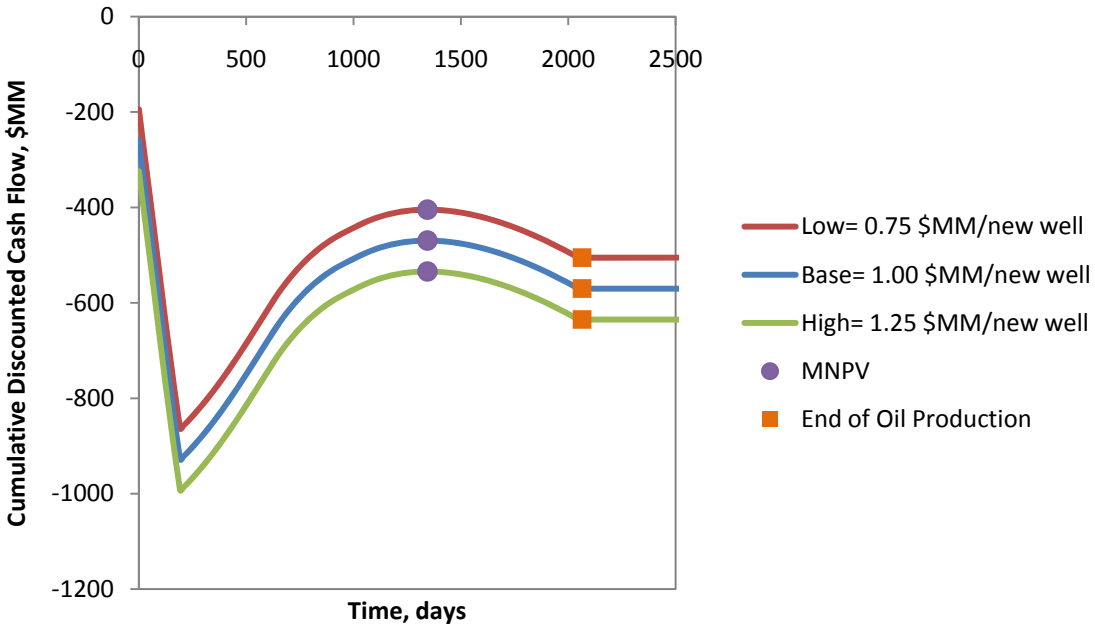

Figure 6-31 Plot of CDCF against Time for a Varying C_I for SP Floods

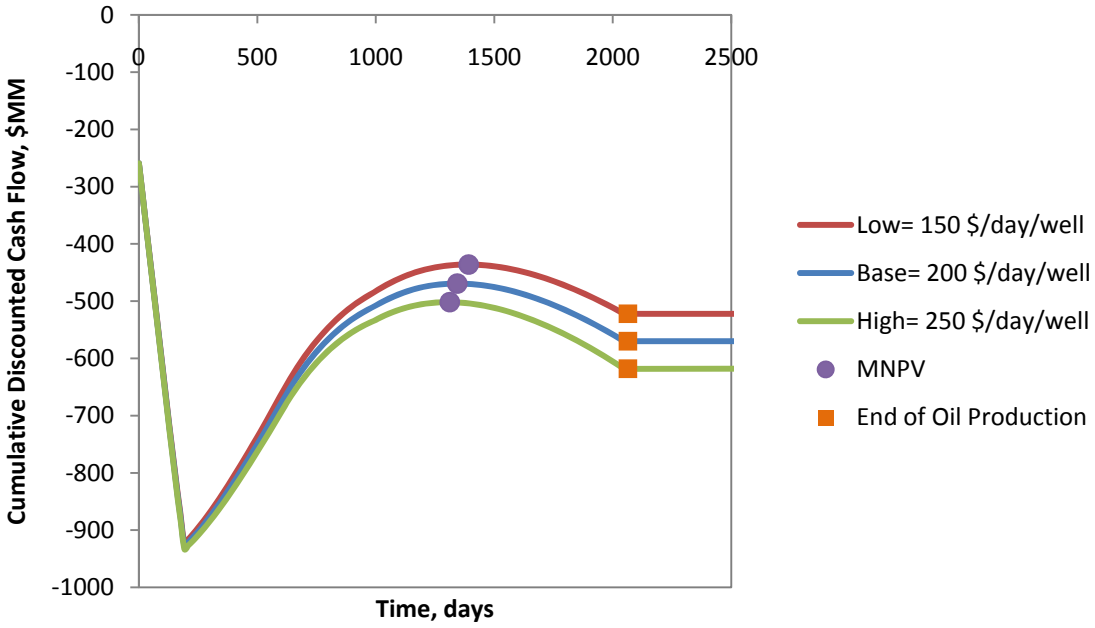

Figure 6-32 Plot of CDCF against Time for a Varying C_M for SP Floods

6.4.2.9 Ad-Valorem Tax

Figure 6-33 is a plot of the CDCF for a varying ad-valorem tax, T_V. The parameter T_V appeared to have some influence on the MNPV of a SP flood. T_V is only applied if the field exists on property owned by the oil producing company, otherwise only royalties are considered. The tax should be considered as a parameter with some uncertainty because even though the tax rate may be well established, the value of the property could vary, leading to variations in taxes. The sensitivity of the tax is small because the total expense it generates is small when compared against the cost of the surfactant.

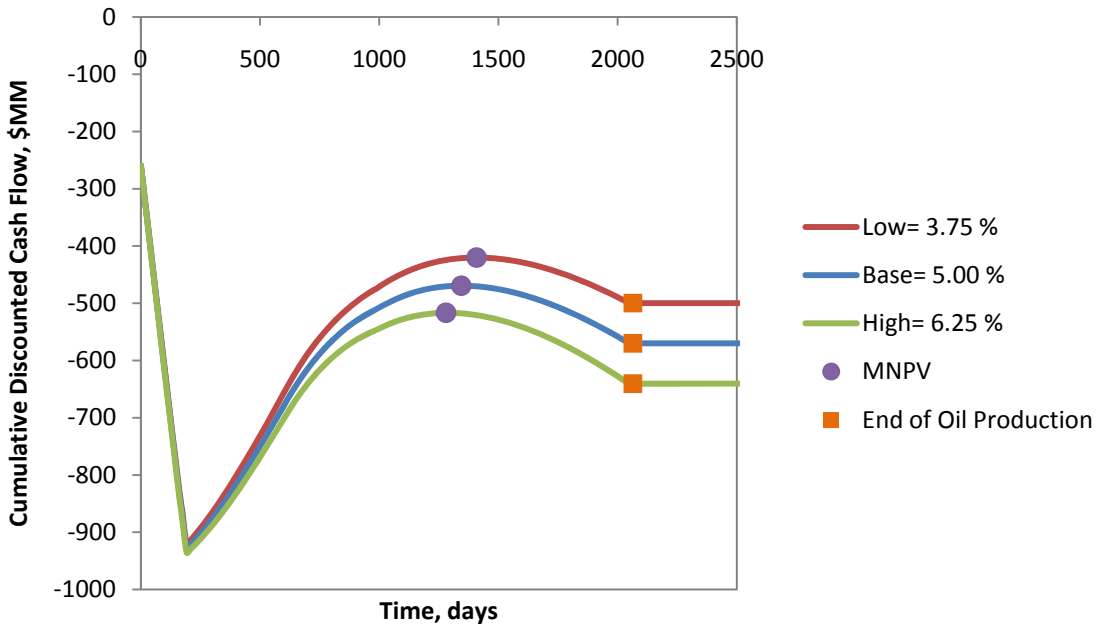

Figure 6-33Plot of CDCF against Time for a Varying T_V for SP Floods

6.5 Sensitivity Analysis of Alkali-Surfactant-Polymer Floods

6.5.1 Setup of Analysis of Alkali-Surfactant-Polymer Flood Analysis

The ASP floods have similar parameters as SP floods. Therefore the ranges provided in Table 6-4 remain applicable for the most part. All variation and inclusions to Table 6-4 are listed in Table 6-6. The ranges were determined the same way as before for the SP flood analysis in Section 6.4 The ASP flood analysis accounts for a total of 29 parameters.

Table 6-6 Summary of Additional Inputs to Table 6-4 Used for the ASP Flood Sensitivity Analysis

#	Var.	Base	Std. Dev.	Range	Unit
11	V_{Chem}	0.40	0.10	0.30 - 0.50	V_p
12	Z_{Sur}	0.30	0.075	0.23 - 0.38	% conc.
27	Z_{Alk}	1.00	0.25	0.75 - 1.25	% conc.
28	C_A	0.40	0.10	0.30 - 0.50	$/lbm
29	C_{Soft}	0.75	0.18	0.57 - 0.93	$/ STB

6.5.2 Results for the Surfactant-Polymer Flood Analysis

The results of the sensitivity analysis for ASP flood parameters are summarized in Table 6-7. Of the 29 parameters analyzed, 14 showed at least some sensitivity. Many of the parameters that are sensitive for the SP flood are also about equally sensitive for ASP floods. Notable parameters that did not experience much change in sensitivity include K_1, K_f, $v_{oB,}$ q_i WS, T_V, T_R, C_I, and C_M. The sensitivity of ΔS_o, V_p, and P_o increased a bit, while the sensitivity of V_{Chem}, Z_{Sur}, and C_{Sur} decreased significantly. The changes in sensitivity are direct results of decrease in the overall influence of the cost injecting

surfactant because there is less surfactant. The injected alkali is also relatively cheap compared to the surfactant and therefore the total cost of injection is lower. The lower injection expenses results in lower sensitivity for any parameter associated with injection costs and higher sensitivity for other parameters.

For ASP floods, V_{Chem} is still a moderately sensitive variable because it directly controls the volume of injected chemicals for both the surfactant and alkali agent. Any parameter that controls the cost of injection of the chemicals has low sensitivity. These parameters include Z_{Sur}, C_{Sur}, Z_{Alk}, and C_{Alk}.

The parameter T_R is the royalty tax. Even though T_R did register some sensitivity, it is not noteworthy because the royalty for a project should be a well understood value that does not often fluctuate with time. Therefore, the parameter will not be treated as one with uncertainty when going into the decision analysis.

Plots of all of the parameters for ASP floods are similar to those shown for SP floods and can be found in Appendix C.

Table 6-7 Summary of Results for the Sensitivity Analysis for ASP Floods

#	Variable	S_i'	Rating
1	ΔS_o	0.144	High
2	K_1	0.066	Moderate
3	K_f	0.028	Low
4	v_{oB}	0.008	--
5	q_i	0.037	Low
6	q_p	0.006	--
7	V_p	0.103	High
8	WS	0.083	Moderate
9	V_{Poly}	0.007	--
10	Z_{Poly}	0.015	--
11	V_{Chem}	0.059	Moderate
12	Z_{Sur}	0.028	Low
13	P_O	0.153	High
14	R_E	0.010	--
15	T_S	0.010	--
16	T_V	0.032	Low
17	T_R	0.028	Low
18	i	0.008	--
19	d	0.009	--
20	C_q	0.002	--
21	C_T	0.000	--
22	C_{WD}	0.008	--
23	C_I	0.043	Low
24	C_M	0.022	Low
25	C_P	0.015	--
26	C_{Sur}	0.028	Low
27	Z_{Alk}	0.018	--
28	C_A	0.018	--
29	C_{Soft}	0.010	--

6.6 Sensitivity Analysis of CO_2 Floods

6.6.1 Setup of CO_2 Flood Analysis

For the CO_2 flood analysis, many of the parameters discussed in the previous analyses continue to apply with the same ranges as mentioned earlier. However, CO_2 floods tend to behave differently and thus must be setup differently. The most significant differences are with v_{oB} and WS. CO_2 floods tend to experience higher v_{oB} values and are designed for higher WS. Table 6-8 is a complete summary of all of the inputs and the ranges analyzed.

Table 6-8 Summary of Inputs Used for CO_2 Flood Sensitivity Analysis

#	Var.	Base	Std. Dev.	Range			Unit
1	ΔS_o	0.10	0.03	0.08	-	0.13	--
2	K_1	3.50	1.0	2.50	-	4.50	--
3	K_f	0.80	0.20	0.60	-	1.00	--
4	v_{oB}	6.00	1.50	4.50	-	7.50	--
5	q_i	1000	250	750	-	1250	STB/day
6	q_p	1000	250	750	-	1250	STB/day
7	V_p	2.00E+08	5.00E+07	1.50E+08	-	2.50E+08	RB
8	WS	30	7	23	-	37	Acres
9	V_{CO2}	0.75	0.25	0.50	-	1.00	V_p
10	Z_{CO2}	3.00	0.75	2.25	-	3.75	--
11	P_O	70.00	17.50	52.50	-	87.50	$/STB
12	R_E	4.00	1.00	3.00	-	5.00	%/yr.
13	T_S	5.0	1.3	3.8	-	6.3	%
14	T_V	5.0	1.3	3.8	-	6.3	%
15	T_R	14.5	2.0	12.5	-	16.5	%
16	i	5.0	1.3	3.8	-	6.3	%/yr.
17	d	10.0	2.5	7.5	-	12.5	%/yr.
18	C_q	0.10	0.03	0.08	-	0.13	$/STB
19	C_T	0.10	0.03	0.08	-	0.13	$/STB
20	C_{WD}	0.15	0.04	0.11	-	0.19	$/STB
21	C_I	1.00E+06	2.50E+05	7.50E+05	-	1.25E+06	$/well
22	C_M	200	50	150	-	250	$/day/well
23	C_{CO2}	4.00	1.0	3.00	-	5.00	$/MCF

6.6.2 Results of CO_2 Flood Analysis

The results of the sensitivity analysis are summarized in Table 6-9. Of the 23 parameters studied, 14 exhibited at least some sensitivity. There is some change in the degree of sensitivity for a few of the parameters when compared to the results from the

ASP and SP analyses. The parameters V_P and P_o are significantly more important than for the other flood types, while ΔS_o is less important. The ΔS_o's importance diminished somewhat because both the WAG ratio (Z_{CO2}) and ΔS_o have a direct impact on v_C and therefore and impact on the shape of the oil history curve. ΔS_o is more influential than the WAG ratio because it also impacts the total volume of oil that is recovered. The significant reduction in the influence of parameter ΔS_o and the overall reduction in expenses for CO_2 lead to a higher relative influence for V_P and P_o when compared against other parameters. The lower expenses are a direct result of lower injection costs, fewer wells for maintenance, and fewer new wells that need to be drilled.

Most of the analyzed parameters behave and alter the base case in the same manner as for the other flood types. Only ΔS_o and Z_{CO2} act differently than for the other flood types because of how both influence v_C and K_2. Plots of all of the parameters for CO_2 floods are similar to those shown for SP floods and can be found in Appendix C.

Table 6-9 Summary of Results for the Sensitivity Analysis for CO_2 Floods

#	Variable	S_i	Rating
1	ΔS_o	0.067	Moderate
2	K_1	0.077	Moderate
3	K_f	0.039	Low
4	v_{oB}	0.048	Low
5	q_i	0.045	Low
6	q_p	0.003	--
7	V_p	0.133	High
8	WS	0.065	Moderate
9	V_{Chem}	0.060	Moderate
10	Z_{Sur}	0.035	Low
11	P_O	0.193	High
12	R_E	0.016	--
13	T_S	0.012	--
14	T_V	0.021	Low
15	T_R	0.035	Low
16	i	0.012	--
17	d	0.015	--
18	C_q	0.006	--
19	C_T	0.000	--
20	C_{WD}	0.011	--
21	C_I	0.019	--
22	C_M	0.029	Low
23	C_{CO2}	0.059	Moderate

6.7 Summary of the Sensitivity Analysis

Table 6-10 is a summary of the most sensitive parameters ordered from most to least sensitive. All of the flood types produced relatively similar results.

The most critical parameters for each flood type are the price of oil, change in oil saturation, and total pore volumes because each of these variables have direct impact on the total earnings of a project. The price of oil scales the profits for a project, while the change in oil saturation and total pore volumes impact the total volume of oil that could be recovered for profit.

The next most influential parameters for all flood types are the well spacing and Koval factor between the oil bank and initial bank, K_1. Both of these parameters have the largest impact on the rate of recovery. Earlier recovery of the oil leads to a better profit margin. The parameters K_f, specific shock velocity of the oil bank, injection rate act in a similar manner, but to a lesser extent.

Of the design parameters, the slug size and concentration of the injected chemicals are influential. For the surfactant-polymer and alkali-surfactant-polymer floods it is the expense generated by larger volumes of injected chemicals that is influential, while for CO_2 floods it the technical concept that the WAG ratio influences the recovery history.

The economic expenses in general are not very sensitive parameters. All flood types are equally dependent on T_V, C_I, C_M, and T_R. Even though each flood showed some sensitivity to T_R, it can be ignored as a parameter with influential uncertainty because the royalty rate should be well known going into a project. The only expense that has a considerable impact on the profitability of a project is the total cost of the surfactant for SP floods because the cost and volume of the required chemical is very

expensive. This expense is controlled by chemical slug size, the concentration of surfactant, and the cost of surfactant. These parameters are also moderately sensitive for ASP flood analyses because of the small volume of surfactant used.

Table 6-10 Summary of Results for the Sensitivity Analysis of All Flood Types

Variable	S_i				Rating	Comments
	SP	ASP	CO_2	Average		
P_O	0.131	0.153	0.193	0.159	High	
ΔS_o	0.123	0.144	0.067	0.112	High	
V_p	0.085	0.103	0.133	0.107	High	
V_{Chem}	0.100	0.059		0.079	Moderate	Important for SP floods
WS	0.071	0.083	0.065	0.073	Moderate	
K_1	0.056	0.066	0.077	0.066	Moderate	Increase with importance as expenses decrease
Z_{Sur}	0.095	0.028		0.061	Moderate	Important for SP floods
C_{Sur}	0.095	0.028		0.061	Moderate	Important for SP floods
V_{CO2}			0.060	0.060	Moderate	
C_{CO2}			0.059	0.059	Moderate	
q_i	0.031	0.037	0.045	0.038	Low	
Z_{CO2}			0.035	0.035	Low	
C_l	0.037	0.043	0.019	0.033	Low	
K_f	0.024	0.028	0.039	0.030	Low	
T_R	0.024	0.028	0.035	0.029	Low	

All of the parameters in Table 6-10 can be considered in a decision analysis because the uncertainty of their values could alter the decision. The only parameter that can be neglected from Table 6-10 for a decision analysis is T_R.

CHAPTER 7: SET UP OF DECISION ANALYSIS FRAMEWORK FOR ENHANCED OIL RECOVERY

7.1 Introduction

A decision analysis allows one to evaluate a decision that involves parameters with uncertainty. For example, enhanced oil recovery (EOR) is usually only profitable if the oil price is high. However, oil price is very difficult to predict because it is based on global economies and energy demands (Belhaj and Lay 2008). A decision analysis applies probabilities to various outcomes as a means to account for the uncertainty. From the assessed probabilities and associated outcomes, one can evaluate whether or not implementing an EOR project is preferred. This chapter discusses the construction of a decision analysis framework that is used to evaluate the value of a pilot for an EOR project.

7.2 Background on Decision Making Process

Deterministic decision making compares the outcome of each alternative and determines the most favorable outcome. The chosen alternative either maximizes satisfaction or minimizes dissatisfaction (Ang and Tang 2007). A decision analysis is made up of different parts including events, probabilities, alternatives, and outcomes.

An event is an occurrence that alters the outcome of a decision (Ang and Tang 2007). For example an increase in the value for the price of oil is an event. An event

could also represent a combination of occurrences, such as a high oil price and low final oil saturation. The success of an EOR project hinges on the outcome of numerous events.

Probabilities are used to characterize the likelihood of an occurrence of an event relative to all other possible mutually exclusive events in the same sample space. The value of a probability is between zero and one, and the sum of probabilities for all mutually exclusive events that comprise the space is equal to one. The set of probabilities for a sample space is called a probability distribution. The distributions can also be described by either a probability mass function (PMF) or a probability density function (PDF). PMFs are applied to discrete sample spaces and PDFs are applied to continuous sample spaces. Figure 7-1 contains examples of a PMF and PDF. With PMFs, each listed event is associated with a value and the probability for the value is the PMF. For PDFs, the area under the curve between two values gives the probability for an event between the two bounding values (Ang and Tang 2007).

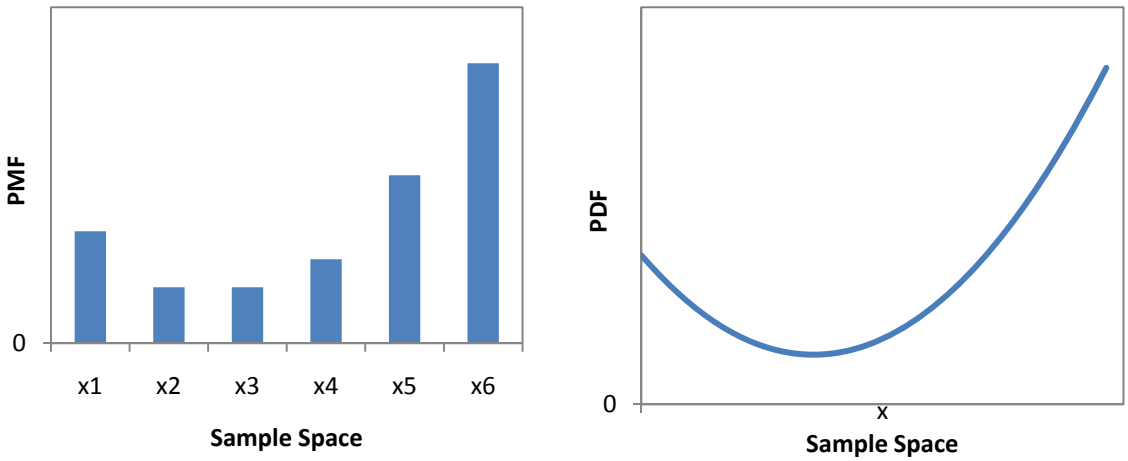

Figure 7-1 Examples of a PMF (Left) and PDF (Right)

A decision is made from a set of alternatives. Examples of alternatives include performing continued water flooding (WF) or implementing EOR. An outcome is a

consequence of a selected alternative and the combination of events that occurs when that alternative is implemented. Generally, consequences are quantified with utility values, where the more preferable the outcome the greater the utility value. For this study, the utility values are expressed as the maximum net present monetary values based on the results from the simplified enhanced oil recovery method (SEORM) and the economic model.

7.2.1 Decision Trees

A decision tree is a graphical representation of the decision making process. It lays out the events, probabilities, alternatives, and outcomes associated with the decision. In a decision tree, square nodes are decision nodes, which denote points where a decision maker makes a decision. Circular nodes are chance nodes, which represent points of uncertainty. Branches that extend from the decision nodes are alternatives and branches that extend from chance nodes are events. The expected utility for an alternative is the summation of the products of the respective probability and utility value for each event (Ang and Tang 1984). Figure 7-2 demonstrates how the different components of a decision tree fit together. Equation 7-1 is an example of the calculation of the expected utility for an alternative.

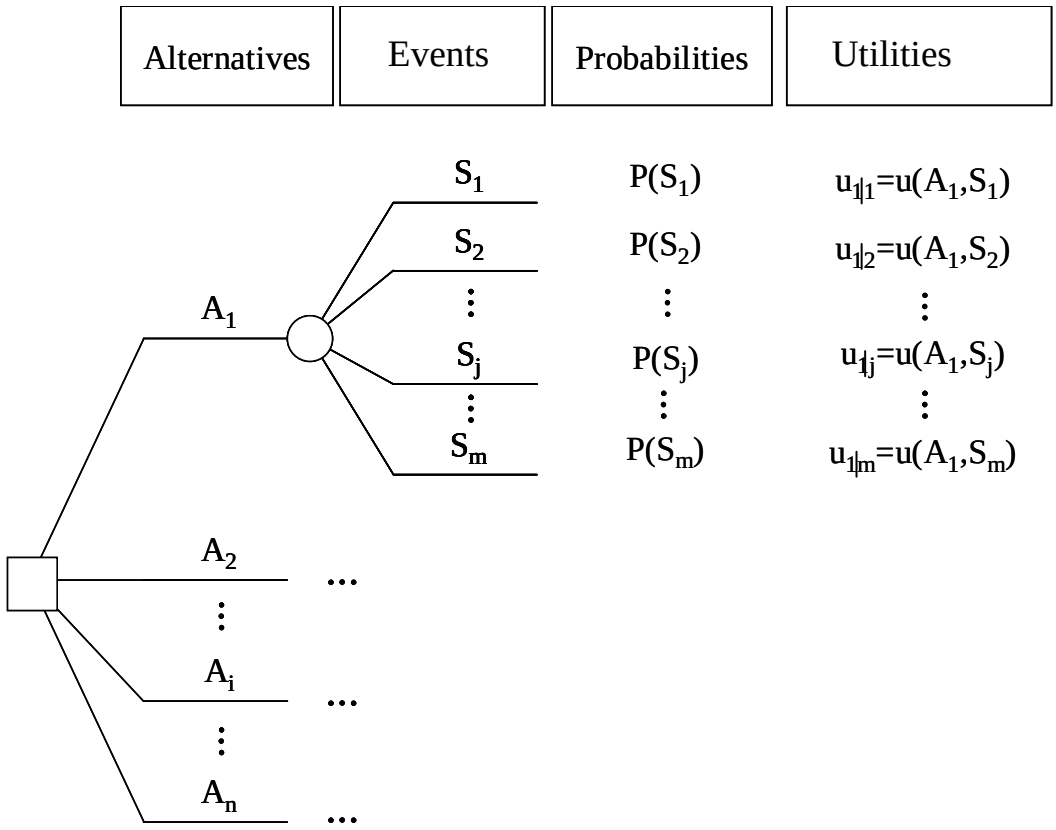

Figure 7-2 Basic Decision Tree (Namhong 2008)

$$E(u_{A_1}) = P(S_1)u_{1|1} + P(S_2)u_{1|2} + \cdots + P(S_j)u_{1|j} + \cdots + P(S_m)u_{1|m}$$

Equation 7-1

7.3 General Discussion of the Enhanced Oil Recovery Decision

This thesis project studies two decisions. One decision, known as the prior decision, is a decision made based on existing information. For the thesis the prior decision is between WF and EOR without any pilot test information. The other decision is the preposterior decision, which is a decision to determine whether or not to obtain additional information. For the thesis, the preposterior is between performing a pilot test and not performing a pilot test.

Pilot tests are small scale-field projects designed to predict the behavior a larger-scale field project. In regards to EOR, they are intended to provide information on the potential of a large-scale project by allowing for better predictions of events.

The events that define the utility values are the input parameters for SEORM and the economic model. As discussed in Chapter 6, there are several sensitive parameters for SEORM and the economic model. For this project, the decision analysis focuses on the three most sensitive parameters for typical EOR projects, the change in oil saturation (ΔS_o), total pore volume (V_P), and price of oil (P_o). From this point forward, the discussion focuses on a decision involving these three parameters. The analysis can be expanded to include more parameters in future work.

7.3.1 The Model for the Water Flood Alternative

The WF alternative is modeled with a simple decline curve analysis. Several options exist for producing a decline curve, including hyperbolic, exponential, and harmonic equations (Walsh and Lake 2003). Each would produce similar results because under most circumstances it is the end of the water flood life is being modeled. Therefore, the simplest approach, an exponential curve, was selected for the model.

For the exponential decline curve analysis it is assumed that the decline rate, D, remains constant. The oil production rate for the water flood, q_{WF}, is

$$q_{WF}(t) = q_{WF|i}e^{-Dt}$$

Equation 7-2

where t is time in terms of years, $q_{WF|i}$ is the initial oil production rate at the start of the water flood in terms of STB/year, and D is in terms of %/year. The cumulative recovery, N_P, can be found by

$$N_P = \frac{(q_{WF|i} - q_{WF})}{D_i}$$

Equation 7-3

where N_P is in units of STB (Walsh and Lake 2003).

It is assumed that the curve begins with a 100% oil cut at the start of the water flood and that it declines to an oil cut that exists at the time that the EOR decision is to be made. Also, it is assumed that the total production rate does not change over time. Based on these assumptions, an assumed age of the water flooding for the field is back calculated. Oil production is assumed to continue until either an economic limit is reached or until the water flood residual oil saturation, S_{or}, is reached. Figure 7-3 is an example decline curve of the oil cut over time for a WF analysis. The economic model discussed in Chapter 5 is also applied to find the utility of the WF alternative.

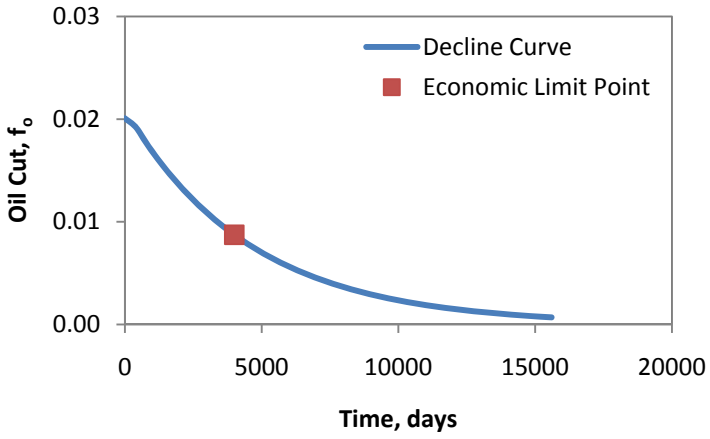

Figure 7-3 Plot of an Example Decline Curve used in the WF Analysis

Figure 7-4 is an example plot of the cumulative discounted cash flow (CDCF) for a water flood, starting at the point when a decision is to be made. The CDCF is based on Equation 4-11. The max net present value (MNPV) is marked to represent the point at which peak profits would be realized. This point coincides with the economic limit point in Figure 7-3. The curve experiences a decline because of two factors. The first is that profits are outweighed by costs, and second is that the cumulative value declines with time. The factors are analogous to those that influence the CDCF for EOR.

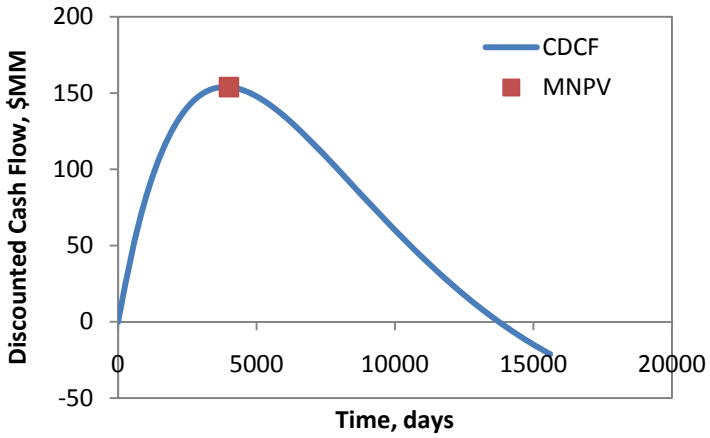

Figure 7-4 Plot of an example CDCF for a WF Analysis

The WF analysis is sensitive to V_P and P_o, but not ΔS_o. V_P alters the assumed volume of the reservoir that is being flooded and therefore impacts the life and ultimate recovery of the WF. The WF utility is also sensitive to P_o because it directly influences the earnings for a project. The parameter ΔS_o has no impact on the WF analysis because ΔS_o is related to the residual oil saturation altered by the EOR process.

7.4 Construction of the Decision Tree Structure for the Analysis

The following is a discussion of the decision tree used in the decision analysis for the thesis project and the meaning of the different components of the tree.

7.4.1 Construction of the Prior Decision Tree

A prior decision is a direct comparison of the utilities of alternatives and it is based on assessed probabilities of events (Min 2008). The analysis is between WF and EOR. If the expected utility for the EOR alternative is greater than the expected utility of the WF alternative, then the analysis suggests that performing an EOR project is the preferable decision. Figure 7-5 is the decision tree of the prior analysis with the three uncertain parameters.

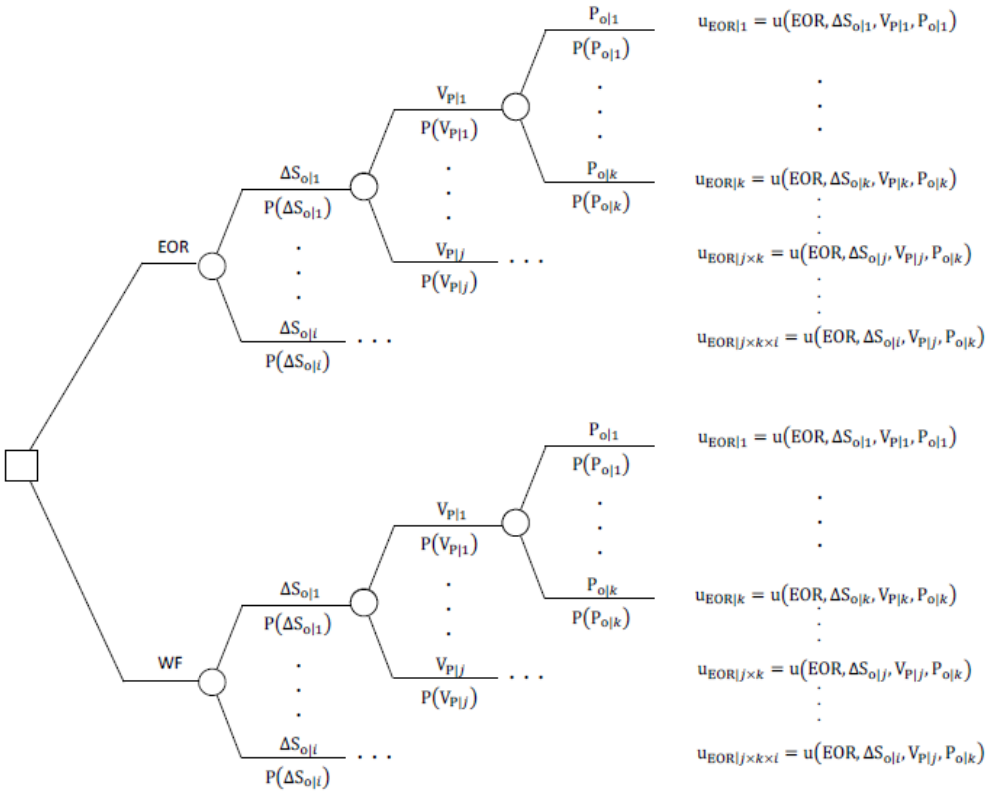

Figure 7-5 The Decision Tree for the Prior Analysis

7.4.2 Construction of the Posterior and Preposterior Decision Trees

A decision that accounts for new information is known as a posterior decision. The posterior decision uses Bayes' theorem for adjusting probabilities.

7.4.2.1 Posterior Decision Tree

A posterior decision provides insight in how new information can alter a decision (Min 2008). For example, one pilot result may suggest that EOR is preferable while another may suggest that WF is preferable. Figure 7-6 is an example of a generic decision tree for a posterior analysis.

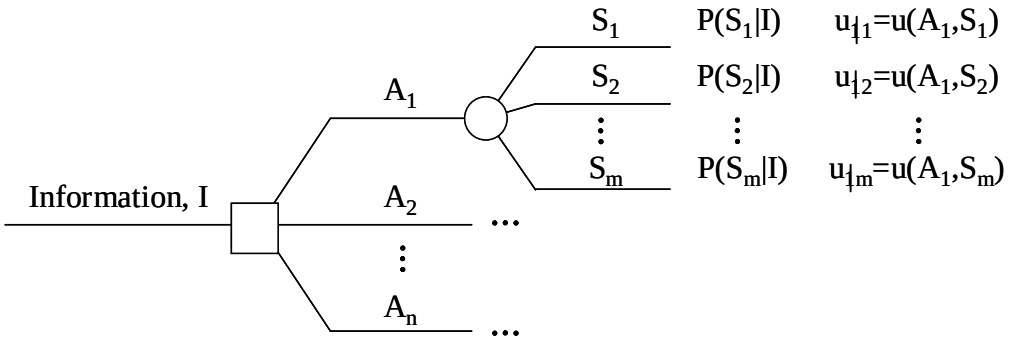

Figure 7-6 Generic Posterior Decision Tree (Min 2008)

New information from a pilot would be included in a posterior tree. Pilots provide some information for some events. For example, a pilot could give some insight on ΔS_o and V_P, but no information about P_o. A decision tree for a posterior analysis must properly include pilot information. Figure 7-7 is part of the decision tree for the posterior analysis of ΔS_o, V_P, and P_o. There are still chance nodes for the ΔS_o and V_P events because pilot information is typically imperfect, and, therefore, there is still some uncertainty about the occurrence of the events.

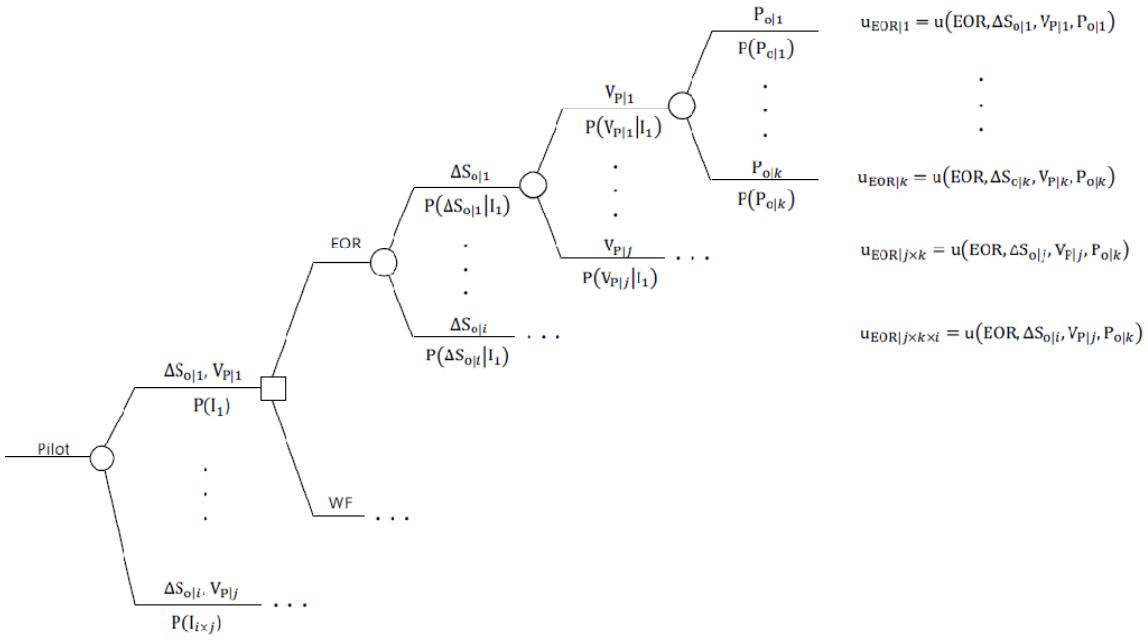

Figure 7-7 Posterior Decision Tree

7.4.2.2 Preposterior Decision

A decision that combines both the prior and posterior decisons is known as a preposterior decision. This type of analysis evaluates "Go - No Go" decisions about performing a pilot. Figure 7-8 is the preposterior decision tree for this problem.

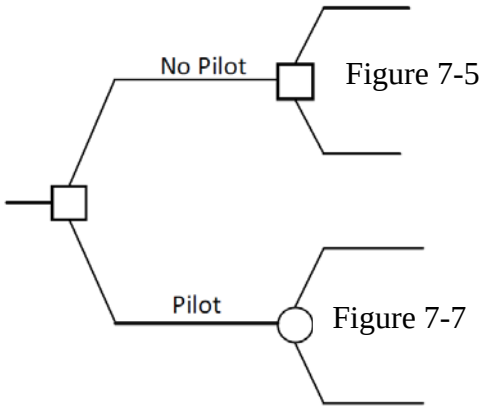

Figure 7-8 Preposterior Decision Tree

A preposterior decision is used to analyze the value of information (VOI) for new information. VOI is defined as the cost of the pilot such that the expected utility of performing the pilot test is equal to that if no additional information is obtained. For this analysis, the VOI of the pilot is the difference in the expected net present values of the "No Pilot" and "Pilot" alternatives. The VOI ranges from zero to an upper bound defined by the value of perfect information (VPI). The VPI means that the pilot perfectly predicts the ΔS_o and V_P values with certainty. If the VOI is equal to zero then the pilot provides no added benefit. If the VOI is a high value, especially if it is much greater than the actual cost of a pilot test, then it suggests that the information from the pilot is expected to be worthwhile (Ang and Tang 1984).

7.5 Non-Informative Prior Probabilities

The prior, posterior, and preposterior decisions are all sensitive to the initial probabilities that are assessed for the events. In this work, the starting point for assessing probabilities assumes complete ignorance, which is the sate of complete uncertainty. Probabilities under the assumption of complete uncertainty are known as non-informative probabilities (Namhong 2008). Available field information is then included to update the starting point distribution to represent the point in time when the EOR and or pilot decision is made.

A common way of handling non-informative probabilities is to follow the principle of insufficient reason (Gilbert et al. 2010). The principle of insufficient reason (PIR) suggests that if there is complete uncertainty about the likelihood of an event then

the event should have a uniform probability distribution. A uniform probability distribution assumes that all events are equally likely. The idea is also known as equiprobability. The challenge in implementing PIR is establishing what sample space to which apply it.

7.5.1 Principle of Insufficient Reason Applied to Input

Typically, PIR is applied to the input of a decision problem, but in a manner that is not rational or consistent. A new concept is to apply PIR to the output of the decision, which provides for rational and consistent results. These two approaches are discussed in the following sections.

7.5.1.1 Rationality

At first glance it may difficult to imagine that PIR applied leads to irrational results; however, it can produce unintended user bias when creating a probability distribution. The user may not apply a bias to likeliness of a particular event, but he or she may show preference to a choice. To better illustrate this issue an example is presented. This example and all subsequent examples assume a surfactant-polymer (SP) flood.

Assume the decision analysis for choosing between EOR and WF is based solely on the possible events for P_o. Four possible values for P_o are assumed; \$60/STB, \$80/STB, \$100/STB, \$120/STB. The decision tree for the analysis is shown in Figure 7-9. Figure 7-10 is a plot of the preferential probabilities of EOR and WF.

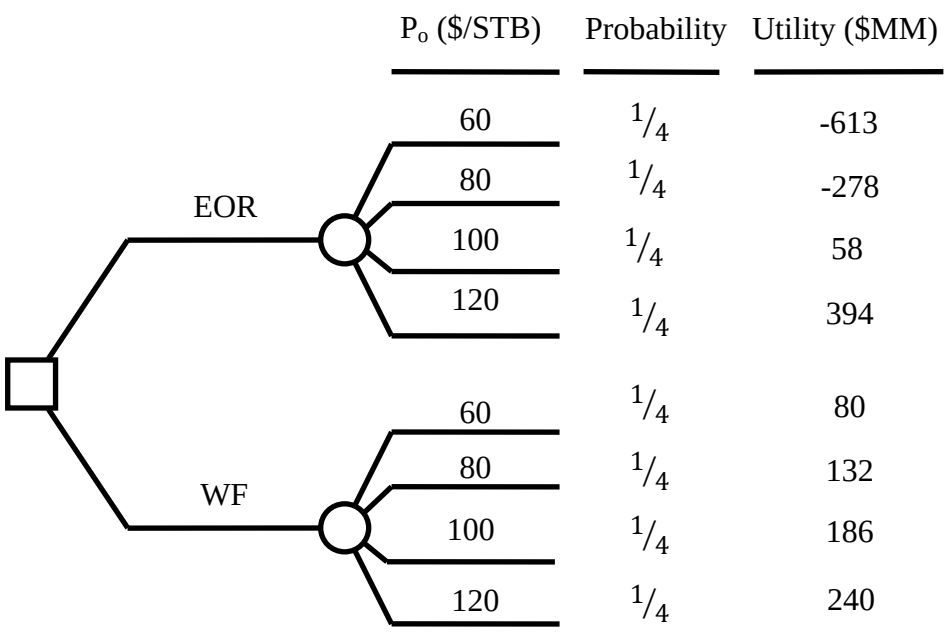

Figure 7-9 Decision Tree for Simple Example Demonstrating Bias in the Principle of Insufficient Reason

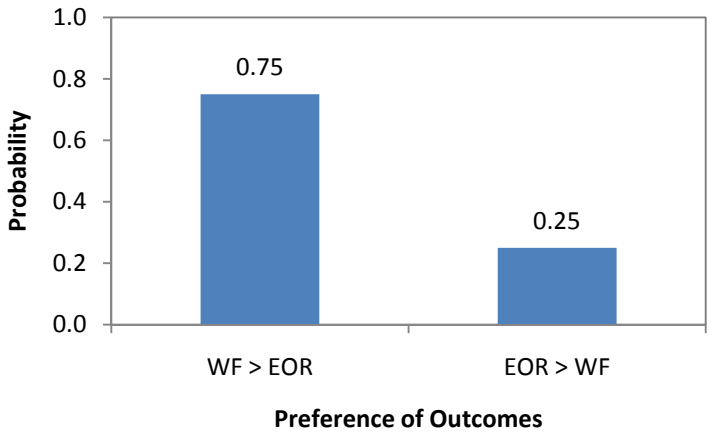

Figure 7-10 Preferential Outcome Plot for the Simple Example Demonstrating Bias

From the analysis the WF alternative is selected for three quarters of the events and EOR is selected for only a quarter of the events. By assigning equal probabilities to each possible P_o, the decision maker makes the WF alternative more likely to be preferred. Therefore, following PIR unintentionally creates bias in the decision because

the decision maker neglects the uncertainty in the decision output when creating a probability distribution for the events.

7.5.1.2 Consistency

Another drawback to applying PIR to the input is that it can create inconsistent probability distributions that vary based on how the events are designated. The following an example illustrates this issue.

For SP floods, two other important parameters are the surfactant slug size, V_{Sur}, and the concentration of surfactant in the slug, Z_{Sur}. These two parameters are about equally influential parameters according to the sensitivity analysis because they both directly influence the amount of injected surfactant, which will be referred to as m_{Sur}. Equation 7-4 is the relationship of m_{Sur} to V_{Sur} and Z_{Sur}.

$$m_{Sur} = V_{Sur} Z_{Sur} V_P \left(351\ {}^{lbm}/_{STB}\right)$$

Equation 7-4

where V_P is the total pore volumes of the reservoir in units of STB. The units for V_{Sur} are in fraction of V_P, Z_{Sur} are in percent of the concentration, and m_{Sur} are in lbm.

There are two ways to apply PIR to account for the economic influence that the injected surfactant has on an SP flood. One approach would be for a decision maker to assume equal probability values for m_{Sur} and the other would be to assume equal probability values for both V_{Sur} and Z_{Sur}. If the decision maker assumes that V_{Sur} is either 0.2 V_P or 0.3 V_P and Z_{Sur} is either 2% conc. or 3% conc., then there would be three possible m_{Sur} values, 1.4V_P lbm/STB, 2.1V_P lbm/STB, and 3.2V_P lbm/STB.

Figure 7-11 is a summary of the different probability distributions based on the possible assumptions. Different probability distributions result depending on how PIR is applied. These types of inconsistencies could lead to significantly different utility values for each alternative and ultimately alter the decision.

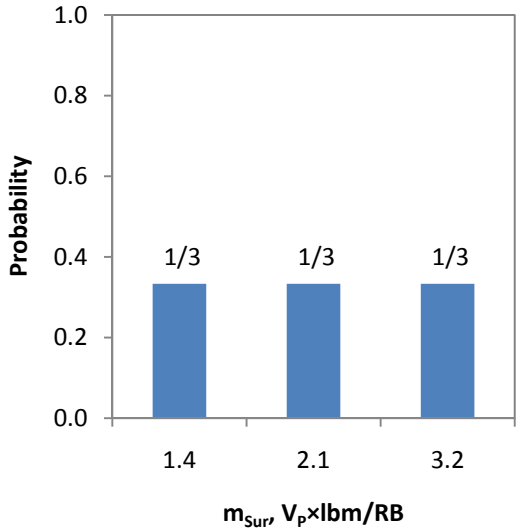

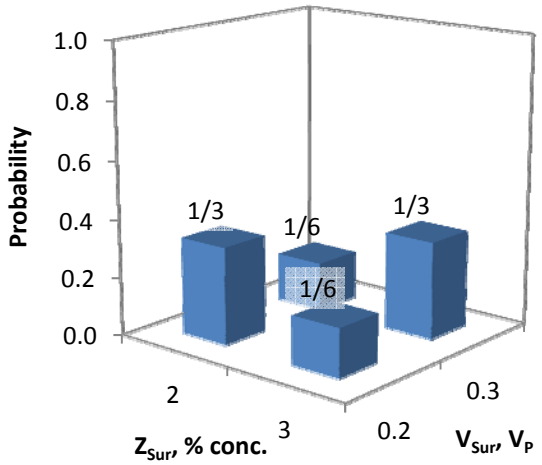

(a) Probability Distribution based on a Uniform Distribution for m_{Sur}

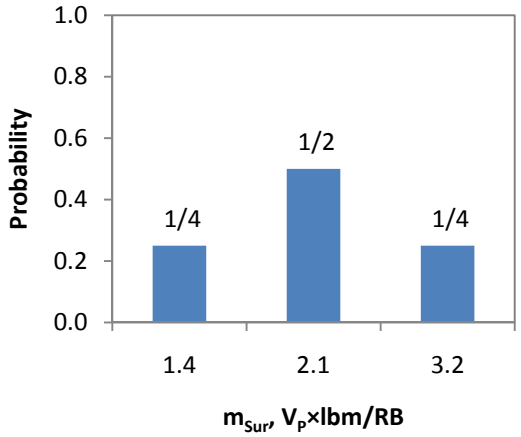

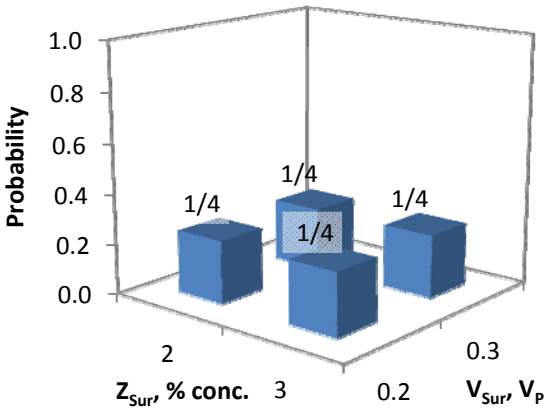

(b) Probability Distribution based on Uniform Distributions for V_{Sur} and Z_{Sur}

Figure 7-11 Demonstration of Inconsistent Probability Distributions Created by Selectively Applying PIR to Input Parameters

A thorough analysis takes into account all possible events so that every possible preference outcome can be realized. For many decision analyses, a continuous number of events are required to represent all events. Analytical solutions are necessary to accurately handle a continuous number of events. Creating analytical solutions can be difficult unless simple equations are used to describe the utility outcomes for each alternative. Therefore, for complicated decision analyses, a decision maker must rely on numerically-based results. A continuous state can be mimicked by studying as many distinct events as possible. Furthermore, for many problems the ranges of values for events would be between negative and positive infinity unless there are boundaries.

An issue with PIR is that it is sensitive to the selected range for an event and the selected number of events studied within that range. An example of this problem can be observed when considering the parameter V_P. If one truly follows the assumptions of complete uncertainty then one has to recognize that V_P can range between zero and infinity. It is not possible to study a V_P equal to infinity, therefore the example looks at a case that ranges between zero and one billion RB. If a decision maker divides the range between into four intervals and another divides it into six intervals, and both apply PIR then they would get different probabilities for each alternative. Table 7-1 is a summary of the results the two analyses and Figure 7-12 is plot of the probability distributions for the outcomes for each analysis.

Table 7-1 Comparison of Two Analyses that Subdivide a Range of V_P Differently

	V_P Event, MMRB	Utilities, $MM		Selection
		EOR	WF	
Four Events	125	-243	132	WF
	375	-45	136	WF
	625	164	137	EOR
	875	363	142	EOR
Six Events	83	-272	124	WF
	250	-148	133	WF
	417	-11	136	WF
	583	129	139	WF
	750	266	142	EOR
	917	395	141	EOR

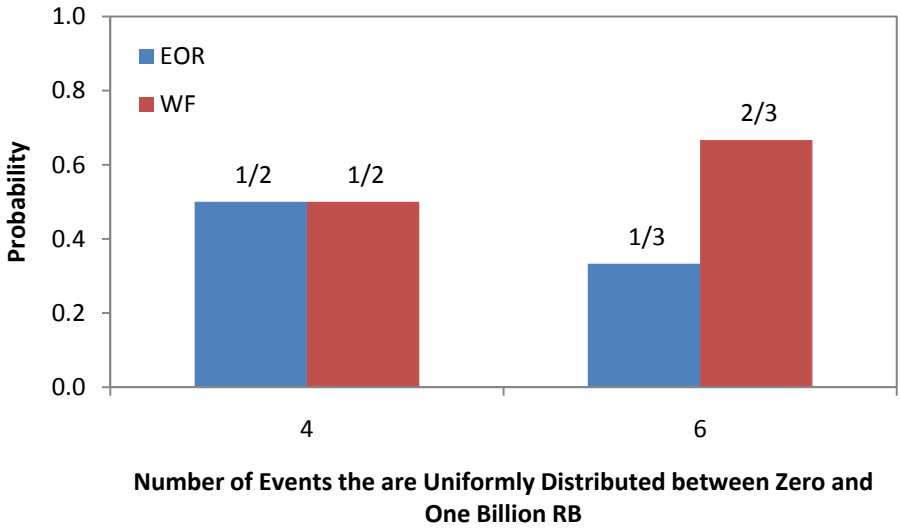

Figure 7-12 Comparison of the Decision Outcomes for Two Analyses that Divide a Range of V_P Differently

By comparing the two analyses it can be seen that the final decision can be altered by simply changing the number of events selected for study within a range of values. Therefore the probability distribution for a continuous number of events could be significantly different from a discrete set of events. This paradox implies a user could

create unwanted bias by predetermining a range of values for each event and by selecting how many events are studied within the range.

Furthermore, applying PIR to the input does not allow a user to truly account for an infinitely wide range. Referring back to the previous example, at about 600 MMRB the decision switches from WF to EOR. This means for any V_P value greater than 600 MMRB, EOR is the preferable choice. If the sample range is set between zero and infinity, then the probability that the WF would be selected goes to zero because it is defined by a limited range and the EOR selection has no limits. Using PIR for a range of input values with an infinite number of events and no limits could create a decision where one alternative approaches a probability of 100%.

7.5.2 The Decision-Based Method

The bias, inconsistency, and instability created by applying PIR to the input can lead to non-informative prior probabilities that may vary from user to user. Non-informative priors should be consistent between decision makers, otherwise similar analyses would produce varying results and potentially cause confusion. Therefore, a robust approach is necessary for establishing the prior distributions. The decision-based method (DBM) attempts to resolve these issues (Min 2008, Gilbert et al. 2010).

7.5.2.1 Theory of the Decision-Based Method

DBM is based on the principle that decision making under complete ignorance should be unbiased and the randomness is with the decision maker's choice and not the input. Therefore, the method applies PIR to the possible preference outcomes, rather than

directly to the possible input values. This approach allows for the probability distribution of the preference outcomes to be uniform, regardless of the number of events, as long as new preference outcomes are not created (Gilbert et al. 2010). For example, in the decision between EOR and WF there are three possible preference outcomes:

$$\text{EOR} > \text{WF}$$
$$\text{WF} > \text{EOR}$$
$$\text{EOR} \sim \text{WF}$$

Equation 7-5

where ">" denotes the preference of one alternative to another and "~" denotes indifference between alternatives. Each of these outcomes have an equal probability, $^1/_3$, assigned to them as long as the events allow them to occur. Figure 7-13 shows three different cases that help illustrate the basis of DBM.

Alt.	Events		
	E_1	E_2	E_3
EOR	500	150	-100
WF	200	150	100

(a) Case 1

Alt.	Events		
	E_1	E_2	E_3
EOR	500	250	-100
WF	200	175	100

(b) Case 2

Alt.	Events			
	E_1	E_2	E_3	E_4
EOR	500	150	-100	-200
WF	200	150	100	75

(c) Case 3

Figure 7-13 Cases that Illustrate the Basis for DBM

In Case 1, there are three events and all three possible preferential outcomes shown in Equation 7-5 occur. Case 2 is a slight alteration of Case 1 where only two preferential outcomes occur, EOR > WF and WF > EOR. These two cases would have a different probability distribution for the preferential outcomes because the number of possible preferential outcomes is different. Case 3 is similar to Case 1 with an added event. Both Cases 1 and 3 have the same probability distribution despite having different

events. A comparison of these three cases, as shown in Figure 7-14, illustrates that it is the outcome of the events and not the number of events that controls the distribution for the preferential outcomes.

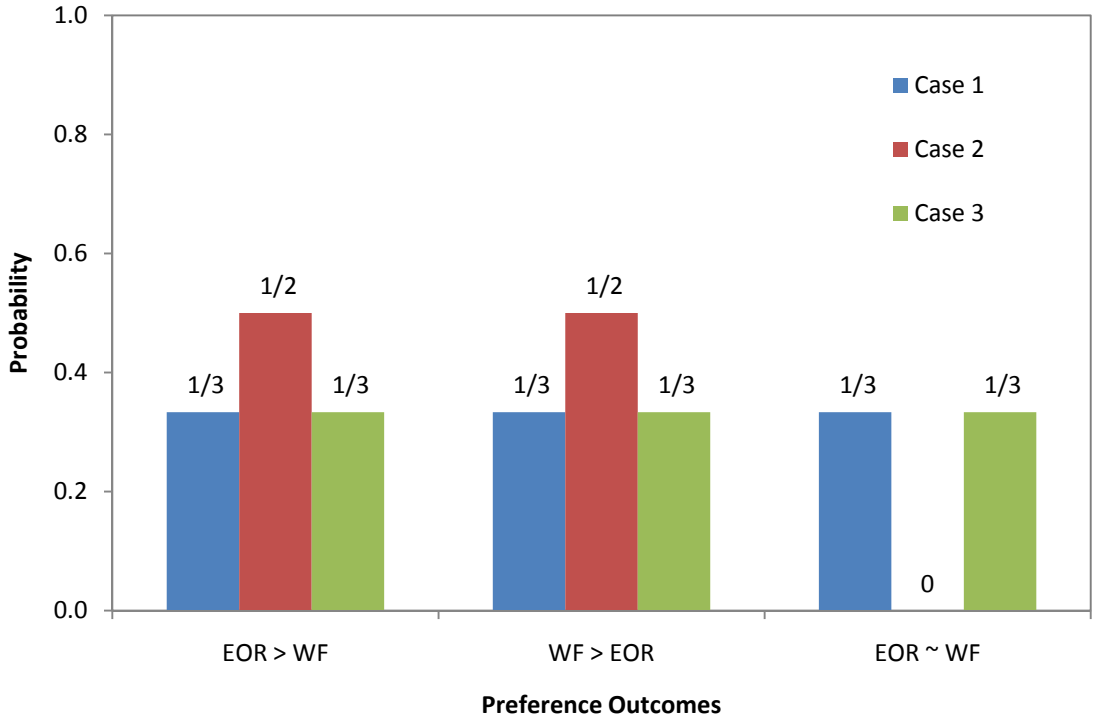

Figure 7-14 Comparison of the Probability Distributions for the Preferential Outcomes for the Example in Figure 7-13

DBM can be extended to include *n* alternatives as shown in Equation 7-6, if all of the preference outcomes are assumed to be mutually exclusive and collectively exhaustive.

$$
\begin{aligned}
&A_1 > \\
&A_2 > \\
&\vdots \\
&A_n > \\
&A_1 \sim A_2 > \\
&A_1 \sim A_3 > \\
&\vdots \\
&A_{n-1} \sim A_n > \\
&\vdots \\
&A_1 \sim A_2 \sim A_3 > \\
&\vdots \\
&A_1 \sim A_2 \sim \ldots \sim A_n >
\end{aligned}
$$

Equation 7-6

The maximum number of preference outcomes, Ω, is

$$\Omega = 2^n - 1$$

Equation 7-7

If all of the preference outcomes exist for a given decision, then the probability of each outcome according to PIR are equally likely and be defined as the inverse of Ω (Min 2008).

Once the probabilities of the preference outcomes are established, the probabilities of the events are determined. Once again PIR is invoked. Each preference outcome is divided by similar sets of outcome utilities. The sets of outcome utilities are treated as equally likely. Each utility set is also subdivided and the events that make up them up are treated as equally likely (Gilbert et al. 2010). Table 7-2 is an example that demonstrates how the probabilities for events are assigned based on the outcomes.

Table 7-2 Decision Matrix Demonstrating How Event Probabilities are Determined

		Events							
		E_1	E_2	E_3	E_4	E_5	E_6	E_7	E_8
Alt. Uti.	EOR	600	350	125	-100	-100	-100	-100	-400
	WF	175	150	125	100	100	100	75	50
Prob.	Event	1/6	1/6	1/3	1/27	1/27	1/27	1/9	1/9
	Uti. Set	1/6	1/6	1/3	1/9			1/9	1/9
	Pref. Out.	1/3		1/3	1/3				
Pref. Out.		EOR > WF		EOR ~ WF	EOR < WF				

For the example in Table 7-2, there are three preference outcomes: EOR > WF, EOR ~ WF, and EOR < WF. The variable E stands for an event, and U stands for a utility set. For the EOR > WF preference, there are two sets of utility values (EOR, WF): U_1= (600, 175) and U_2 = (300, 150). Based on the concept of randomness, each of these outcomes would be equally likely. The probability U_1 would equal U_2 and the sum of the probabilities would equal the probability of EOR > WF. U_1 consists of only E_1 and therefore the probability of E_1 is equal to the probability of U_1. The same applies for E_2 and U_2. These relationships are summarized by Equation 7-8 through Equation 7-11.

$$P(EOR < WF) = P(U_1) + P(U_2) = {}^1/_3$$

Equation 7-8

$$P(U_1) = P(U_2) = {}^1/_6$$

Equation 7-9

$$P(E_1) = P(U_1) = {}^1/_6$$

Equation 7-10

$$P(E_2) = P(U_2) = {}^1/_6$$

Equation 7-11

where P stands for the probability of an outcome or event. For the EOR ~ WF preference outcome, there is only one utility set, U_3 = (125, 125), and there is only one event, E_3, that can lead to the preference outcome. Therefore

$$P(EOR \sim WF) = P(U_3) = P(E_3) = {}^1/_3$$

Equation 7-12

Finally, for the preference outcome EOR < WF, there are three distinct utility sets and there are five events that lead to the preference outcome. The utility sets are U_4 = (-100, 100), U_5 = (-100, 75), and U_6 = (-400, 50). Utilities U_5 and U_6 are associated with one event and U_4 is associated with three. Following the same process as before

$$P(EOR < WF) = P(U_4) + P(U_5) + P(U_6) = {}^1/_3$$

Equation 7-13

$$P(U_4) = P(U_5) = P(U_6) = {}^1/_9$$

Equation 7-14

$$P(U_4) = P(E_4) + P(E_5) + P(E_6) = {}^1/_9$$

Equation 7-15

$$P(E_4) = P(E_5) = P(E_6) = {}^1/_{27}$$

Equation 7-16

$$P(U_7) = P(E_7) = {}^1/_9$$

Equation 7-17

$$P(U_8) = P(E_8) = {}^1/_9$$

Equation 7-18

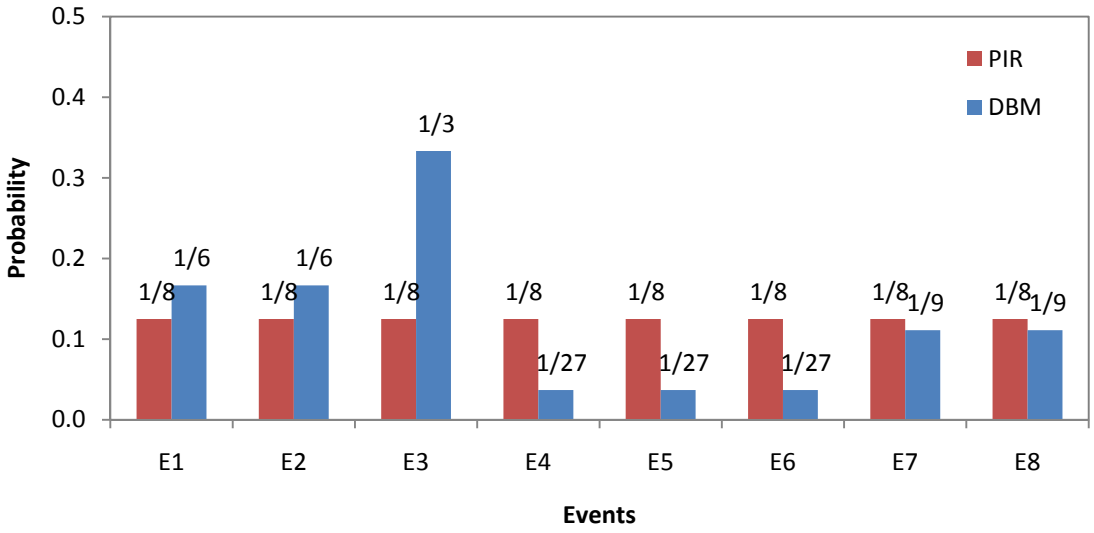

Figure 7-15 Comparison of the Probability Distribution for DBM and PIR for the Example in Table 7-2

By following DBM and keeping strictly to the probabilities that are established, the expected utilities for each alternative change when compared to applying PIR to the inputs. Table 7-3 is a summary of the comparison of expected values for the two methods. DBM suggests that the decision maker would select the EOR alternative while the PIR applied to the input prefers the WF alternative.

Table 7-3 Comparison of DBM and PIR in Terms of the Expected Utilities

Assumption	Alternative Utilities	
	EOR	WF
Decision Based Method	133	121
Principle of Insufficient Reason	34	109

Another observation from the previous example is that DBM suggests a higher likelihood for E_3 than any other event. The method's emphasis of E_3 implies that the event is significant to the decision. DBM increased the weight for E_3 to maintain a uniform probability distribution for the preference outcomes. By giving more weight to

certain events, it allows a decision maker to pick out the events of interest and determine how the final decision can be affected by them.

The probability distributions created with DBM also suggest that the parameters are not necessarily independent. Therefore, the probability for a given set of events that involves multiple parameters is not simply the product of the marginal probabilities of each parameter.

7.5.2.2 Example of DBM Dealing with Rationality and Consistency

DBM was introduced because of issues with unintended bias and inconsistency which are inherent with PIR. The example shown in Figure 7-11 will be used to demonstrate how DBM overcomes these issues. Table 7-4 and Table 7-5 summarize the probabilities determined with DBM assuming that the events are either defined by V_{Sur} and Z_{Sur} or m_{Sur}. Recall that m_{Sur} is related to V_{Sur} and Z_{Sur} as shown in Equation 7-4. Figure 7-16 is a collection of the probability distributions common for the results from both Table 7-4 and Table 7-5.

Regardless of which set of events are used to approach the decision, the probabilities are the same and thus consistency is maintained. Furthermore, the probability distribution of the preference outcomes is uniform and therefore there is no bias between the choices.

Table 7-4 Decision Matrix Assuming the Events are Defined by V_{Sur} and Z_{Sur}

		Events							
		E_1		E_2		E_3		E_4	
		V_{Sur}	Z_{Sur}	V_{Sur}	Z_{Sur}	V_{Sur}	Z_{Sur}	V_{Sur}	Z_{Sur}
		0.2	**2**	**0.2**	**3**	**0.3**	**2**	**0.3**	**3**
Alt. Uti.	EOR	273		59		59		-260	
	WF	127		127		127		127	
Prob.	Event	1/2		1/8		1/8		1/4	
	Uti. Set	1/2		1/4				1/4	
	Pref. Out.	1/2		1/2					
Pref. Out.		EOR > WF		EOR < WF					

Table 7-5 Decision Matrix Assuming the Events are Defined by m_{Sur}

		Events		
		E_1	E_2	E_3
		m_{Sur}	m_{Sur}	m_{Sur}
		1.4	**2.1**	**3.2**
Alt. Uti.	EOR	273	59	-260
	WF	127	127	127
Prob.	Event	1/2	1/4	1/4
	Uti. Set	1/2	1/4	1/4
	Pref. Out.	1/2	1/2	
Pref. Out.		EOR > WF	EOR < WF	

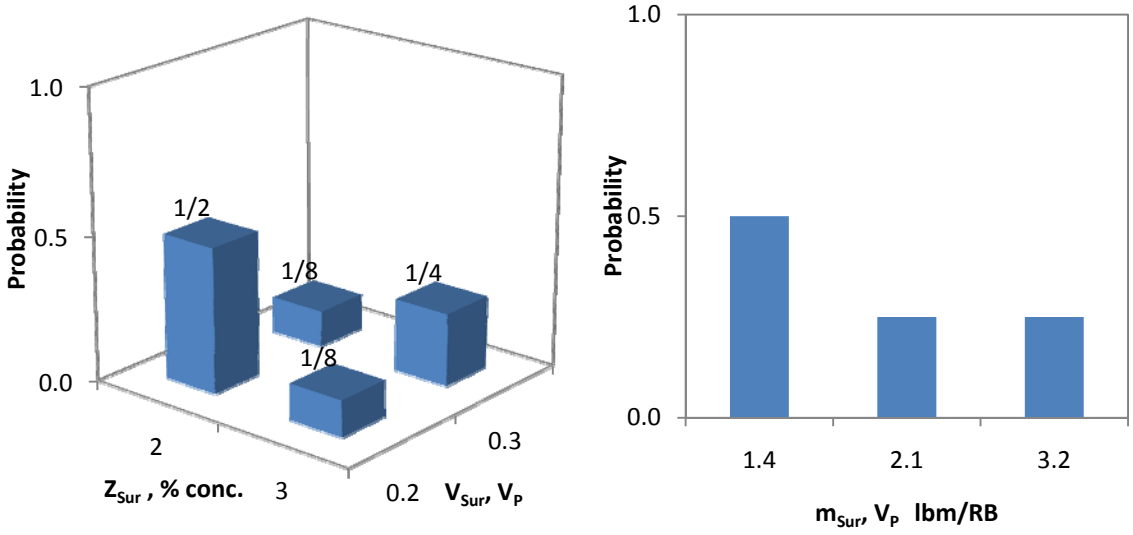

(a) Probability Distribution of Z_{Sur} and V_{Sur}

(b) Probability Distribution of m_{Sur}

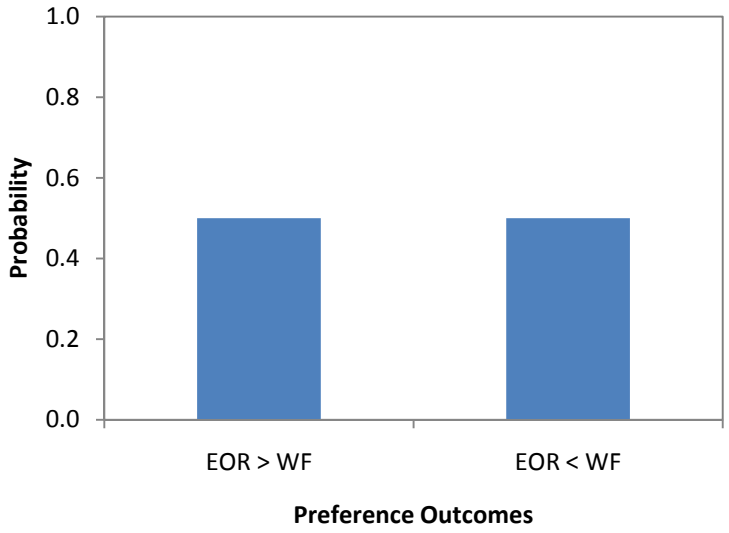

(c) Probability Distribution of the Prefence Outcomes

Figure 7-16 Plots of Probability Distributions

To demonstrate that DBM can handle a continuous distribution and an infinite range, the issue discussed in section 7.5.1.2 will be used as an example. V_P is taken from zero to a hundred billion RB. Dividing a hundred billion RB into even intervals would create very large intervals unless a very large number of intervals were used. It is already

shown that DBM can handle inconsistency and therefore considering V_P or the $\log(V_P)$ would produce the same result for the same range of values studied. By using $\log(V_P)$, the low values of V_P as well as the high ones can be considered. Figure 7-17 is a plot that compares how the number of intervals influence the PDF for $\log(V_P)$ when using DBM. As the number of intervals increases, the resolution of the PDF improves and approaches a constant shape.

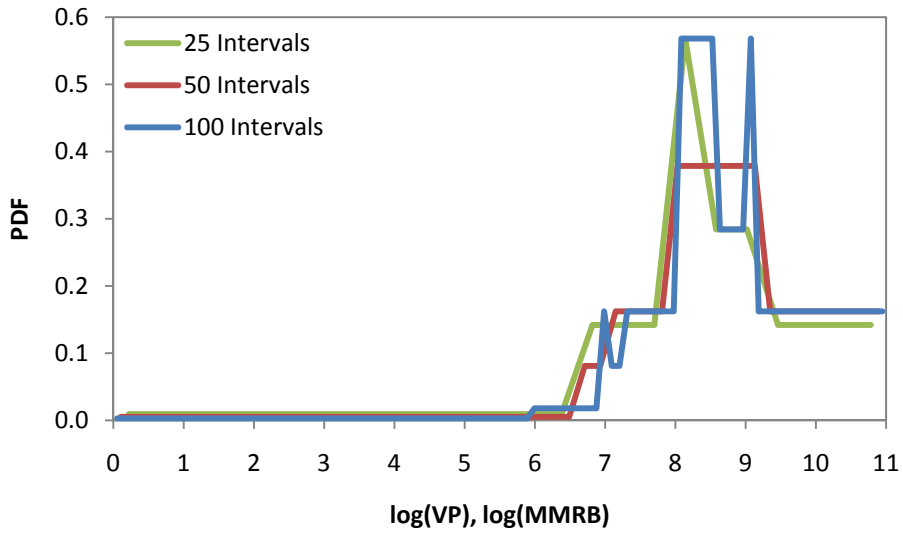

Figure 7-17 Comparison of the PDF for DBM with Varying Intervals

Table 7-6 is a comparison of the expected utilities for the different intervals. As the number of intervals approaches infinity, the expected utility approaches a constant.

Table 7-6 Comparison of the Expected Utilities for DBM with Varying Intervals

Number of Intervals	Decision Based Method	
	EOR	WF
25	-2829	164
50	-3193	179
100	-3161	187

Even though the decision looks at a very wide range of possible events, the probability of one alternative being selected over another remains the same because the preference outcomes are assumed to be equally likely. Therefore, DBM is able to handle a range with limits at positive and negative infinity.

Therefore, the problems that exist when PIR is applied to inputs have been addressed with DBM.

7.5.3 Applying Monte Carlo Simulation to the Decision Based Method

When working with DBM and input parameters that come from a continuous space, the calculus of analytically deriving the continuous joint probability distribution can be cumbersome. This problem is especially true when dealing with multiple input parameters at a time. Applying Monte Carlo simulation provides a method to work around the problem.

Monte Carlo simulation is a technique that uses random sampling to create a representative sample of events (Ang and Tang 2007). For example, if a probability distribution exists, then Monte Carlo simulation can be applied to randomly select a set of events based on the probability distribution for simulations. Monte Carlo is used at different stages of the decision analysis process because many simulations must be performed.

To apply Monte Carlo simulation to DBM, the following procedure is followed. The first step is to assume that all of the inputs have a uniform probability distribution. A random number generator is then used to select values for each parameter. Each selected

set represents one sample. For each sample set of input parameters, outcomes for EOR and WF are calculated. Several samples are collected and the number of preferential outcomes, the number of outcome sets, and the number of events for each outcome set is then calculated. In order to be able to keep track of all of the samples, especially when working with multiple input parameters, each parameter range is divided into a certain number of intervals. Again, the larger the number of intervals is per parameter, the better the resolution for the probability distribution. The sample sets are organized into the intervals and then probabilities are determined with DBM for only sampled intervals. For example, if $\log(V_P)$ is divided into 100 intervals and a Monte Carlo simulation is run with 50 samples, then only the intervals represented by the selected samples are used in DBM. This example is also illustrated in Figure 7-18. The Monte Carlo simulation is able to capture the generic shape of the distribution and produce relatively similar expected values as shown in Table 7-7.

Table 7-7 Comparison of the Expected Values for a Monte Carlo Simulation and a Complete Analysis

	Decision Based Method	
	EOR ($MM)	WF ($MM)
100 Intervals	-3161	187
100 Intervals (50 MC Simulations)	-3325	185

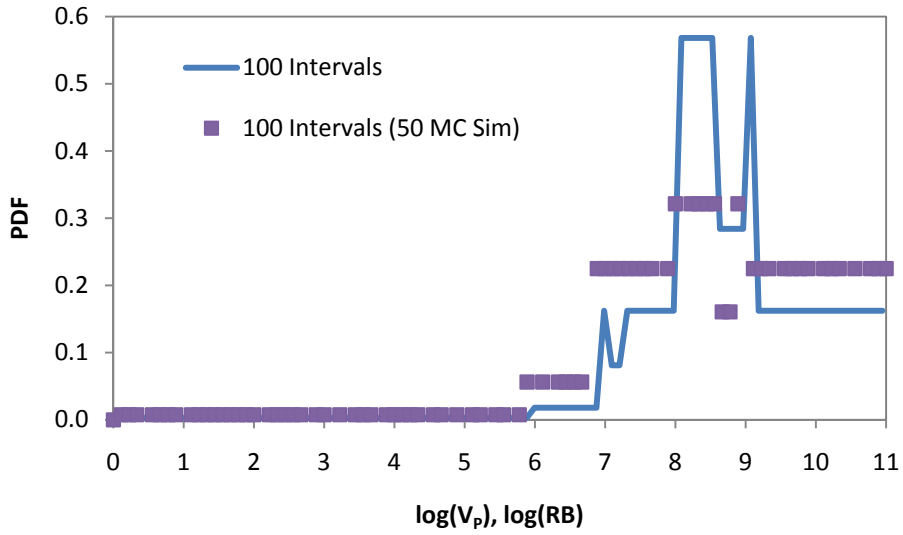

Figure 7-18 Comparison of the Monte Carlo Simulation and a Complete Analysis

7.6 Bayes' Theorem

As new information is obtained, such as production history up to the EOR decision, an EOR pilot test, research, etc., the probability distributions for events may be updated. Bayes' theorem is applied to update existing information. For this study, the probability distributions are updated at several points. One point is to update the non-informative probability distribution based on any experience or knowledge about the field or EOR process. Another point is to update the probability distributions again based on new information determined from the results from the pilot tests.

7.6.1 Bayes' Theorem Definition

Bayes' theorem is used to relate new information to an existing probability of a sample space, as shown in

$$P(A_i|I_j) = \frac{P(I_j|A_i)P(A_i)}{P(I_j)}$$

Equation 7-19

where $P(A_i|I_j)$ is the updated probability of event A_i given the information I_j, $P(A_i)$ is original probability of event A_i, $P(I_j|A_i)$ is the likelihood function that relates the probability distribution of A and I to each other, and $P(I_j)$ is the probability of the information about event A_i. Based on the total probability theorem, $P(I_j)$ is defined to be

$$P(I_j) = \sum_{1}^{i} P(I_j|A_i)P(A_i)$$

Equation 7-20

The updated probability is also known as the posterior probability and is based on the original probability and the likelihood function (Ang and Tang 2007).

The likelihood function acts like a filter that is used to narrow the original distribution based on the new information. The probability of every possible event in the likelihood function ranges between zero and one. There are two limiting cases for the function, no new information and perfect information. If the likelihood distribution is uniform, then it is suggested that there is no new information that alters the original probability distribution. If the likelihood distribution applies a probability of one to a particular event but zero to all others, then it suggests perfect information, and the updated distribution only has the event occurring.

The limiting cases can offer some good information; however, it is not reasonable to assume either limiting case for a decision analysis because a pilot or any source of

information will provide some input, but not perfect input. For this study, an example likelihood function is used for illustrative purposes.

7.6.2 Bayes' Theorem Example

The following is an example of Bayesian application. A field is being assessed for EOR. There is some understanding about the field's V_P from previous measurements and experience with the field. Figure 7-19 is the initial probability distribution. An EOR pilot is then performed and it appears the original prediction for V_P needs to be adjusted. A likelihood function, Figure 7-20, is then developed and applied to the initial distribution. The adjusted posterior probability is shown in Figure 7-21. The new probability distribution is different from the original distribution and so is the expected outcome. The expected V_P shifts from 350 MMRB for the prior distribution to 267 MMRB for the posterior distribution.

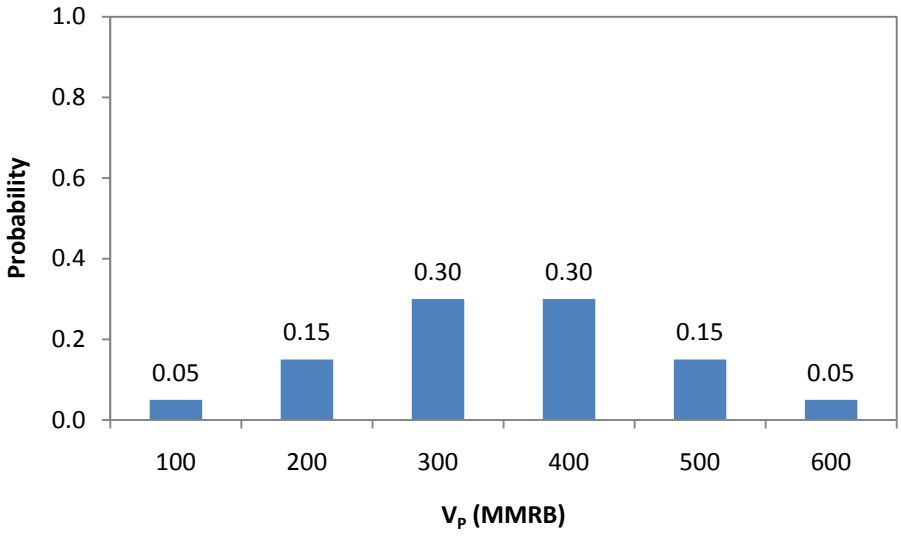

Figure 7-19 Prior Probability Distribution for the Bayes' Theorem Example

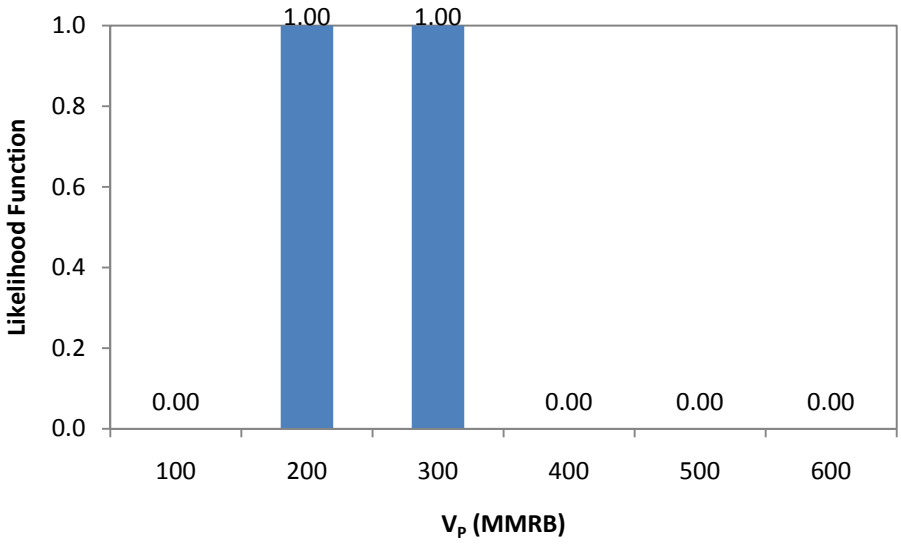

Figure 7-20 Likelihood Function from Testing for the Bayes' Theorem Example

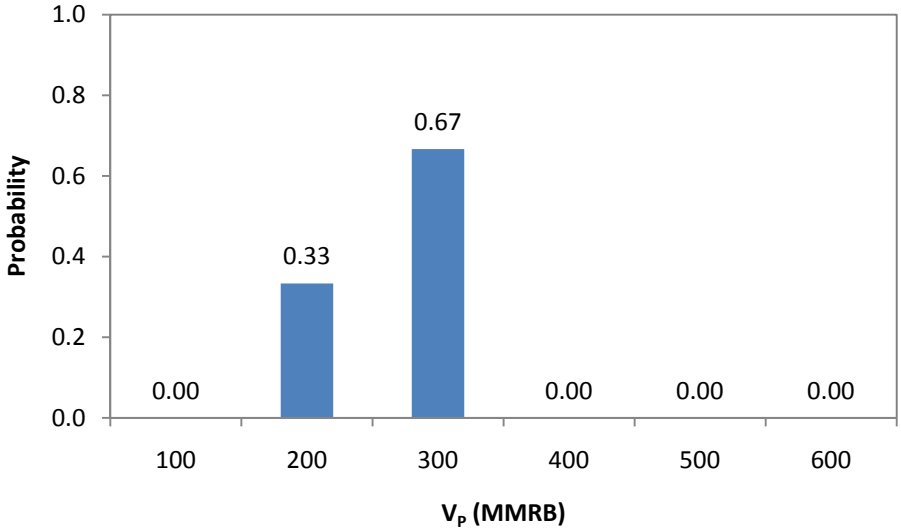

Figure 7-21 Posterior Probability Distribution for the Bayes' Theorem Example

7.7 Summary

The decision analysis for this study involves several decisions including one between enhanced oil recovery and continued water flooding and a "Go" versus "No Go" for a pilot. This study focuses on three parameters, ΔS_o, P_o, and V_P because they are the

most influential parameters based on the sensitivity analysis of the simplified enhanced oil recovery method and the economic model, which are used to determine the value of any outcome. The method and construction of the decision framework discussed in this chapter could allow one to expand the decision analysis to account for more parameters.

An important step in the decision analysis is to establish non-informative prior probabilities so that a starting point can be set for the probability distribution of all of the events. It is pointed out that simply assuming all events for input parameters are equally likely and assuming arbitrary ranges of values for the events is not an adequate approach because it creates inconsistent probability distribution between users. Therefore the decision based method is recommended and applied to the decision analysis.

The probabilities established with the decision based method can then be adjusted or updated with either existing or new information through the use of Bayes' theorem. From the decision based method and Bayes' theorem, every probability distribution for every part of the decision can be determined. Chapter 8 discusses the entire decision making process step by step with a simple example.

CHAPTER 8: EXAMPLE OF THE DECISION ANALYSIS

8.1 Introduction

This chapter provides a generic discussion as to how to perform a decision analysis that uses the decision based method (DBM) to create non-informative prior probabilities and adapt those probabilities with Bayes' theorem. The example discussed in this chapter focuses on three parameters, ultimate change in oil saturation (ΔS_o), price of oil (P_o), and total pore volumes (V_P). The selected ranges for each parameter are divided into five intervals. Five intervals are used to keep the example simple and easy for demonstrative purposes.

8.2 Performing the Decision Analysis for the Thesis Decision

A generic procedure is presented for performing the analysis through two similar examples. Example A works with a non-informative probability distribution for the prior decision, and assumes a perfect pilot. Example B works through with an informed probability distribution for the prior decision and assumes perfect information from the pilot. The three input parameters, ΔS_o, V_P, and P_o, define the events for the decision. The alternatives are enhanced oil recovery (EOR) and continued water flooding (WF). The following outlines the steps taken and any additional assumptions made throughout the analysis.

8.3 Outline for Example A

8.3.1 Step 1: Setup the Decision Tree

The first step is to setup the decision tree for the decision analysis. Construction of the decision tree is discussed in Chapter 7. A decision tree establishes the frame work of the decision. The decision for this study is a preposterior decision that looks at a "Go," "No Go" decision for a performing a pilot. A preposterior decision also involves a prior decision and posterior decisions.

8.3.2 Step 2: Establish the Conditions for the Enhanced Oil Recovery Decision

The next step is to determine the generic conditions for the EOR decision, which entails assuming values to use for the parameters in the simplified enhanced oil recovery method (SEORM), the economic model, and the water flood model, as shown in Table 8-1. Only parameters that are involved in the analysis do not have to be assumed. Table 8-2 is a summary of the values used in the example.

Table 8-1 Summary of Inputs for the Decision Analysis

Model	Flood	Par.	Description	Units
SEORM	All	ΔS_o	Change in oil saturation over life of EOR flood	--
		K_1	Koval factor for mobilized oil & initial banks	--
		K_f	Scale factor for determining K_2	--
		v_{oB}	Specific shock velocity of mobilized oil bank	--
		q_i	Injection rate (constant for entire flood)	STB/day
		q_p	Production rate (constant for entire flood)	STB/day
		V_p	Total pore volume of reservoir	RB
WF	WF	D	Decline Rate	%/yr.
	WF	q_{WFli}	Oil production at start of water flood	STB/yr.
Flood Design	All	WS	Well spacing	Acres
	SP and ASP	V_{Poly}	Polymer slug size	V_p
		Z_{Poly}	Polymer concentration	ppm
		V_{Chem}	Surfactant or alkali slug size (SP,ASP)	V_p
		Z_{Sur}	Surfactant concentration (SP, ASP)	% conc.
	ASP	Z_{Alk}	Alkali agent concentration	% conc.
	CO_2	V_{CO2}	CO_2 slug size	V_p
		Z_{CO2}	CO_2 WAG ratio	--
Economic Model	All	P_O	Price of Oil	$/STB
		R_E	Escalation Factor	%/yr.
		T_S	Severance Tax	%
		T_V	Ad-Valorem Tax	%
		T_R	Royalty Rate	%
		i	Inflation Rate	%/yr.
		d	Discount Rate	%/yr.
		C_q	Fluid Injection Cost	$/STB
		C_T	Oil Treatment Cost	$/STB
		C_{WD}	Water Disposal Cost	$/STB
		C_I	Start Up Cost	$/well
		C_M	Maintenance Cost	$/day/well
	SP & ASP	C_P	Polymer Price	$/lbm
		C_{Sur}	Surfactant Price	$/lbm
	ASP	C_A	Alkali Price	$/lbm
		C_{Soft}	Softening Cost	$/STB
	CO_2	C_{CO2}	CO_2 Price	$/MCF
	All	Cap	Economic Cap to the Profits Realized	--

Table 8-2 Base Case Values for the Example of the Decision Making Process

Oil Saturations	
S_{oI}	0.70
S_{oR}	0.35
S_{or}	0.30
S_{oF}	0.25
ΔS_o	0.10

Flood Behavior	
K_1	2.00
K_2	3.50
v_{oB}	2.50
v_C	1.33
K_f	0.86
f_{oI}	0.02

Fractional Flow Inputs		
k^o_{rw}	0.20	
k^o_{ro}	0.80	
n	2.0	
m	2.0	
μ_o	5.0	cp
μ_w	1.0	cp
μ_c (Inj. Chem.)	50.0	cp

Reservoir Properties		
V_p	200	MMRB
OOIP	140	MMSTB
B_o	1.00	RB/STB
Original WS	40	acres
New WS	20	acres
Field Size	5000	acres
D (for WF)	10	%/year

Economic Inputs		
Surfactant		
Z_{Sur}	2.5	% conc.
C_{Sur}	2.00	$/lbm
Polymer		
Z_{Poly}	1000	ppm
C_{Poly}	1.00	$/lbm
Other Economic Inputs		
P_o	80	$/STB
R_E	3	%/yr
T_S	5	%
T_V	0	%
T_R	12.5	%
d	10	%/yr
i	3	%/yr
C_q	0.1	$/STB
C_T	0.1	$/STB
C_{WD}	0.15	$/STB
C_I	1.25	$MM/well
C_M	250	$/well/day
Cap for EOR: 200%		
Cap for WF: 300%		

Flood Injection Inputs				
Fluid	SP	Polymer	Water Flood	
q_I	250	250	250	MSTB/day
q_P	280	280	280	MSTB/day
Slug Size	0.20	0.75	1.60	Frac. V_p

8.3.3 Step 3: Establish the Non-Informative Prior Probability Distributions for the Analyzed Parameters

The non-informative prior probability distribution is determined with the decision based method (DBM). DBM is recommended to avoid bias or other issues with the initial probability distributions for ΔS_o, V_P, and P_o.

8.3.3.1 Applying the Decision-Based Method to the Study's Decision

DBM is used to determine the initial probability distributions for the events of the parameters analyzed, because of its robustness when compared to the principle of insufficient reason. The following is a discussion of how DBM is applied and the sensitivity of the probability distributions.

8.3.3.2 Sensitivity Analysis of the Decision Based Method

The following explores the sensitivity of DBM by studying the parameters individually, in pairs, and all together, and the sensitivity involved with alterations to the ranges and the number of events considered. The base case values for the decision analysis are in Table 8-2. The parameters highlighted are altered in the sensitivity analysis.

There are only two preference outcomes EOR > WF and EOR < WF. The preference outcome of EOR ~ WF is not possible because it represents an infinitesimally small portion of the full outcome space since it only occurs at the intersection of the EOR utility with the WF utility. The intersection of the values of EOR and WF utilities represent a line for a surface. The overlap represents an infinitesimally small area on the surface. Therefore, there is a zero chance of the indifference outcome occurring. The sensitivity analysis looks to see how different step intervals and the parameters influence the prior probability distributions.

8.3.3.3 Sensitivity of Parameter Intervals

The complete sample space for the parameters cannot be captured by a discrete number of events. Instead each parameter is assumed to be defined by a continuous set of events. The ranges of the sets must include all possible values between the bounding conditions or to infinity in the positive and negative directions. For the analysis, large values are used to represent infinity. Table 8-3 is a summary of the ranges used in the analysis. The parameters ΔS_o and V_P are not taken down to zero because errors occur with SEORM.

Table 8-3 Summary of the Starting Ranges Used in the Sensitivity Analysis of DBM

Parameter	Physical Ranges		Analysis Range		Units
	Lower Bound	Upper Bound	Lower Bound	Upper Bound	
ΔS_o	0	0.35	0.01	0.35	--
P_o	0	∞	1	1.0E+8	$/STB
V_P	0	∞	1	1.0E+11	RB

The log of parameter V_P and P_o are divided into intervals because a very large range of values is being considered. For each parameter, 25, 50, and 100 step intervals are studied. Figure 8-1 and Figure 8-2 are plots that demonstrate the sensitivity for ΔS_o and P_o, respectively. It appears that at 100 intervals there is not significant change and that 50 intervals is a good approximation of a continuous set. V_P is not represented because for all possible events where V_P is the only changing input parameter, the utility value of EOR is never greater than the utility value of the WF, as shown in Figure 8-3.

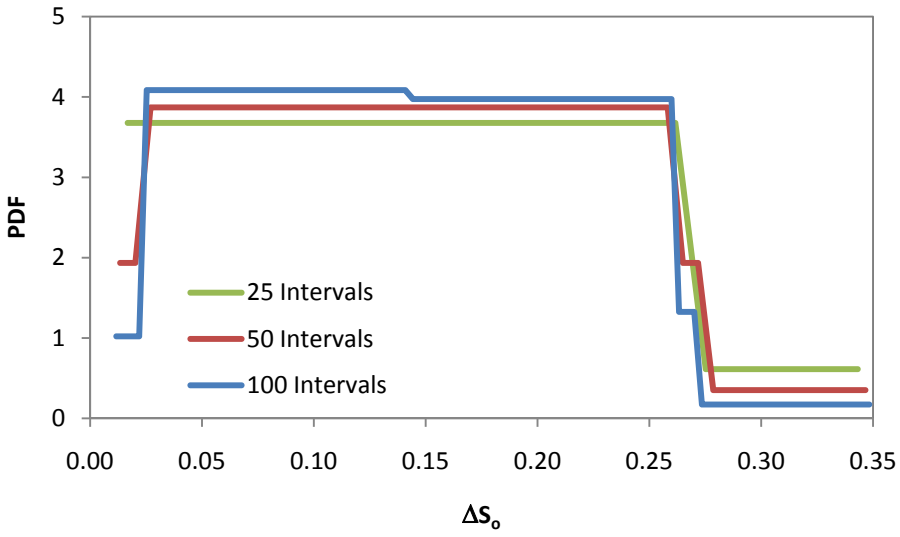

Figure 8-1 Plot Comparing the Interval Steps for the Parameter ΔS_o

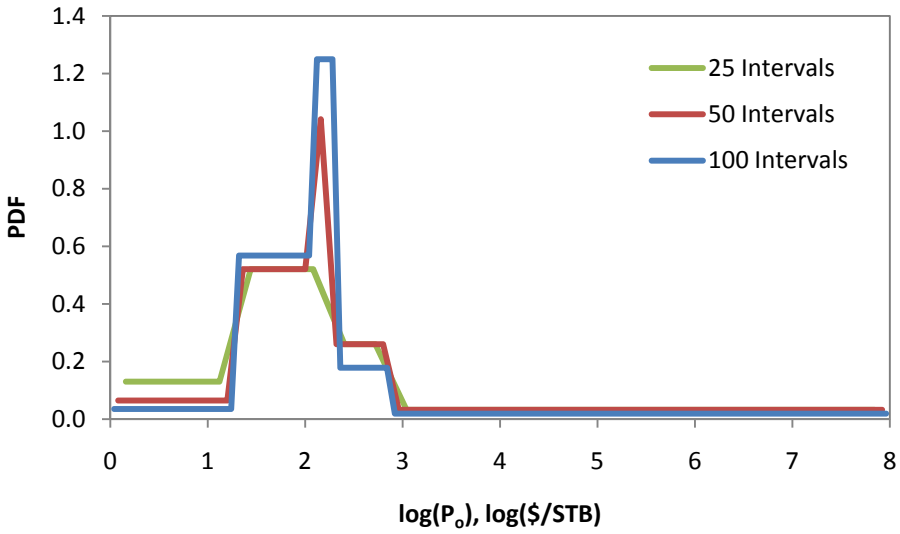

Figure 8-2 Plot Comparing the Interval Steps for the Parameter P_o

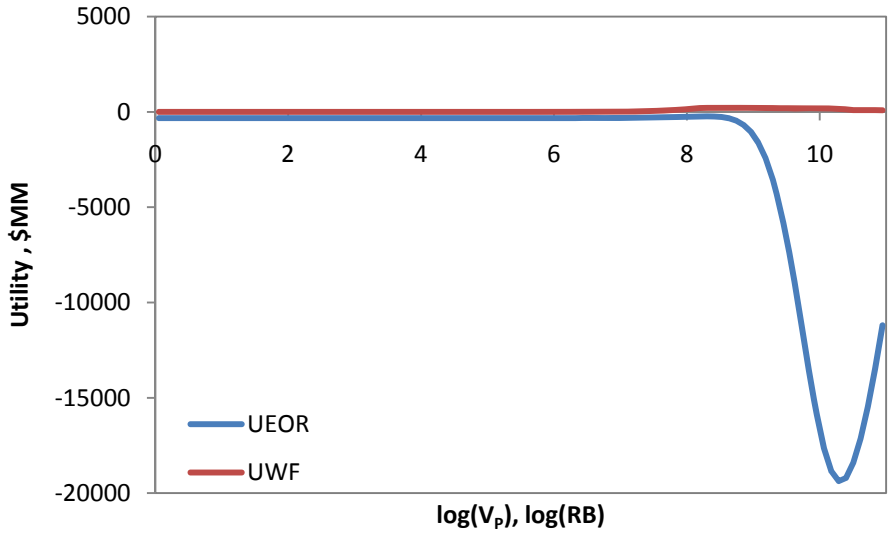

Figure 8-3 Plot Comparing the Utility Values for Parameter V_P

Even though no value of V_P alters the decision when it is considered solely, it does become a factor when more parameters are included in the analysis.

8.3.3.4 Sensitivity of Parameter Combinations

The simplest analyses are those involving a single parameter defining the events. For example, Figure 8-4 is a plot of both utility values for EOR and WF and the PDF for the parameter ΔS_o. The PDF value changes at four distinct points. The first change occurs at a very low ΔS_o, at about 0.02. Between 0.01 and 0.02, the utility set is constant because neither the utility for EOR or WF changes. Any ΔS_o event within that range leads to the same outcome; therefore, the entire range is treated as equally likely and as a unique utility set. The EOR utility begins to rise because at ΔS_o = 0.02 there is some profit after the surfactant slug is completely injected.

The second change is when the decision switches from WF to EOR at about 0.14 ΔS_o. Between 0.02 and 0.14, all of the utility sets are considered unique, but have the same preferential outcome and, therefore, all are treated as equally likely.

The third change occurs at about ΔS_o = 0.26, when the utility sets become constant again. Between 0.14 and 0.26 all of the utility sets have the same preferential outcome and each set is unique and treated as equally likely.

There is one last change in the PDF at ΔS_o = 0.27 because there are a few similar utility sets between 0.26 and 0.27. After 0.27, all utility sets have a similar utility value and thus each event within the range is treated as equally likely.

The PDF suggests that events between 0.02 and 0.26 are the most significant to the decision because there are many unique utility outcomes and, therefore, more uncertainty in the preference than at the ends of the distribution.

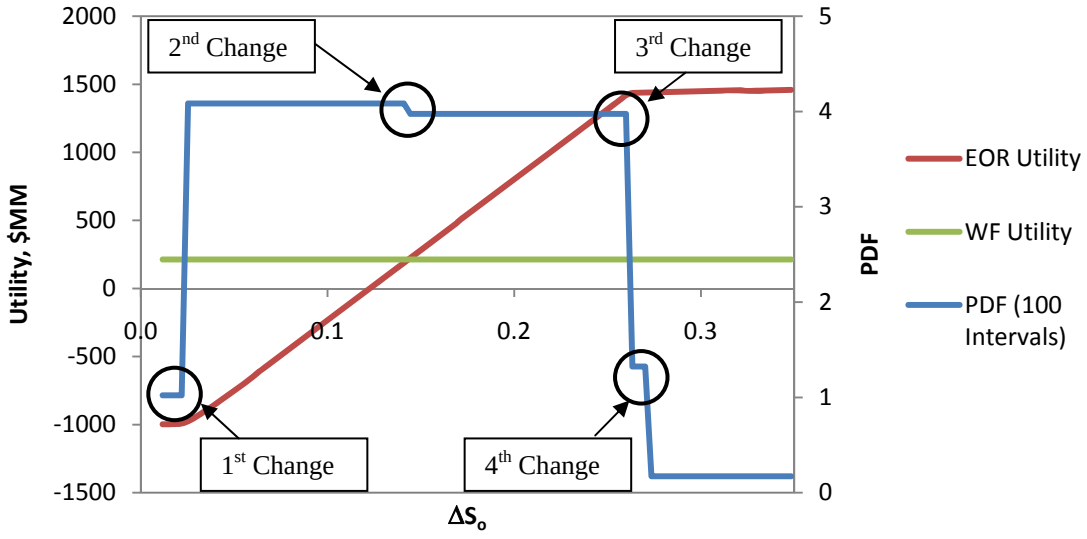

Figure 8-4 Plot of the PDF against the Utilities for ΔS_o

The marginal probability distribution of ΔS_o changes significantly when new parameters are introduced, as shown in Figure 8-5. A marginal PDF is a PDF of single parameter with the probabilities of all other parameters consolidated. It appears that when either parameters P_o or V_P are introduced, the marginal PDF changes considerably from the case where ΔS_o is the only parameter. The addition of parameter P_o creates a relatively linear PDF that gently slopes downward, thus no particular range of ΔS_o values is more important to the decision. Before when ΔS_o is the sole parameter, any event less than 0.24 leads to WF being the preferred alternative. With P_o considered, even low ΔS_o values have the potential for conditions where EOR is preferred as long as P_o is very high. At low ΔS_o there is a wider range of P_o where the decision may switch between WF and EOR than at high ΔS_o values because there is a narrower range for P_o where the switch in preference occurs. Therefore, at low ΔS_o values there is more uncertainty than at high ΔS_o values.

If V_P is included, then the distribution changes to where there are a couple of plateaus. At low ΔS_o, less than 0.14, it appears there are not many circumstances where the decision switches from WF to EOR and thus there is not much uncertainty as to what the preference is. At larger ΔS_o values the range of V_P values where the switch occurs is larger and, therefore, there is more uncertainty. It appears that at about $\Delta S_o = 0.26$, the range of V_P values where the preference switches begin to shrink, leading to more certainty in the preferred outcome and lower PDFs. At large ΔS_o values, it is more likely that EOR is preferred than WF, thus there is less uncertainty.

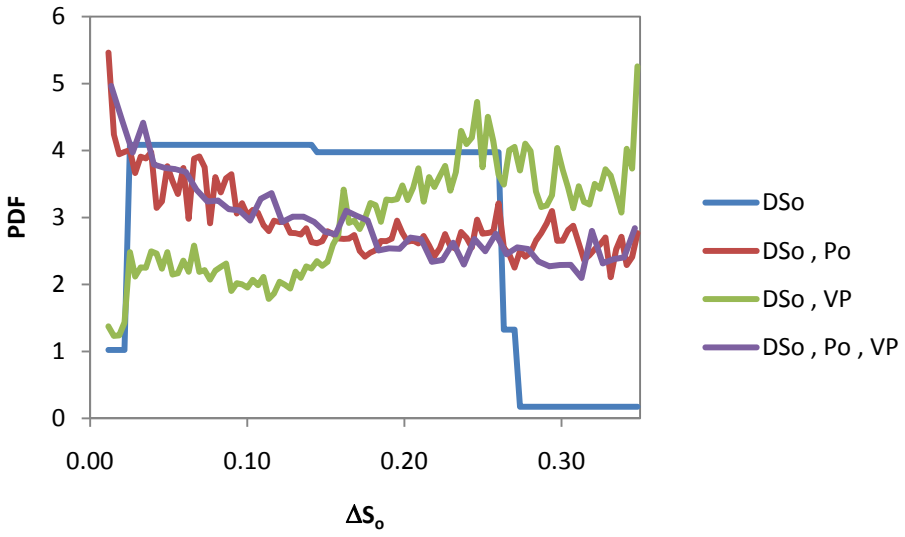

Figure 8-5 Plot Comparing the Marginal PDFs of ΔS_o with Various Parameter Combinations

It is also important to study the joint PDFs of the variable combinations. Figure 8-6 and Figure 8-7 are plots of the PDF for ΔS_o and $\log(V_P)$, and ΔS_o and $\log(P_o)$, respectively. Both of these plots suggest that there are combinations of parameters that are not significant to the decision. For the ΔS_o and $\log(V_P)$ combination, any event with a $\log(V_P)$ value that is less than six is of very low significance because regardless of what ΔS_o is, the decision will be for WF since the V_P is too small to allow EOR to ever be more profitable than WF. Furthermore, at such low V_P the outcome sets are very similar. The most significant events are between seven and nine for $\log(V_P)$ and 0.15 and 0.35 for ΔS_o because this is where the largest mix of switches in preference occurs as well as the fewest similar outcome sets. For any ΔS_o value less than 0.15 there does not appear to be scenarios where EOR is selected. When ΔS_o is greater than 0.15 there is considerable variability in the preferred alternative because for any ΔS_o value there is a limited range of V_P where EOR is preferred. If the field is too small, then there is not

enough oil to recover for the project to be profitable. If the field is too large, then it takes too long to recover oil profitably in terms of the time value of money.

For the ΔS_o and $\log(P_o)$ combination, any event that has a $\log(P_o)$ greater than four is of minimal importance because every combination events within the range creates a condition where EOR is preferred. Furthermore, the utility sets in this range are similar. The most important events are between $\log(P_o)$ values of zero and three. In this range of $\log(P_o)$ value, all ΔS_o values are significant to the decision, because EOR can be preferred for almost any ΔS_o value as long as P_o is large enough. Therefore, there is considerable uncertainty in what the preference is.

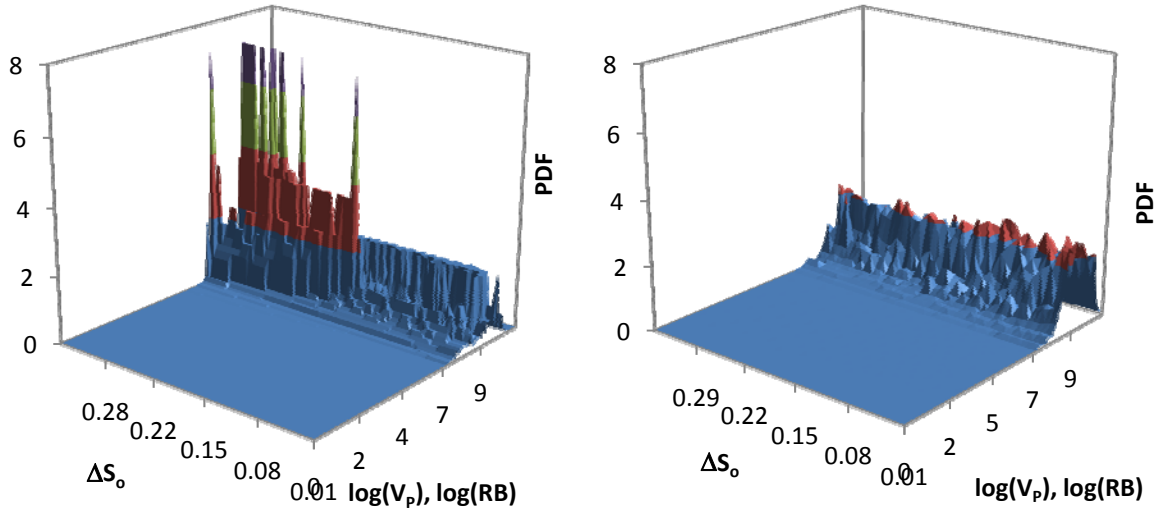

(a) ΔS_o and $\log(V_P)$ Analyzed **(b) ΔS_o, $\log(V_P)$ and P_o Analyzed**

Figure 8-6 Joint PDF Plots of ΔS_o and $\log(V_P)$ Combination for Two (a) and Three (b) Parameter Analyses

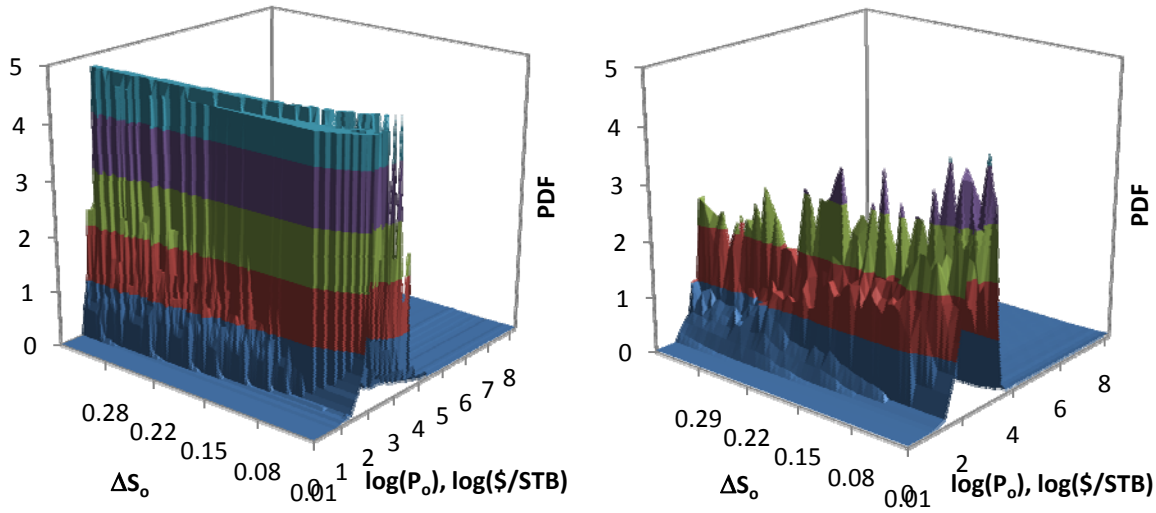

(a) ΔS_o and P_o Analyzed **(b) ΔS_o, log(V_P) and P_o Analyzed**

Figure 8-7 Joint PDF Plots of ΔS_o and P_o Combination for Two (a) and Three (b) Parameter Analyses

It is also important to study how the combination of all three parameters influences the distributions. Referring back to Figure 8-5, it appears that the marginal probability distribution of ΔS_o for all three changing parameters is similar to when only ΔS_o and P_o are changing. The distribution suggests that V_P does not alter the marginal distribution as significantly as P_o. This observation is most likely a result of how only a small range of V_P is important to the decision (between seven and nine log(V_P)) and for any V_P within that range, the joint PDF of ΔS_o and P_o are likely to have similar forms. Therefore, when all joint PDFs of ΔS_o and P_o for all V_P values are consolidated together, as shown in Figure 8-7 (b), there is similar emphasis for certain ranges of events as in Figure 8-7 (a). Both plots appear to have somewhat different shapes, but they both produce similar marginal distributions for ΔS_o because both have emphasis on low ΔS_o values and between log(P_o) values of one and four.

The joint PDFs also change once all three parameters are considered in the analysis. Figure 8-6 and Figure 8-7 show the joint PDFs for analyses with three parameters as well. For the ΔS_o and $\log(V_P)$ joint PDF, the range of interest does not change significantly. However; the emphasis of the distributions are different. The joint PDF of ΔS_o and $\log(V_P)$ with P_o consolidated, Figure 8-6 (b), suggests there is higher uncertainty at lower ΔS_o values. The uncertainty is greater because at various P_o, scenarios where a low ΔS_o can lead to an EOR as the preferred outcome increases. Higher ΔS_o values are less likely to have scenarios where WF is preferred over EOR than lower ΔS_o values will have scenarios where EOR is preferred over WF.

For the ΔS_o and P_o joint PDF there is some change when all three parameters are considered. Overall, both joint PDFs place a similar amount of emphasis in similar ranges of interest. Each V_P interval is likely have a slightly different range of interest for $\log(P_o)$ and ΔS_o. Therefore, the peak values for the joint PDF is reduced because consolidation of all of the V_P intervals creates a slightly more uniform distribution over the $\log(P_o)$ range of interest.

The probability distributions for other parameter combinations can be found in Appendix D.

8.3.3.5 Sensitivity of Parameter Ranges

Altering the ranges of the parameters can also have an impact on the probability distributions. As is seen in Figure 8-6 and Figure 8-7, there are regions of values where the probability approaches zero. Combinations of events that create these conditions are

essentially representing the limits to the parameters' ranges. Any combination of events that exist in the regions of zero probability is meaningless to the decision and is ignored. If these regions are removed and the ranges for the parameters are reduced, they still create probability distributions similar to the distributions based on the complete ranges. However, if the ranges are narrowed too much and important outcomes are removed, then the distributions are changed.

Table 8-4 is a summary that compares the ranges used in the sensitivity analysis. The "complete" ranges are full range of possible values, the "selected" ranges are carefully altered ranges that do not remove important combinations of events, and the "narrowed" ranges are arbitrarily altered.

Table 8-4 Summary of the Ranges used in the Sensitivity Analysis for DBM

Parameter	Complete Range		Selected Range		Narrowed Range	
	Low	High	Low	High	Low	High
ΔS_o	0.01	0.35	0.01	0.35	0.05	0.25
$\log(P_o)$, log($/STB)	0	8	0	4	1	3
$\log(V_P)$, log(RB)	0	11	6	11	7	9

Figure 8-8 is a collection of plots comparing the different ranges for $\log(P_o)$ and $\log(V_P)$. The "complete" range and the "selected" ranges produce very similar results, while the "narrowed" ranges produce a significantly different distribution. The main differences between in the plots from the "complete" and "selected" ranges are a result of improved resolution because of the finer intervals for the "selected" range.

From the sensitivity analyses it appears that as long as enough intervals are used and that wide enough ranges are applied that do not eliminate important outcomes, then a consistent result can be attained.

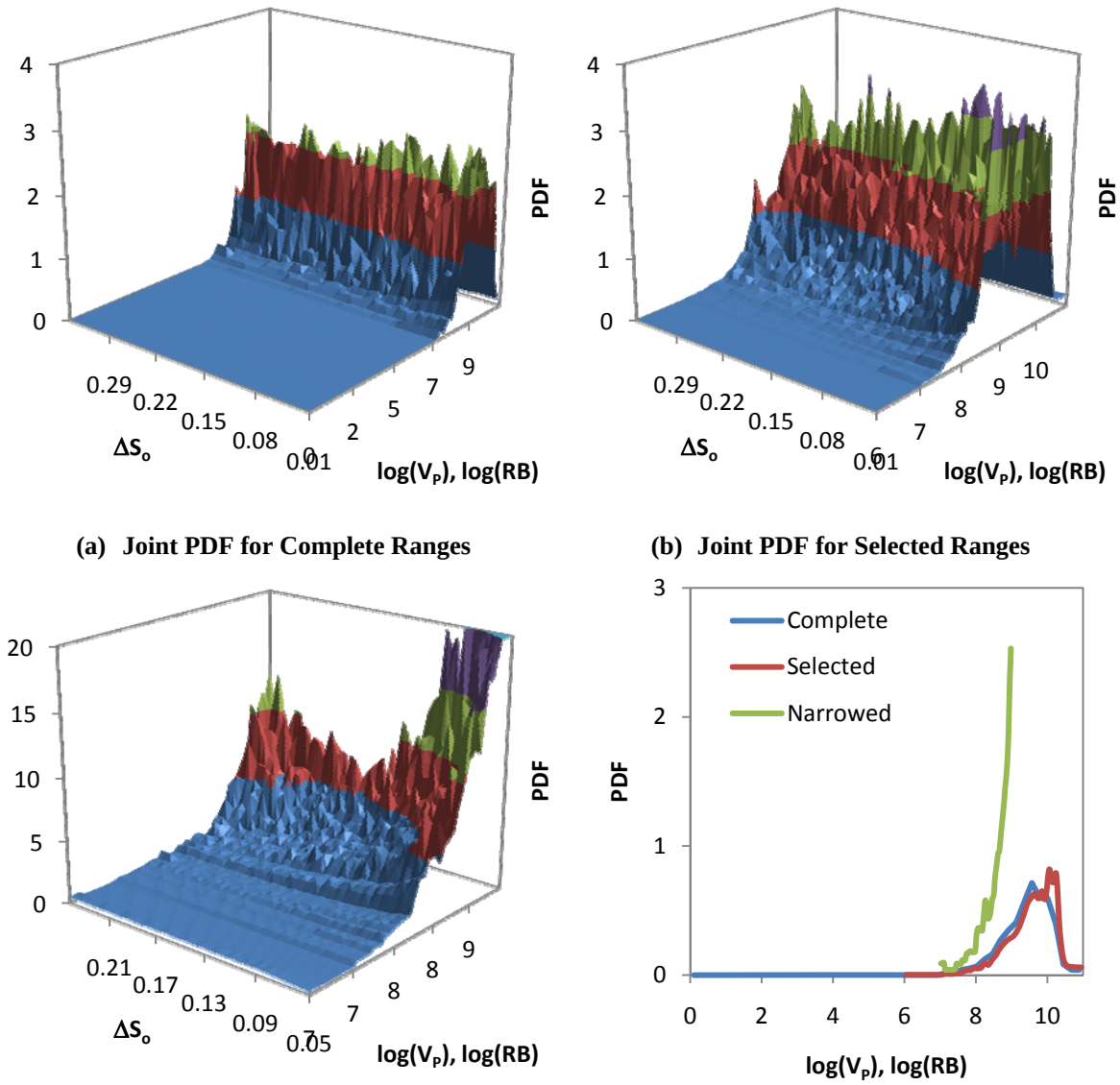

(a) Joint PDF for Complete Ranges

(b) Joint PDF for Selected Ranges

(c) Joint PDF for Narrowed Ranges

(d) Marginal PDF Comparing Ranges

Figure 8-8 Plots Comparing the Sensitivity of DBM to the Ranges for Parameters

8.3.3.6 Applying Monte Carlo Simulation to the Decision Based Method with Multiple Parameters

To best recreate a continuous sample set, a numerical analysis that breaks up the range into 50 intervals is used. This involves analyzing 125,000 event combinations,

which means 125,000 simulations with SEORM. More intervals would produce more refined distributions; however, the computation time becomes a limitation and the Excel data sheet used for the calculations becomes difficult to handle. Monte Carlo simulation could be used to deal with these issues, especially as more parameters are included in the analysis.

Following the Monte Carlo procedure discussed in Chapter 7 for a single parameter, the process is expanded for multiple parameters. An example of the results is demonstrated with the previous DBM example with the "Selected" ranges for the inputs. The example works with 40,000 Monte Carlo simulations, which is a fraction of the 125,000 simulations needed for the full evaluation.

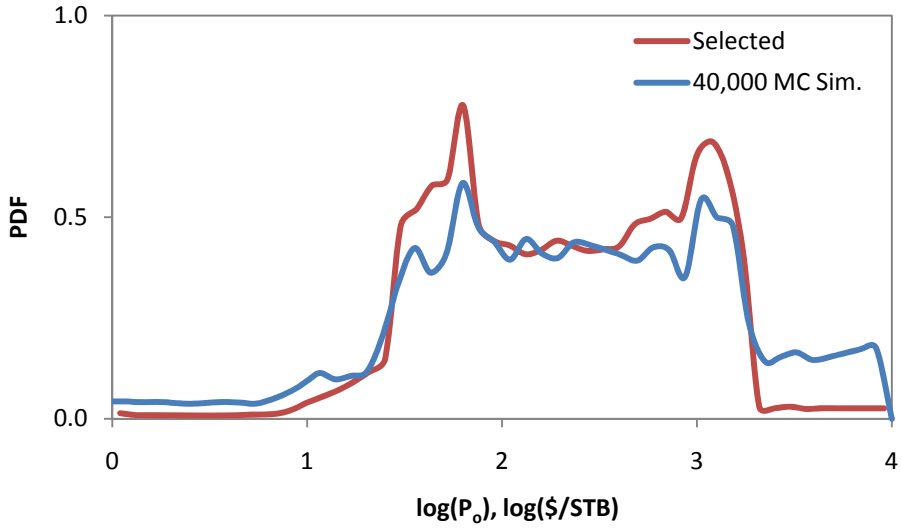

Figure 8-9 Comparison of a Rigorous Analysis Against Monte Carlo Simulated Result for Approximating the Marginal PDF of log(P_o)

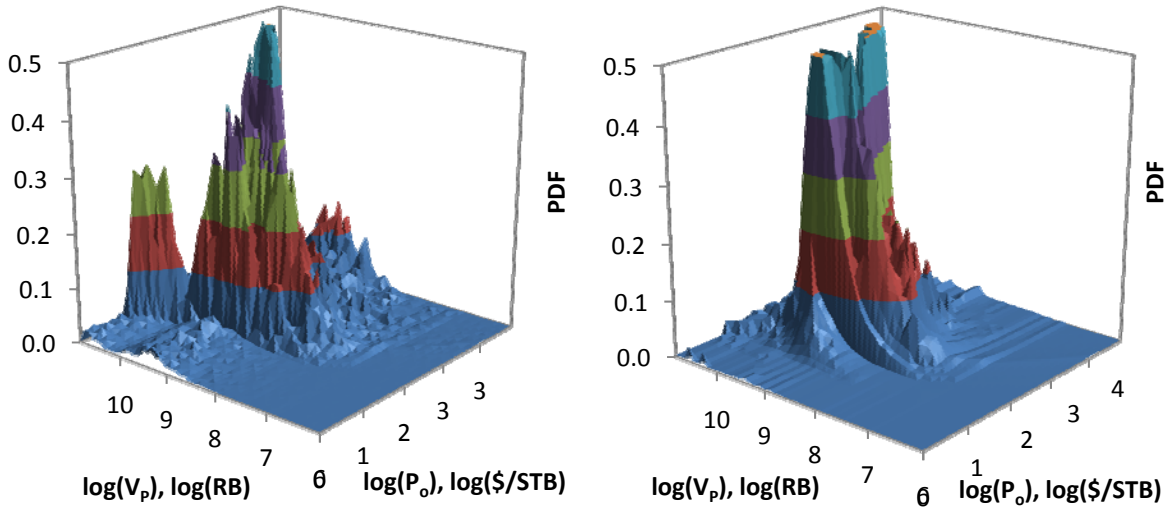

(a) Monte Carlo Simulated Result **(b) Rigorous Analysis**

Figure 8-10 Comparison of a Rigorous Analysis Against Monte Carlo Simulated Result for Approximating the Joint PDF of $\log(V_P)$ and $\log(P_o)$

It appears that at about 40,000 simulations relatively general representations of the probability distributions begin to form. More simulations provide considerably better resolution; however, it does provide a decent rough approximation that could be used for preliminary analyses. More plots comparing the Monte Carlo results with the full analyses are in Appendix D.

8.3.3.7 Summary of Sensitivity Analysis for the Decision Based Method

DBM is moderately sensitive to the number of intervals selected. For good resolution, a large number of intervals are recommended; however, this can lead computational times that may be limiting. Monte Carlo simulation can assist with this issue.

Carefully studying the distributions created with DBM can provide insight into which parameters are most influential and the parameters influence the probability

distributions. Based on the sensitivity analysis, it appears that P_o may be the most influential parameter. ΔS_o also appears to provide relatively identifiable points where the decision typically changes.

When working with DBM, it is important to recognize how the selected ranges for each input parameter influences the probability distributions. As long as important events that alter the decision are not eliminated, similar distributions can be generated with ranges reduced from more complete ranges. It is preferred to determine an appropriate range that wide enough to capture all important events, but narrow enough to allow for good resolution.

8.3.3.8 Applying the Decision Based Method for Example A

For the example DBM is applied, with five intervals for each input parameter and 125 event combinations for all three input parameters. The range for each parameter follows the ranges used for the "selected" ranges in Table 8-4. A plot of the probability distribution is shown in Figure 8-11. In the figure, the distribution is laid out so that event can be represented.

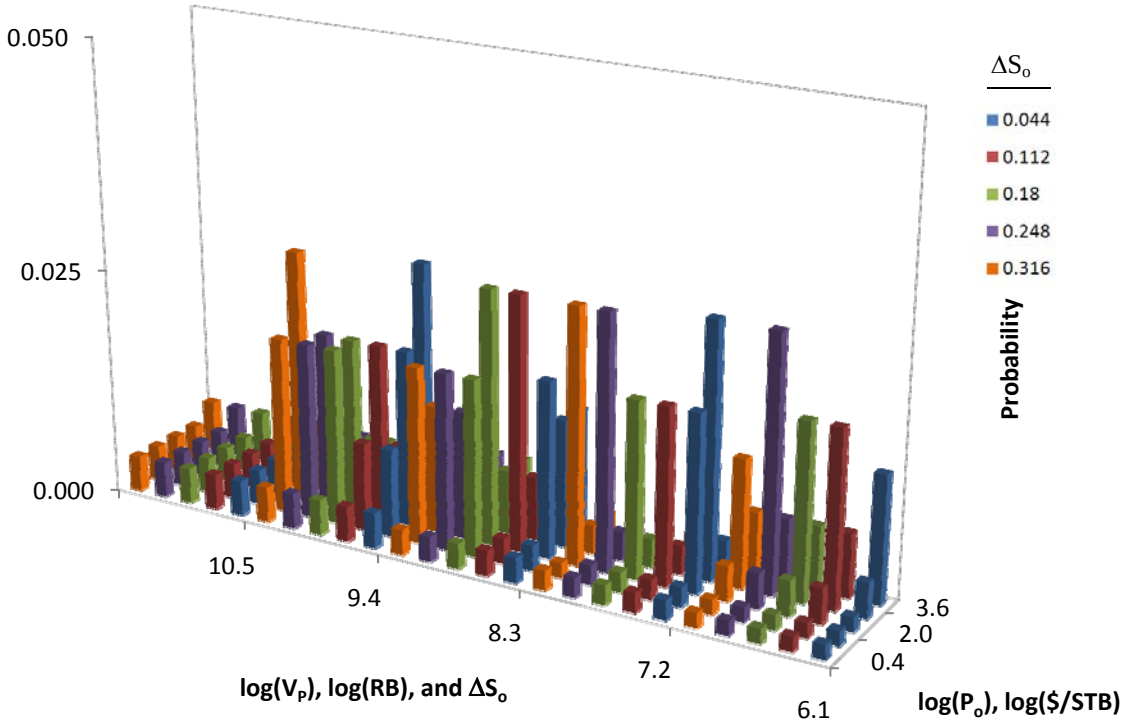

Figure 8-11 Probability Distribution for the Non-Informative Prior Probabilities

8.3.4 Step 4: Determine the Expected Utilities of the Alternatives for the Non-Informative Prior Decision

The non-informed prior probability distributions created with DBM assume there is no information about the field in any form. The expected utilities are calculated from the utilities and probabilities as shown in Equation 8-1.

$$u_{A_1} = P(\Delta S_{o|1}, P_{o|1}, V_{P|1})u_{A_1|1} + \cdots + P(\Delta S_{o|1}, P_{o|1}, V_{P|h})u_{A_1|h} + \cdots + P(\Delta S_{o|1}, P_{o|j}, V_{P|h})u_{A_1|h\times j} + \cdots + P(\Delta S_{o|i}, P_{o|j}, V_{P|h})u_{A_1|h\times j\times i}$$

Equation 8-1

To obtain accurate expected values, the parameters should be divided into several intervals. With the expected utilities calculated the decision is then made between WF and EOR. The alternative with the largest expected utility is the selected alternative.

For this example the expected utility for the EOR alternative is $-959 MM and for the WF alternative it is $115 MM, which means WF is preferred. The expected utility for EOR is so low because there is an upper cap limit set on the profits, but there is no cap to the potential loses. Furthermore, there are considerable expenses associated with SP flooding including upfront costs and high injection costs. Water flooding does not have such expenses and it is assumed that if there is no profitable recovery the water flooding is immediately terminated, which means the lowest value for WF is zero.

8.3.5 Step 5: Set Up the Posterior Decision

The posterior decision is designed to account for new information from a pilot test. For the decision analysis in this study, the pilot test provides information about ΔS_o and V_P but no information about P_o. Therefore, the posterior analysis considers every possible combination of ΔS_o and V_P that could be realized for the pilot. For each pilot realization, a decision between EOR and WF is analyzed. Because there is new information from the pilot, the probability distribution from the prior decision is updated. The distribution is updated through Bayes' theorem with likelihood functions.

For this example, the likelihood functions assume that the values from the pilot provide perfect information. Therefore, if the pilot suggests a value for a particular parameter, then that event is representative of what will happen for a full scale project.

These distributions only apply to ΔS_o and V_P because no new information exists for P_o. Instead the likelihood function for P_o is uniform.

The following demonstrates the likelihood distributions for a particular pilot realization. Consider that the results from the pilot are ΔS_o is 0.04 and $\log(V_P)$ is 8.5. Then the likelihood functions would be as shown in Table 8-5. The likelihood probability distribution function is shown in Figure 8-12.

Table 8-5 Example of the Likelihood Distributions

ΔS_o	Likelihood Distribution	$\log(P_o)$ log($/STB)	Likelihood Distribution	$\log(V_P)$ log(RB)	Likelihood Distribution
0.04	1.0	0.4	1.0	6.5	0.0
0.11	0.0	1.2	1.0	7.2	0.0
0.18	0.0	2.0	1.0	8.3	1.0
0.25	0.0	2.8	1.0	9.4	0.0
0.32	0.0	3.6	1.0	10.5	0.0

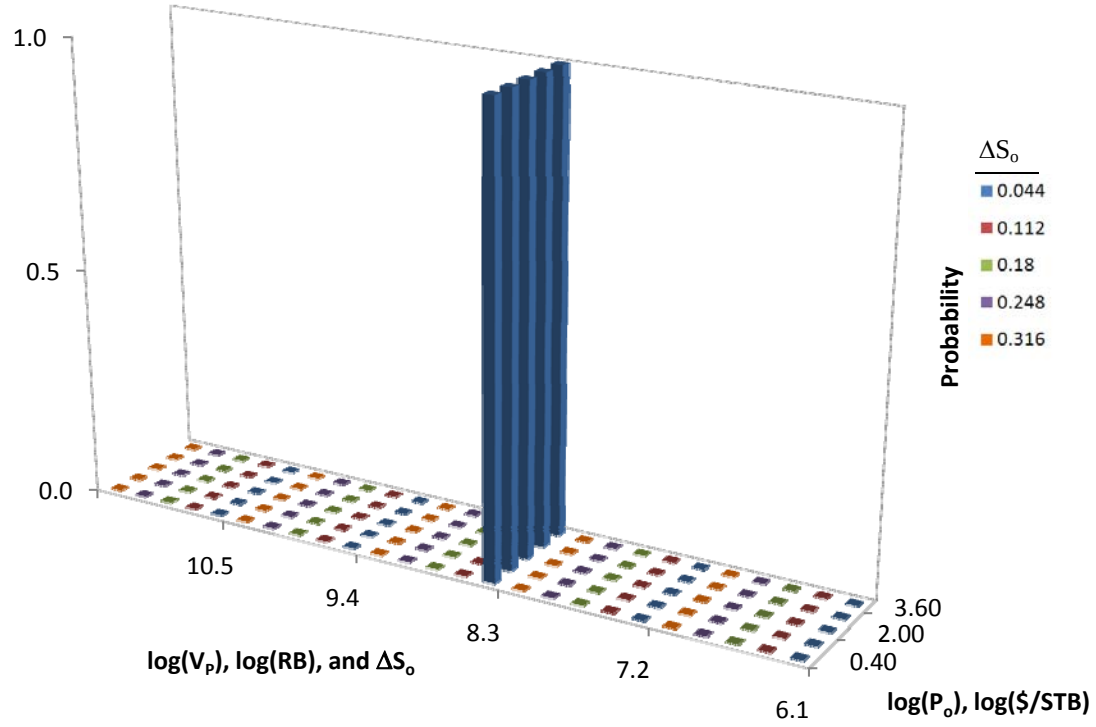

Figure 8-12 Example of the Likelihood Function

By applying the likelihood function to the prior probability distribution through Bayes' theorem, an updated probability distribution is created for the posterior decision. This distribution is shown in Figure 8-13. The new distribution puts heavy emphasis on the event ΔS_o = 0.04, $\log(V_P)$ = 8.5, and $\log(P_o)$ = 2.0, 2.8, and 3.6. There are three significant P_o values because they are emphasized in the prior probability distribution, as well, Figure 8-13.

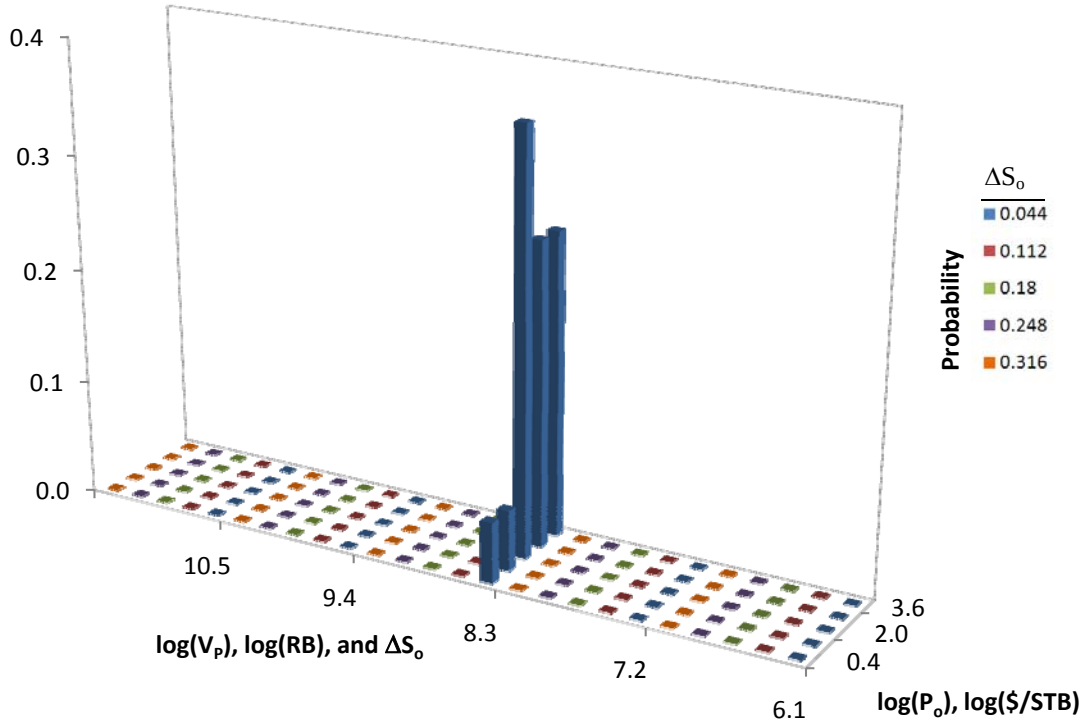

Figure 8-13 Example Updated Probability Distribution for the Posterior Decision

8.3.6 Step 6: Determine the Expected Utilities of the Alternatives from the Posterior Analysis

The expected utility values for each posterior branch are then determined. An additional assumption involved with the posterior decision is that time passes before a pilot could be started, completed and the results analyzed. Therefore, the EOR process is delayed. The calculated EOR utilities reflect the delay and include profits made from a continued water flood and any expenses or profits involved with the pilot itself. Equation 8-2 represents the equation for calculating the utility of EOR with the pilot,

$$U_{EOR|Pilot} = U_{WF\ during\ delay} + U_{Pilot} + U_{Delayed\ EOR}$$

Equation 8-2

where $U_{WF\ during\ delay}$ represents earnings during the delay from continued water flooding, U_{Pilot} are the earnings or loses from the pilot project itself, and $U_{Delayed\ EOR}$ is the utility from the field EOR project with a delayed start. U_{Pilot} does not account for any costs associated with research, lab testing, publicity, or expenses associated with preparing for a pilot test. The delay does reduce the overall value of an EOR project because of decreasing value on delayed earnings. The WF utility with the pilot, $U_{WF|Pilot}$, includes expenses or profits from the pilot as well as the earnings from water flooding, U_{WF} .

$$U_{WF|Pilot} = U_{WF} + U_{Pilot}$$

Equation 8-3

The calculation of the expected value for each posterior decision is analogous to the calculation for the prior decision. Table 8-6 is a summary of the results for the posterior decisions for the example. With all of the expected utilities calculated, a decision is made for each posterior decision. Again the alternatives with the highest expected utility are selected. The EOR alternative is selected fewer times than the WF alternative. EOR is preferred for 30% of the events.

Table 8-6 Summary of the Expected Values from Posterior Decisions for the Example

Event, E_j		Expected Utilities, $MM		Probability of Information, $P(I_j)$
ΔS_o	$\log(V_P)$	EOR	WF	
0.04	6.5	-185	4	0.023
0.04	7.5	-184	43	0.033
0.04	8.5	502	254	0.033
0.04	9.5	-608	212	0.042
0.04	10.5	-3878	75	0.028
0.11	6.5	-102	4	0.054
0.11	7.5	-88	39	0.030
0.11	8.5	529	244	0.030
0.11	9.5	-1524	176	0.038
0.11	10.5	-3875	75	0.038
0.18	6.5	-55	4	0.053
0.18	7.5	-11	40	0.047
0.18	8.5	553	181	0.064
0.18	9.5	-1849	145	0.050
0.18	10.5	-3873	75	0.050
0.25	6.5	-5	4	0.066
0.25	7.5	66	41	0.045
0.25	8.5	513	157	0.055
0.25	9.5	-1274	146	0.055
0.25	10.5	-3872	75	0.063
0.32	6.5	29	4	0.021
0.32	7.5	158	43	0.021
0.32	8.5	569	157	0.021
0.32	9.5	-602	155	0.021
0.32	10.5	-3872	75	0.021

8.3.7 Step 7: Set Up of the Preposterior Decision

Once the prior and posterior decisions are completed, the preposterior decision is set up. The branch representing the "No Pilot" choice is simply the decision made from the prior analysis and the expected utility associated with it. The branch representing the "Pilot" choice is represented by the expected utility for the pilot. The expected utility is

the sum product of the probability of information for each pilot test and the selected expected utility values for each posterior decision. For this example, the probabilities for each pilot are shown in Table 8-6. These probabilities are determined with the total probability theorem

$$P(I_j) = \sum_{i=1}^{n} P(I_j|E_i)P(E_i)$$

Equation 8-4

where $P(I_j)$ is the probability of information I for pilot event *j*, which represents a combination ΔS_o and V_P, $P(I_j|E_i)$ is the probability of information I_j given event E_i, and $P(E_i)$ is the probability for event E for event *i*, which represents a particular combination of ΔS_o, V_P, and P_o. $P(I_j|E_i)$ is the likelihood function for the pilot's information and $P(E_i)$ is from the prior probabilities. Based on the conditions used for this example, the expected value for the "No Pilot" alternative is $115 MM and for the "Pilot" alternative it is $210 MM.

8.3.8 Step 8: Determine the Value of Information

With both the expected utilities for the "No Pilot" and "Pilot" the value of information (VOI) can be calculated. The VOI is equal to the expected utility of the "Pilot" alternative minus the utility of the selected alternative for the "No Pilot" decision.

$$VOI = \sum_j \max\left[E(U_{WF|Pilot}), E(U_{EOR|Pilot})\right] = \sum_j \left[\max(U_{WF|Pilot}, U_{EOR|Pilot})P(E_j)\right]$$

Equation 8-5

It is up to the user to determine what the minimum the VOI should to be to follow through with the pilot decision. The VOI ranges from zero to positive infinity, with zero meaning the pilot provides no benefit. It is beneficial to run a value of perfect information (VPI) analysis because the VPI represents the most value a pilot could provide. Example A is a VPI analysis.

For Example A, the expected value of the "No Pilot" alternative is $115 MM and for the "Pilot" alternative it is $210 MM. Therefore, the VPI is $95 MM, which suggests the pilot offers information that is at most expected to be worth $95 MM. If this value is above the original threshold established for a pilot's value, then more detailed analyses where existing information and imperfect pilot information is assumed. Otherwise, the decision is to not perform a pilot.

8.4 Updating the Non-Informative Prior, Example B

After step three, another step may be added to create a more realistic analysis. The decision maker may decide to add any information that may be readily available. For example, if the user has a good understanding of a limited range for P_o or some idea about the V_P for the field based on water flood history, then this information may be represented with a likelihood function and applied through Bayes' theorem.

For Example B, it is assumed that the decision maker has some understanding about the parameters. Table 8-7 is a summary of the assumed probability distribution based on previous experience. Figure 8-14 is a plot of the likelihood function assumed from prior experiences. Simple functions are used to illustrate how limiting the ranges

for the parameters influence the prior probability distributions. Through Bayes' theorem, the non-informative distribution is updated with the information from the assumed distributions, creating the updated prior distribution shown in Figure 8-15.

Table 8-7 Example Likelihood Functions for Each Parameter Based on Existing Information

ΔS_o	Likelihood	$\log(P_o)$ log($/STB)	Likelihood	$\log(V_P)$ log(RB)	Likelihood
0.04	1.0	0.4	0.0	6.5	0.00
0.11	1.0	1.2	1.0	7.5	1.0
0.18	1.0	2.0	1.0	8.5	1.0
0.25	0.00	2.8	0.0	9.5	1.0
0.32	0.00	3.6	0.0	10.5	0.00

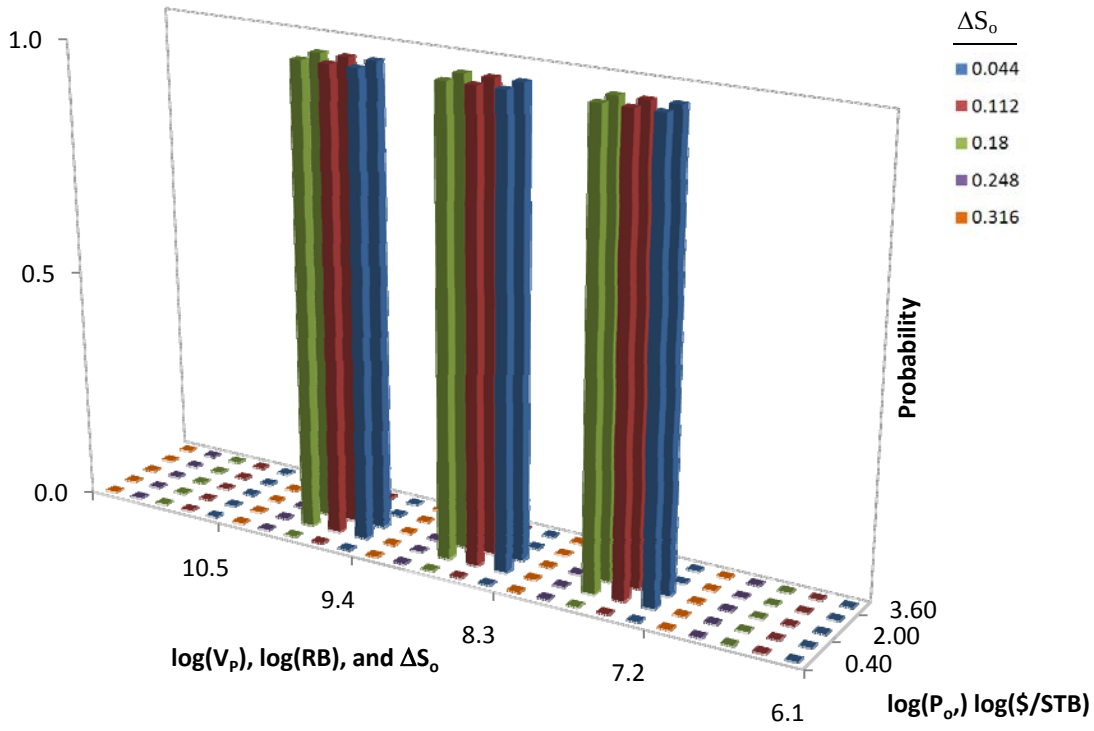

Figure 8-14 Likelihood Function for the Information Based on Experience

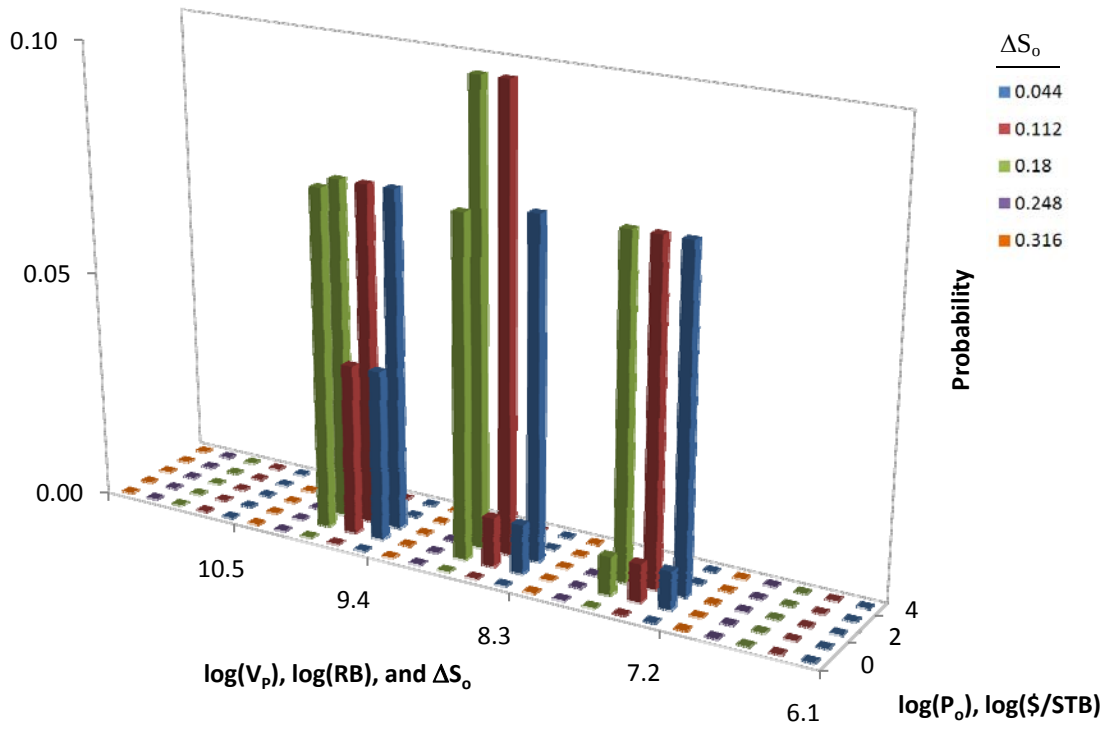

Figure 8-15 Probability Distribution of the Update Prior Distribution Based on Information from Experience

The new information acts like a filter, eliminating several events from consideration. Of the remaining events, the ones with the most weight are $\log(P_o) = 2$ log($/STB), $\log(V_P) = 8.3$ and 9.4 log(RB), and $\Delta S_o = 0.18$. The expected values of the decision are summarized in Table 8-8.

Table 8-8 Comparison of VPI Analyses for Examples A and B

	"No Pilot" Alternative			"Pilot" Alternative	VPI
	U_{EOR} ($MM)	U_{WF} ($MM)	Selected ($MM)	Expected Value ($MM)	($MM)
Example A	-959	115	115	210	95
Example B	-2182	134	134	165	31

The new information has removed some of the uncertainty that existed with the original prior distribution and therefore the adjusted prior distribution is less sensitive to perfect information from the pilot. Example B demonstrates how a pilot, or any source of new information, is typically most valuable when no other information exists.

For Example B, the likelihood function that adjusts the non-informative prior is designed to remove events that are known to be impossible. Arbitrarily filtering events can lead to unintended bias in the decision. Therefore, a reasonable and rational approach that accounts for existing information from case histories (Chapter 4) and any existing information about the field is needed for creating consistent and unbiased likelihood functions.

8.5 Applying Monte Carlo Simulation to the Decision Analysis

To perform a complete decision analysis, a decision maker has to evaluate many combinations of events and their simulations. A thorough analysis requires many simulations and lots of computation time. Monte Carlo is recommended to be used in the decision analyses because there are a large number of simulations that have to be performed, in particular with the preposterior analyses.

The simple example used for this chapter has three parameters with five events each. Each posterior analysis therefore has 125 event combinations. A complete posterior decision analysis would involve analyzing 25 potential pilot results. Each pilot result involves 125 event combinations that are also analyzed. All together, the posterior decision analysis requires 3125 events to be analyzed. A spreadsheet can handle the

computations for such an analysis; however, if a more thorough analysis is required, one with 50 events per each parameter, then there would be 2500 pilot events each with 125,000 events for each posterior decision. That leads to 312,500,000 simulated events for all of the posterior decisions. This full enumeration involves a staggering amount of simulations with SEORM and calculations for a spreadsheet. The run time for calculations becomes prohibitively long. Monte Carlo simulation provides considerable assistance in reducing the computation time without sacrificing much on accuracy.

To apply Monte Carlo to the decision analysis, first the prior and the preposterior probability distributions need to be determined. It is from these distributions that random samples of events for the input parameters are selected. With the prior distribution the expected value of the prior decision can be approximated. The preposterior distribution is calculated from probability of information for each possible pilot realization, and with it pilot realizations are randomly selected. For each pilot realization a posterior distribution is calculated from the prior probability distribution and the pilot's likelihood function. Again, random samples are selected from the posterior decision distributions and used to approximate the expected value of the posterior decision.

Programs were developed in Excel® that handle the calculations for the decision making process and can either perform a rigorous analysis that goes through every possible combination of events or a Monte Carlo simulation based analysis.

8.5.1 Monte Carlo Simulation Example

The following is an example of Monte Carlo being applied to the prior decision for the example decision discussed in this chapter. The expected utilities for the complete analysis, which takes into account all 125 events, are shown in Table 8-9. The table also shows the results from Monte Carlo simulations of various sizes. As the number of simulations increases, the accuracy of the results increases. It appears good accuracy requires about 1000 simulations, and therefore for this example Monte Carlo does not provide an advantage.

Table 8-9 Comparison of Monte Carlo Results for Calculating the Utility of Prior Decision for a Simple Example

		Expected Utilities ($MM)	
		UEOR	UWF
Complete (125 Simulations)		-959	115
# of Simulations	10	-645	100
	100	-1025	113
	1000	-962	116
	10,000	-958	115

Results from a more thorough analysis are presented as well. This analysis has three parameters divided into 50 intervals and therefore required 125,000 simulations for an accurate result. Table 8-10 shows the results of the complete analysis as well as from Monte Carlo simulations. Again the accuracy improves with more simulations, with a good result occurring with about 1000 simulations. In this case, this is only a fraction of what is necessary for a complete enumeration. Therefore, considerable time can be saved without a significant loss in accuracy.

Table 8-10 Comparison of Monte Carlo Results for Calculating the Utility of Prior Decision for a Complex Example

		Expected Utilities ($MM)	
		UEOR	UWF
Complete (125,000 Simulations)		-391	175
# of Simulations	100	-315	152
	1000	-370	182
	10,000	-395	174
	50,000	-395	174

Monte Carlo could also be used to assist with the preposterior decision. For the simpler problem with only five intervals, only 3125 simulations are necessary for a complete enumeration. As shown in Table 8-11, it once again appears that running a full analysis instead of Monte Carlo is preferred because a relatively few number of simulations are required. The numbers within parentheses in the table refers to the number of simulations for both the prior and posterior decisions. However, the Monte Carlo simulator does produce a reasonably accurate answer if the proper number of simulations is applied for both the prior and posterior decisions.

Table 8-11 Comparison of Monte Carlo Results for Calculating the Utility of Preposterior Decision for a Simple Example

		Expected Utilities ($MM)	
		"No Go"	"Go"
Complete (3125 Simulations)		115	210
# of Simulations	10,000 (1000/10)	115	180
	25,000 (1000/25)	116	220
	50,000 (1000/50)	114	205
	100,000 (1000/100)	115	213
	1,000,000 (1000/1000)	115	212

For more thorough preposterior analyses, Monte Carlo simulation must be used because the computing becomes prohibitively long. The calculation time becomes more

extensive because of the calculation time associated with the simulations and distributions.

8.6 Summary

Decision making involves several steps and components. The first step is to set up the decision in the form of a decision framework so that all of the information and how it is interrelated can be easily seen. The decision analysis for this thesis project involves several other decisions before the final one of "Go" versus "No Go" for a pilot. The next step is to establish non-informative prior probabilities so that a starting point can be set for the probability distribution of all of the events. The non-informative prior may then be updated with any existing data with Bayes' theorem. A prior decision is first completed the utility of the selected alternative is the utility of the "No Go" alternative for the preposterior decision.

The posterior distributions are then established based on potential pilot outcomes. Each posterior decision is evaluated. The utility of the "Go" alternative for the preposterior decision is based on the preferred utilities for each posterior decision and the probabilities for each pilot realization.

Each decision requires considerable numeration because the events are supposed to be from a continuous set. Many simulations can create staggeringly long simulation times. Therefore, Monte Carlo simulation is being used to limit the number of simulations and computation time, without sacrificing accuracy.

Examples A and B presented in the chapter, demonstrate how the value of information from a pilot is sensitive to the available information prior to the decision. With more information applied early on in the decision analysis, the less valuable the pilot information becomes in these examples. A rational and reasonable methodology for determining likelihood functions to update existing probability distributions that includes information from case histories and field specific information from primary and secondary production data would be valuable.

CHAPTER 9: CONCLUSIONS AND FUTURE WORK

9.1 Review of the Research

This study was focused on developing decision support for enhanced oil recovery (EOR) projects. To perform a decision analysis, there needed to be a way to determine the utility or monetary outcome of an EOR project based on potential reservoir characteristics. Therefore, the first step was to create a simple model that can handle forecasting oil production for three different forms of isothermal EOR methods, surfactant-polymer (SP), alkali-surfactant-polymer (ASP), and CO_2 flooding. This model is known as the simplified enhanced oil recovery method (SEORM). It was evaluated with field data to ensure that it is able to create accurate oil production history curves based on reservoir properties. An economic model was also created as means to determine the economic value of a project. A sensitivity analysis was then performed to better understand how the parameters of SEORM and the economic model influence the value of a project. The decision tree and the decision making process were then set up and explained. Finally, a simple example was used to demonstrate the decision making process for determining the value of information of a pilot. The process discussed in this study was designed to avoid bias, inconsistency, and other issues common with establishing probability distributions for events with uncertainty.

9.2 Conclusions

There are essentially two sets of conclusions that can be drawn from this research. The first set involves SEORM and the other set is from the decision analysis.

9.2.1 Conclusions about the Simplified Enhanced Oil Recovery Method

SEORM is designed to be a simple in that it only requires a few physically meanigful parameters to characterize an oil production history curve. The method is simple with only four fitting parameters for SP, ASP, and CO_2 floods. Assuming an incomplete fractional flow curve, for SP and ASP flood the change in oil saturation (ΔS_o), two Koval factors (K_1 and K_2), and the specific shock velocity of the oil bank (v_{oB}) are assumed. The Koval factors and v_{oB} capture the heterogeneity and mobility issues. For CO_2 floods, ΔS_o, K_1, v_{oB}, and total pore volume of the reservoir (V_P) must be assumed for the fit. If the fractional flow curve is known, then v_{oB} is not assumed, which reduces the number of fitting parameters to three.

Based on the evaluation with existing field data, the method appears to work very well in creating oil production history curves that fit pilot and field data. SEORM appears to be capable of creating most potential oil production history curves that could occur. The method is based on fractional flow theory, and the strong fits further suggest that fractional flow theory can be a good indicator of a field's performance.

Several generic correlations between the field properties and performance are noted based on the evaluation fittings. First it is observed that larger scale fields tend to perform less efficiently than smaller fields. This observation is based on the fact there is a general tendency for large fields to have lower change in oil saturation, higher Koval factor values, and higher specific shock velocities than smaller fields.

Another observation is that SP and ASP floods behave quite differently from CO_2 floods. SP and ASP floods tend to have K_2 values that vary between K_1 and $K_{2,max}$, which implies that the oil bank typically arrives at the producer before the injected chemical bank. For CO_2 floods, the best fits are with K_2 equal to $K_{2,max}$, which implies the solvent and oil banks arrive at the producers the same time. SP and ASP floods also have better sweep and shorter flood lives in terms of dimensionless time than CO_2 floods because SP and ASP floods have lower Koval factors and specific shock velocities than CO_2 floods. These trends are consistent with field experiences.

The sensitivity analysis of SEORM and the economic model for the three flood types shows that the most influential parameters are ΔS_o, price of oil (P_o), and V_P. These variables are most important because they directly influence profit potential for a project. The next most important parameters deal with the injected volume and concentration of the injected chemicals or solvent because the cost of the injected fluids is the most significant expense.

9.2.2 Conclusions about the Decision Making Process

The decision analysis for this thesis project involves several decisions including one between "Go" and "No Go" for a pilot and others between EOR and continued water flooding. An important early step for the decision analysis is to set up the non-informative prior probabilities as a starting point for the probability distribution of all of the events. Following the principle of insufficient reason (PIR) and assuming all input values are equally likely with arbitrarily assumed ranges of values for the events is not an

adequate approach because it creates inconsistent probability distribution between users. The decision-based method (DBM) addresses the inadequacies because it applies (PIR) to the output of the decision and it is recommended decision analysis.

Some non-informative prior distributions for the input parameters change in oil saturation (ΔS_o), oil price (P_o), and total pore volumes (V_P) are created with DBM. The method demonstrates that there are positive and negative infinite limits for P_o and V_P. It also shows correlations between the parameters, suggesting that the inputs are not independent when it comes to altering the final decision. For example, if P_o is very high, then low ΔS_o values can still allow for EOR to be preferred over continued water flooding.

The simple example in the thesis demonstrates that the value of information for a pilot diminishes as more information is applied early to the decision. Therefore, the pilot is most valuable under conditions where there is little experience or understanding about a reservoir's properties.

9.3 Recommendations for Future Work

It is recommended that SEORM be evaluated with more field data, especially with ASP floods. More evaluations can provide a more representative sample set for determining representative ranges of SEORM's input parameters. The extra evaluations can improve confidence in the method's accuracy for creating representative oil production curves. More evaluations may also assist with determining potential trends between SEORM's inputs and measurable reservoir characteristics. If trends can be

developed then basic means for approximating the parameter values can be used for more accurate and reasonable forecasting.

Another recommendation is to adjust the evaluations of SEORM for SP and ASP floods to allow V_P to be an adjustable parameter. Currently it is not recommended to allow V_P to be an adjustable parameter because several significantly different satisfactory fits can be created. If the evaluation process is adjusted so that the number of fits is limited then potentially more accurate and more representative fits can be created.

Another recommendation is for the decision analyses to take into account more variables with more intervals for the parameters are performed. This study focused on establishing the method of decision making so that consistent probability distributions can be created. More analyses are required to study how the parameters and different conditions alter the decision.

Finally, it is recommended that reasonable and rational approach be created for determining likelihood functions that represent information. There is currently no process for creating likelihood functions based on existing information. Typically, the distributions come from judgment based on past experiences; however, this can lead to unintended bias and is a questionable approach. A process is needed so the distributions can be created in consistent manner.

APPENDIX A: EVALUATION FITS

A.1 Fitted Pilot Scale Surfactant-Polymer Floods

The following is the full set of pilot scale SP flood project that were fitted with SEORM along with the inputs used for the fits. All of the tables have colored cells. The light blue cells are values fitted with SEORM. The light green cells are values provided in the literature. The light purple cells are the values fitted for the fractional flow curve. All other cells are calculated values based on the other inputs.

Several plots are provided for every fit, including ones for oil cut, oil saturation, oil production rate, oil recovery, and the fitted fractional flow curve.

A.1.1 Benton Pilot

Table A-1 Summary of Inputs for Benton Pilot

Oil Saturations			Fractional Flow Inputs		
S_{oI}	0.80		k^o_{rw}	0.15	
S_{oR}	0.35		k^o_{ro}	0.80	
S_{or}	0.30		n	2.0	
S_{oB}	0.48		m	2.0	
S_{oF}	0.26		μ_o	3.5	cp
ΔS_o	0.09		μ_w	0.8	cp
Oil Cuts			μ_c (Inj. Chem.)	5.0	cp
f_{oI}	0.02		**Reservoir Properties**		
f_{oB}	0.29		V_p	4970	RB
f_{oF}	0.00		OOIP	3976	STB
Flood Behavior			B_o	1.00	RB/STB
K_1	1.58		Well Spacing	1.0	acres
K_2	2.45		Field Size	1.0	acres
v_{oB}	2.11		**Other Inputs**		
v_C	1.36		Z_{Sur}	2.7	% conc.
K_f	1.00		Z_{Poly}	275	ppm

Flood Injection Inputs				
Fluid	Surfactant	Polymer	Water	
q_I	80	60	75	STB/day
q_P	80	60	75	STB/day
Slug Size	0.28	3.30	0.00	Frac. V_p

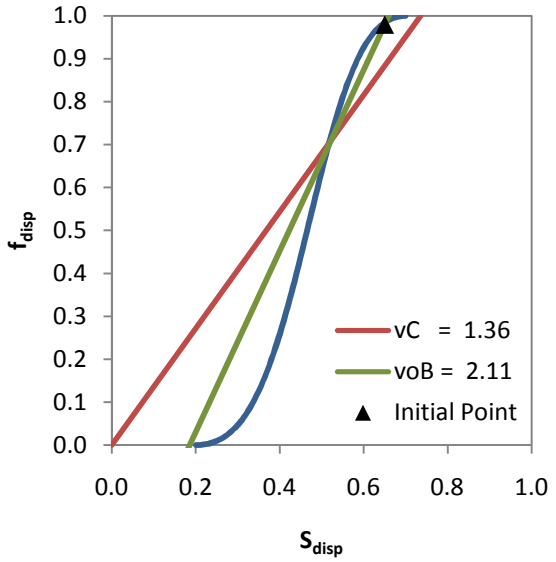

Figure A-1 Fractional Flow Curve for Benton Pilot

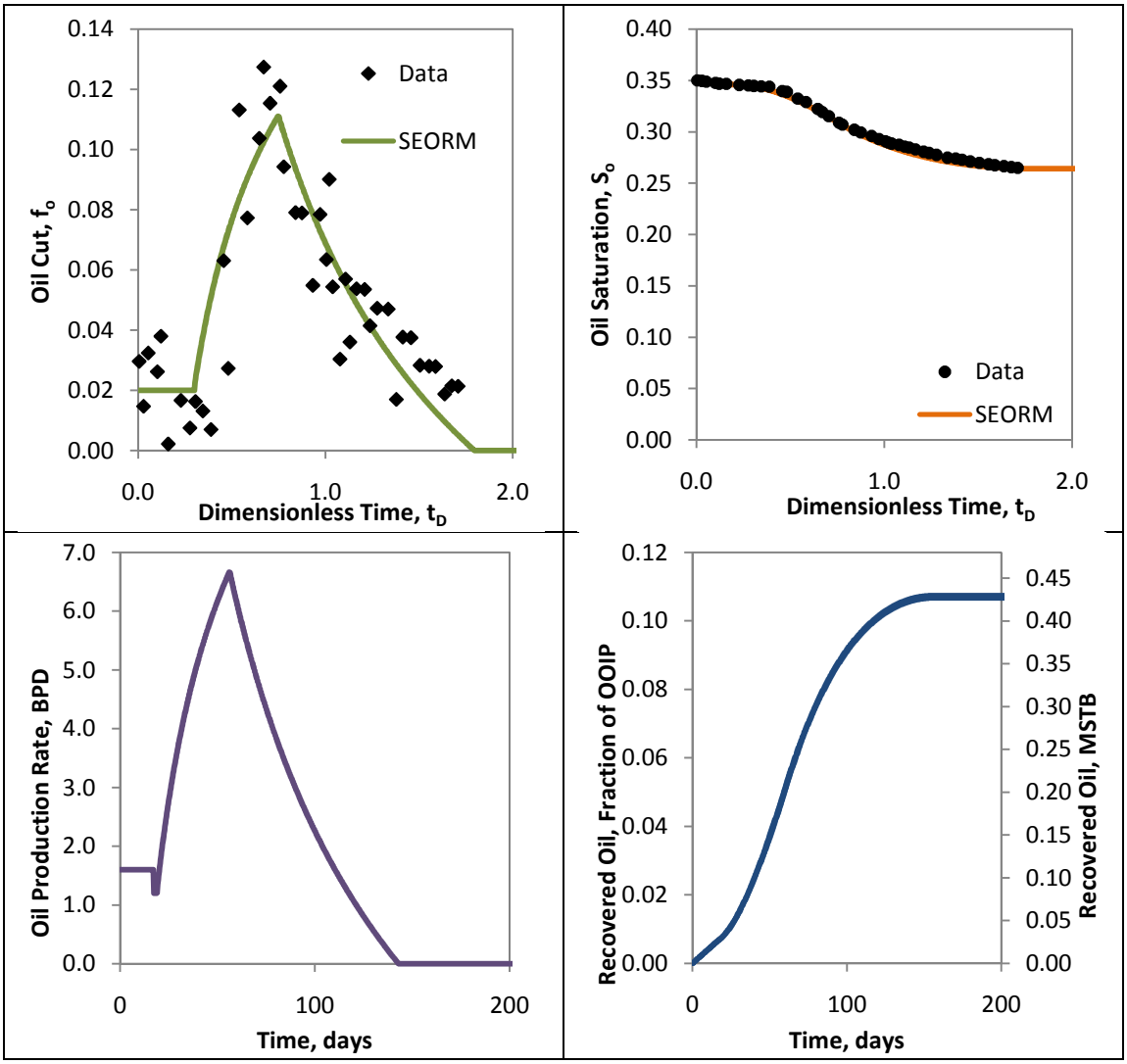

Figure A-2 Plots for Fitted Benton Pilot Data

References: French et al. 1973, Lake et al. 1981

A.1.2 Berryhill Pilot

Table A-2 Summary of Inputs for Berryhill Pilot

Oil Saturations			Fractional Flow Inputs		
S_{oI}	0.71		k^o_{rw}	0.18	
S_{oR}	0.30		k^o_{ro}	0.80	
S_{or}	0.27		n	3.0	
S_{oB}	0.41		m	2.0	
S_{oF}	0.22		μ_o	4.0	cp
ΔS_o	0.08		μ_w	1.0	cp
Oil Cuts			μ_c (Inj. Chem.)	50.0	cp
f_{oI}	0.01		**Reservoir Properties**		
f_{oB}	0.25		V_p	724000	RB
f_{oF}	0.00		OOIP	514040	STB
Flood Behavior			B_o	1.00	RB/STB
K_1	2.50		Well Spacing	4.5	acres
K_2	3.90		Field Size	18	acres
v_{oB}	2.10		**Other Inputs**		
v_C	1.28		Z_{Sur}	5	% conc.
K_f	0.88		Z_{Poly}	1000	ppm

Flood Injection Inputs				
Fluid	Surfactant	Polymer	Water	
q_I	1000	700	1000	STB/day
q_P	1500	1500	1000	STB/day
Slug Size	0.10	0.35	2.59	Frac. V_p

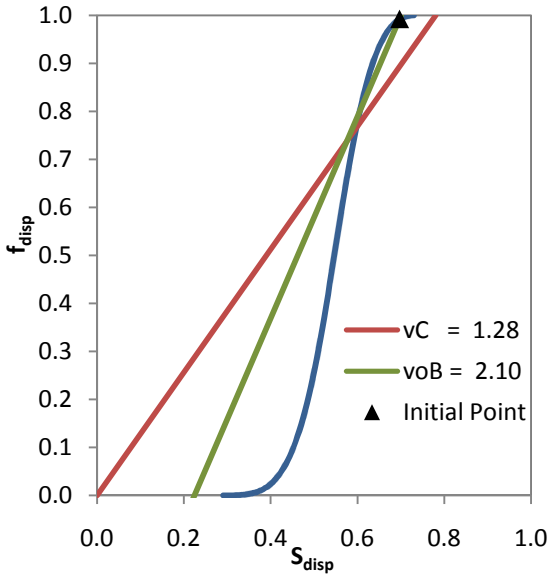

Figure A-3 Fractional Flow Curve for Berryhill Pilot

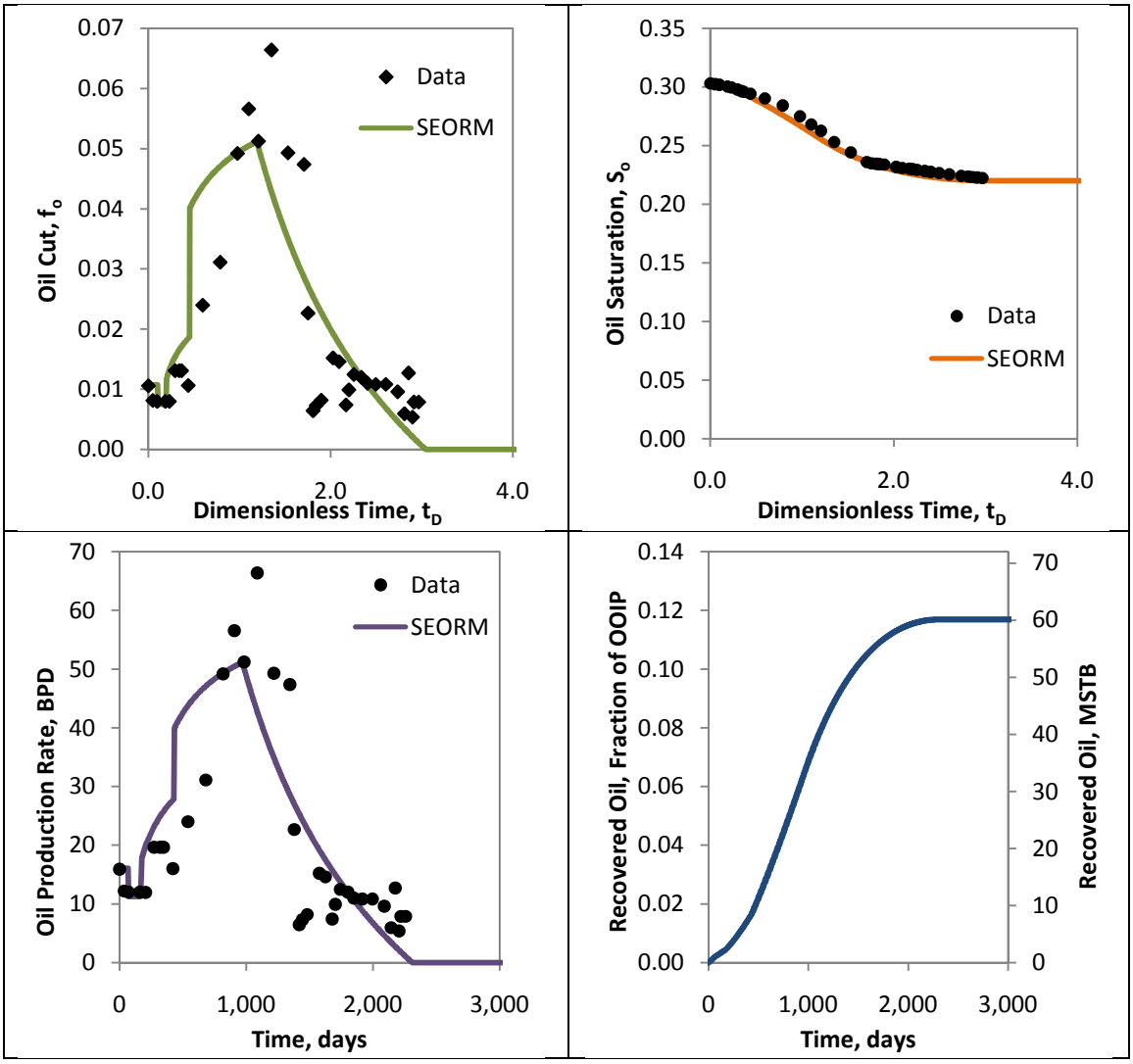

Figure A-4 Plots for Fitted Berryhill Pilot Data

References: Crawford and Crawford 1985, Bae 1995, Bae and Syed 1988

A.1.3 Big Muddy Pilot

Table A-3 Summary of Inputs for Big Muddy Pilot

Oil Saturations			Fractional Flow Inputs		
S_{oI}	0.53		k^o_{rw}	0.10	
S_{oR}	0.32		k^o_{ro}	0.80	
S_{or}	0.31		n	6.0	
S_{oB}	0.34		m	2.0	
S_{oF}	0.22		μ_o	4.0	cp
ΔS_o	0.10		μ_w	0.7	cp
Oil Cuts			μ_c (Inj. Chem.)	12.0	cp
f_{oI}	0.01		**Reservoir Properties**		
f_{oB}	0.15		V_p	140000	RB
f_{oF}	0.00		OOIP	73500	STB
Flood Behavior			B_o	1.00	RB/STB
K_1	1.2		Well Spacing	1.0	acres
K_2	2.1		Field Size	1.0	acres
v_{oB}	8.1		**Other Inputs**		
v_C	1.28		Z_{Sur}	2.5	% conc.
K_f	0.14		Z_{Poly}	600	ppm

Flood Injection Inputs				
Fluid	Surfactant	Polymer	Water	
q_I	150	170	320	STB/day
q_P	150	170	320	STB/day
Slug Size	0.25	0.50	0.92	Frac. V_p

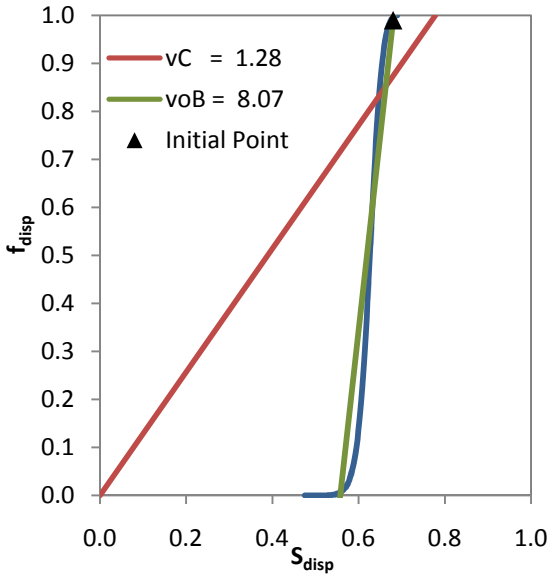

Figure A-5 Fractional Flow Curve for Big Muddy Pilot

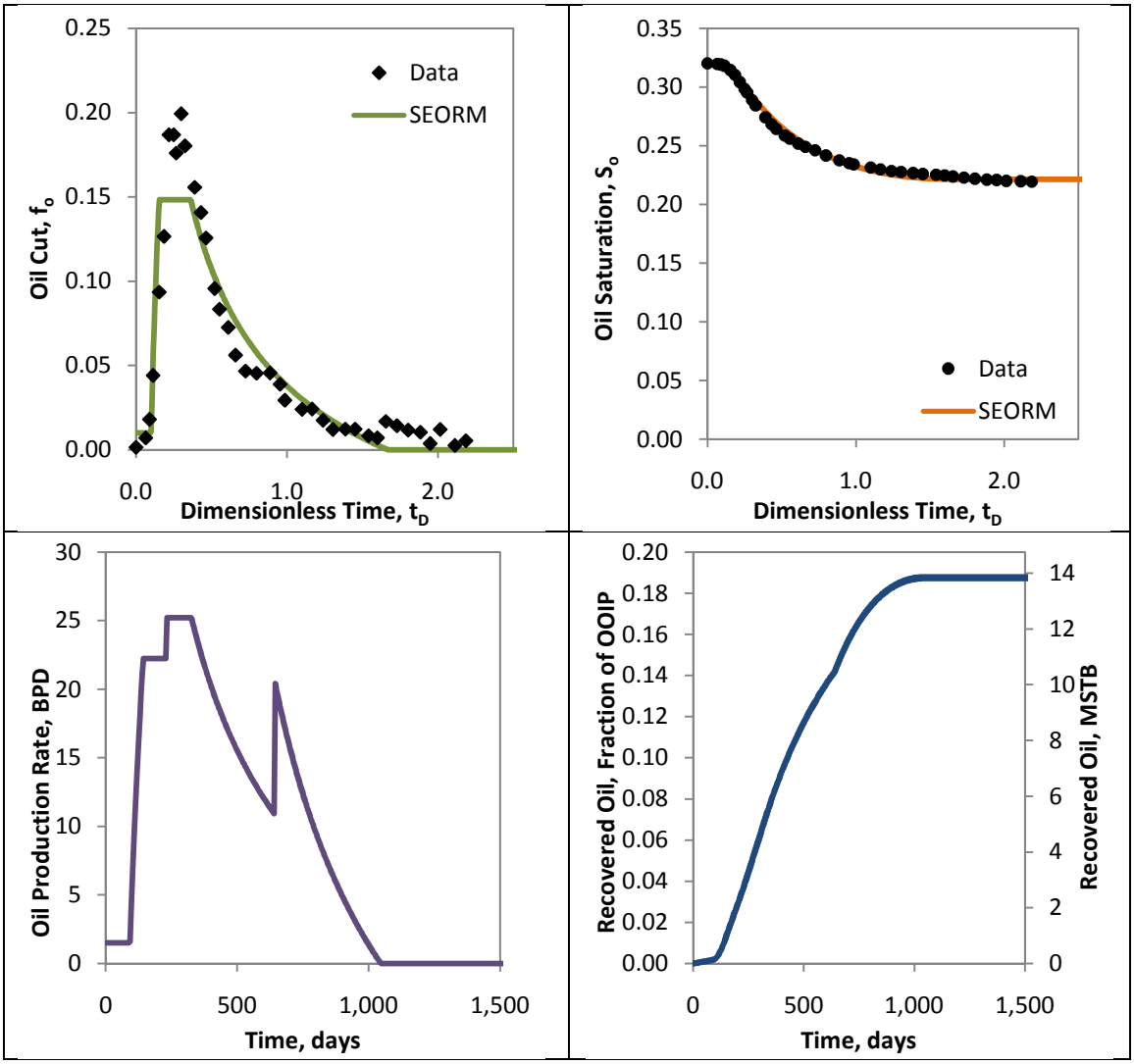

Figure A-6 Plots for Fitted Big Muddy Pilot Data

References: Saad et al. 1989, Ferrell et al. 1988, Haller 1955

A.1.4 Borregos Pilot

Table A-4 Summary of Inputs for Borregos Pilot

Oil Saturations			Fractional Flow Inputs		
S_{oI}	0.68		k^o_{rw}	0.20	
S_{oR}	0.31		k^o_{ro}	0.90	
S_{or}	0.27		n	2.0	
S_{oB}	0.34		m	2.0	
S_{oF}	0.22		μ_o	0.4	cp
ΔS_o	0.09		μ_w	0.4	cp
Oil Cuts			μ_c (Inj. Chem.)	1.0	cp
f_{oI}	0.05		**Reservoir Properties**		
f_{oB}	0.15		V_p	7200	RB
f_{oF}	0.00		OOIP	3527.5	STB
Flood Behavior			B_o	1.39	RB/STB
K_1	1.85		Well Spacing	1.25	acres
K_2	2.00		Field Size	1.25	acres
v_{oB}	3.65		**Other Inputs**		
v_C	1.28		Z_{Sur}	2.3	% conc.
K_f	0.04		Z_{Poly}	0	ppm

Flood Injection Inputs				
Fluid	Surfactant	Polymer	Water	
q_I	50	50	50	STB/day
q_P	50	50	50	STB/day
Slug Size	0.47	0.00	1.09	Frac. V_p

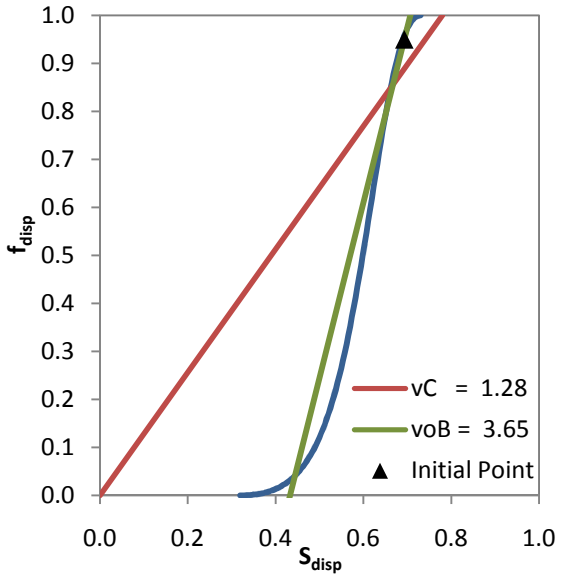

Figure A-7 Fractional Flow Curve for Borregos Pilot

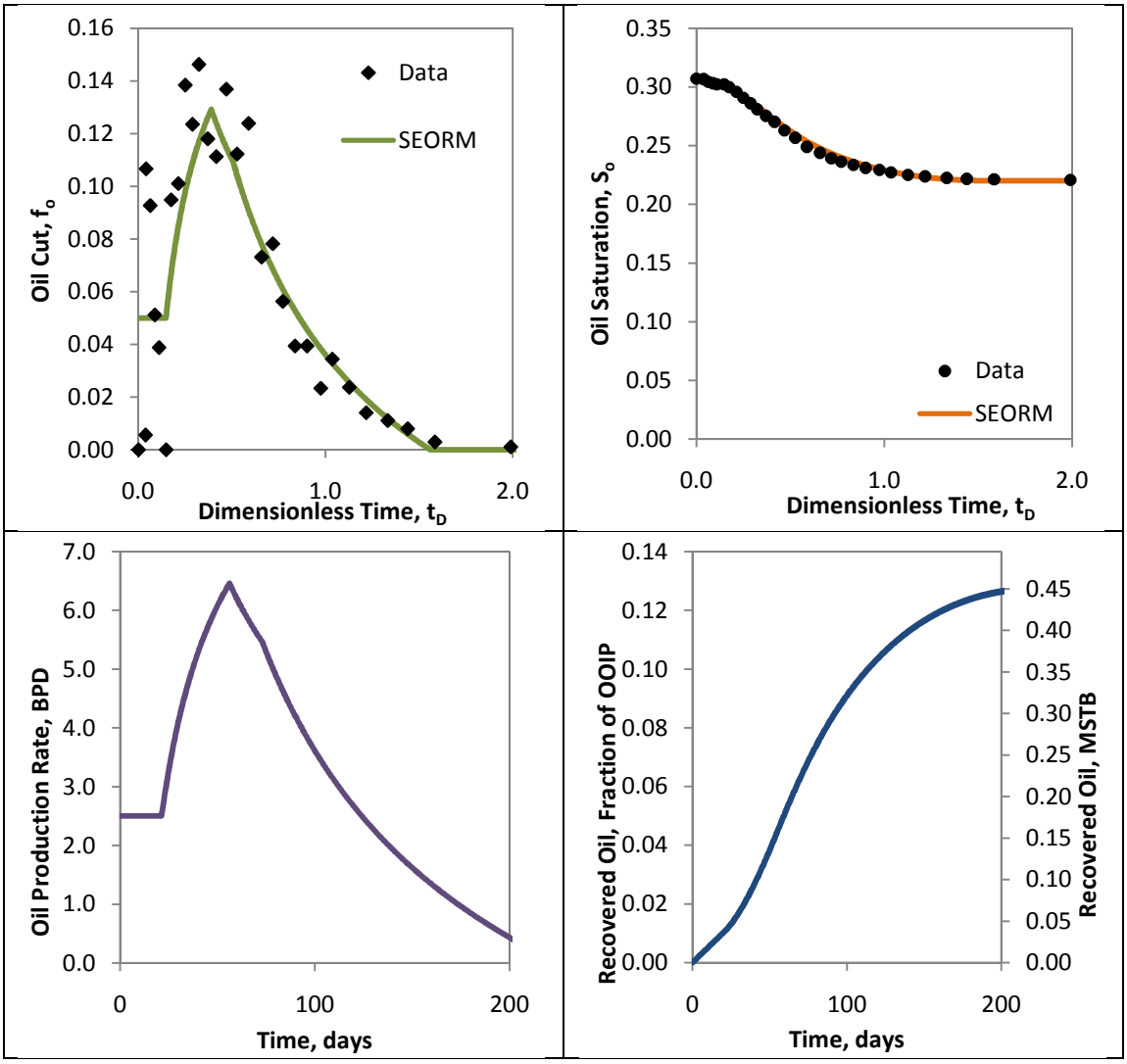

Figure A-8 Plots for Fitted Borregos Pilot Data

References: Pursley and Graham 1975

A.1.5 Chateaurenard Pilot

Table A-5 Summary of Inputs for Chateaurenard Pilot

Oil Saturations			Fractional Flow Inputs		
S_{oI}	0.80		k^o_{rw}	0.06	
S_{oR}	0.50		k^o_{ro}	1.00	
S_{or}	0.37		n	3.0	
S_{oB}	0.62		m	2.0	
S_{oF}	0.00		μ_o	40.0	cp
ΔS_o	0.50		μ_w	0.73	cp
Oil Cuts			μ_c (Inj. Chem.)	55.0	cp
f_{oI}	0.07		**Reservoir Properties**		
f_{oB}	0.71		V_p	1400	MRB
f_{oF}	0.00		OOIP	1120	MSTB
Flood Behavior			B_o	1.00	RB/STB
K_1	2.01		Well Spacing	4.9	acres
K_2	5.19		Field Size	19.4	acres
v_{oB}	3.80		**Other Inputs**		
v_C	1.00		Z_{Sur}	3	% conc.
K_f	0.57		Z_{Poly}	1500	ppm

Flood Injection Inputs				
Fluid	Surfactant	Polymer	Water	
q_I	1100	960	960	STB/day
q_P	1100	1250	1250	STB/day
Slug Size	0.038	10.41	6.89	Frac. V_p

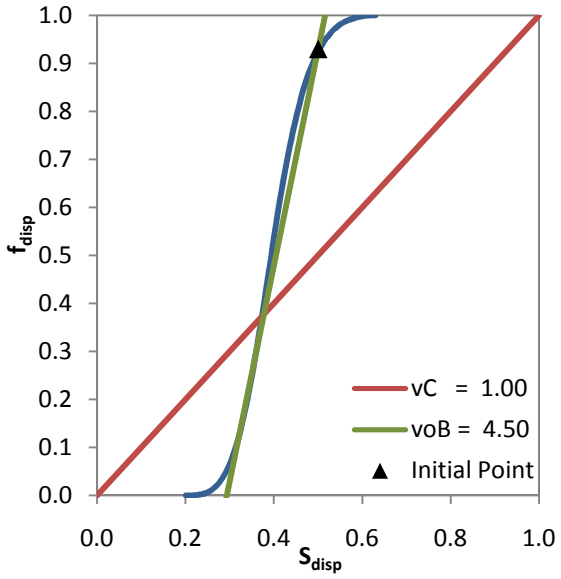

Figure A-9 Fractional Flow Curve for Chateaurenard Pilot

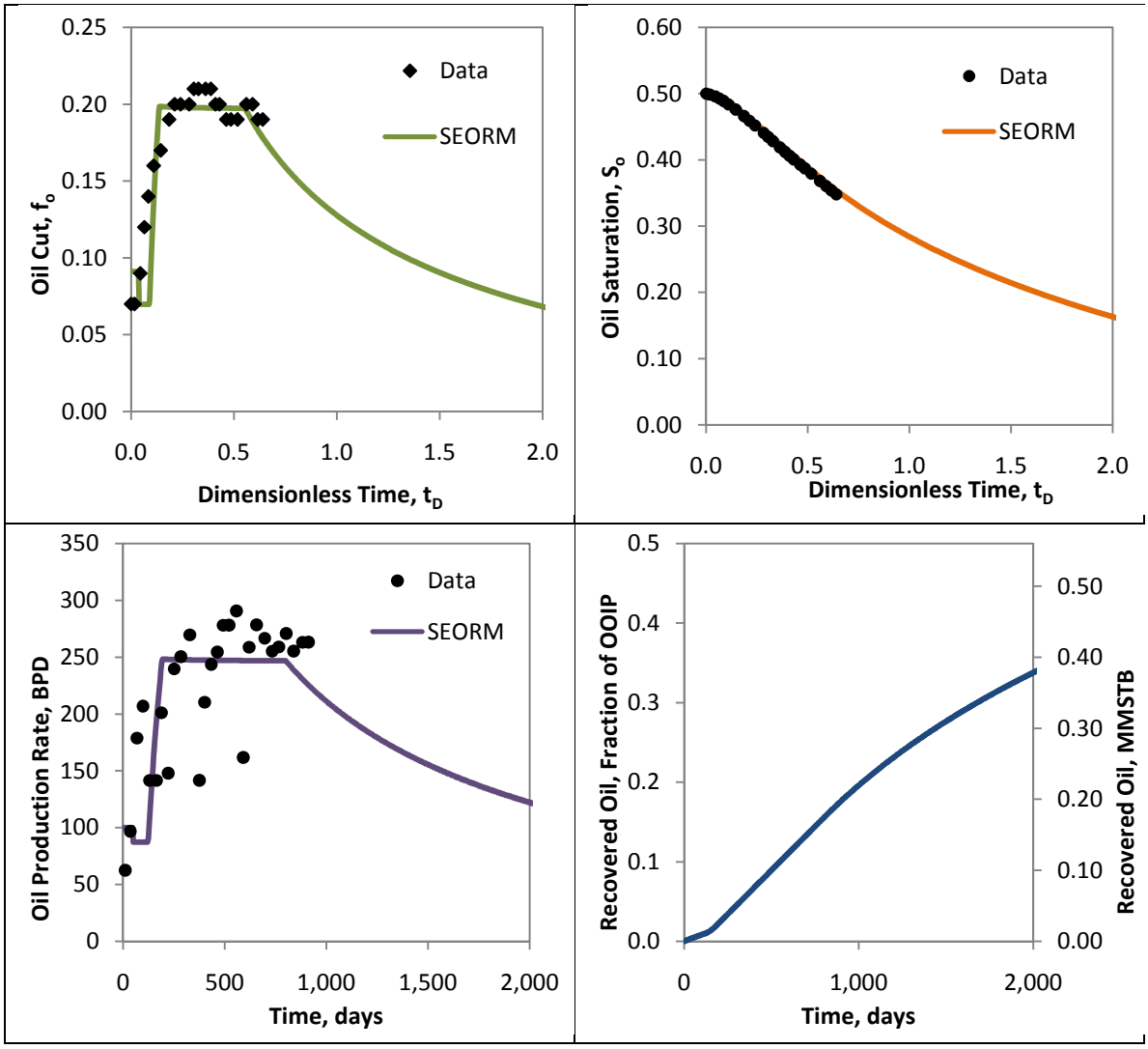

Figure A-10 Plots for Fitted Chateaurenard Pilot Data

References: Putz et al. 1981, Chapotin et al. 1986, and Putz et al. 1988

A.1.6 Loudon Pilot

Table A-6 Summary of Inputs for Loudon Pilot

Oil Saturations			Fractional Flow Inputs		
S_{oI}	0.68		k^o_{rw}	0.17	
S_{oR}	0.24		k^o_{ro}	1.00	
S_{or}	0.16		n	2.0	
S_{oB}	0.34		m	2.0	
S_{oF}	0.08		μ_o	5.0	cp
ΔS_o	0.17		μ_w	1.0	cp
Oil Cuts			μ_c (Inj. Chem.)	40.0	cp
f_{oI}	0.04		**Reservoir Properties**		
f_{oB}	0.29		V_p	17200	RB
f_{oF}	0.00		OOIP	11610	STB
Flood Behavior			B_o	1.00	RB/STB
K_1	1.31		Well Spacing	0.7	acres
K_2	1.83		Field Size	0.7	acres
v_{oB}	2.42		**Other Inputs**		
v_C	1.08		Z_{Sur}	2.2	% conc.
K_f	0.32		Z_{Poly}	1000	ppm

Flood Injection Inputs				
Fluid	Surfactant	Polymer	Water	
q_I	78	75	75	STB/day
q_P	78	75	75	STB/day
Slug Size	0.30	1.25	0.14	Frac. V_p

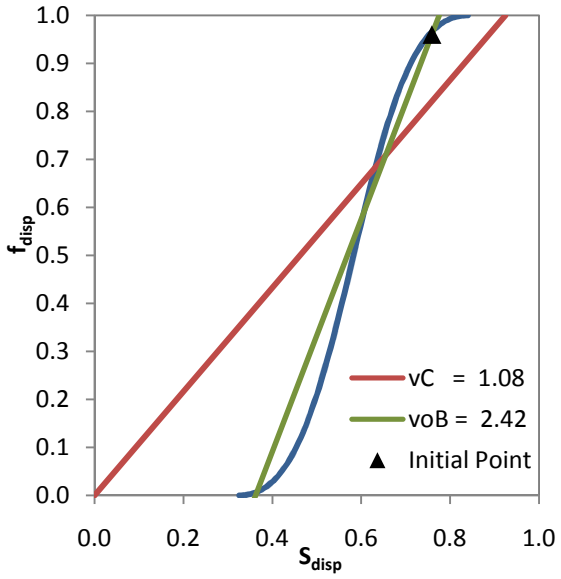

Figure A-11 Fractional Flow Curve for Loudon Pilot

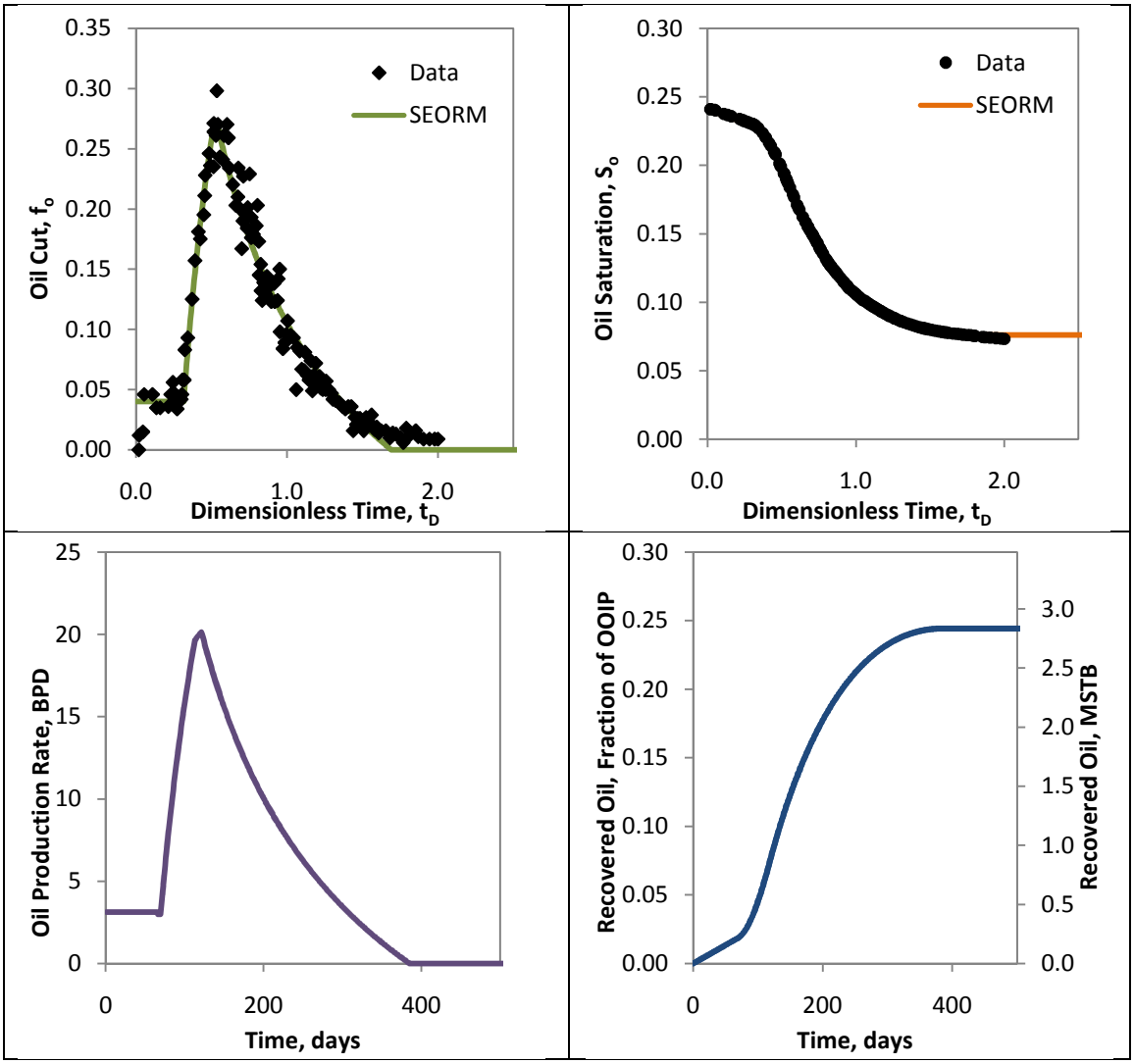

Figure A-12 Plots for Fitted Loudon Pilot Data

References: Reppert et al. 1990

A.1.7 Manvel Pilot

Table A-7 Summary of Inputs for Manvel Pilot

Oil Saturations			Fractional Flow Inputs		
S_{oI}	0.58		k^o_{rw}	0.20	
S_{oR}	0.30		k^o_{ro}	0.45	
S_{or}	0.25		n	2.0	
S_{oB}	0.38		m	2.3	
S_{oF}	0.25		μ_o	4.0	cp
ΔS_o	0.05		μ_w	1.0	cp
Oil Cuts			μ_c (Inj. Chem.)	50.0	cp
f_{oI}	0.01		**Reservoir Properties**		
f_{oB}	0.17		V_p	695000	RB
f_{oF}	0.00		OOIP	403100	STB
Flood Behavior			B_o	1.00	RB/STB
K_1	3.72		Well Spacing	2.75	acres
K_2	5.58		Field Size	5.5	acres
v_{oB}	2.00		**Other Inputs**		
v_C	1.33		Z_{Sur}	2.5	% conc.
K_f	1.00		Z_{Poly}	1000	ppm

Flood Injection Inputs				
Fluid	Surfactant	Polymer	Water	
q_I	2000	2000	2000	STB/day
q_P	3500	3500	3500	STB/day
Slug Size	0.25	0.50	3.19	Frac. V_p

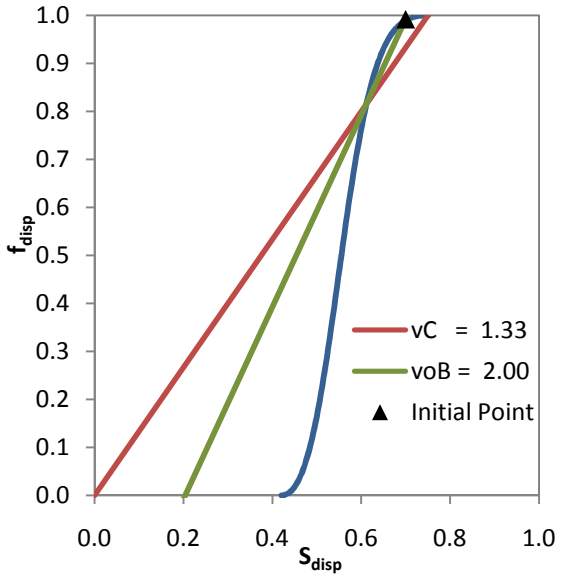

Figure A-13 Fractional Flow Curve for Manvel Pilot

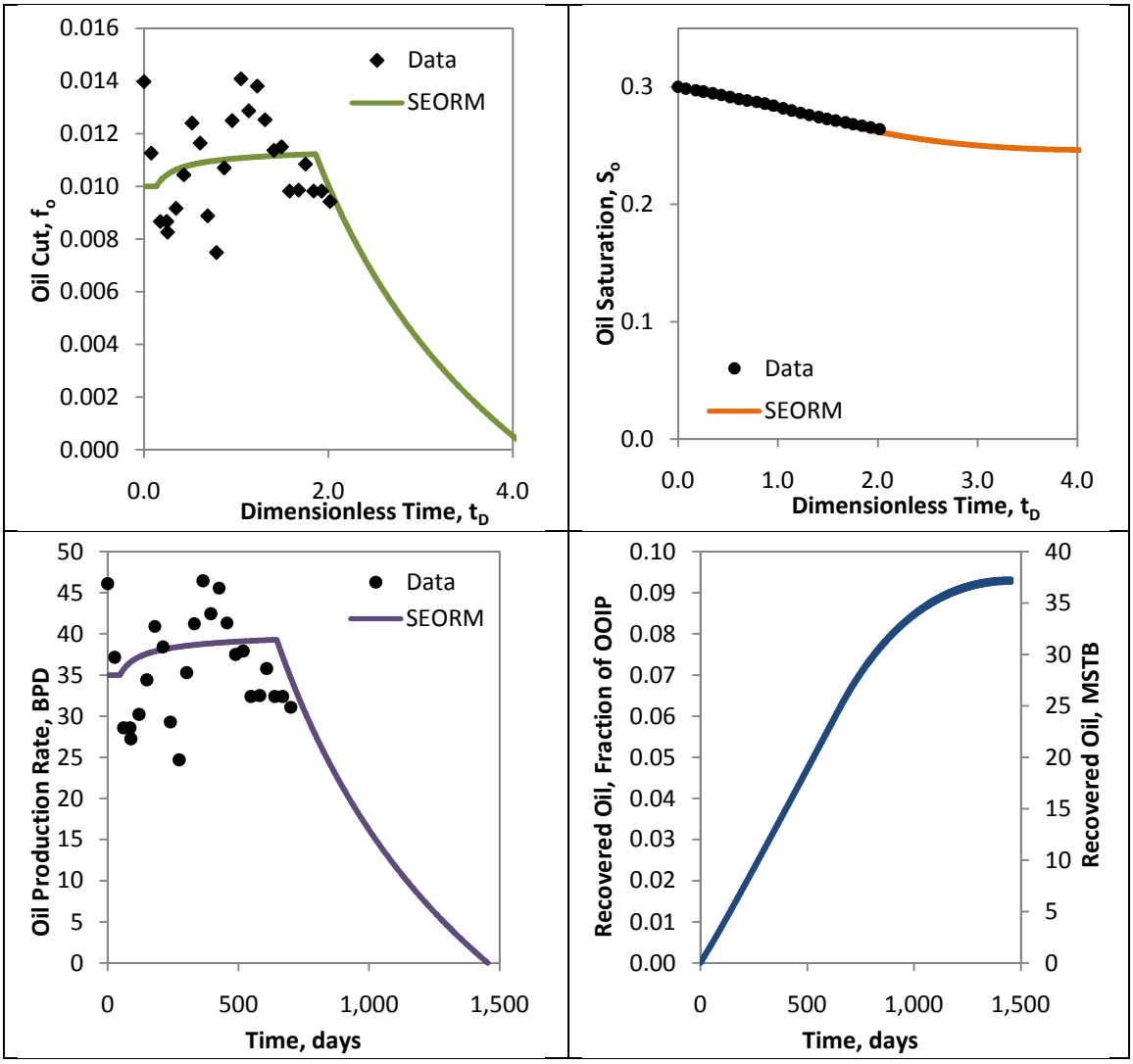

Figure A-14 Plots for Fitted Manvel Pilot Data

References: Widmyer and Pindell 1981

A.1.8 Robinson Pilot

Table A-8 Summary of Inputs for Robinson Pilot

Oil Saturations			Fractional Flow Inputs		
S_{oI}	0.75		k^o_{rw}	0.15	
S_{oR}	0.40		k^o_{ro}	0.80	
S_{or}	0.32		n	3.0	
S_{oB}	0.48		m	2.0	
S_{oF}	0.26		μ_o	7.0	cp
ΔS_o	0.14		μ_w	1.0	cp
Oil Cuts			μ_c (Inj. Chem.)	30.0	cp
f_{oI}	0.05		**Reservoir Properties**		
f_{oB}	0.30		V_p	27000	RB
f_{oF}	0.00		OOIP	20250	STB
Flood Behavior			B_o	1.00	RB/STB
K_1	1.50		Well Spacing	0.75	acres
K_2	2.55		Field Size	0.75	acres
v_{oB}	3.00		**Other Inputs**		
v_C	1.35		Z_{Sur}	10	% conc.
K_f	0.57		Z_{Poly}	1200	ppm

Flood Injection Inputs				
Fluid	Surfactant	Polymer	Water	
q_I	50	60	80	STB/day
q_P	60	60	80	STB/day
Slug Size	0.09	1.90	0.00	Frac. V_p

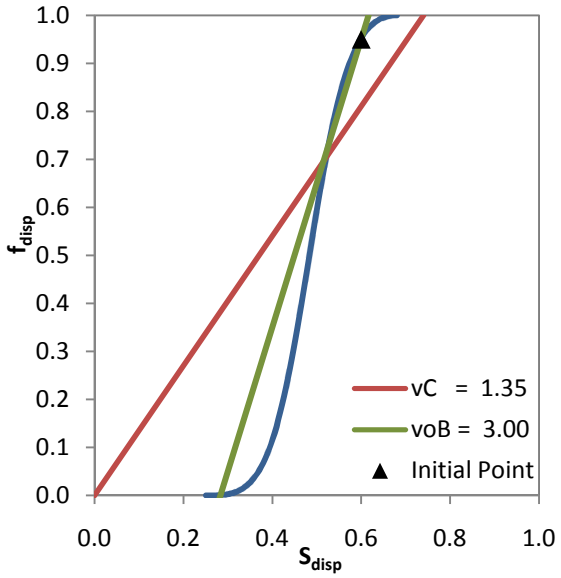

Figure A-15 Fractional Flow Curve for Robinson Pilot

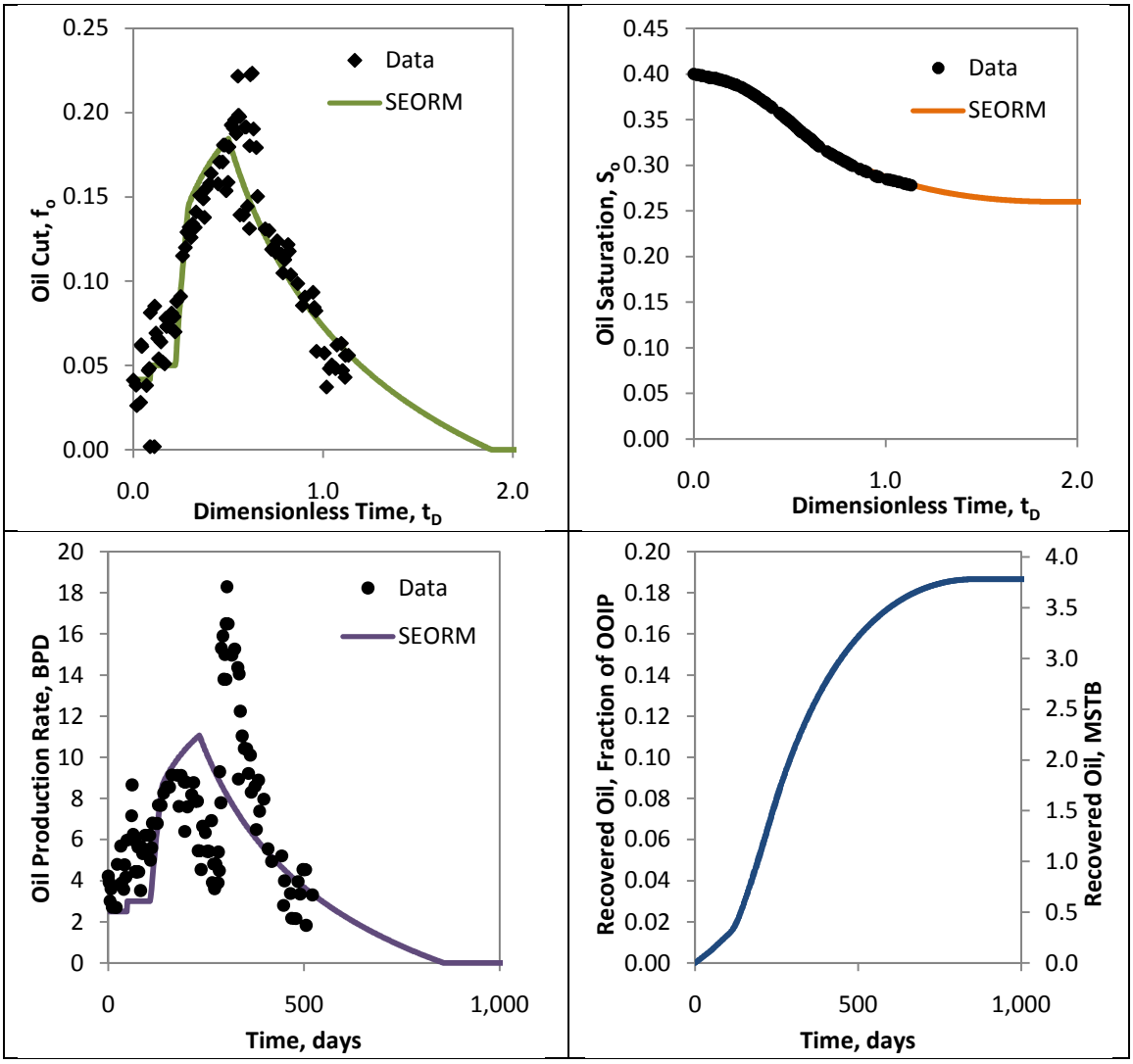

Figure A-16 Plots for Fitted Robinson Pilot Data

References: Gogarty and Surkalo 1972, Stover 1988

A.1.9 Sloss Pilot

Table A-9 Summary of Inputs for Sloss Pilot

Oil Saturations			Fractional Flow Inputs		
S_{oI}	0.79		k^o_{rw}	0.20	
S_{oR}	0.30		k^o_{ro}	1.00	
S_{or}	0.30		n	3.0	
S_{oB}	0.50		m	3.0	
S_{oF}	0.15		μ_o	0.8	cp
ΔS_o	0.15		μ_w	0.3	cp
Oil Cuts			μ_c (Inj. Chem.)	5.0	cp
f_{oI}	0.01		**Reservoir Properties**		
f_{oB}	0.42		V_p	120000	RB
f_{oF}	0.00		OOIP	79000	STB
Flood Behavior			B_o	1.20	RB/STB
K_1	2.00		Well Spacing	9.0	acres
K_2	3.37		Field Size	9.0	acres
v_{oB}	2.00		**Other Inputs**		
v_C	1.18		Z_{Sur}	5	% conc.
K_f	0.98		Z_{Poly}	1500	ppm

Flood Injection Inputs				
Fluid	Surfactant	Polymer	Water	
q_I	225	110	130	STB/day
q_P	225	110	130	STB/day
Slug Size	0.07	1.67	1.13	Frac. V_p

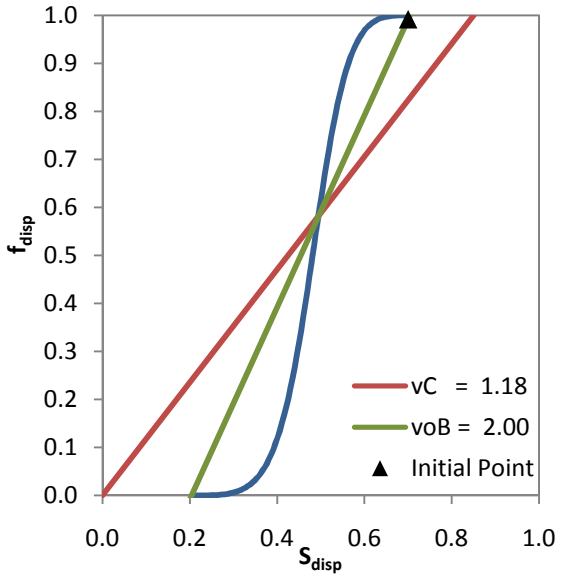

Figure A-17 Fractional Flow Curve for Sloss Pilot

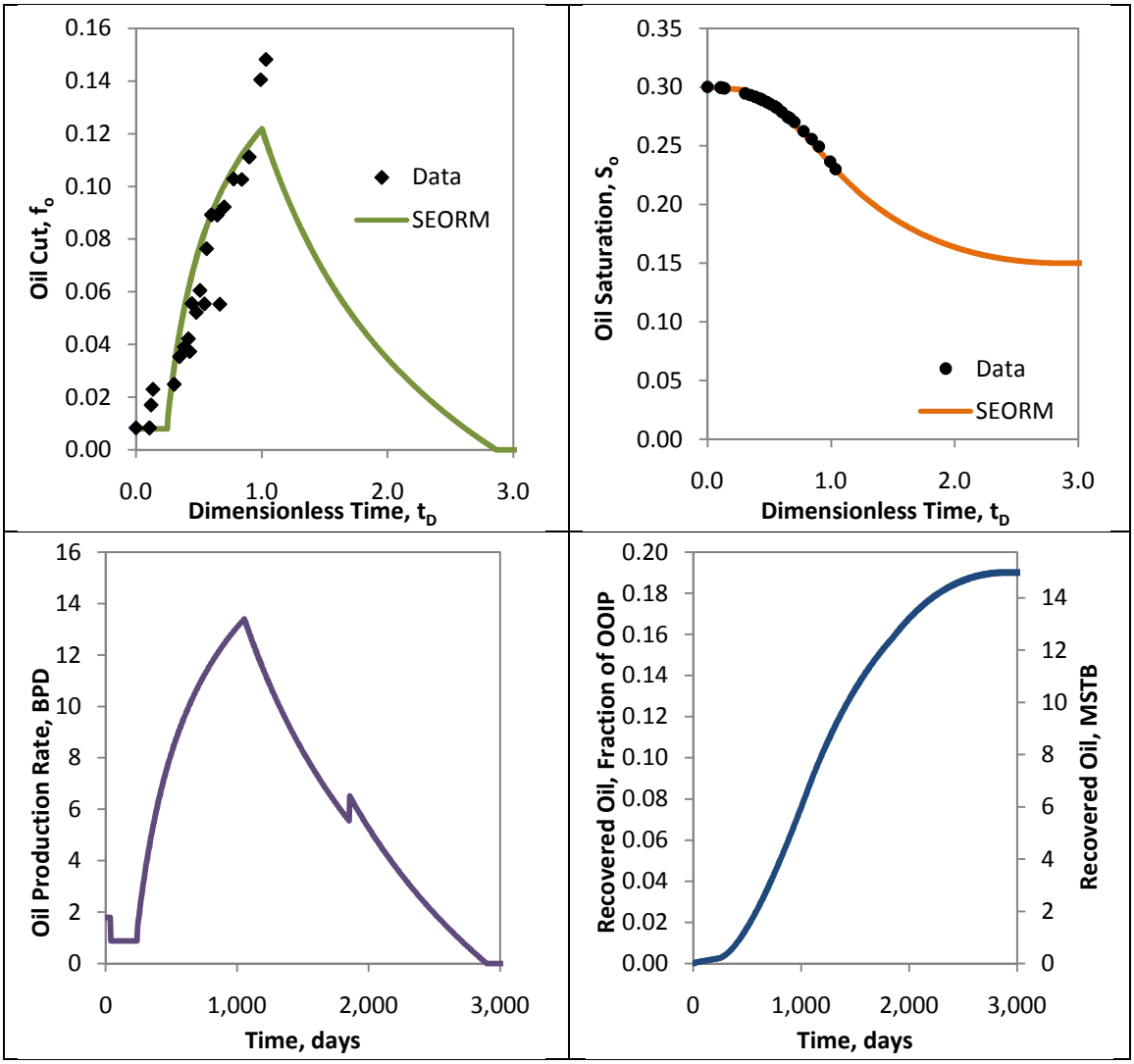

Figure A-18 Plots for Fitted Sloss Pilot Data

References: Wanosik 1978

A.1.10 Wilmington Pilot

Table A-10 Summary of Inputs for Wilmington Pilot

Oil Saturations			Fractional Flow Inputs		
S_{oI}	0.85		k^o_{rw}	0.20	
S_{oR}	0.35		k^o_{ro}	0.70	
S_{or}	0.25		n	5.0	
S_{oB}	0.50		m	2.0	
S_{oF}	0.23		μ_o	25.0	cp
ΔS_o	0.12		μ_w	1.0	cp
Oil Cuts			μ_c (Inj. Chem.)	40.0	cp
f_{oI}	0.02		**Reservoir Properties**		
f_{oB}	0.35		V_p	1E+06	RB
f_{oF}	0.00		OOIP	1E+06	STB
Flood Behavior			B_o	1.00	RB/STB
K_1	1.71		Well Spacing	2.6	acres
K_2	2.85		Field Size	10.3	acres
v_{oB}	2.17		**Other Inputs**		
v_C	1.30		Z_{Sur}	13.4	% conc.
K_f	0.99		Z_{Poly}	2500	ppm

Flood Injection Inputs				
Fluid	Surfactant	Polymer	Water	
q_I	2000	2000	2000	STB/day
q_P	4500	3500	3500	STB/day
Slug Size	0.13	0.93	1.14	Frac. V_p

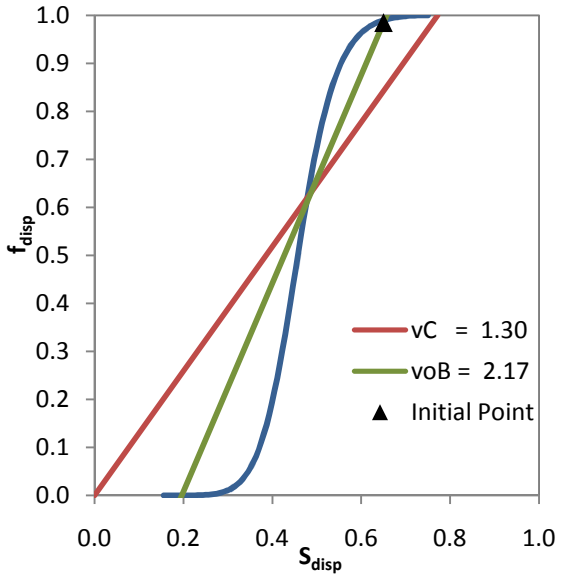

Figure A-19 Fractional Flow Curve for Wilmington Pilot

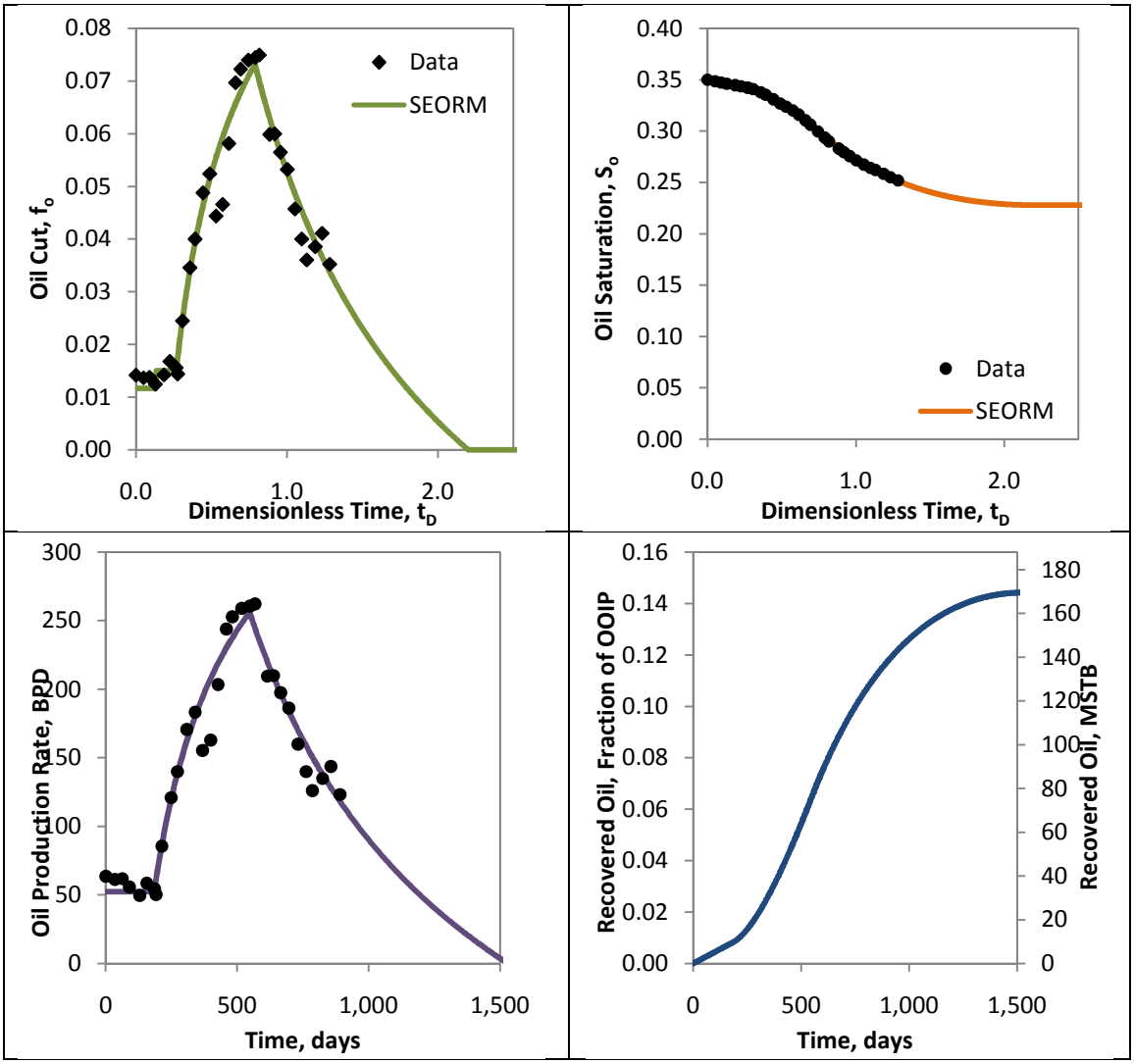

Figure A-20 Plots for Fitted Wilmington Pilot Data

References: Aguey 1982

A.2 Fitted Field Scale Surfactant-Polymer Floods

The following is the full set of field scale SP flood project that were fitted with SEORM along with the inputs used for the fits. The tables follow the same color scheme mentioned earlier. Several plots are provided for every fit, including ones for oil cut, oil saturation, oil production rate, oil recovery, and the fitted fractional flow curve.

A.2.1 M-1 2.5 Acre Field

Table A-11 Summary of Inputs for M-1 2.5 Acre Field

Oil Saturations			Fractional Flow Inputs		
S_{oI}	0.75		k^o_{rw}	0.15	
S_{oR}	0.40		k^o_{ro}	0.80	
S_{or}	0.32		N	3.0	
S_{oB}	0.45		M	2.0	
S_{oF}	0.31		μ_o	7.0	cp
ΔS_o	0.09		μ_w	1.0	cp
Oil Cuts			μ_c (Inj. Chem.)	25.0	cp
f_{oI}	0.05		**Reservoir Properties**		
f_{oB}	0.20		V_p	9E+06	RB
f_{oF}	0.00		OOIP	7E+06	STB
Flood Behavior			B_o	1.00	RB/STB
K_1	1.62		Well Spacing	2.5	acres
K_2	2.42		Field Size	200	acres
v_{oB}	3.10		**Other Inputs**		
v_C	1.45		Z_{Sur}	10	% conc.
K_f	0.43		Z_{Poly}	750	ppm

Flood Injection Inputs				
Fluid	Surfactant	Polymer	Water	
q_I	1470	4360	3800	STB/day
q_P	1470	4360	3800	STB/day
Slug Size	0.10	1.05	0.52	Frac. V_p

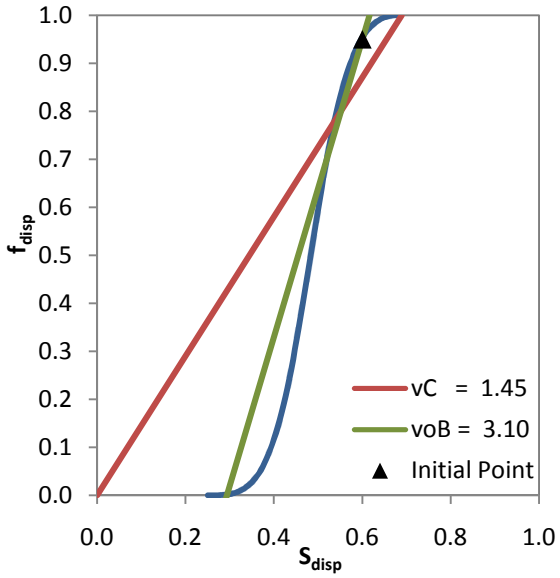

Figure A-21 Fractional Flow Curve for 1-M 2.5 Acre Field

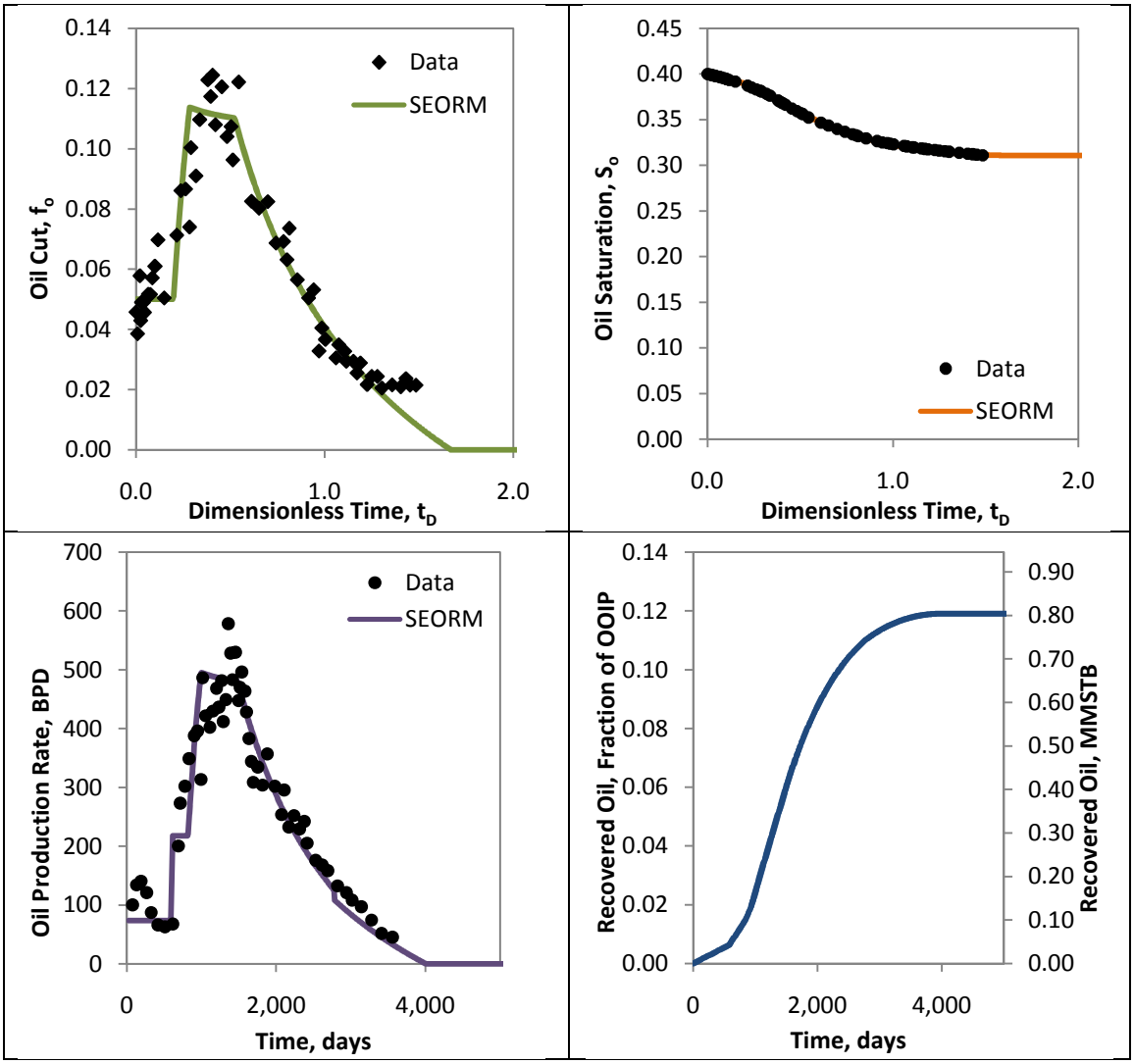

Figure A-22 Plots for Fitted 1-M 2.5 Acre Field Data

References: Gogarty and Surkalo 1972, Stover 1988

A.2.2 M-1 5.0 Acre Field

Table A-12 Summary of Inputs for M-1 5.0 Acre Field

Oil Saturations			Fractional Flow Inputs		
S_{oI}	0.75		k^o_{rw}	0.15	
S_{oR}	0.40		k^o_{ro}	0.80	
S_{or}	0.32		n	3.0	
S_{oB}	0.44		m	2.0	
S_{oF}	0.32		μ_o	7.0	cp
ΔS_o	0.08		μ_w	1.0	cp
Oil Cuts			μ_c (Inj. Chem.)	25.0	cp
f_{oI}	0.05		**Reservoir Properties**		
f_{oB}	0.17		V_p	9E+06	RB
f_{oF}	0.00		OOIP	7E+06	STB
Flood Behavior			B_o	1.00	RB/STB
K_1	1.60		Well Spacing	5.0	acres
K_2	2.40		Field Size	200	acres
v_{oB}	3.20		**Other Inputs**		
v_C	1.47		Z_{Sur}	10	% conc.
K_f	0.43		Z_{Poly}	1000	ppm

Flood Injection Inputs				
Fluid	Surfactant	Polymer	Water	
q_I	1260	1820	1820	STB/day
q_P	1260	1820	1820	STB/day
Slug Size	0.10	1.00	0.53	Frac. V_p

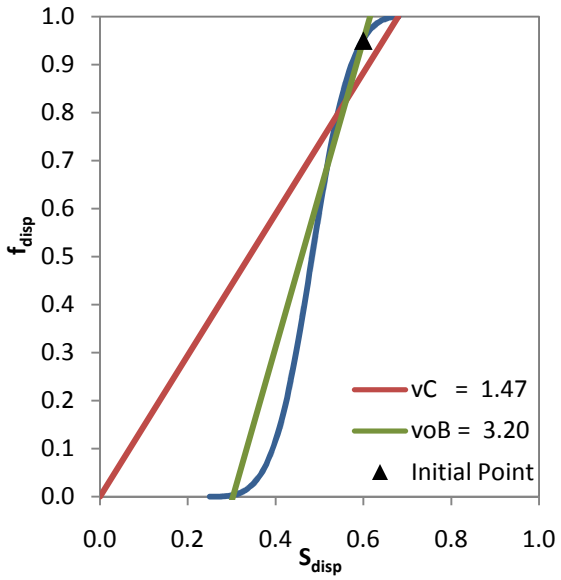

Figure A-23 Fractional Flow Curve for 1-M 5.0 Acre Field

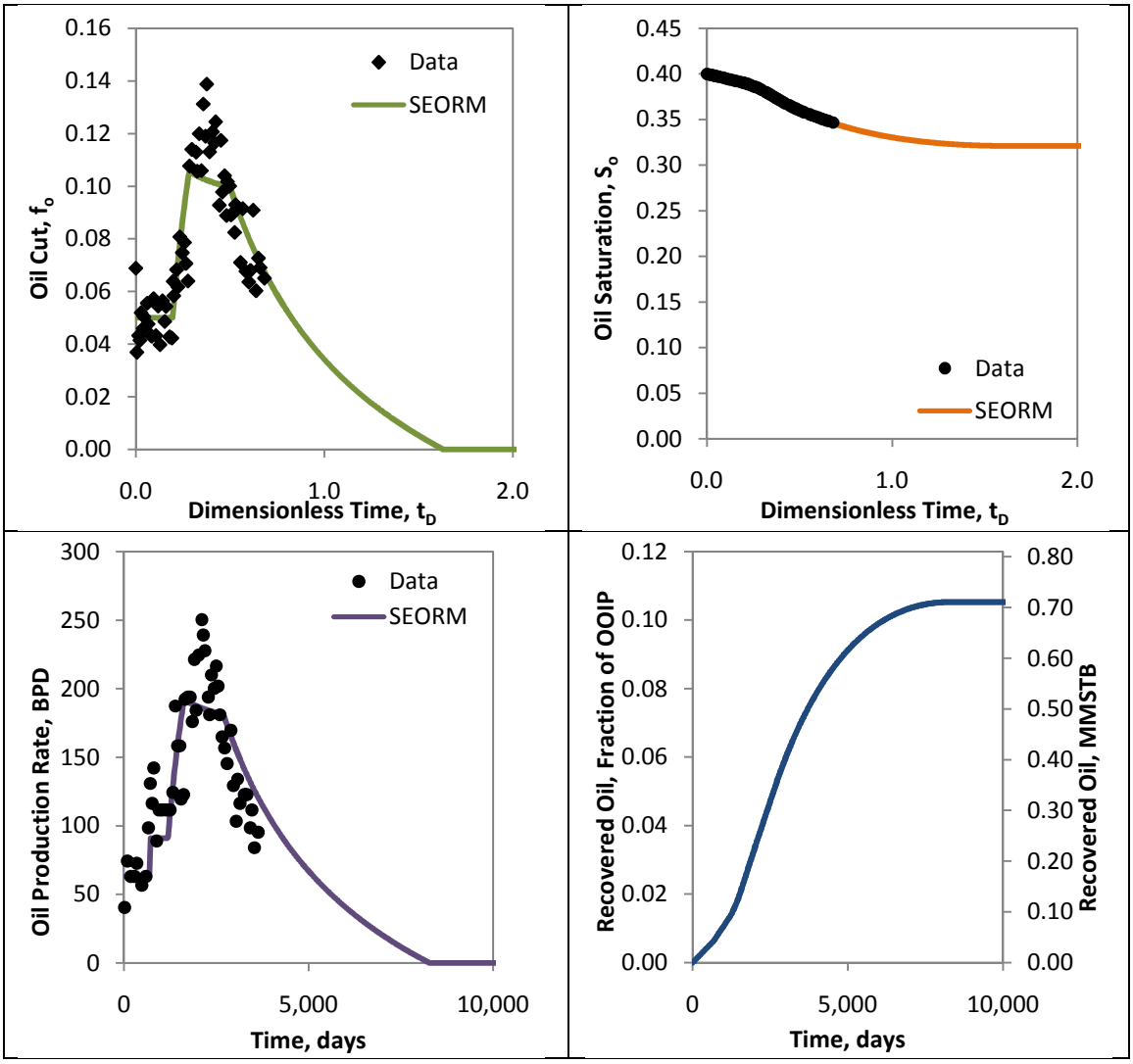

Figure A-24 Plots for Fitted 1-M 5.0 Acre Field Data

References: Gogarty and Surkalo 1972, Stover 1988

A.2.3 Bell Creek Field

Table A-13 Summary of Inputs for Bell Creek Field

Oil Saturations			Fractional Flow Inputs		
S_{oI}	0.80		k^o_{rw}	0.18	
S_{oR}	0.33		k^o_{ro}	0.80	
S_{or}	0.24		n	1.8	
S_{oB}	0.47		m	2.0	
S_{oF}	0.20		μ_o	6.0	cp
ΔS_o	0.13		μ_w	1.2	cp
Oil Cuts			μ_c (Inj. Chem.)	30.0	cp
f_{oI}	0.03		**Reservoir Properties**		
f_{oB}	0.36		V_p	9E+06	RB
f_{oF}	0.00		OOIP	7E+06	STB
Flood Behavior			B_o	1.03	RB/STB
K_1	1.25		Well Spacing	20	acres
K_2	2.00		Field Size	179	acres
v_{oB}	2.00		**Other Inputs**		
v_C	1.25		Z_{Sur}	8.1	% conc.
K_f	0.99		Z_{Poly}	950	ppm

Flood Injection Inputs				
Fluid	Surfactant	Polymer	Water	
q_I	2800	7300	7300	STB/day
q_P	8900	17800	17800	STB/day
Slug Size	0.05	0.93	0.74	Frac. V_p

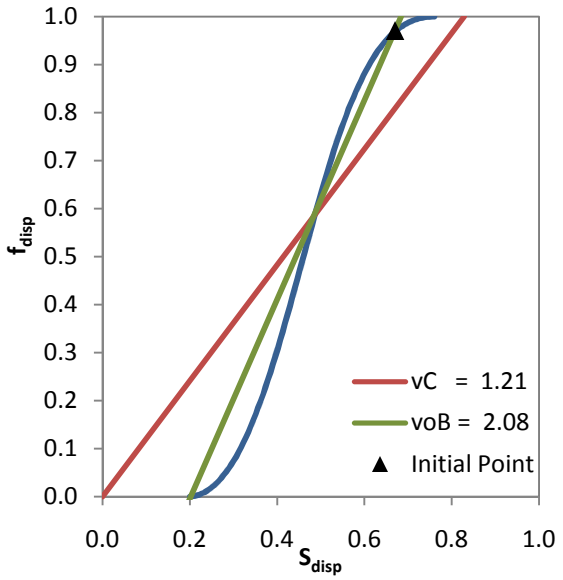

Figure A-25 Fractional Flow Curve for Bell Creek Field

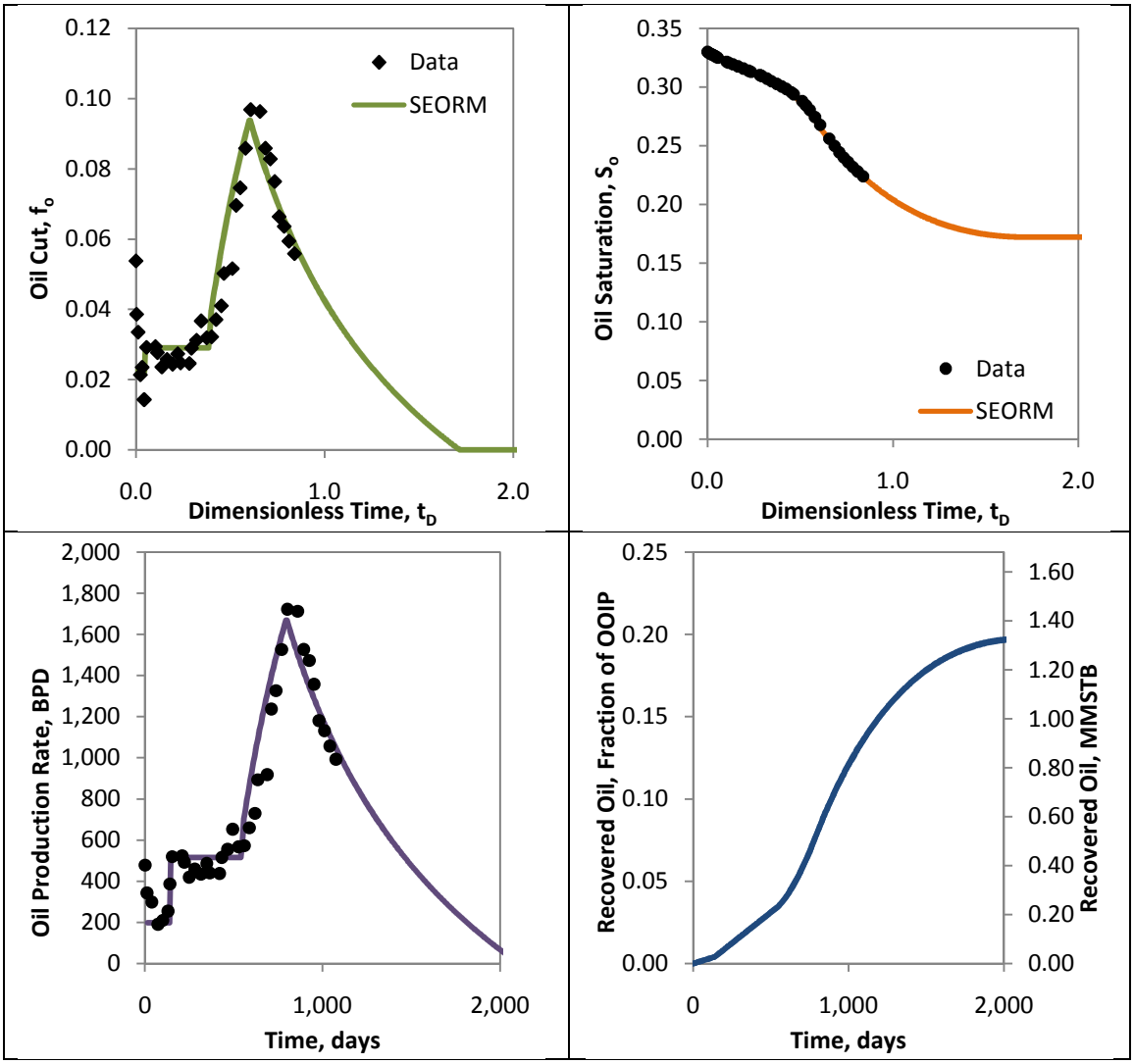

Figure A-26 Plots for Fitted Bell Creek Field Data

References: Hartshorne and Nikonchik 1984, Vargo 1978

A.2.4 Berryhill Field

Table A-14 Summary of Inputs for Berryhill Field

Oil Saturations			Fractional Flow Inputs		
S_{oI}	0.71		k^o_{rw}	0.15	
S_{oR}	0.30		k^o_{ro}	0.80	
S_{or}	0.27		n	3.0	
S_{oB}	0.39		m	2.0	
S_{oF}	0.22		μ_o	4.0	cp
ΔS_o	0.09		μ_w	1.0	cp
Oil Cuts			μ_c (Inj. Chem.)	40.0	cp
f_{oI}	0.01		**Reservoir Properties**		
f_{oB}	0.22		V_p	1E+07	RB
f_{oF}	0.00		OOIP	9E+06	STB
Flood Behavior			B_o	1.00	RB/STB
K_1	3.75		Well Spacing	4.4	acres
K_2	7.36		Field Size	92	acres
v_{oB}	2.50		**Other Inputs**		
v_C	1.27		Z_{Sur}	5	% conc.
K_f	1.00		Z_{Poly}	1000	ppm

Flood Injection Inputs				
Fluid	Surfactant	Polymer	Water	
q_I	13000	22000	30000	STB/day
q_P	15000	25000	34000	STB/day
Slug Size	0.10	0.70	4.98	Frac. V_p

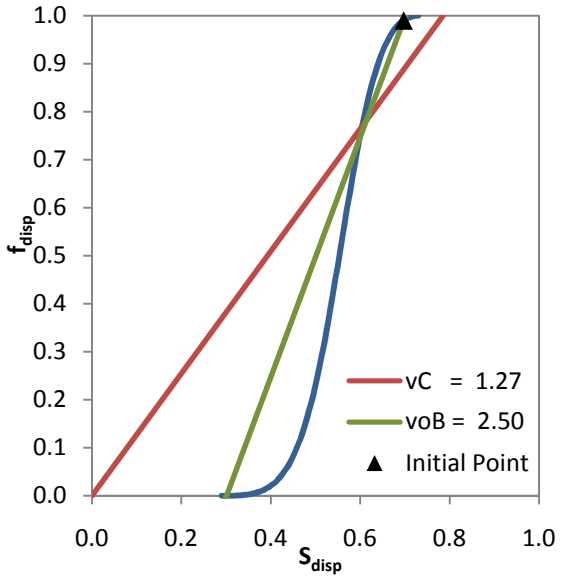

Figure A-27 Fractional Flow Curve for Berryhill Field

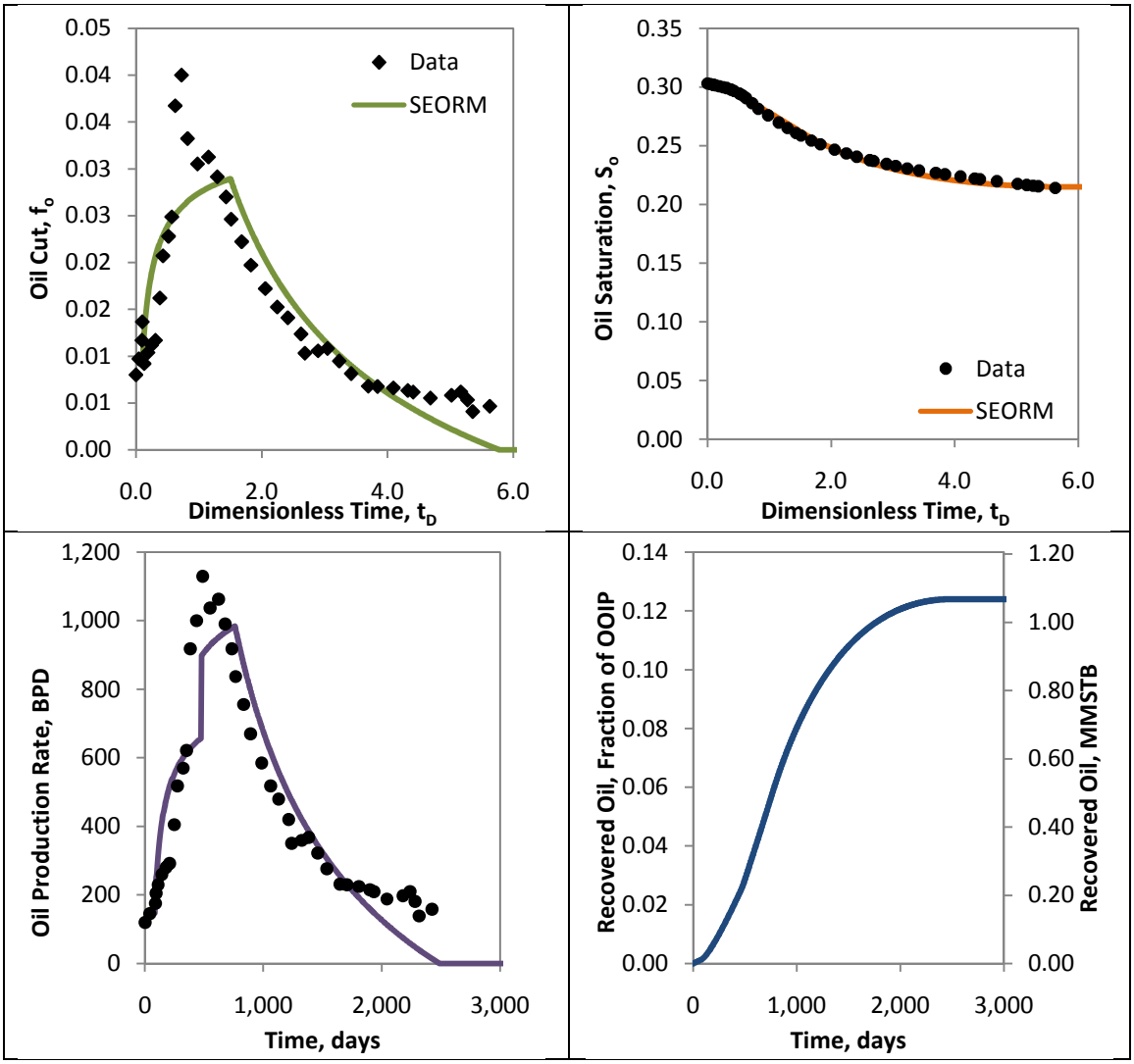

Figure A-28 Plots for Fitted Berryhill Field Data

References: Crawford and Crawford 1985, Bae 1995, Bae and Syed 1988

A.2.5 Big Muddy Field

Table A-15 Summary of Inputs for Big Muddy Field

Oil Saturations			Fractional Flow Inputs		
S_{oI}	0.53		k^o_{rw}	0.10	
S_{oR}	0.32		k^o_{ro}	0.80	
S_{or}	0.31		n	6.0	
S_{oB}	0.33		m	2.0	
S_{oF}	0.23		μ_o	4.0	cp
ΔS_o	0.09		μ_w	0.7	cp
Oil Cuts			μ_c (Inj. Chem.)	12.0	cp
f_{oI}	0.01		**Reservoir Properties**		
f_{oB}	0.14		V_p	9E+06	RB
f_{oF}	0.00		OOIP	5E+06	STB
Flood Behavior			B_o	1.00	RB/STB
K_1	1.50		Well Spacing	10	acres
K_2	4.10		Field Size	90	acres
v_{oB}	8.70		**Other Inputs**		
v_C	1.30		Z_{Sur}	3	% conc.
K_f	0.30		Z_{Poly}	1000	ppm

Flood Injection Inputs				
Fluid	Surfactant	Polymer	Water	
q_I	1900	1700	1500	STB/day
q_P	3850	3150	2700	STB/day
Slug Size	0.10	0.18	2.88	Frac. V_p

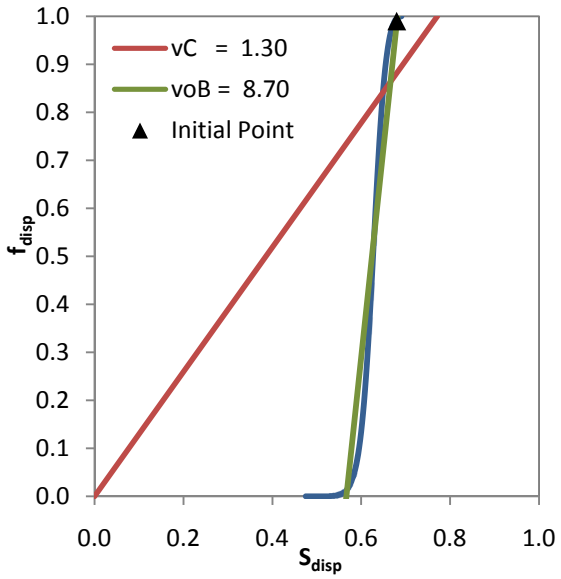

Figure A-29 Fractional Flow Curve for Big Muddy Field

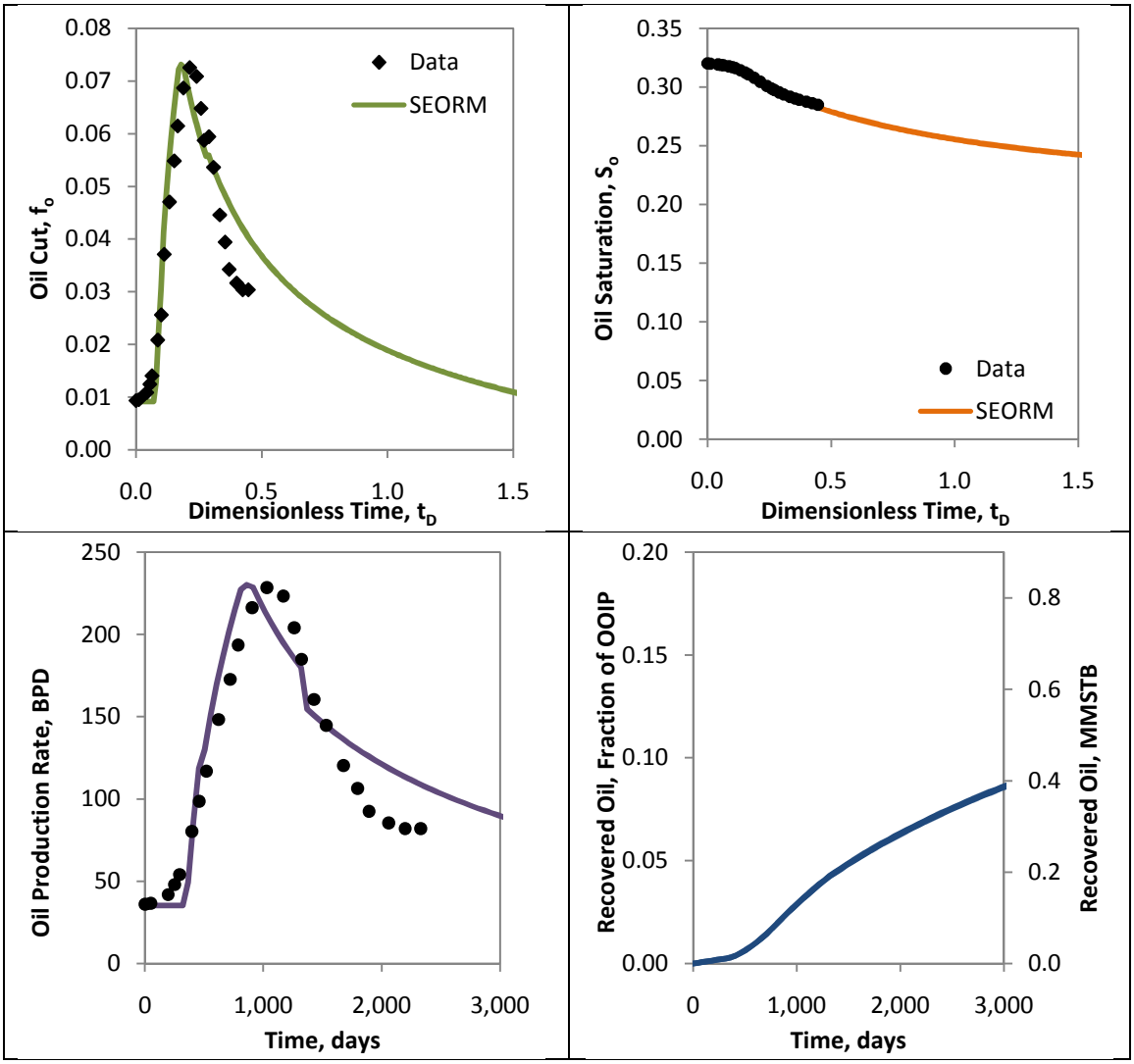

Figure A-30 Plots for Fitted Big Muddy Field Data

References: Saad et al. 1989, Ferrell et al. 1988, Haller 1955

A.2.6 Altered Big Muddy Field

Table A-16 Summary of Inputs for Altered Big Muddy Field

Oil Saturations			Fractional Flow Inputs		
S_{oI}	0.53		k^o_{rw}	0.10	
S_{oR}	0.32		k^o_{ro}	0.80	
S_{or}	0.31		n	6.0	
S_{oB}	0.35		m	2.0	
S_{oF}	0.24		μ_o	4.0	cp
ΔS_o	0.09		μ_w	0.7	cp
Oil Cuts			μ_c (Inj. Chem.)	12.0	cp
f_{oI}	0.01		**Reservoir Properties**		
f_{oB}	0.14		V_p	5E+06	RB
f_{oF}	0.00		OOIP	3E+06	STB
Flood Behavior			B_o	1.00	RB/STB
K_1	1.75		Well Spacing	10	acres
K_2	2.30		Field Size	90	acres
v_{oB}	5.00		**Other Inputs**		
v_C	1.31		Z_{Sur}	3	% conc.
K_f	0.11		Z_{Poly}	1000	ppm

Flood Injection Inputs				
Fluid	Surfactant	Polymer	Water	
q_I	1900	1700	1500	STB/day
q_P	3850	3150	2700	STB/day
Slug Size	0.10	0.18	1.48	Frac. V_p

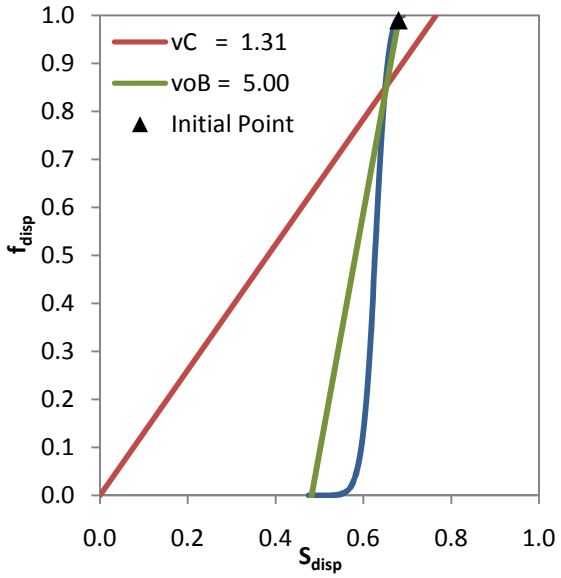

Figure A-31 Fractional Flow Curve for Altered Big Muddy Field

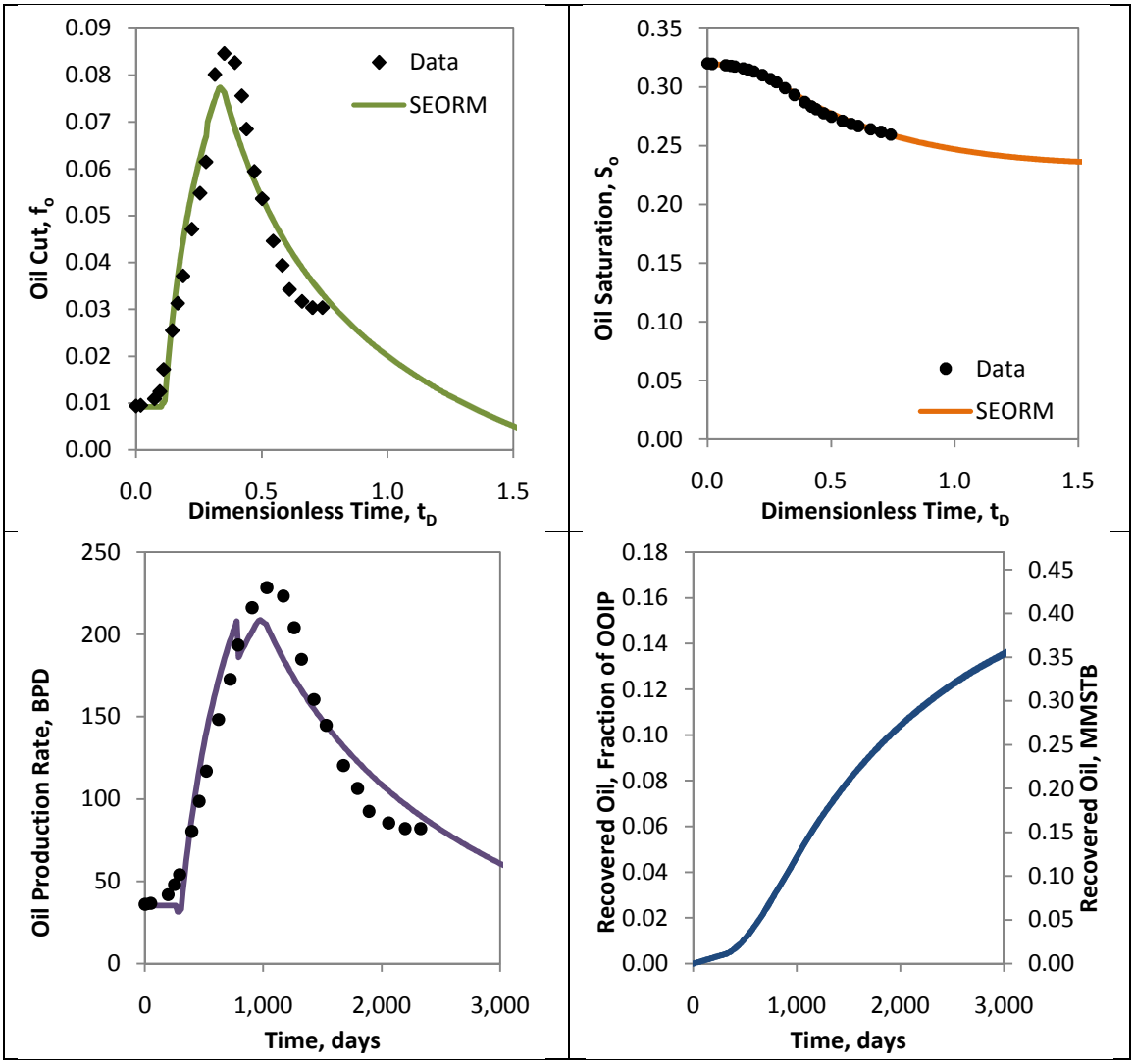

Figure A-32 Plots for Fitted Altered Big Muddy Field Data

References: Saad et al. 1989, Ferrell et al. 1988, Haller 1955

A.2.7 Bradford 7 Field

Table A-17 Summary of Inputs for Bradford 7 Field

Oil Saturations			Fractional Flow Inputs		
S_{oI}	0.65		k^o_{rw}	0.10	
S_{oR}	0.40		k^o_{ro}	0.80	
S_{or}	0.38		n	3.0	
S_{oB}	0.45		m	2.0	
S_{oF}	0.28		μ_o	5.0	cp
ΔS_o	0.13		μ_w	1.0	cp
Oil Cuts			μ_c (Inj. Chem.)	20.0	cp
f_{oI}	0.01		**Reservoir Properties**		
f_{oB}	0.24		V_p	2E+06	RB
f_{oF}	0.00		OOIP	1E+06	STB
Flood Behavior			B_o	1.00	RB/STB
K_1	1.59		Well Spacing	2.9	acres
K_2	5.00		Field Size	46	acres
v_{oB}	4.50		**Other Inputs**		
v_C	1.38		Z_{Sur}	12	% conc.
K_f	0.95		Z_{Poly}	660	ppm

Flood Injection Inputs				
Fluid	Surfactant	Polymer	Water	
q_I	1175	1400	1500	STB/day
q_P	1800	3200	2200	STB/day
Slug Size	0.05	1.20	2.37	Frac. V_p

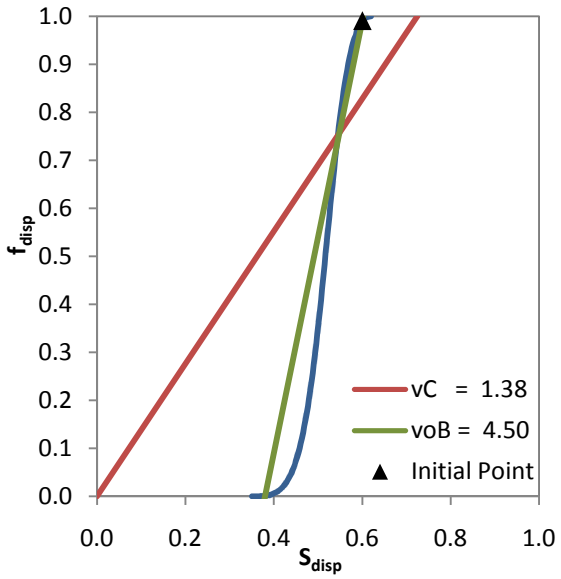

Figure A-33 Fractional Flow Curve for Bradford 7 Field

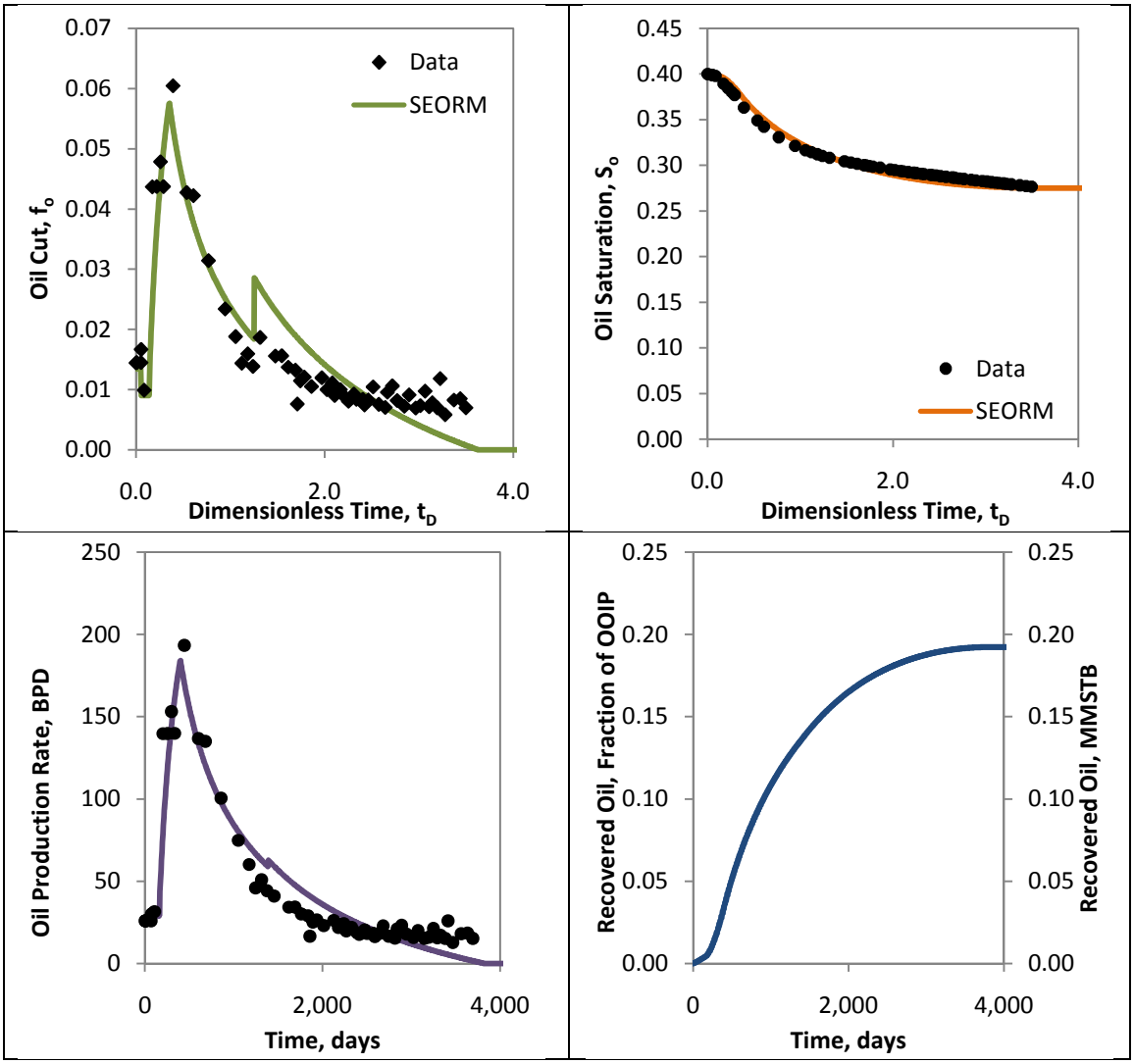

Figure A-34 Plots for Fitted Bradford 7 Field Data

References: Danielson et al. 1976, Guckert and Warren 1982, Ondrusek 1988

A.2.8 Bradford 8 Field

Table A-18 Summary of Inputs for Bradford 8 Field

Oil Saturations			Fractional Flow Inputs		
S_{oI}	0.65		k^o_{rw}	0.20	
S_{oR}	0.40		k^o_{ro}	0.80	
S_{or}	0.38		n	2.0	
S_{oB}	0.47		m	2.0	
S_{oF}	0.35		μ_o	5.0	cp
ΔS_o	0.06		μ_w	1.0	cp
Oil Cuts			μ_c (Inj. Chem.)	60.0	cp
f_{oI}	0.01		**Reservoir Properties**		
f_{oB}	0.20		V_p	6E+06	RB
f_{oF}	0.00		OOIP	4E+06	STB
Flood Behavior			B_o	1.00	RB/STB
K_1	1.50		Well Spacing	4	acres
K_2	2.25		Field Size	220	acres
v_{oB}	2.50		**Other Inputs**		
v_C	1.52		Z_{Sur}	4.8	% conc.
K_f	0.77		Z_{Poly}	5000	ppm

Flood Injection Inputs				
Fluid	Surfactant	Polymer	Water	
q_I	3000	2500	2500	STB/day
q_P	4000	4000	4000	STB/day
Slug Size	0.10	1.00	0.39	Frac. V_p

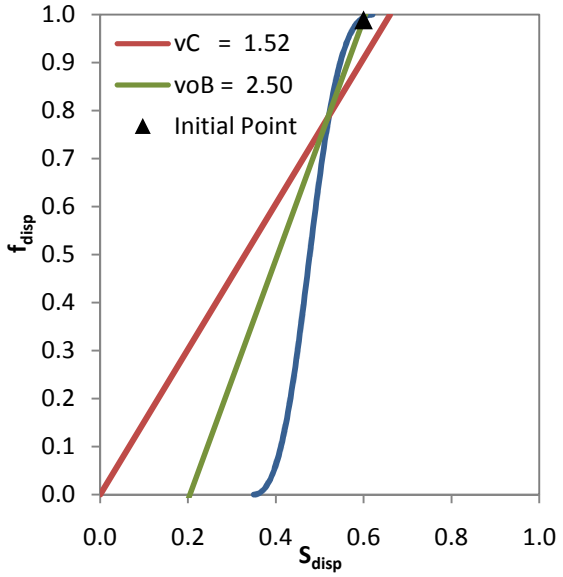

Figure A-35 Fractional Flow Curve for Bradford 8 Field

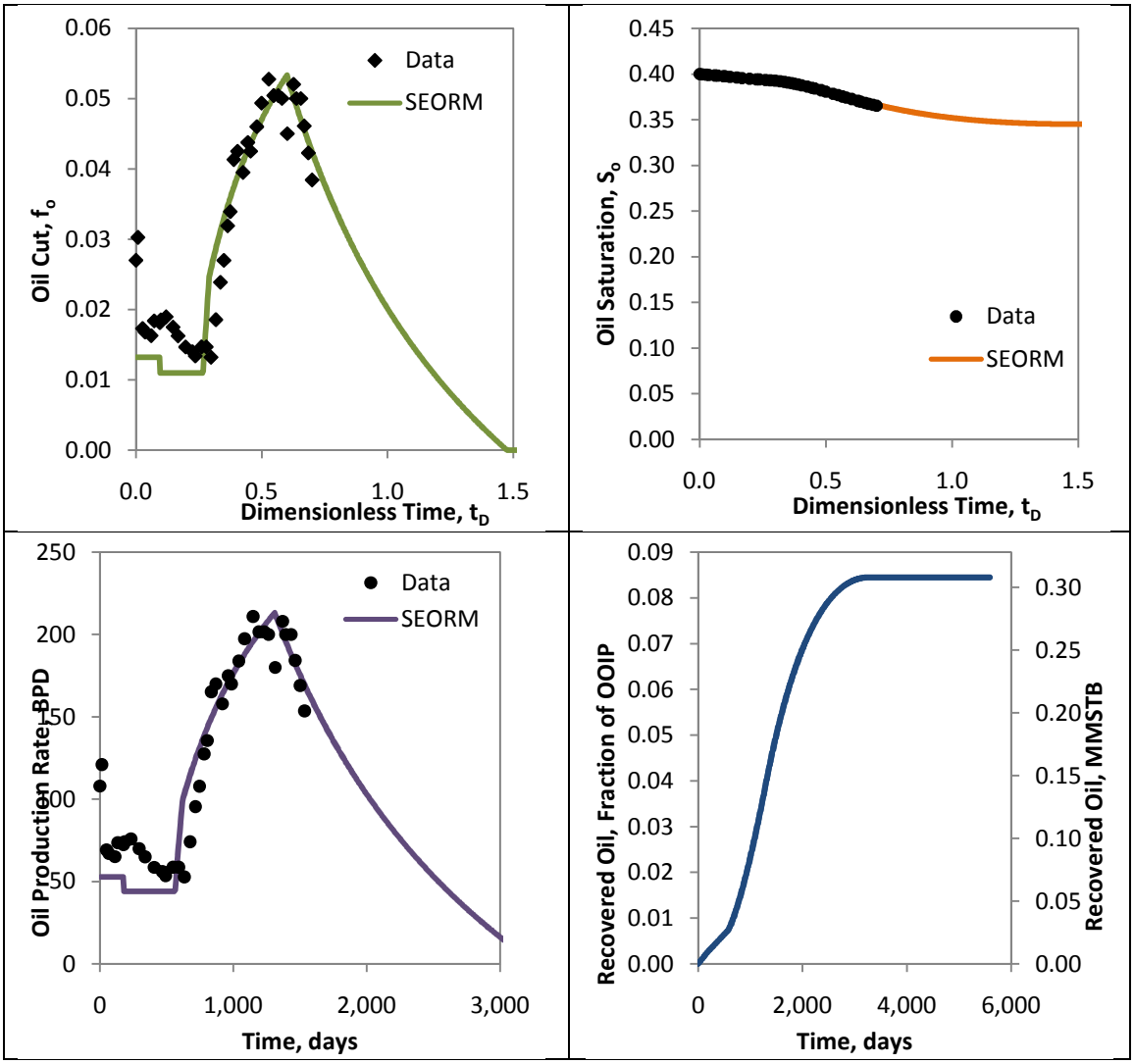

Figure A-36 Plots for Fitted Bradford 8 Field Data

Reference: Danielson et al. 1976, Guckert and Warren 1982, Ondrusek 1988

A.2.9 North Burbank Field

Table A-19 Summary of Inputs for North Burbank Field

Oil Saturations			Fractional Flow Inputs		
S_{oI}	0.60		k^o_{rw}	0.60	
S_{oR}	0.34		k^o_{ro}	0.85	
S_{or}	0.27		n	3.0	
S_{oB}	0.39		m	2.0	
S_{oF}	0.27		μ_o	3.3	cp
ΔS_o	0.07		μ_w	0.6	cp
Oil Cuts			μ_c (Inj. Chem.)	50.0	cp
f_{oI}	0.01		**Reservoir Properties**		
f_{oB}	0.17		V_p	5E+06	RB
f_{oF}	0.00		OOIP	3E+06	STB
Flood Behavior			B_o	1.00	RB/STB
K_1	2.00		Well Spacing	10	acres
K_2	4.30		Field Size	90	acres
v_{oB}	3.00		**Other Inputs**		
v_C	1.37		Z_{Sur}	6	% conc.
K_f	0.97		Z_{Poly}	1500	ppm

Flood Injection Inputs				
Fluid	Surfactant	Polymer	Water	
q_I	7000	5000	5000	STB/day
q_P	13000	13000	13000	STB/day
Slug Size	0.06	0.52	2.56	Frac. V_p

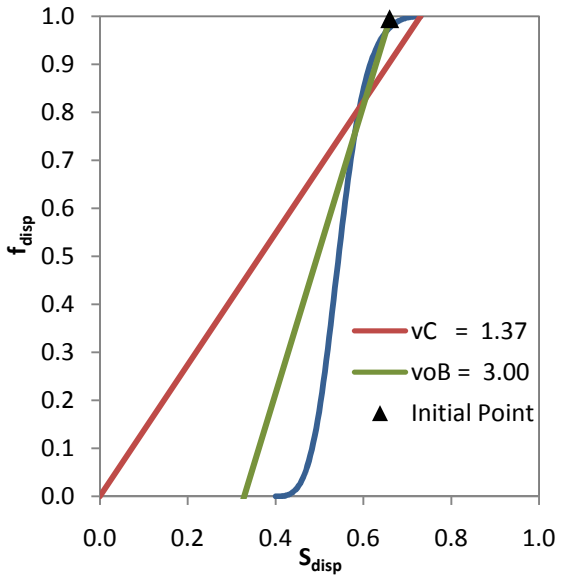

Figure A-37 Fractional Flow Curve for North Burbank Field

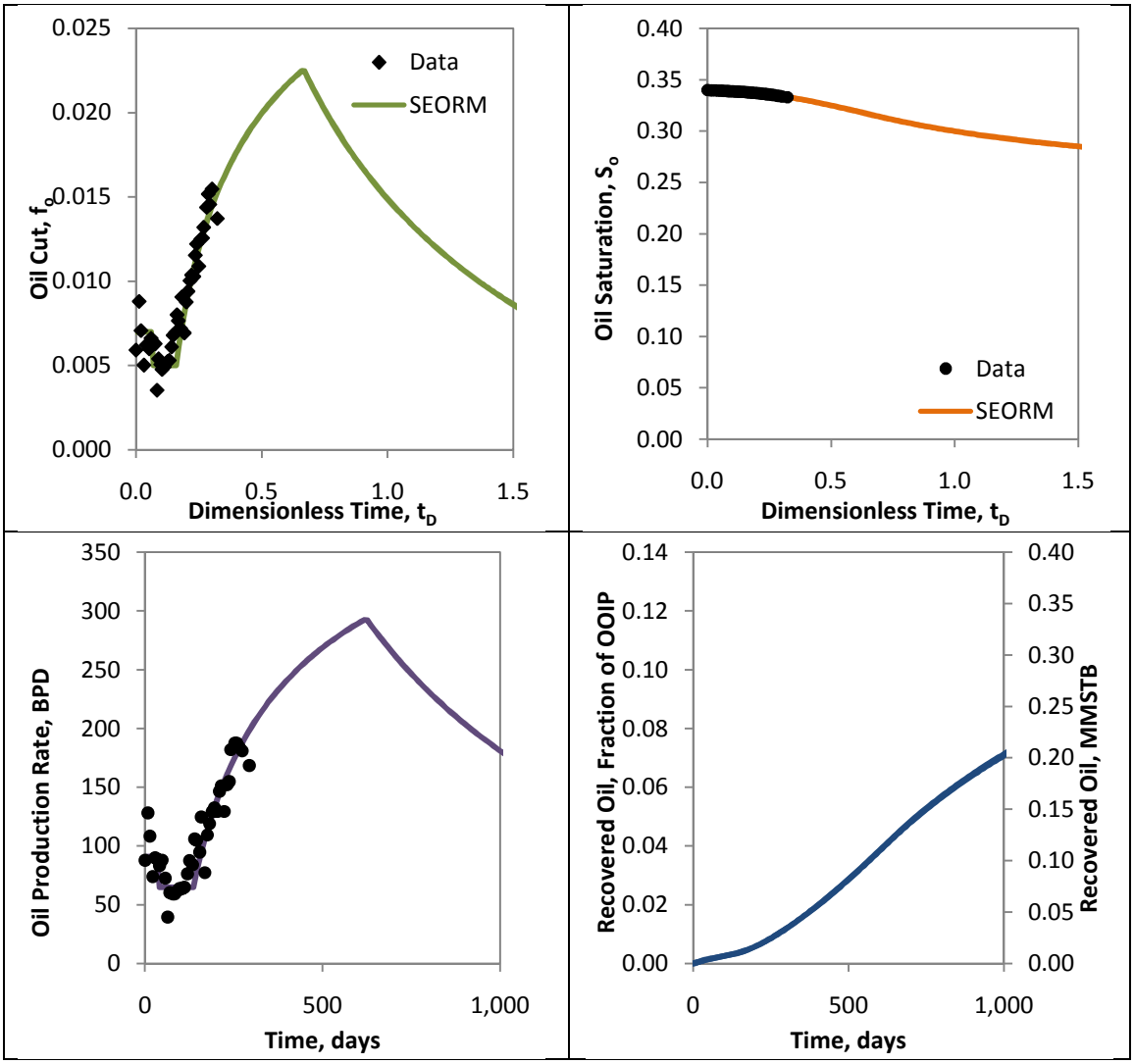

Figure A-38 Plots for Fitted North Burbank Field Data

References: Trantham et al. 1978, Trantham et al. 1980

A.2.10 Salem Field

Table A-20 Summary of Inputs for Salem Field

Oil Saturations			Fractional Flow Inputs		
S_{oI}	0.67		k^o_{rw}	0.20	
S_{oR}	0.30		k^o_{ro}	0.60	
S_{or}	0.27		n	2.0	
S_{oB}	0.44		m	2.0	
S_{oF}	0.17		μ_o	3.6	cp
ΔS_o	0.13		μ_w	1.0	cp
Oil Cuts			μ_c (Inj. Chem.)	40.0	cp
f_{oI}	0.01		**Reservoir Properties**		
f_{oB}	0.33		V_p	4E+06	RB
f_{oF}	0.00		OOIP	2E+06	STB
Flood Behavior			B_o	1.00	RB/STB
K_1	3.67		Well Spacing	5	acres
K_2	6.93		Field Size	60	acres
v_{oB}	2.28		**Other Inputs**		
v_C	1.20		Z_{Sur}	3.6	% conc.
K_f	0.99		Z_{Poly}	1400	ppm

Flood Injection Inputs				
Fluid	Surfactant	Polymer	Water	
q_I	5000	7000	7000	STB/day
q_P	5000	10000	12000	STB/day
Slug Size	0.18	0.80	4.71	Frac. V_p

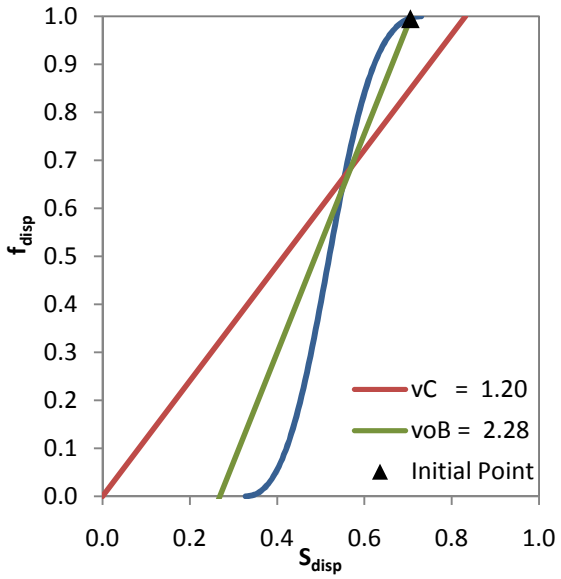

Figure A-39 Fractional Flow Curve for Salem Field

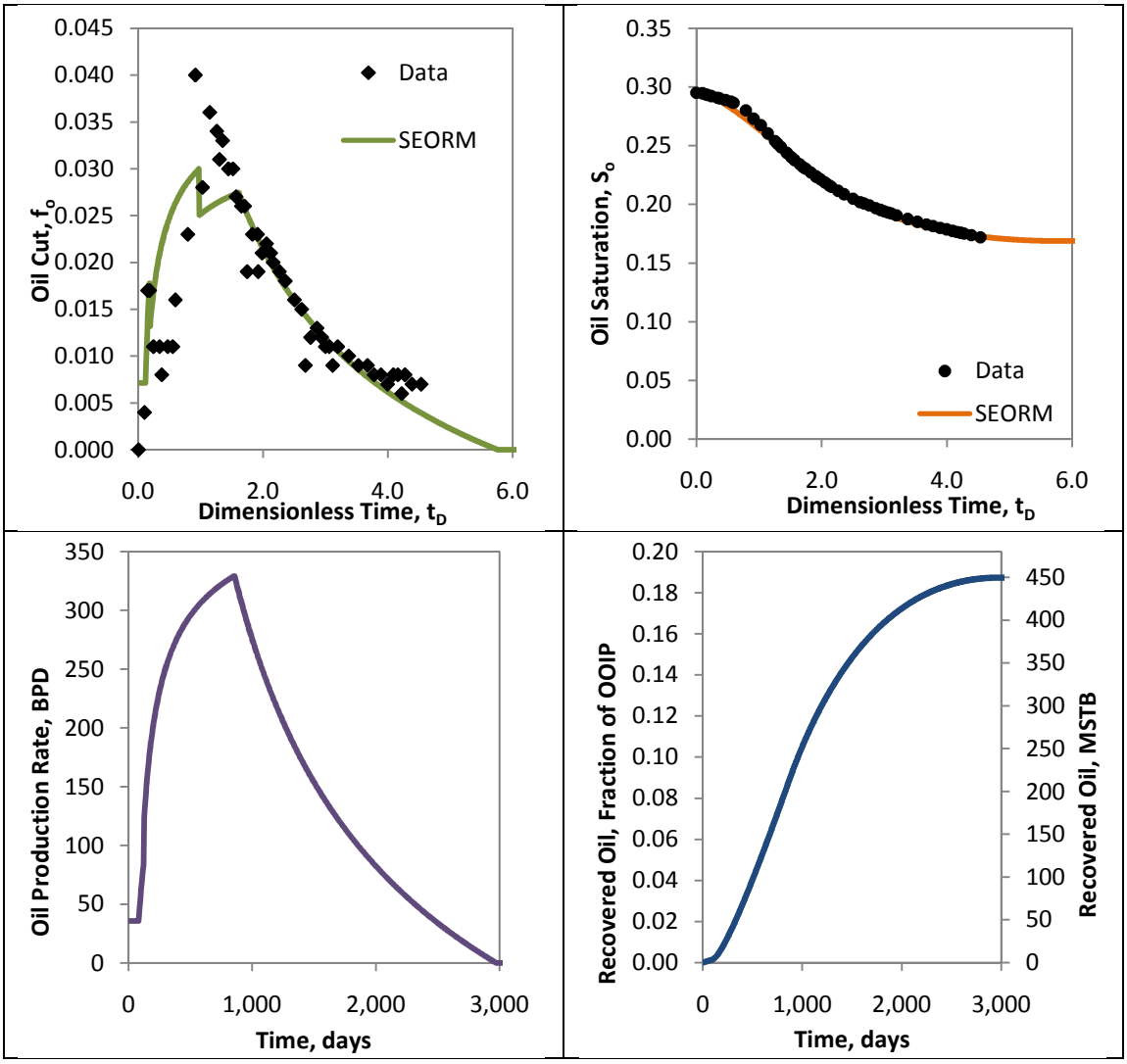

Figure A-40 Plots for Fitted Salem Field Data

References: Widmyer et al. 1988, Strange and Talash 1977

A.3 Fitted Pilot Scale Alkali-Surfactant-Polymer Floods

The following is the full set of pilot scale ASP flood projects that were fitted with SEORM along with the inputs used for the fits. The tables follow the same color scheme mentioned earlier. Several plots are provided for every fit, including ones for oil cut, oil saturation, oil production rate, oil recovery, and the fitted fractional flow curve.

A.3.1 Cambridge Pilot

Table A-21 Summary of Inputs for Cambridge Pilot

Oil Saturations			Fractional Flow Inputs		
S_{oI}	0.78		k^o_{rw}	0.20	
S_{oR}	0.66		k^o_{ro}	0.80	
S_{or}	0.31		n	2.0	
S_{oB}	0.59		m	2.0	
S_{oF}	0.22		μ_o	10.0	cp
ΔS_o	0.44		μ_w	1.0	cp
Oil Cuts			μ_c (Inj. Chem.)	--	cp
f_{oI}	0.75		**Reservoir Properties**		
f_{oB}	0.48		V_p	6E+06	RB
f_{oF}	0.00		OOIP	5E+06	STB
Flood Behavior			B_o	1.00	RB/STB
K_1	2.01		Well Spacing	4.0	acres
K_2	2.80		Field Size	4.0	acres
v_{oB}	4.00		**Other Inputs**		
v_C	1.28		Z_{Sur}	0.1	% conc.
K_f	0.19		Z_{Poly}	1000	ppm
Flood Injection Inputs			Z_{alk}	1.25	% conc.

Fluid	Alk. & Sur.	Polymer	Water	
q_I	1400	1400	1400	STB/day
q_P	1400	1400	1400	STB/day
Slug Size	0.30	0.31	1.58	Frac. V_p

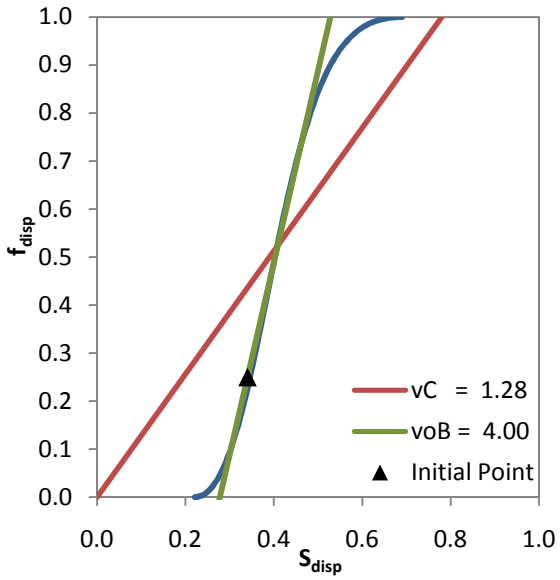
1.0
0.9
0.8
0.7
0.6
0.5
0.4
0.3
0.2
0.1
0.0
f_{disp}
0.0
0.2
0.4
0.6
0.8
1.0
S_{disp}
vC = 1.28
voB = 4.00
Initial Point

Figure A-41 Fractional Flow Curve for Cambridge Pilot

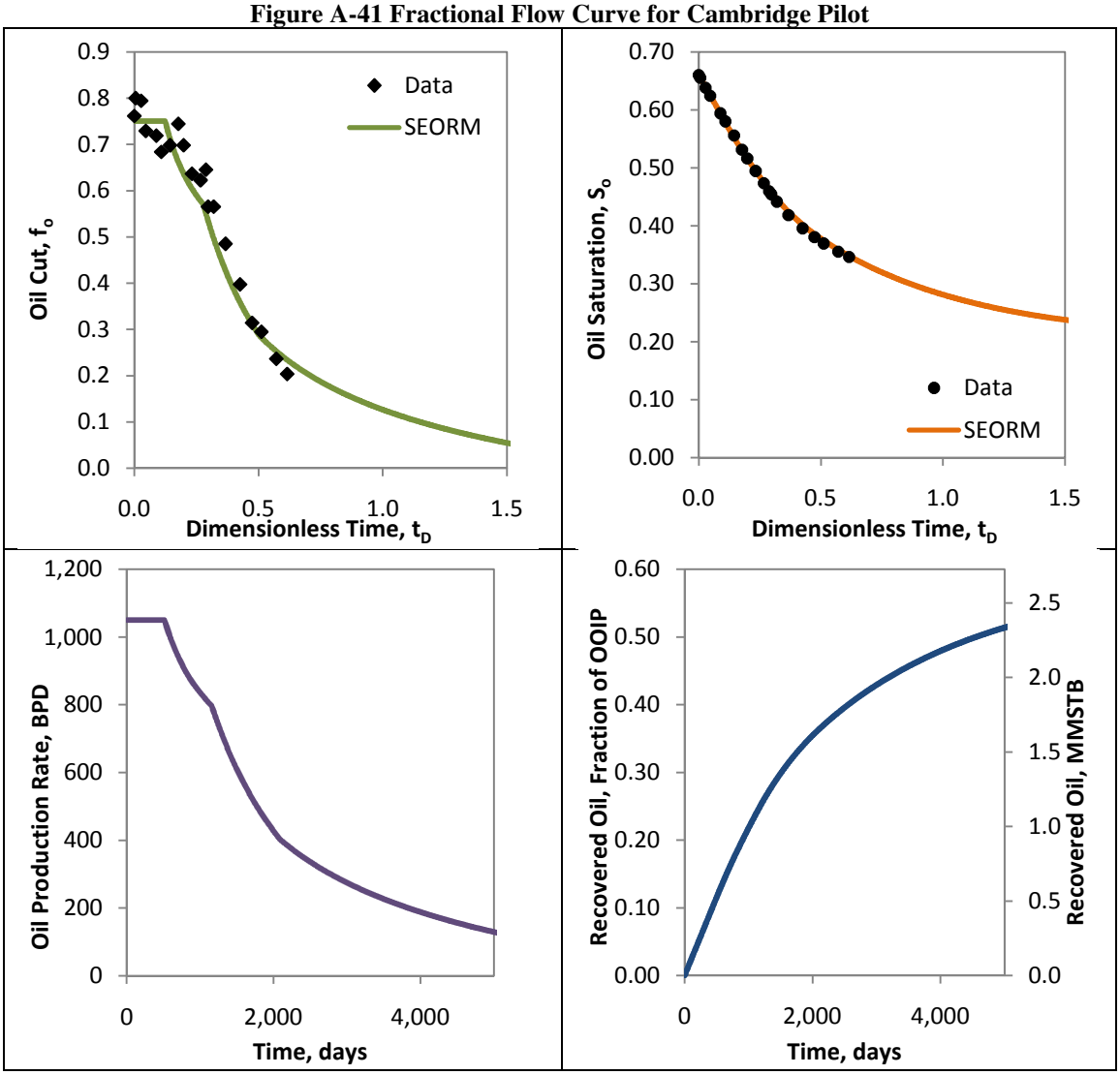

Figure A-42 Plots for Fitted Cambridge Pilot Data

References: Vargo et al. 2000

A.3.2 Karamay Pilot

Table A-22 Summary of Inputs for Karamay Pilot

Oil Saturations			Fractional Flow Inputs		
S_{oI}	0.60		k^o_{rw}	0.20	
S_{oR}	0.34		k^o_{ro}	0.80	
S_{or}	0.24		n	3.0	
S_{oB}	0.47		m	3.0	
S_{oF}	0.05		μ_o	24.3	cp
ΔS_o	0.29		μ_w	1.0	cp
Oil Cuts			μ_c (Inj. Chem.)	--	cp
f_{oI}	0.01		**Reservoir Properties**		
f_{oB}	0.44		V_p	250000	RB
f_{oF}	0.00		OOIP	150000	STB
Flood Behavior			B_o	1.00	RB/STB
K_1	2.50		Well Spacing	1.9	acres
K_2	6.00		Field Size	7.7	acres
v_{oB}	3.40		**Other Inputs**		
v_C	1.05		Z_{Sur}	0.3	% conc.
K_f	0.63		Z_{Poly}	1000	ppm
Flood Injection Inputs			Z_{alk}	1.40	% conc.

Fluid	Alk. & Sur.	Polymer	Water	
q_I	380	380	380	STB/day
q_P	380	380	380	STB/day
Slug Size	0.34	0.17	5.20	Frac. V_p

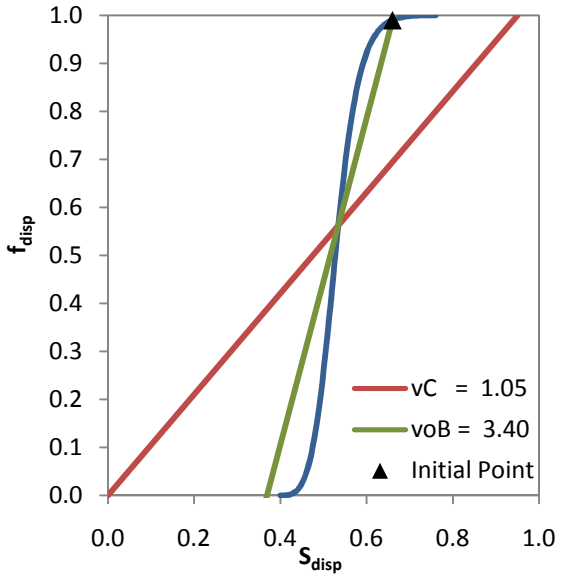

Figure A-43 Fractional Flow Curve for Karamay Pilot

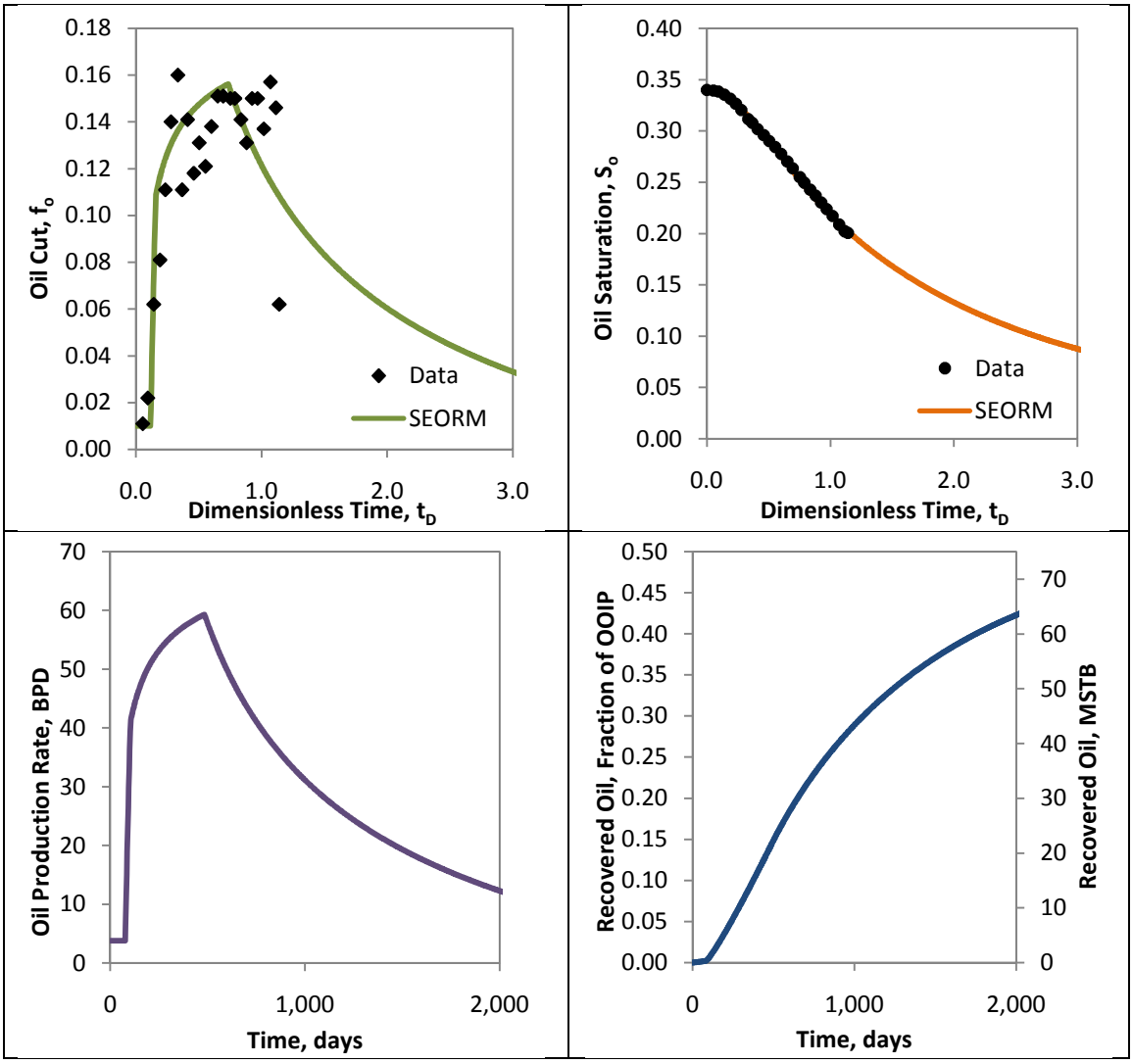

Figure A-44 Plots for Fitted Karamay Pilot Data

References: Qi et al. 2000

A.3.3 Tanner Pilot

Table A-23 Summary of Inputs for Tanner Pilot

Oil Saturations			Fractional Flow Inputs		
S_{oI}	0.8		k^o_{rw}	0.18	
S_{oR}	0.61		k^o_{ro}	0.80	
S_{or}	0.45		n	3.0	
S_{oB}	0.59		m	2.0	
S_{oF}	0.42		μ_o	11.0	cp
ΔS_o	0.19		μ_w	1.0	cp
Oil Cuts			μ_c (Inj. Chem.)	--	cp
f_{oI}	0.35		**Reservoir Properties**		
f_{oB}	0.30		V_p	3E+06	RB
f_{oF}	0.00		OOIP	2E+06	STB
Flood Behavior			B_o	1.02	RB/STB
K_1	2.54		Well Spacing	40	acres
K_2	2.54		Field Size	40	acres
v_{oB}	5.00		**Other Inputs**		
v_C	1.71		Z_{Sur}	0.1	% conc.
K_f	0.00		Z_{Poly}	800	ppm
Flood Injection Inputs			Z_{alk}	1.00	% conc.

Fluid	Alk. & Sur.	Polymer	Water	
q_I	750	750	750	STB/day
q_P	800	800	800	STB/day
Slug Size	0.25	0.25	0.99	Frac. V_p

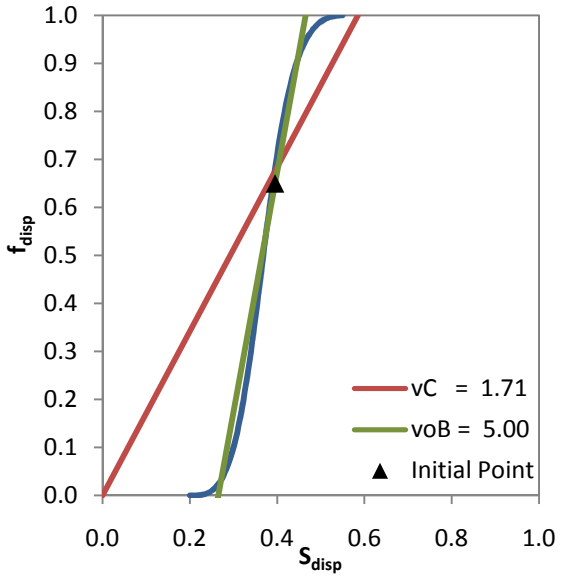

Figure A-45 Fractional Flow Curve for Tanner Pilot

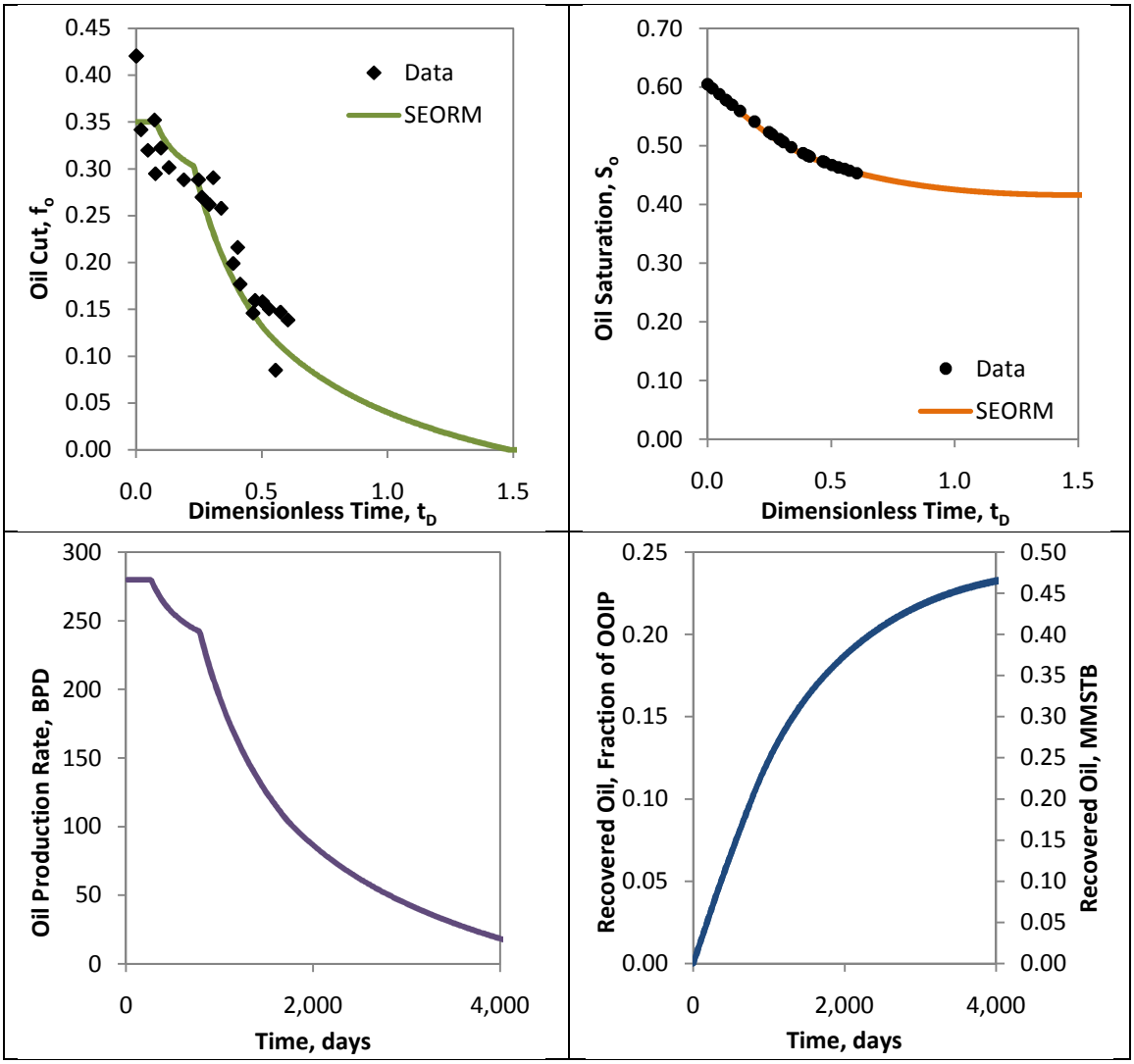

Figure A-46 Plots for Fitted Tanner Pilot Data

References: Pitts et al. 2006

A.4 Fitted Pilot and Field Scale Carbon Dioxide Floods

The following is the full set of pilot and field scale CO_2 flood projects that were fitted with SEORM along with the inputs used for the fits. The tables follow the same color scheme mentioned earlier. Several plots are provided for every fit, including ones for oil cut, oil saturation, oil production rate, oil recovery, and the fractional flow curve.

A.4.1 Lost Soldier Field

Table A-24 Summary of Inputs for Lost Soldier Field

Oil Saturations			Fractional Flow Inputs		
S_{oI}	0.90		k^o_{rw}	0.15	
S_{oR}	0.50		k^o_{ro}	0.90	
S_{or}	0.48		n	4.0	
S_{oB}	0.59		m	1.5	
S_{oF}	0.20		μ_o	1.4	cp
ΔS_o	0.30		μ_w	1.0	cp
Oil Cuts			μ_c (Inj. Chem.)	0.1	cp
f_{oI}	0.04		**Reservoir Properties**		
f_{oB}	0.65		Provided V_P	3.0E+08	RB
f_{oF}	0.00		Fitted V_P	1.3E+08	RB
Flood Behavior			OOIP	1E+08	STB
K_1	5.40		B_o	1.12	RB/STB
K_2	22.50		Well Spacing	10	acres
v_{oB}	7.00		Field Size	100	acres
v_C	1.68		**Other Inputs**		
fK	1.00		Z_{CO2}	1	WAG

Flood Injection Inputs			
Fluid	CO_2	Water	
q_I	100000	100000	STB/day
q_P	100000	100000	STB/day
Slug Size	0.50	12.91	Frac. V_p

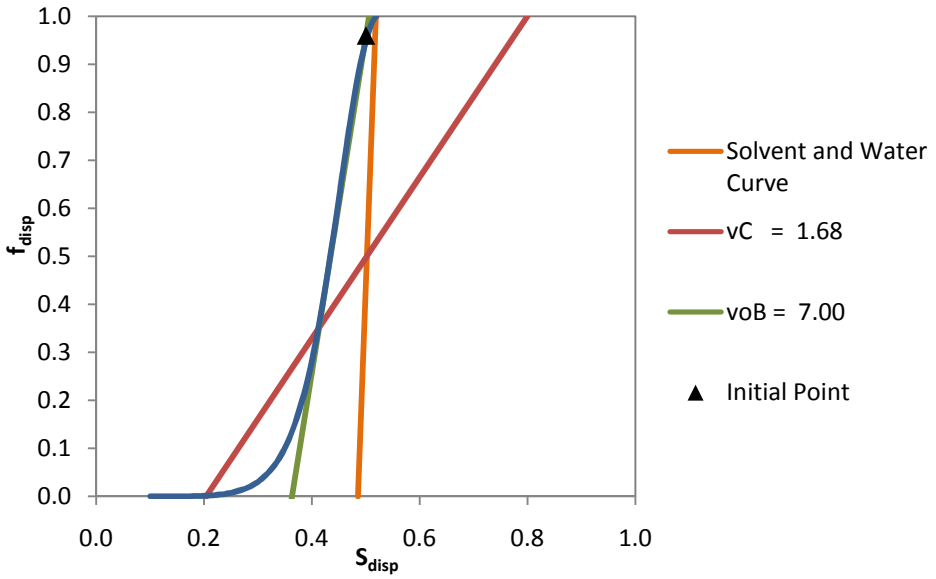

Figure A-47 Fractional Flow Curve for Lost Soldier Field

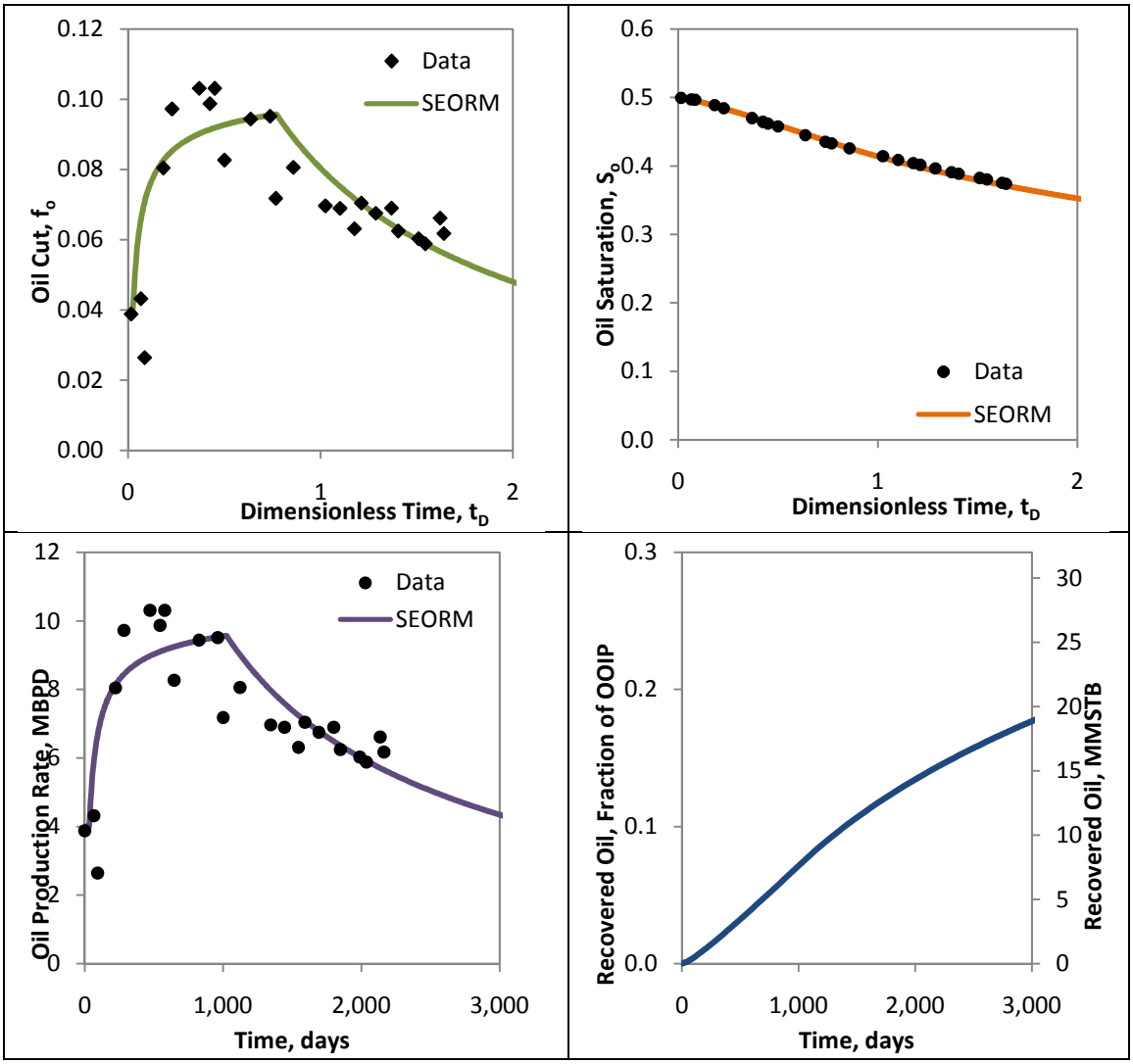

Figure A-48 Plots for Fitted Lost Soldier Field Data

References: Masoner and Wackowski 1995, Walsh and Lake 2008

A.4.2 Rangely Field

Table A-25 Summary of Inputs for Rangely Field

Oil Saturations		Fractional Flow Inputs		
S_{oI}	0.80	k^o_{rw}	0.10	
S_{oR}	0.50	k^o_{ro}	0.70	
S_{or}	0.47	n	5.0	
S_{oB}	0.57	m	2.0	
S_{oF}	0.33	μ_o	1.5	cp
ΔS_o	0.17	μ_w	1.0	cp
Oil Cuts		μ_c (Inj. Chem.)	0.1	cp
f_{oI}	0.05	**Reservoir Properties**		
f_{oB}	0.71	Provided V_P	1.9E+09	RB
f_{oF}	0.00	Fitted V_P	1.6E+09	RB
Flood Behavior		OOIP	1E+09	STB
K_1	6.90	B_o	1.00	RB/STB
K_2	23.00	Well Spacing	10	acres
v_{oB}	10.00	Field Size	2590	acres
v_C	3.00	**Other Inputs**		
fK	1.00	Z_{CO2}	1	WAG

Flood Injection Inputs			
Fluid	CO_2	Water	
q_I	525000	375000	STB/day
q_P	525000	375000	STB/day
Slug Size	0.50	7.17	Frac. V_p

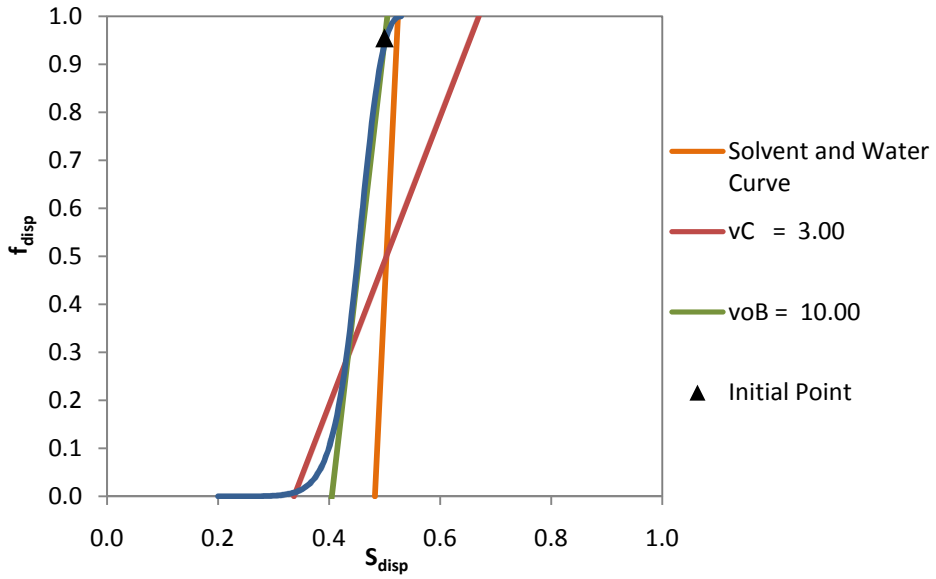

Figure A-49 Fractional Flow Curve for Rangely Field

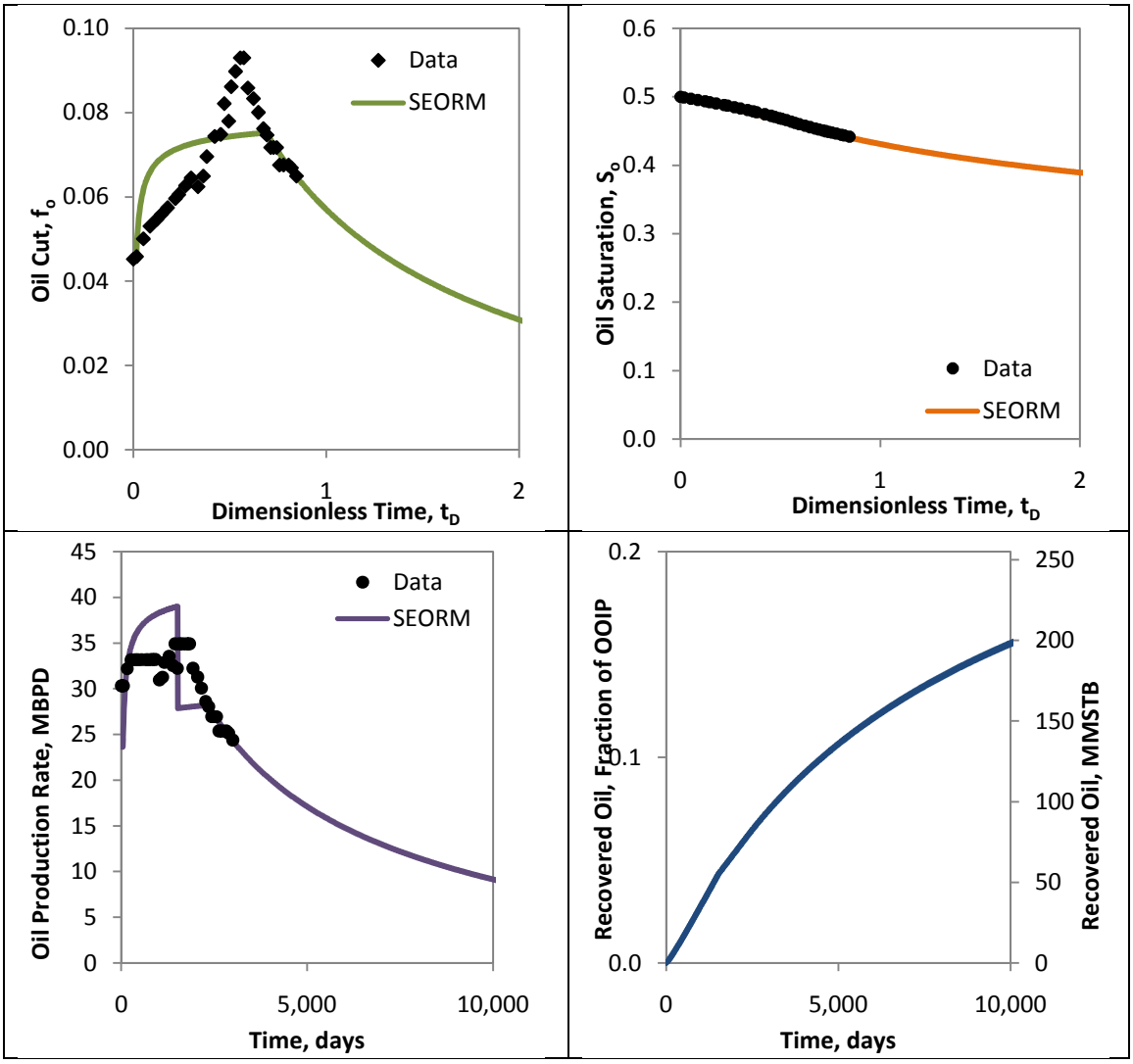

Figure A-50 Plots for Fitted Lost Soldier Field Data

References: Walsh and Lake 2008

A.4.3 SACROC 4 Field

Table A-26 Summary of Inputs for SACROC 4 Field

Oil Saturations			Fractional Flow Inputs		
S_{oI}	0.78		k^o_{rw}	0.28	
S_{oR}	0.46		k^o_{ro}	0.34	
S_{or}	0.42		n	1.5	
S_{oB}	0.55		m	2.0	
S_{oF}	0.29		μ_o	0.4	cp
ΔS_o	0.17		μ_w	0.7	cp
Oil Cuts			μ_c (Inj. Chem.)	0.1	cp
f_{oI}	0.03		**Reservoir Properties**		
f_{oB}	0.35		Provided V_P	5.4E+07	RB
f_{oF}	0.00		Fitted V_P	2.4E+07	RB
Flood Behavior			OOIP	1E+07	STB
K_1	2.30		B_o	1.51	RB/STB
K_2	6.35		Well Spacing	40	acres
v_{oB}	3.75		Field Size	600	acres
v_C	1.35		**Other Inputs**		
fK	0.99		Z_{CO2}	3	WAG

Flood Injection Inputs			
Fluid	CO_2	Water	
q_I	28000	28000	STB/day
q_P	28000	28000	STB/day
Slug Size	0.50	4.20	Frac. V_p

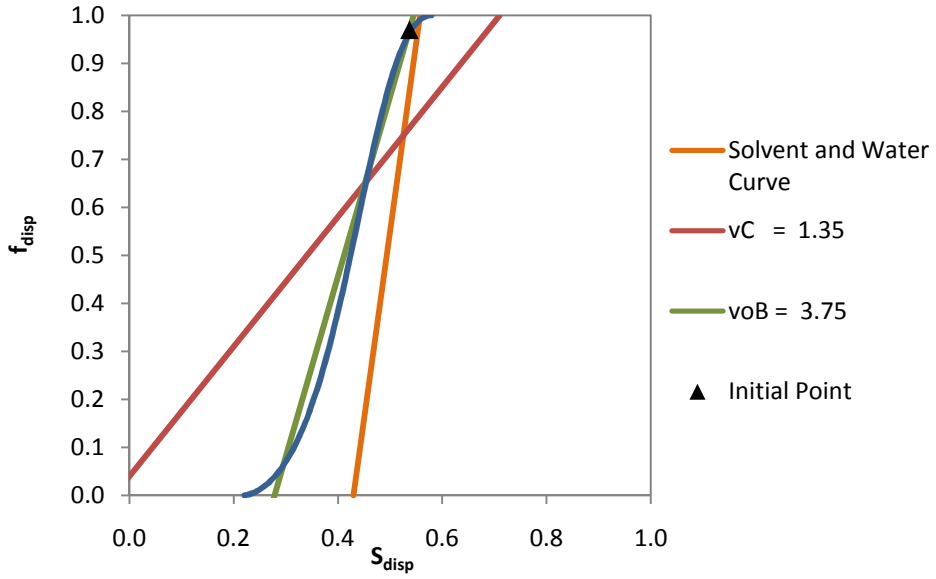

Figure A-51 Fractional Flow Curve for SACROC 4 Field

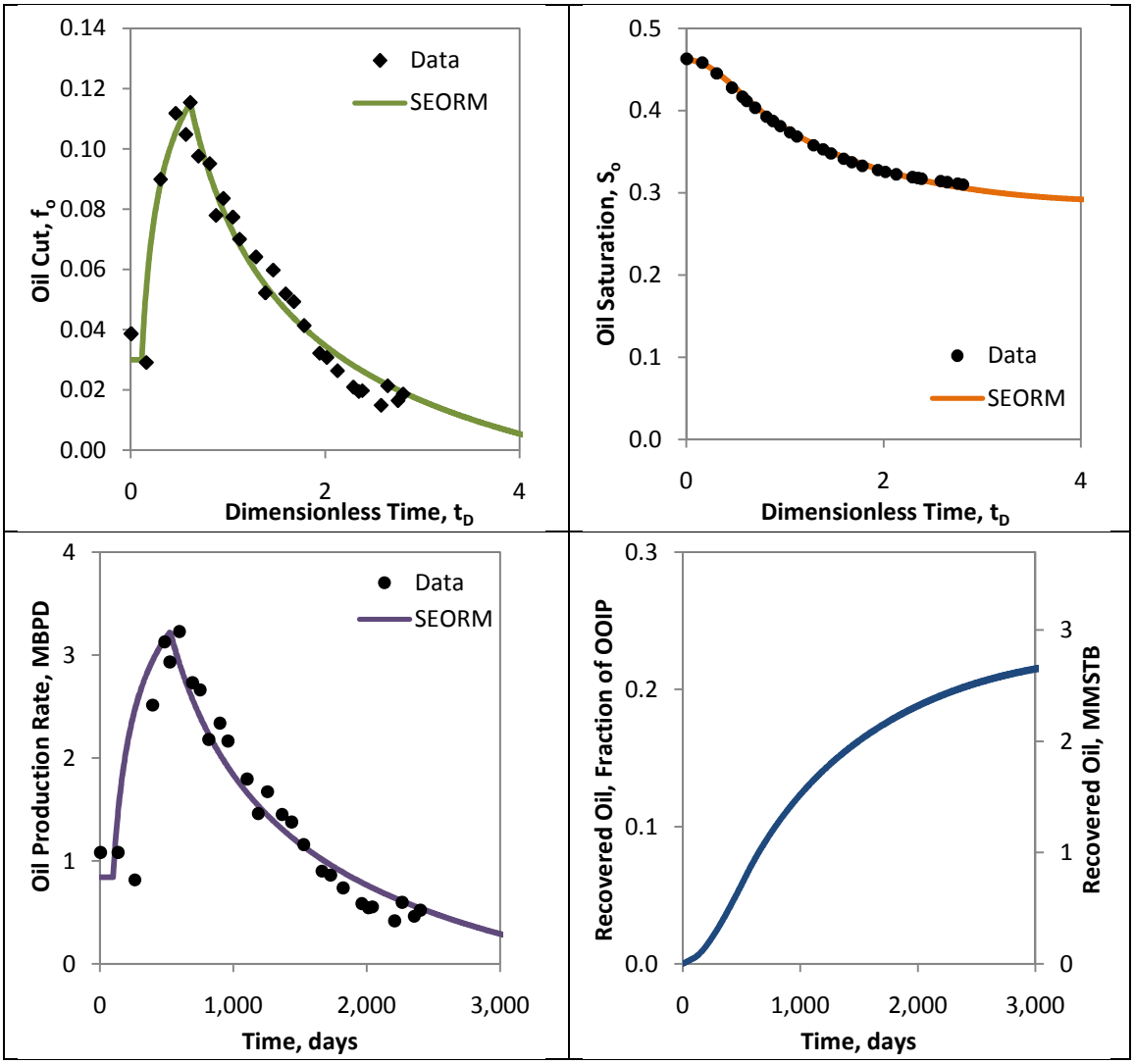

Figure A-52 Plots for Fitted SACROC 4 Field Data

References: Paul and Lake 1984, Langston and Young 1988, Walsh and Lake 2008

A.4.4 SACROC 17 Field

Table A-27 Summary of Inputs for SACROC 17 Field

Oil Saturations			Fractional Flow Inputs		
S_{oI}	0.78		k^o_{rw}	0.28	
S_{oR}	0.46		k^o_{ro}	0.34	
S_{or}	0.42		n	1.5	
S_{oB}	0.53		m	2.0	
S_{oF}	0.33		μ_o	0.4	cp
ΔS_o	0.13		μ_w	0.7	cp
Oil Cuts			μ_c (Inj. Chem.)	0.1	cp
f_{oI}	0.03		**Reservoir Properties**		
f_{oB}	0.25		Provided V_P	1.6E+08	RB
f_{oF}	0.00		Fitted V_P	7.1E+07	RB
Flood Behavior			OOIP	4E+07	STB
K_1	3.00		B_o	1.51	RB/STB
K_2	7.70		Well Spacing	40	acres
v_{oB}	3.20		Field Size	2700	acres
v_C	1.24		**Other Inputs**		
fK	0.99		Z_{CO2}	5	WAG

Flood Injection Inputs			
Fluid	CO_2	Water	
q_I	50000	50000	STB/day
q_P	50000	50000	STB/day
Slug Size	0.50	5.71	Frac. V_p

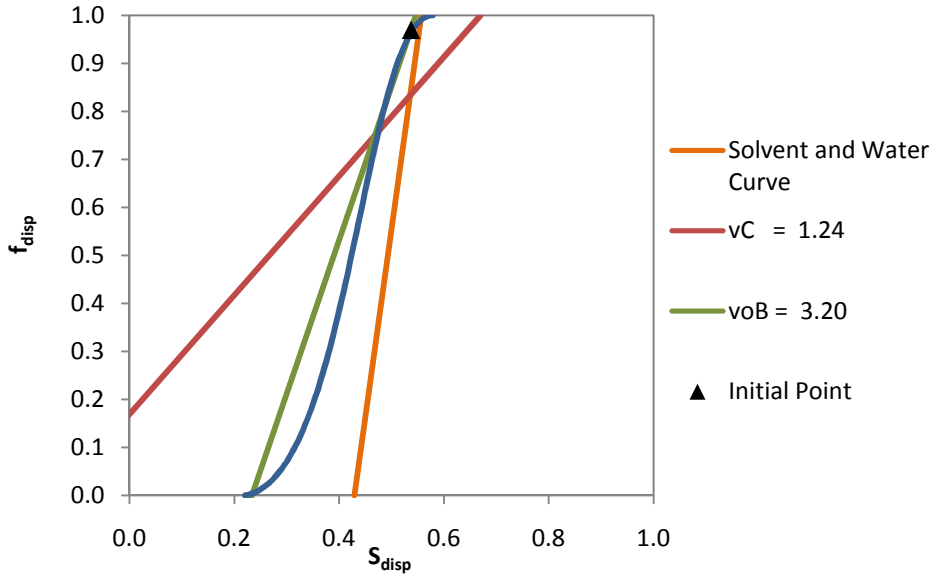

Figure A-53 Fractional Flow Curve for SACROC 17 Field

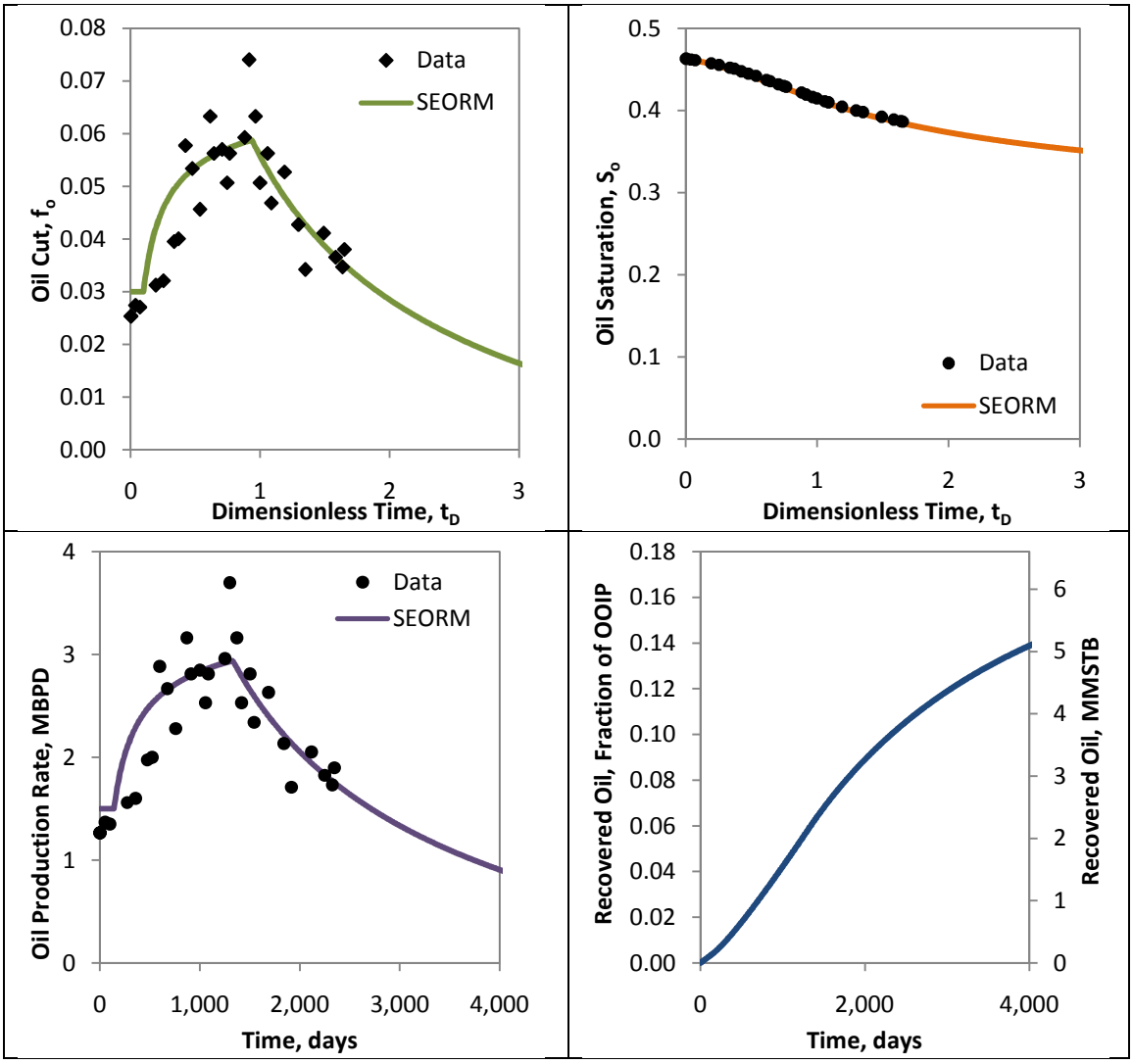

Figure A-54 Plots for Fitted SACROC 17 Field Data

References: Paul and Lake 1984, Langston and Young 1988, Walsh and Lake 2008

A.4.5 Slaughter Pilot

Table A-28 Summary of Inputs for Slaughter Pilot

Oil Saturations			Fractional Flow Inputs		
S_{oI}	0.92		k^o_{rw}	0.30	
S_{oR}	0.55		k^o_{ro}	1.00	
S_{or}	0.44		n	1.5	
S_{oB}	0.83		m	2.5	
S_{oF}	0.23		μ_o	2.0	cp
ΔS_o	0.32		μ_w	0.7	cp
Oil Cuts			μ_c (Inj. Chem.)	0.1	cp
f_{oI}	0.05		**Reservoir Properties**		
f_{oB}	0.91		Provided V_P	8.6E+05	RB
f_{oF}	0.00		Fitted V_P	7.2E+05	RB
Flood Behavior			OOIP	538537	STB
K_1	2.40		B_o	1.23	RB/STB
K_2	4.90		Well Spacing	3	acres
v_{oB}	3.10		Field Size	12	acres
v_C	1.52		**Other Inputs**		
fK	1.01		Z_{CO2}	1	WAG

Flood Injection Inputs			
Fluid	CO_2	Water	
q_I	520	520	STB/day
q_P	520	520	STB/day
Slug Size	0.50	2.72	Frac. V_p

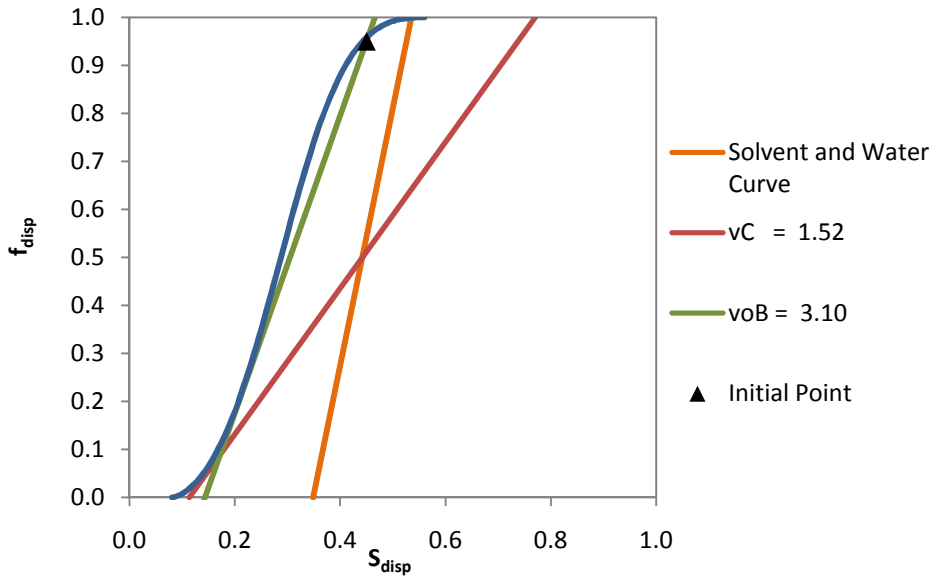

Figure A-55 Fractional Flow Curve for Slaughter Pilot

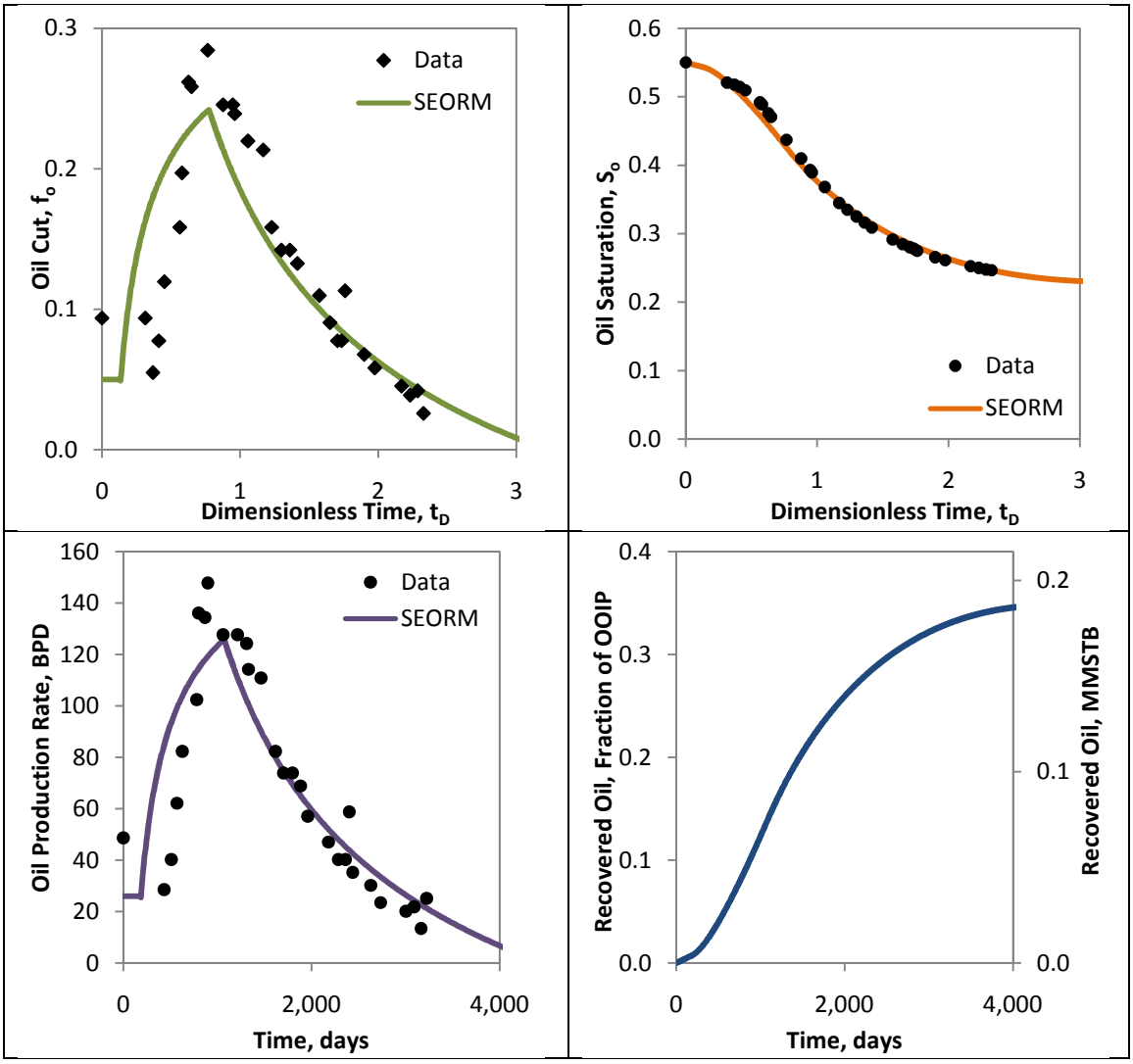

Figure A-56 Plots for Fitted Slaughter Pilot Data

References: Paul and Lake 1984, Rowe et al. 1982, Walsh and Lake 2008

A.4.6 Twofreds Pilot

Table A-29 Summary of Inputs for Twofreds Pilot

Oil Saturations		Fractional Flow Inputs		
S_{oI}	0.54	k^o_{rw}	0.20	
S_{oR}	0.46	k^o_{ro}	0.60	
S_{or}	0.44	n	2.0	
S_{oB}	0.50	m	4.0	
S_{oF}	0.38	μ_o	1.5	cp
ΔS_o	0.08	μ_w	1.0	cp
Oil Cuts		μ_c (Inj. Chem.)	0.0	cp
f_{oI}	0.01	**Reservoir Properties**		
f_{oB}	0.65	Provided V_P	3.4E+07	RB
f_{oF}	0.00	Fitted V_P	4.0E+07	RB
Flood Behavior		OOIP	2E+07	STB
K_1	3.14	B_o	1.18	RB/STB
K_2	8.96	Well Spacing	40	acres
v_{oB}	15.00	Field Size	80	acres
v_C	5.32	**Other Inputs**		
fK	1.02	Z_{CO2}	1	WAG

Flood Injection Inputs			
Fluid	CO_2	Water	
q_I	4300	4300	STB/day
q_P	4300	4300	STB/day
Slug Size	0.50	1.18	Frac. V_p

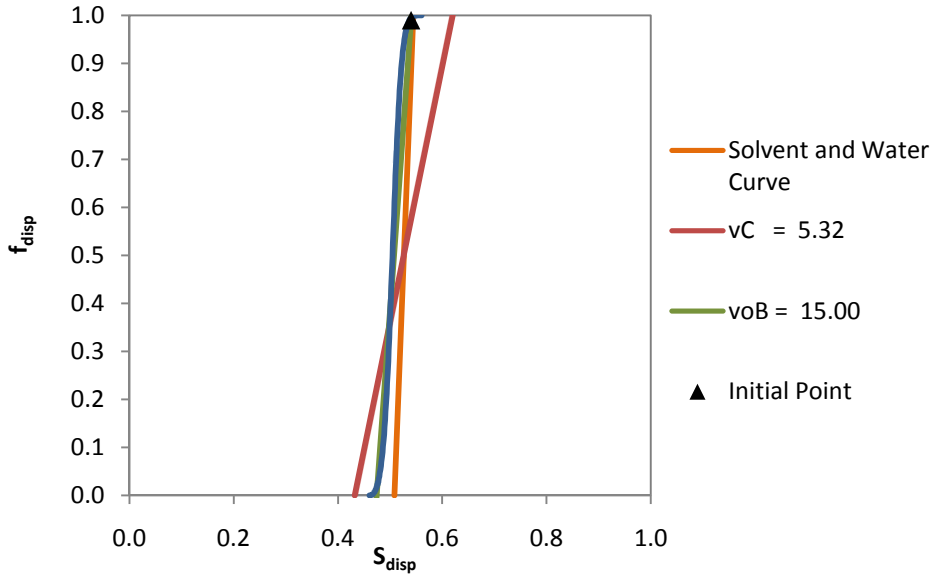

Figure A-57 Fractional Flow Curve for Twofreds Pilot

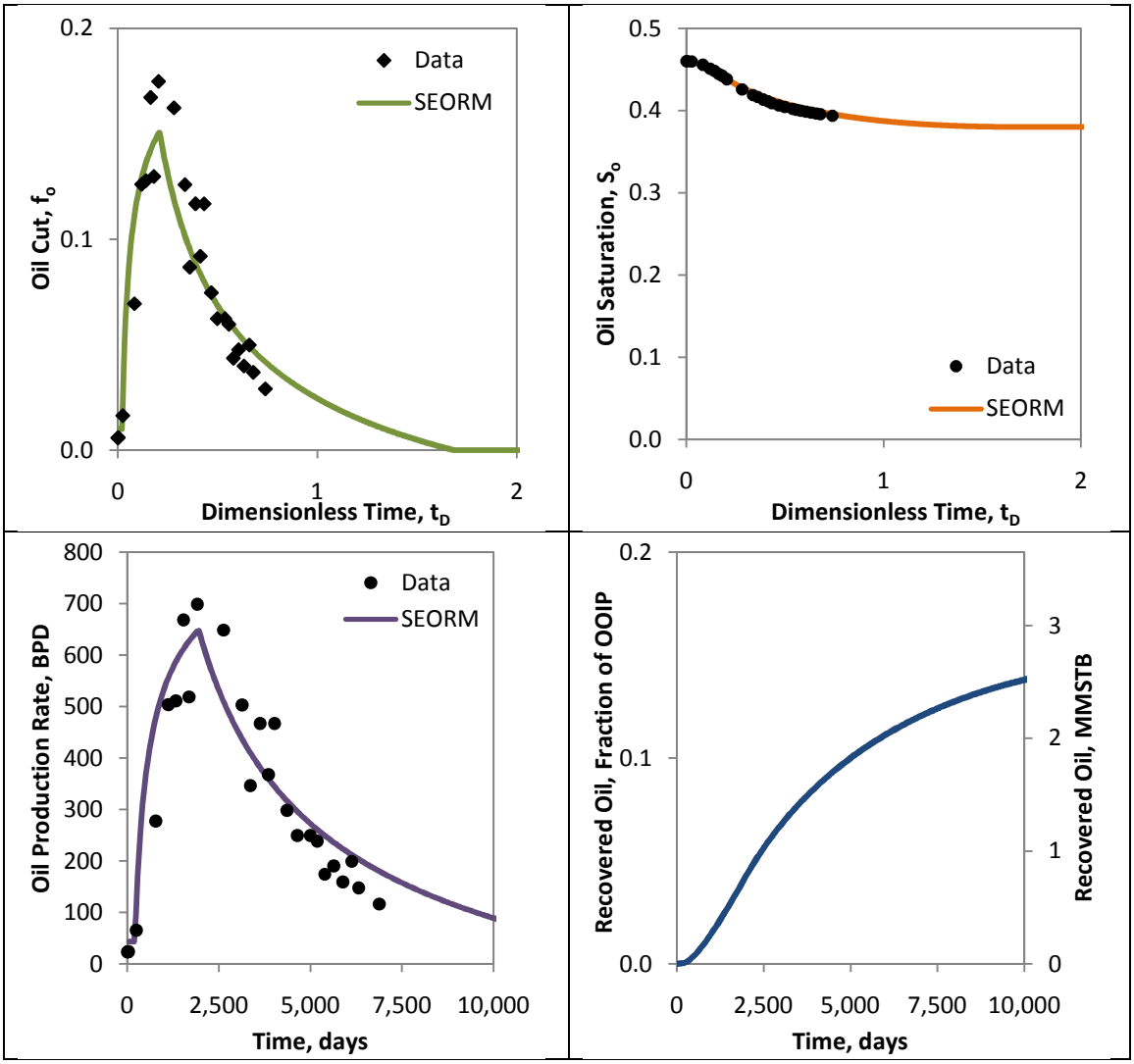

Figure A-58 Plots for Fitted Twofreds Pilot Data

References: Flanders and DePauw 1993, Walsh and Lake 2008

A.4.7 Wertz Field

Table A-30 Summary of Inputs for Wertz Field

Oil Saturations		Fractional Flow Inputs		
S_{oI}	0.90	k^o_{rw}	0.10	
S_{oR}	0.49	k^o_{ro}	0.90	
S_{or}	0.47	n	4.0	
S_{oB}	0.59	m	2.0	
S_{oF}	0.24	μ_o	1.3	cp
ΔS_o	0.25	μ_w	1.0	cp
Oil Cuts		μ_c (Inj. Chem.)	0.1	cp
f_{oI}	0.03	**Reservoir Properties**		
f_{oB}	0.67	Provided V_P	2.2E+08	RB
f_{oF}	0.00	Fitted V_P	8.3E+07	RB
Flood Behavior		OOIP	6E+07	STB
K_1	7.00	B_o	1.16	RB/STB
K_2	25.00	Well Spacing	10	acres
v_{oB}	7.00	Field Size	370	acres
v_C	1.94	**Other Inputs**		
fK	0.98	Z_{CO2}	1	WAG

Flood Injection Inputs			
Fluid	CO_2	Water	
q_I	140000	140000	STB/day
q_P	140000	140000	STB/day
Slug Size	0.50	12.40	Frac. V_p

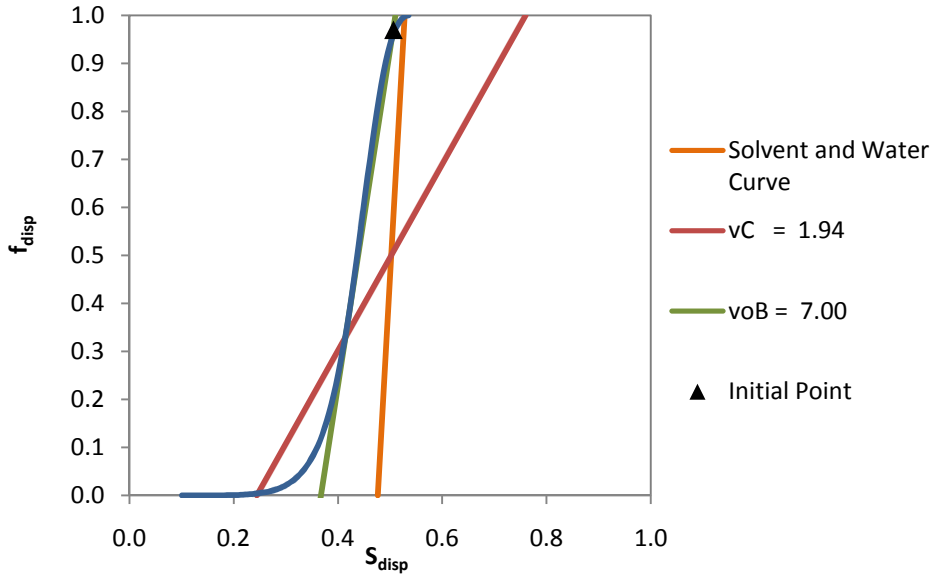

Figure A-59 Fractional Flow Curve for Wertz Field

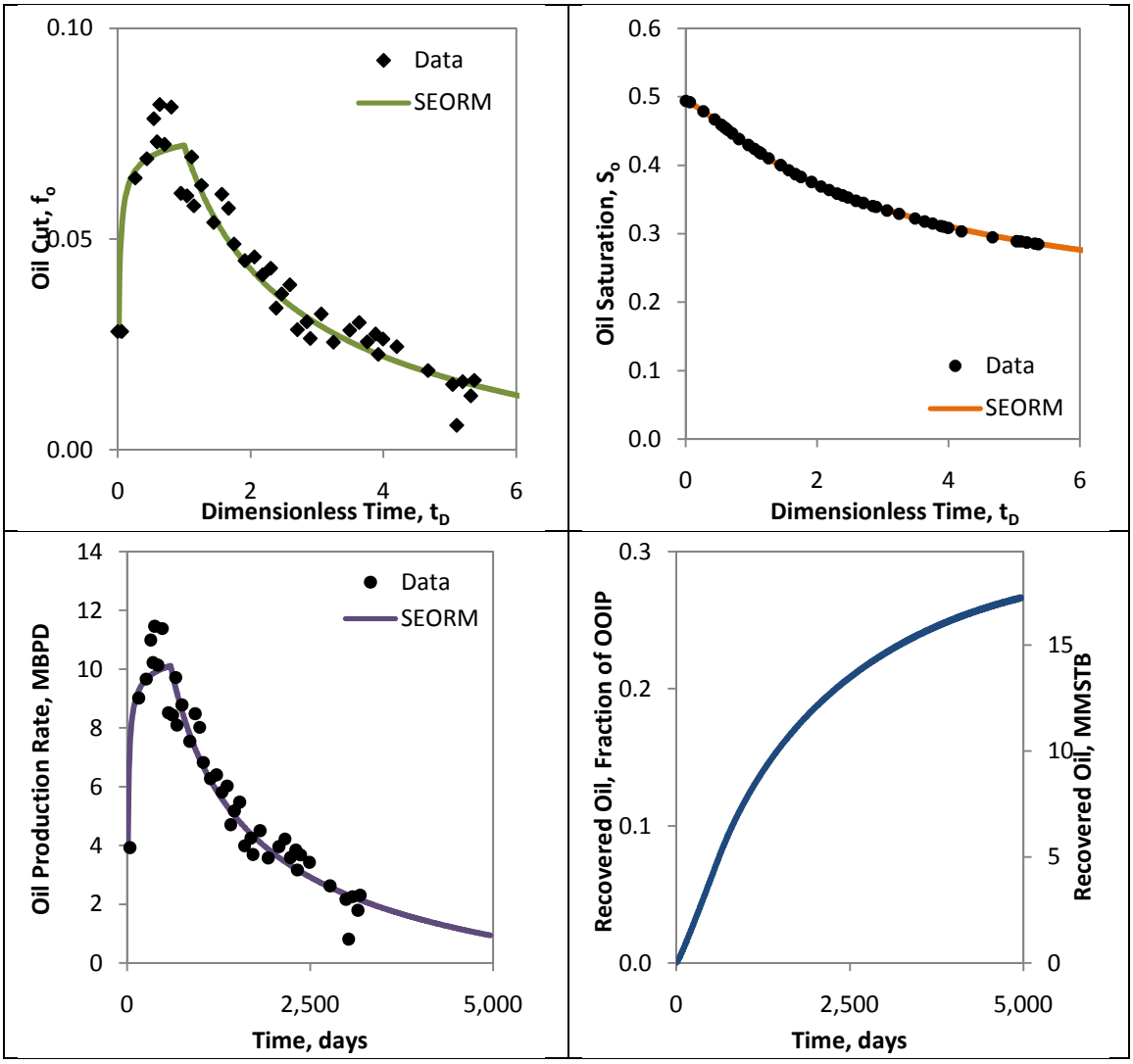

Figure A-60 Plots for Fitted Wertz Field Data

References: Kleinsteiber 1990, Walsh and Lake 2008

A.4.8 West Sussex Pilot

Table A-31 Summary of Inputs for West Sussex Pilot

Oil Saturations		Fractional Flow Inputs		
S_{oI}	0.73	k^o_{rw}	0.20	
S_{oR}	0.43	k^o_{ro}	0.70	
S_{or}	0.38	n	2.0	
S_{oB}	0.56	m	2.5	
S_{oF}	0.36	μ_o	1.4	cp
ΔS_o	0.07	μ_w	1.0	cp
Oil Cuts		μ_c (Inj. Chem.)	0.1	cp
f_{oI}	0.03	**Reservoir Properties**		
f_{oB}	0.69	Provided V_P	3.2E+05	RB
f_{oF}	0.00	Fitted V_P	3.0E+05	RB
Flood Behavior		OOIP	191601	STB
K_1	2.70	B_o	1.14	RB/STB
K_2	3.90	Well Spacing	9.6	acres
v_{oB}	5.00	Field Size	9.6	acres
v_C	3.42	**Other Inputs**		
fK	0.96	Z_{CO2}	4	WAG

Flood Injection Inputs			
Fluid	CO_2	Water	
q_I	350	350	STB/day
q_P	350	350	STB/day
Slug Size	0.50	0.64	Frac. V_p

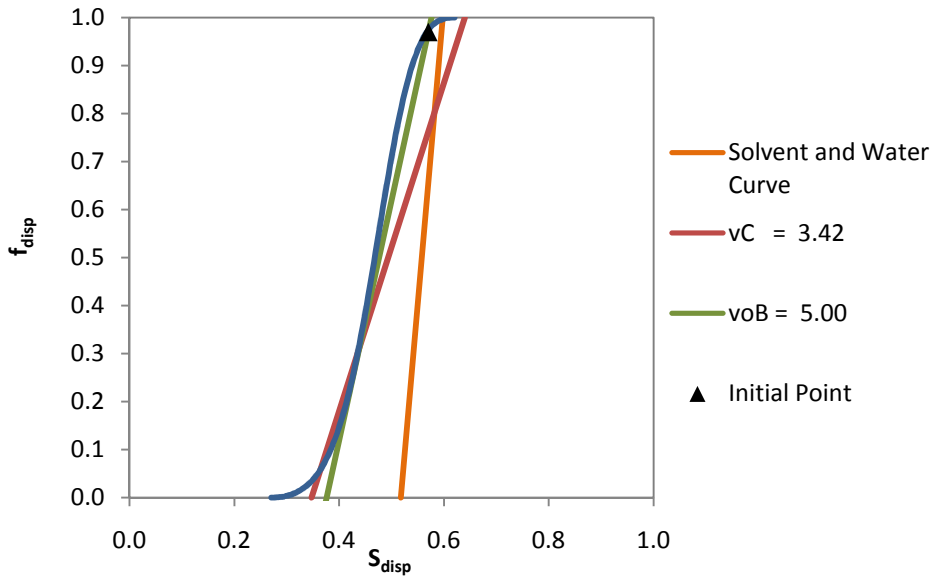

Figure A-61 Fractional Flow Curve for West Sussex Pilot

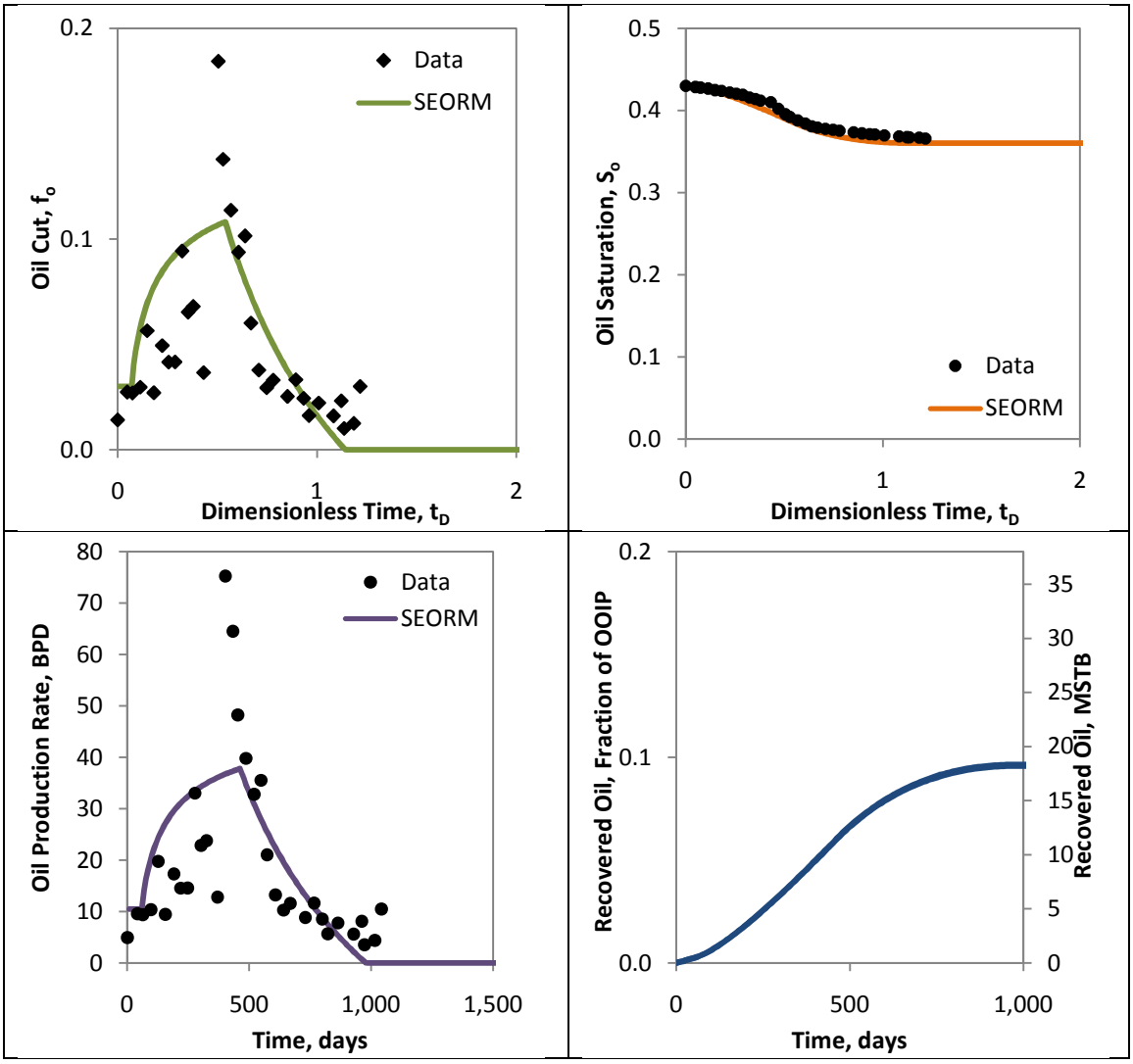

Figure A-62 Plots for Fitted West Sussex Pilot Data

References: Hoiland et al. 1986, Walsh and Lake 2008

APPENDIX B: RELATIONSHIPS BETWEEN RESERVOIR CHARACTERISTICS AND FITTING PARAMETERS

B.1 Introduction

As a means to help put in perspective what the fitting parameters for the simplified enhanced oil recovery method (SEORM) mean, attempts were made to determine if relationships exist between the parameters and various reservoir characteristics. From a review of the fits, it appears that no trends seem to exist. This does not mean that the parameters do not capture certain aspects of a reservoir's properties, but rather it suggests that the parameters may capture combinations of the characteristics. Going into considerable detail about determining if relationships exist is out of the scope of this research project. Coming up with basic ranges for the fitted parameters is enough to allow one to perform a decision analysis that can simulate any potential outcome. It may be interesting to see if meaningful relationships can be developed as SEORM is fitted to more data.

B.2 Trend fits

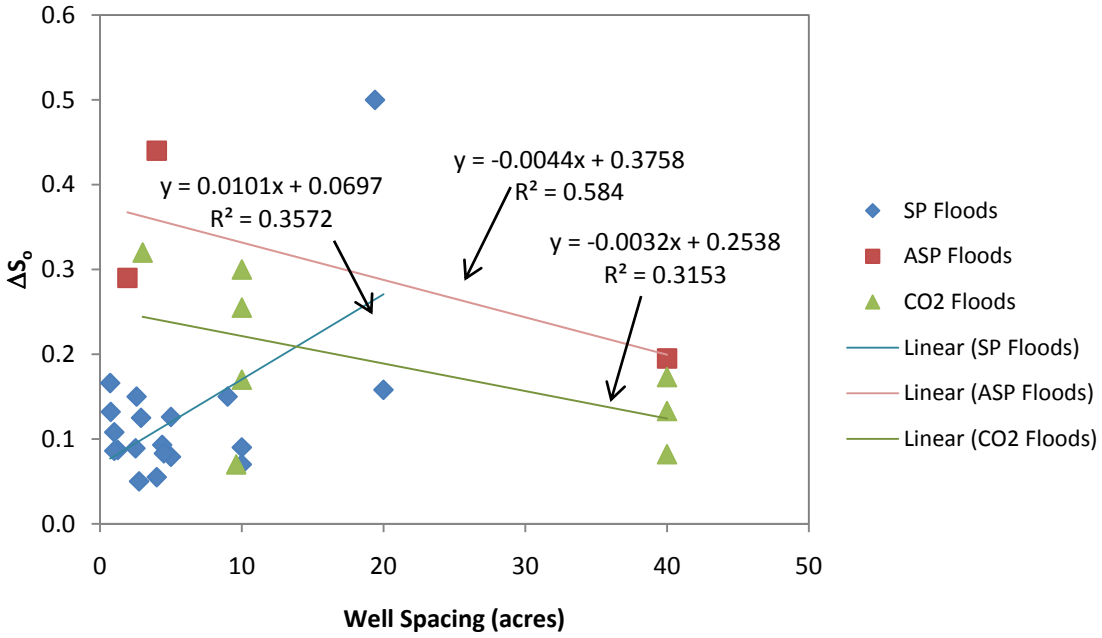

Figure B-1 ΔS_o against Well Spacing for Each Flood Type

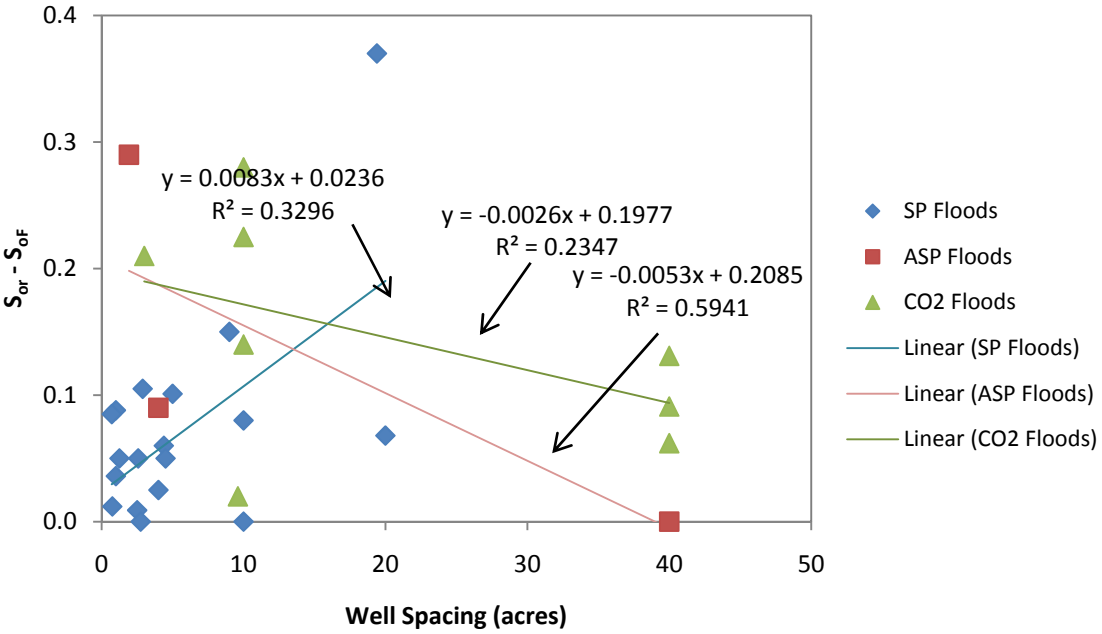

Figure B-2 S_{or}-S_{oF} against Well Spacing for Each Flood Type

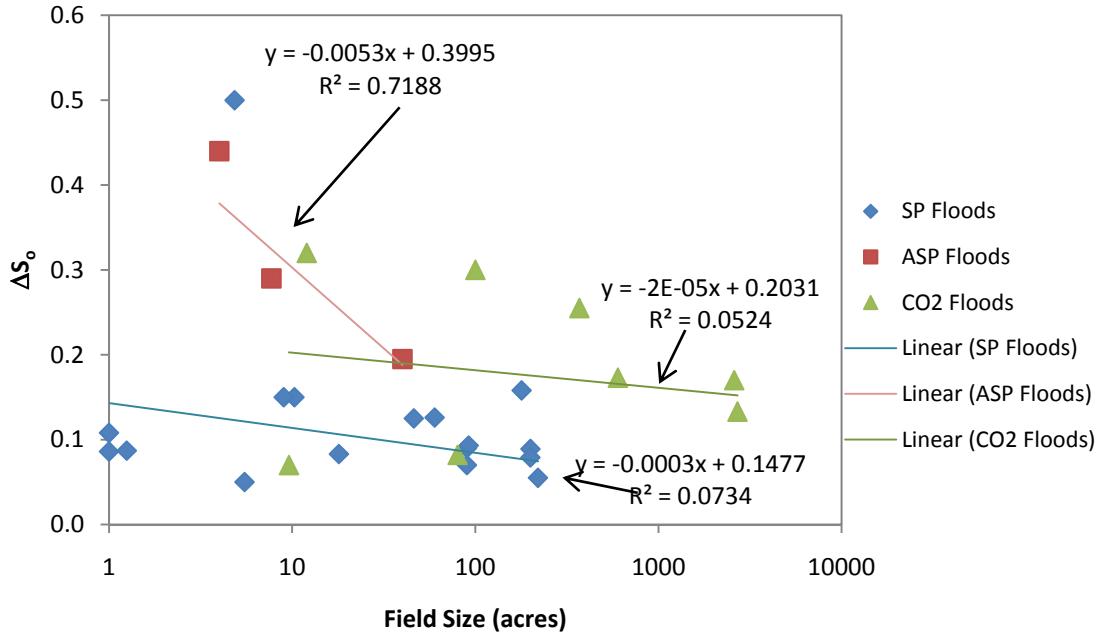

Figure B-3 ΔS_o against Field Size for Each Flood Type

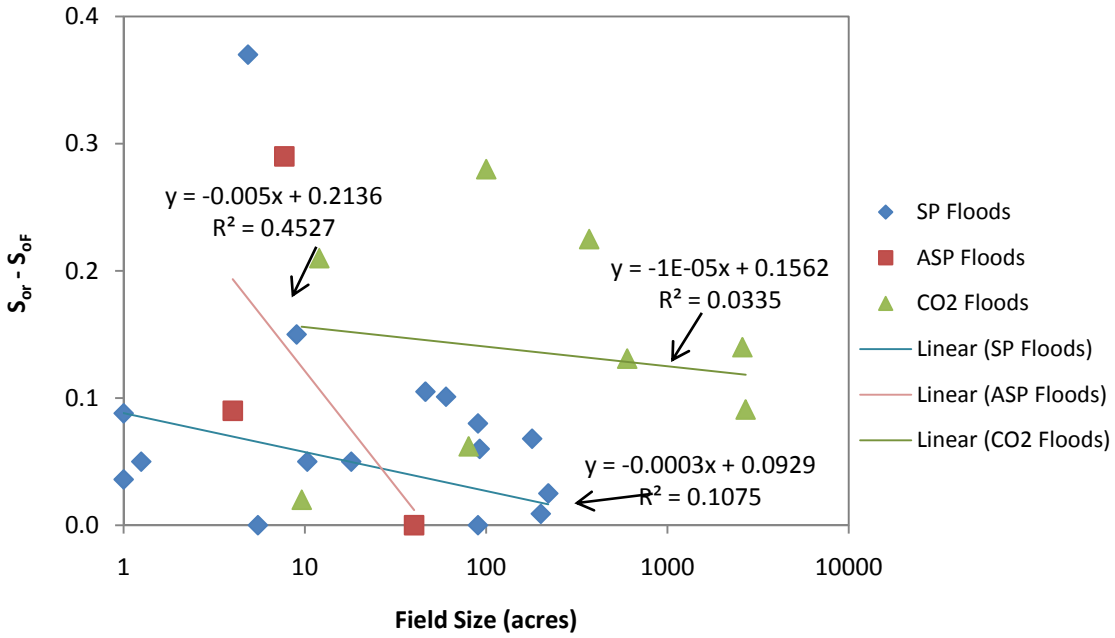

Figure B-4 S_{or}-S_{oF} against Field Size for Each Flood Type

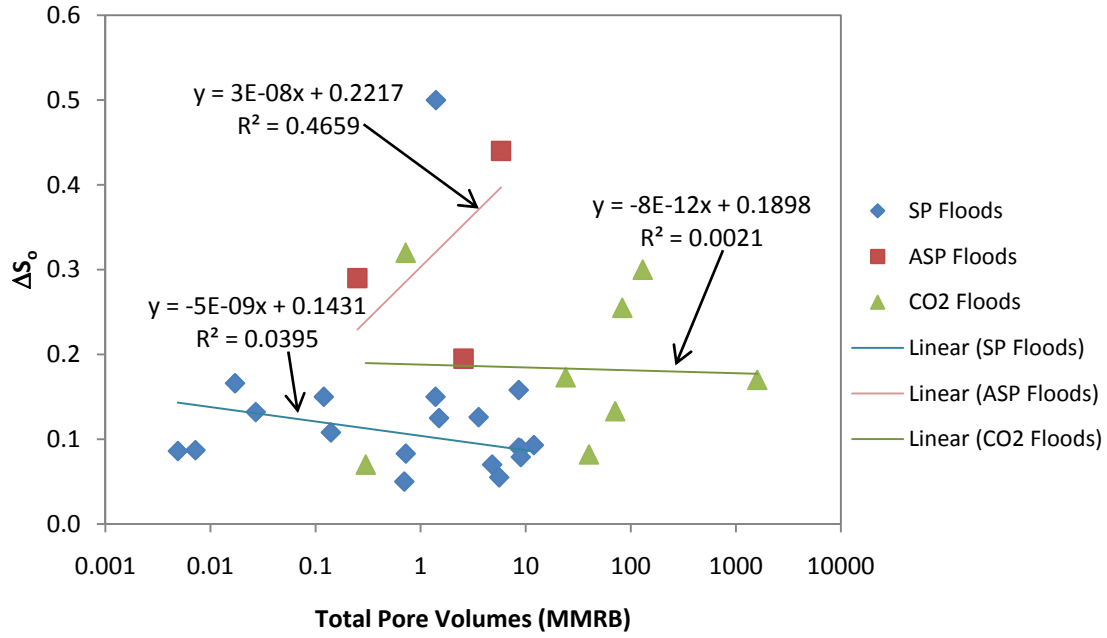

Figure B-5 ΔS_o against Total Pore Volumes for Each Flood Type

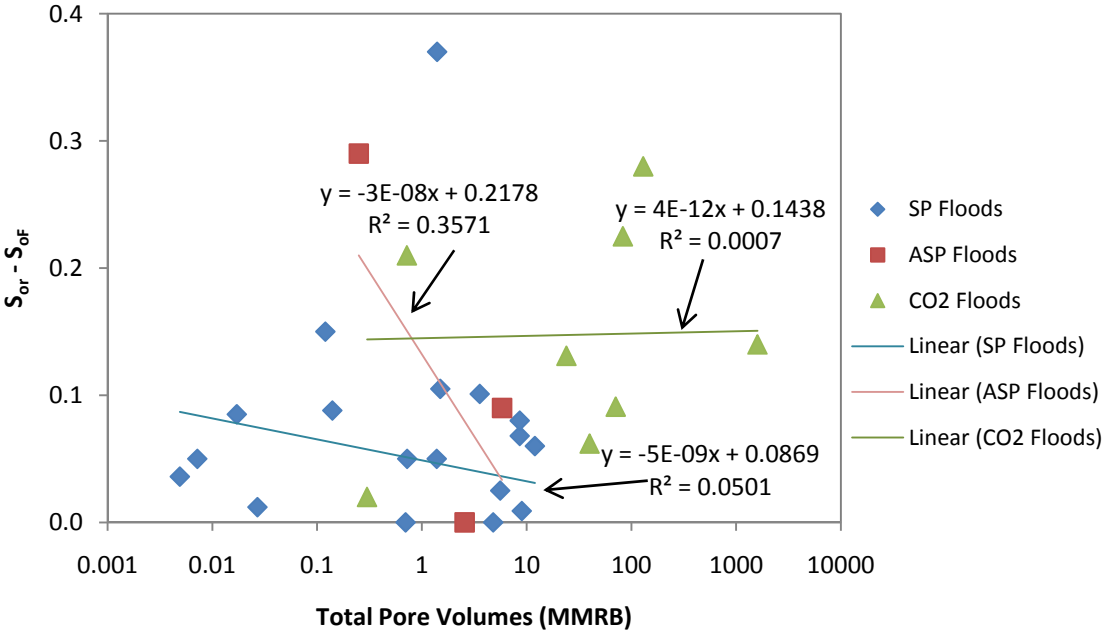

Figure B-6 S_{or}-S_{oF} against Total Pore Volumes for Each Flood Type

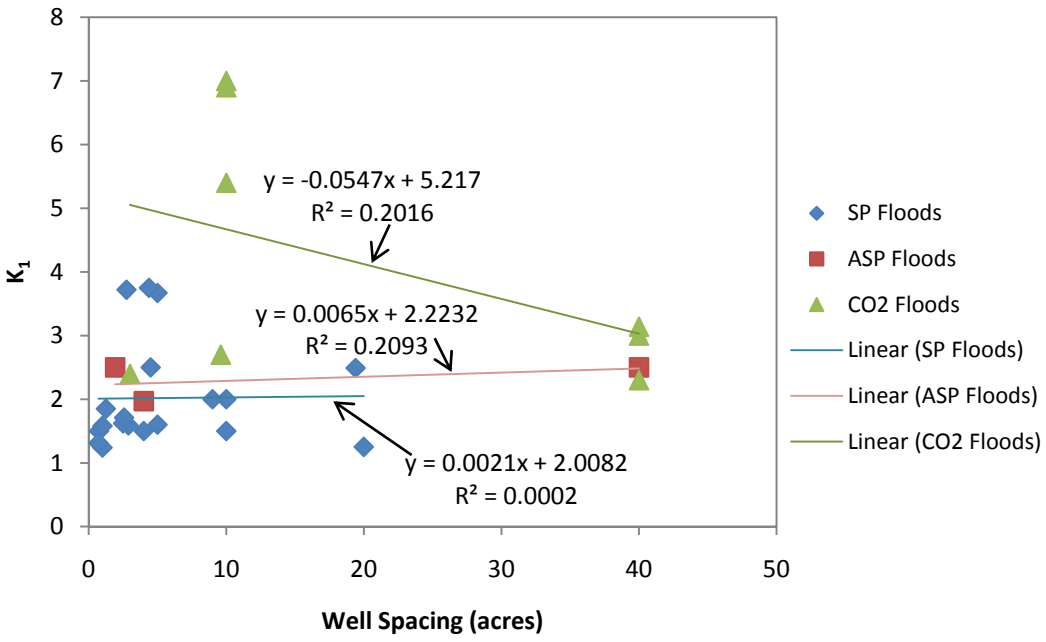

Figure B-7 K_1 against Well Spacing for Each Flood Type

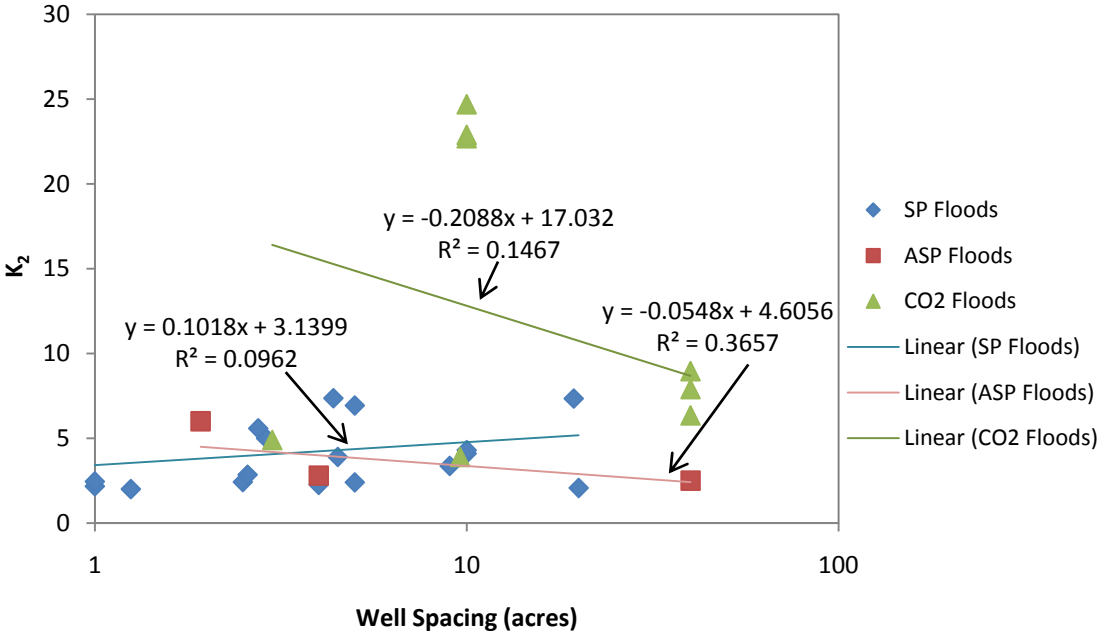

Figure B-8 K_2 against Well Spacing for Each Flood Type

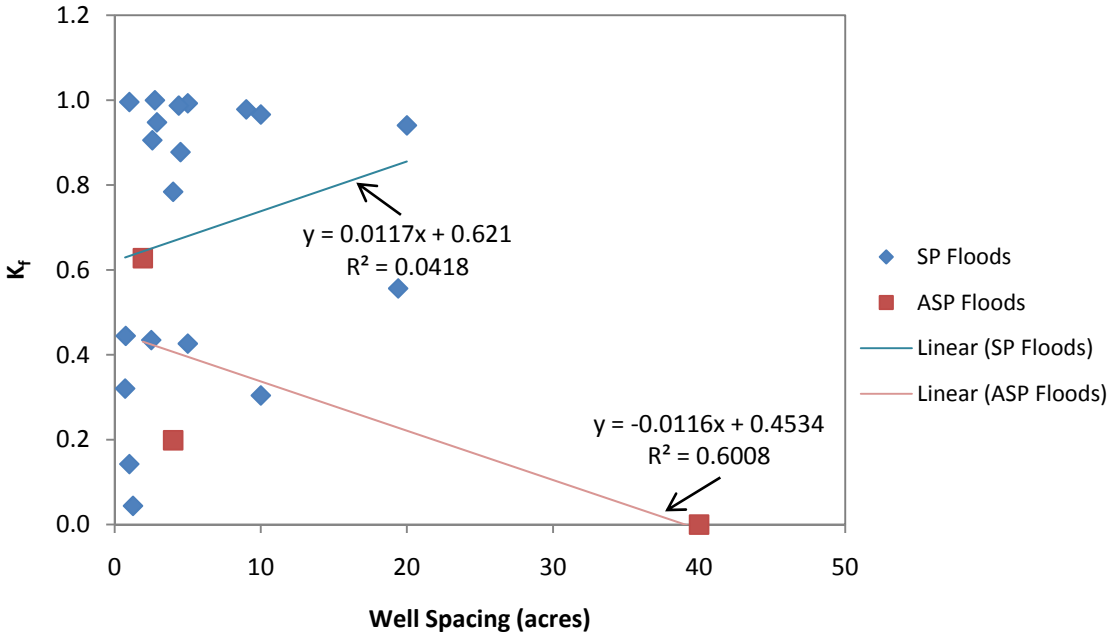

Figure B-9 K_f against Well Spacing for SP and ASP Flood Types

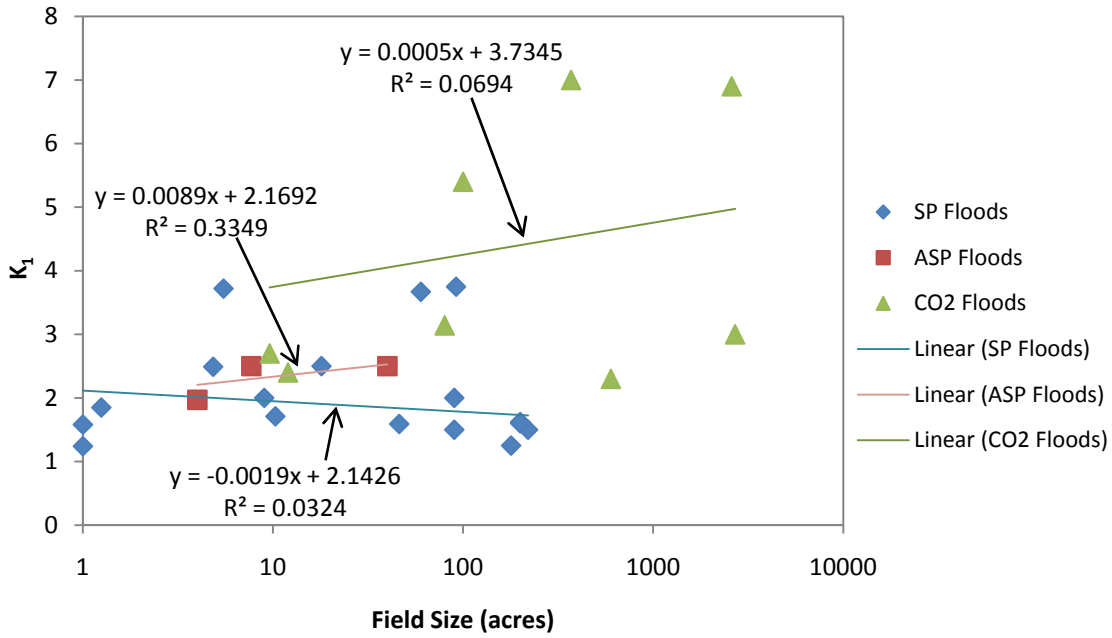

Figure B-10 K_1 against Field Size for Each Flood Type

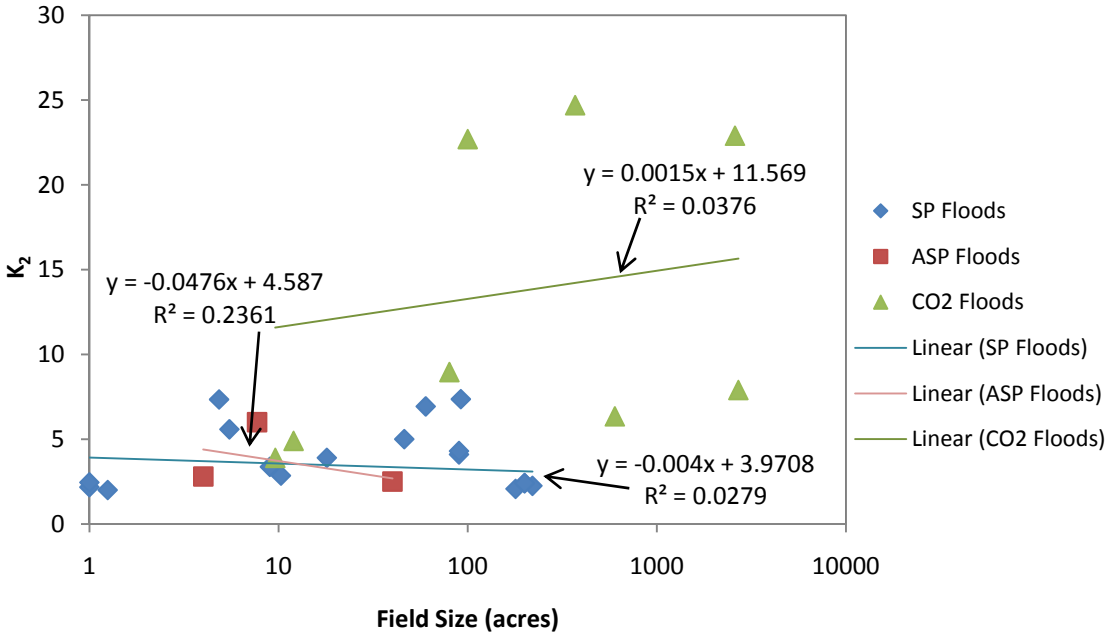

Figure B-11 K_2 against Field Size for Each Flood Type

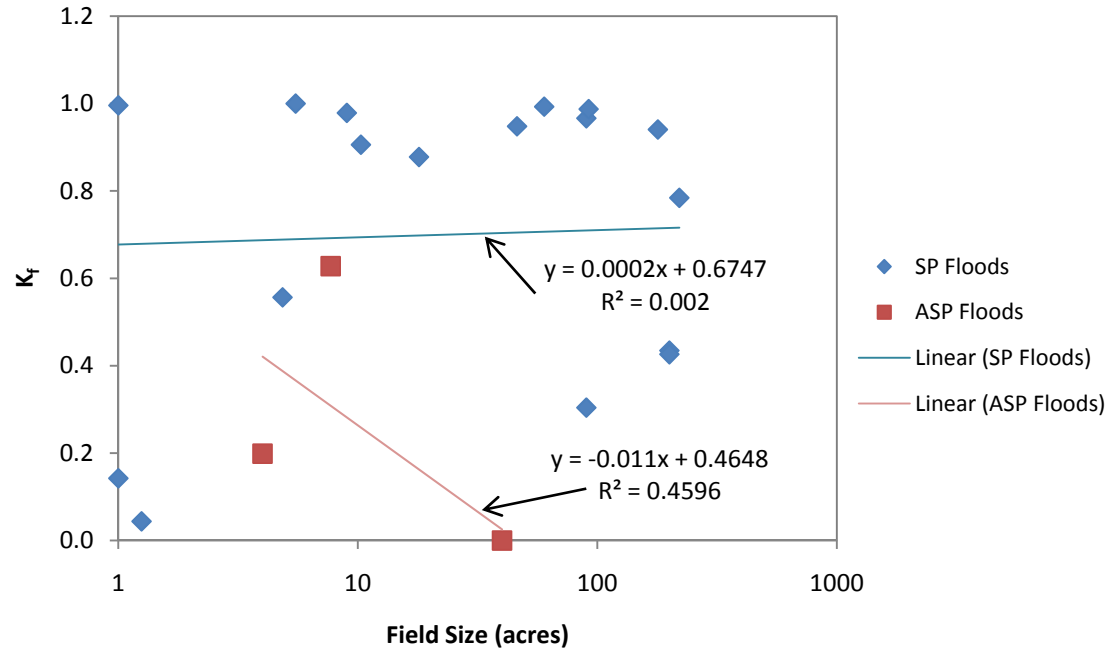

Figure B-12 K_f against Field Size for SP and ASP Floods

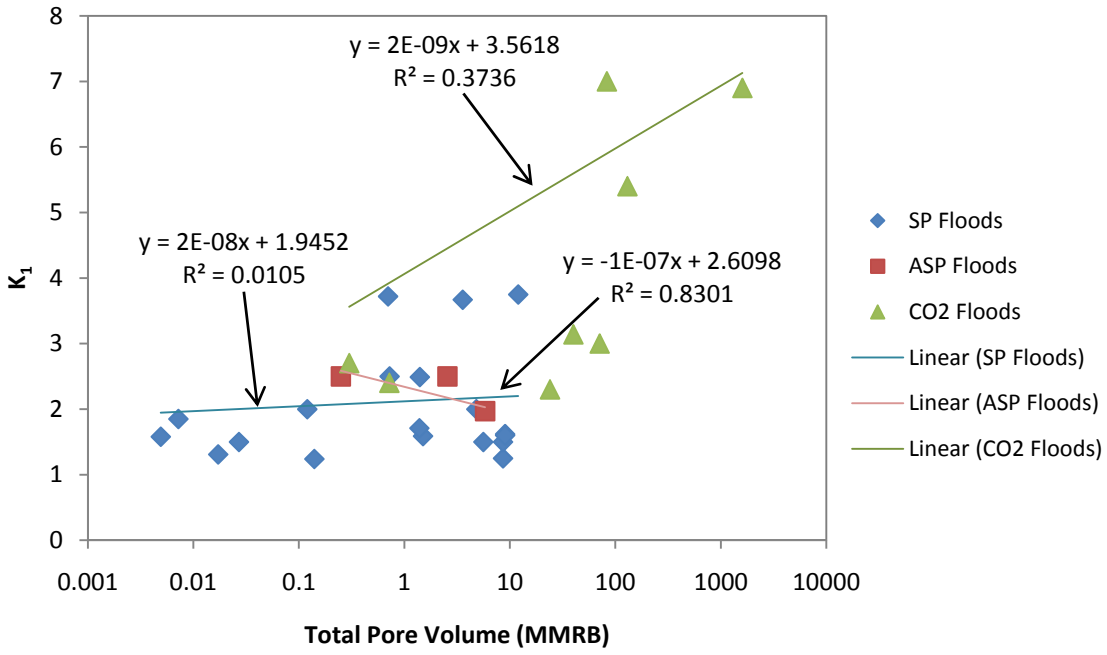

Figure B-13 K_1 against Total Pore Volume for Each Flood Type

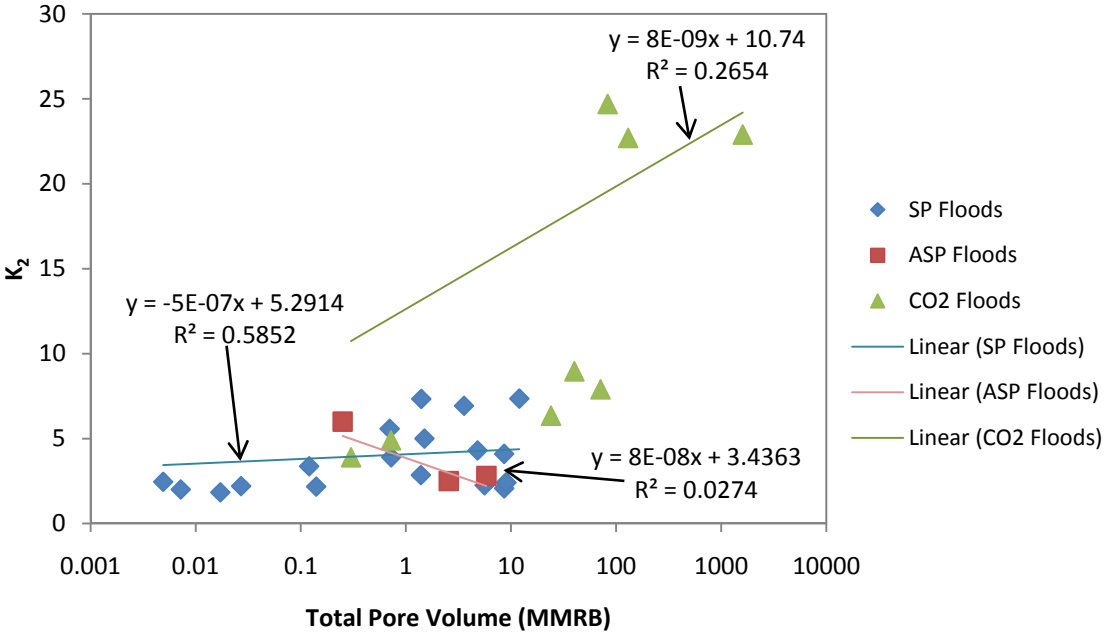

Figure B-14 K_2 against Total Pore Volume for Each Flood Type

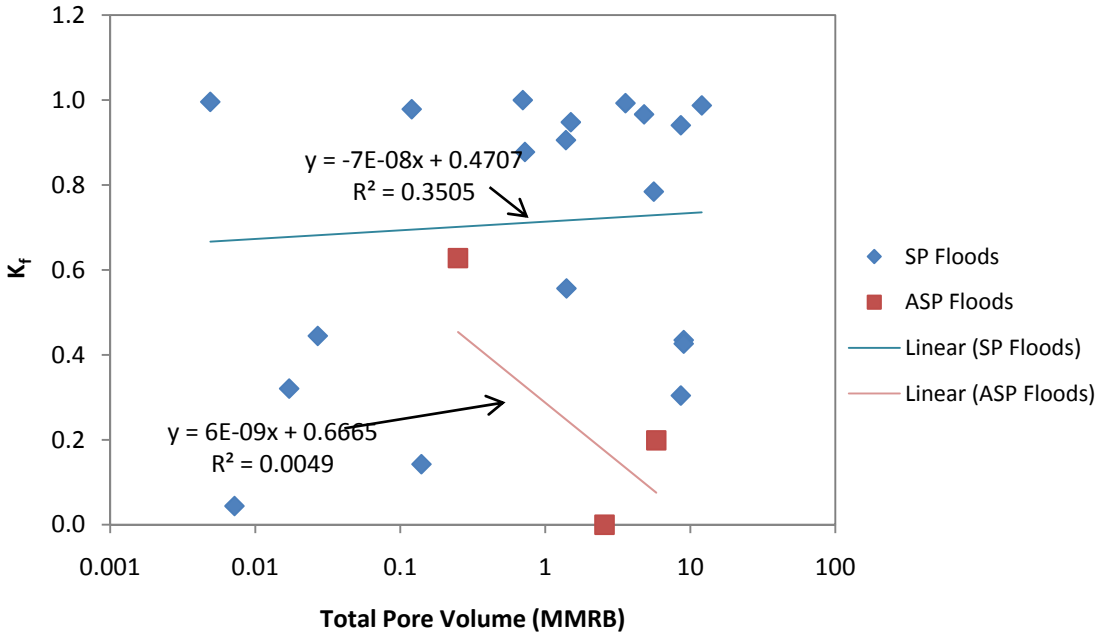

Figure B-15 K_f against Total Pore Volume for SP and ASP Floods

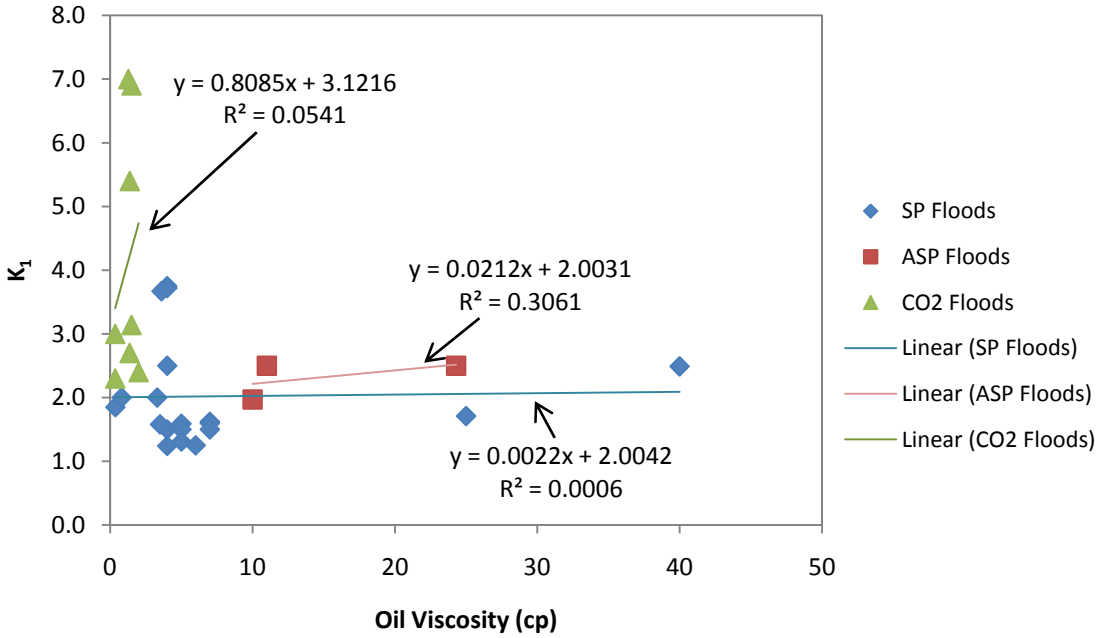

Figure B-16 K_1 against Oil Viscosity for Each Flood Type

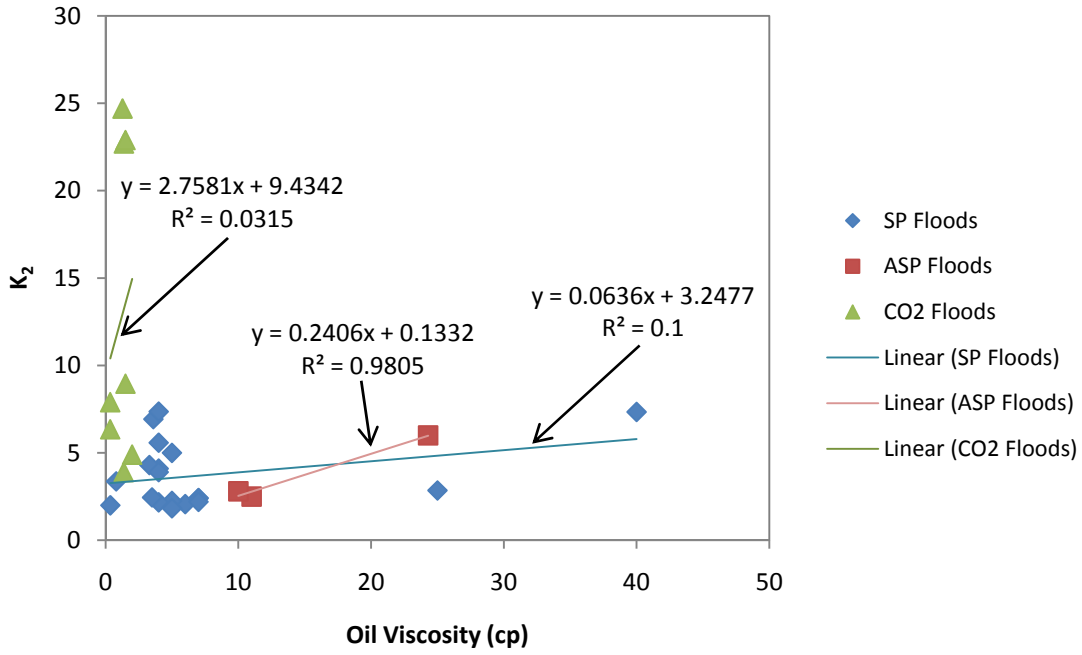

Figure B-17 K_2 against Oil Viscosity for Each Flood Type

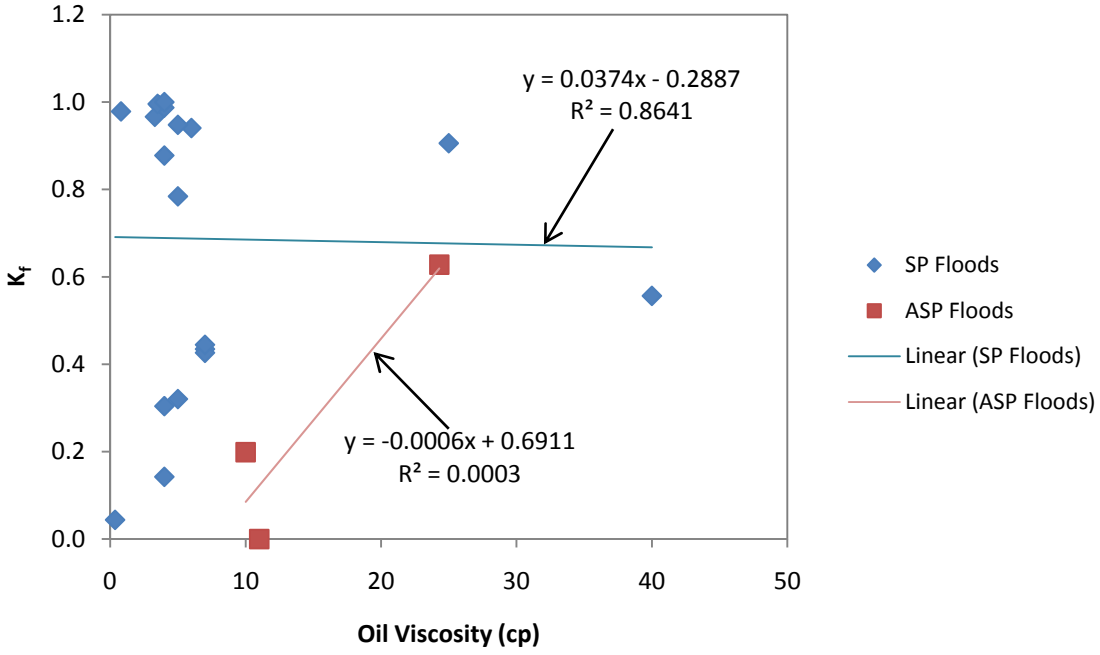

Figure B-18 K_f against Oil Viscosity for SP and ASP Floods

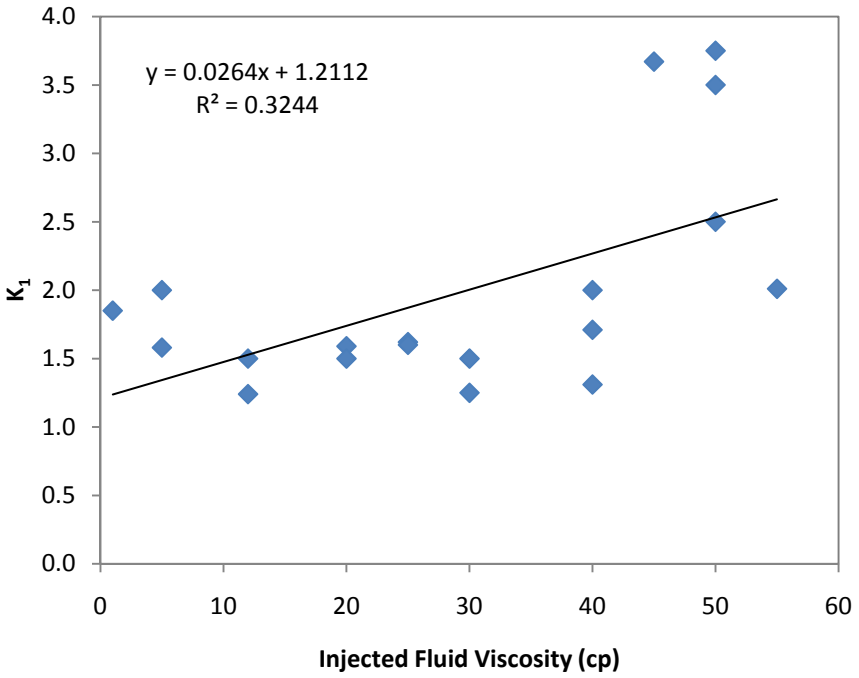

Figure B-19 K_1 against Injected Fluid Viscosity for Surfactant Polymer Floods

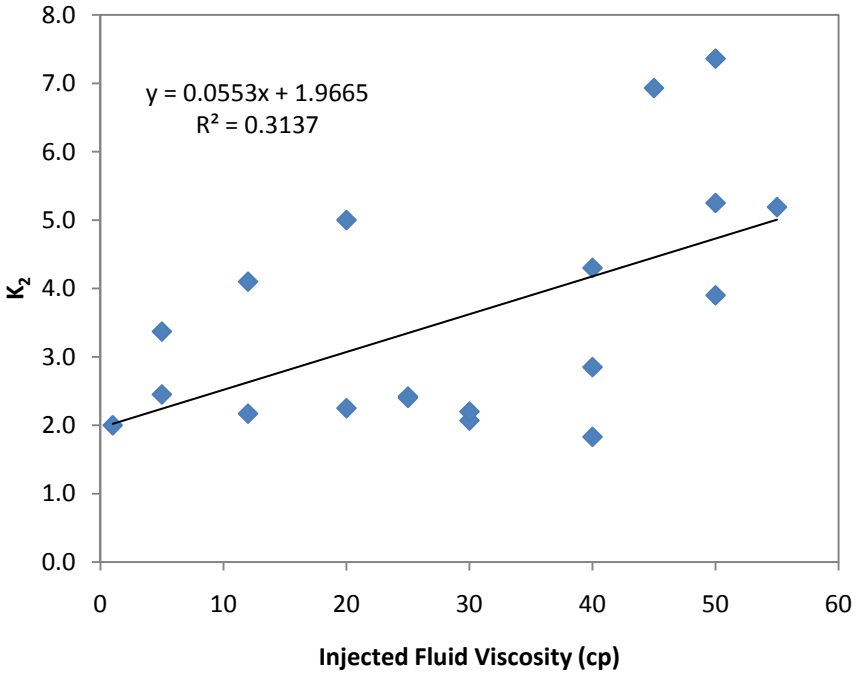

Figure B-20 K_2 against Injected Fluid Viscosity for Surfactant Polymer Floods

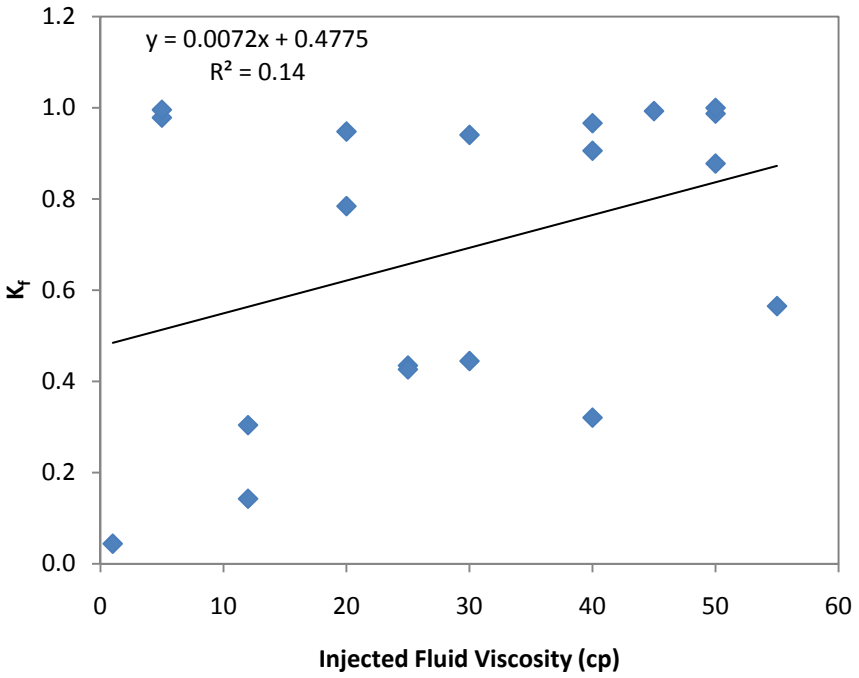

Figure B-21 K_f against Injected Fluid Viscosity for Surfactant Polymer Floods

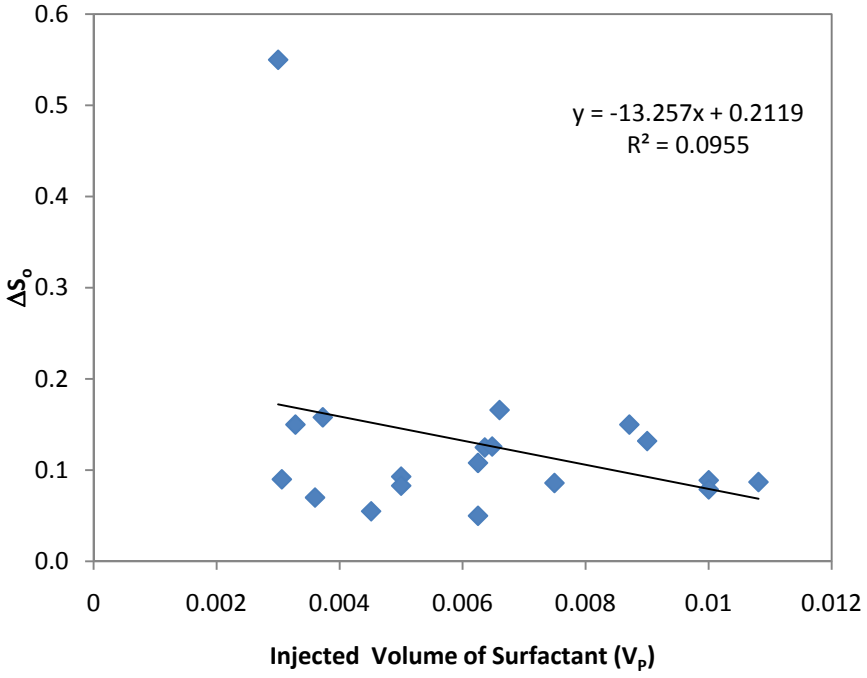

Figure B-22 ΔS_o against Injected Volume of Surfactant for Surfactant Polymer Floods

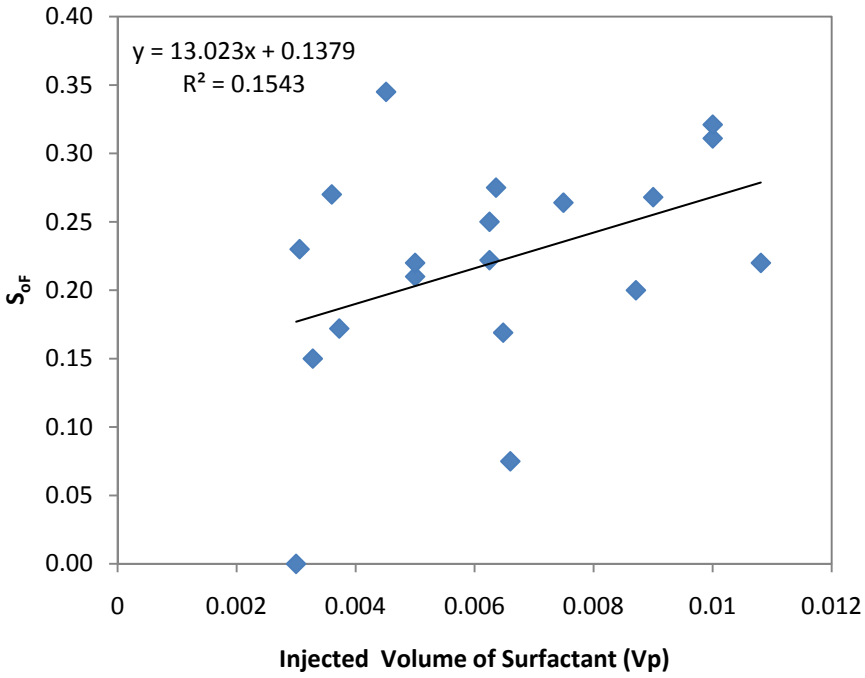

Figure B-23 S_{oF} against Injected Volume of Surfactant for Surfactant Polymer Floods

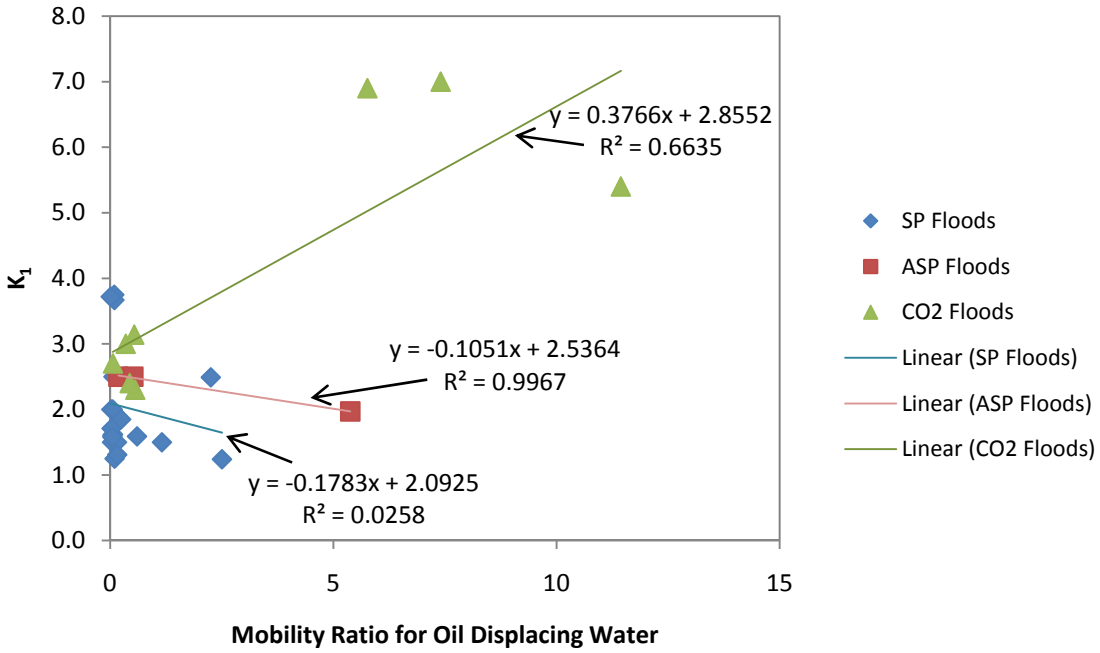

Figure B-24 K_1 against End Point Mobility Ratio for Oil Displacing Water for All Types of Floods

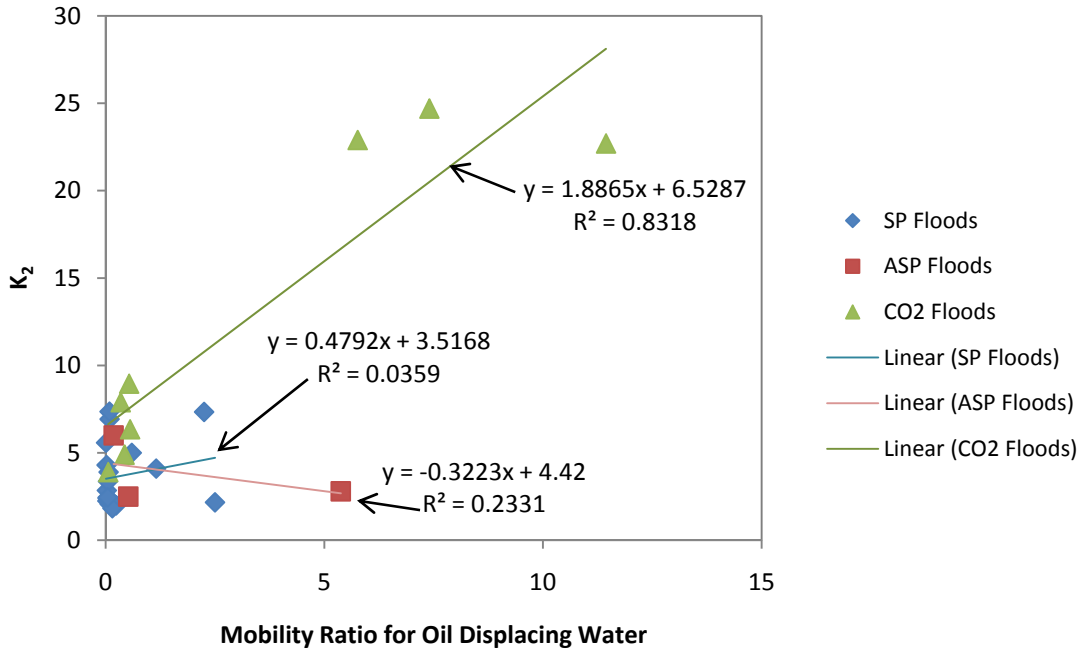

Figure B-25 K_2 against End Point Mobility Ratio for Oil Displacing Water for All Types of Floods

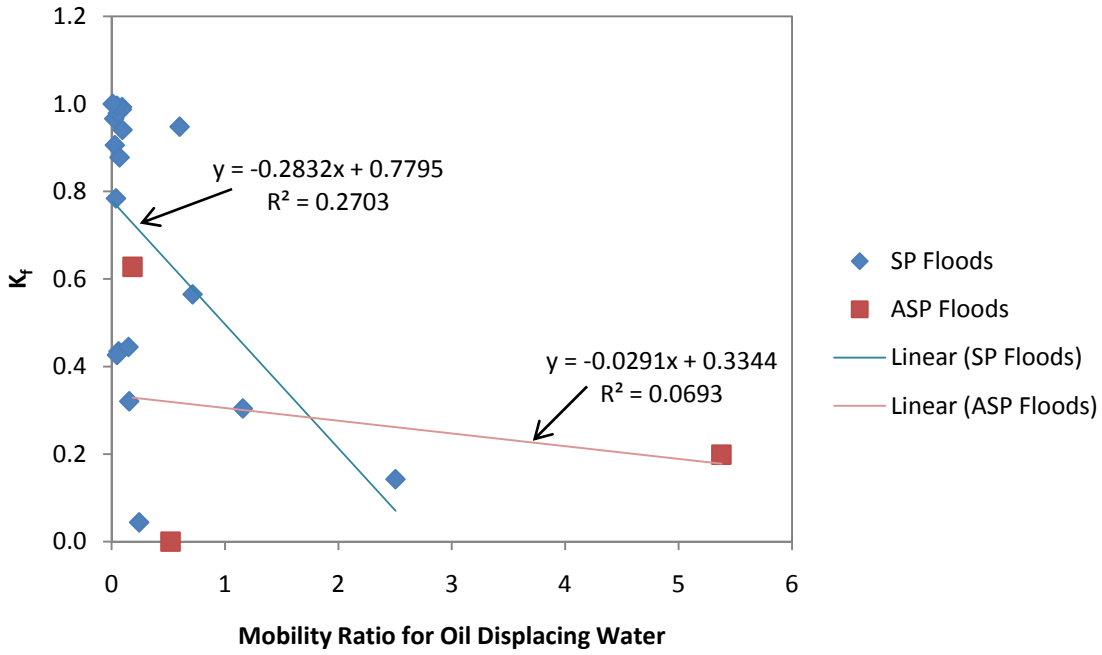

Figure B-26 K_f against End Point Mobility Ratio for Oil Displacing Water for SP and ASP Floods

APPENDIX C: SENSITIVITY ANALYSIS PLOTS

C.1 Introduction

The following is a collection of all of the plots created for the sensitivity analysis. These plots are discussed in more detail in Chapter 6.

C.2 Sensitivity Analysis Plots for Surfactant-Polymer Floods

The following are all of the plots produced for the sensitivity analysis of all of the parameters associated with surfactant-polymer floods.

C.2.1 Sensitivity Plots for the Parameters of the Simplified Enhanced Oil Recovery Method

These plots include analyses of the following parameters: change in oil saturation, total pore volumes, heterogeneity factors, and the specific shock velocity of the oil bank.

C.2.1.1 Change in Oil Saturation

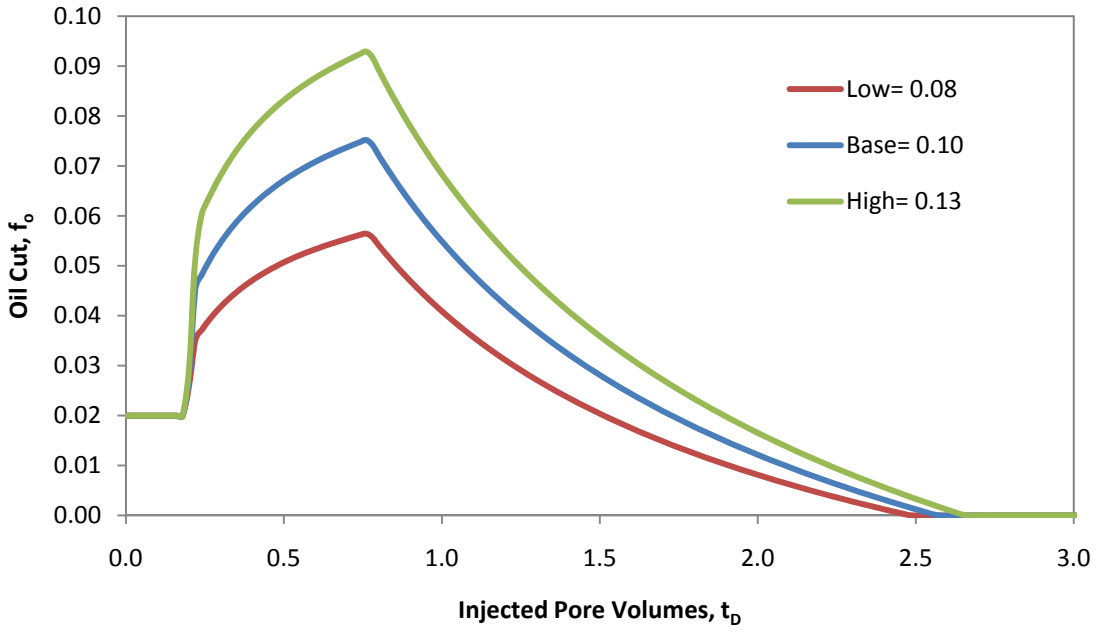

Figure C-1 Plot of Oil Cut against Dimensionless Time for Varying ΔS_o for SP Floods

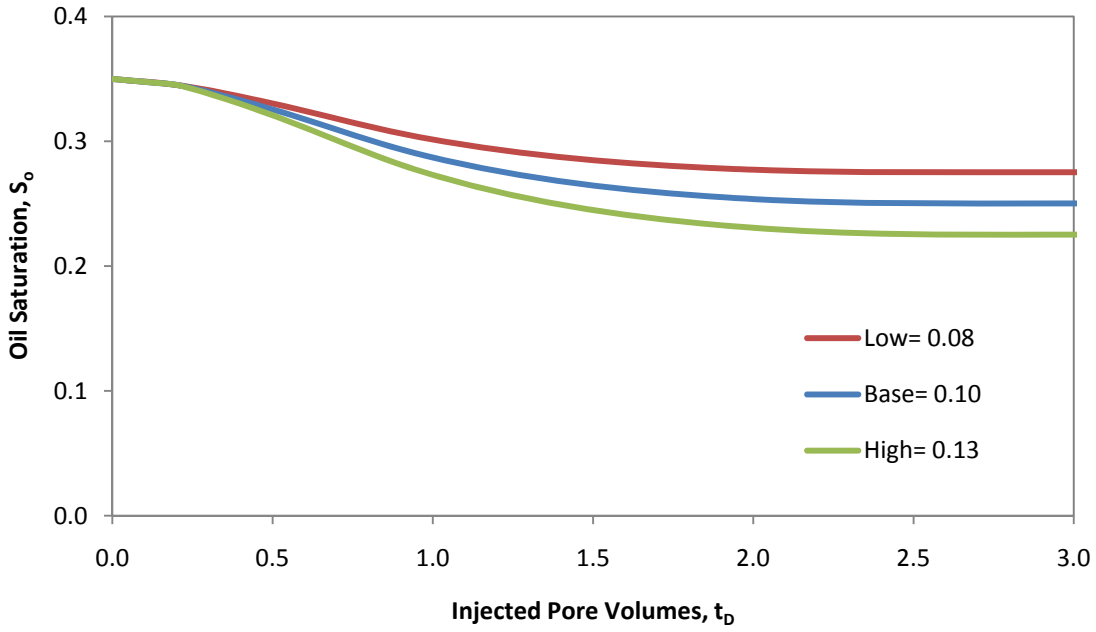

Figure C-2 Plot of Oil Saturation against Dimensionless Time for Varying ΔS_o for SP Floods

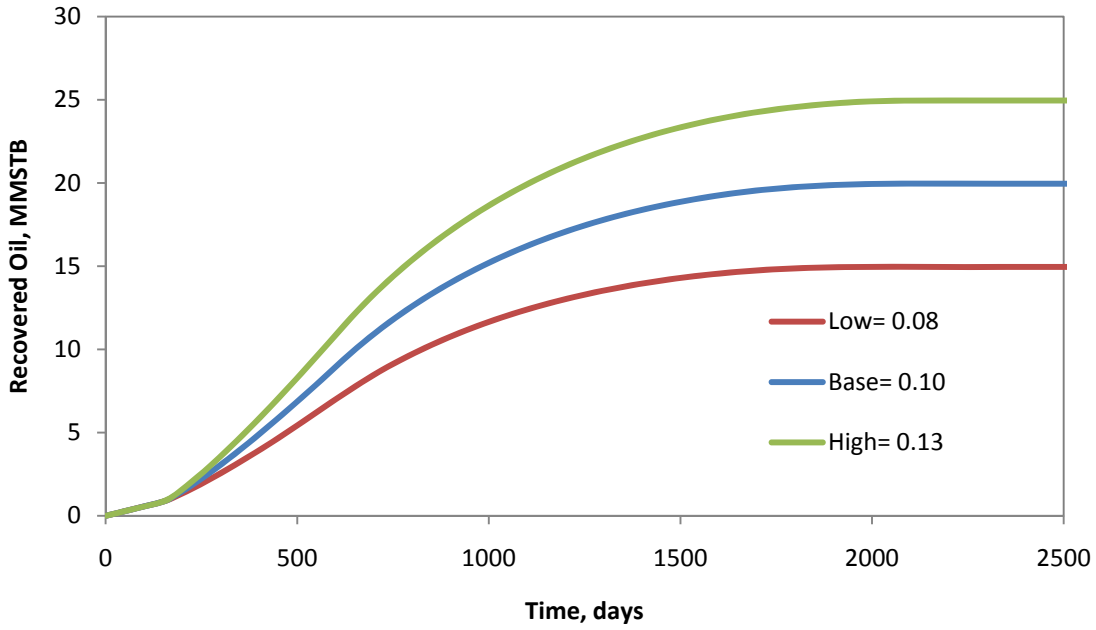

Figure C-3 Plot of Oil Recovery against Time for Varying ΔS_o for SP Floods

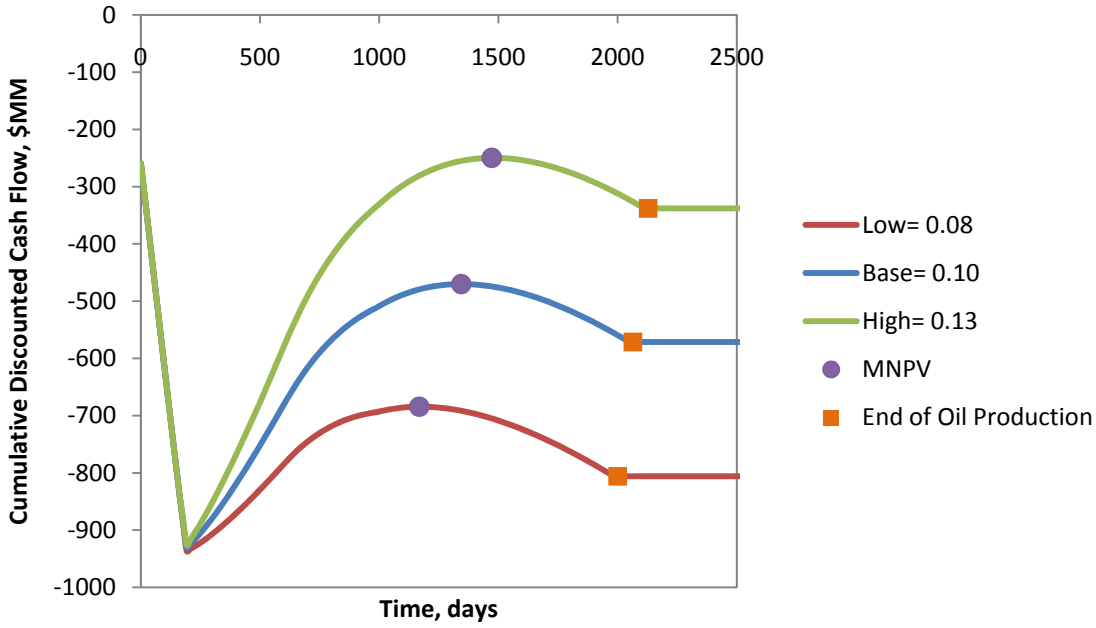

Figure C-4 Plot of CDCF against Time for Varying ΔS_o for SP Floods

C.2.1.2 Total Pore Volumes

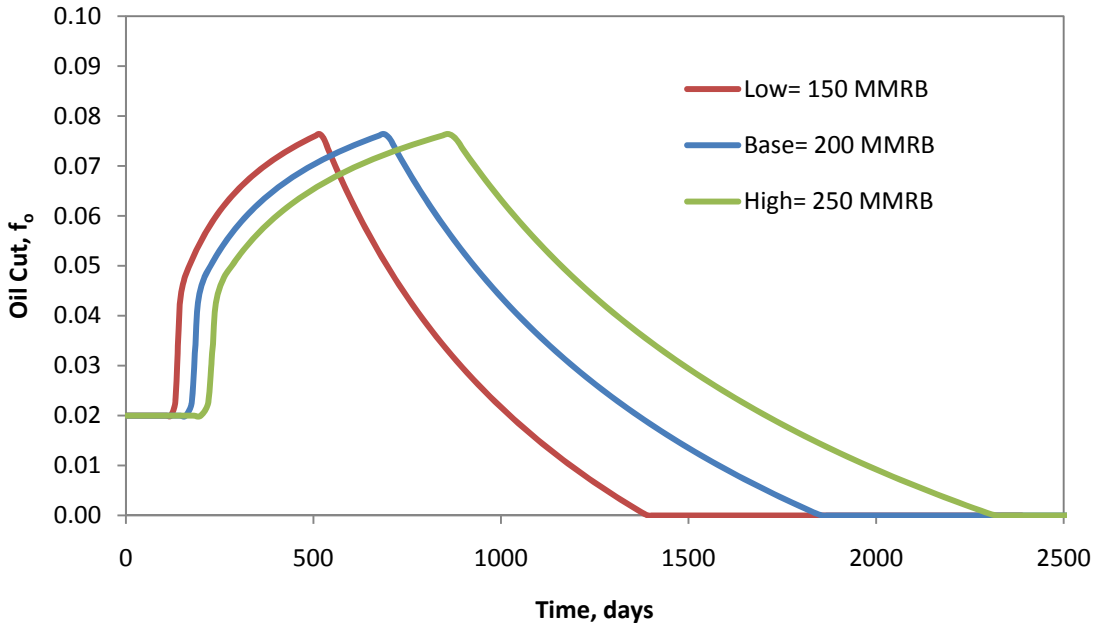

Figure C-5 Plot of Oil Cut against Time for a Varying V_p for SP Floods

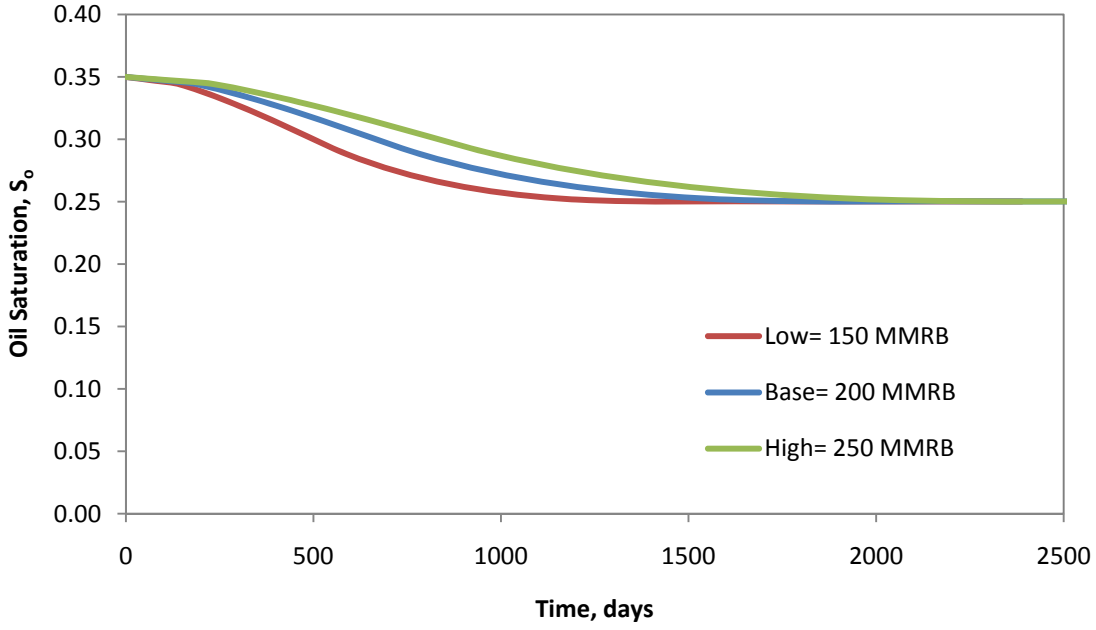

Figure C-6 Plot of Oil Saturation against Time for a Varying V_p

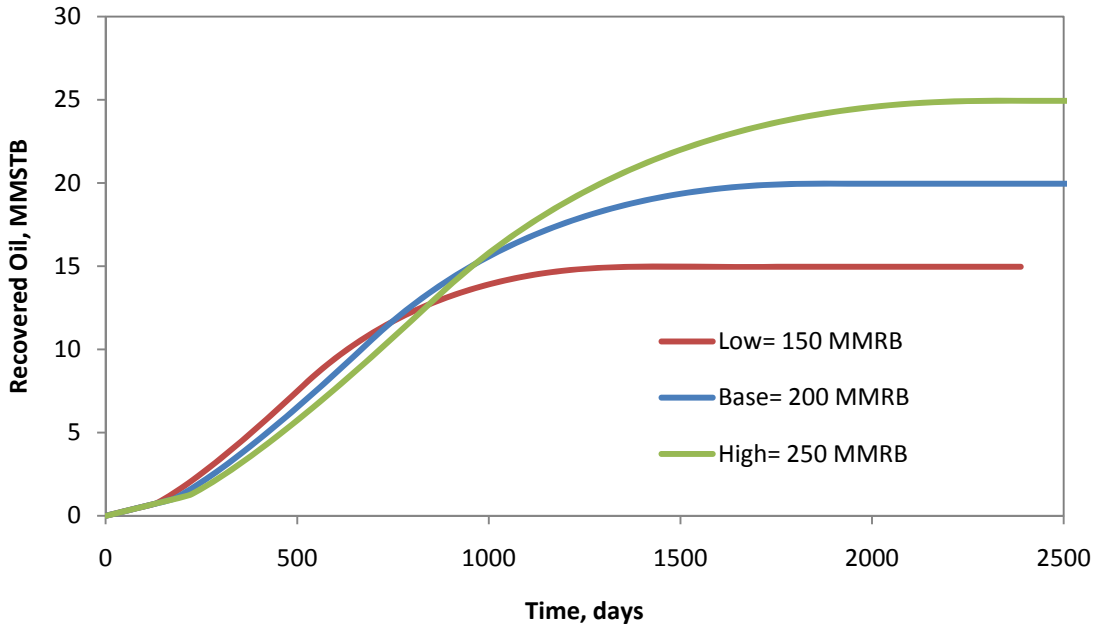

Figure C-7 Plot of Oil Recovery against Time for a Varying V_p for SP Floods

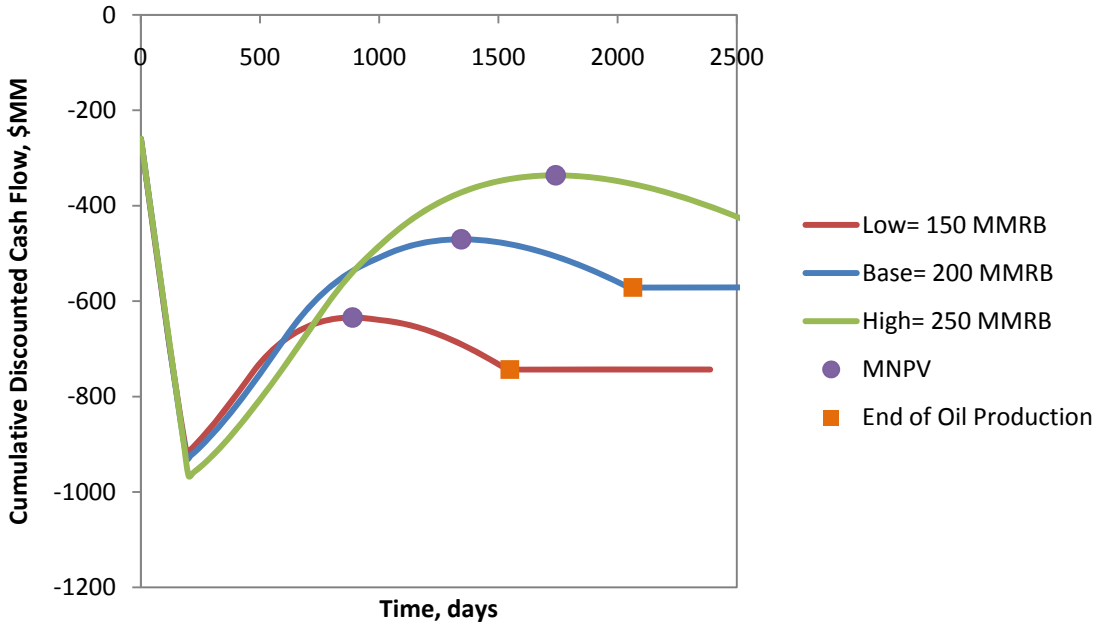

Figure C-8 Plot of CDCF against Time for a Varying V_p for SP Floods

C.2.1.3 Heterogeneity Factors

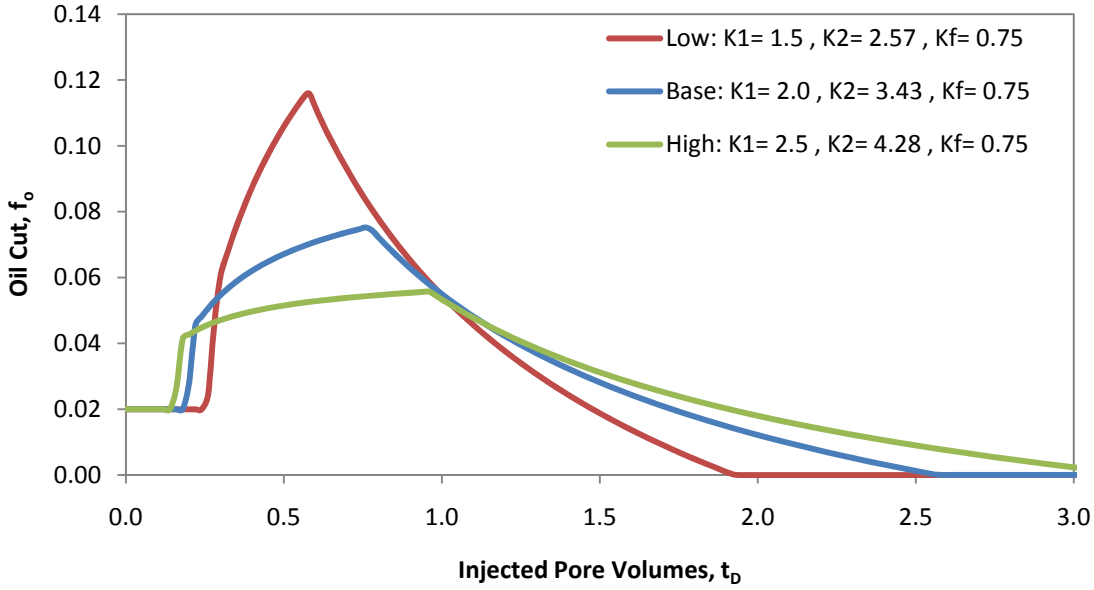

Figure C-9 Plot of Oil Cut against Dimensionless Time for a Varying K_1 for SP Floods

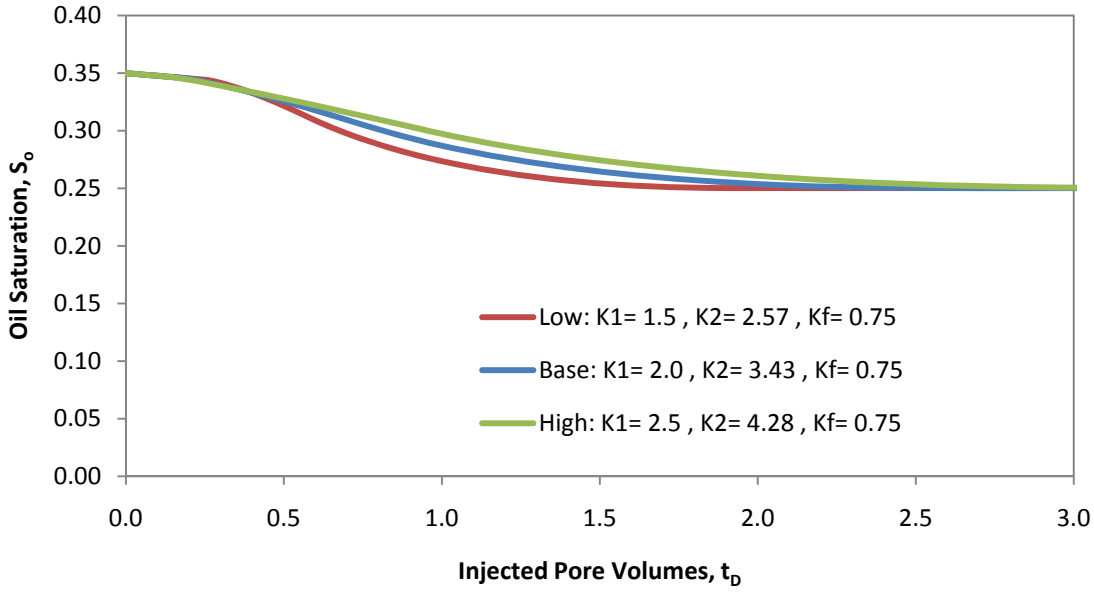

Figure C-10 Plot of Oil Saturation against Dimensionless Time for a Varying K_1 for SP Floods

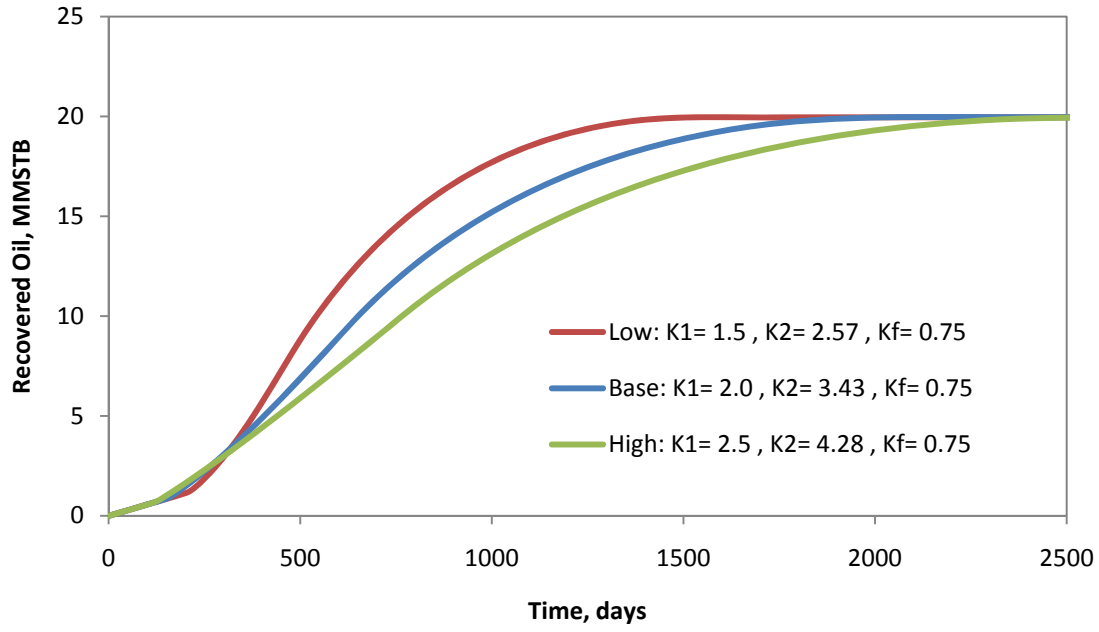

Figure C-11 Plot of Oil Recovery against Time for a Varying K_1 for SP Floods

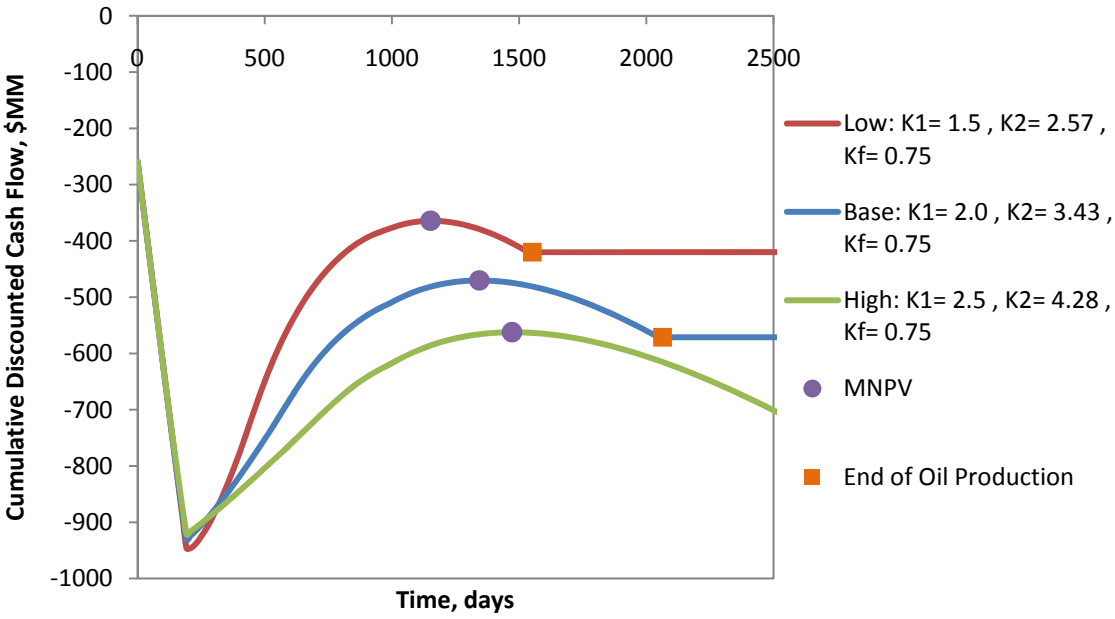

Figure C-12 Plot of CDCF against Time for a Varying K_1 for SP Floods

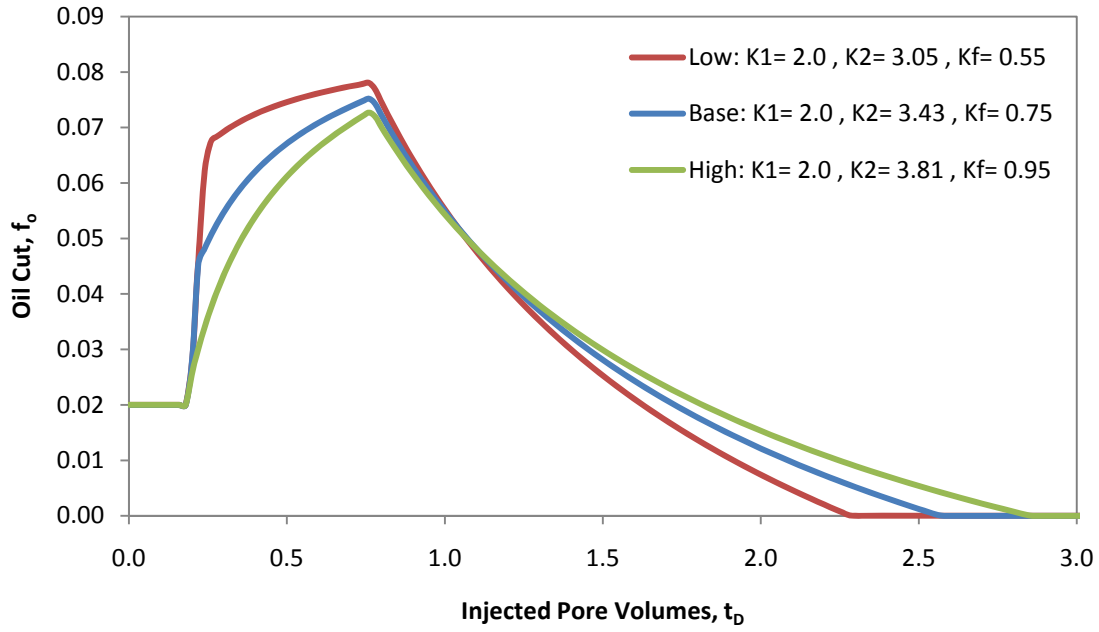

Figure C-13 Plot of Oil Cut against Dimensionless Time for a Varying K_f for SP Floods

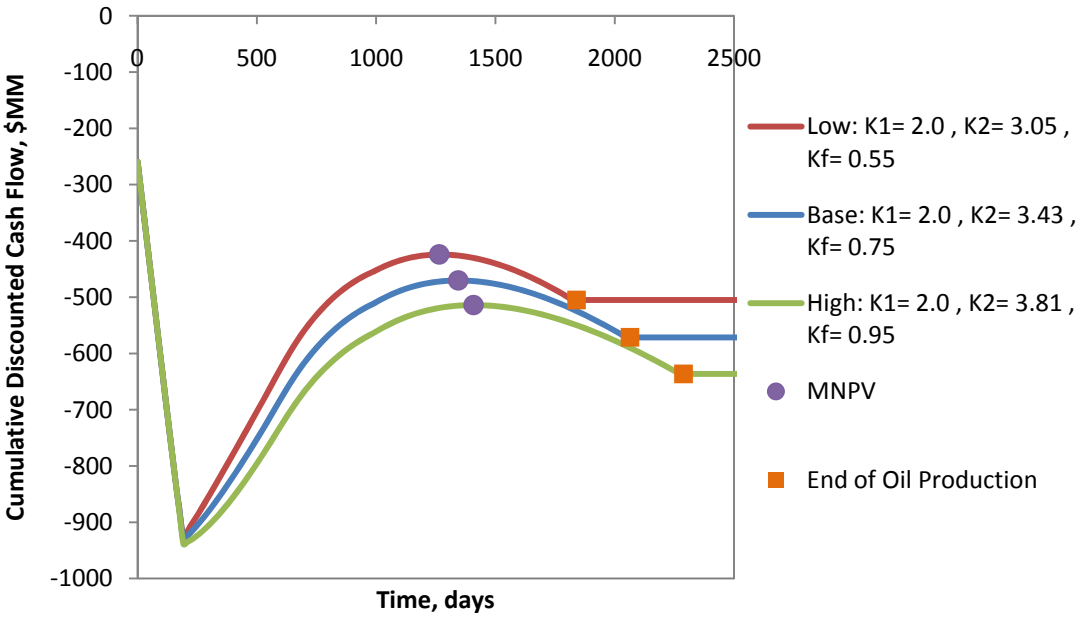

Figure C-14 Plot of CDCF against Time for a Varying K_f for SP Floods

C.2.1.4 Specific Shock Velocity of Oil Bank

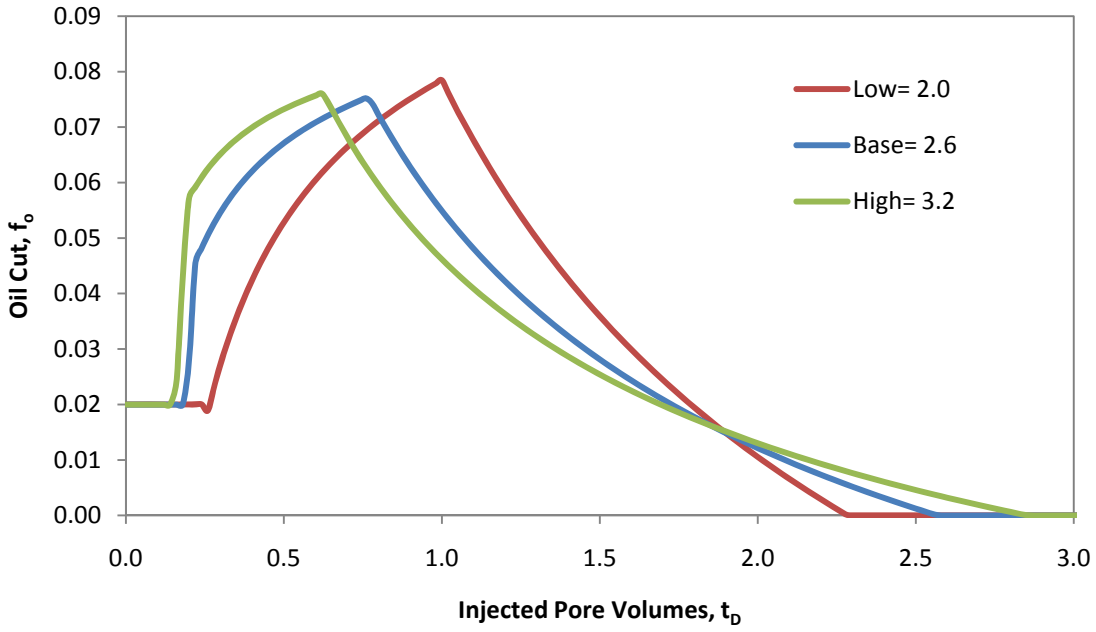

Figure C-15 Plot of Oil Cut against Dimensionless Time for a Varying v_{oB} for SP Floods

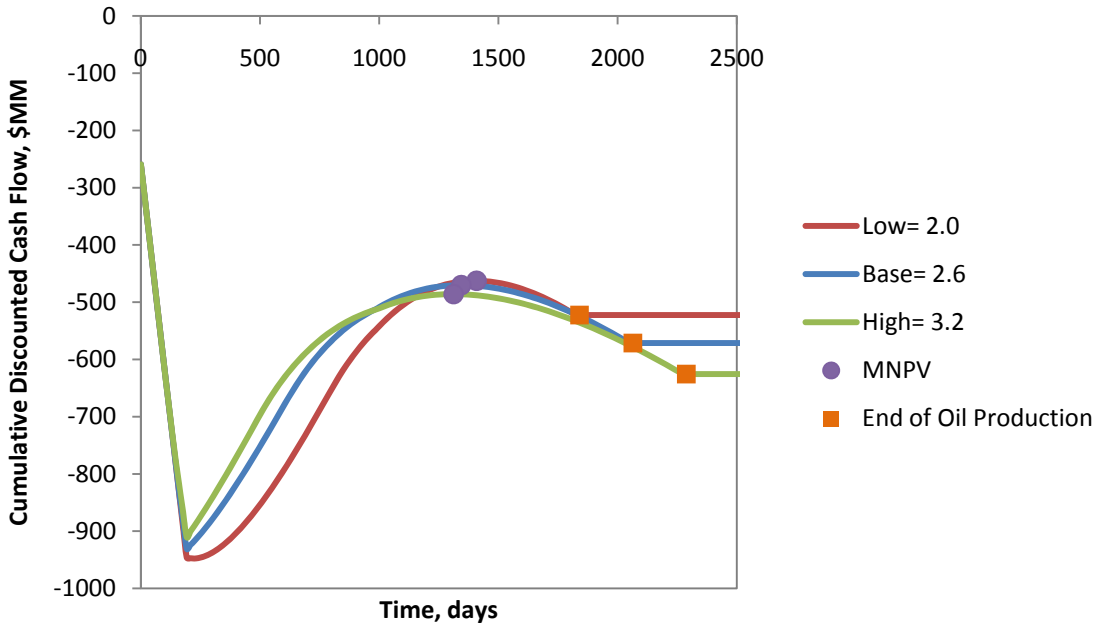

Figure C-16 Plot of CDCF against Time for a Varying v_{oB} for SP Floods

C.2.2 Sensitivity Plots of the Design Parameters

These plots include analyses of the following design parameters: well spacing, injection rate, production rate, pore volumes for the injected chemicals, and concentrations for the chemicals.

C.2.2.1 Well Spacing

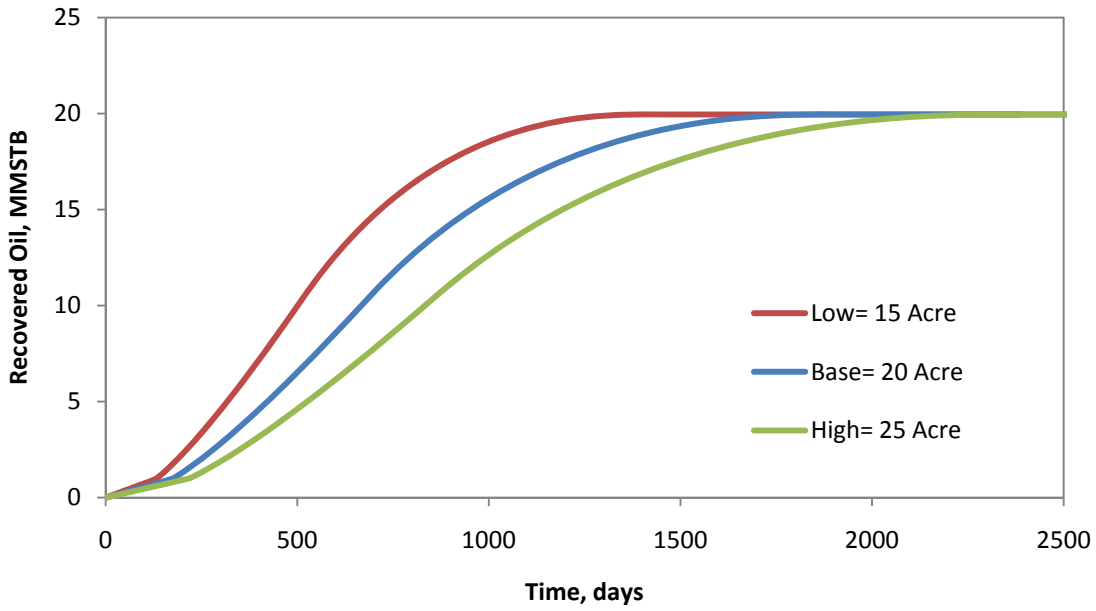

Figure C-17 Plot of Oil Recovery against Time for a Varying WS for SP Floods

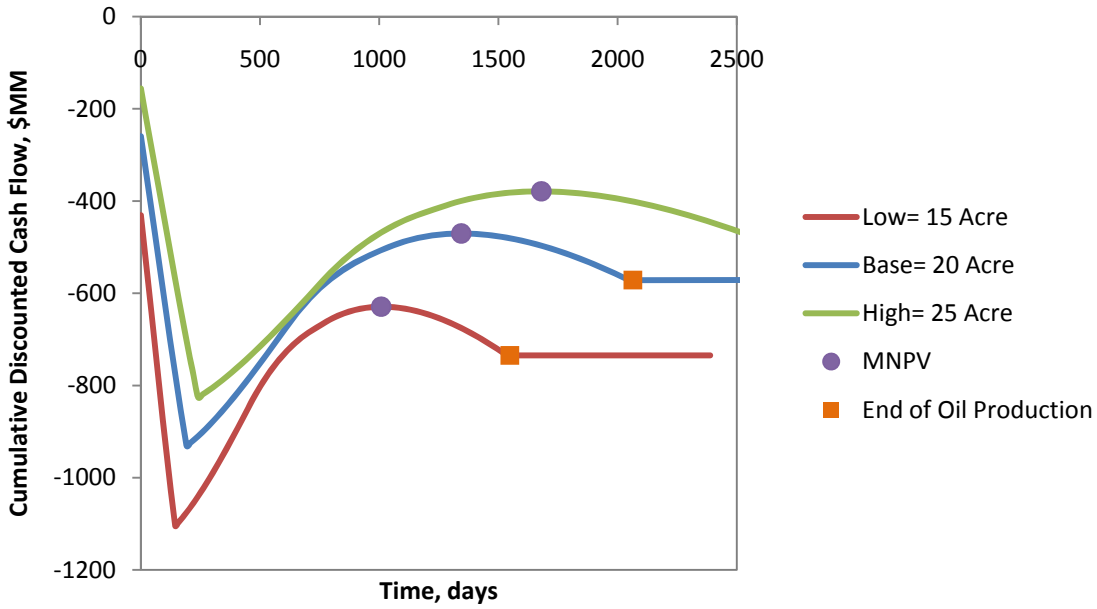

Figure C-18 Plot of CDCF against Time for Varying WS for SP Floods

C.2.2.2 Injection Rate

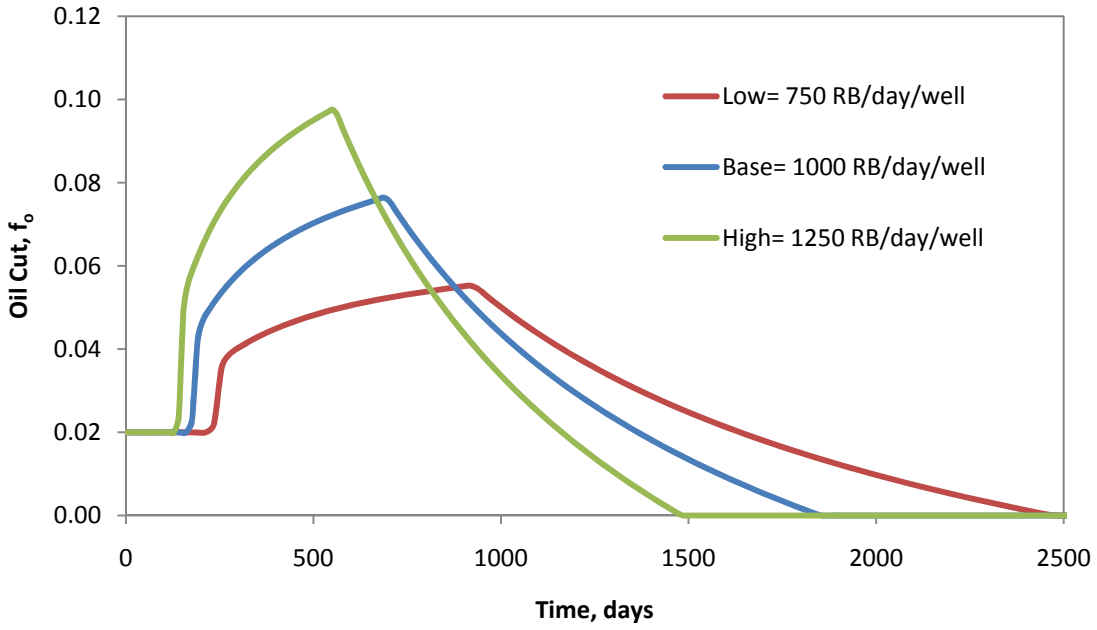

Figure C-19 Plot of Oil Cut against Time for a Varying q_i for SP Floods

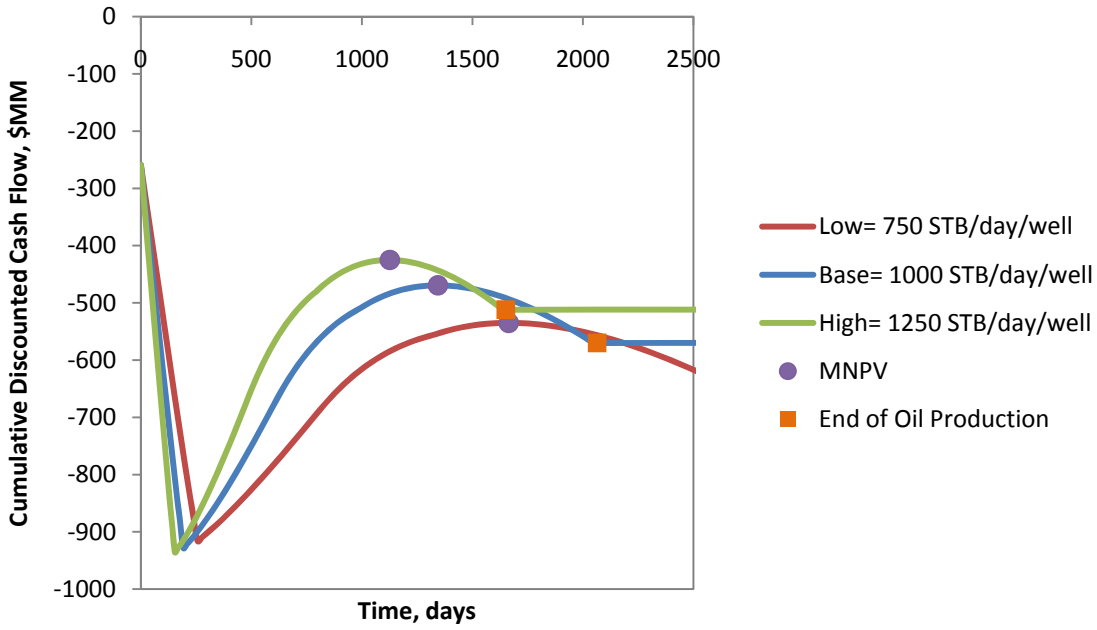

Figure C-20 Plot of CDCF against Time for a Varying q_i for SP Floods

C.2.2.3 Production Rate

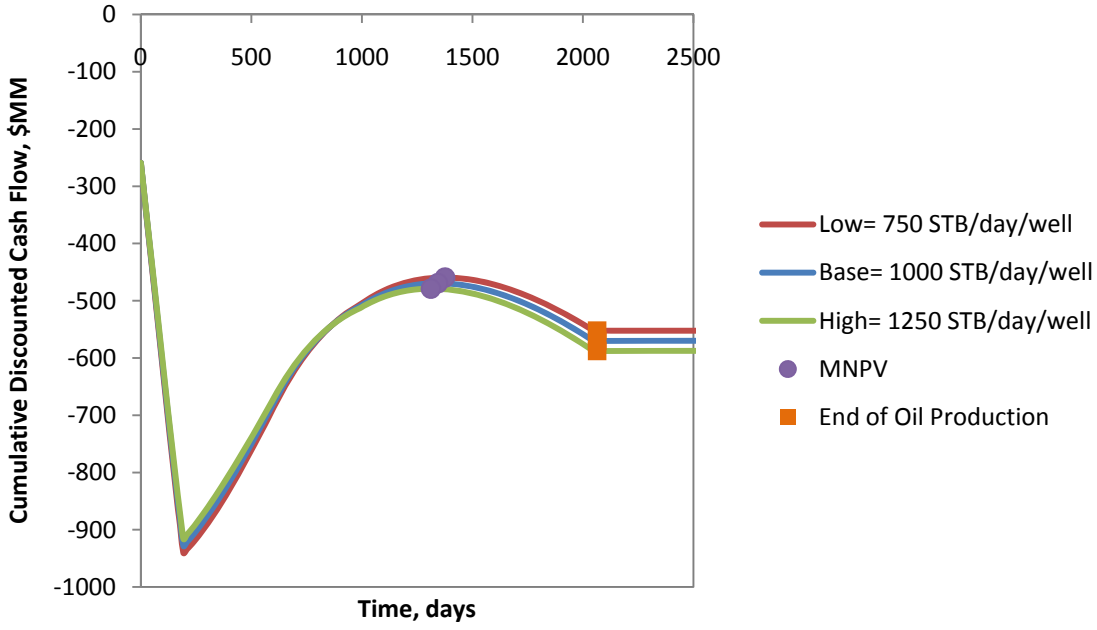

Figure C-21 Plot of CDCF against Time for Varying q_p for SP Floods

C.2.2.4 Surfactant-Polymer and Polymer Slug Sizes

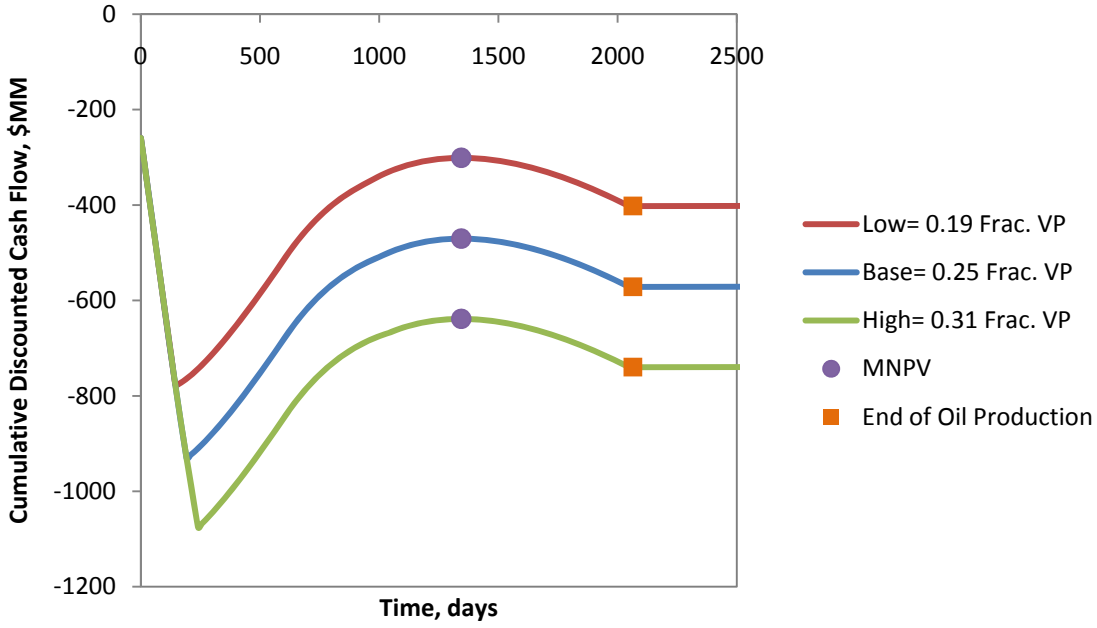

Figure C-22 Plot of CDCF against Time for Varying V_{Chem} for SP Floods

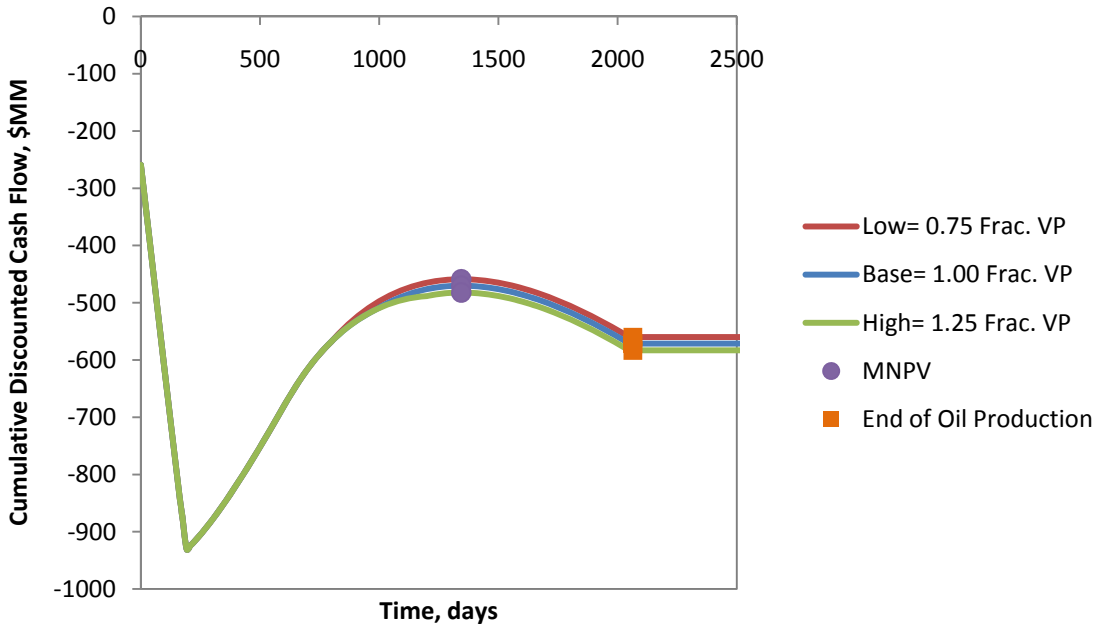

Figure C-23 Plot of CDCF against Time for Varying V_{Poly} for SP Floods

C.2.2.5 Concentrations of Surfactant and Polymer

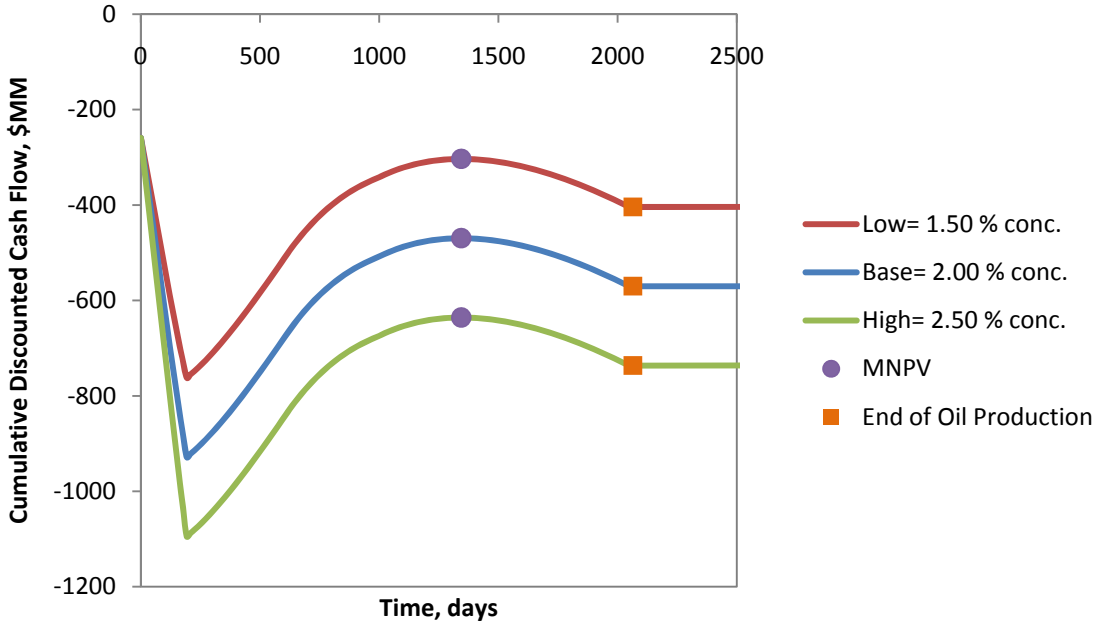

Figure C-24 Plot of CDCF against Time for Varying Z_{Sur} for SP Floods

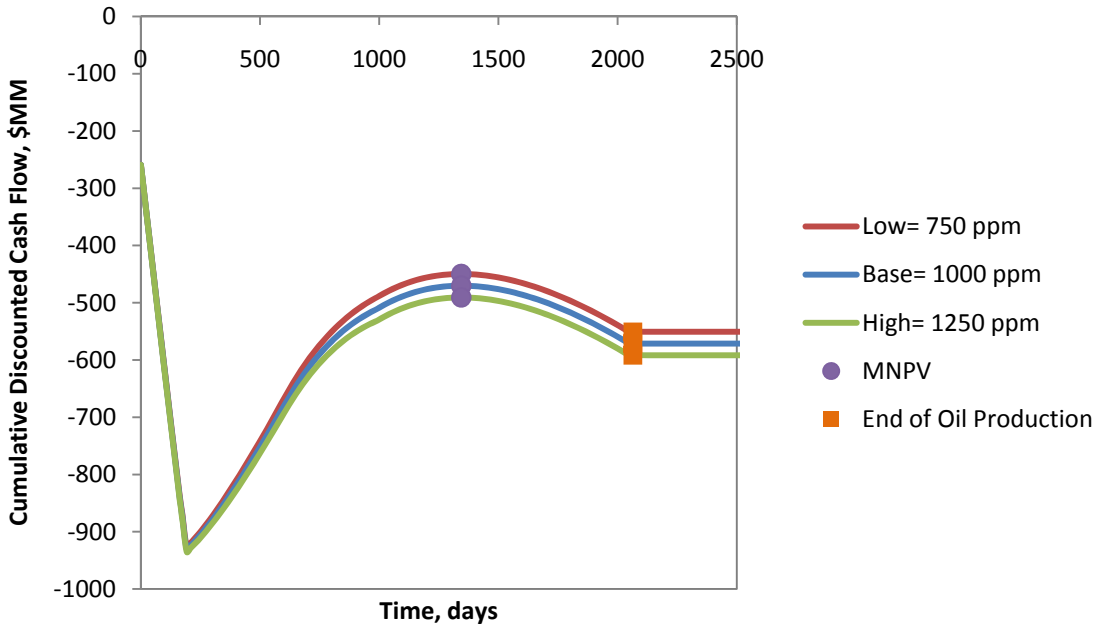

Figure C-25 Plot of CDCF against Time for Varying Z_{Poly} SP Floods

C.2.3 Sensitivity Plots for Economic Parameters

The following plots are for the following economic parameter: price of oil, escalation factor, price of surfactant, price of polymer, cost of injection, cost of treatment, cost of water disposal, upfront costs, maintenance costs, royalties, ad-valorem tax, severance tax, inflation, and discount rate.

C.2.3.1 Price of Oil and Escalation Factor for the Price of Oil

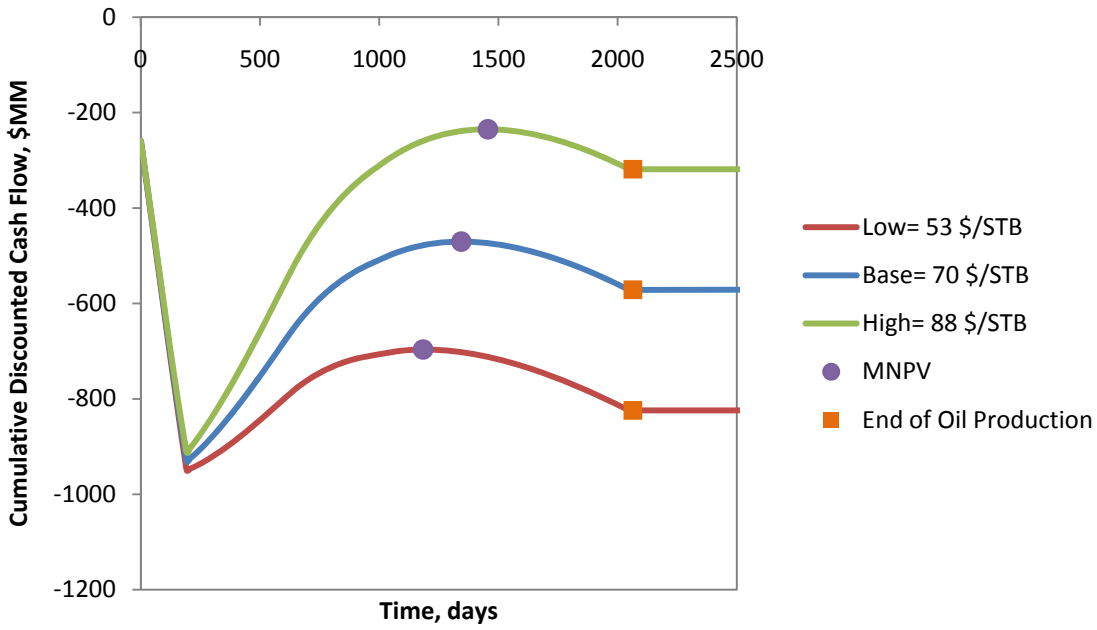

Figure C-26 Plot of CDCF against Time for Varying P_o for SP Floods

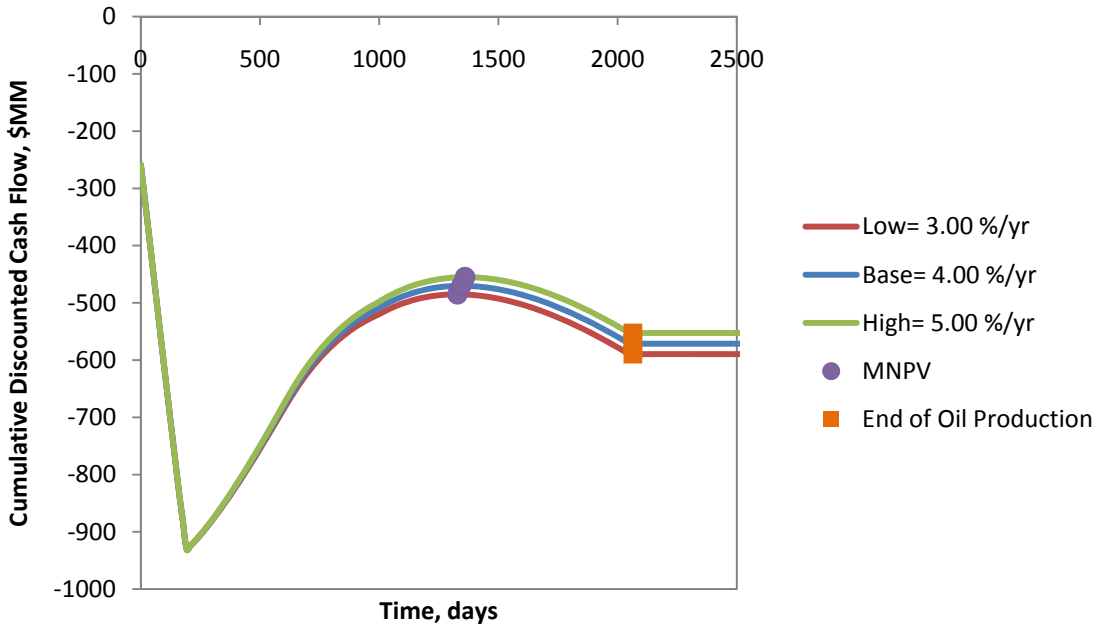

Figure C-27 Plot of CDCF against Time for Varying R_E for SP Floods

C.2.3.2 Price of Surfactant and Polymer

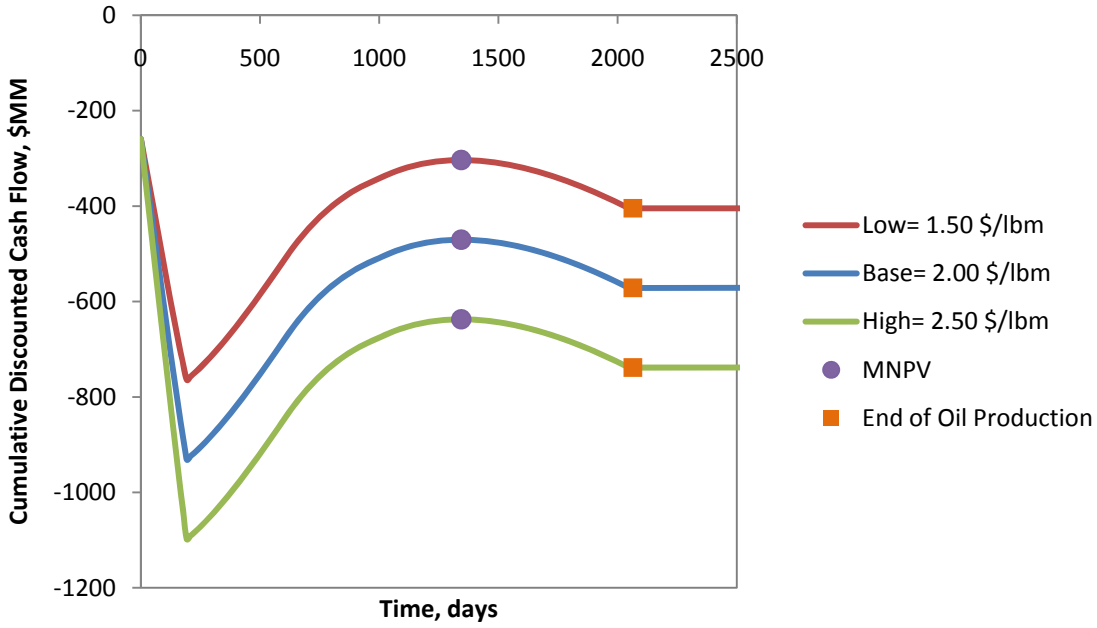

Figure C-28 Plot of CDCF against Time for Varying C_{Sur} for SP Floods

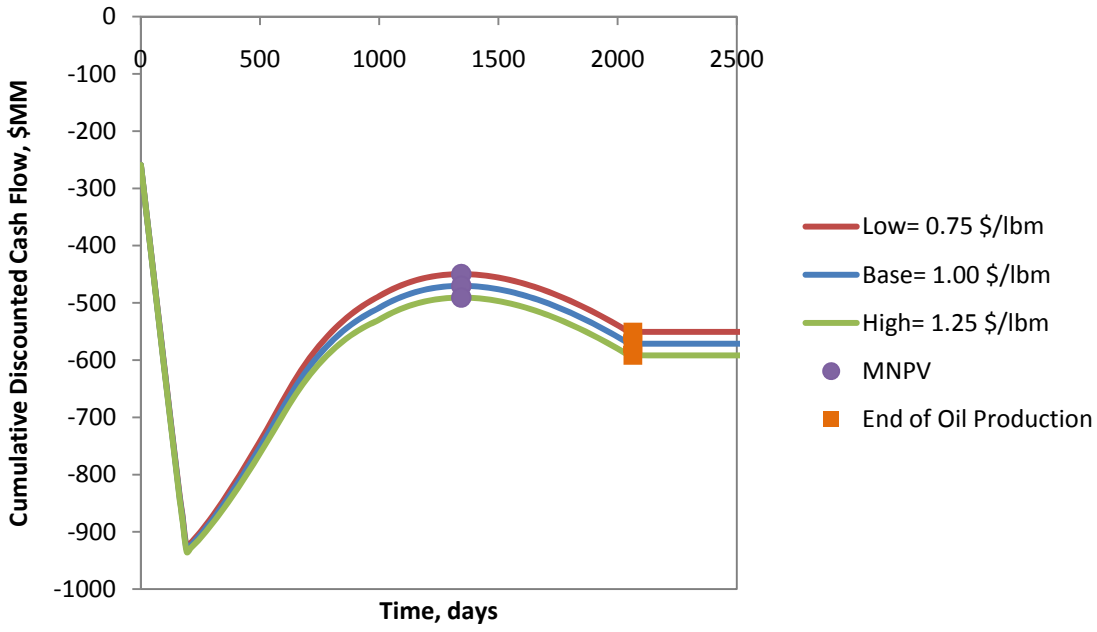

Figure C-29 Plot of CDCF against Time for Varying C_{Poly} for SP Floods

C.2.3.3 Costs of Injection, Treatment, Water Disposal

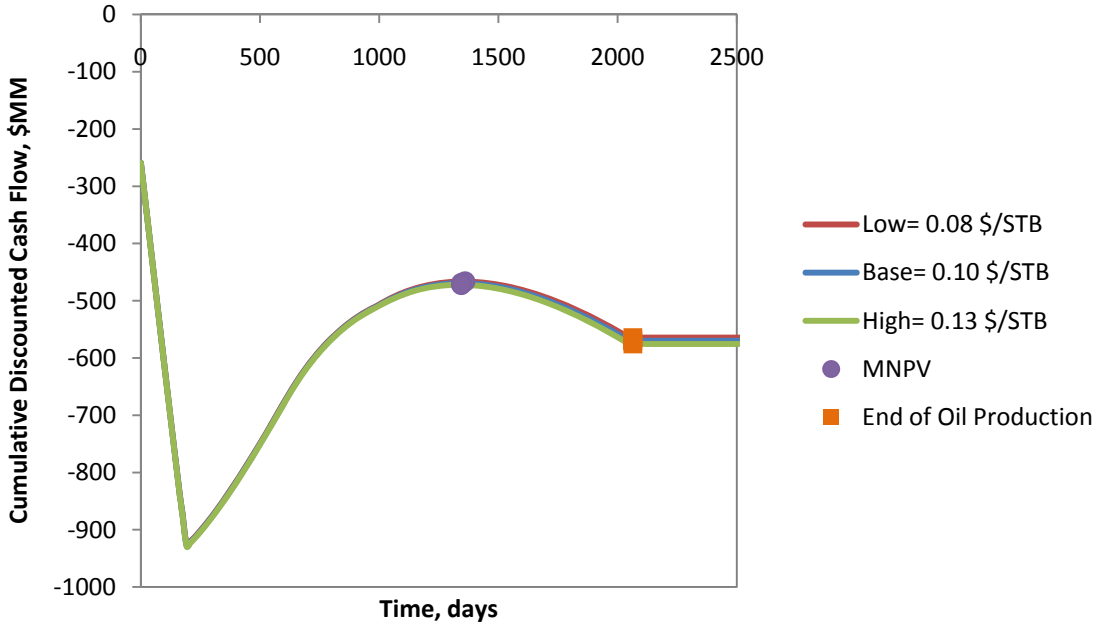

Figure C-30 Plot of CDCF against Time for Varying C_q for SP Floods

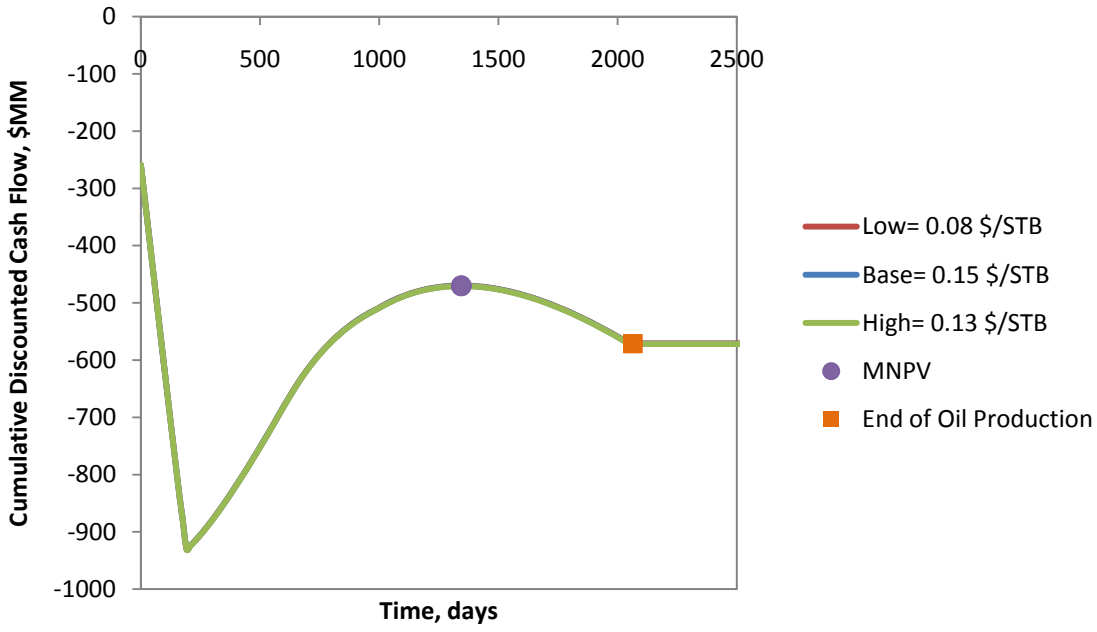

Figure C-31 Plot of CDCF against Time for Varying C_T for SP Floods

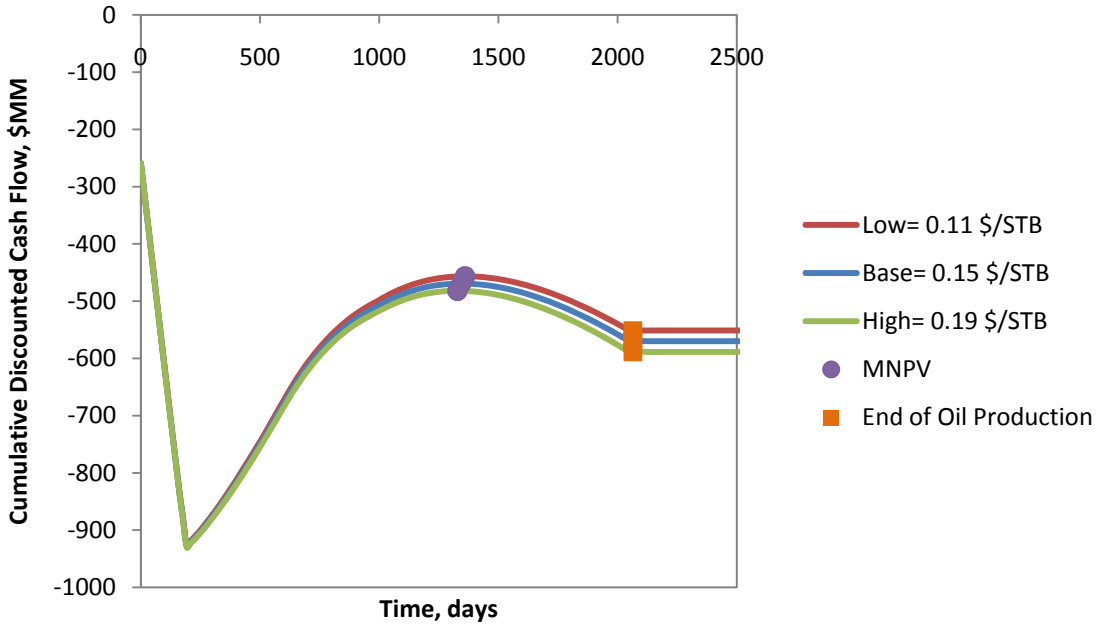

Figure C-32 Plot of CDCF against Time for Varying C_{WD} for SP Floods

C.2.3.4 Upfront and Maintenance Costs

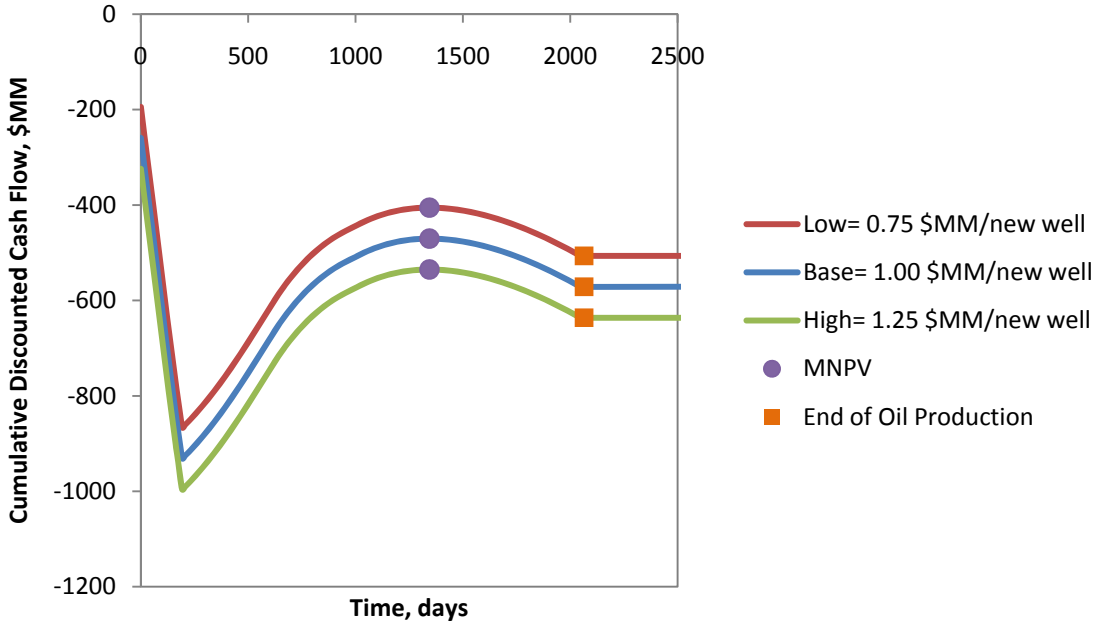

Figure C-33 Plot of CDCF against Time for a Varying C_I for SP Floods

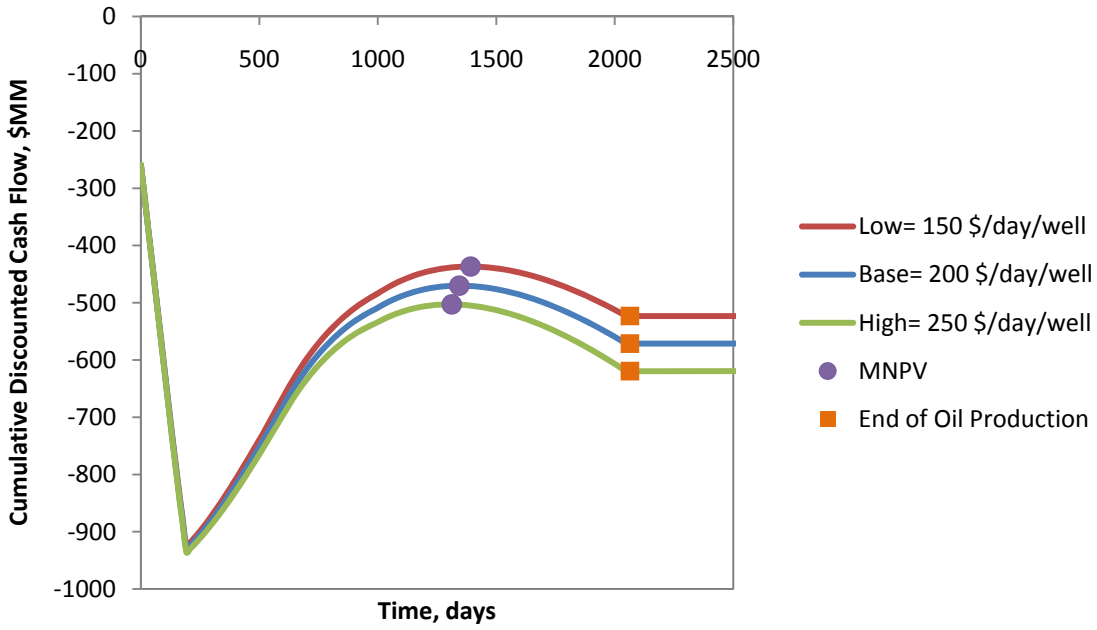

Figure C-34 Plot of CDCF against Time for a Varying C_M for SP Floods

C.2.3.5 Royalty, Ad-Valorem Tax, Severance Tax

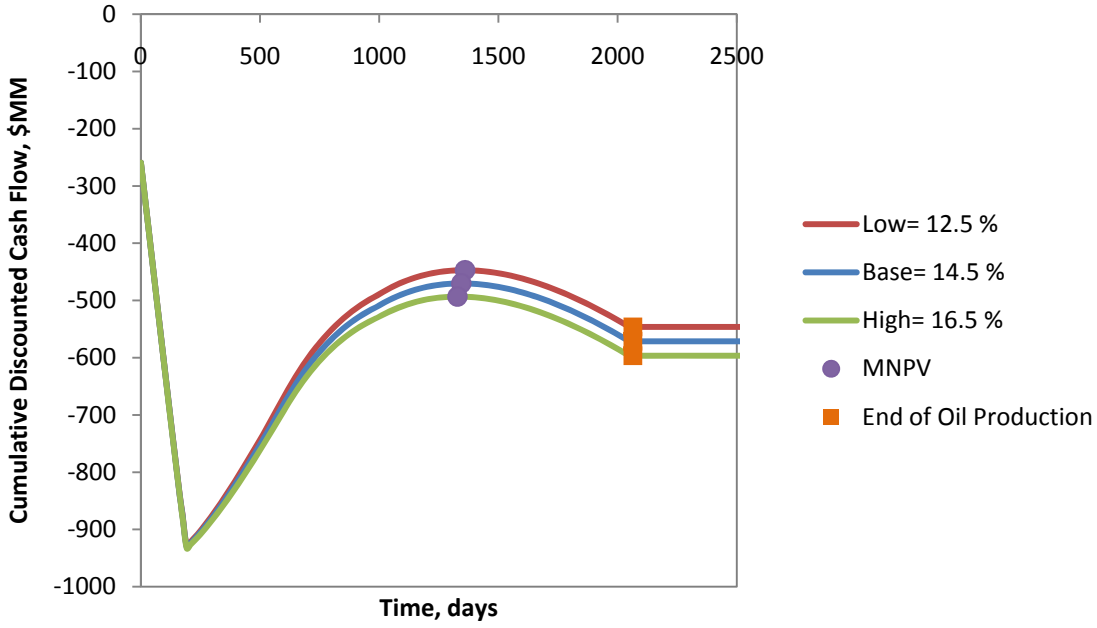

Figure C-35 Plot of CDCF against Time for a Varying T_R for SP Floods

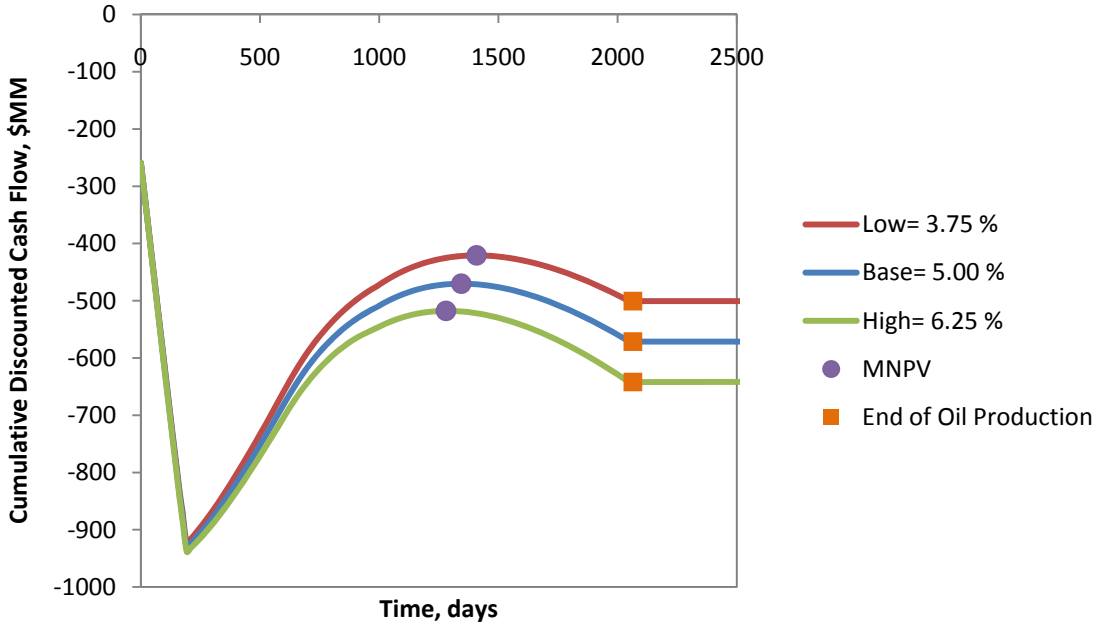

Figure C-36 Plot of CDCF against Time for a Varying T_V for SP Floods

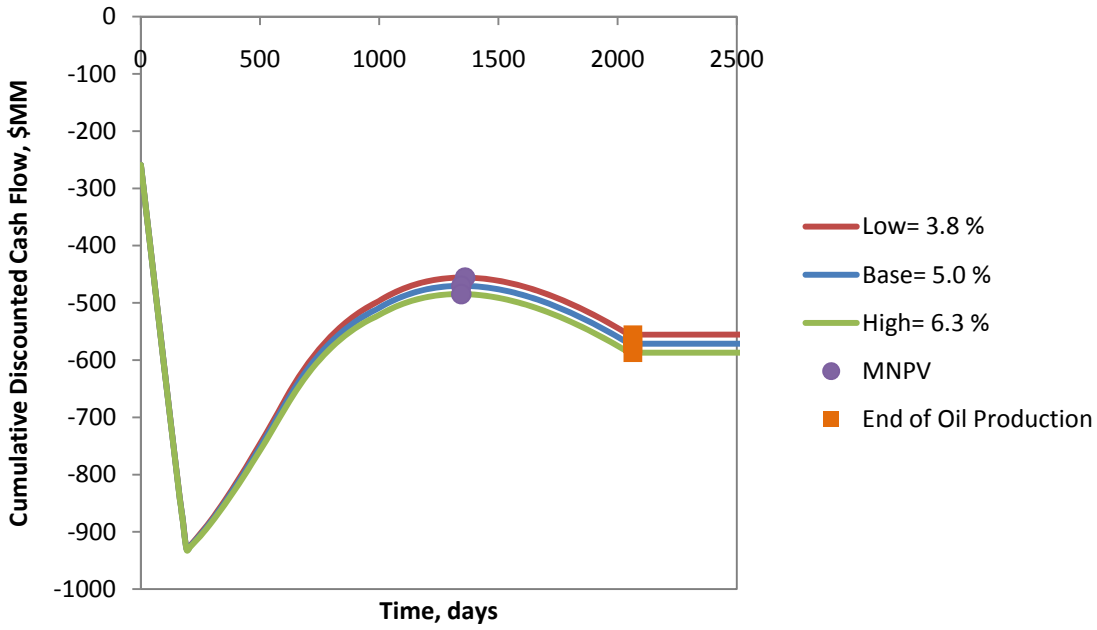

Figure C-37 Plot of CDCF against Time for a Varying T_S for SP Floods

C.2.3.6 Inflation and Discount Rate

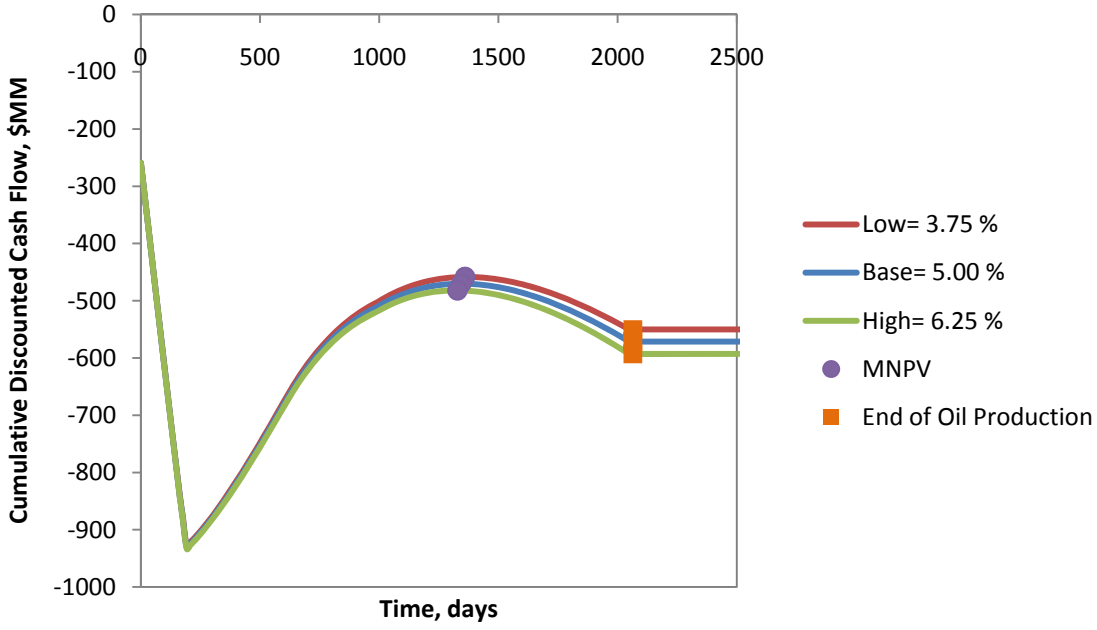

Figure C-38 Plot of CDCF against Time for a Varying i for SP Floods

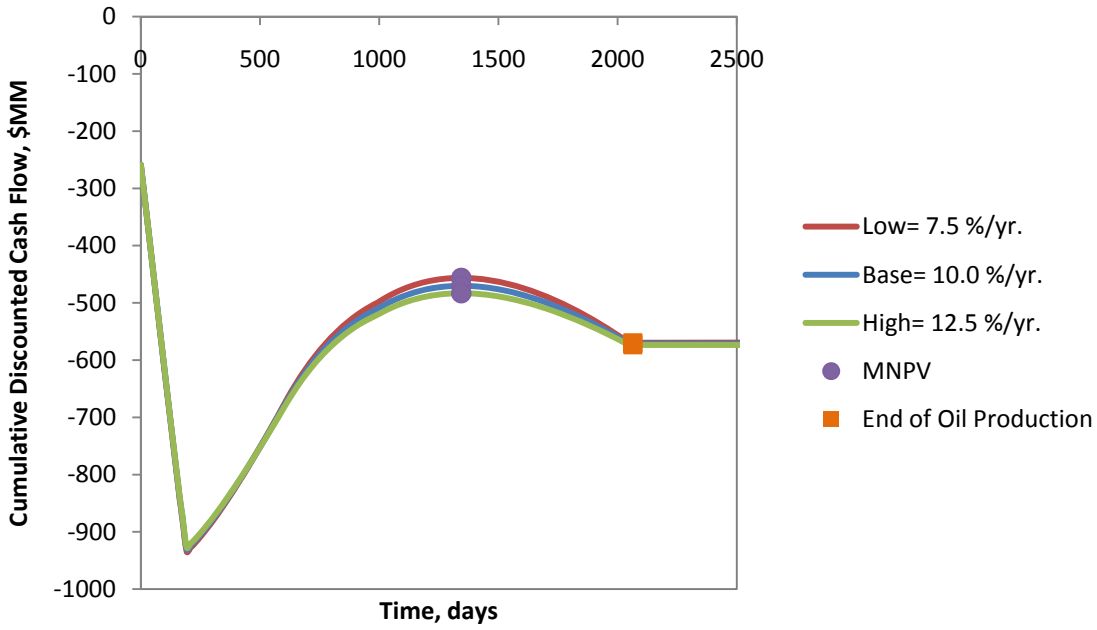

Figure C-39 Plot of CDCF against Time for a Varying d for SP Floods

C.3 Sensitivity Analysis Plots for Alkaline-Surfactant-Polymer Floods

The following are all of the plots produced for the sensitivity analysis of all of the parameters associated with alkali-surfactant-polymer floods.

C.3.1 Sensitivity Analysis Plots of the Parameters for the Simplified Enhanced Oil Recovery Method

These plots include analyses of the following parameters: change in oil saturation, total pore volumes, heterogeneity factors, and the specific shock velocity of the oil bank.

C.3.1.1 Change in Oil Saturation

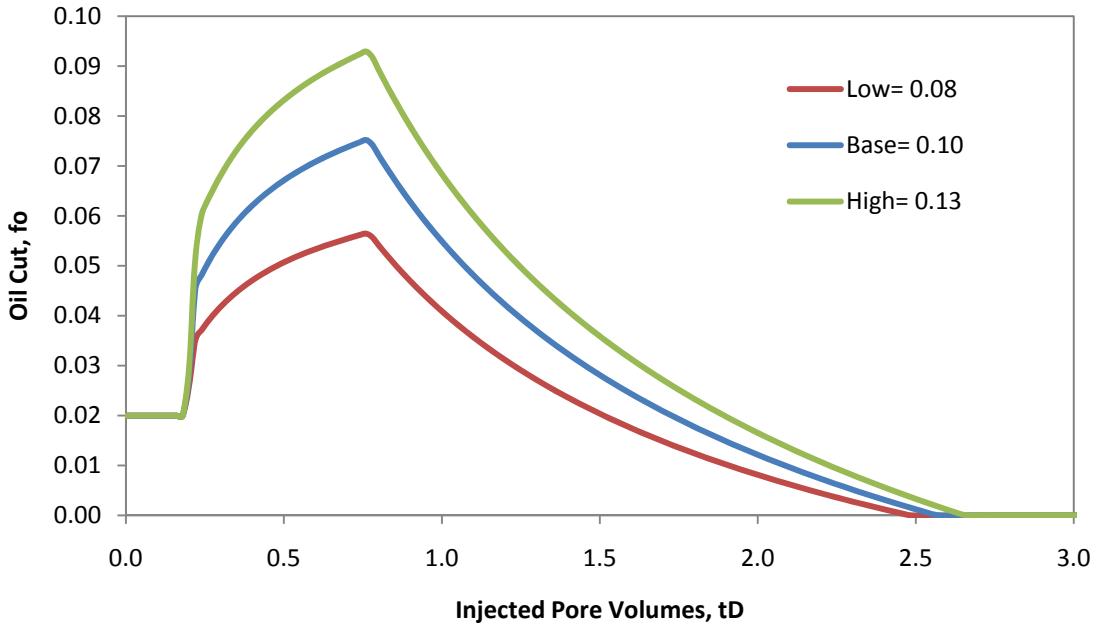

Figure C-40 Plot of Oil Cut against Dimensionless Time for Varying ΔS_o for ASP Floods

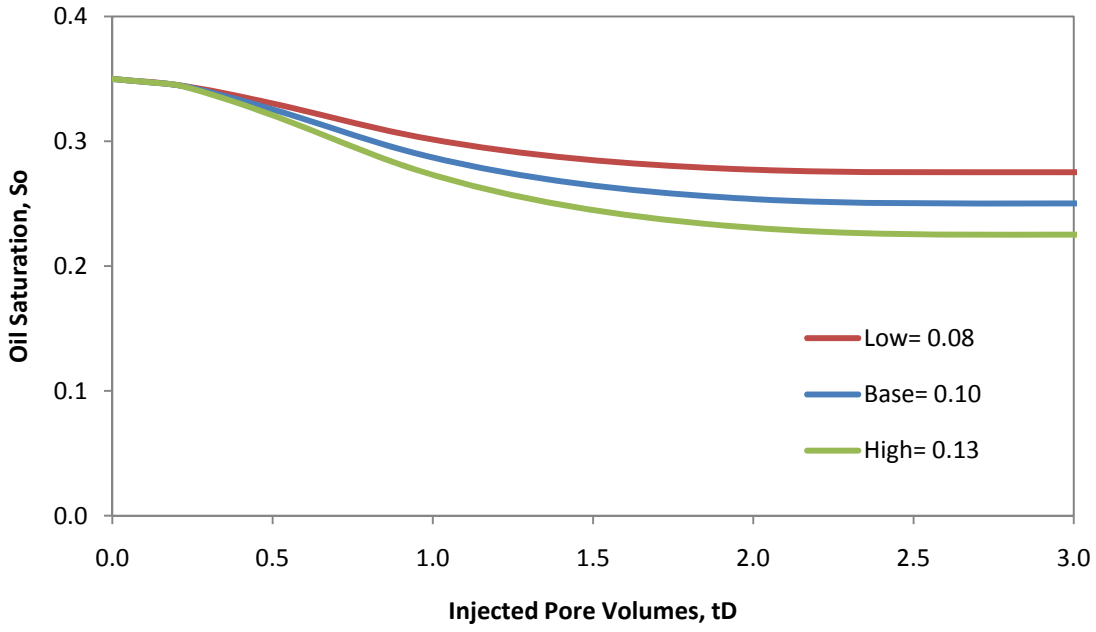

Figure C-41 Plot of Oil Saturation against Dimensionless Time for Varying ΔS_o for ASP Floods

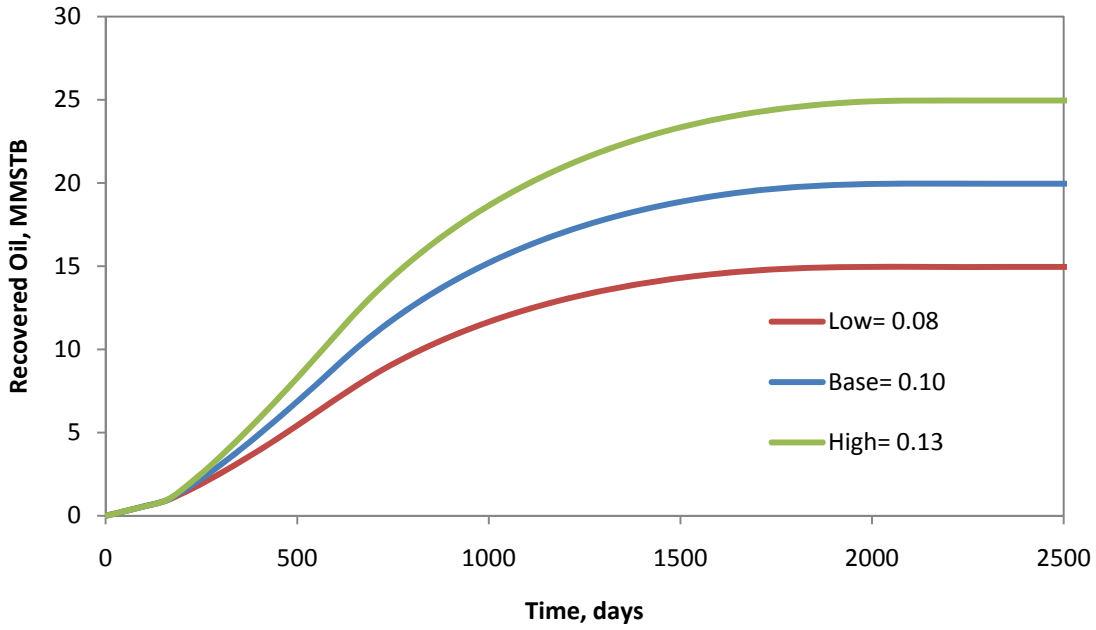

Figure C-42 Plot of Oil Recovery against Time for Varying ΔS_o for ASP Floods

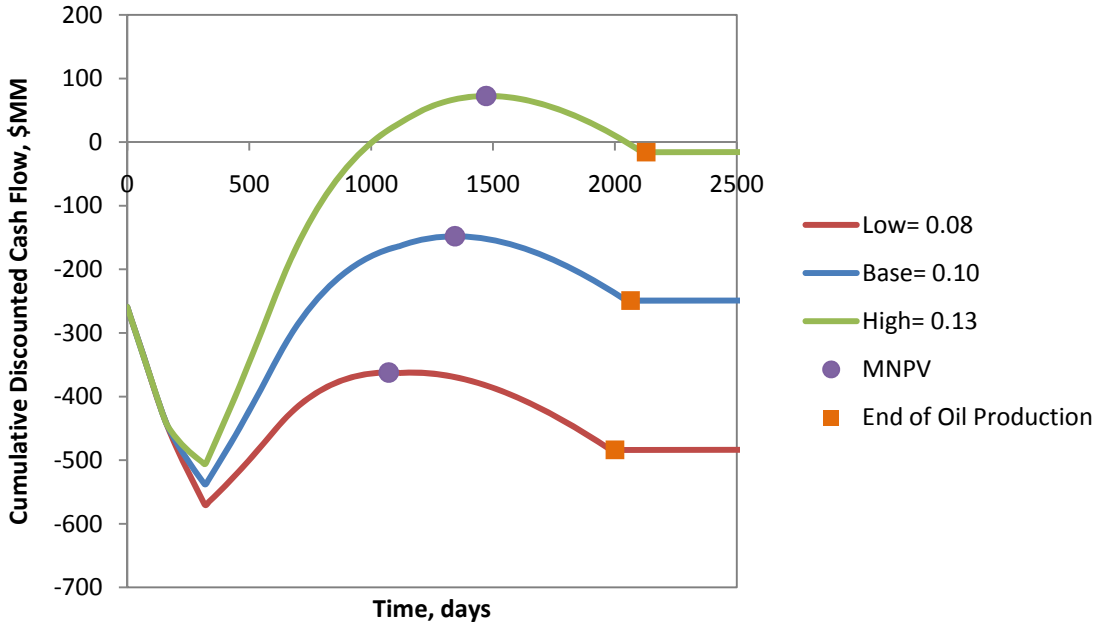

Figure C-43 Plot of CDCF against Time for Varying ΔS_o for ASP Floods

C.3.1.2 Total Pore Volumes

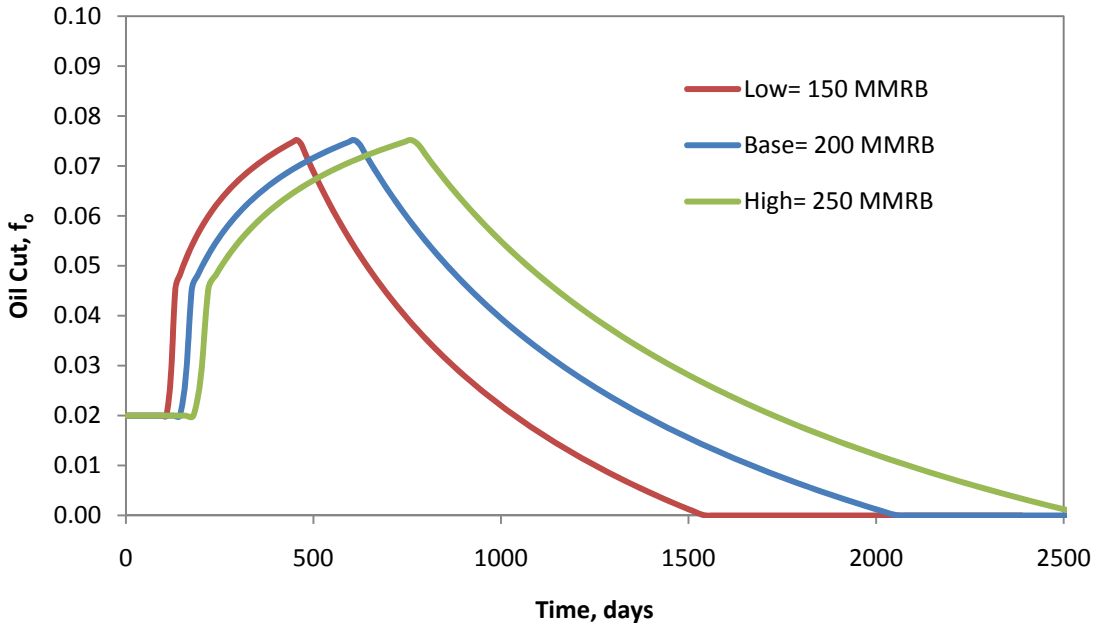

Figure C-44 Plot of Oil Cut against Time for a Varying V_p for ASP Floods

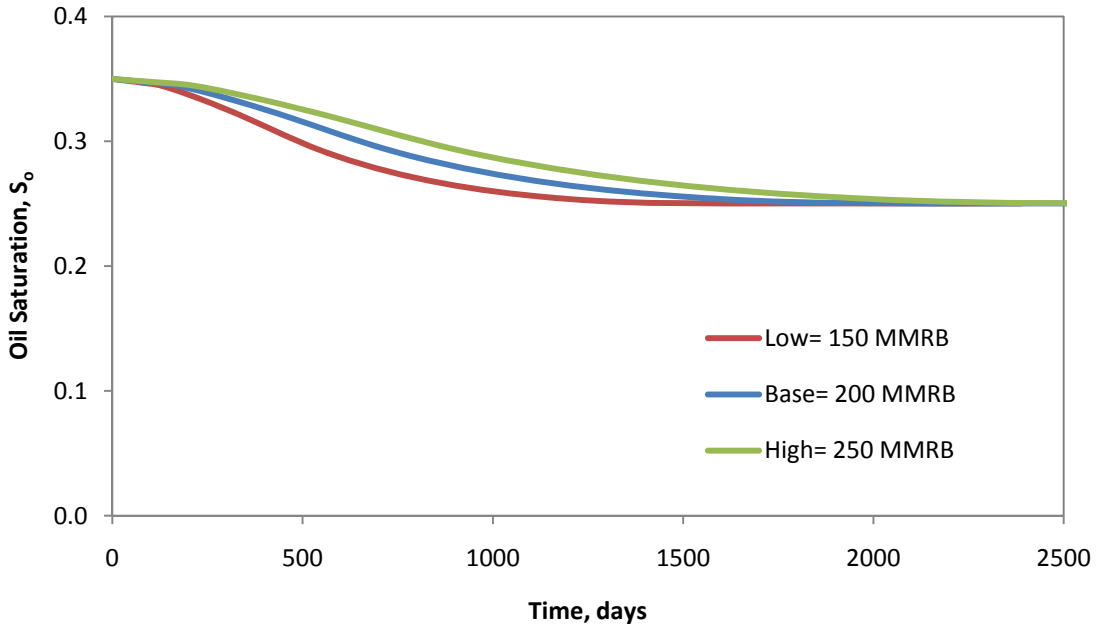

Figure C-45 Plot of Oil Saturation against Time for a Varying V_p for ASP Floods

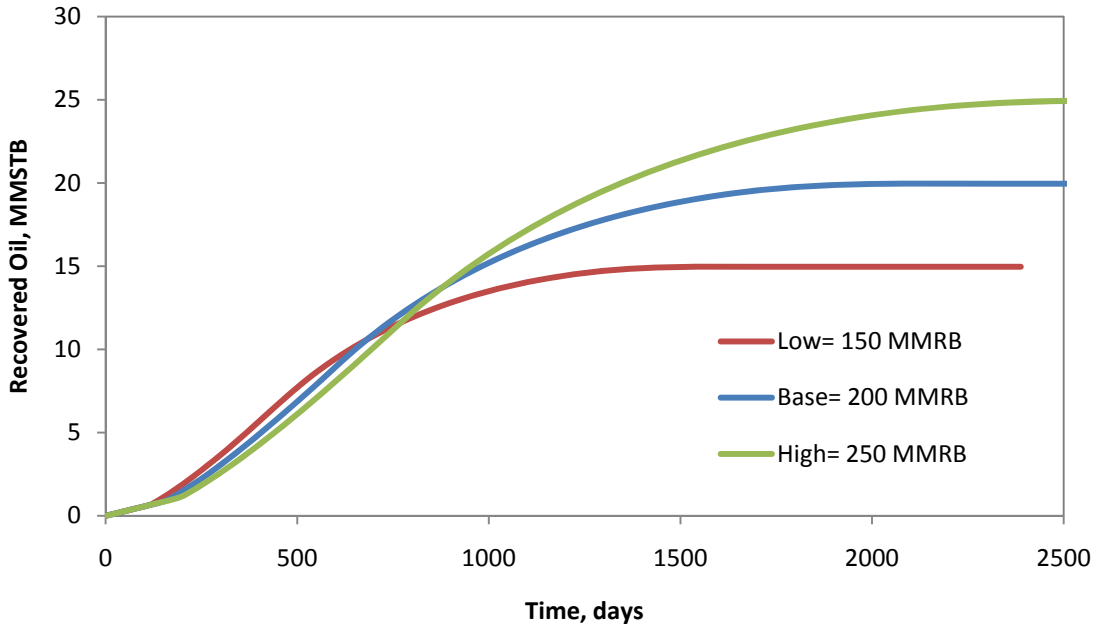

Figure C-46 Plot of Oil Recovery against Time for a Varying V_p for ASP Floods

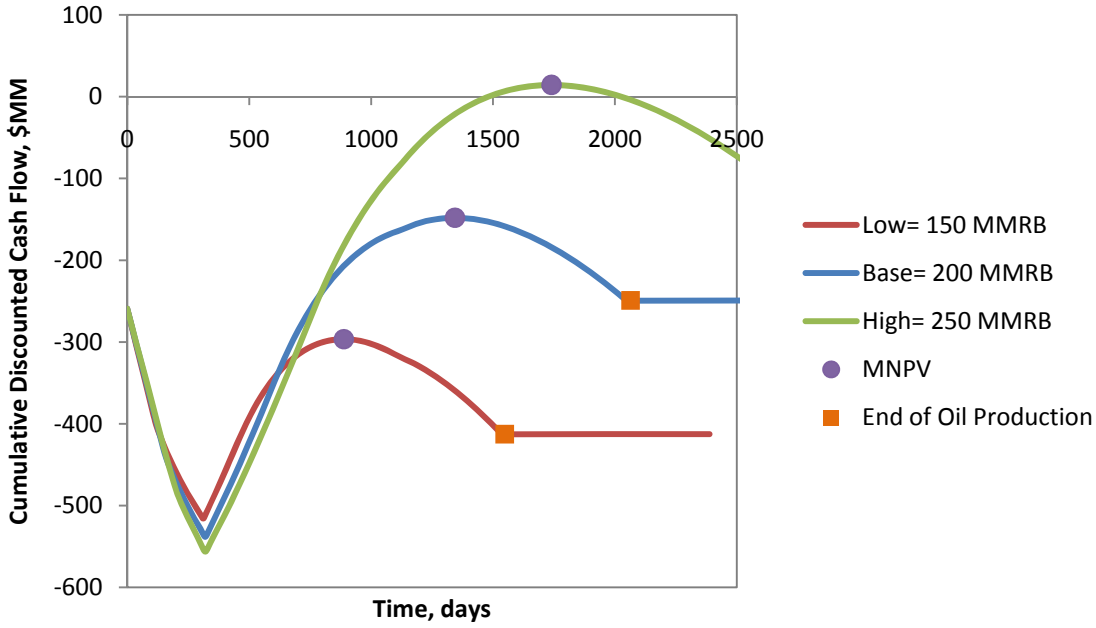

Figure C-47 Plot of CDCF against Time for a Varying V_p for ASP Floods

C.3.1.3 Heterogeneity Factors

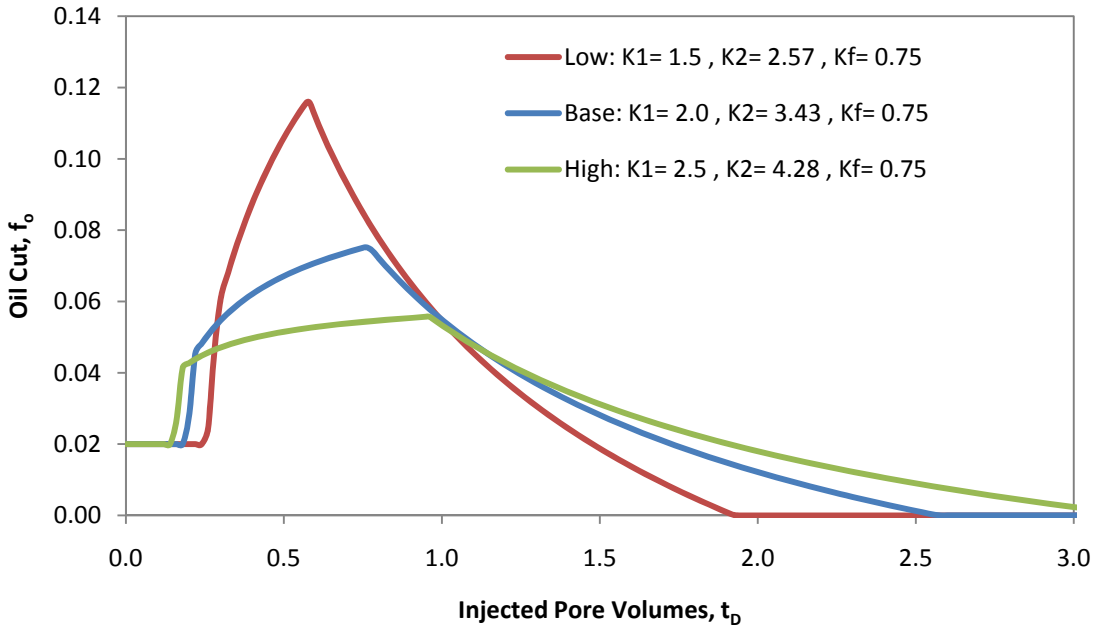

Figure C-48 Plot of Oil Cut against Dimensionless Time for a Varying K_1 for ASP Floods

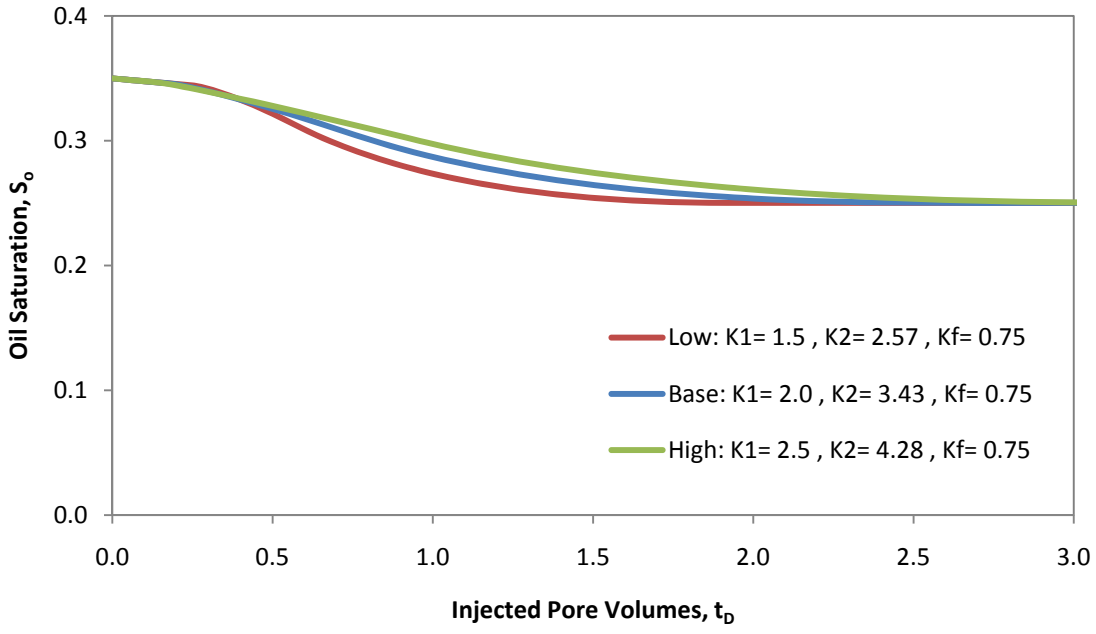

Figure C-49 Plot of Oil Saturation against Dimensionless Time for a Varying K_1 for ASP Floods

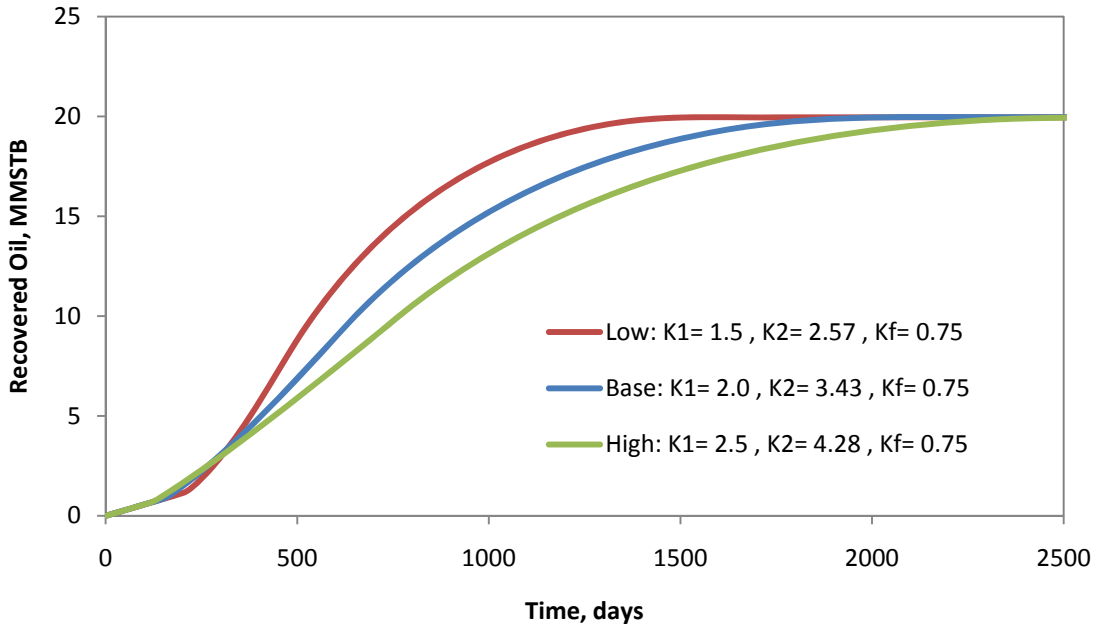

Figure C-50 Plot of Oil Recovery against Time for a Varying K_1 for ASP Floods

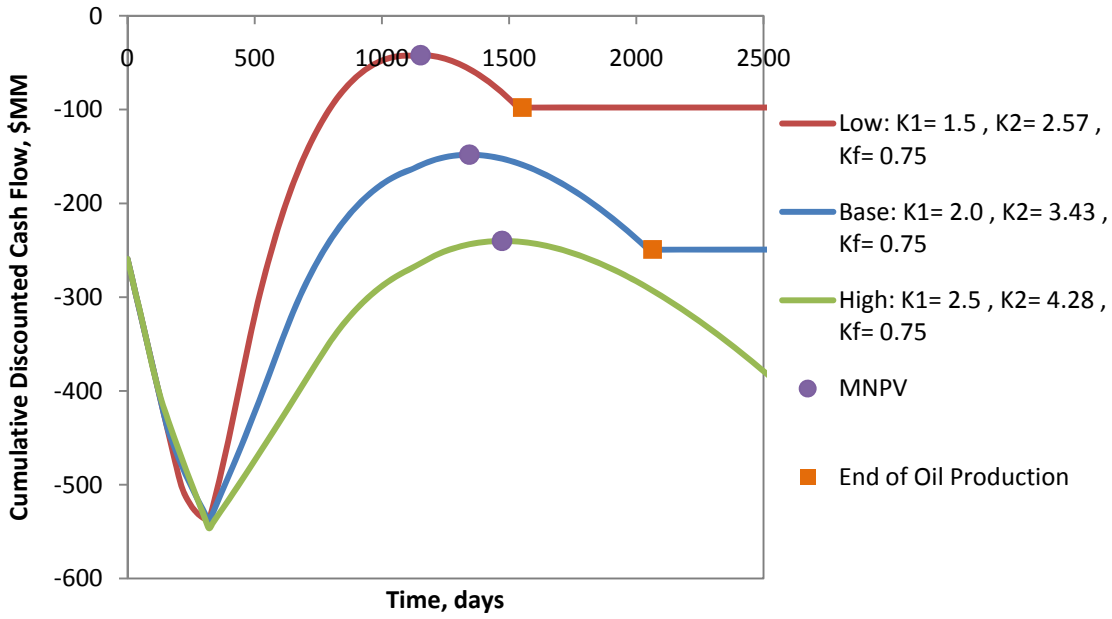

Figure C-51 Plot of CDCF against Time for a Varying K_1 for ASP Floods

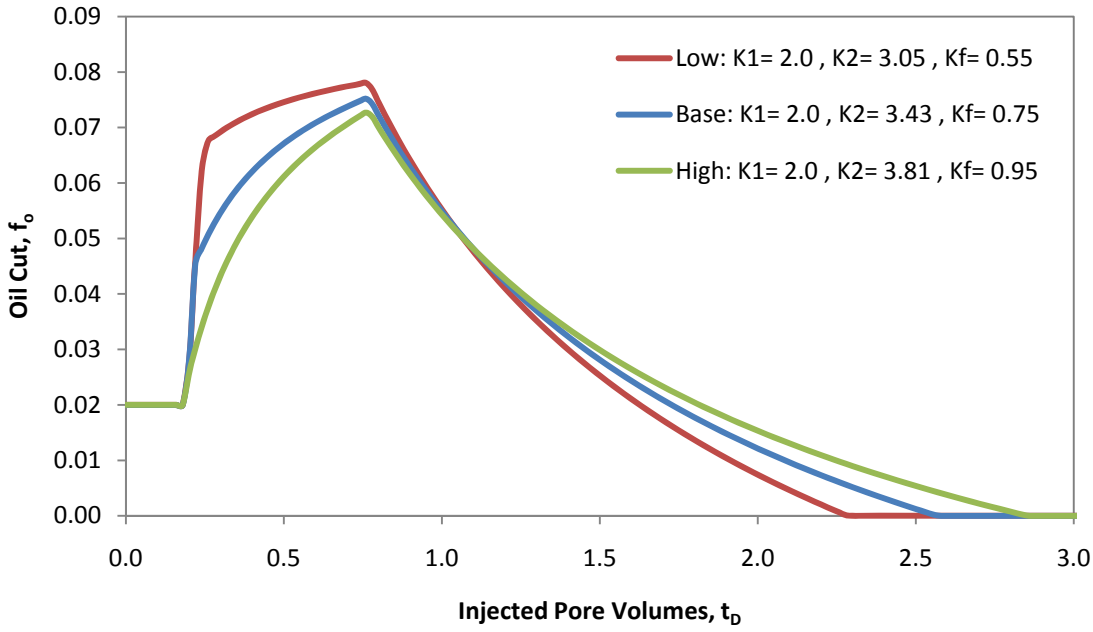

Figure C-52 Plot of Oil Cut against Dimensionless Time for a Varying K_f for ASP Floods

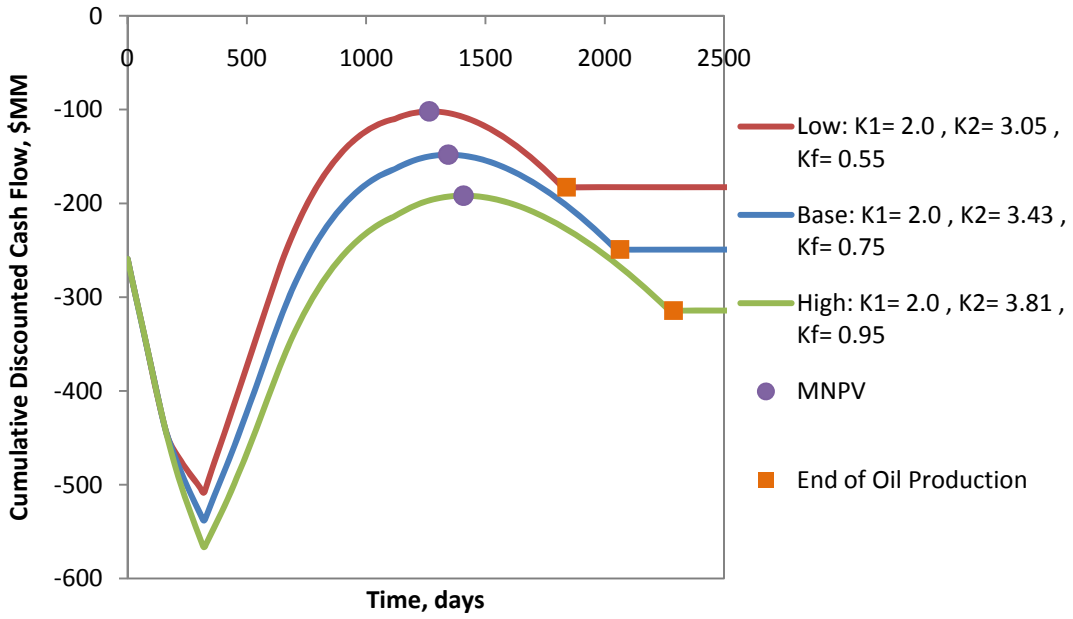

Figure C-53 Plot of CDCF against Time for a Varying K_f for ASP Floods

C.3.1.4 Specific Shock Velocity of Oil Bank

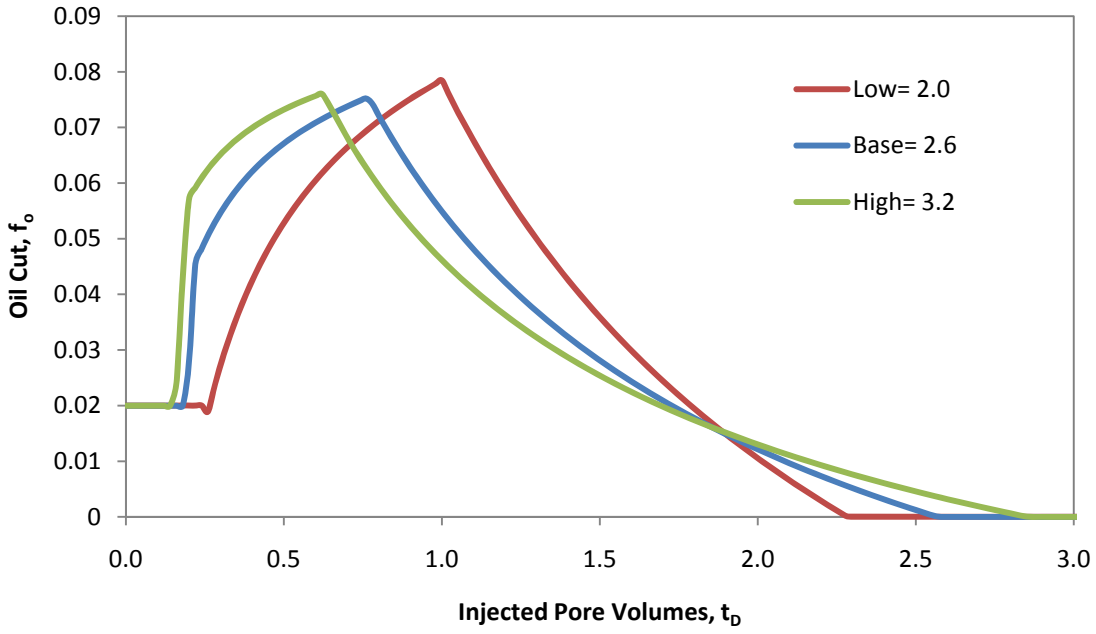

Figure C-54 Plot of Oil Cut against Dimensionless Time for a Varying v_{oB} for ASP Floods

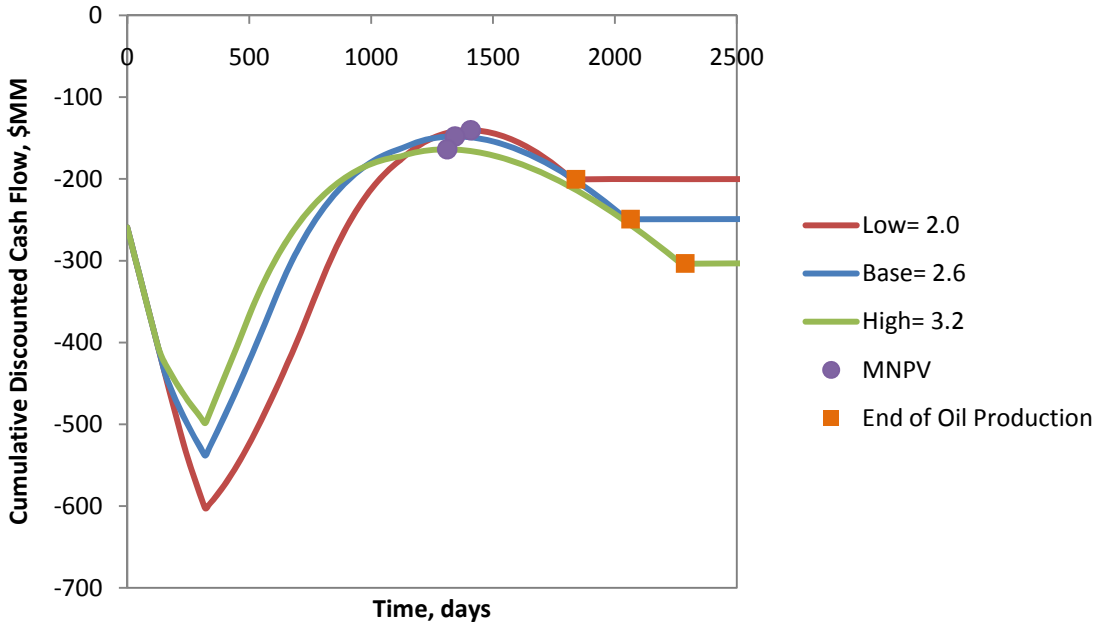

Figure C-55 Plot of CDCF against Time for a Varying v_{oB} for ASP Floods

C.3.2 Sensitivity Plots of the Design Parameters

These plots include analyses of the following design parameters: well spacing, injection rate, production rate, pore volumes for the injected chemicals, and concentrations for the chemicals.

C.3.2.1 Well Spacing

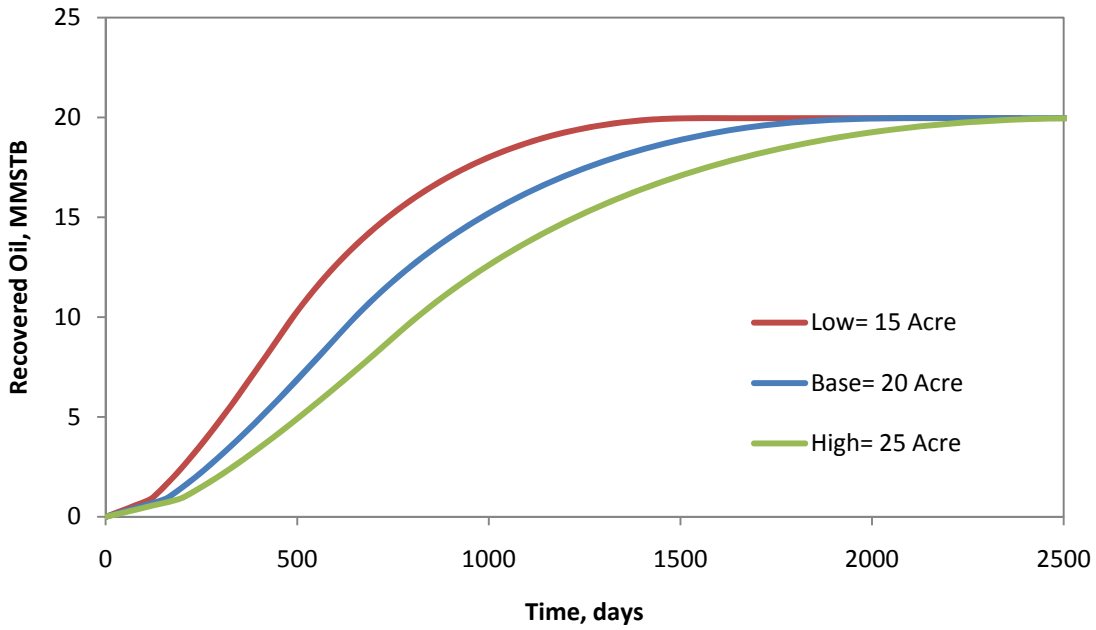

Figure C-56 Plot of Oil Recovery against Time for a Varying WS for ASP Floods

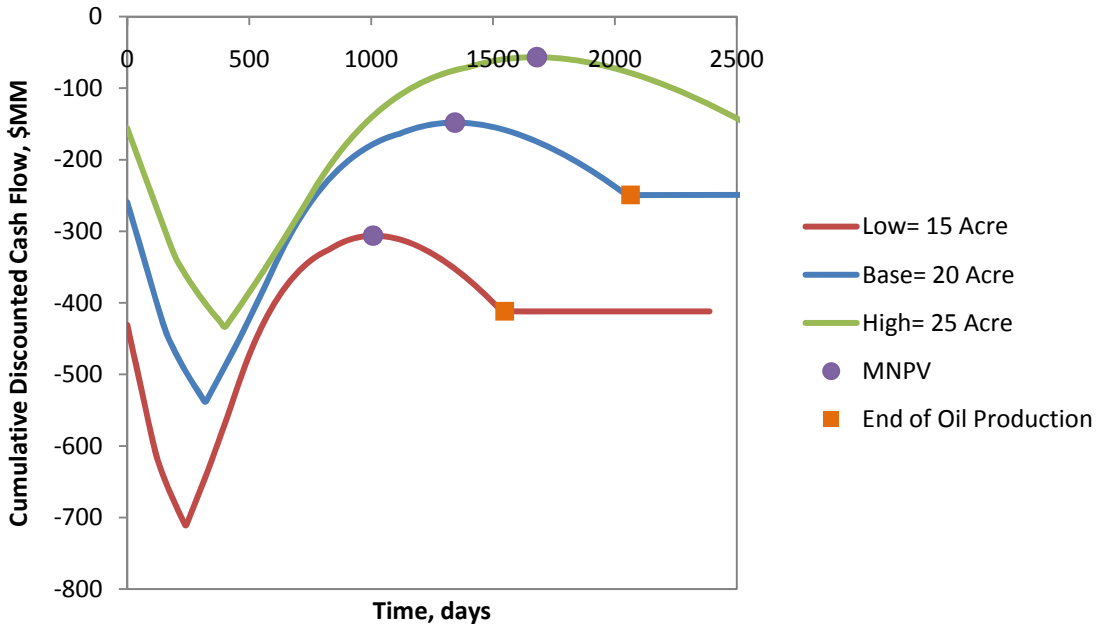

Figure C-57 Plot of CDCF against Time for Varying WS for ASP Floods

C.3.2.2 Injection Rate

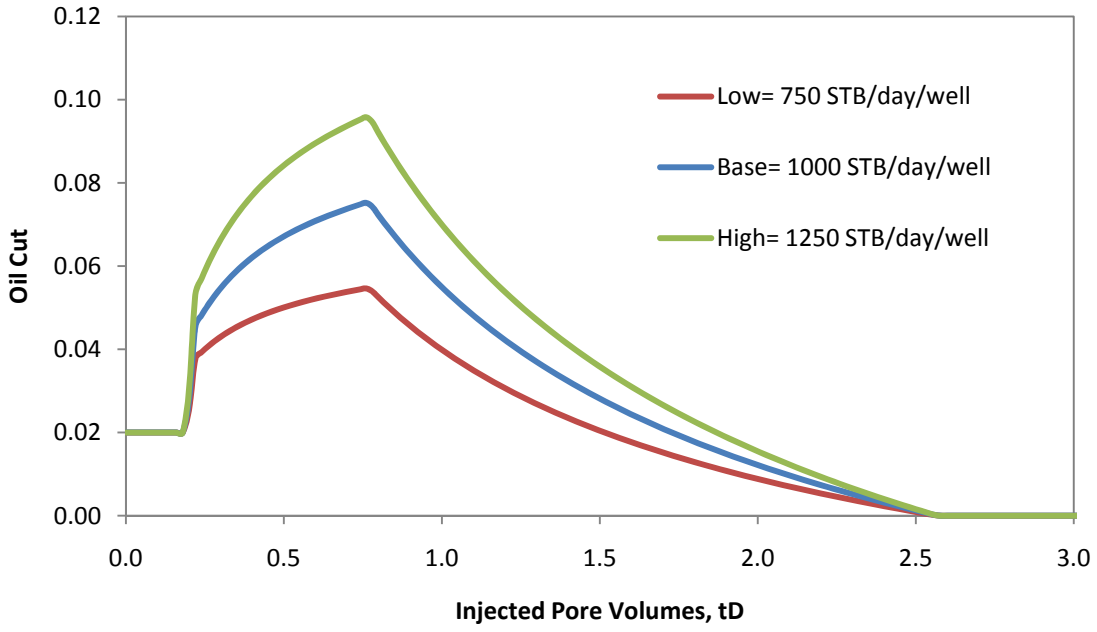

Figure C-58 Plot of Oil Cut against Time for a Varying q_i for ASP Floods

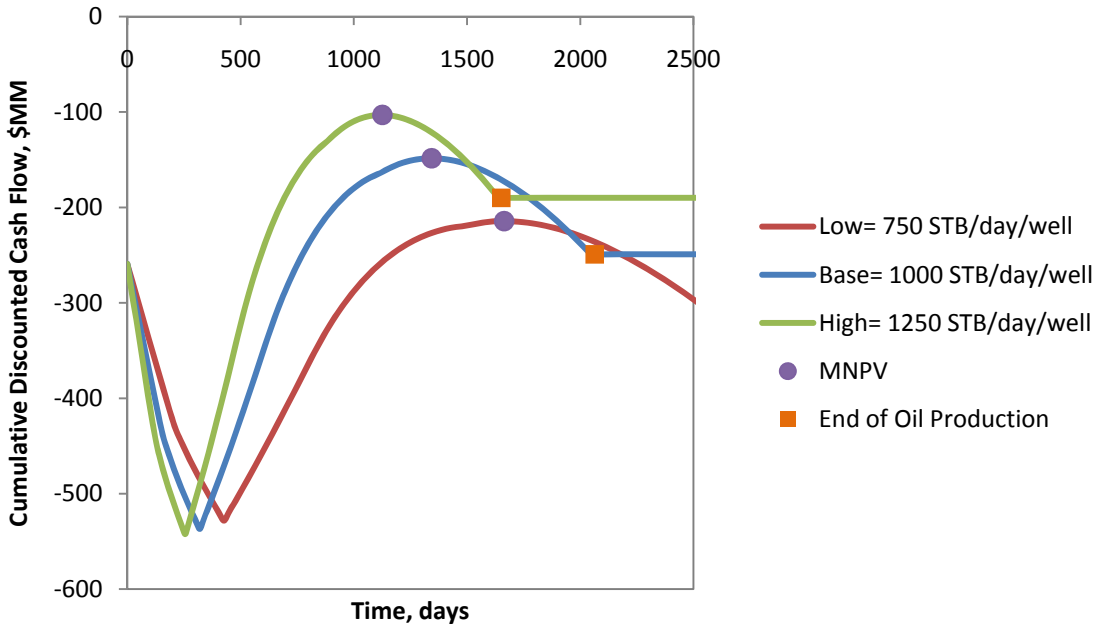

Figure C-59 Plot of CDCF against Time for a Varying q_i for ASP Floods

C.3.2.3 Production Rate

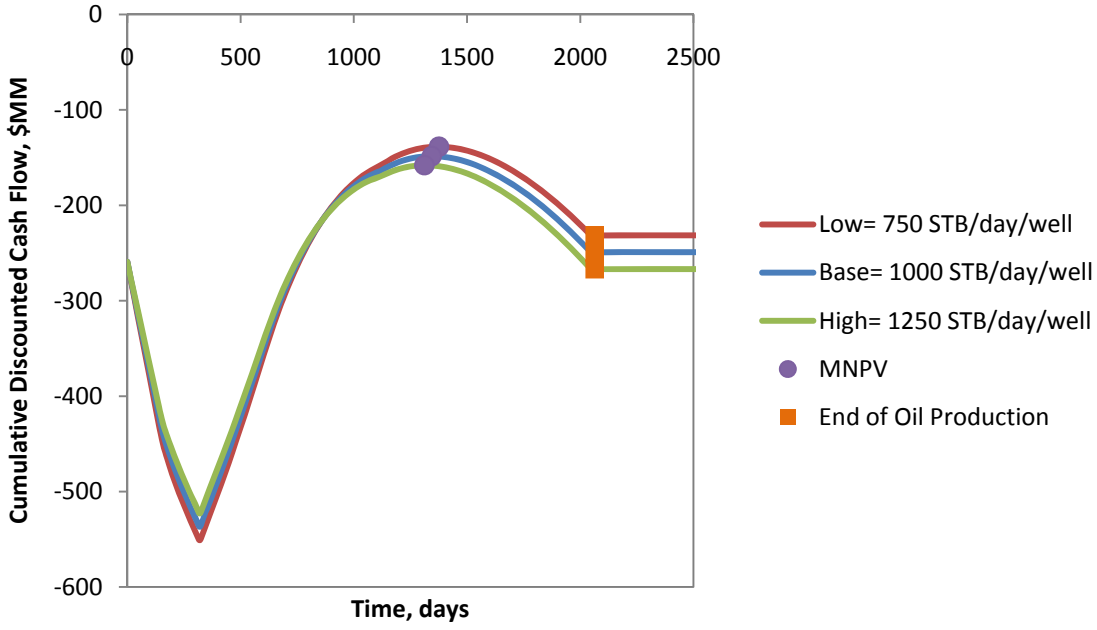

Figure C-60 Plot of CDCF against Time for Varying q_p for ASP Floods

C.3.2.4 Alkali-Surfactant-Polymer and Polymer Slug Sizes

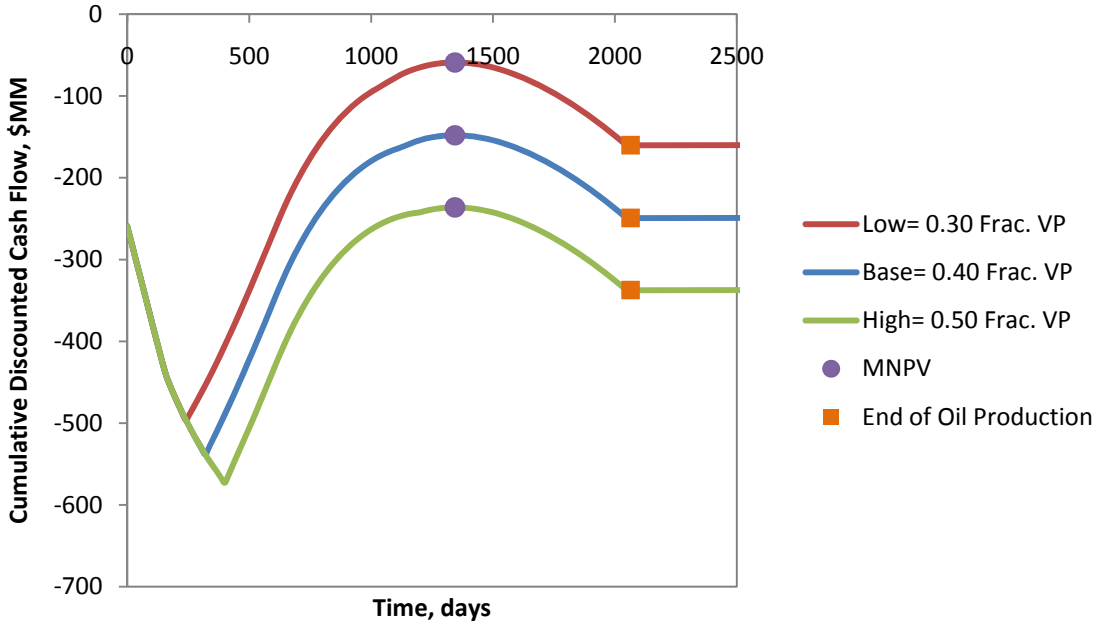

Figure C-61 Plot of CDCF against Time for Varying V_{Chem} for ASP Floods

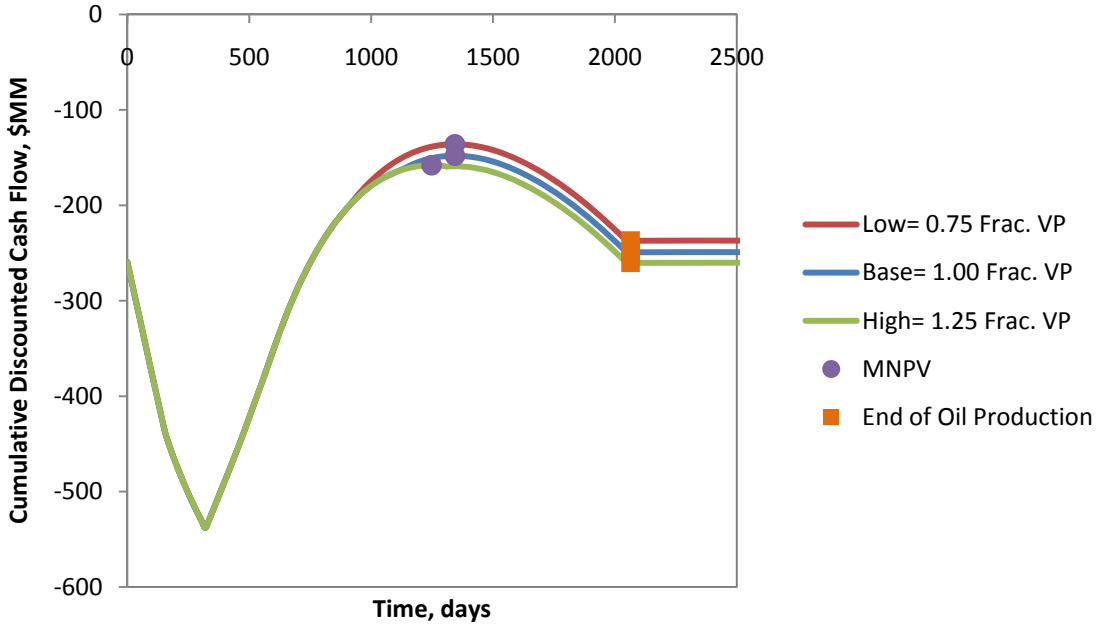

Figure C-62 Plot of CDCF against Time for Varying V_{Poly} for ASP Floods

C.3.2.5 Concentrations of Surfactant, Alkali, and Polymer

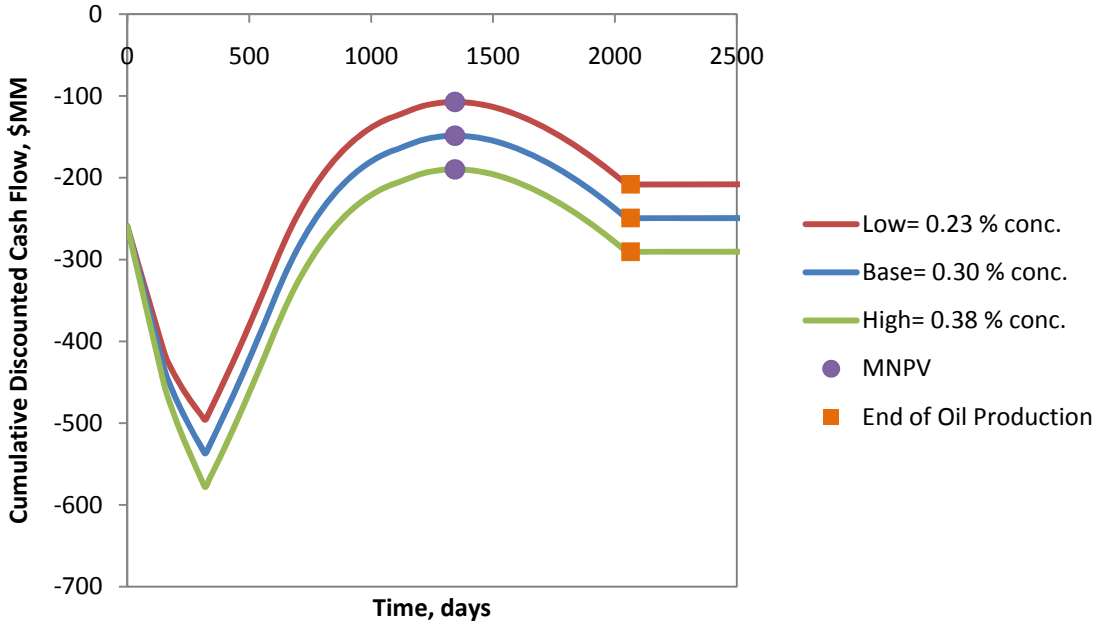

Figure C-63 Plot of CDCF against Time for Varying Z_{Sur} for ASP Floods

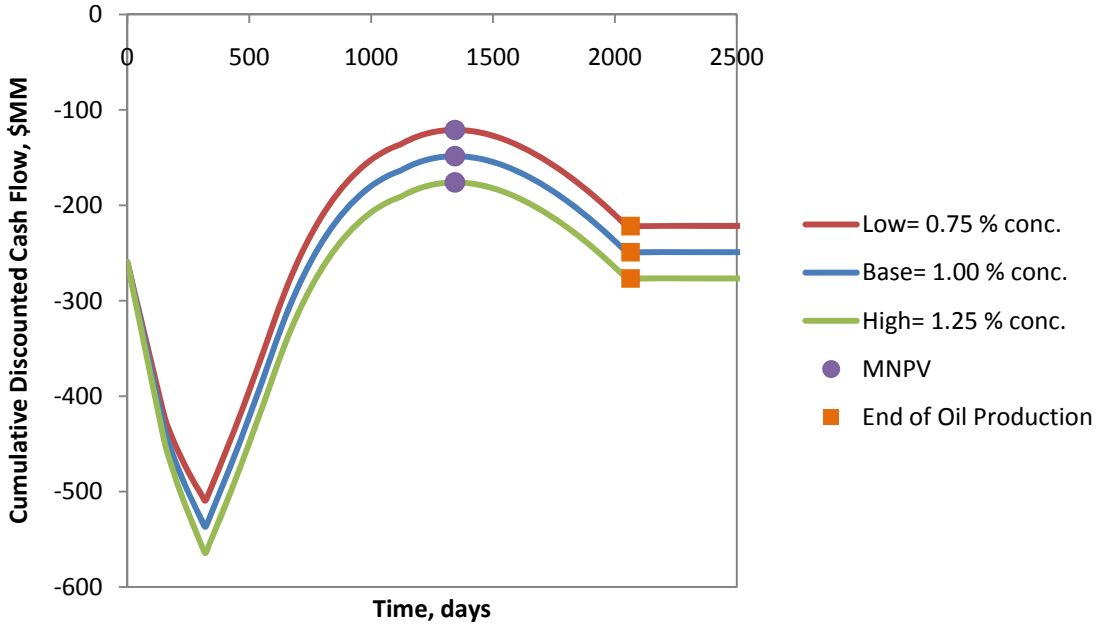

Figure C-64 Plot of CDCF against Time for Varying Z_{Alk} ASP Floods

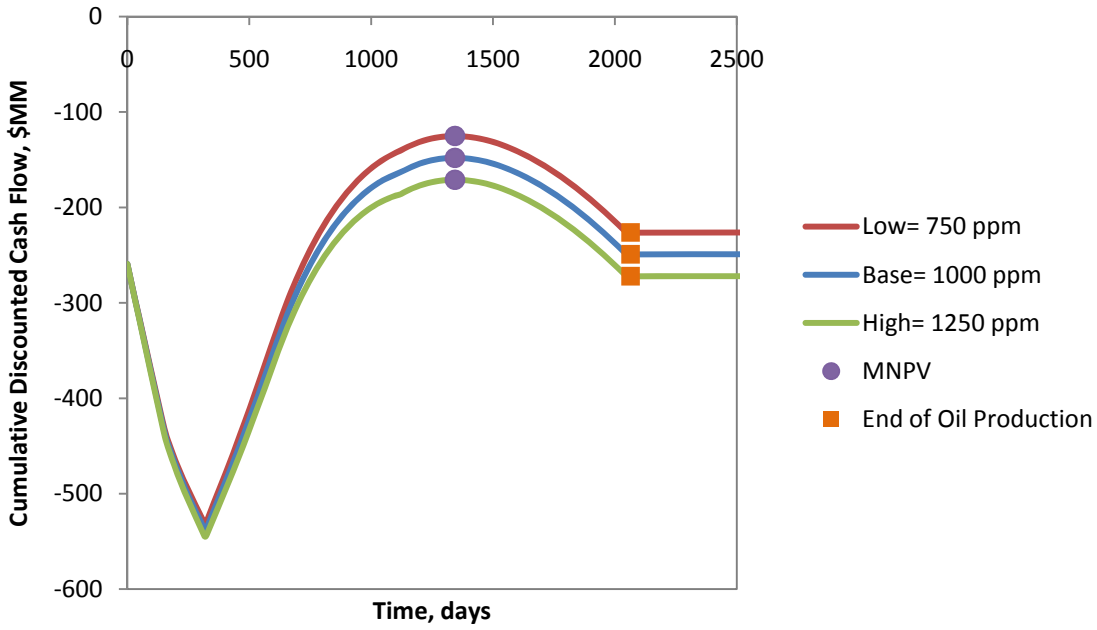

Figure C-65 Plot of CDCF against Time for Varying Z_{Poly} ASP Floods

C.3.3 Sensitivity Plots for Economic Parameters

The following plots are for the following economic parameter: price of oil, escalation factor, price of surfactant, price of polymer, cost of injection, cost of treatment, cost of water disposal, upfront costs, maintenance costs, royalties, ad-valorem tax, severance tax, inflation, and discount rate.

C.3.3.1 Price of Oil and Escalation Factor for the Price of Oil

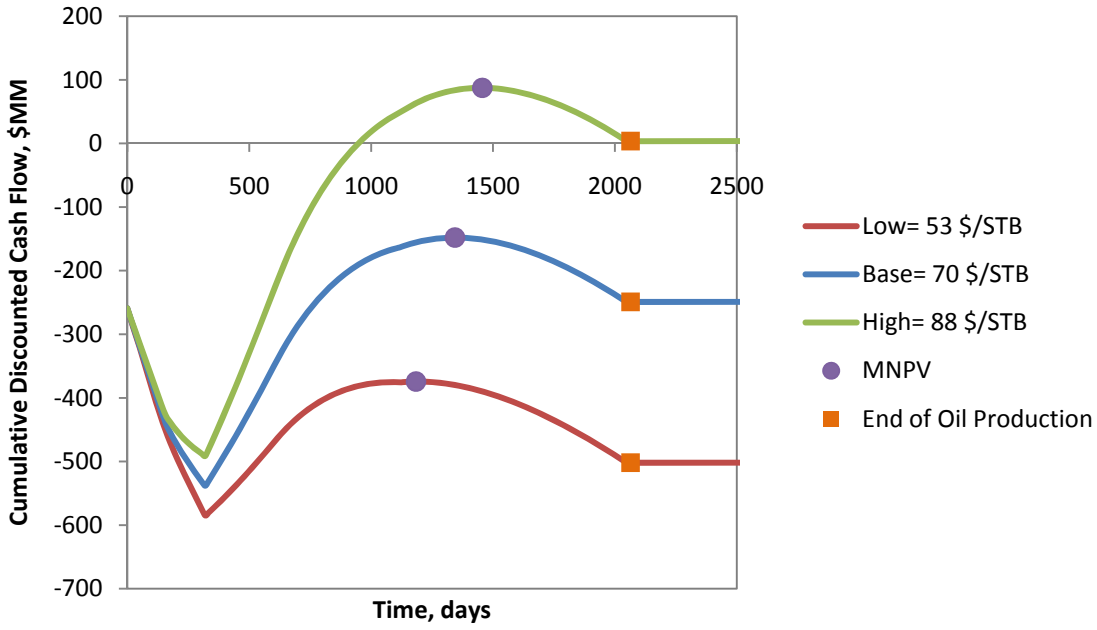

Figure C-66 Plot of CDCF against Time for Varying P_o for ASP Floods

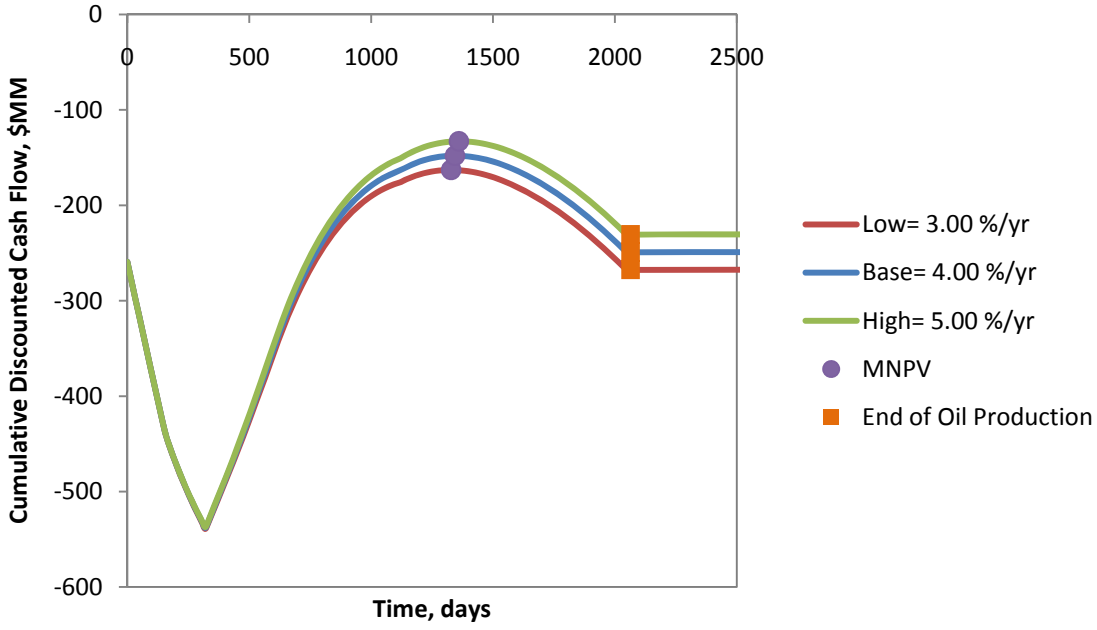

Figure C-67 Plot of CDCF against Time for Varying R_E for ASP Floods

C.3.3.2 Price of Surfactant, Alkali, and Polymer

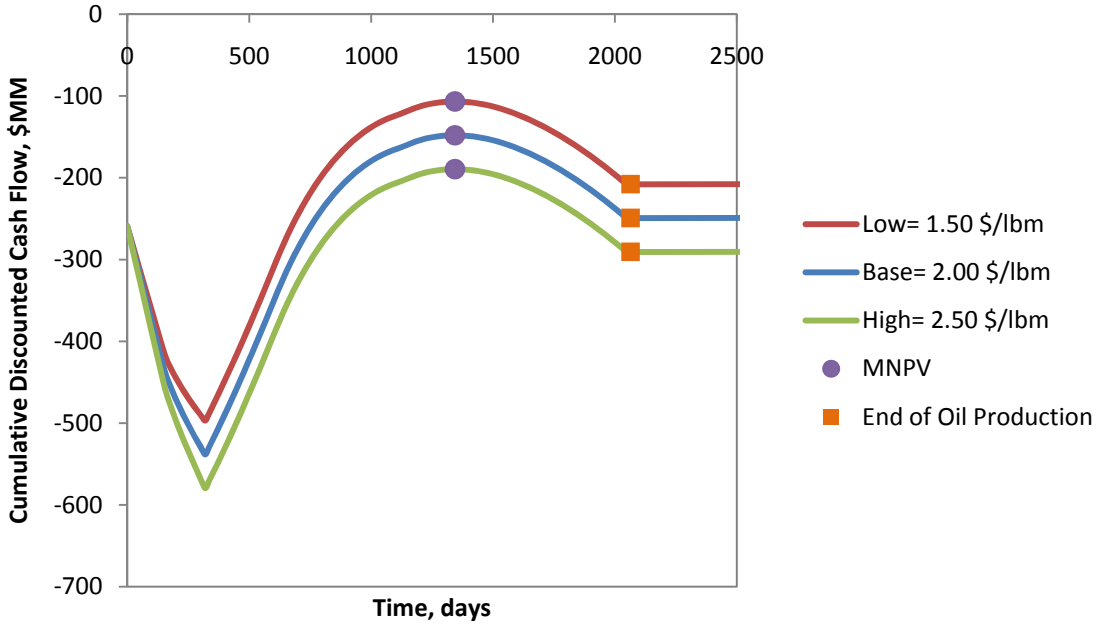

Figure C-68 Plot of CDCF against Time for Varying C_{Sur} for ASP Floods

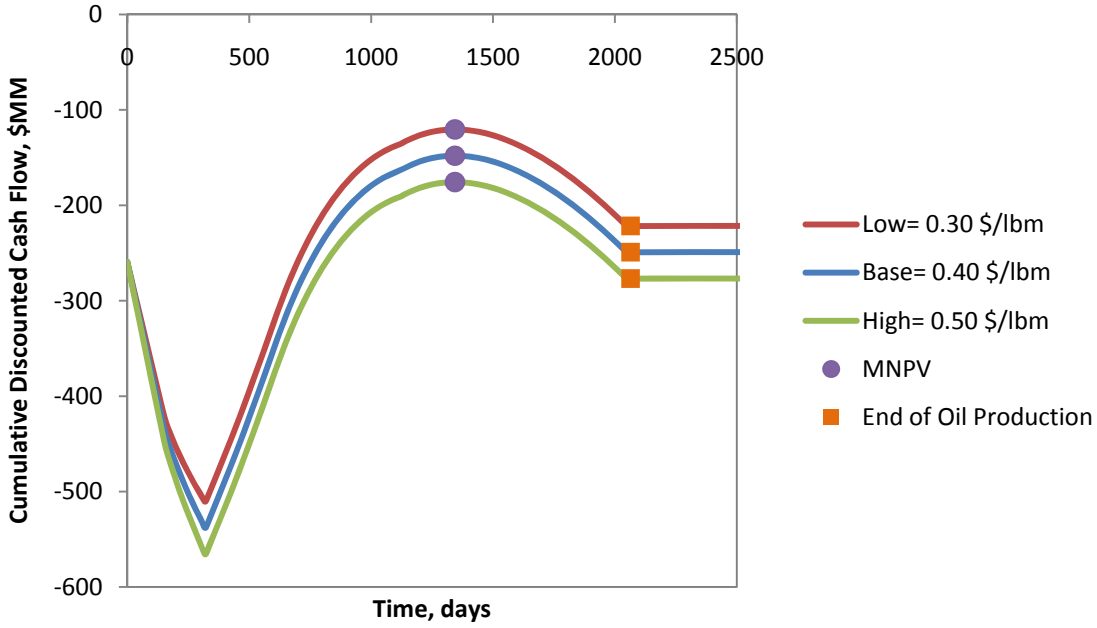

Figure C-69 Plot of CDCF against Time for Varying C_{Alk} for ASP Floods

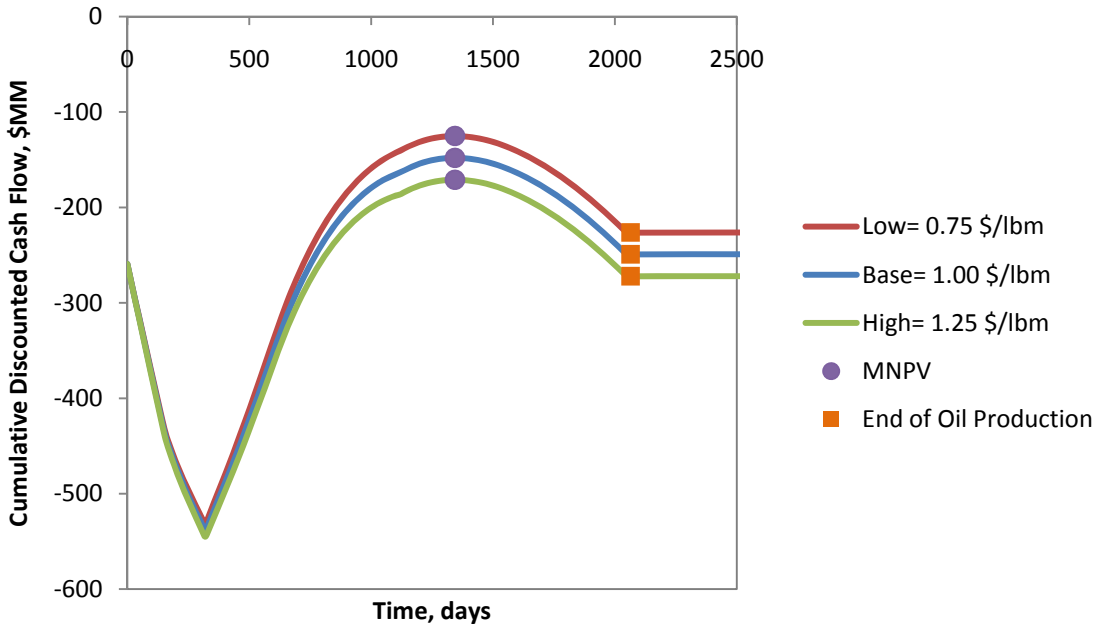

Figure C-70 Plot of CDCF against Time for Varying C_{Poly} for ASP Floods

C.3.3.3 Costs of Injection, Treatment, Water Disposal, and Softening

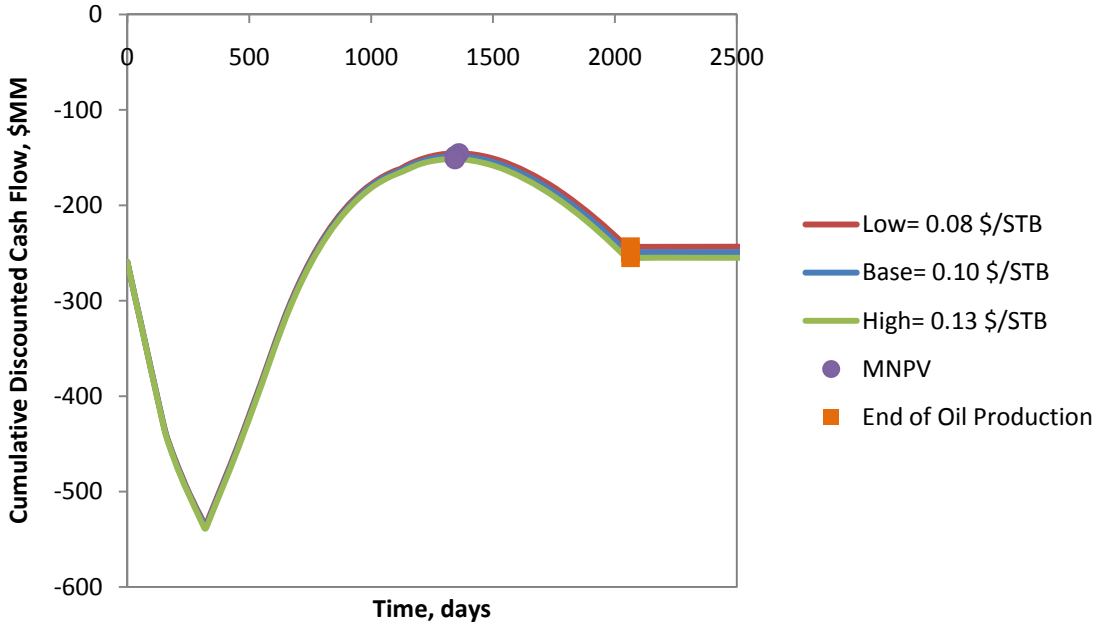

Figure C-71 Plot of CDCF against Time for Varying C_q for ASP Floods

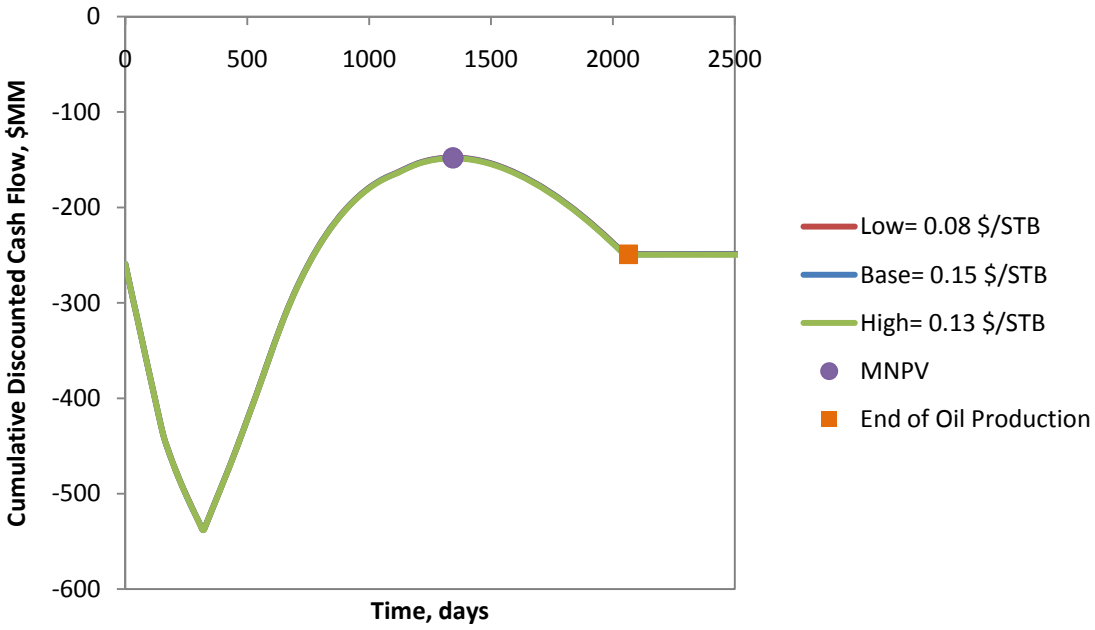

Figure C-72 Plot of CDCF against Time for Varying C_T for ASP Floods

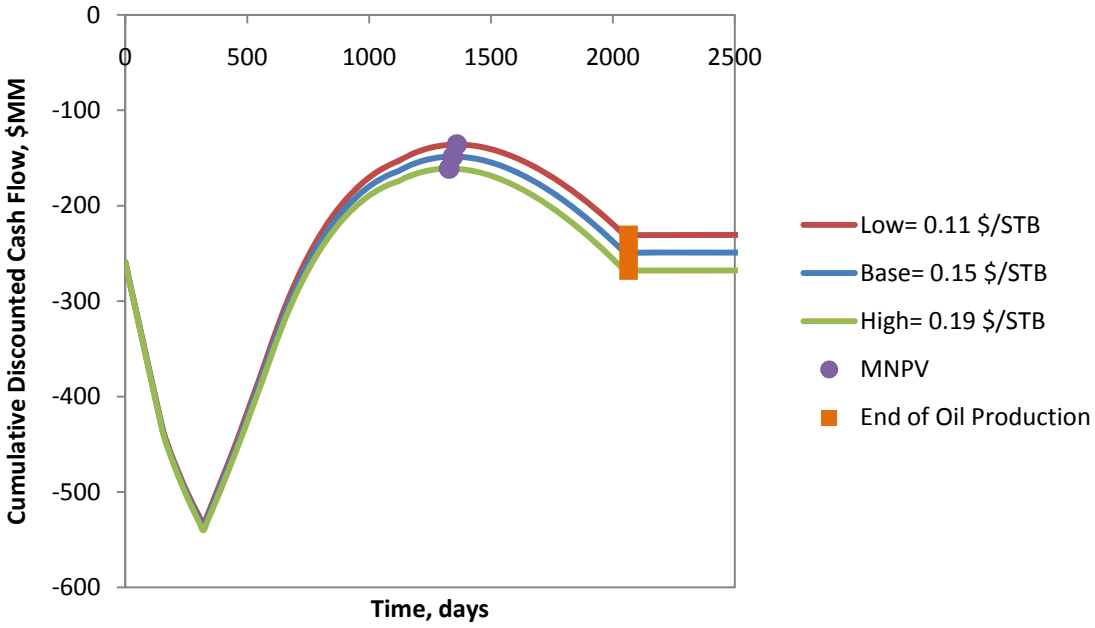

Figure C-73 Plot of CDCF against Time for Varying C_{WD} for ASP Floods

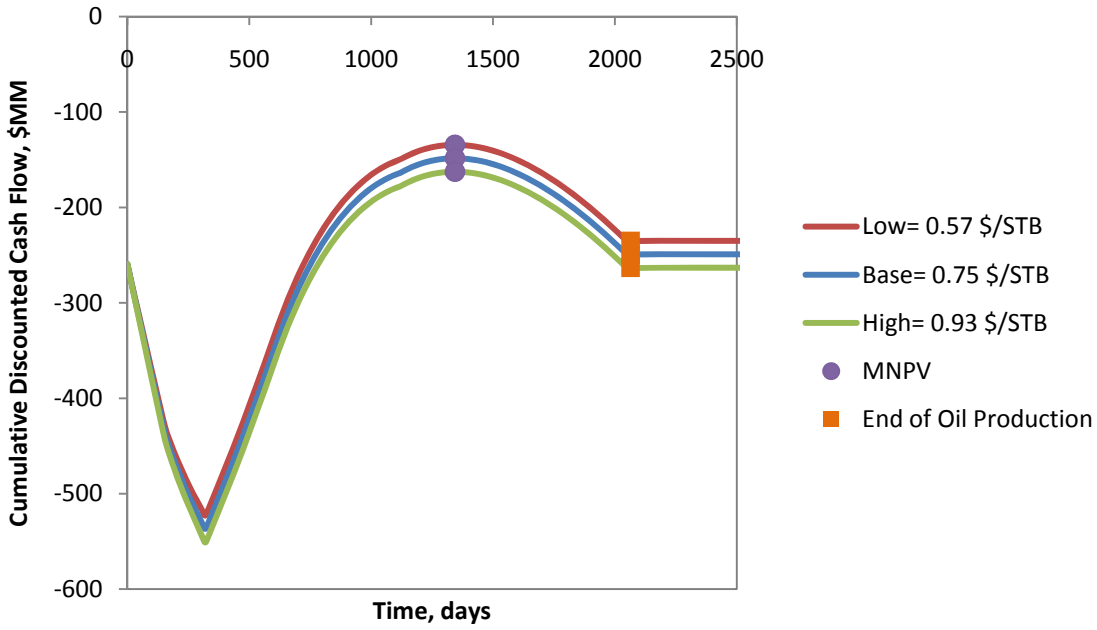

Figure C-74 Plot of CDCF against Time for Varying C_{Soft} for ASP Floods

C.3.3.4 Upfront and Maintenance Costs

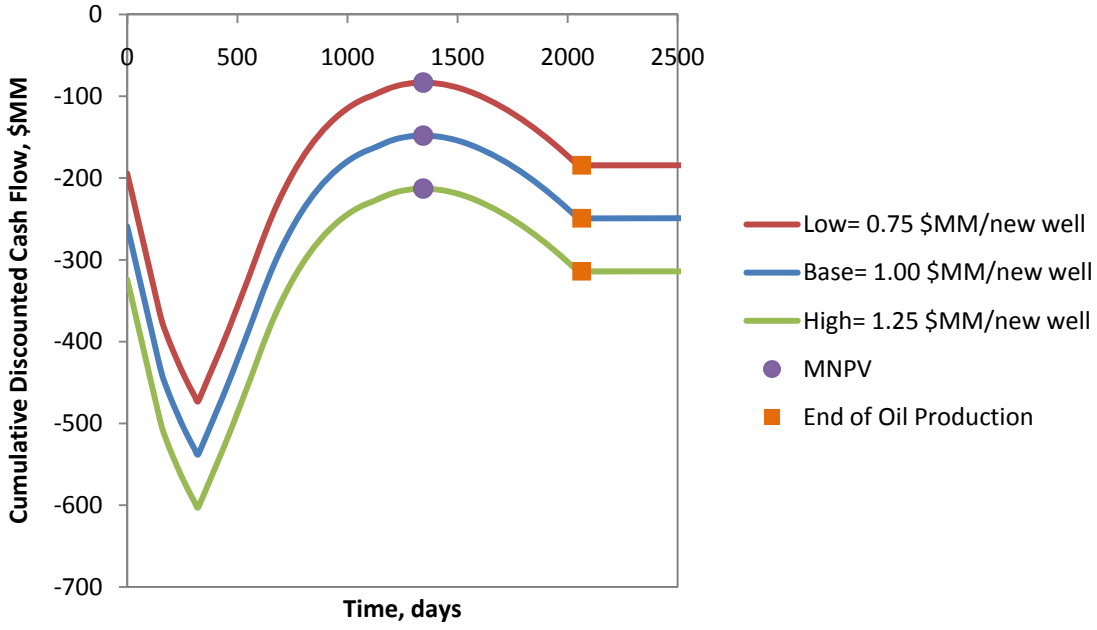

Figure C-75 Plot of CDCF against Time for a Varying C_I for ASP Floods

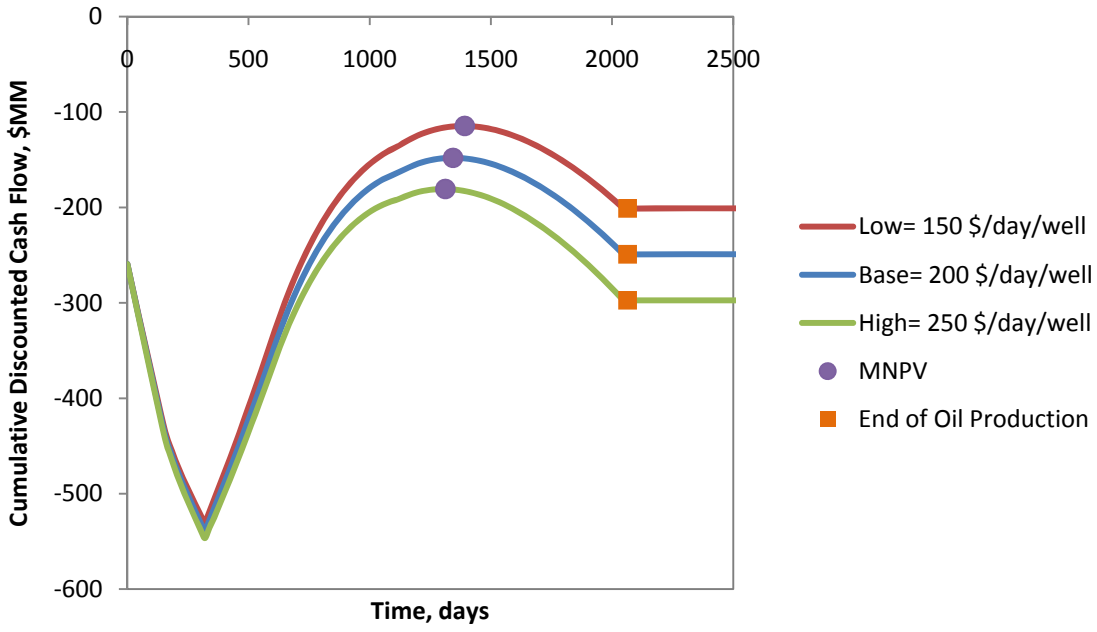

Figure C-76 Plot of CDCF against Time for a Varying C_M for ASP Floods

C.3.3.5 Royalty, Ad-Valorem Tax, Severance Tax

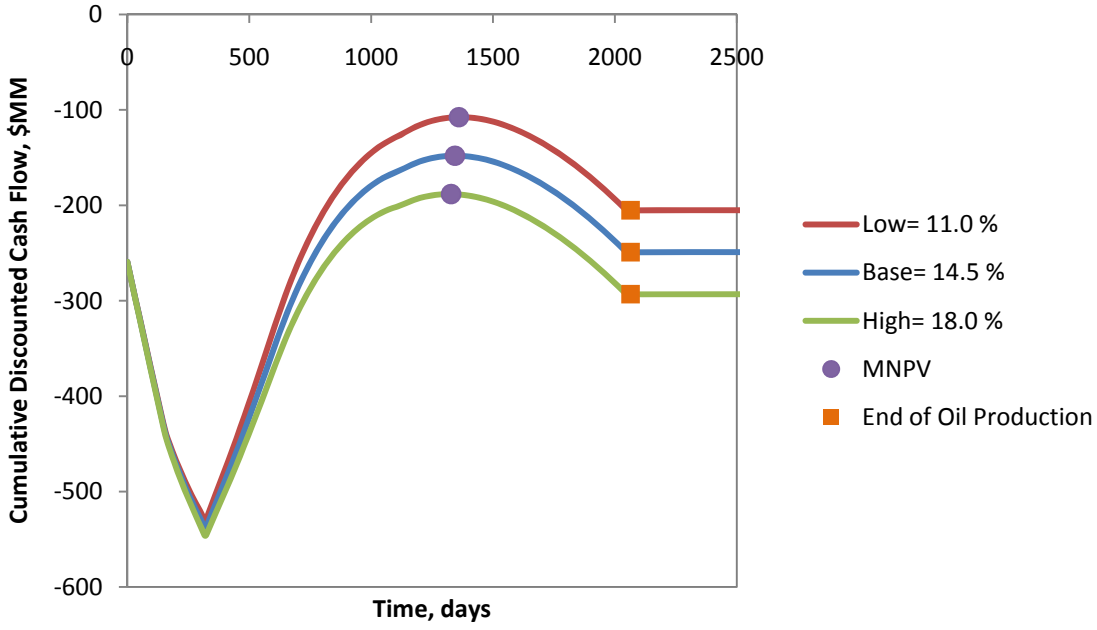

Figure C-77 Plot of CDCF against Time for a Varying T_R for ASP Floods

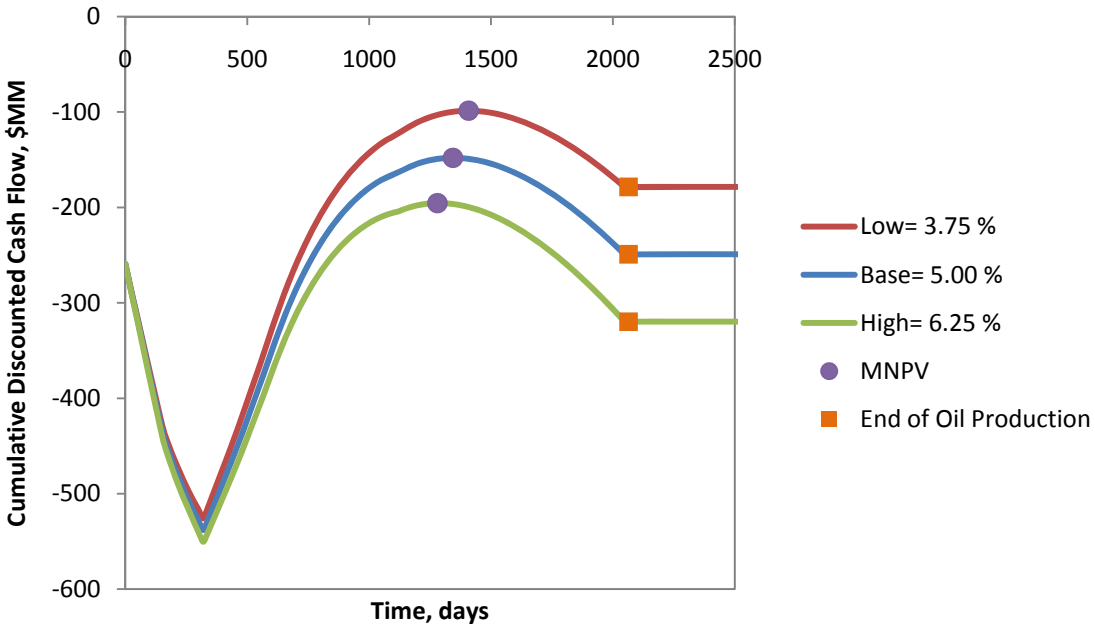

Figure C-78 Plot of CDCF against Time for a Varying T_V for ASP Floods

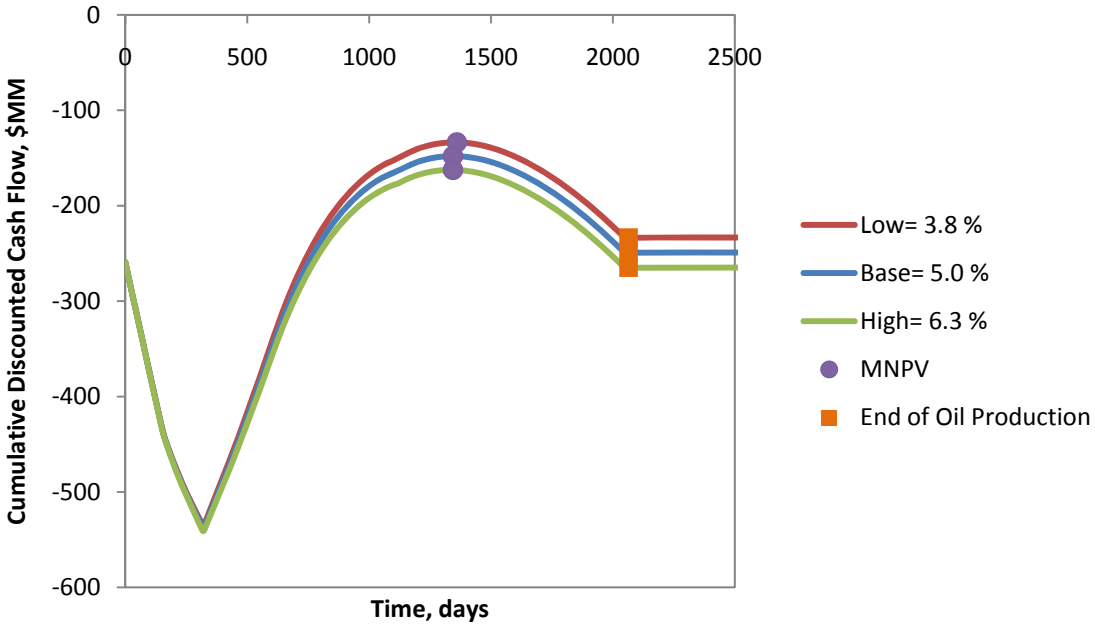

Figure C-79 Plot of CDCF against Time for a Varying T_S for ASP Floods

C.3.3.6 Inflation and Discount Rate

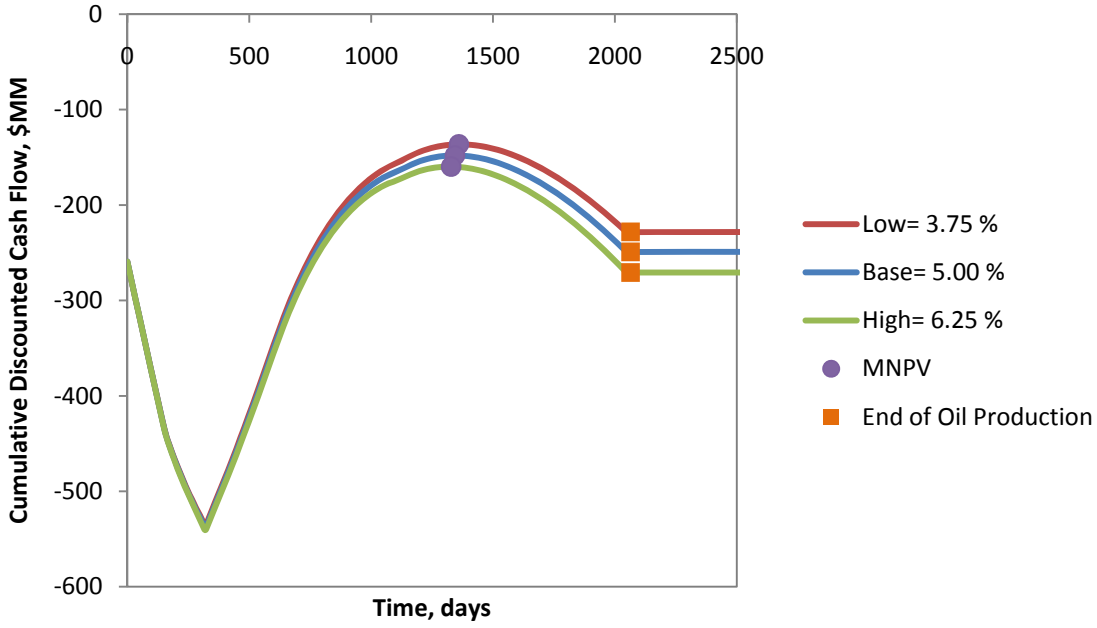

Figure C-80 Plot of CDCF against Time for a Varying i for ASP Floods

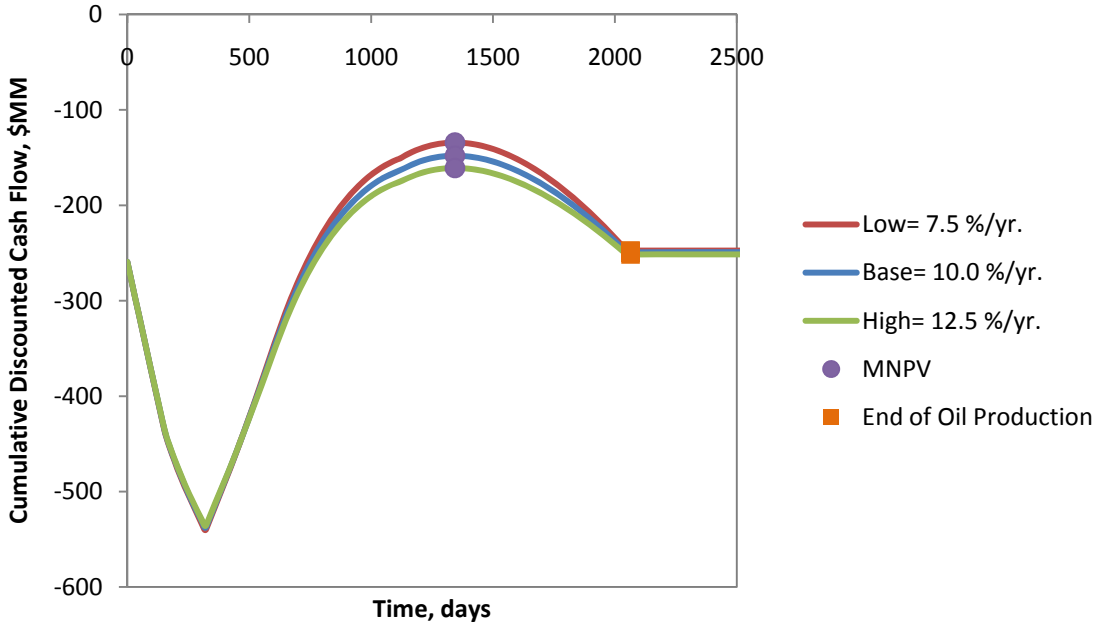

Figure C-81 Plot of CDCF against Time for a Varying d for ASP Floods

C.4 Sensitivity Analysis Plots for CO_2 Floods

The following are all of the plots produced for the sensitivity analysis of all of the parameters associated with CO_2 floods.

C.4.1 Sensitivity Analysis Plots of the Parameters for the Simplified Enhanced Oil Recovery Method

These plots include analyses of the following parameters: change in oil saturation, total pore volumes, heterogeneity factors, and the specific shock velocity of the oil bank.

C.4.1.1 Change in Oil Saturation

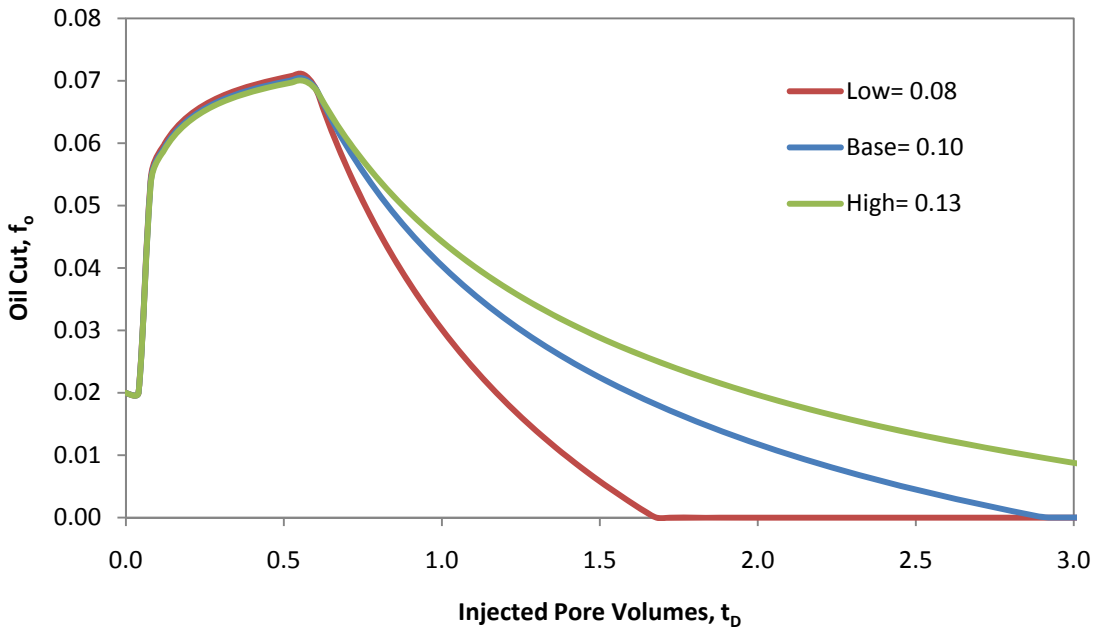

Figure C-82 Plot of Oil Cut against Dimensionless Time for Varying ΔS_o for CO_2 Floods

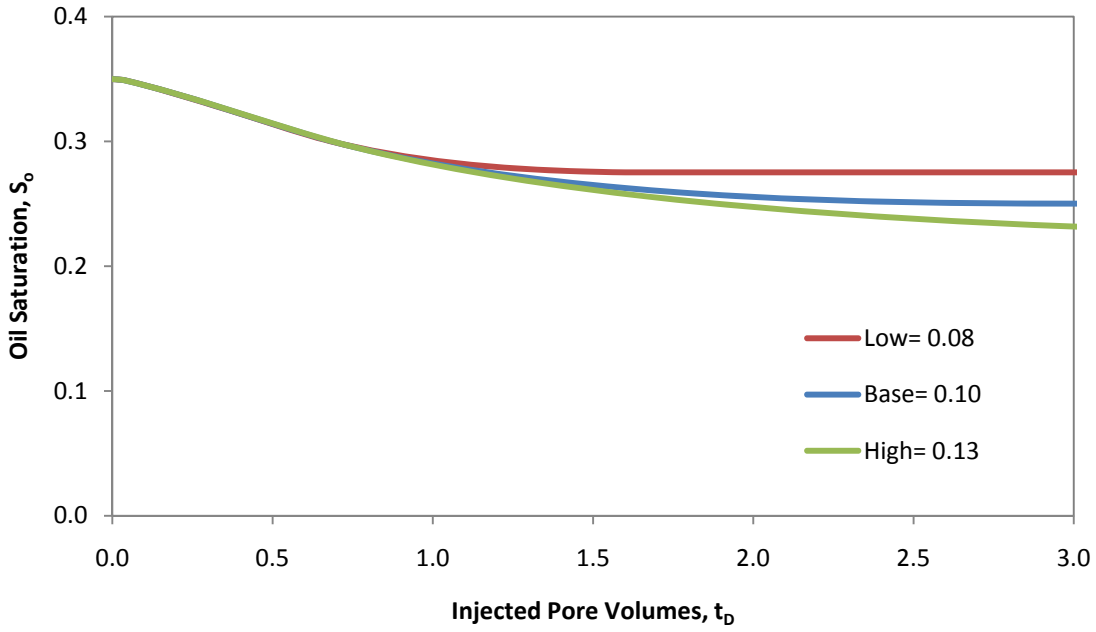

Figure C-83 Plot of Oil Saturation against Dimensionless Time for Varying ΔS_o for CO_2 Floods

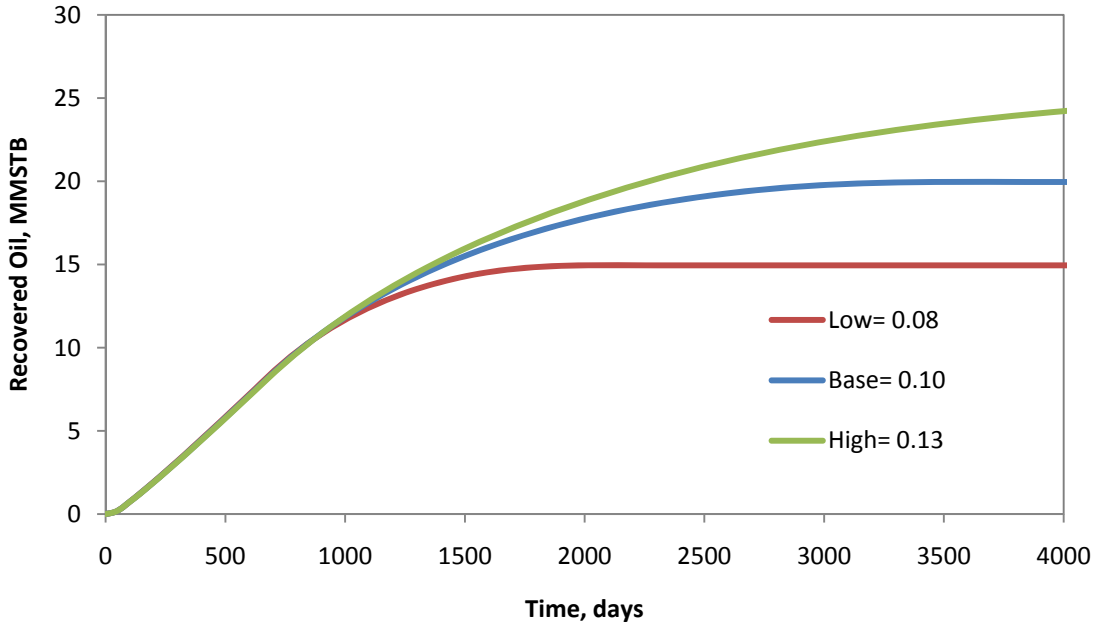

Figure C-84 Plot of Oil Recovery against Time for Varying ΔS_o for CO_2 Floods

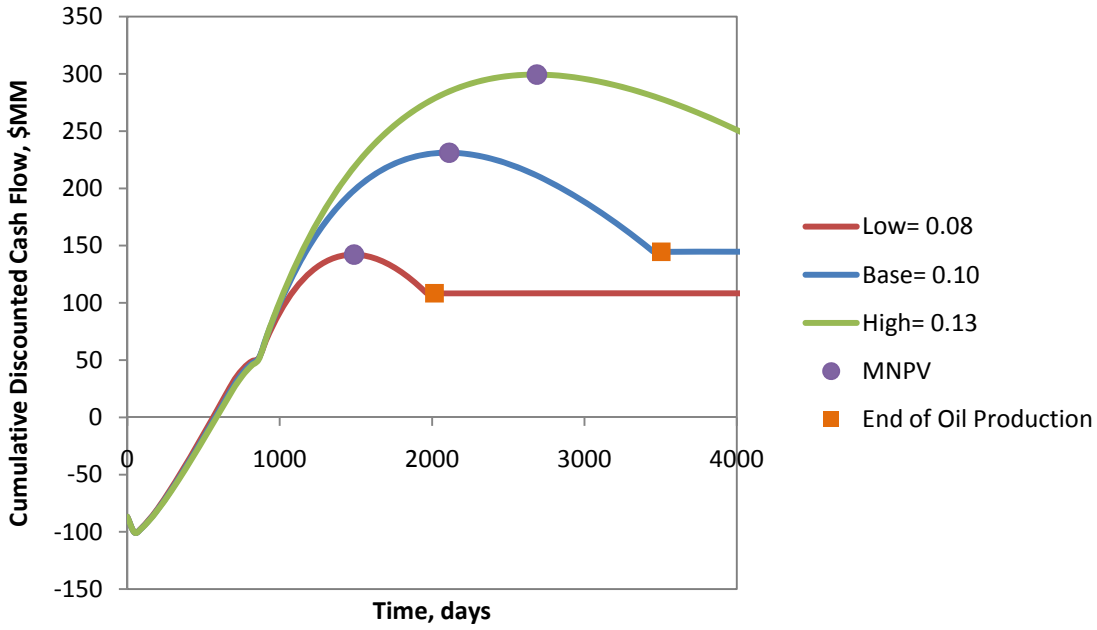

Figure C-85 Plot of CDCF against Time for Varying ΔS_o for CO_2 Floods

C.4.1.2 Total Pore Volumes

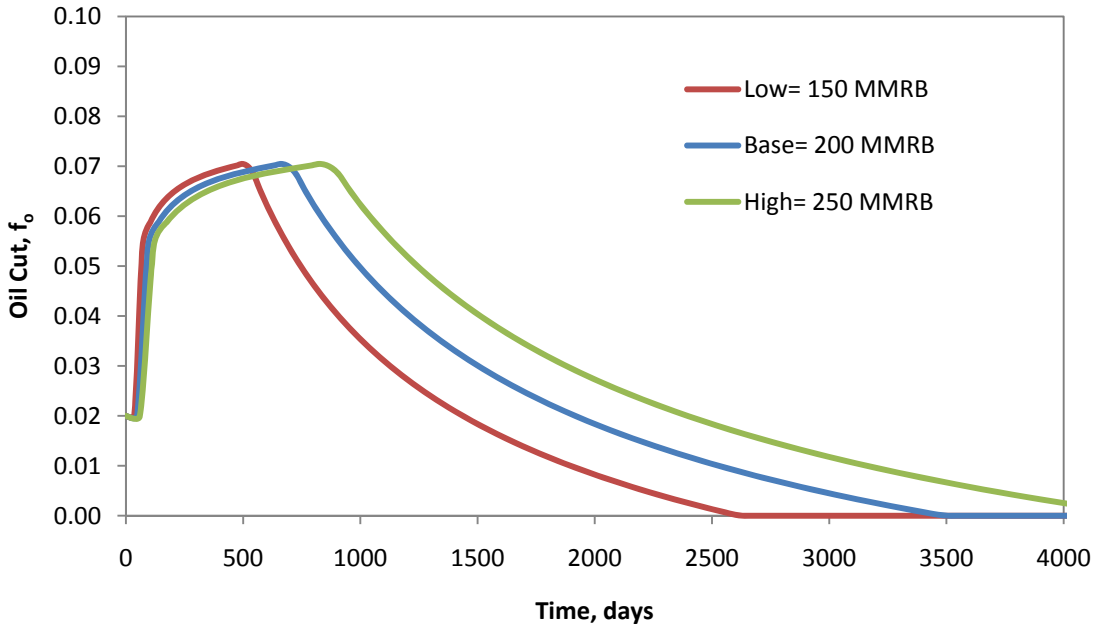

Figure C-86 Plot of Oil Cut against Time for a Varying V_p for CO_2 Floods

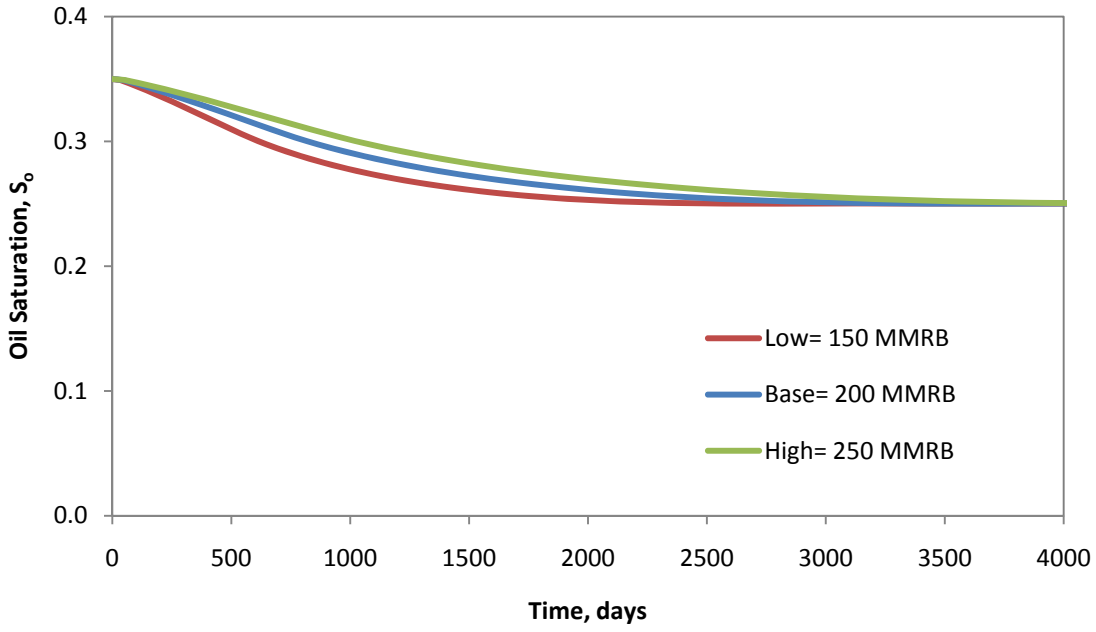

Figure C-87 Plot of Oil Saturation against Time for a Varying V_p for CO_2 Floods

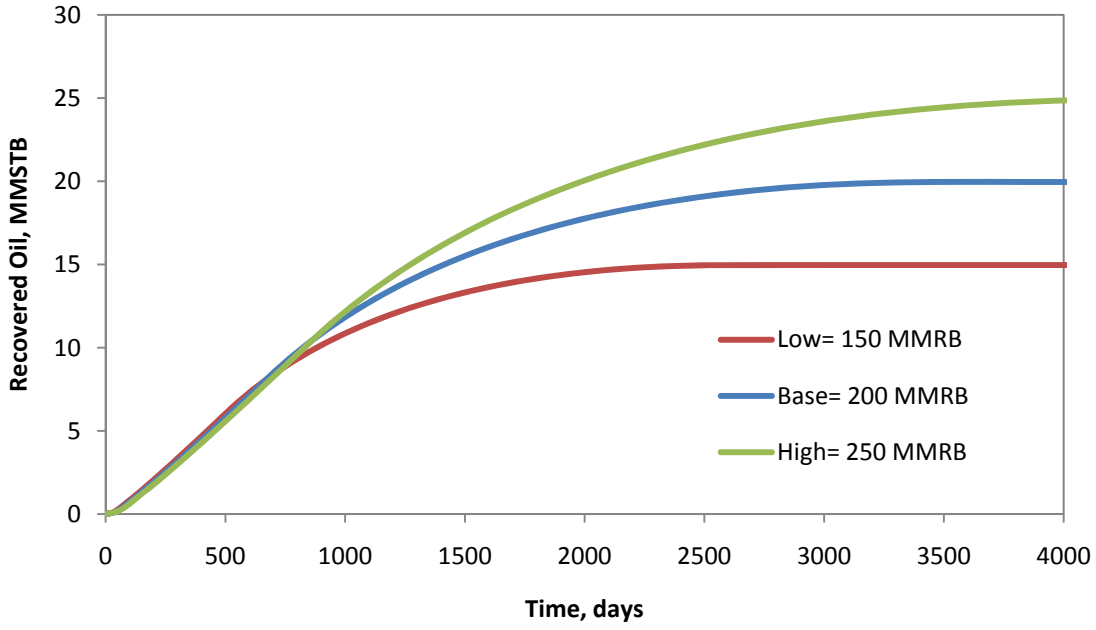

Figure C-88 Plot of Oil Recovery against Time for a Varying V_p for CO_2 Floods

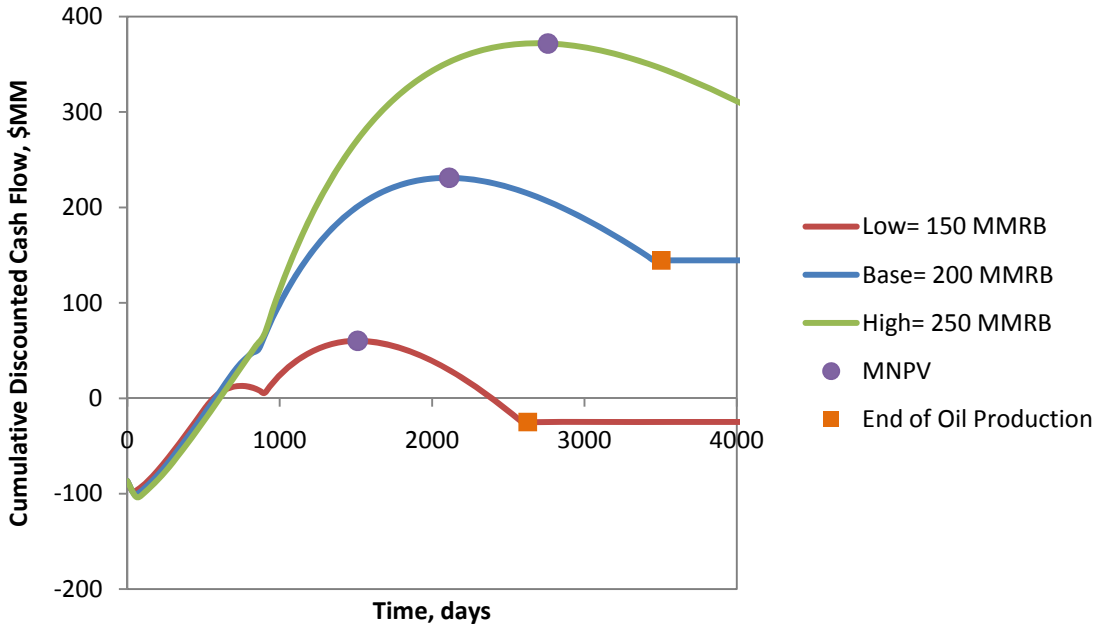

Figure C-89 Plot of CDCF against Time for a Varying V_p for CO_2 Floods

C.4.1.3 Heterogeneity Factors

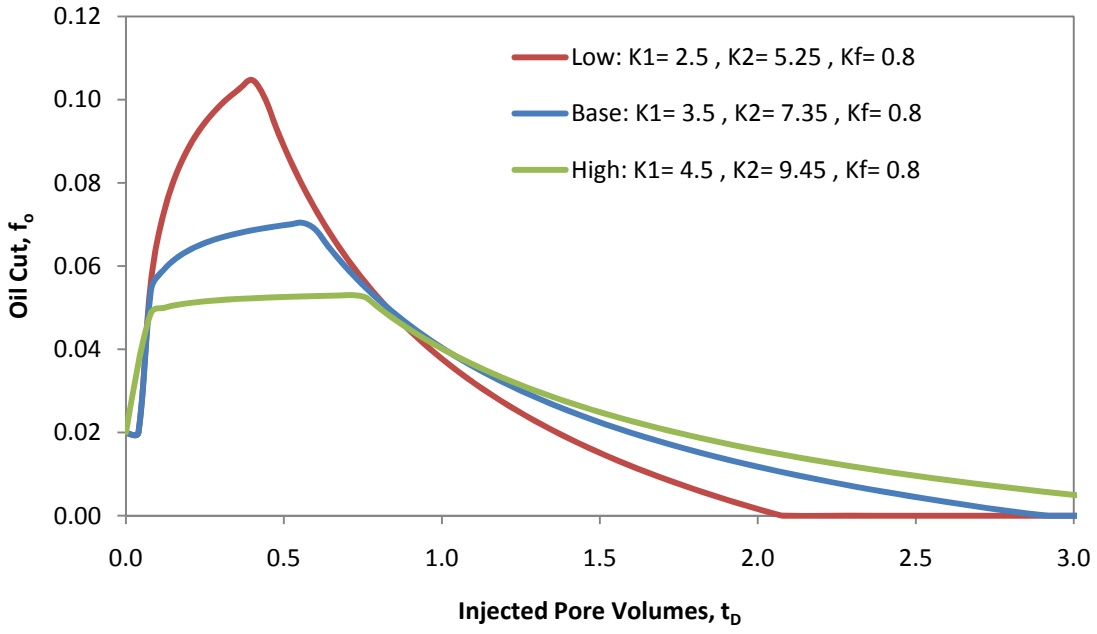

Figure C-90 Plot of Oil Cut against Dimensionless Time for a Varying K_1 for CO_2 Floods

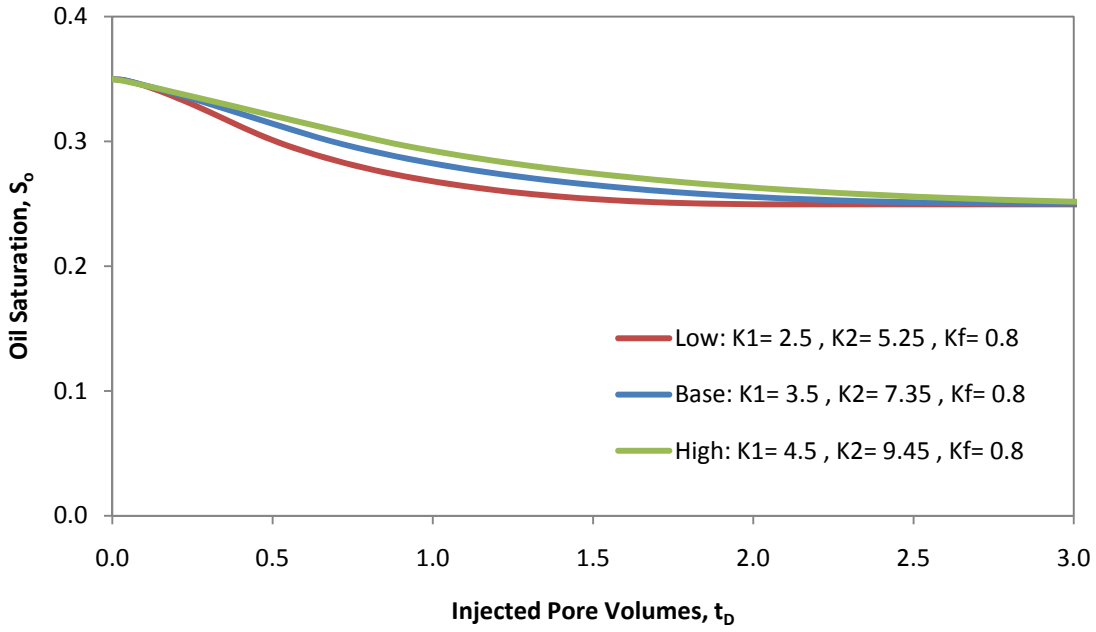

Figure C-91 Plot of Oil Saturation against Dimensionless Time for a Varying K_1 for CO_2 Floods

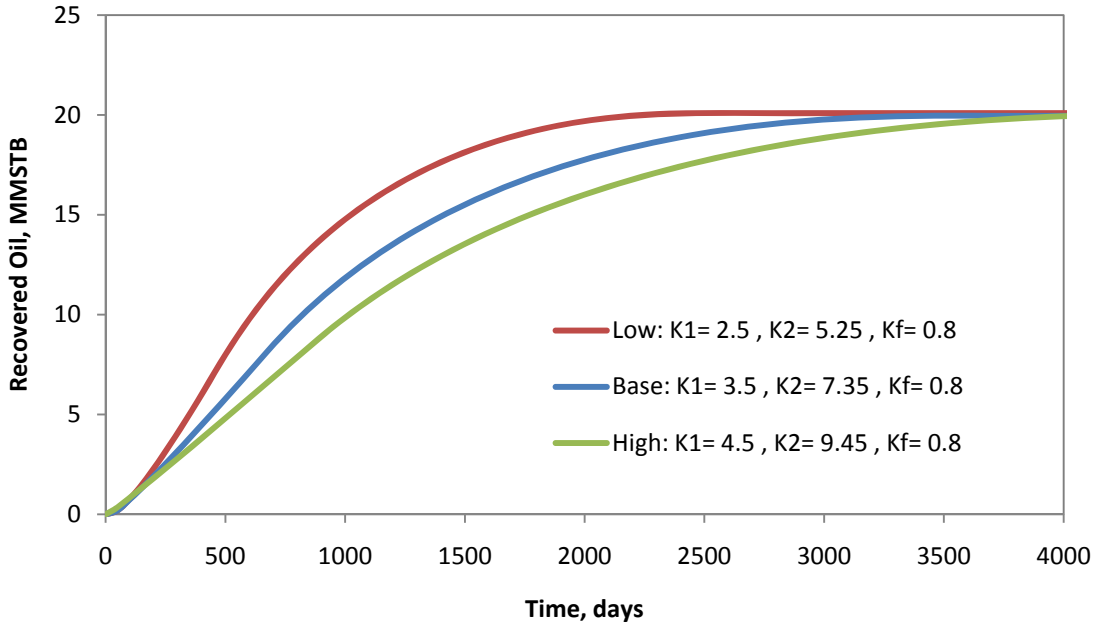

Figure C-92 Plot of Oil Recovery against Time for a Varying K_1 for CO_2 Floods

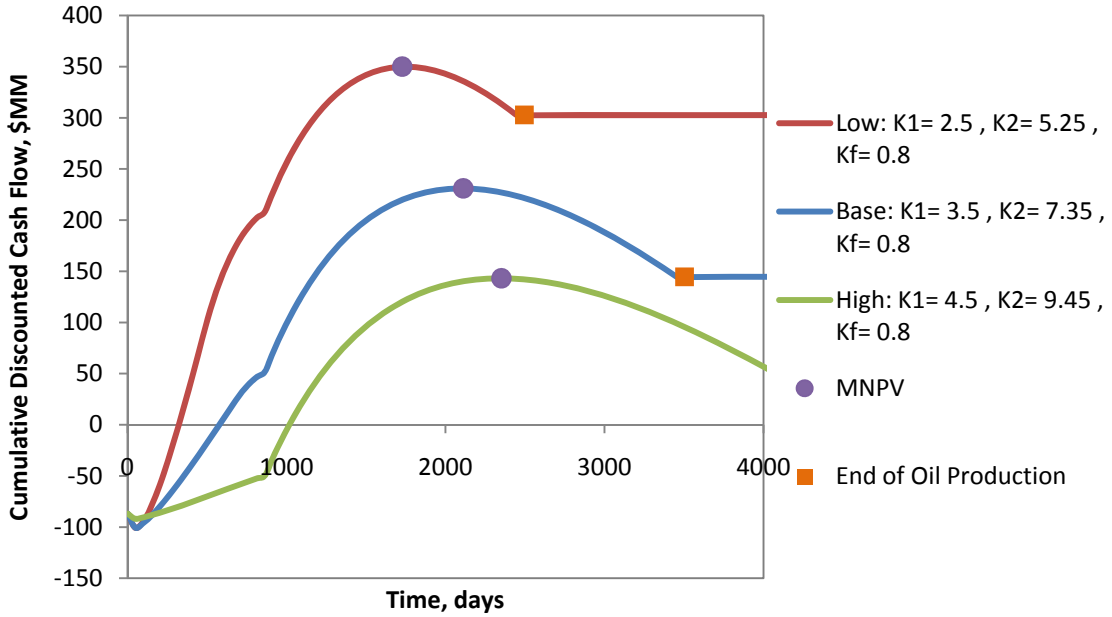

Figure C-93 Plot of CDCF against Time for a Varying K_1 for CO_2 Floods

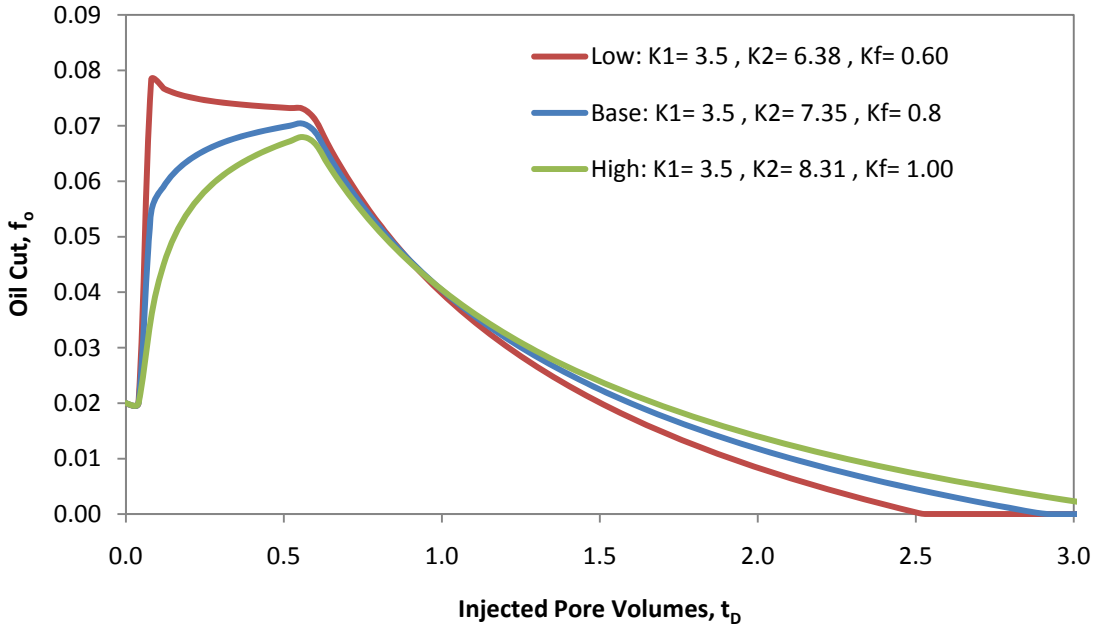

Figure C-94 Plot of Oil Cut against Dimensionless Time for a Varying K_f for CO_2 Floods

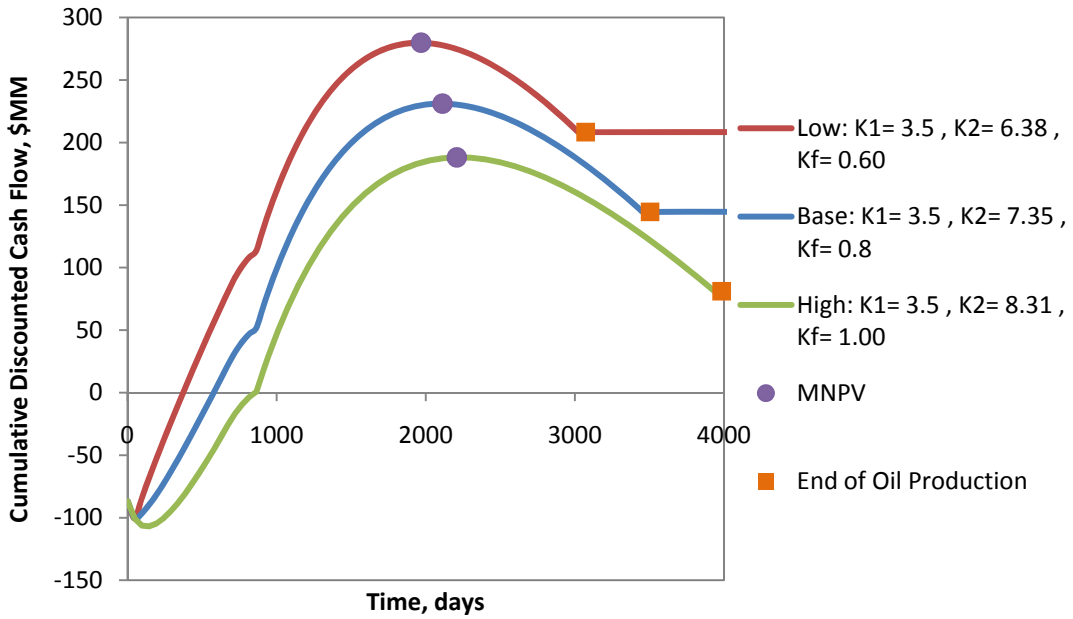

Figure C-95 Plot of CDCF against Time for a Varying K_f for CO_2 Floods

C.4.1.4 Specific Shock Velocity of Oil Bank

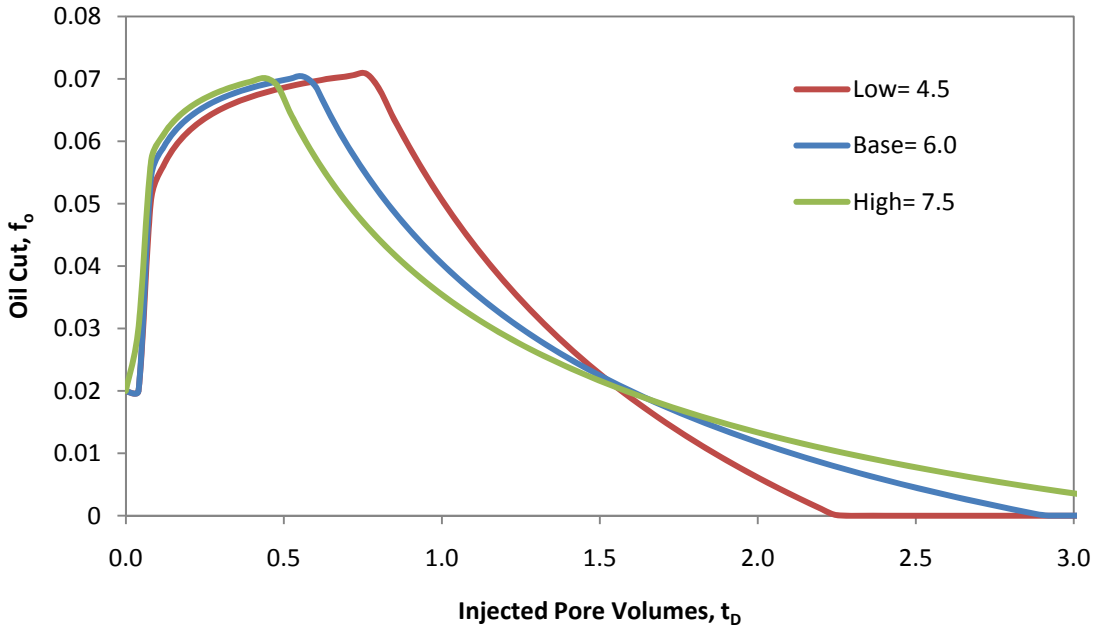

Figure C-96 Plot of Oil Cut against Dimensionless Time for a Varying v_{oB} for CO_2 Floods

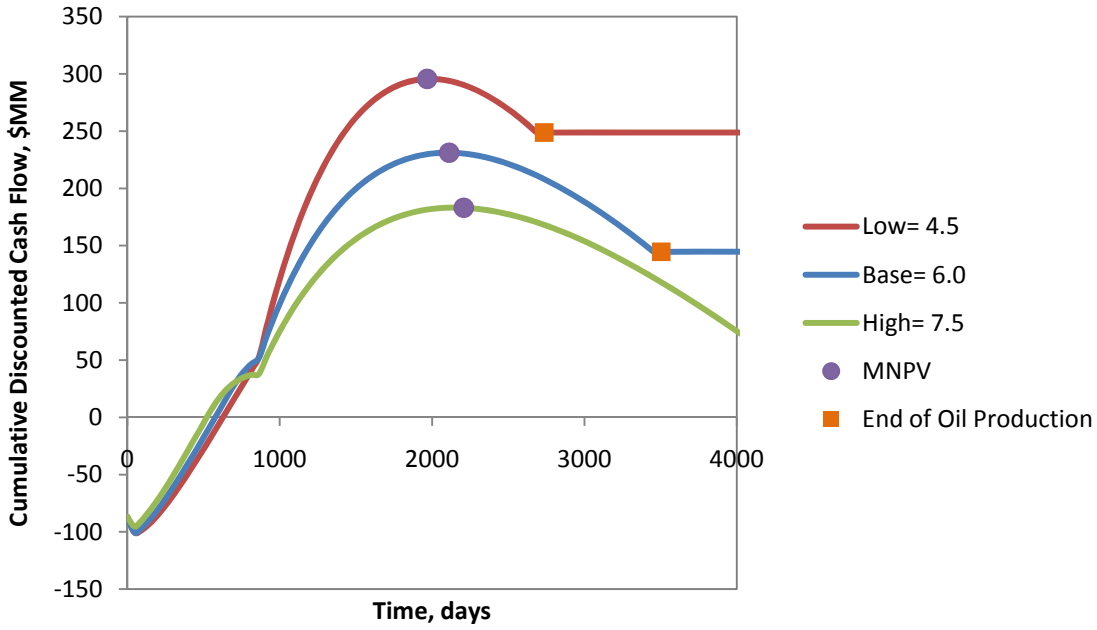

Figure C-97 Plot of CDCF against Time for a Varying v_{oB} for CO_2 Floods

C.4.2 Sensitivity Plots of the Design Parameters

These plots include analyses of the following design parameters: well spacing, injection rate, production rate, pore volumes for the injected chemicals, and water to gas (WAG) ratio.

C.4.2.1 Well Spacing

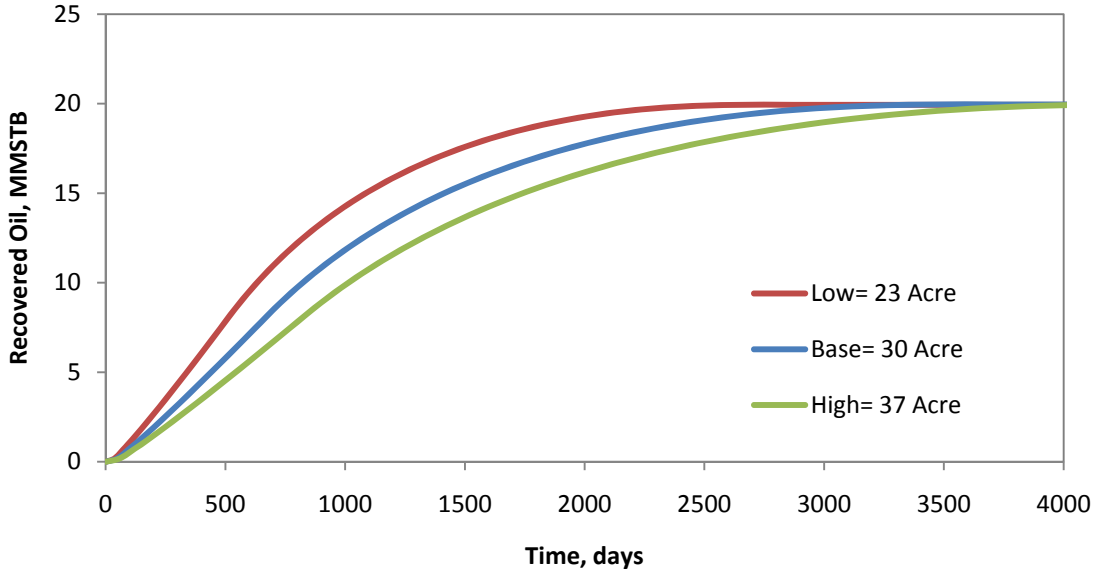

Figure C-98 Plot of Oil Recovery against Time for a Varying WS for CO_2 Floods

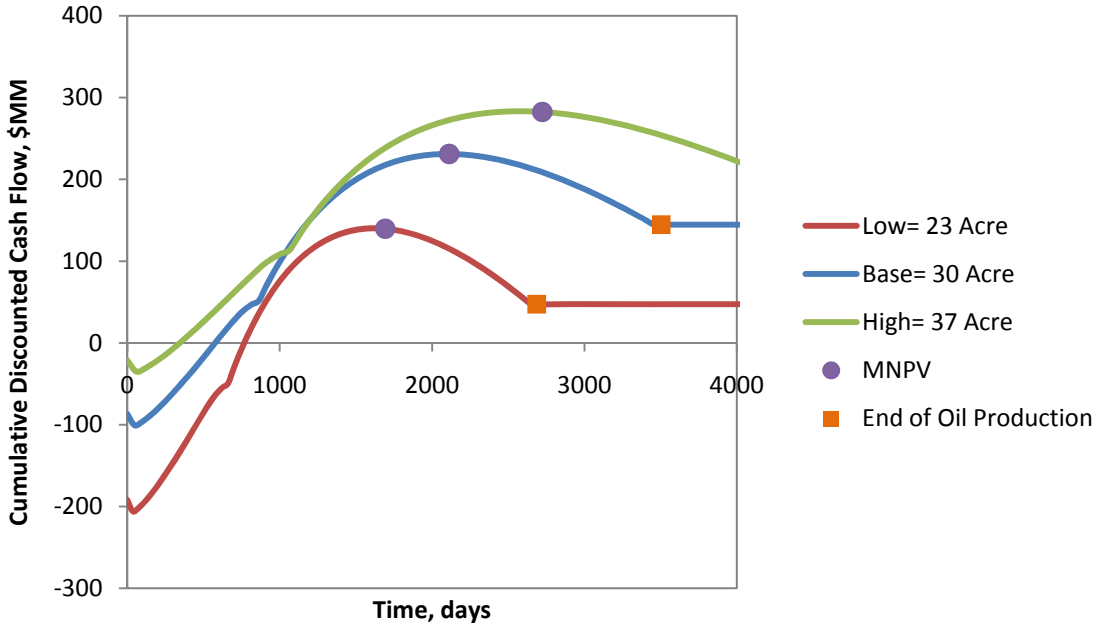

Figure C-99 Plot of CDCF against Time for Varying WS for CO_2 Floods

C.4.2.2 Injection Rate

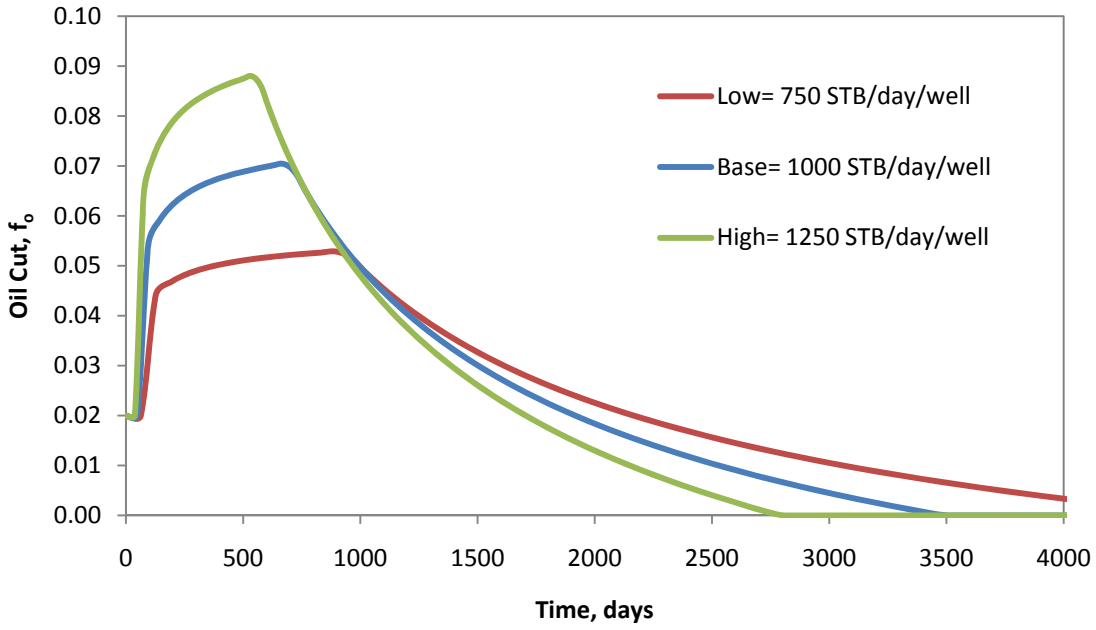

Figure C-100 Plot of Oil Cut against Time for a Varying q_i for CO_2 Floods

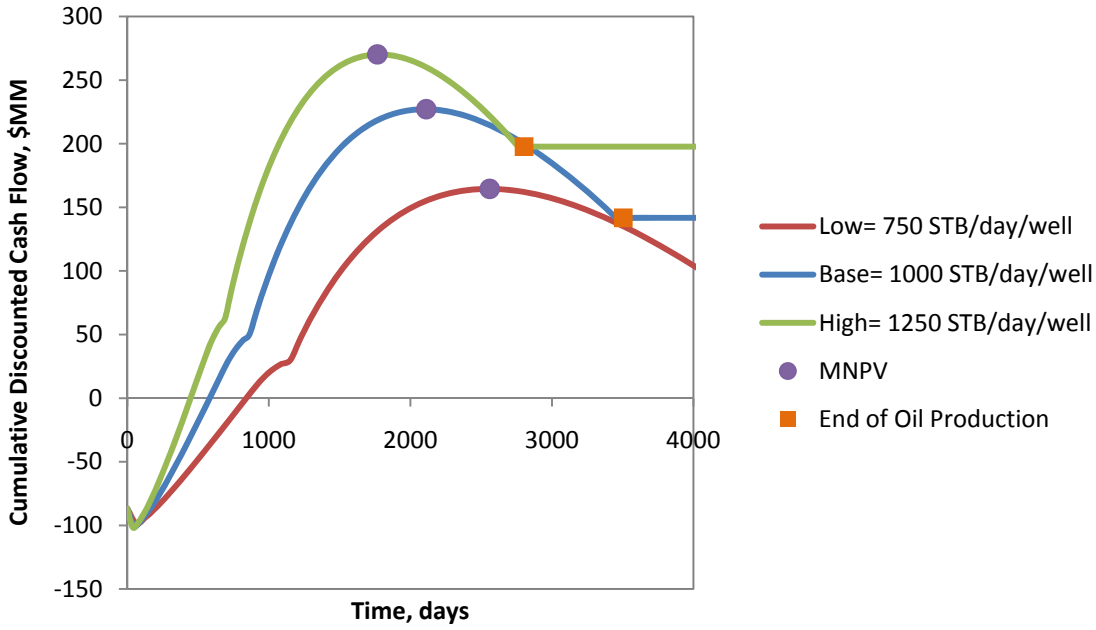

Figure C-101 Plot of CDCF against Time for a Varying q_i for CO_2 Floods

C.4.2.3 Production Rate

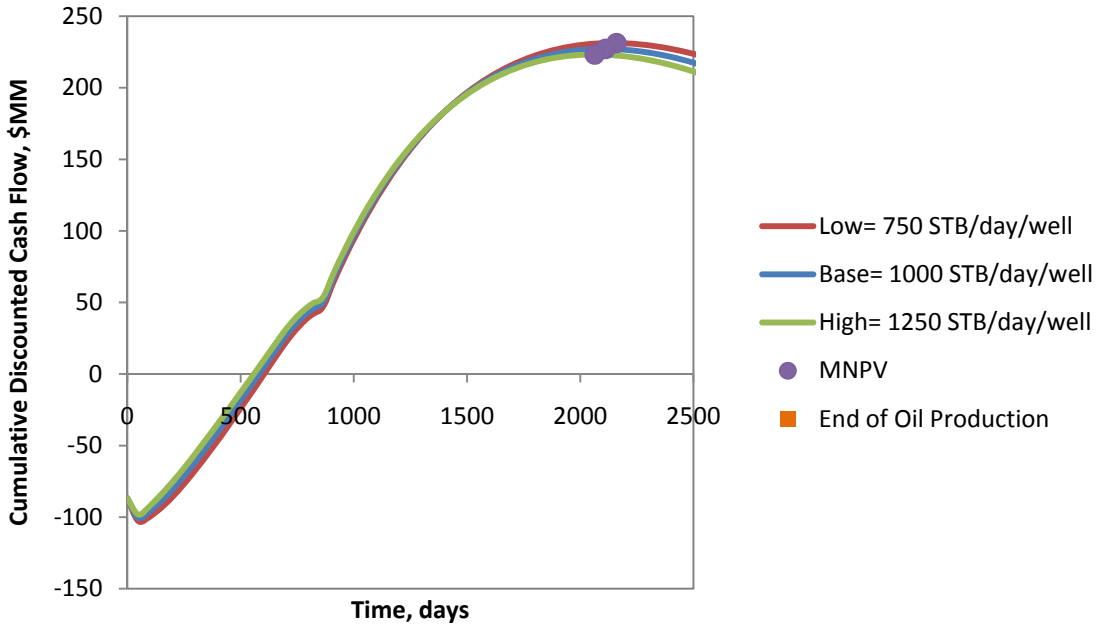

Figure C-102 Plot of CDCF against Time for Varying q_p for CO_2 Floods

C.4.2.4 CO_2 Slug Sizes

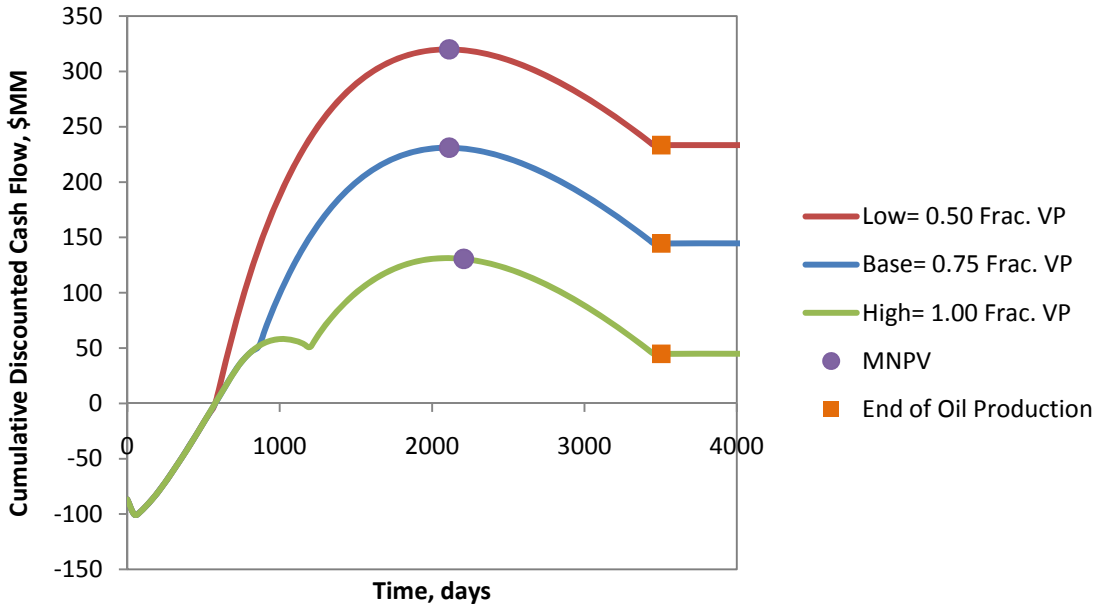

Figure C-103 Plot of CDCF against Time for Varying V_{CO2} for CO_2 Floods

C.4.2.5 WAG Ratio

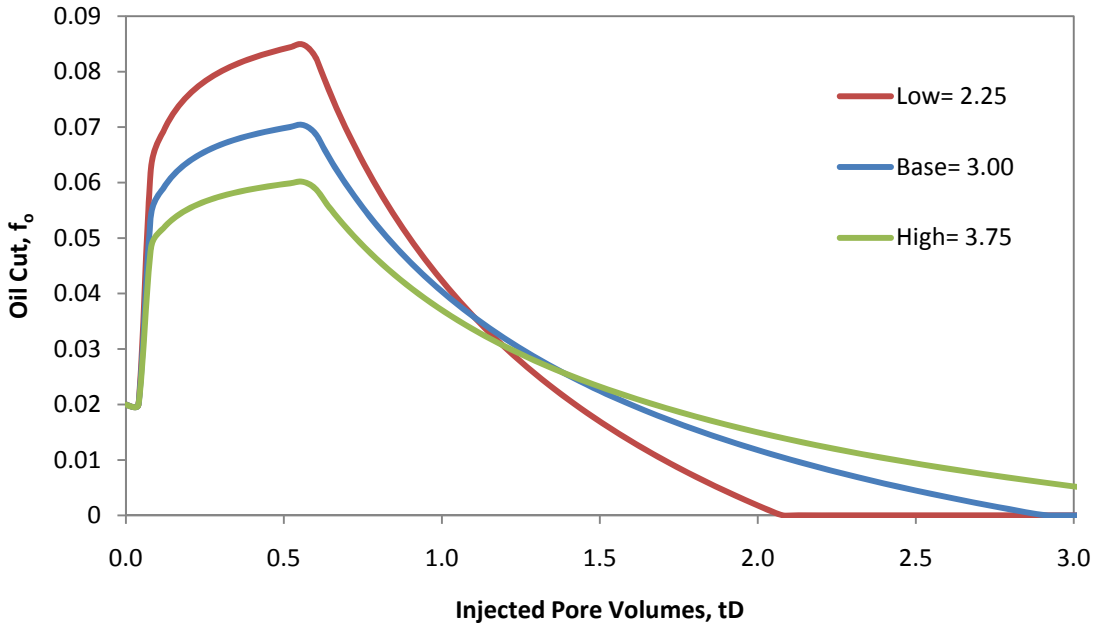

Figure C-104 Plot of Oil Cut against Dimensionless Time for Varying Z_{CO2} (WAG) for CO_2 Floods

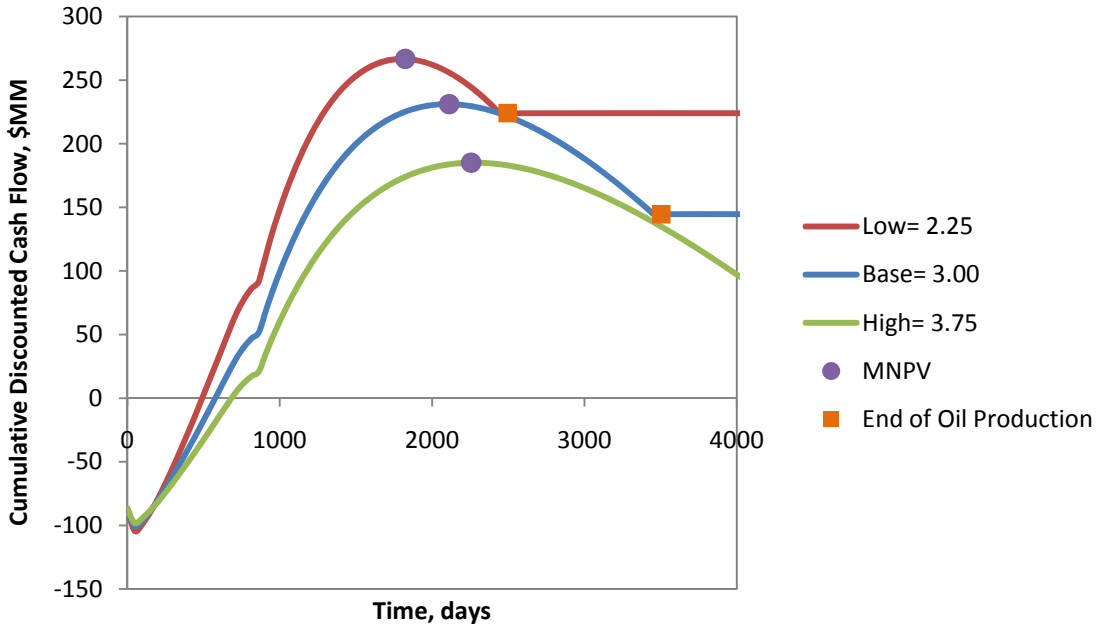

Figure C-105 Plot of CDCF against Time for Varying Z_{CO2} (WAG) for CO_2 Floods

C.4.3 Sensitivity Plots for Economic Parameters

The following plots are for the following economic parameter: price of oil, escalation factor, price of CO_2, cost of injection, cost of treatment, cost of water disposal, upfront costs, maintenance costs, royalties, ad-valorem tax, severance tax, inflation, and discount rate.

C.4.3.1 Price of Oil and Escalation Factor for the Price of Oil

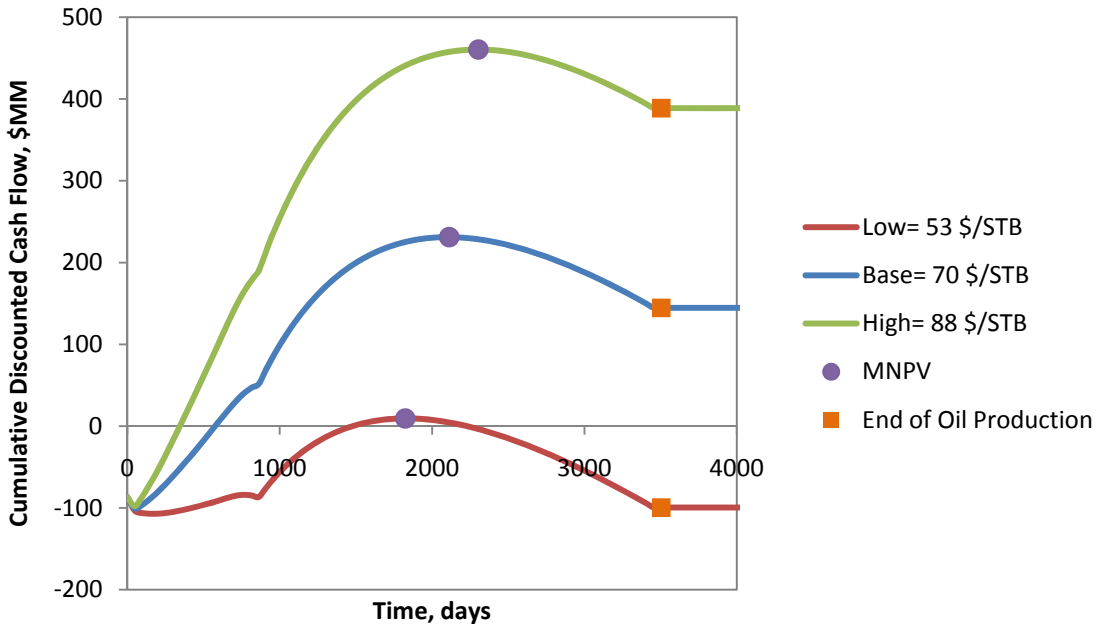

Figure C-106 Plot of CDCF against Time for Varying P_o for CO_2 Floods

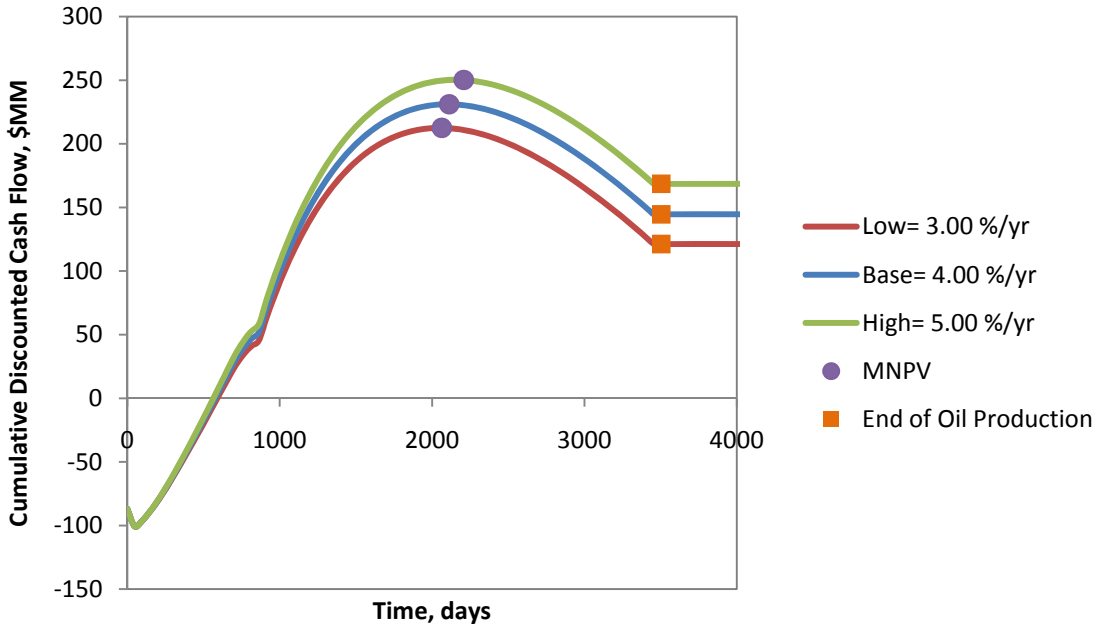

Figure C-107 Plot of CDCF against Time for Varying R_E for CO_2 Floods

C.4.3.2 Price of CO_2

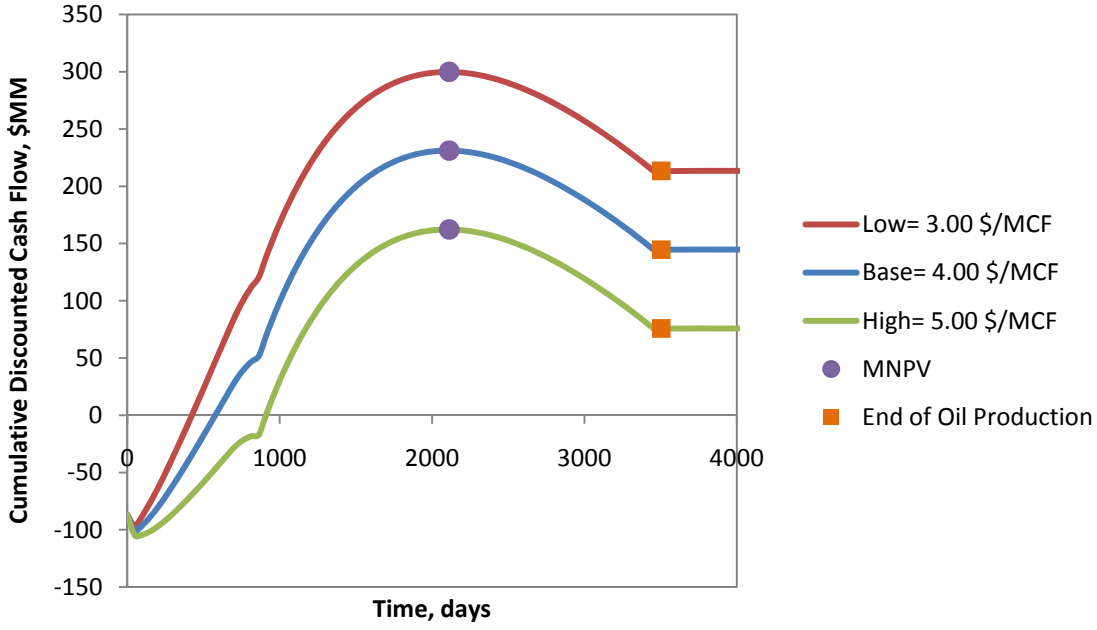

Figure C-108 Plot of CDCF against Time for Varying C_{CO2} for CO_2 Floods

C.4.3.3 Costs of Injection, Treatment, and Water Disposal, and Softening

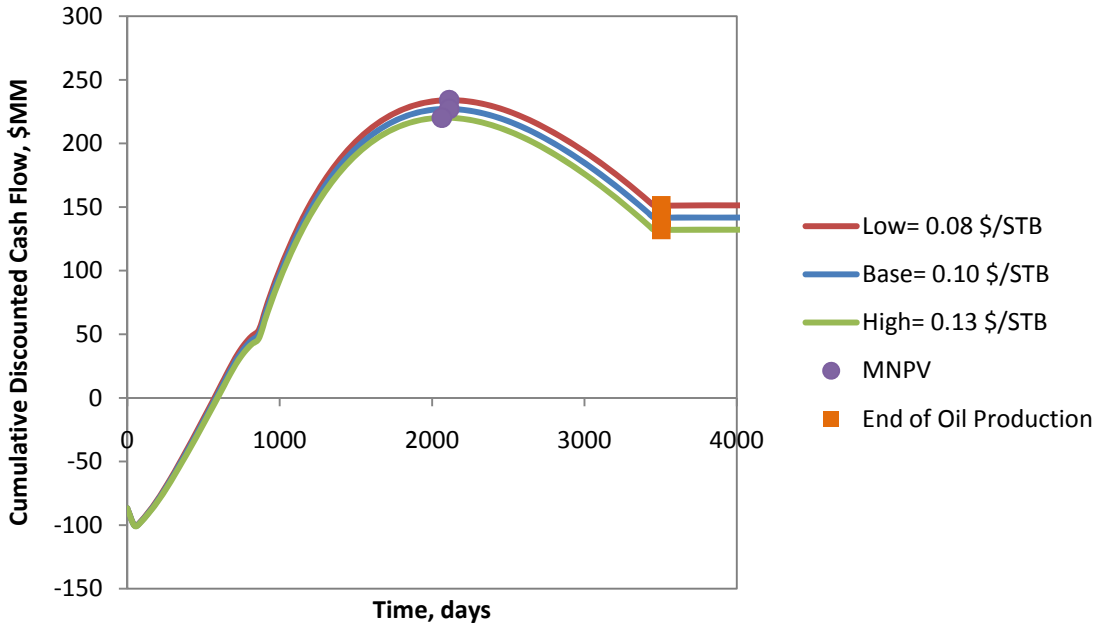

Figure C-109 Plot of CDCF against Time for Varying C_q for CO_2 Floods

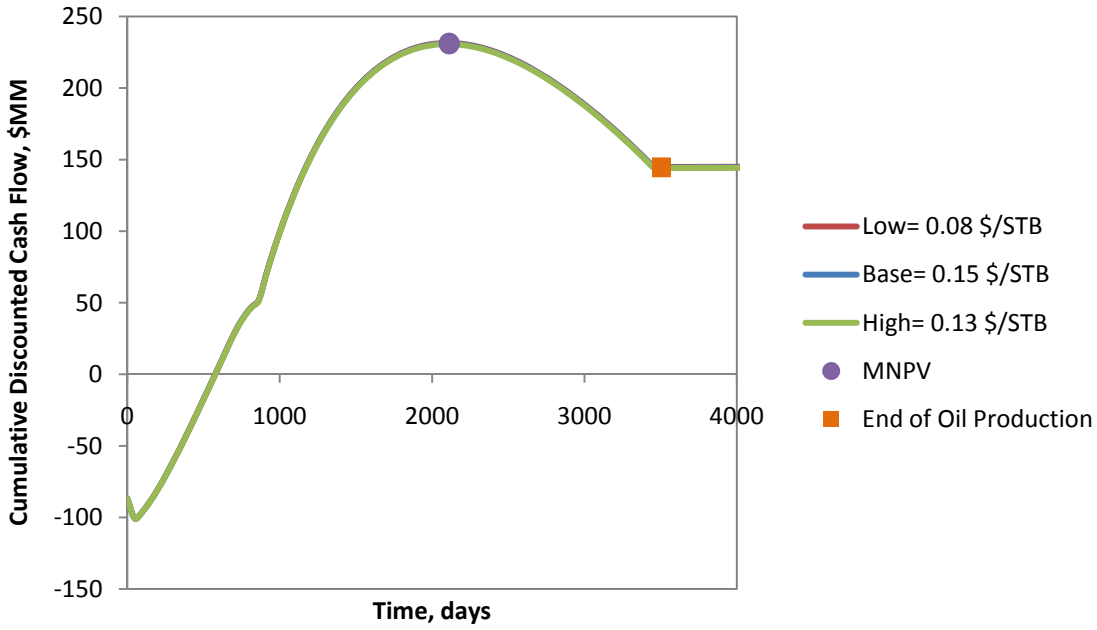

Figure C-110 Plot of CDCF against Time for Varying C_T for CO_2 Floods

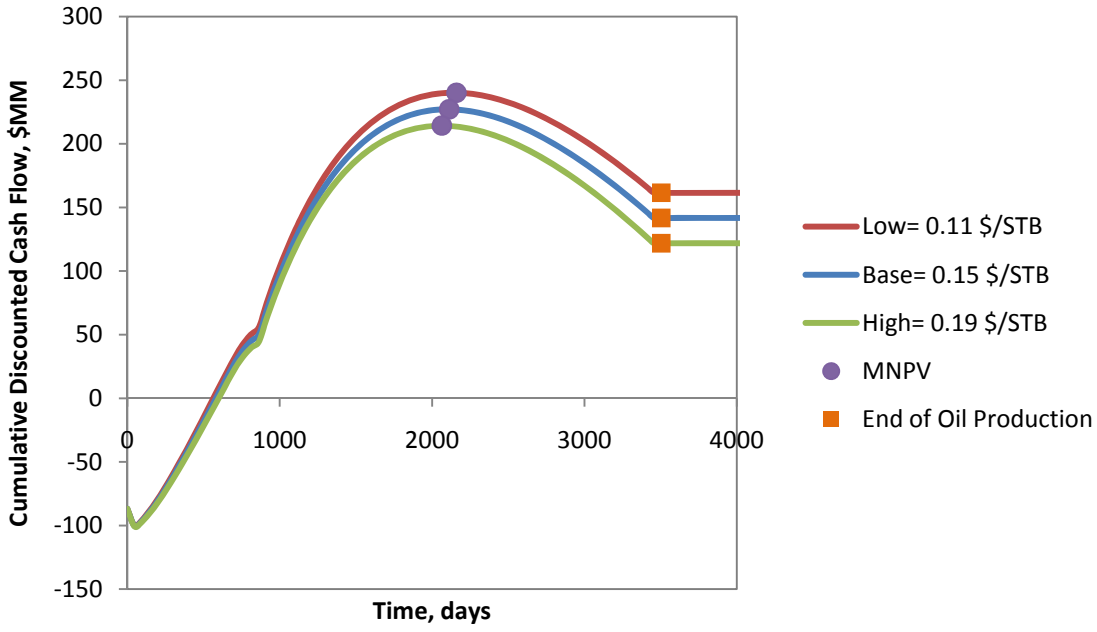

Figure C-111 Plot of CDCF against Time for Varying C_{WD} for CO_2 Floods

C.4.3.4 Upfront and Maintenance Costs

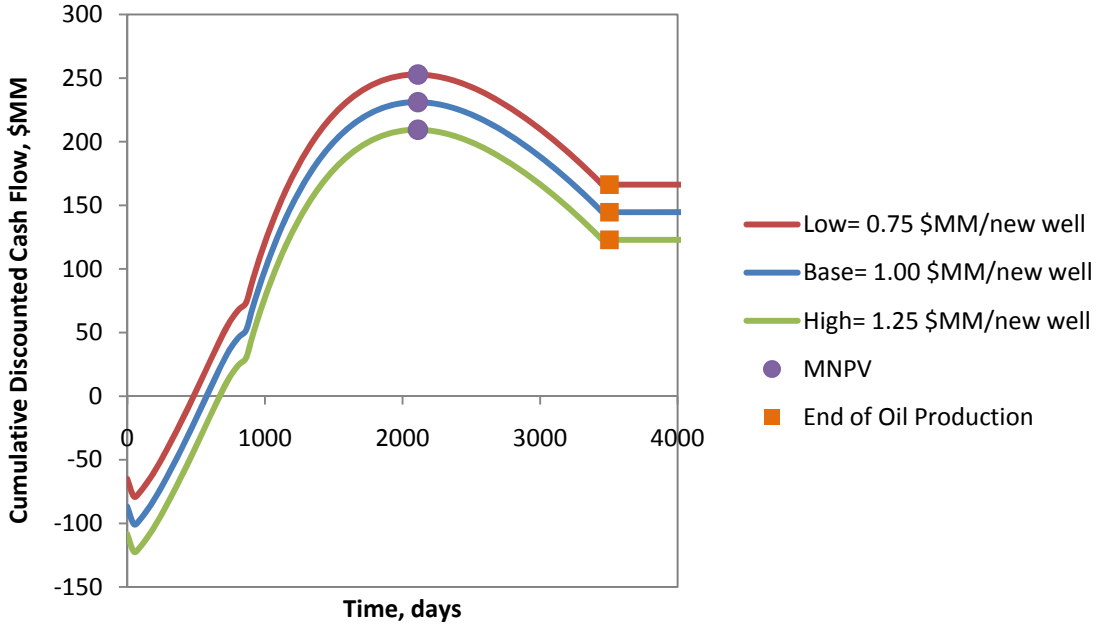

Figure C-112 Plot of CDCF against Time for a Varying C_I for CO_2 Floods

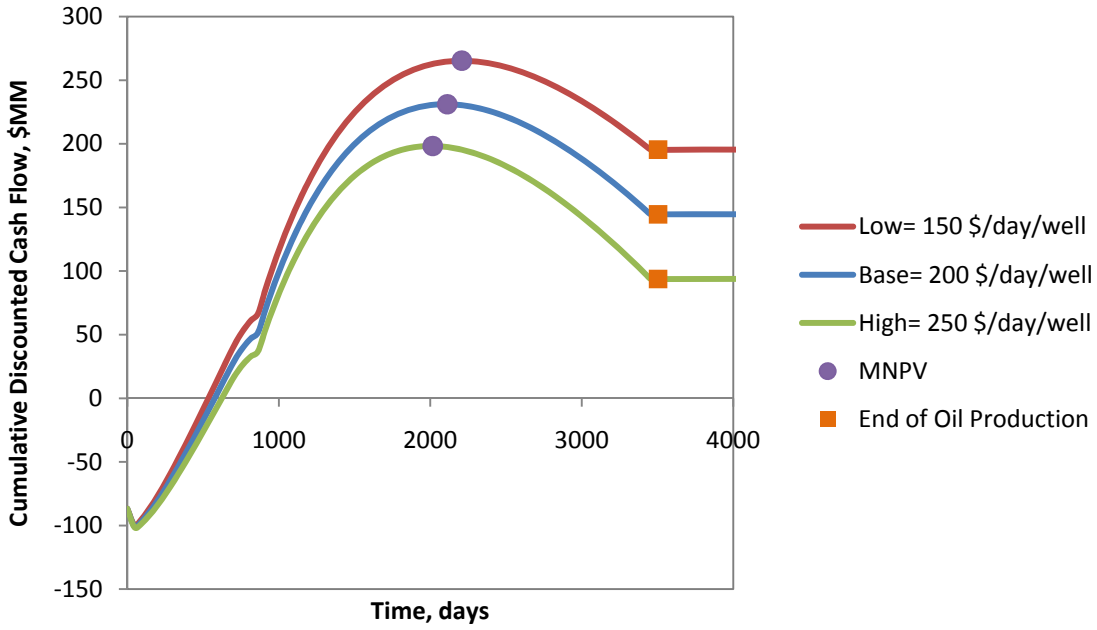

Figure C-113 Plot of CDCF against Time for a Varying C_M for CO_2 Floods

C.4.3.5 Royalty, Ad-Valorem Tax, Severance Tax

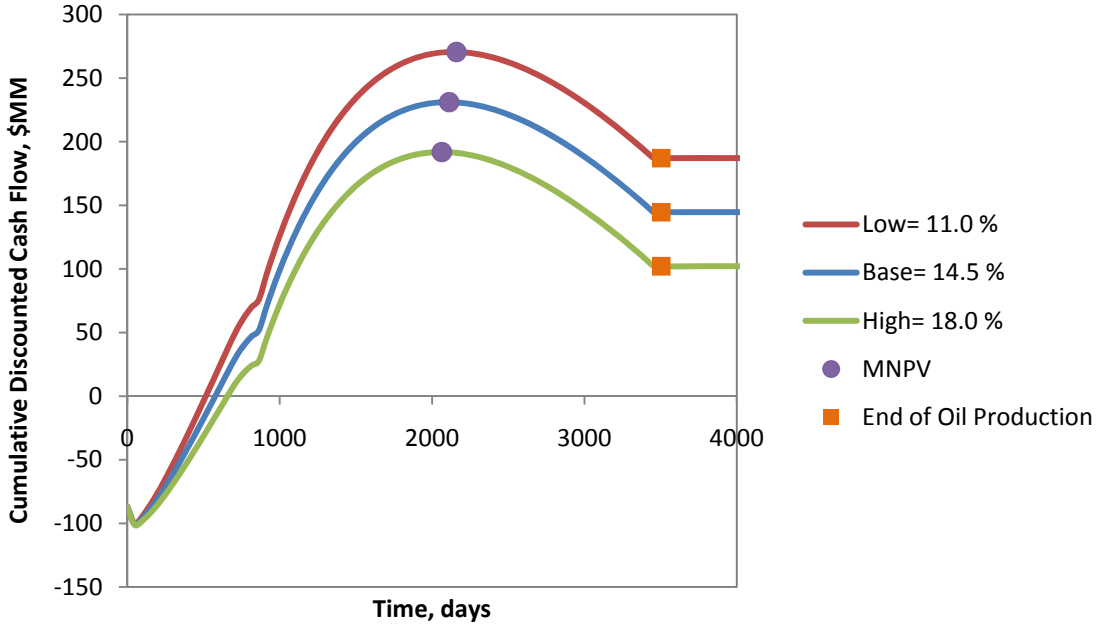

Figure C-114 Plot of CDCF against Time for a Varying T_R for CO_2 Floods

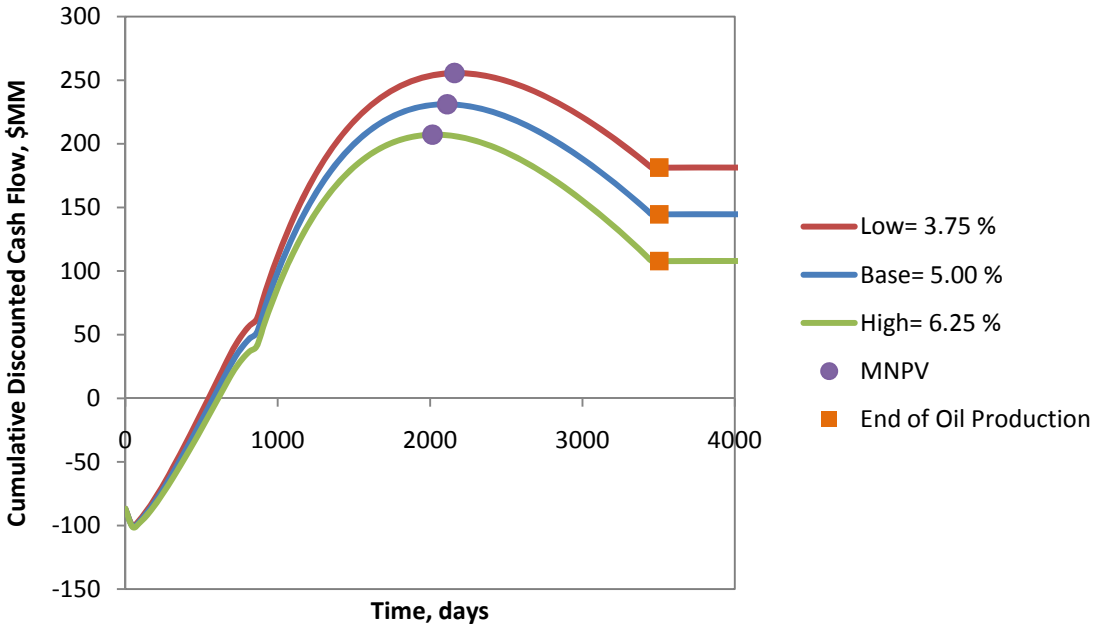

Figure C-115 Plot of CDCF against Time for a Varying T_V for CO_2 Floods

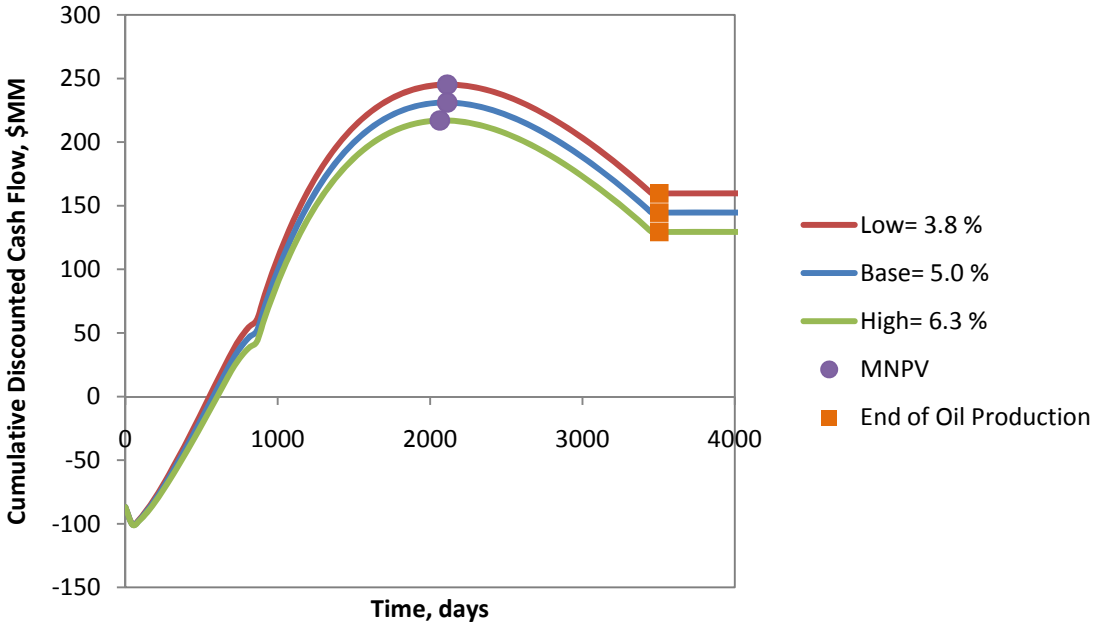

Figure C-116 Plot of CDCF against Time for a Varying T_S for CO_2 Floods

C.4.3.6 Inflation and Discount Rate

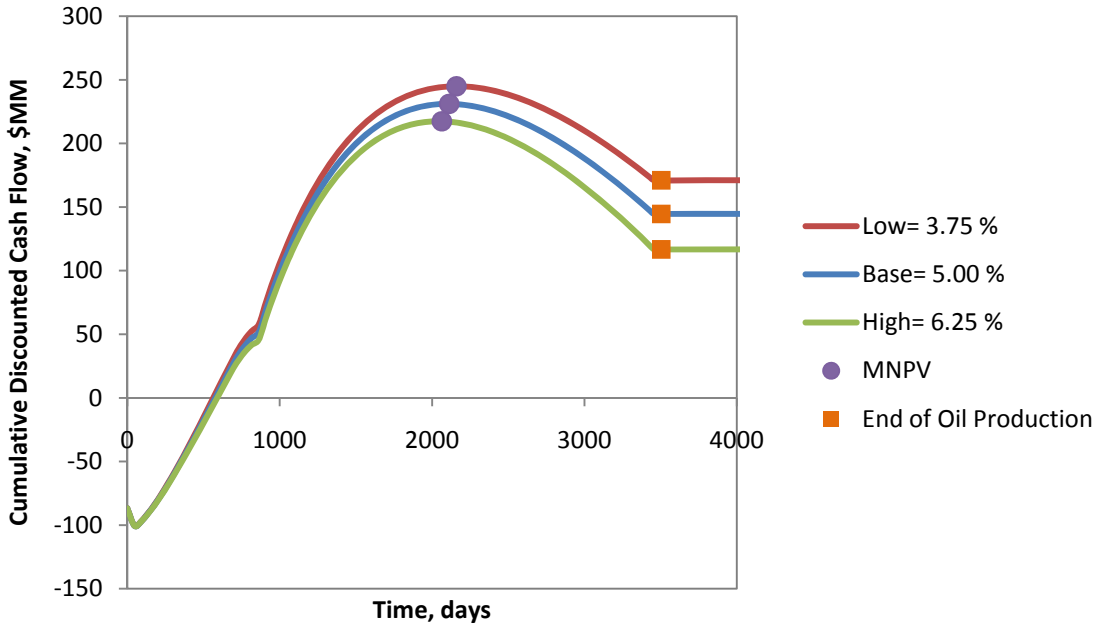

Figure C-117 Plot of CDCF against Time for a Varying i for CO_2 Floods

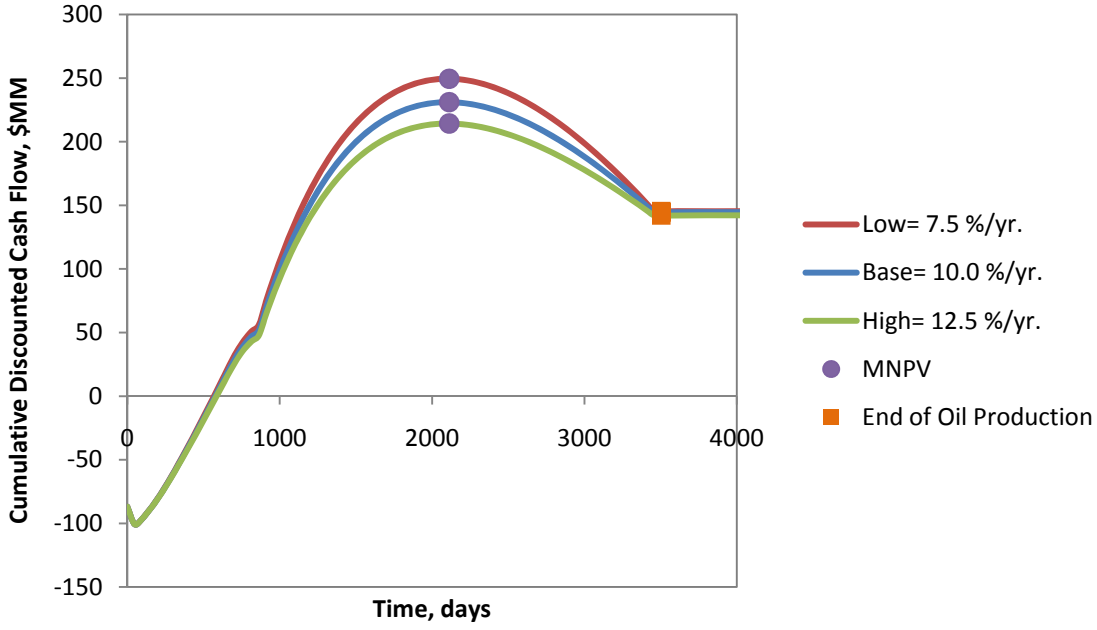

Figure C-118 Plot of CDCF against Time for a Varying d for CO_2 Floods

APPENDIX D: EXTRA PLOTS FOR THE DEMONSTRATION OF THE DECISION BASED METHOD

D.1 Introduction

The following is a collection of all of the plots created for the example of the decision based method (DBM) in Chapter 8. The significance of these plots is discussed in Chapter 8 and is briefly reviewed throughout this appendix. The example for demonstrating DBM is based on three parameters, change in oil saturation (ΔS_o), total pore volumes (V_P), and price of oil (P_o), and two alternatives, enhanced oil recovery (EOR) and water flooding (WF).

D.2 Plots of Analyses with a Single Parameter

The following are plots of the probability density functions (PDF) and cumulative density functions (CDF) created with DBM when only one parameter is considered.

D.2.1 Plots of Probability Density Functions against Utilities for Single Parameters

Figure D-1 and Figure D-2 are plots that show that the PDF reflects changes in the utility values for EOR and WF. These help to demonstrate how the PDFs created with DBM are sensitive to changes in decision and to utility set outcomes.

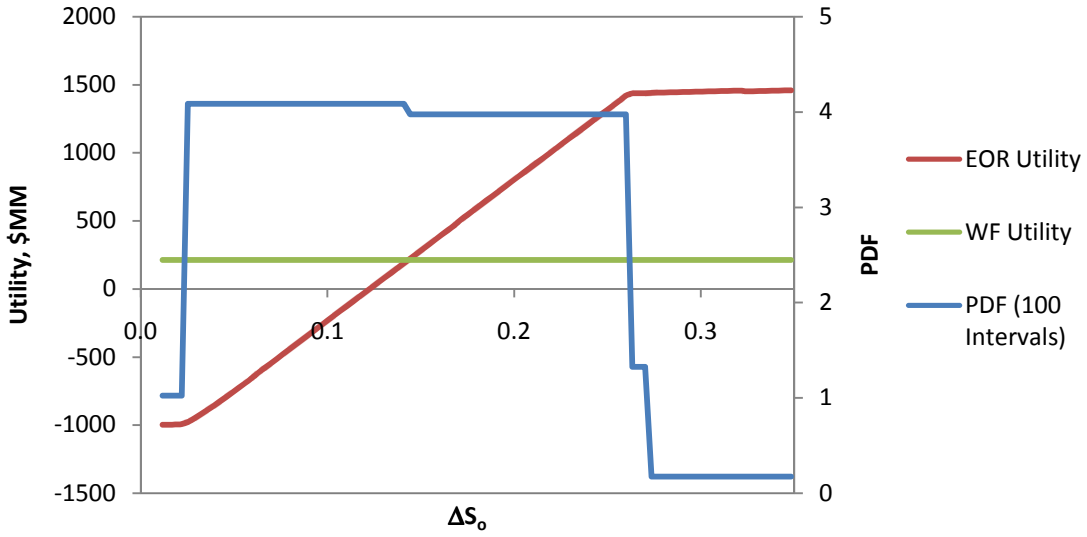

Figure D-1 Plot of the PDF against the Utilities for ΔS_o

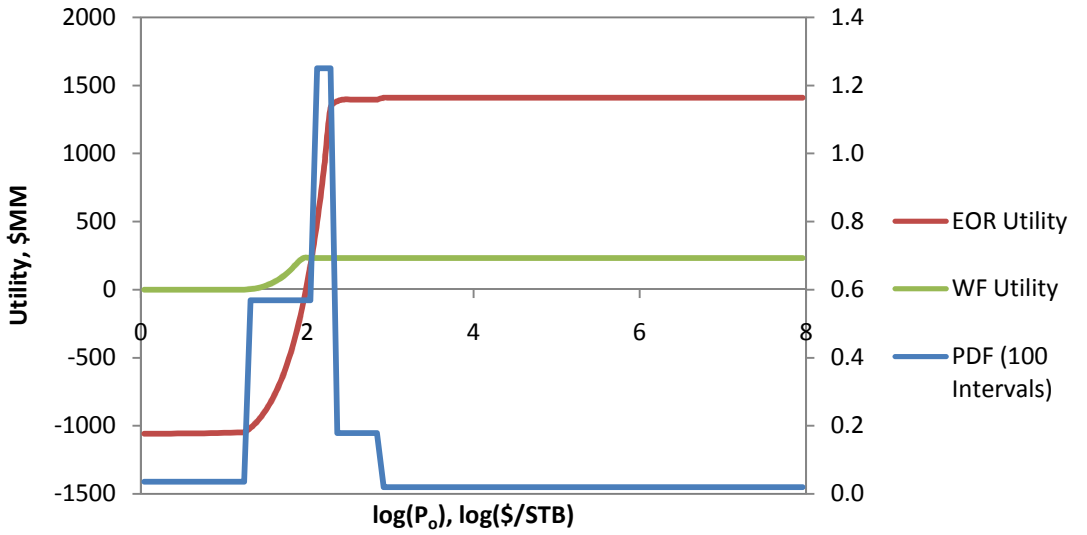

Figure D-2 Plot of the PDF against the Utilities for P_o

D.2.2 Plots Demonstrating Sensitivity to Resolution for a Single Parameter

The following plots demonstrate how sensitive DBM is to the number of intervals used for each parameter in the analysis. The higher resolution allows for more accuracy in determining at which points the decision and the utility set outcomes changes.

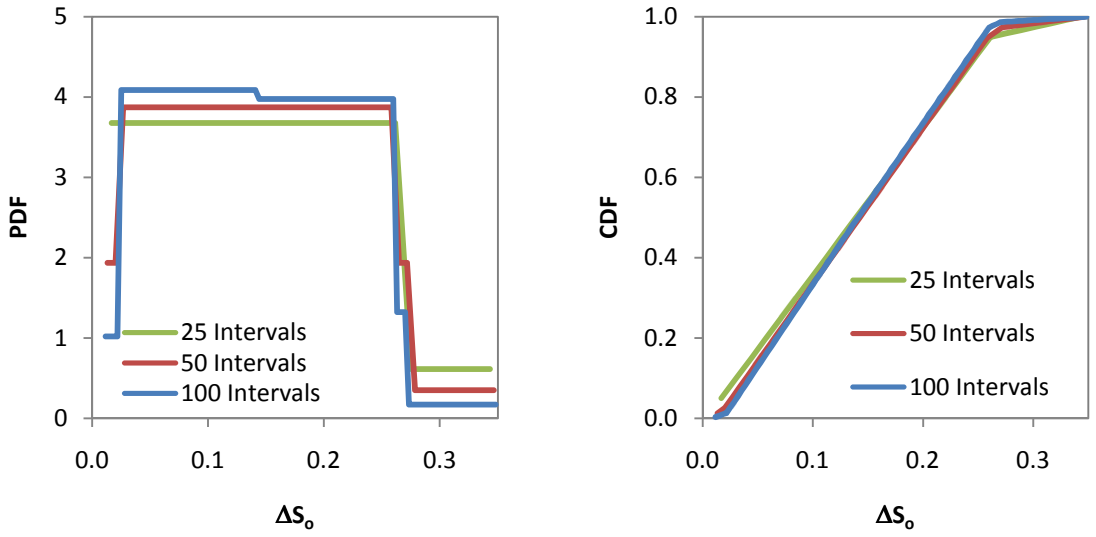

(a) PDF **(b) CDF**

Figure D-3 Plots of the PDF and CDF for ΔS_o with Varying Resolution

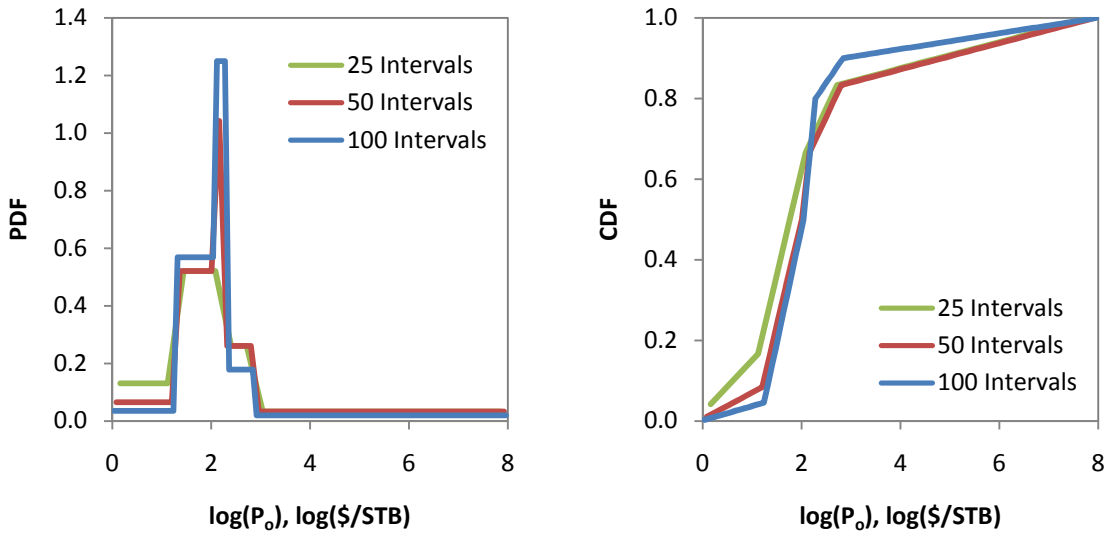

(a) PDF **(b) CDF**

Figure D-4 Plots of the PDF and CDF for P_o with Varying Resolution

D.3 Two Parameter Analyses

The following are plots of the joint PDFs and CDFs for analyses that consider two varying parameters. These plots help show how different parameter combinations produce different probability distributions because the kinds of outcomes vary considerably between the different combinations.

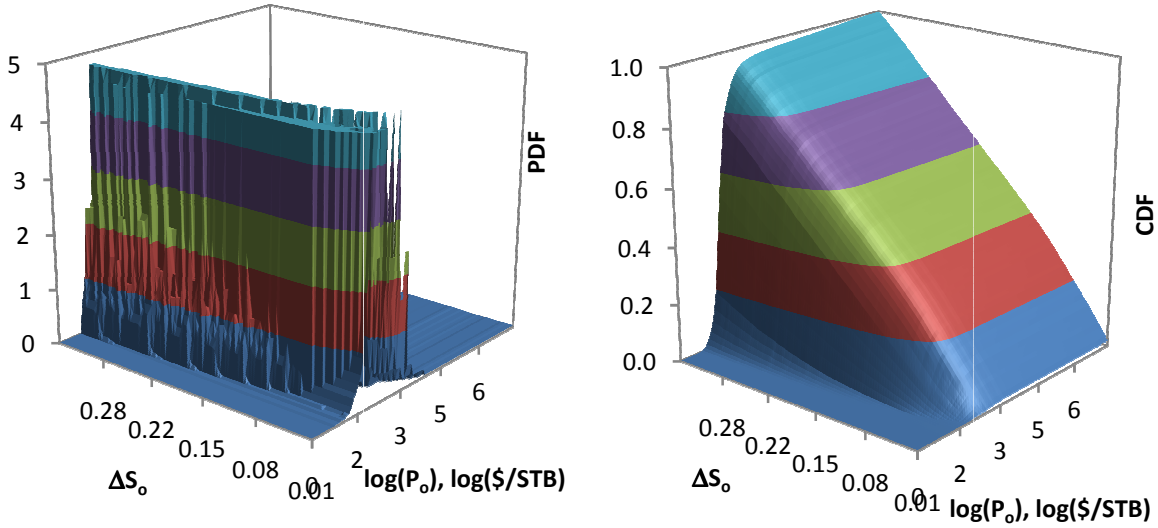

(a) Joint PDF **(b) Joint CDF**

Figure D-5 Plots of the Joint PDF and CDF for the Combination of ΔS_o and P_o

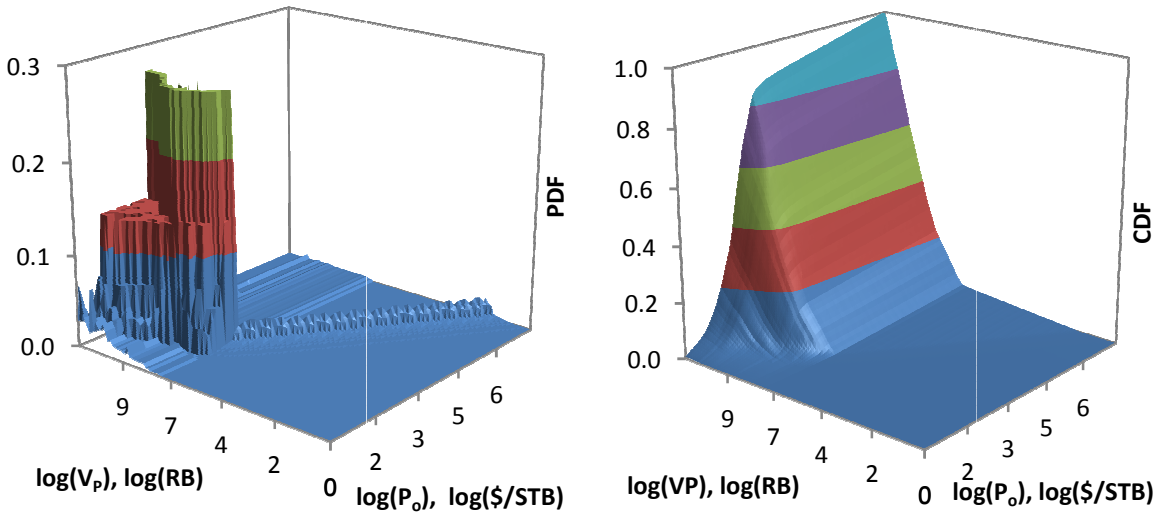

(a) Joint PDF **(b) Joint CDF**

Figure D-6 Plots of the Joint PDF and CDF for the Combination of V_P and P_o

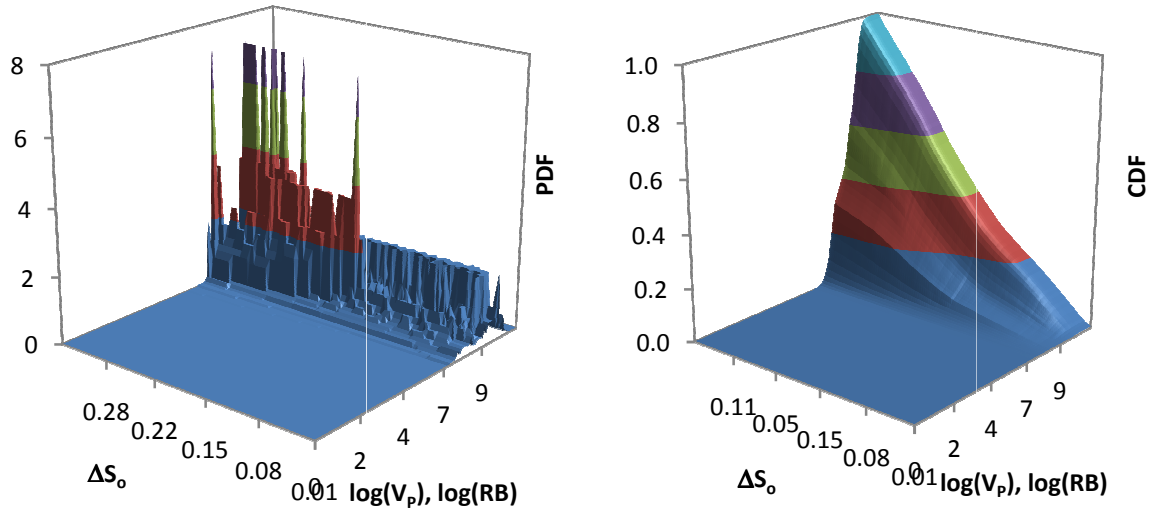

(a) Joint PDF **(b) Joint CDF**

Figure D-7 Plots of the Joint PDF and CDF for the Combination of ΔS_o and V_P

D.4 Three Parameter Analyses

The following plots illustrate how the probability distributions change when all three parameters are considered. Analyses were also performed to demonstrate how sensitive DBM is to the selected ranges for each parameter. The complete range attempts to look at all possible values. The plots created with this range are used for comparisons between other analyses. The selected range is based on a narrow range of value that encompasses all possible outcome sets, and therefore neglects meaningless events. The narrowed range is a narrower set of ranges that are arbitrarily selected. Table D-1 is a summary of the different ranges used for the sensitivity analysis.

Table D-1 Summary of the Ranges used in the Sensitivity Analysis for DBM

Parameter	Complete Range		Selected Range		Narrowed Range	
	Low	High	Low	High	Low	High
ΔS_o	0.01	0.35	0.01	0.35	0.05	0.25
log(P_o), log($/STB)	0	8	0	4	1	3
log(V_P), log(RB)	0	11	6	11	7	9

There is minimal difference between distributions based on the complete and selected ranges because the outcomes and the utility sets that influence the decision are the same between the two sets of ranges. However, there is considerable difference between the narrowed range and the other two because several important outcomes have been eliminated, which alters the probability distributions.

D.4.1 Three Parameter Analyses with Complete Ranges

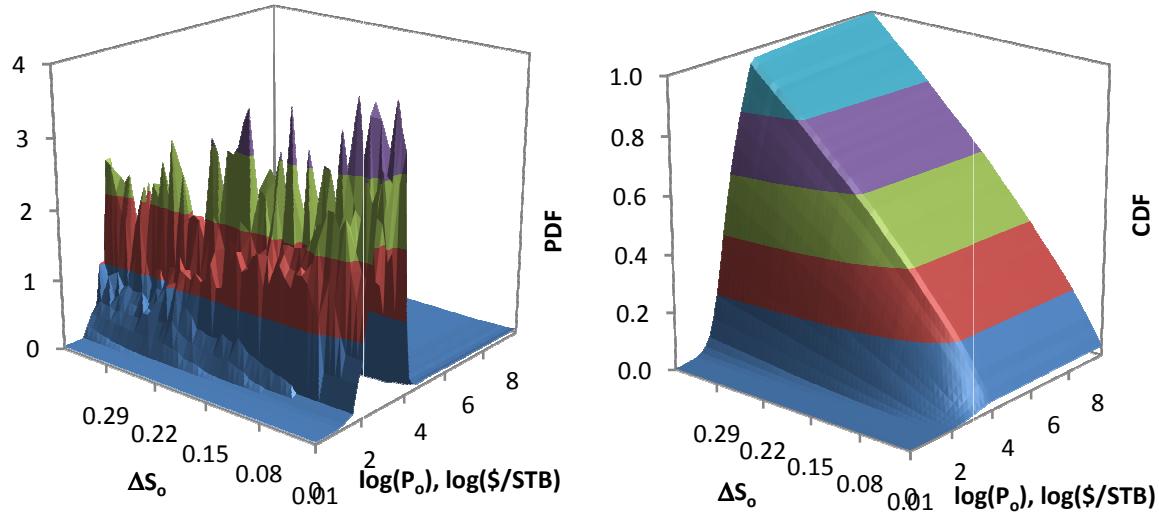

(a) Joint PDF (b) Joint CDF

Figure D-8 Plots of the Joint PDF and CDF for ΔS_o and P_o based on the Combination of ΔS_o, P_o, and V_P with Complete Ranges

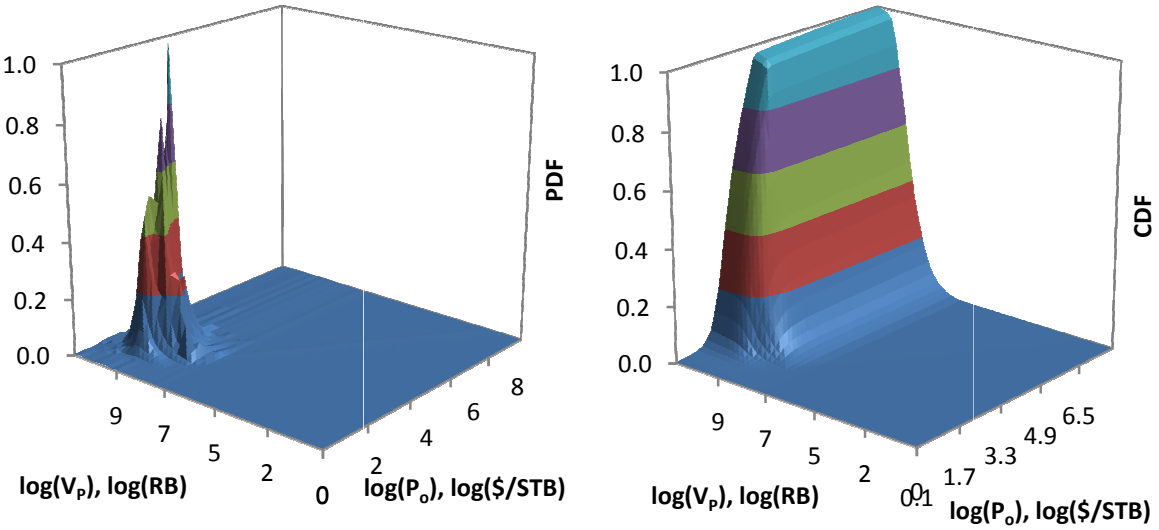

(a) Joint PDF (b) Joint CDF

Figure D-9 Plots of the Joint PDF and CDF for V_P and P_o based on the Combination of ΔS_o, P_o, and V_P with Complete Ranges

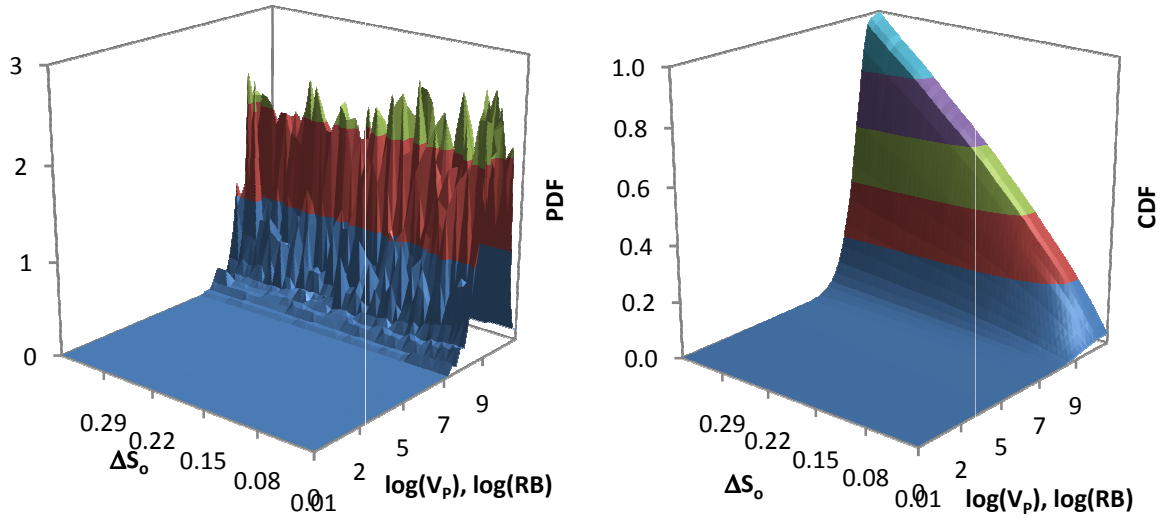

(a) Joint PDF **(b) Joint CDF**

Figure D-10 Plots of the Joint PDF and CDF for ΔS_o and V_P based on the Combination of ΔS_o, P_o, and V_P with Complete Ranges

D.4.2 Three Parameter Analyses with Selected Ranges

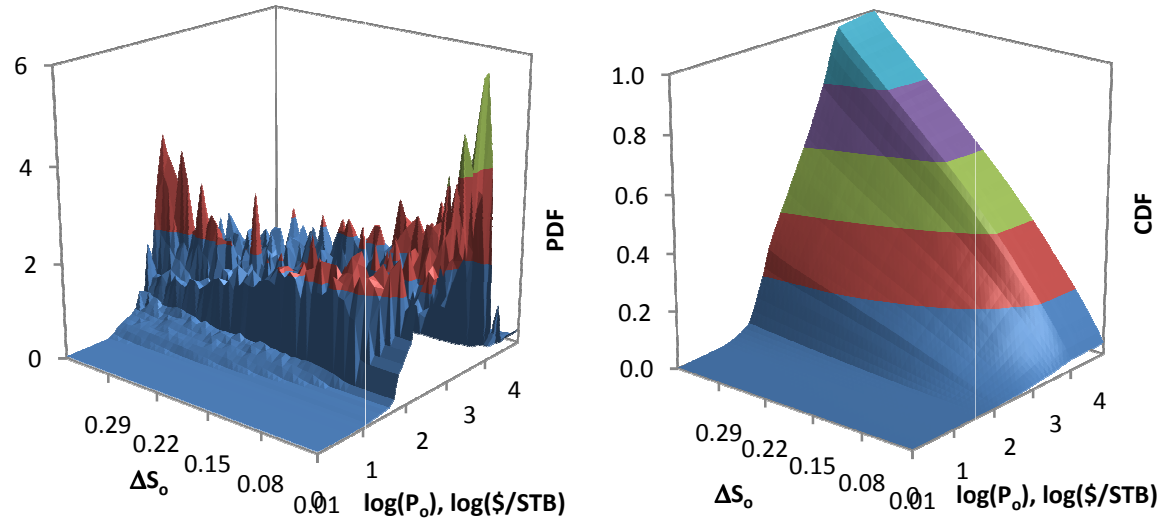

(a) Joint PDF **(b) Joint CDF**

Figure D-11 Plots of the Joint PDF and CDF for ΔS_o and P_o based on the Combination of ΔS_o, P_o, and V_P with Selected Ranges

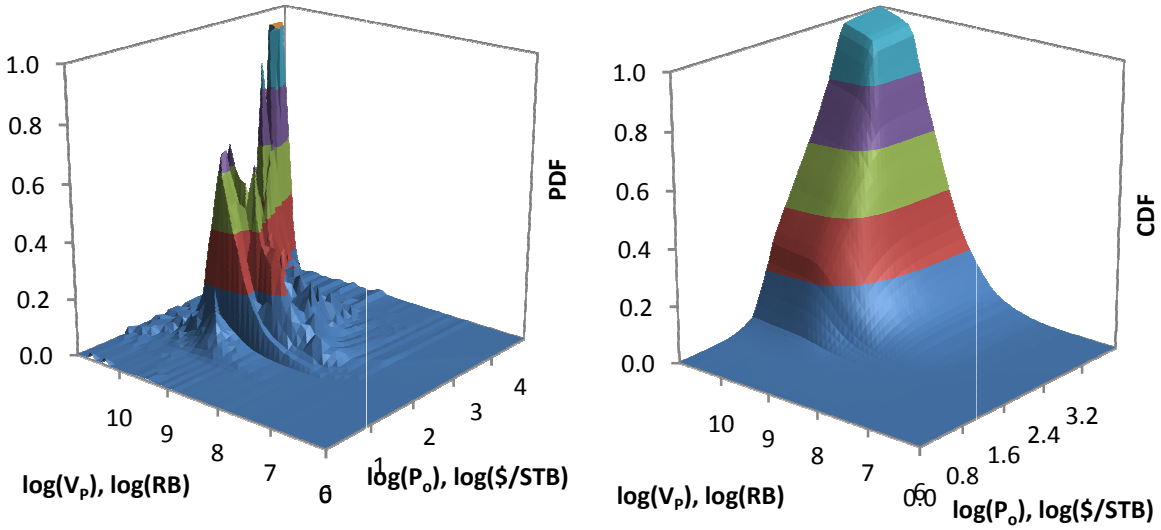

(a) Joint PDF (b) Joint CDF

Figure D-12 Plots of the Joint PDF and CDF for V_P and P_o based on the Combination of ΔS_o, P_o, and V_P with Selected Ranges

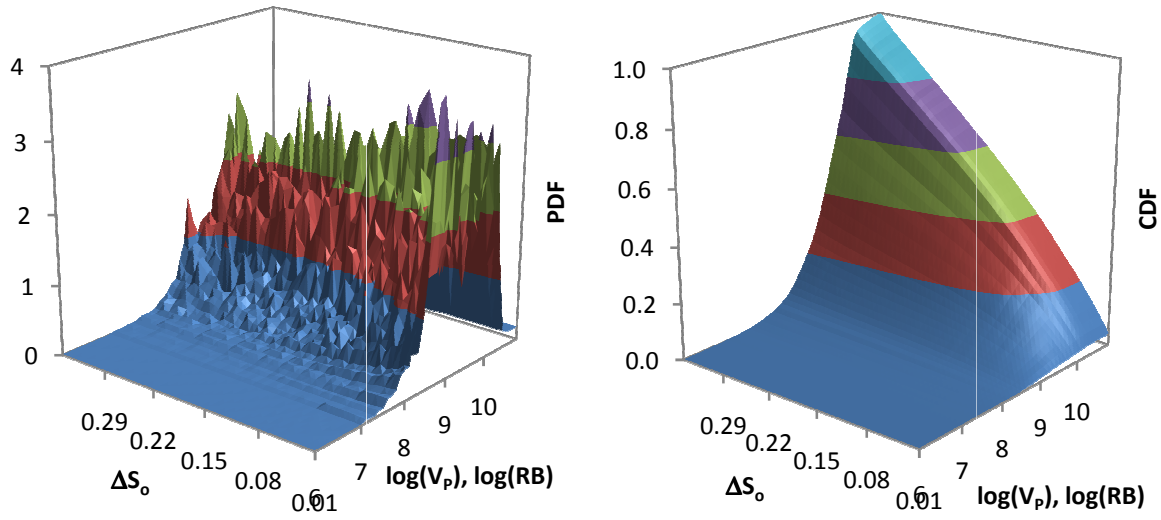

(a) Joint PDF (b) Joint CDF

Figure D-13 Plots of the Joint PDF and CDF for ΔS_o and V_P based on the Combination of ΔS_o, P_o, and V_P with Selected Ranges

D.4.3 Three Parameter Analyses with Narrowed Ranges

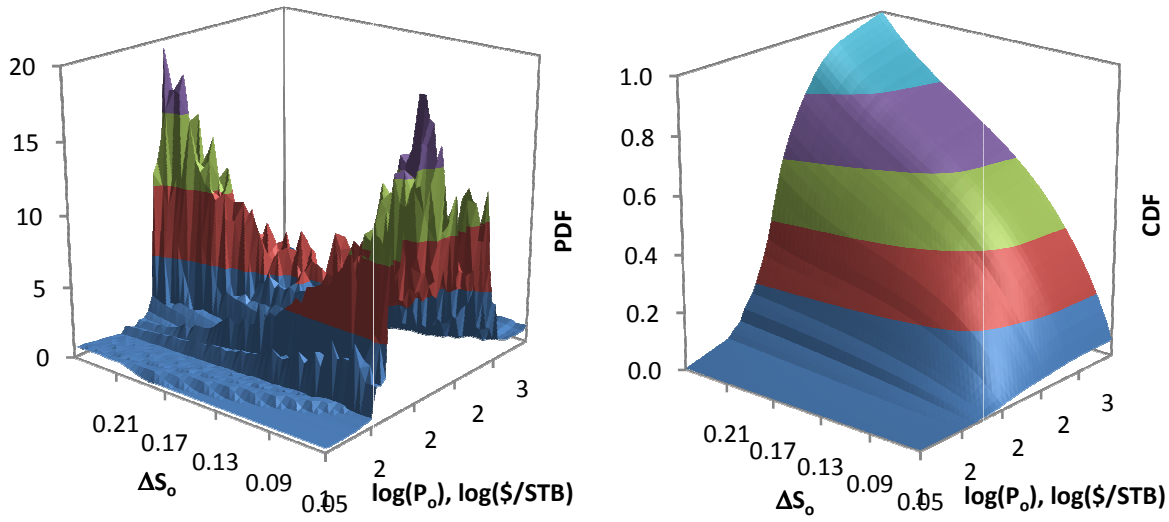

(a) Joint PDF (b) Joint CDF

Figure D-14 Plots of the Joint PDF and CDF for ΔS_o and P_o based on the Combination of ΔS_o, P_o, and V_P with Narrowed Ranges

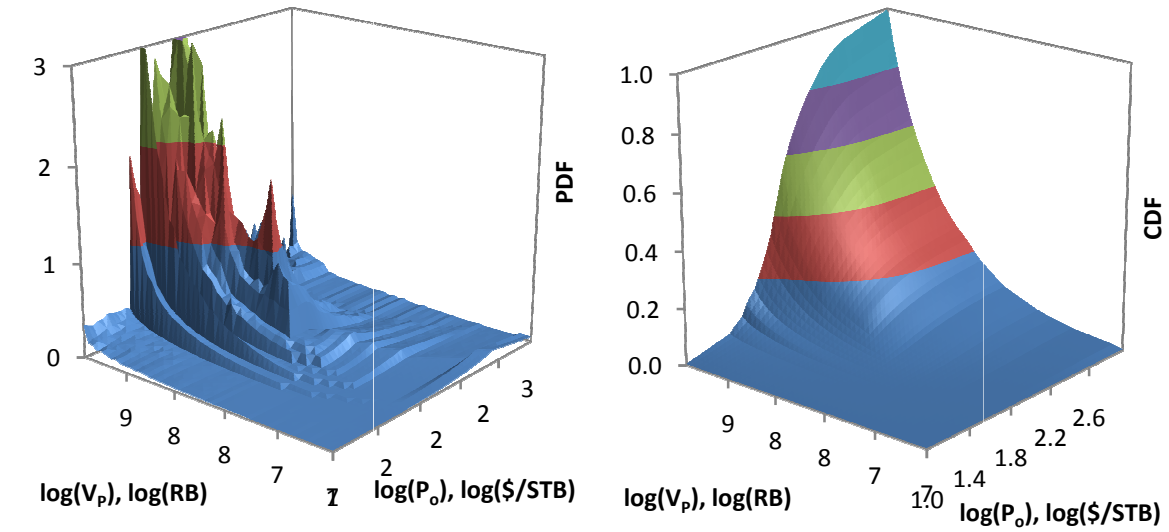

(a) Joint PDF (b) Joint CDF

Figure D-15 Plots of the Joint PDF and CDF for V_P and P_o based on the Combination of ΔS_o, P_o, and V_P with Narrowed Ranges

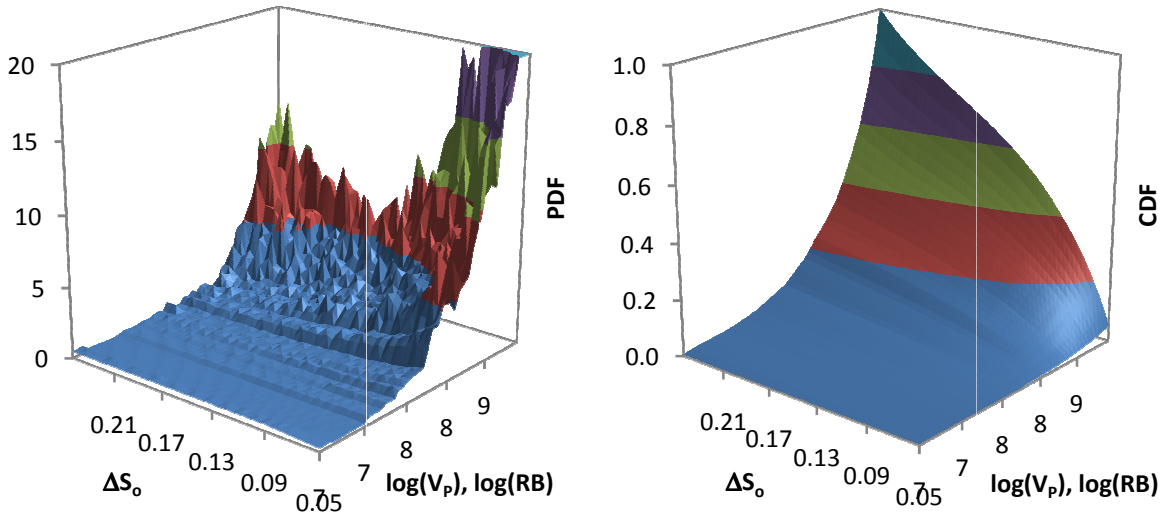

(a) Joint PDF **(b) Joint CDF**

Figure D-16 Plots of the Joint PDF and CDF for ΔS_o and V_P based on the Combination of ΔS_o, P_o, and V_P with Narrowed Ranges

D.4.4 Comparison of All Three Range Types

The following are plots of the marginal PDFs for the three parameters. These plots allow for an easy way to see how the ranges influence the distributions.

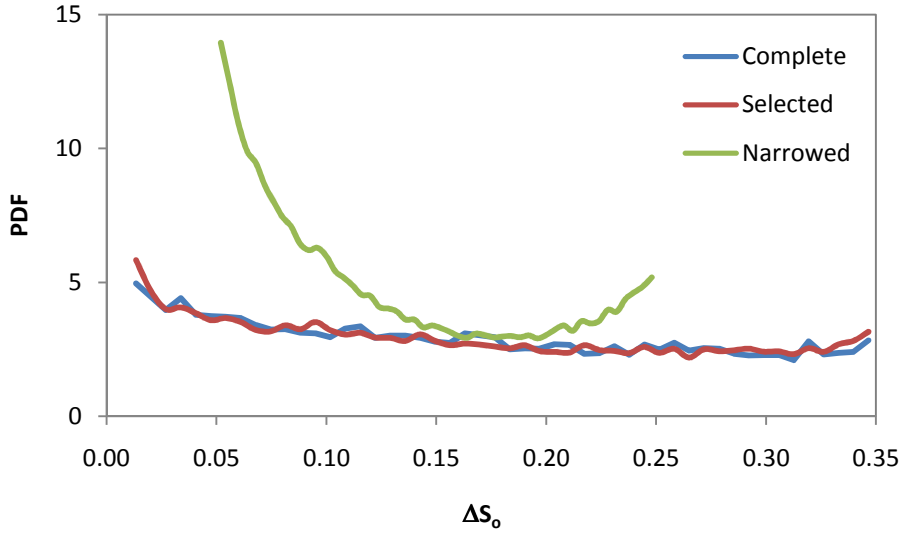

Figure D-17 Plots of the Marginal PDF for ΔS_o based on the Combination of ΔS_o, P_o, and V_P with Various Ranges

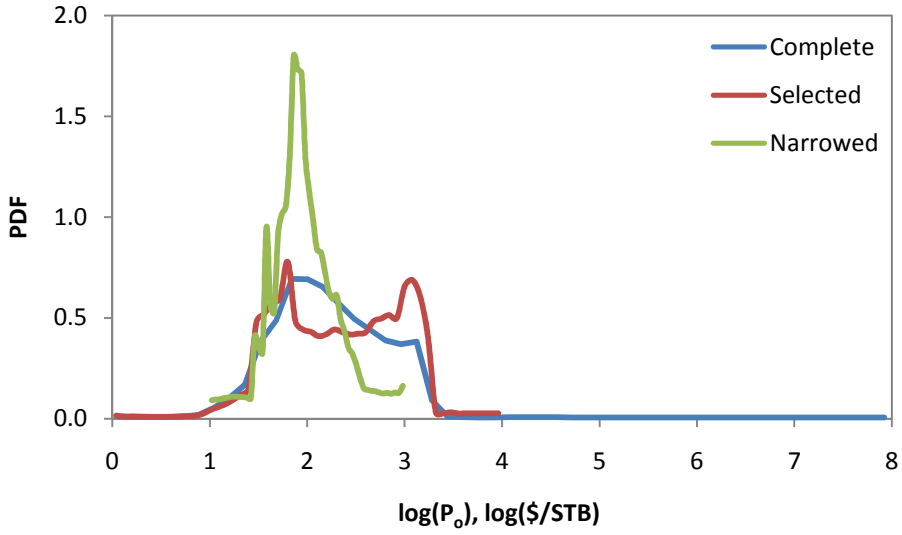

Figure D-18 Plots of the Marginal PDF for P_o based on the Combination of ΔS_o, P_o, and V_P with Various Ranges

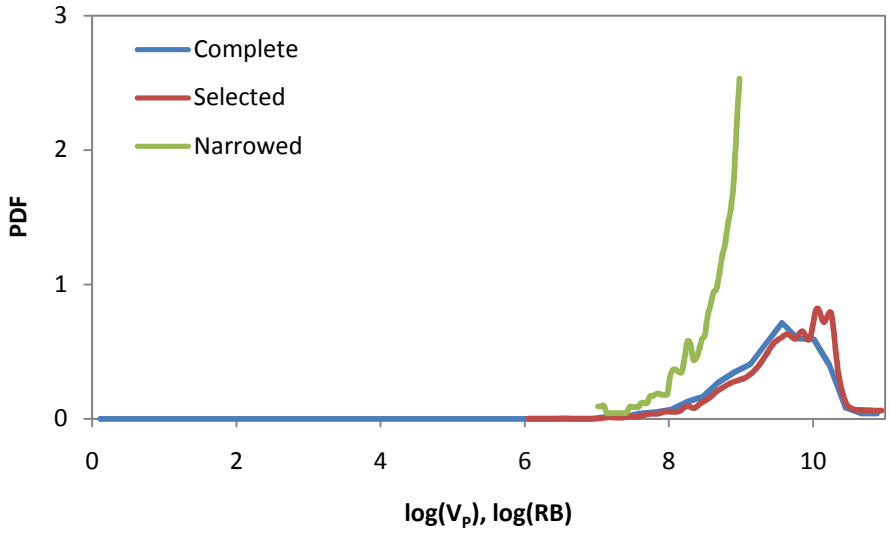

Figure D-19 Plots of the Marginal PDF for V_P based on the Combination of ΔS_o, P_o, and V_P with Various Ranges

D.5 Monte Carlo Comparisons

The following are plots the results of a Monte Carlo simulation for DBM with the "selected" ranges. The Monte Carlo simulation is with 40,000 randomly selected points.

D.5.1 Monte Carlo Comparisons for Joint PDFs and CDFs

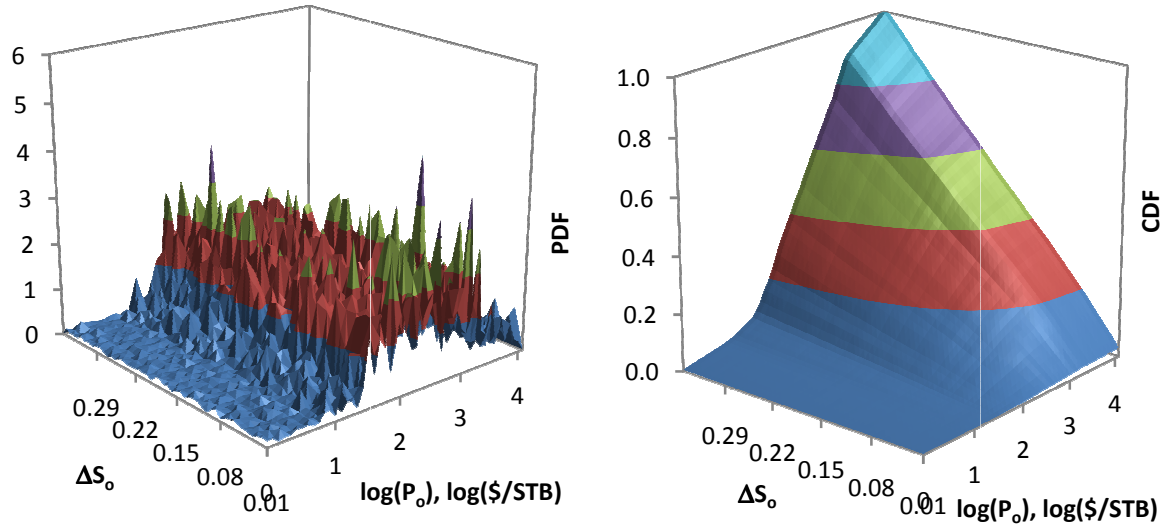

(a) Joint PDF **(b) Joint CDF**

Figure D-20 Plots of the Joint PDF and CDF from Monte Carlo Simulation for ΔS_o and P_o based on the Combination of ΔS_o, P_o, and V_P with Selected Ranges

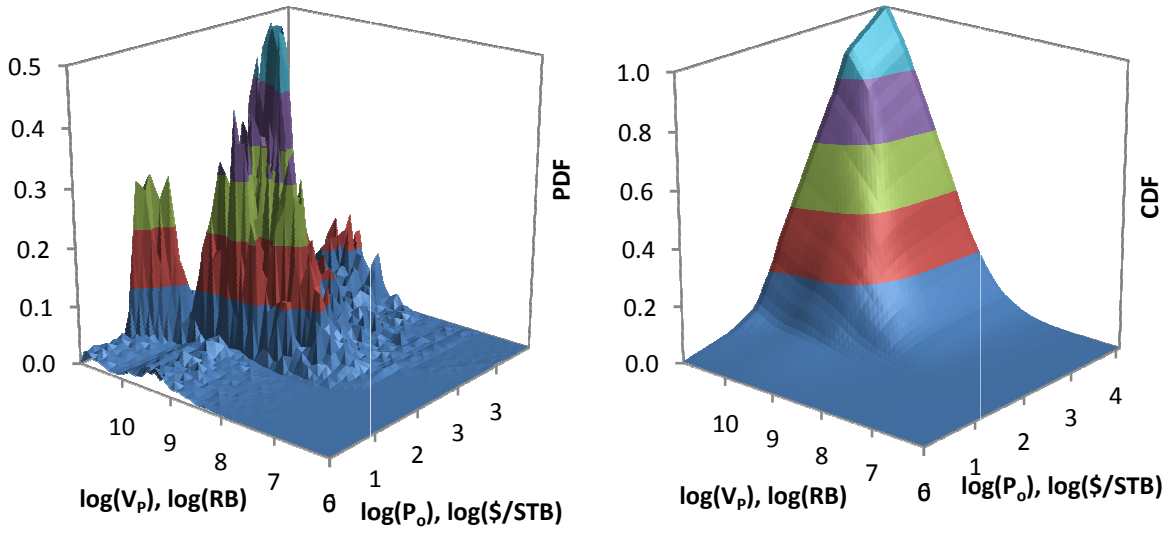

(a) Joint PDF **(b) Joint CDF**

Figure D-21 Plots of the Joint PDF and CDF from Monte Carlo Simulation for V_P and P_o based on the Combination of ΔS_o, P_o, and V_P with Selected Ranges

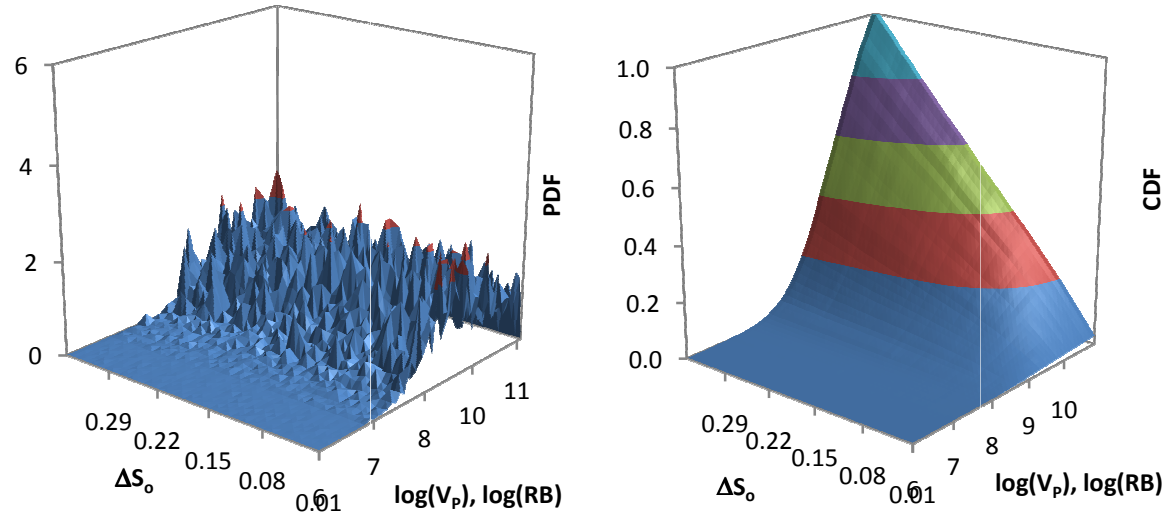

(a) Joint PDF **(b) Joint CDF**

Figure D-22 Plots of the Joint PDF and CDF from Monte Carlo Simulation for ΔS_o and V_P based on the Combination of ΔS_o, P_o, and V_P with Selected Ranges

D.5.2 Monte Carlo Comparisons for Marginal PDFs and CDFs

The comparison of the rigorous analysis and the Monte Carlo analysis is more easily seen with the marginal PDFs and CDFs.

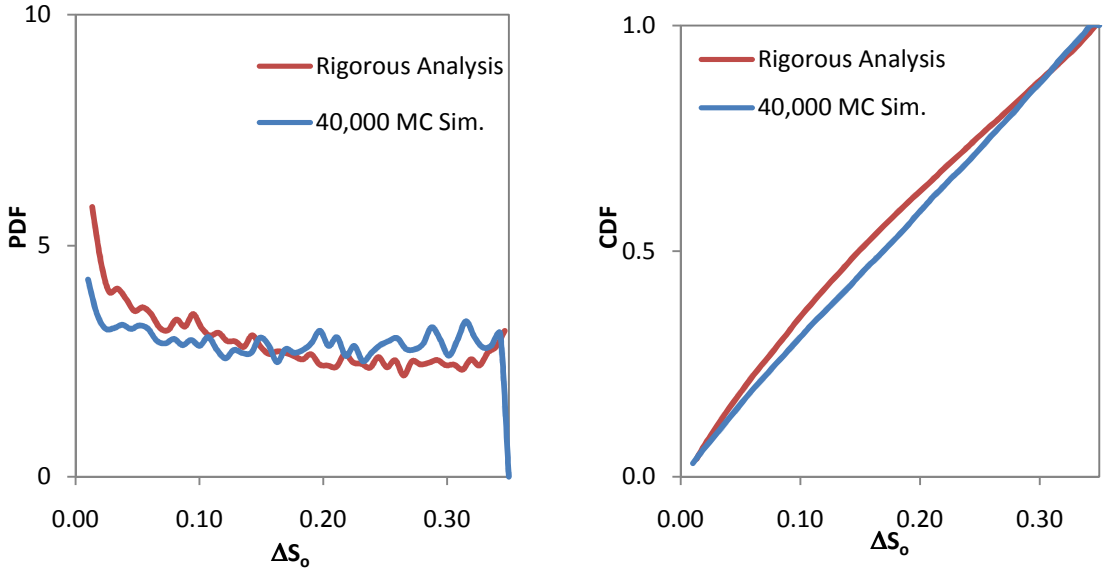

Figure D-23 Comparison of the Marginal PDFs and CDFs for the Rigorous and Monte Carlo Simulations for ΔS_o

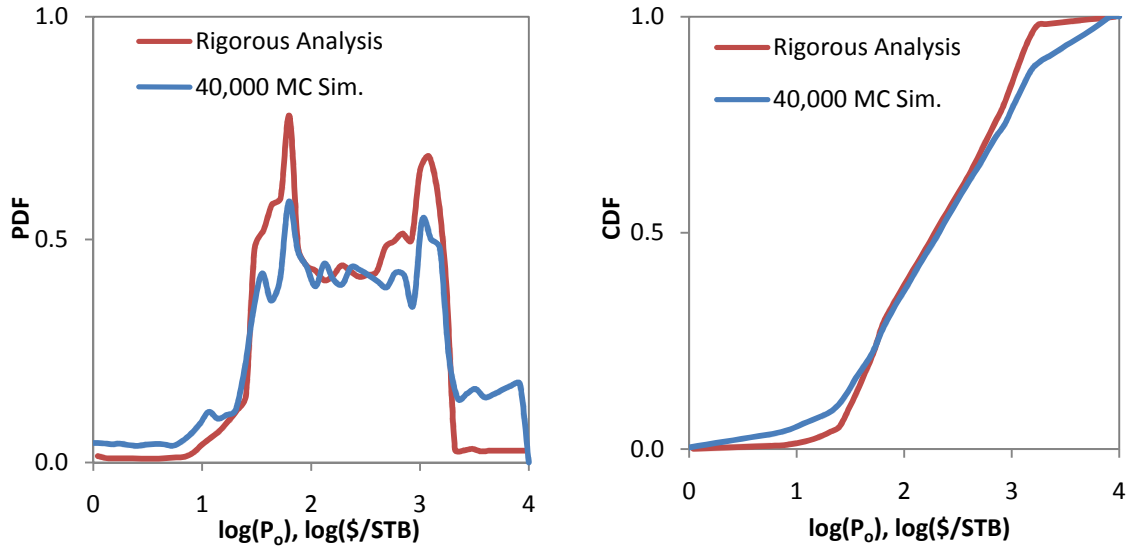

(a) Joint PDF (b) Joint CDF

Figure D-24 Comparison of the Marginal PDFs and CDFs for the Rigorous and Monte Carlo Simulations for P_o

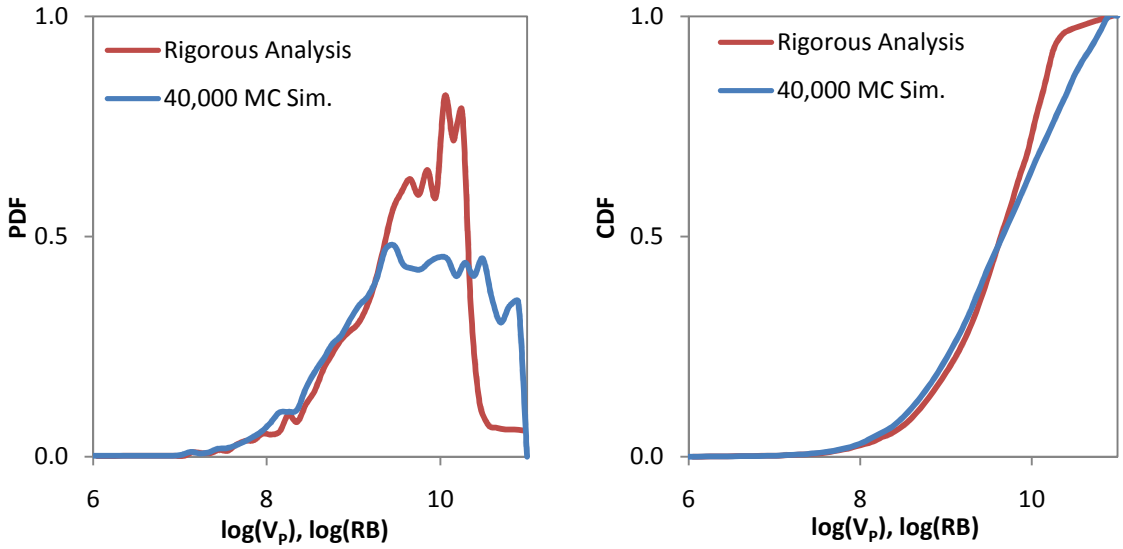

(a) Joint PDF (b) Joint CDF

Figure D-25 Comparison of the Marginal PDFs and CDFs for the Rigorous and Monte Carlo Simulations for V_P

APPENDIX E: NOMENCLATURE

E.1 Introduction

The following is a summary of all of the abbreviated terms, parameters, and units used throughout the thesis.

E.2 Units

Table E-1 is a list of abbreviated units used throughout the thesis.

Table E-1 List of Abbreviated Units

BOPD	Barrels of oil per day
BPD	Barrels per day
CF	Cubic feet
cp	Centipoises
lb	Pound
M	Thousand
MM	Million
RB	Reservoir barrel
STB	Stock-tank barrel
WAG	Water alternating gas ratio

E.3 Abbreviations and Acronyms

Table E-2 is a list of abbreviations and acronyms used throughout the thesis.

Table E-2 List of Abbreviations and Acronyms

ASP	Alkali-surfactant-polymer
CDCF	Cumulative discounted cash flow
CDCFM	Cumulative discounted cash flow method
CDF	Cumulative distribution function
CFPM	Chemical flood predictive model
CO_2	Carbon dioxide
COV	Coefficient of variation
DBM	Decision based method
EOR	Enhanced oil recovery
MNPV	Max net present value
NPV	Net present value
OOIP	Original oil at place (at time of discovery)
PDF	Probability density function
PIR	Principle of insufficient reason
PMF	Probability mass function
SEORM	Simplified enhanced oil recovery method
SP	Surfactant-polymer
VOI	Value of information
VPI	Value of perfect information
WF	Water flooding

E.4 Parameters and Variables

Table E-3 is a list of the parameters associated with the simplified enhanced oil recovery method. More details can be found in Chapter 3.

Table E-3 List of Parameters Associated with SEORM

S_{oF}	Average oil saturation at the end of the EOR flood
K_1	The Koval factor for the flow between the mobilized oil and initial banks
K_2	The Koval factor for the flow between the injected and mobilized oil banks
K_f	Scale factor for determining K_2
v_{oB}	Specific shock velocity of mobilized oil bank
V_p	Total pore volume of reservoir
ΔS_o	Change in oil saturation over life of EOR flood

Table E-4 is a list of the parameters associated with the design inputs for an enhanced oil recovery project. These parameters are typically controlled and determined by the designers of the flood. More details can be found in Chapter 3 and 5.

Table E-4 List of Parameters Associated with Design Inputs for an EOR Project

q_i	Injection rate (constant for entire flood)
q_p	Production rate (constant for entire flood)
V_{Chem}	Surfactant or alkali slug size (For SP and ASP floods)
V_{CO2}	CO_2 slug size
V_{Poly}	Polymer slug size
WS	Well spacing
Z_{CO2}	CO_2 WAG ratio
Z_{Alk}	Alkali agent concentration
Z_{Poly}	Polymer concentration
Z_{Sur}	Surfactant concentration (For SP and ASP floods)

Table E-5 is a list of the economic parameters used to develop economic values of projects. More information on the parameters can be found in Chapter 5.

Table E-5 List of Economic Parameters

C_A	Unit price of alkali
C_{CO2}	Unit price of CO_2 price
C_I	Start up cost per new well
C_M	Maintenance cost per well
C_P	Polymer price
C_q	Fluid injection cost
C_{Soft}	Softening Cost
C_{Sur}	Unit price of surfactant
C_T	Oil treatment cost
C_{WD}	Water disposal cost
d	Real discount rate (without inflation)
i	Inflation
P_O	Price of oil
R_E	Escalation factor for the price of oil
T_R	Royalty
T_S	Severance tax
T_V	Ad-valorem tax

Table E-6 is a list of the variables that are used as part of the statistical analyses. More details about the variables can be found in Chapters 4, 6, and 7.

Table E-6 List of Statistical Variables

A	An alternative for a decision analysis
E	An event for a decision analysis
I	Information for a decision analysis
R^2	Coefficient of determination
S	Sensitivity index, used for the sensitivity analysis
U	Utility, the value associated with an outcome in a decision analysis
μ	Mean
σ	Standard deviation

Table E-7 is a list of all other parameters and variables used in derivations and other mathematical explanations.

Table E-7 List of Other Parameters and Variables used throughout the Thesis

A	Cross-sectional area of a reservoir
b	Number of wells
B_o	Formation volume factor for oil
C	Channeling variable
D	Decline rate in oil production
d	Real discount rate (Inflation is not included)
E	Effective viscosity
F_{disp}	Fractional flow of the displacing fluid
f_o	Oil cut at producer
F_{oB}	Fractional flow of the oil bank
f_{oB}	Peak oil cut for mobilized oil bank
F_{oF}	Fractional flow of the chasing fluids
f_{oF}	Oil cut at the end of EOR flood, assumed to be zero
f_{oI}	Oil cut at start of EOR flood
FV	Future value
H	Heterogeneity factor
I	Information for a decision analysis
J_{disp}	Saturation velocity of the displacing fluid
K	Koval factor
K_{disp}	Koval factor for displacing fluid
K_f	Koval scale factor
k^o_{ro}	End point relative permeability of oil
k^o_{rw}	End point relative permeability of water
L	Distance between injector and producer
m	Corey type exponent for oil
m_A	Mass of injected alkali
m_P	Mass of injected polymer
m_{Sur}	Mass of injected surfactant
n	Corey type exponent for water
N_C	Capillary number

N_P	Cumulative produced oil
PV	Present value
q	Volumetric flow
q_I	Injection rate
q_P	Production rate
q_{WF}	Injection rate for water flooding
S	Relative saturation of the system
S'_i	Magnitude of influence of a parameter i
SA	Surface area of project, field size
S_{disp}	Saturation of the displacing fluid
S_{oB}	Oil saturation within the mobilized oil bank
S_{oF}	Average oil saturation at the end of the EOR flood
S_{oI}	Average oil saturation at the start of EOR flood
S_{or}	Average residual oil saturation at the end of water flooding
S_{or}	Residual oil saturation
S_{wr}	Residual water saturation
t	Time
t_D	Dimensionless time in terms of injected pore volume
u_{disp}	Interstitial velocity for the displacing fluid
v	Effective flow rate
v_C	The specific shock velocity of the injected chemical bank
v_{disp}	The specific shock velocity of the displacing fluid
v_{oB}	The specific shock velocity of the mobilized oil bank
V_p	Total pore volume of reservoir
x	Distance from injector
x_D	Relative distance between injector and producer
ϕ	Porosity
μ_o	Viscosity of oil
μ_w	Viscosity of water
ν	Viscosity ratio
σ	Surface tension

References

Aguey, Omar Jose. "Field Performance Analysis of Micellar Polymer Pilot Flood." *SPE California Regional Meeting.* San Fransisco: Society of Petroleum Engineers, 1982.

American Petroleum Institute. "Oil and Natural Gas Royalties." *The API Website.* http://www.api.org/aboutoilgas/sectors/explore/oilandnaturalgas.cfm (accessed March 1, 2010).

Anderson, Glen, Mojdeh Delshad, Chrissi King, Hourshad Mohammadi, and Gary Pope. "Optimization of Chemical Flooding in a Mixed-Wet Dolomite Reservoir." *Symposium on Improved Oil Recovery.* Tulsa: SPE/DOE, 2006.

Ang, Alfredo Hua sing, and Wilson H. Tang. *Probability Concepts in Engineering: Emphasis on Applications in Civil and Environmental Engineering.* New York: Wiley, 2007.

Ang, Alfredo, and Wilson Tang. *Probability Concepts in Engineering Planning and Design.* Vol. 2. New york: John Wiley and Sons, 1984.

Austad, Tor, and Jess Milter. "Surfactant Flooding in Enhanced Oil Recovery." In *Surfactants: Fundamentals and Applications in the Petroleum Industry*, by Laurier L. Schramm, 203-249. Cambridge: Cambridge University Press, 2000.

Bae, J.H. "Glenn Pool Surfactant Flood Expansion Project: A Technical Summary." *SPE Reservoir Engineering* 10, no. 2 (1995): 123-128.

Bae, J.H., and E.U. Syed. "Glenn Pool Surfactant Flood Pilot Test: Part 2 - Field Operations." *SPE Reservoir Engineering* 3, no. 3 (1988): 771-777.

Belhaj, Hadi, and T. Lay. "Future Projection of Energy Prices: A Predictive Model." *Western Regional and Pacific Section AAPG Joint Meeting.* Bakersfield: SPE, 2008.

Borah, M.T., and M.D. Gregory. "A Summary of the Big Muddy Field Low-Tension Flood Demonstration." *SPE Rocky Mountain Regional Meeting.* Casper: Society of Petroleum Engineers, Inc, 1988.

Bosch, Maria, Joan Montllor-Serrats, and Maria Tarrazon. "NPV as a Function of the IRR: The Value Drivers of Investment Projects." *Journal of Applied Finance* 17, no. 2 (2007): 41-45.

Brooks, R. H., and A. T. Corey. "Hydraulic Properties of Porous Media." *Hydrology Papers.* Colorado: Colorado State University, 1964.

Buckley, S.E., and M.C. Leverett. "Mechanism of Fluid Displacement in Sands." *Petroleum Transactions, AIME*, 1942: 107-116.

Chapotin, D., J. Lomer, and A. Putz. "The Chateaurenard (France) Industrial Microemulsion Pilot Design and Performance." *Fifth Symposium on Enhanced Oil Recovery of the Society of Petroleum Engineers and the Department of energy.* Tulsa: Society of Petroleum Engineers, 1986.

Crawford, C.C., and M.E. Crawford. "Wm. Berryhill Micellar Polymer Project: A Case History." *SPE Annual Technical Conference and Exhibition.* Las Vegas: Society of Petroleum Engineers, 1985.

Danielson, H.H., W.T. Paynter, and H.W. Milton. "Tertiary Recovery by the Maraflood Process in the Bradford Field." *Journal of Petroleum Technology* 28, no. 2 (1976): 129-138.

Department of Energy. "EIA - Forecasts and Analysis of Energy Data." *Energy Information Administration - EIA - Official Energy Statistics from the U.S. Government.* http://www.eia.doe.gov/oiaf/forecasting.html (accessed March 1, 2010).

Ferrell, H.H., D.W. King, and C.Q. Sheely. "Analysis of the Low-Tension Pilot at Big Muddy Field, Wyoming." *SPE Formation Evaluation* 3, no. 2 (1988): 315-321.

Flanders, W.A., and R.M. DePauw. "Update Case History: Performance of the Twofreds Tertiary CO2 Project." *SPE Annual Technical Conference and Exhibition.* Houston: Society of Petroleum Engineers, Inc., 1993.

Forbes. "Tax Terms." *Investopedia.* http://www.investopedia.com (accessed March 1, 2010).

French, M.S., G.L. Stegemeier, R.C. Ueber, and H.J. Hill. "Field Test of an Aqueous Surfactant System For Oil Recovery, Benton Field, Illinois." *Journal of Petroleum Technology* 25, no. 2 (1973): 195-204.

Gilbert, Robert B., Min Namhong, and Larry W. Lake. *A Sound Foundation for Assessing Probabilities.* Austin: The University of Texas at Austin, 2008.

Goda, H., and P. Behrenbrunch. "Using a Modified Brooks-Corey Model to Study Oil-Water Relative Permeability for Diverse Pore Structures." *SPE Asia Pacific Oil and Gas Conference and Exhibition.* Perth, 2004.

Gogarty, W.B., and H. Surkalo. "A Field Test of Micellar Solution Flooding." *Journal of Petroleum Technology* 24, no. 9 (1972): 1161-1169.

Guckert, Larry, and Warren T. Paynter. "Micellar-Polymer Flooding Projects in the Bradford Field." *International Petroleum Exhibition and Technical Symposium.* Beijing: Society of Petroleum Engineers, 1982.

Haller, R.W. "Big Muddy Water Flood." *Journal of Petroleum Technology* 7, no. 11 (1955): 9-12.

Hartshorne, J.M. "Micellar/Polymer Flood Shows Success in Bell Creek Field." *SPE Annual.* Houston: Society of Petroleum Engineers of AIME, 1984.

Hoiland, R.C., H.D. Joyner, and J.L. Stalder. "Case History of a Successful Rocky Mountain Pilot CO2 Flood." *SPE Enhanced Oil Recovery Symposium.* Tulsa: Society of Petroleum Engineers, 1986.

Kleinstelber, Stanley W. "The Wertz Tensleep CO2 Flood: Design and Initial Performance." *Journal of Petroleum Technology* 42, no. 5 (1990): 630-636.

Koval, E.J. "A Method for Predicting the Performance of Unstable Miscible Displacement in Heterogeneous Media." *SPE Journal* 3, no. 2 (1963): 145 - 154.

Lake, Larry W. *Enhanced Oil Recovery.* Alexandria: Prentice Hall, 1989.

Lake, Larry W. "Enhanced Oil Recovery Fundamentals." Houston, Texas: Shell, November 2008.

Lake, Larry W., James R. Johnston, and George L. Stegemeier. "Simulation and Performance Prediction of a Large-Scale Surfactant/Polymer Project." *SPE Journal* 21, no. 6 (1981): 731-739.

Langston, M.V., and D.N. Young. "Definitive CO2 Flooding Response in the SACROC Unit." *SPE Enhanced Oil Recovery Symposium.* Tulsa: Society of Petroleum Engineers, 1988.

Langston, M.V., S.F. Hoadley, and D.N. Young. "Definitive CO2 Flooding Response in the SACROC Unit." *SPE Enhanced Oil Recovery Symposium.* Tulsa: Society of Petroleum Engineers , 1988.

Masoner, L.O., and R.K. Wackowski. "Rangely Weber Sand Unit CO2 Project Update." *SPE Reservoir Engineering* 10, no. 3 (1995): 203-207.

Min, Namhong. *A Method to Establish Non-Informative Prior Probabilities for Risk-Based Decision Analysis.* PhD Thesis, Austin: The University of Texas at Austin, 2008.

Mohan, Hitesh, Marshall Carolus, and Khosrow Biglarbigi. "The Potential for Additional Carbon Dioxide Flooding Projects in the United States." *Symposium on Improved Oil Recovery.* Tulsa: SPE/DOE, 2008.

Ondrusek, P.S. "Micellar/Polymer Flooding in the Bradford Field." *Journal of Petroleum Technology* 40, no. 8 (1988): 1061-1067.

Paul, G.W., and Larry W. Lake. "A Simplified Predictive Model for CO2 Miscible Flooding." *Annual Technical Conference and Exhibition.* Houston: SPE, 1984.

Pitts, M.J., P. Dowling, K. Wyatt, H. Surkalo, and C. Adams. "Alkaline-Surfactant-Polymer Flood of the Tanner Field." *SPE/DOE Symposium on Improved Oil Recovery.* Tulsa: Society of Petroleum Engineers, 2006.

Pope, Gary. "The Application of Fractional Flow Theory to Enhanced Oil Recovery." *SPE Journal* 20, no. 3 (1980): 191-205.

Pursley, S.A., and H.L. Graham. "Borregos Field Surfactant Pilot Test." *Journal of Petroleum Technology* 27, no. 6 (1975): 695-700.

Putz, A. G., J. M. Lecourtier, and L. Bruckert. "Interpretation of High Recovery Obtained in a New Polymer Flood in the Chateaurenard Field." *Annual Technical Conference and Exhibition of the Society of Petroleum Engineers.* Houston: Society of Petroleum Engineers, 1988.

Putz, A., J.P. Chevalier, G. Stock, and J. Philippot. "A Field Test of Microemulsion Flooding, Chateaurenard Field, France." *Journal of Petroleum Technology* 33, no. 4 (1981): 710-718.

Qi, Qiao, Gu Hongjun, Li Dongwen, and Dong Ling. "The Pilot Test of ASP Combination Flooding in Karamay Oil Field." *International Oil and Gas Conference and Exhibition in China.* Beijing: Society of Petroleum Engineers Inc., 2000.

Reppert, T.R., J.R. Bragg, J.R. Wilkinson, T.M. Snow, N.K. Maer, and W.W. Gale. "Second Ripley Surfactant Flood Pilot Test." *SPE/DOE Enhanced Oil Recovery Symposium.* Tulsa: Society of Petroleum Engineers, Inc., 1990.

Rowe, Hunter G., Derryl S. York, and Joseph C. Ader. "Slaughter Estate Unit Tertiary Pilot Performance." *Journal of Petroleum Technology* 34, no. 3 (1982): 613-620.

Saad, Naji, Gary A. Pope, and Kamy Sepehrnoori. "Simulation of Big Muddy Surfactant Pilot." *SPE Reservoir Engineering* 4, no. 1 (1989): 24-34.

Singh, Vijay P., Sharad K. Jain, and Aditya Tyagi. *Risk and Reliability Analysis: A Handbook for Civil and Environmental Engineers.* Reston, Virginia: ASCE Press/America, 2007.

Strange, L.K., and A.W. Talash. "Analysis of Salem Low-Tension Waterflood Test." *Journal of Petroleum* 29, no. 11 (1977): 1380-1384.

Trantham, J.C., and H.L. Patterson. "The North Burbank Unit, Tract 97 Surfactant/Polymer Pilot Operation and Control." *Journal of Petroleum Technology* 30, no. 7 (1978): 1068-1074.

Trantham, J.C., C.B. Threlkeld, and H.L. Patterson. "Reservoir Description for a Surfactant/ Polymer Pilot in a Fractured, Oil-Wet Reservoir - North Burbank Unit Tract 97." *Journal of Petroleum Technology* 32, no. 9 (1980): 1647-1656.

Vargo, J.J. "Site Selection, Reservoir Definition and Estimation of Tertiary Target Oil for the Bell Creek Unit "A" Micellar-Polymer Project." *SPE Symposium on Improved Methods of Oil Recovery*. Tulsa: American Institute of Mining, Metallurgical, and Petroleum Engineers, Inc., 1978.

Vargo, Jay, et al. "Alkaline-Surfactant-Polymer Flooding of the Cambridge Minnelusa Field." *SPE Reservoir Evaluation & Engineering* 3, no. 6 (2000): 552-558.

Walsh, Mark P., and Larry W. Lake. "Applying Fractional Flow Theory to Solvent Flooding and Chase Fluids." *Journal of Petroleum Science and Engineering* 2 (1989): 281-303.

Walsh, Mark P., and Larry W. Lake. *Enhanced Oil Recovery Field Data Literature Search.* Technical Report, Austin: Department of Petroleum and Geosystems Engineering of the University of Texas at Austin, 2008.

Walsh, Mark, and Larry W. Lake. *A Generalized Approach To Primary Hydrocarbon Recovery Of Petroleum Exploration & Production.* Amsterdam: Elsevier, 2003.

Wanosik, J.L. "Sloss Micellar Pilot: Project Design and Performance." *SPE Symposium on Improved Methods of Oil Recovery*. Tulsa: American Institute of Mining, Metallurgical, and Petroleum Engineers, Inc., 1978.

White, J.R., R.L. Gorring, and A.S. Odeh. "A General Approach to Estimating the Cost of Recovering Crude Oil by Surfactant Waterflood Techniques." *Journal of Petroleum Technology* 38, no. 2 (1986): 208-216.

Widmyer, R.H, D.B. Williams, and J.W. Ware. "Performance Evaluation of the Salem Unit Surfactant/Polymer Pilot." *Journal of Petroleum Technology* 40, no. 9 (1988): 1217-1226.

Widmyer, Richard, and Robert G. Pindell. "Manvel Enhanced Recovery Pilot Performance Evaluation." *SPE/DOE Enhanced Oil Recovery Symposium.* Tulsa: Society of Petroleum Engineers, 1981.

Wyatt, Kon, Malcom Pitts, and Harry Surkalo. "Economics of Field Proven Chemical Flooding Technologies." *Symposium on Improved Oil Recovery* . Tulsa: SPE/DOE, 2008.

VITA

Panos Andonyadis was born in Baltimore, Maryland. After he completed his high school studies at Oakton High School in Vienna, Virginia, he went to Virginia Tech where he earned a Bachelor of Engineering degree with high honors in May, 2008. During the summers between 2004 and 2008, he completed multiple internships with various civil engineering firms, including time with companies such as ECS and CDM. In the fall of 2008, he enrolled into the Graduate School at The University of Texas at Austin to earn a Master of Engineering in the field of Geotechnical Engineering.

Permanent Address: 3104 Ashburton Avenue

Herndon, Virginia 20171

USA

Email: andonyad@gmail.com

This thesis was typed by Panos Andonyadis.